I. SYNTHESIS AND UTILIZATION OF DIAZOCOMPOUNDS FOR
APPLICATIONS IN SOLUTION-PHASE AND GAS-PHASE CHEMISTRY
II. PROGRESS TOWARD THE COMMUNESIN ALKALOIDS

Thesis by

Jeremy Allen May

In Partial Fulfillment of the Requirements for the

Degree of

Doctor of Philosophy

CALIFORNIA INSTITUTE OF TECHNOLOGY

Pasadena, California

2005

(Defended July 22, 2005)

To my family and

the many teachers who prepared my way

ACKNOWLEDGEMENTS

Most important to my graduate career, of course, was the mentorship of Professor Brian Stoltz. When visiting Caltech, Brian made an offer I couldn't refuse to help him set up his lab that next summer. That summer I was able to work alongside Brian and catch some of his amazing interest in the subject of chemistry (as well as see some incredible technique). I always appreciated that he could motivate just by the excitement he exuded as he would come up with a two-page list of experiments to try. As the years have progressed, Brian has shown great patience and faith in allowing me to fill many of my own lists while making key suggestions to keep me on track. The greatest principle that Brian has exemplified is that you should never try to just meet what is required, but should exceed expectations such that there is no doubt of your success.

Along with Brian, Professor Peter Beal deserves credit for guiding me to graduate school. He took me on as an inexperienced undergraduate and showed me how to do science. His ability to teach logical, scientific thought is unparalleled. It was in his lab that I first learned how organic chemistry is performed. I also wish to extend thanks to the faculty who've worked with me as my thesis advisory committee. Professor Dave Macmillan was also very influential in bringing me to Caltech and was always glad to call on me in class when I was at my most tired. The openness with which his lab received the new Stoltz lab aided us immensely. Professor Jack Beauchamp has worked closely with me in a collaboration and has always been willing to overlook my ignorance and still invite me to his house for barbeques. Other than with Brian, I think I've talked with Professor Bob

Grubbs one-on-one more than I have with any other faculty in the department. He has the talent of getting me exited to go to the lab and do chemistry and then getting me excited to escape the lab and jump up a wall somewhere.

I've had the great pleasure to work with incredible collaborators during graduate school. Ryan Julian and I spent many hours talking chemistry in the lab. He has the incredible talent to find fascinating, undiscovered gems of chemistry, and then the ability to get Jack to read his writing no matter how many drafts it takes. Ryan and his wife Jen have become great friends and were great adventure companions in the Tetons. I look forward to continued scientific and personal interactions.

In collaboration with the Peters Group, Ted Betley was gracious enough to let me attempt some transformations with their catalysts and even to use his glovebox. Ryan Zeidan worked closely with me for years on nomofungin and the communesins, so he's one of the few in this world who knows my pain. He is a good friend and a pretty decent quarterback. Shyam Krishnan deserves the most thanks as he is willing to continue the work on the communesins, despite the setbacks that I have seen. An undergrad who pursued my crazy research ideas for three summers, Brian Underwood was a bright, willing student who is now on to big things. I appreciate his willingness to keep trying.

When the Stoltz lab congealed, there were four of us bright young hopefuls. Neil Garg is someone whose approach to chemistry is a true example to me. He is thorough and creative, and he'll be tough competition in a couple of years. On the other hand, I

consider him a good friend, and I'll remember the time spent thinking up smooth things, hitting Lee's hoagie house, or chowing on pizza during Star Wars with him and Lindsey. Eric Feirreira is an incredibly hard worker who has worked to develop an impressive knowledge of the chemical literature. He has also introduced me to some of my favorite music and was always one whom I could talk culture with. Sarah Spessard worked next to me for years and was always up for a conversation. She showed me what determination in the face of a difficult problem is and how to achieve results. She could also play a mean game of name-that-song. Dr. Haiming Zhang was an incredible friend in the lab with whom many hours were spent talking chemistry. He was also willing to talk about anything else on my mind, and I'll always look forward to talking to him again.

Raissa Trend deserves special thanks for her friendship. I can always count on Raissa to be honest with me, which is a quality I value above almost all others. I always have learned something in talking with her, and she's willing to help someone who needs it. Truthfully, this thesis couldn't have been printed without her. Another colleague who greatly influenced my chemical outlook was Dr. Richmond Sarpong. He is full of ideas and personality, and he's one of the nicest guys I'll ever meet. Dan Caspi is one of the world's great problem solvers. He made many routines to facilitate the functioning of the lab, especially for us neophytes attempting to put an electronic thesis together. I also want to thank everyone in the Stoltz lab who was willing to read for me and offer insight to my chemistry. Their contributions made this document much better.

ABSTRACT

Advances in the synthesis and use of diazo compounds are first discussed. The development of non-carbonyl stabilized diazo equivalents has allowed for carbene reactivity to be localized at carbons not adjacent to carbonyls. Consequently, a new tandem sequence, the Bamford-Stevens/Claisen reaction, has been developed that incorporates selective Z-enol enol-ether formation with a thermal- or Lewis acid-promoted Claisen reaction. Bamford-Stevens/Claisen/Carbonyl Ene and Bamford-Stevens/Claisen/Cope reactions have also been realized.

Also discussed is the application of diazocompounds to gas-phase chemistry with peptides. Crown ethers are used for binding to primary amines, and a diazomalonate is incorporated for generation of a highly reactive carbene within a non-covalent complex. Intermolecular insertion reactions can then occur in these complexes. Electrospray ionization mass spectrometry and density functional theory (DFT) are utilized to evaluate these reactions for small molecules and peptides, as well as metal-promoted Wolff Rearrangement in the gas phase.

Finally, the biosynthesis of the calycanthaceous alkaloids is examined. The development of an approach to the alkaloid communesin B (2) is presented. The approach is based on considerations of a possible biosynthetic sequence involving an oxidative coupling of tryptamine with a derivative of the ergot alkaloid aurantioclavine. Structure revision is also suggested for the recently isolated microfilament disrupting alkaloid nomofungin. Crystallographic evidence is presented for products from the proposed inverse-demand Diels-Alder reaction.

TABLE OF CONTENTS

LIST OF ABBREVIATIONS

$[a]_D$	specific rotation at wavelength of sodium D line
Ac	acetyl, acetate
app.	apparent
aq.	aqueous
atm	atmosphere
Bn	benzyl
Boc	*tert*-butyloxycarbonyl
br	broad
Bu	butyl
n-Bu	butyl
t-Bu	*tert*-Butyl
c	concentration for specific rotation measurements
°C	degrees Celsius
calc'd	calculated
CCDC	Cambridge Crystallographic Data Centre
CDI	1,1'-carbonyldiimidazole
CI	chemical ionization
Cy	cyclohexyl
d	doublet
dba	dibenzylideneacetone
dppb	1,4-bis(diphenylphosphino)butane
dec	decomposition
DMAP	4-dimethylaminopyridine
DMF	*N,N*-dimethylformamide
DMSO	dimethyl sulfoxide
EC_{50}	50% effective concentration
ee	enantiomeric excess
eNOS	endothelial nitric oxide synthase
equiv	equivalent
ESI	electrospray ionization
Et	ethyl
FAB	fast atom bombardment

g	gram(s)
gCOSY	gradient-selected Correlation Spectroscopy
h	hour(s)
HIV	human immunodeficiency virus
HRMS	high resolution mass spectroscopy
HPLC	high performance liquid chromatography
HSV	herpes simplex virus
hν	light
Hz	hertz
iNOS	inducible nitric oxide synthase
IR	infrared (spectroscopy)
J	coupling constant
l	wavelength
L	liter
m	multiplet or milli
m	meta
m/z	mass to charge ratio
m	micro
Me	methyl
MHz	megahertz
min	minute(s)
mol	mole(s)
mp	melting point
Ms	methanesulfonyl (mesyl)
MS	molecular sieves
nbd	norbornadiene
NBS	*N*-bromosuccinimide
NMO	*N*-methylmorpholine *N*-oxide
NMR	nuclear magnetic resonance
NOE	Nuclear Overhauser Effect
NOESY	Nuclear Overhauser Enhancement Spectroscopy
NOS	nitric oxide synthase
nNOS	neural nitric oxide synthase
[O]	oxidation
p	para
PDC	pyridinium dichromate

Ph	phenyl
pH	hydrogen ion concentration in aqueous solution
PhH	benzene
ppm	parts per million
PP	protein phosphatase
Pr	propyl
i-Pr	isopropyl
pyr	pyridine
q	quartet
rt	room temperature
R_f	retention factor
s	singlet or strong
SEM	(trimethylsilyl)ethoxymethyl
t	triplet
TBAF	tetrabutylammonium fluoride
TBS	*tert*-butyldimethylsilyl
Tf	trifluoromethanesulfonyl (trifyl)
TFA	trifluoroacetic acid
THF	tetrahydrofuran
TIPS	triisopropylsilyl
TLC	thin layer chromatography
TMS	trimethylsilyl
Tr	triphenylmethyl (trityl)
Ts	*p*-toluenesulfonyl (tosyl)
UV	ultraviolet
w	weak

CHAPTER 1

Non-Carbonyl Stabilized Diazo Compounds in the Tandem Bamford-Stevens/Claisen Reaction[1]

1.1 Background

1.1.1 Cascade Reactions

Tandem reactions comprise a powerful synthetic strategy that offers complex organic transformations through a sequence of simple steps. These multi-step processes increase synthetic efficiency by eliminating the handling and purification of compound between steps, and they can provide transformations not available otherwise.[2] The driving force for these reactions is often a thermodynamic sink as provided by carbon-carbon bond formation, aromatization, and other such events. Tandem reactions are usually primed by incorporation of functionality that offers the driving force for the succeeding reactions, such as a zwitterionic dipole, strained bonds, or a carbene. Through this process, multiple carbon-carbon (C-C) bonds can be formed through highly ordered and stereoselective transformations.

1.1.2 Diazo Chemistry

1.1.2.1 Diazo Compounds

A powerful activating group for organic transformations is the diazo group. The loss of dinitrogen drives formation of a relatively reactive carbene, which can be used in a variety of rearrangements and bond-forming reactions. Diazo functionality has been incorporated in diazoesters, diazoketones, and diazoalkanes in some limited cases (Figure 1.1.1). Diazoalkanes are rare without an element of stabilization, such as a carbonyl or

aromatic ring, for the diazo group. Robust preparations are known for a few of these compounds.[3,4]

Figure 1.1.1: Commonly Available Diazo Compounds.

Carbonyl Stabilized:

1   2   3   4   5

Diazoalkanes:

6   7   8
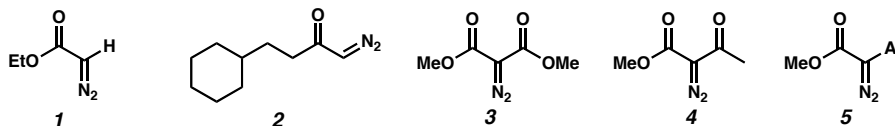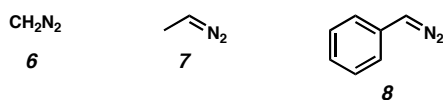
1.1.2.2 Useful Catalysts for Diazo Chemistry

Though common dediazotization catalysts include Lewis acids or Cu(0)- and Cu(II)-based complexes, controlled carbene chemistry has been greatly advanced by the advent of rhodium(II) carboxylate catalysts (i.e., **12**, Figure 1.1.2), which offer significant control over energetic intermediates.[5] The electronic nature of these catalysts can be varied by incorporation of a variety of ligands. Thus, the catalyst can be tuned to promote a specific reaction pathway, whether insertion or cycloaddition. Chiral catalysts that promote enantioselective reactions are also known.[5]

Figure 1.1.2: Typical Dediazotization Catalysts.

BF₃·Et₂O
9

Cu₍ₛ₎
10

Cu(OTf)₂
11

12

13

X=CH₂, O
*Other ligands
omitted for clarity.*

14
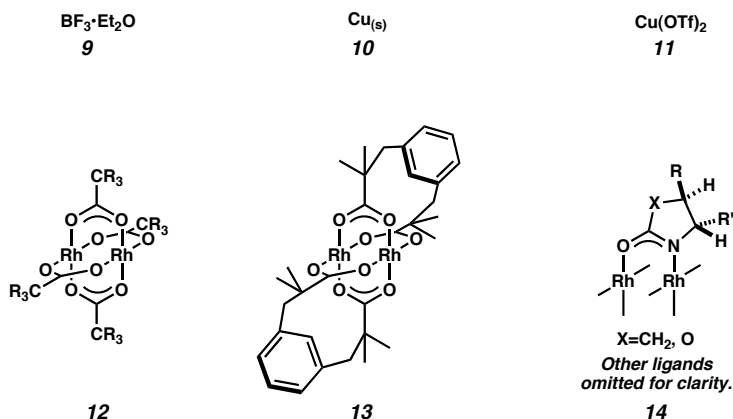
1.1.2.3 Typical Tandem Reactions from Diazo Compounds

Insertions, cycloadditions, and rearrangements to initiate cascade chemistry are available from diazo compounds. Both heteroatom-hydrogen and carbon-hydrogen insertions have been characterized, and both diastereoselective and enantioselective versions of these reactions are possible.[5] Insertions have been used to initiate cascade reactions, as is the case in the Wood version of the Claisen reaction (Scheme 1.1.1).[6] Here, initial oxygen association with the carbene of an allylic alcohol generates the allyl-enol **16**, which can then undergo a Claisen rearrangement to form ketoester **17**. Enol intermediate **16** is activated, so the Claisen reaction occurs at relatively low temperature.

Scheme 1.1.1: Common Diazo Initiated Tandem Reactions.
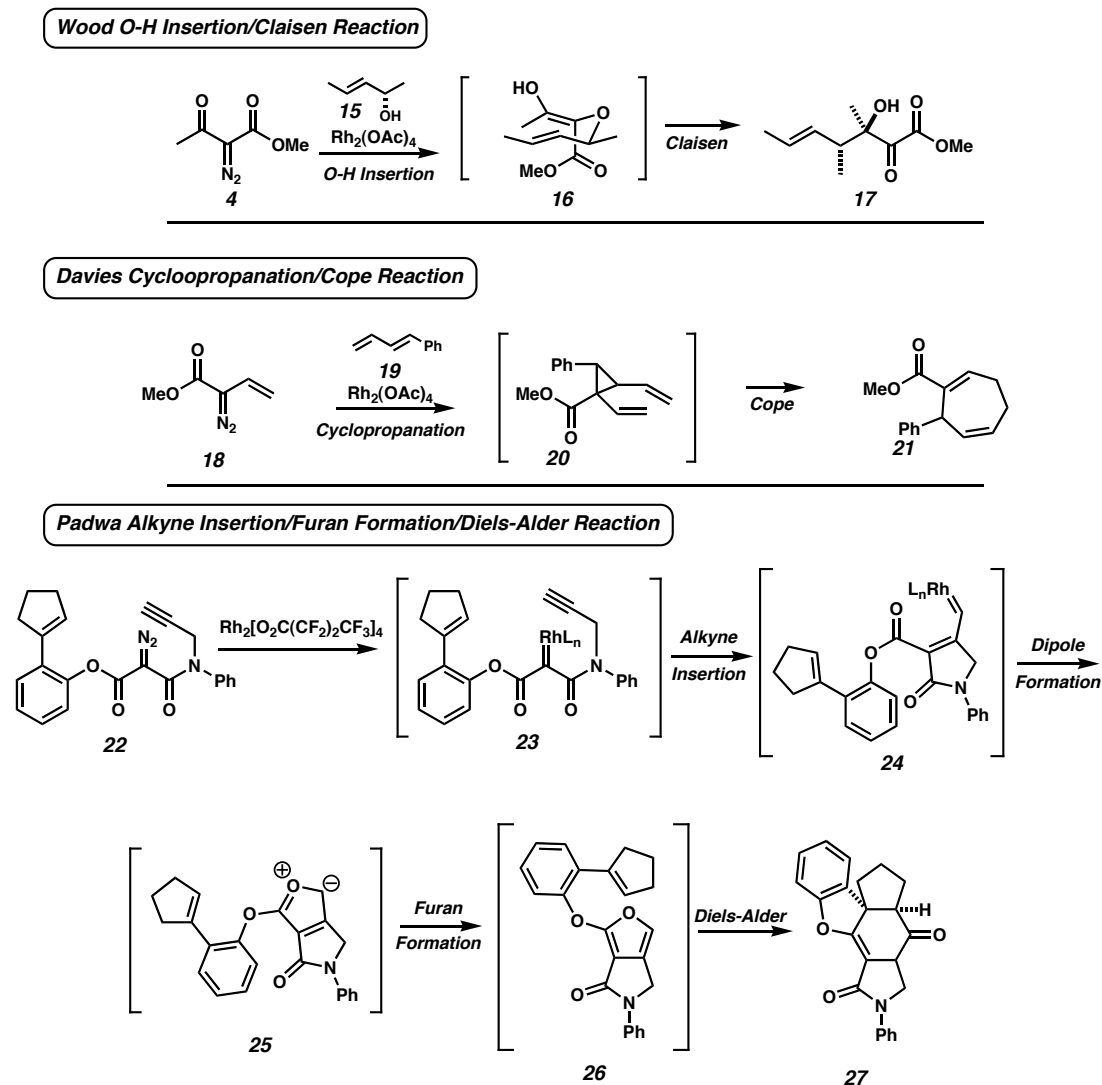
Cycloadditions, such as cyclopropanation, have also initiated tandem sequences.[7] Davies et al. has used a tandem 1,3-diene cyclopropanation/Cope sequence to generate unsaturated seven-membered rings (e.g, **21**). Furthermore, dipole formation and subsequent rearrangements have been used in many cascade reactions. Padwa has demonstrated that carbene insertion into triple bonds generates a new carbene **24**, which can then associate with proximal carbonyls, forming 1,3-dipole **25**.[8] In the example shown in Scheme 1.1.1, this dipole rearranges to furan **26**, which then reacts with a

pendant diene through an intramolecular Diels-Alder reaction. This sampling of tandem reactions demonstrates the versatility of carbenes for generating reactive intermediates that can then promote cascade reactions.

1.1.3 Alternative Methods for Generating Alkyl Carbenes

1.1.3.1 The Need for Stabilization

Associated with the excellent reactivity found in diazo chemistry is the great instability associated with such compounds. Diazoalkanes themselves can be quite unstable or even explosive. Some stability is achieved using α-diazo carbonyl compounds, where the adjacent carbonyl provides resonance stabilization to the diazo group (Scheme 1.1.2). Aromatic groups can also offer stabilization, as in **8**. For synthetic applications, though, the requirement for an adjacent stabilizing group limits the potential use of dinitrogen as a tandem sequence initiator in many synthetic environments. If the reactivity of a diazo group could be accessed from an alternative mode of stabilization, then carbene generation could occur at many carbon centers previously inaccessible by current methods.

Scheme 1.1.2: Resonance Stabilization of Diazo Compounds by an α-Carbonyl.
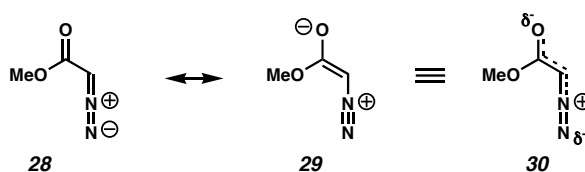
1.1.3.2 Tosyl Hydrazones

Recently, such non-stabilized diazo equivalents have been sought that still afford reactive carbenes. Tosylhydrazones, formed from the condensation of a ketone (**31**) with tosylhydrazide (**32**), have been used as one possible diazo equivalent (Scheme 1.1.3).[9]

The tosyl group stabilizes the diazo group for safe handling and thus acts essentially as a diazo protecting group. The in situ generation of a diazo alkane occurs by initial deprotonation with base and subsequent spontaneous loss of the tosyl group as sulfinate **35**. The drawback with tosylhydrazones is the strong base needed to initiate diazoalkane formation, as this can potentially affect other functionality present in organic structures. Furthermore, use of tosylhydrazones in tandem sequences has not been reported.

Scheme 1.1.3: Tosyl Hydrazones as Masked Diazo Compounds.
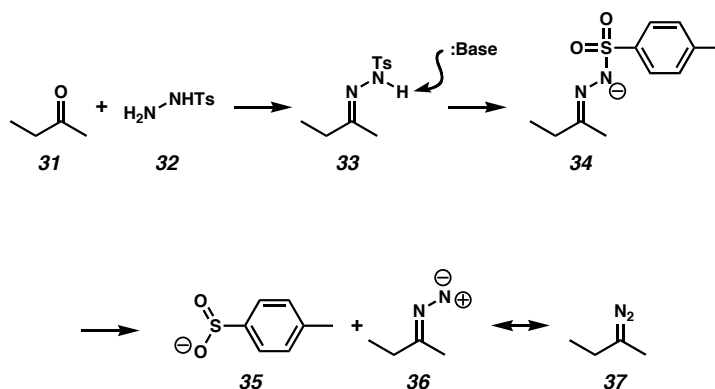
1.1.3.3 Eschenmoser Hydrazones

1.1.3.3.1 Carbene Generation

In the 1960s, Eschenmoser developed an alternative, aziridine-protected hydrazone **40** that is triggered to reveal the latent diazo group **43** (Scheme 1.1.4).[10] Mechanistically, this occurs either via a retro-[1,3]-cycloaddition or by radical fragmentation to release stilbene (**41**) or styrene (**47**) and expose the diazo group. Experimentally, the release of stilbene or styrene is promoted either under thermal (about 80 °C) or photolytic (UV irradiation) conditions. The aziridinyl imines were initially used by Eschenmoser in connection with the fragmentation of epoxy hydrazones (Scheme 1.1.5). Subsequent studies saw the Eschenmoser hydrazones used as precursors

for carbene formation.[11] A few uses of *N*-aziridinyl imines are found in synthetic organic

transformations, as well (see Section 1.1.3.3.2).

Scheme 1.1.4: Eschenmoser Hydrazones.
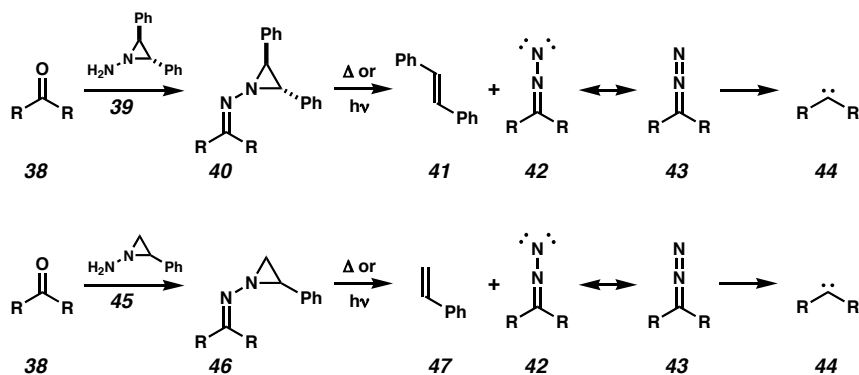
Scheme 1.1.5: Eschenmoser Hydrazone Applications.
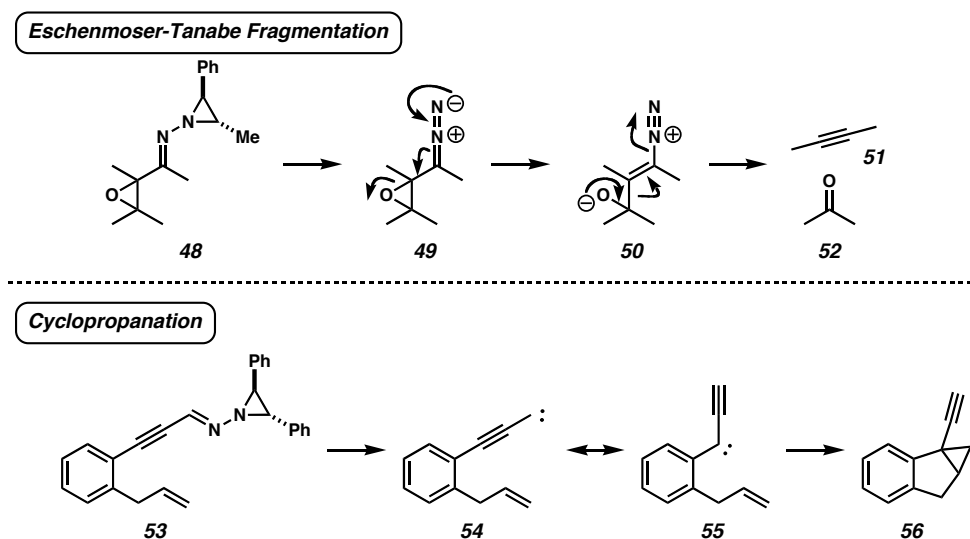
1.1.3.3.2 Eschenmoser Hydrazones Used with Catalysis

Our desire was to couple carbene generation from Eschenmoser hydrazones with

rhodium(II) catalysis for controlled reactivity (Scheme 1.1.6). However, only a few cases

demonstrate aziridinyl imine use with rhodium(II) catalysis.[12] Danishefsky et al. coupled

carbene generation from the hydrazone with a $Rh_2(OAc)_4$ catalyzed reductive cyclization

reaction to generate a seven-membered ring (**59**, Scheme 1.1.7). Sarkar et al. modified

the Bamford-Stevens reaction for use with an aziridinyl imine and Rh(II) catalyst to produce allylsilanes **61** with moderate selectivity. Attempts to pursue this reaction with tosylhydrazones failed.

Scheme 1.1.6: Eschenmoser Hydrazones Coupled with Rhodium Catalysts.

Can this reaction be coupled with known catalysts to generate the desired reativity?
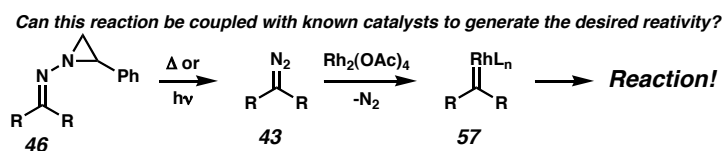
We hypothesized that use of the rhodium catalyst could be made general with Eschenmoser hydrazones. Moreover, because of the thermal activation of these motifs, we anticipated that they would be amenable to a variety of thermally allowed transformations that would be synthetically useful and would accommodate tandem reactivity. To this end, we sought to develop the use of Eschenmoser hydrazones in the context of a natural product synthetic endeavor.

Scheme 1.1.7: Hydrazones with Catalyst Control.
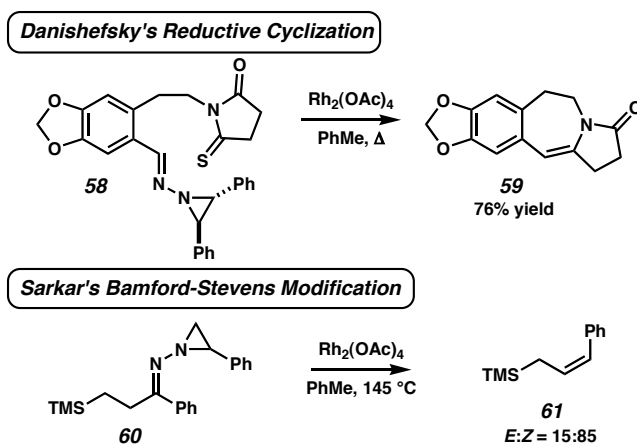
1.2 The Synthetic Use of Masked Diazo Alkanes

1.2.1 Inspiration from Incarvillateine

1.2.1.1 Natural Product Retrosynthesis

Incarvillateine (**62** Figure 1.2.1), an alkaloid isolated from *Incarvillea sinensis*, posseses analgesic properties through interactions with opiate receptors.[13] This natural product contains a cyclobutane core with inversion symmetry decorated by two pendant aromatic rings and two identical alkaloid bicycles. A retrosynthetic analysis of the bicycles reveals the opportunity for a novel cyclization reaction of a carbene generated from masked diazo alkane (**67**).

Figure 1.2.1 Incarvillateine Retrosynthesis.
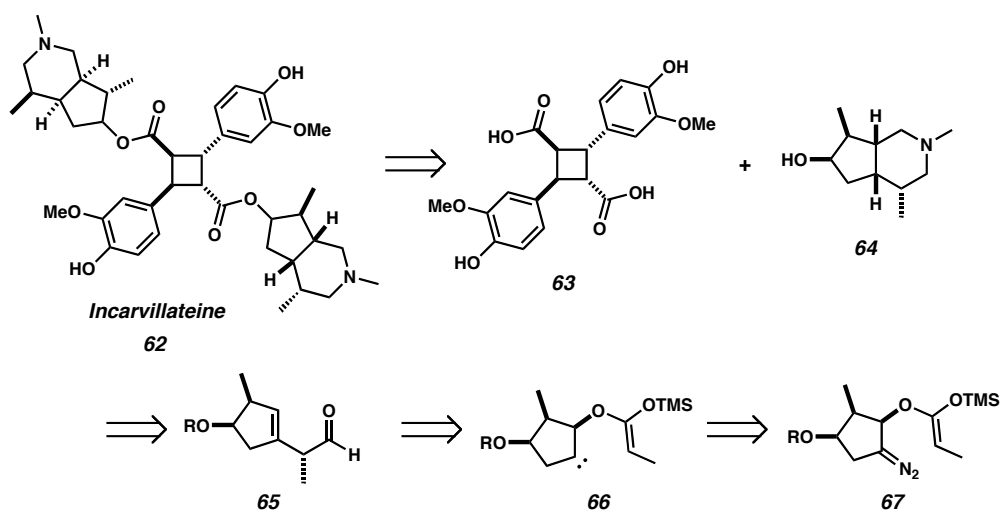
1.2.1.2 The Incarvillateine-Inspired Methodology

This reaction, in theory, would be approached by generating silyl ketene acetal **69** (Scheme 1.2.1). Decomposition of the Eschenmoser hydrazone and interception of the resulting diazo alkane with a Rh(II) catalyst would afford rhodium-carbene **70**. A carbene-based [2,3]-rearrangement of this intermediate would form a new carbon-carbon bond as shown in the product **65**.

Scheme 1.2.1: A Novel Diazo-Initiated [2,3]-Rearrangement.
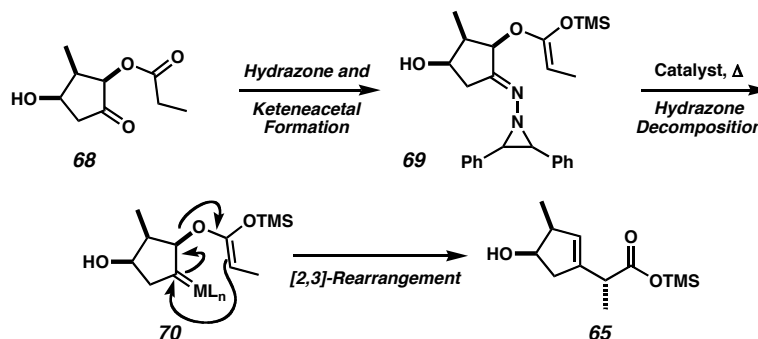
1.2.1.3 Background for the Incarvillateine-Inspired Methodology

Though the use of a ketene acetal is unprecedented for such a reaction, an all-carbon equivalent has been demonstrated by Padwa et al. (Scheme 1.2.2). In that system, intermediate **72** undergoes a pseudo electrocyclization to form the indene **74**. The difference between the proposed transformation and Padwa's is the movement of π-electrons in the styrene instead of a C-O bond fragmentation for the ketene acetal. To test the significance of this difference, simplified model systems were envisioned and pursued.

Scheme 1.2.2: Precedent for a Similar [2,3]-Rearrangement.
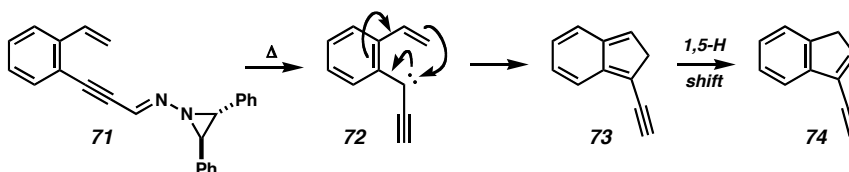
1.2.2 Modeling Reactivity for the Proposed [2,3]-Rearrangement

1.2.2.1 The Desired Model System

Simplified ketene acetal **77** was envisioned to originate from acetylated α-hydroxyacetophenone (**75**, Scheme 1.2.3). The proposed reaction conditions were hoped to generate the metallocarbene **77** and initiate the [2,3]-rearrangement to the ester **78**.

Scheme 1.2.3: Proposed Model Transformation.
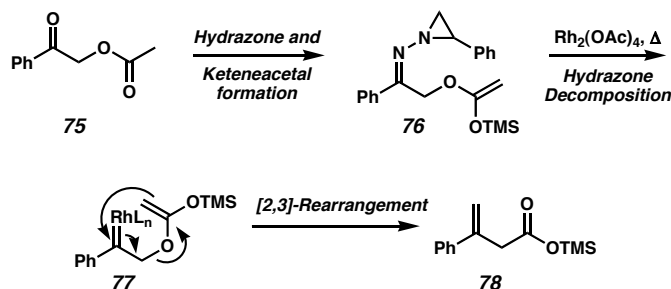
1.2.2.2 Synthetic Efforts toward the Model System

The acetophenone acetate **75** was readily synthesized, and treatment with aminoaziridine salt **80** afforded hydrazone **81** (Scheme 1.2.4). Unfortunately, approaches to prepare the silyl ketene acetal **76** through standard silylketene acetal formation conditions, such as base and silyl triflates, met with resistance.

Scheme 1.2.4: Substrate Synthesis.
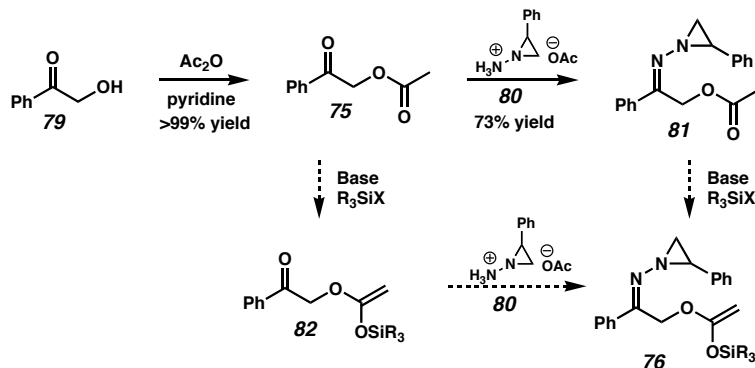
1.2.2.3 Use of Hydrazone 81 as the Model System

The presence of the aziridinyl imine in **81** could allow insight into the feasibility of rhodium-carbene formation in a tandem reaction if subjected to the proposed reaction conditions. To this end, a simple probe reaction based on this substrate was envisioned (Scheme 1.2.5). Should the Rh(II) catalyst be able to intercept a transient diazo species formed from thermal hydrazone decomposition, the attached ester carbonyl could

associate to form dipole **86** in an analogous manner to dipole formation with ketones and aldehydes (e.g., Padwa's example, Scheme 1.1.1).   Dimethylacetylenedicarboxylate (DMAD), a known dipolarophile, offers the possibility of a [2,3]-cycloaddition to trap the intermediate dipole and form bicyclic acetal **84**.

Scheme 1.2.5: Test Reaction for Rhodium Carbene Formation.
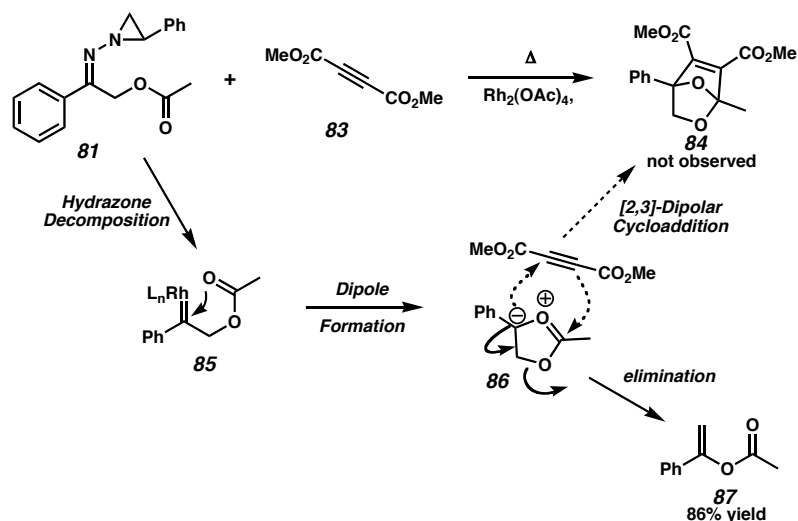
When hydrazone **81** was exposed to the proposed conditions, however, enol acetate **87** was the only observed product.[14] **87** was also observed in the absence of DMAD, but only general decomposition was seen in the absence of $Rh_2(OAc)_4$. Therefore, rhodium must be participating in the reaction, but DMAD is just a spectator. A likely mechanism that fulfills these observations is initial formation of the proposed dipole **86**, which is followed by a rapid elimination rather than cyclization with DMAD. Such a mechanism, though not anticipated, supported the viability of aziridinyl imines as diazoalkane precursors and the strategy of a nucleophile interacting with the electrophilic Rh carbene.

1.2.3 Exploring the Reactivity of α-Oxygenated Hydrazones

1.2.3.1 Revisiting the Incarvillateine [2,3]-Rearrangement

To revisit our initially proposed [2,3]-rearrangement, we envisioned that use of the ketene acetal **88** would mimic the reaction of the α-acetate and could allow for carbene interaction with the nucleophilic π-electrons instead of the lone pairs of the acetate carbonyl and form a new dipole (i.e., **89 → 90**, Scheme 1.2.6). The dipole intermediate could then undergo elimination in similar fashion to **86** to produce the ester **91**. The net reaction would be the same as the originally proposed [2,3]-rearrangement, but mechanistically it would proceed in a stepwise fashion. Thus, a synthetically accessible α-ketene or enol substituent was needed to test this reactivity.

Scheme 1.2.6: Revisiting the [2,3]-Rearrangement.
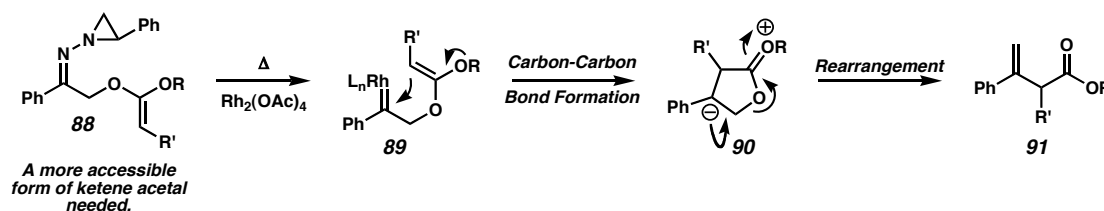
1.2.3.2 Synthesis of a Suitable Substrate

A convenient substrate was available from the coupling of 2-methyltetronic acid (**93**) and 2-bromoacetophenone (**92**) under basic conditions (Scheme 1.2.7). The resulting ketone **94** was then condensed with the aziridinyl imine acetic acid salt **80**, generating the desired enol-ether hydrazone **95**.

Scheme 1.2.7: The α-Enol Ether Hydrazone.
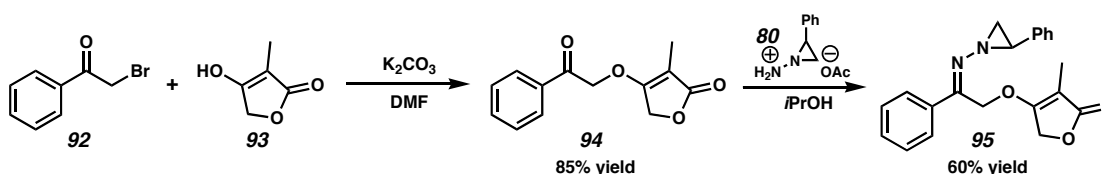
1.2.3.3 Rediscovery of the Bamford-Stevens Reaction

When exposed to the conditions necessary for the rearrangement in Scheme 1.2.5, formation of the desired substituted styrene **97** was not observed (Scheme 1.2.8). Instead, a [1,2]-hydride shift, mechanistically similar to the Bamford-Stevens reaction, occurred from intermediate **96** to form enol ether **98**. Interestingly, only the Z-isomer of the enol ether was detectible, indicating that the reaction is kinetically controlled to form the non-thermodynamically favored isomer. Moreover, the presence of Rh(II) in the reaction was essential for Z-selectivity and to avoid general decomposition, implying rhodium carbene formation is also necessary for controlled reactivity.

Scheme 1.2.8: The Bamford-Stevens Mechanism is Operative.
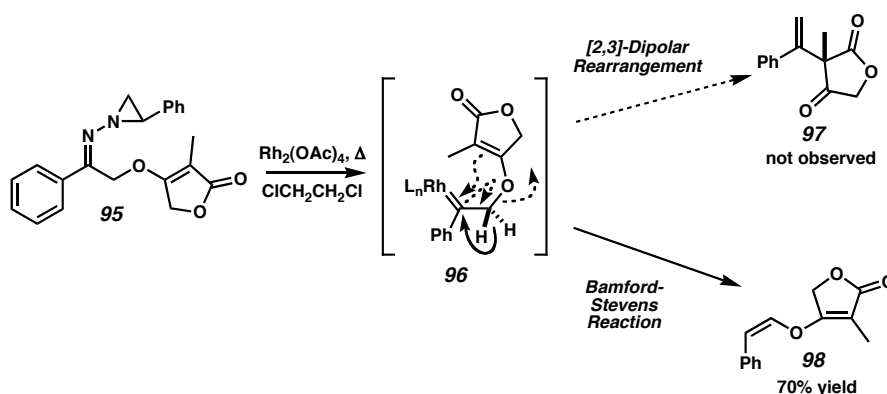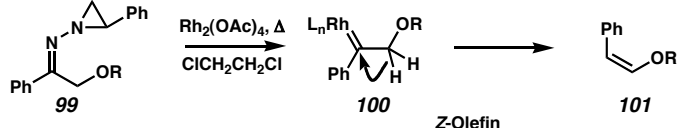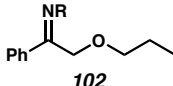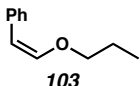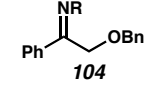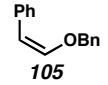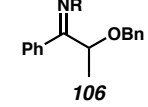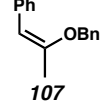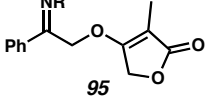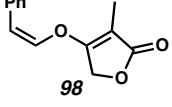
1.2.4 Z-Enol Ethers from Eschenmoser Hydrazones

The production of Z-enol ethers from α-oxygenated Eschenmoser hydrazones in the presence of Rh(II) carboxylates proved to be general for multiple ethers (Table 1.2.1). Alkyl ethers **102** and **104** provide exclusively the Z-ethers in good yield. Importantly, the more substituted hydrazone **106** provides the trisubstituted enol ether **107** as one isomer in useful yield. The stereochemistry of the resulting vinyl ether was determined from the coupling constants of the vinylic hydrogens. When rhodium was omitted from the

reaction conditions, a mixture of *E*- and *Z*-enol ethers was obtained in a lower yield. Furthermore, the *E*-isomer was the major isomer without rhodium, allowing the comparison of coupling constants for the vinylic hydrogens of the *E*- and *Z*-isomers.

Table 1.2.1: Reactivity in the Bamford-Stevens Reaction.

Entry	Substrate	Z-Olefin Product	Yield
1	102	103	70%
2	104	105	81%
3	106	107	63%
4	95	98	70%

1.2.5 The Origin of Selectivity in the Bamford-Stevens Reaction

Rhodium appears to play an integral role in the selectivity of this reaction. Without a Rh(II) carboxylate dimer present, *E* and *Z* mixtures were observed and yields were decreased. Two possibilities of the origin of the stereoselectivity present themselves: steric influences or electronic direction (Scheme 1.2.9). In the steric model, the α-substitution is oriented distant to the Rh metal center (**108**). A 1,2-hydride shift with substituents in this orientation, followed by a rapid dissociation of the catalyst, generates the *Z*-enol ether **101**. If an electronic factor (e.g., dipole minimization) is dominant, then an *anti*-orientation in transition state **109** is expected. Hydride shift and metal dissociation again lead to the observed stereochemistry.

Scheme 1.2.9: Selectivity in the Bamford-Stevens Reaction.
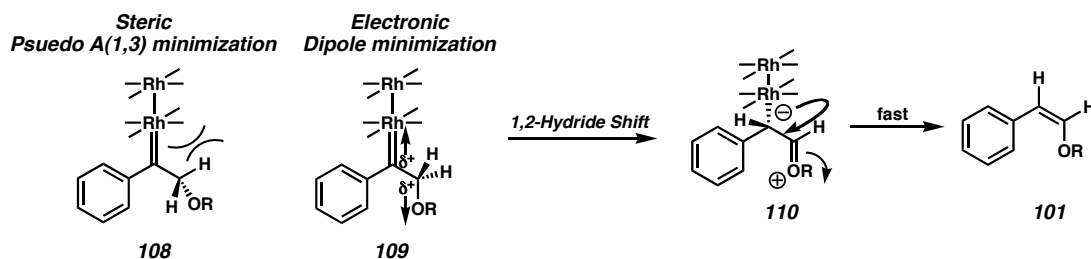
For substrate **106**, however, dissimilarity could arise between the two postulated influences (Scheme 1.2.10). With additional substitution α to the metal carbene, the larger of these substituents would be most inclined to rotate away from the metal center (**115**). As methyl groups are similar in size to alkoxy groups, the expected change in the ratio of orientations for the intermediate **117** to **112** would be transmitted to an altered *E/Z* ratio in the product. By comparison, in the electronic controlled pathway, the oxygen group would still dominate the interaction, and a similar *E/Z* ratio is expected for the product. As Z-vinyl ether **1133** is exclusively observed in the reaction of **106**, electronic factors likely dominate the Bamford-Stevens transformation.

Scheme 1.2.10: Considerations of Selectivity in the Bamford-Stevens Reaction.
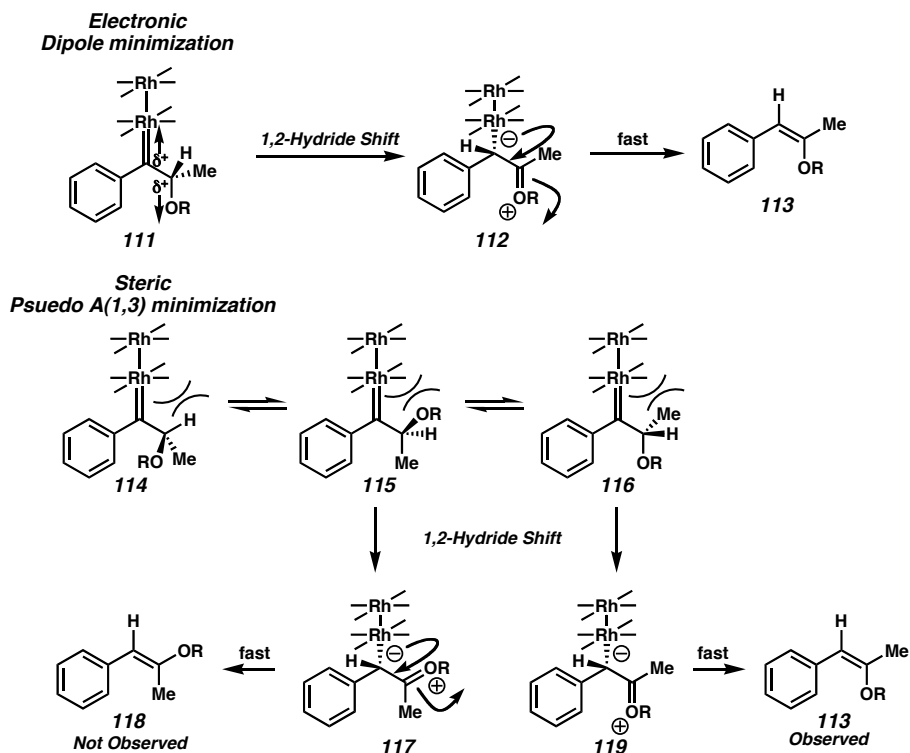
Further evidence for oxagenic electronic factors is found in a comparison of these Bamford-Stevens substrates to those of Sarkar (see Scheme 1.1.7). For α,α-disubstituted substrate **111** (Scheme 1.2.11), the reaction proceeds as above. For C,C-disubstituted intermediate **119**, however, no oxygen is present to provide electronic effects. Thus, **119** would equilibrate based on steric considerations and provide product **122** with little selectivity, as observed. Thus, if the α-alkoxy substrate **106** were only subject to non-bonding interactions in the selectivity-determining step, exclusive formation of the *Z*-isomer would not occur.

Scheme 1.2.11: Comparison of Bamford-Stevens Substrates.
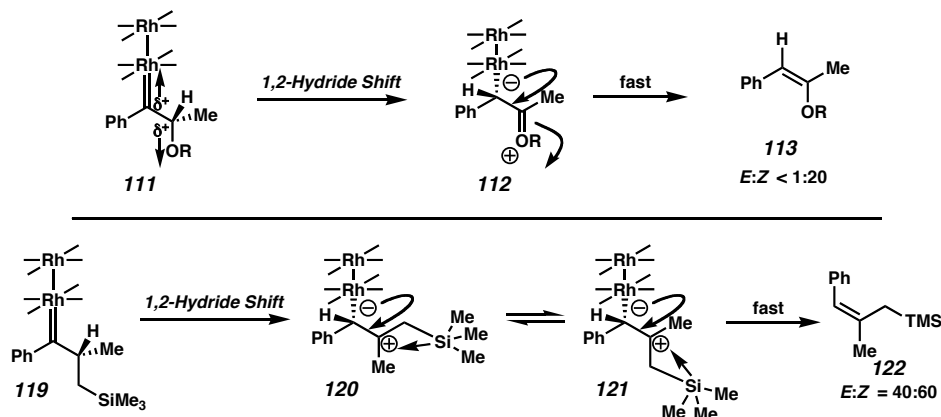
1.3 The Tandem Bamford-Stevens Claisen Sequence

1.3.1 Principles for Consideration

A selective method for *Z*-enol ether formation lends itself to a variety of synthetic transformations. One such transformation is the ubiquitous Claisen reaction, which is a [3,3]-sigmatropic rearrangement of an allyl-vinyl ether to produce a γ,δ-unsaturated carbonyl (Scheme 1.3.1).[15] This reaction proceeds through an ordered, chair-like transition state that transmits stereochemical information from the starting material to the product. Approaches to allyl-vinyl ether synthesis typically use thermodynamic couplings such as a mercury catalyzed vinyl transfer (**125 → 127**) or a Michael/retro-Michael substitution (**128 → 1331**) to generate vinyl ethers under thermodynamic control.

Scheme 1.3.1: Characteristics of the Claisen Reaction.
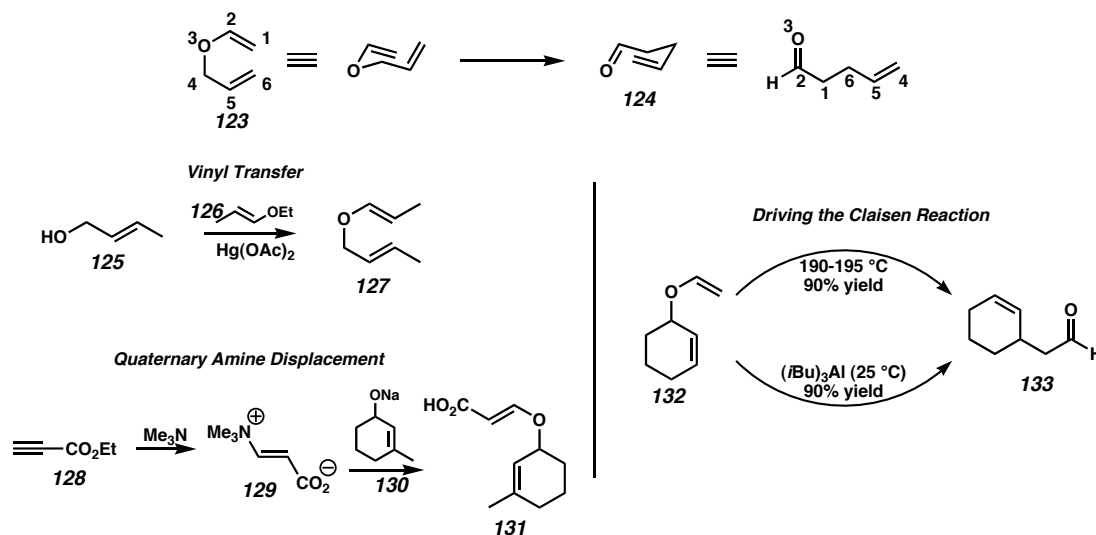
As no convenient method for generating the thermodynamically disfavored *Z*-vinyl ethers is known, aldehydic Claisen rearrangement products are generally only available as certain diastereomers that derive from *E*-vinyl ethers. Thus, the coupling of our rhodium-catalyzed Bamford-Stevens reaction to a Claisen rearrangement could allow access to previously unattainable diastereomers. Moreover, the combination of the Bamford-Stevens reaction and the Claisen reaction in a tandem sequence, as illustrated in Scheme 1.3.2, transforms a simple α-allyloxy ketone **144** into a γ,δ-unsaturated aldehyde **148**, forming a new C-C bond in the process.

Scheme 1.3.2: A Tandem Bamford-Stevens/Claisen Reaction.
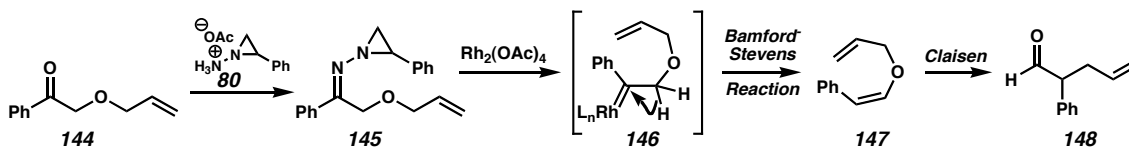
1.3.2 Starting Material Synthesis

The desired α-allyloxy hydrazones could be generated from acid chlorides by diazomethane addition and then OH-insertion of the appropriate allylic alcohols (Scheme

1.3.3). However, increased steric hindrance on the diazoketone or allylic alcohol resulted in lowered yields.

Scheme 1.3.3: OH Insertion of an Allylic Alcohol.
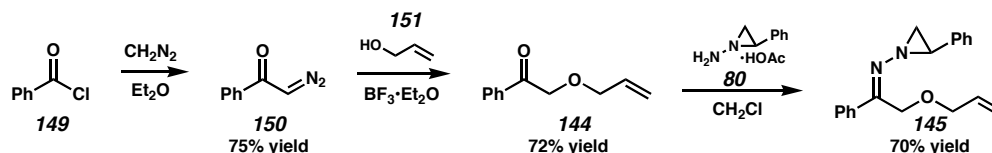
An alternative approach reacted the allylic alcohols first with the sodium salt of 2-chloroacetic acid (Scheme 1.3.4). This reaction tolerated secondary alcohols as well as α-substitution on the acetic acid. The 2-allyloxy acid product was then transformed to a Weinreb amide (**154 → 157**), which accommodated the addition of a variety of nucleophiles. Aziridinyl imine formation proceeded as previously.

Scheme 1.3.4: Nucleophile Addition to a Weinreb Amide.
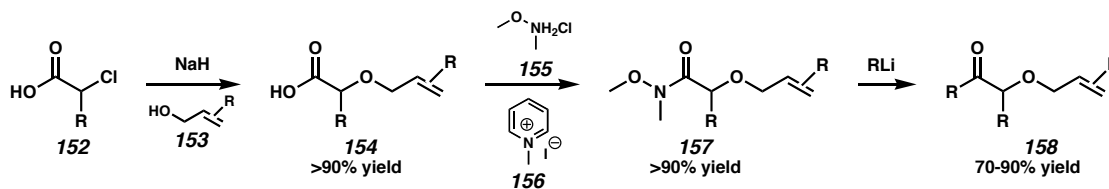
1.3.3 Initial Trial

The aziridinyl imine **145**, formed from 2-allyloxyacetophenone, provided a suitable substrate for the tandem Bamford-Stevens/Claisen reaction (Scheme 1.3.5). Upon exposure to the identical conditions used for the rearrangement of hydrazone **95** and for the Bamford-Stevens substrates in Table 1.2.1, the desired aldehyde **148** was formed. Authenticity of the product was established by comparison to an authentic sample using thin layer chromatography and ^{1}H NMR. Accompanying the desired product, however, was formation of a cyclopropane **159** from cycloaddition on the allyl

ether olefin. Furthermore, the Bamford-Stevens product, Z-enol ether **147**, was isolable

from the reaction. Importantly, the rhodium catalyst was again essential to the reaction

for any controlled reactivity. In the absence of rhodium, the reaction mixture

decomposed to an intractable concoction. To find conditions that favored one pathway

over the other, a series of variations in experimental parameters was made.

Scheme 1.3.5: The Tandem Reaction Outcome.
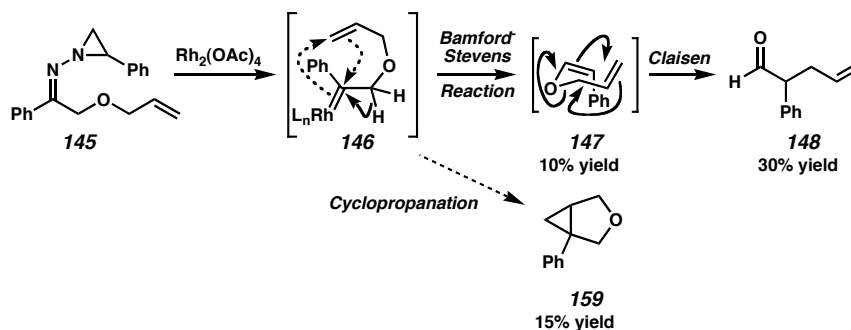
1.4 Reaction Optimization

1.4.1 Testing Catalysts

Several known carbene reaction catalysts were employed in the Bamford-

Stevens/Claisen reaction to identify catalyst preference for a Bamford-Stevens 1,2-

hydride shift or cyclopropanation (Table 1.4.1). For these trials, both thermal and

photolytic aziridine decomposition was performed to obtain a comprehensive indication

of catalyst potential.

Rh(II) and $Cu_{(s)}$ catalysts favored the Bamford-Stevens elimination most strongly,

though Cu caused low yields and generated several unidentifiable byproducts. Thermal

activation was important for this selectivity, as photolytic conditions generally favored

cyclopropane formation for all the catalysts. Interestingly, photolytic activation was

capable of forming a significant amount of cyclopropane without catalyst, whereas

thermal conditions required a competent catalyst to avoid decomposition. The testing of

catalysts demonstrates that Rh(II) plays an integral role in the reaction mechanism and

can provide control over reactive intermediates.

Table 1.4.1: The Influence of Various Catalysts.
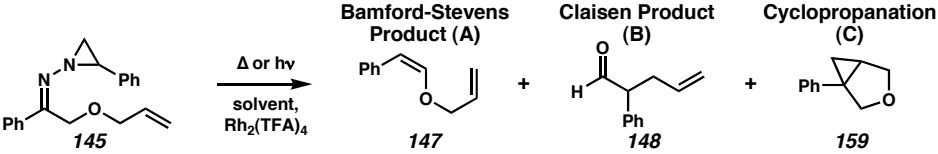
Catalyst	Thermal (147+148:159)	Photolytic (147+148:159)
Rh$_2$(OAc)$_4$	3.8 : 1	1 : 3.7
Rh$_2$(TFA)$_4$	2.8 : 1	1.2 : 1
Pd(OAc)$_2$	1.66 : 1	1 : 2.5
Cu(OTf)$_2$	unknown products	1 : 1.4
(nbd)PdCl$_2$	no product	1 : 1.6
Cu(s)	>8 : 1 (but low yield)	1 : 4.8
no catalyst	unknown products	1 : 5.8

1.4.2 Testing Solvents

Solvents also play an important role in the selective formation and/or reaction of

intermediate **146** (Table 1.4.2). Several common organic solvents were employed in the

reaction, again under both thermal and photolytic conditions. In general, thermal

activation again favored the Bamford-Stevens pathway, and photolysis favored

cyclopropanation. Solvent polarity had a pronounced effect on product distribution, as

did the presence of a Rh(II) catalyst. As above, little difference was seen between

Rh$_2$(OAc)$_4$ and the more electron-deficient Rh$_2$(TFA)$_4$. Polar, aprotic solvents, including

N-methylpyrrolidinone, dimethylformamide, acetonitrile, and dichloroethane, promoted

the hydride shift most effectively. Conversely, non-polar solvents like

carbontetrachloride, especially under photolytic conditions, favored reaction with the nearby olefin.

Table 1.4.2: Solvent Effects on Reaction Pathway.

Solvent	Thermal (147 + 148 : 159)[a]			Photolytic (147 + 148 : 159)[a]		
	Rh$_2$(OAc)$_4$	Rh$_2$(TFA)$_4$	no catalyst	Rh$_2$(OAc)$_4$	Rh$_2$(TFA)$_4$	no catalyst
N-Methylpyrrolidinone	6.0 : 1	3.9 : 1	1 : 1.1	2.1 : 1	1.5 : 1	1 : >10
Acetonitrile	5.3 : 1	7.0 : 1	other	--	--	--
Dimethylformamide	5.2 : 1	1.8 : 1	1 : >10	1 : 1.3	1.6 : 1	1 : 2.0
Dioxane	3.7 : 1	4.6 : 1	1 : >10 + other	--	--	--
Dimethylacetamide	5.4 : 1	1.5 : 1	1 : 7.1	2.5 : 1	1.7 : 1	1 : 4.4
t-Butanol	2.1 : 1	3.9 : 1	1 : 7.7	1 : 1.3	1.7 : 1	1 : 2.9
Toluene	3.0 : 1	3.6 : 1	1 : 4.3	1 : 1.7	1 : 1.4	1 : 2.1
Dichloromethane	--	--	--	1.3 : 1	1 : 1.4	1 : 2.5
Hexane	--	--	--	1 : 2.2	1 : 1.9	1 : 2.5
Pinacolone	3.9 : 1	2.7 : 1	1 : 2.1 +other 9.9	1 : ~1.5	1.5 : 1	1 : ~5
Dichloroethane	3.8 : 1	2.8 : 1	other	1 : 3.7	1.5 : 1	1 : 5.8
Isopropylacetate	1 : 1	4.0 : 1	other	--	--	--
Heptane	2.1 : 1	2.8 : 1	1 : >10+ other	1 : 3.9	1 : 4.4	1 : 3.3
Nitromethane	2.3 : 1	1 : >10	1 : >10	--	--	--
Methylcyclohexane	--	--	--	--	1 : 5.1	--
Carbontetrachloride	1.9 : 1	1.7 : 1	1 : >10+ other	1 : 8.5	1 : >10	1 : 2.2
Dimethylsulfoxide	1 : 5.2	1 : 6.1	1 : >10	1 : 3.7	decomposition	1 : 2.9

[a]Product Ratios Determined from the ^{1}H of the Crude Reaction Mixture.

1.5 Substrate Scope

1.5.1 Tandem Bamford-Stevens/Claisen Reactions

With a better-defined understanding of the influence the reaction conditions had on the reaction pathway, more substrates were synthesized. We quickly found that terminally substituted allylic ethers were less likely to undergo cyclopropanation, though cyclopropane products could be isolated if favorable conditions were used (see section 1.8.2).

Aromatic-substituted allylic ethers **163**, **165**, **167**, **169**, and **173** reacted cleanly as desired in the tandem Bamford-Stevens/Claisen reaction (Table 1.5.1). As the thermal Claisen rearrangement in these cases was rapid, intermediate **161** was not observed. Excellent diastereoselectivity was seen for the terminally substituted allylic ethers **163** and **165**, as would be expected from the *Z*-enol ether of the Bamford-Stevens reaction coupled to the chair-like Claisen rearrangement transition state. Similarly, the secondary ethers **167** and **169** showed a high degree of selectivity; importantly, the **167** class of substrates, if enantioenriched ethers are used, could transmit this stereochemical information to produce enantioenriched aldehydes.

Table 1.5.1: Aromatic Allylic Ethers in the B-S/Claisen Reaction.

Entry	Substrate	Product	Yield(dr)[a]
1	163	164	87% (>20:1)
2	165	166	82% (>20:1)
3	167	168	79% (>20:1)
4	169	170	72% (8:1)
5	171	172	76% (3:1)
6	173	174	73% (7:1)[b]

[a]*Diastereomer Ratios Determined from the ^{1}H of the Crude Reaction Mixture.*
[b]*Rh$_2$(OAc)$_4$, NMP, 200 °C, 1 h.*

Hydrazone **171** differed from the other aromatic substrates with a low diastereomeric ratio observed in the product (cf. Entry 3). This outcome was not unreasonable, as internal allylic substitution would form a *syn*-pentane interaction with the substituent on the *Z*-vinyl ether in the Claisen reaction chair-like transition state as seen in intermediate **176** (Scheme 1.5.1). Though normally the chair-like conformation[16]

is energetically preferred, the unfavorable interaction destabilizes transition state **176**, making a switch to the boat-like transition state **177** more facile. As these two states lead to different product diastereomers, the decreased difference in transition state energy erodes the reaction diastereoselectivity.

Scheme 1.5.1: Erosion of Diastereoselectivity for Internal Olefin Substitution.
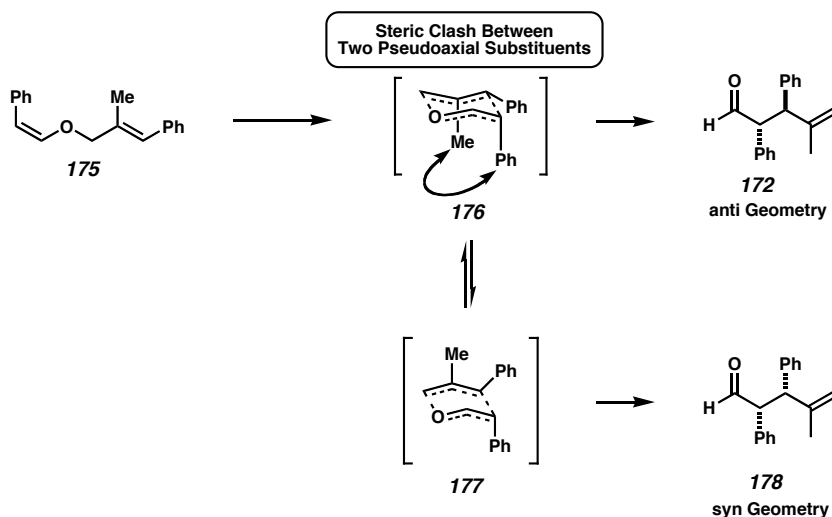
Importantly, benzylic hydrazones were not required for the Bamford-Stevens reaction. With *N*-methylpyrrolidinone as solvent and the reaction run at 200 °C, aliphatic hydrazone **173** reacted smoothly to form aldehyde **174** in one hour (entry 6). Apparently, conjugation to the hydrazone increases the rate of decomposition. Thus, the order of reactivity for the hydrazones was benzylic, styrenyl, allylic, and then aliphatic (see section 1.6.3 for styrenyl and allylic examples).

1.5.2 Tandem Thermal Bamford-Stevens/Lewis Acid Claisen Reactions

For the aliphatic-substituted allylic ethers (Table 1.5.2), the Claisen reaction was slower. In these cases, a buildup of the 1,5-diene intermediate **161** was seen, with a small amount of product formation. After two hours at 130 °C all the hydrazone had reacted. At this point, the reaction could be maintained at high temperature until the Claisen

reaction proceeded to completion (entries 7 and 8). Alternatively, the reaction could be

cooled to –40 °C (with the addition of a small amount of dichloromethane to maintain the

solvent in a liquid state), followed by addition of a Lewis acid for rapid promotion of the

Claisen rearrangement (entries 9 and 10).[17] When Me$_2$AlCl was added, the Claisen

cyclization proceeded rapidly, within five minutes in many cases, to provide the products

shown with good diastereoselectivity.

Table 1.5.2: Aliphatic-Substituted B-S/Claisen Reaction Substrates.

Entry	Substrate	Product	Yield(dr)[a]
7	**179**	**180**	71%
8	**181**	**182**	86%
9	**183**	**184**	63% (7:1)[b]
10	**185**	**186**	72% (6:1)[b]

[a]*Diastereomer Ratios Determined from the ^{1}H of the Crude Reaction Mixture.*
[b]*Subsequent Treatment with Me$_2$AlCl at –40 °C.*

As **180** and **182** demonstrate, quaternary carbon centers were readily formed. *Cis* olefins in the allylic arm of the ether successfully relayed that stereochemical information to the product **184**. Substrates **181** and **185** demonstrate that rings were tolerated in the tandem reaction.

1.6 Higher Order Tandem Reactions

1.6.1 Tandem Bamford-Stevens/Claisen/Reduction Reactions

When diisobutylaluminum hydride (DIBAL) was used in place of Me$_2$AlCl in the above reaction with substrate **183**, the Lewis acidic nature of DIBAL accelerated the Claisen rearrangement as before, and then the metal-hydride immediately reduced the aldehydic Claisen reaction product to form alcohol **188** (Scheme 1.6.1). This transformation is especially useful if unstable aldehydes are formed in the course of the reaction. Furthermore, the reduction allows for further orthogonality to the Claisen reaction; the Ireland Claisen reaction generates acid products, the Bamford-Stevens/Claisen reaction generates aldehydes, and the Bamford-Stevens/Claisen/Reduction reaction generates alcohols.

Scheme 1.6.1: The Tandem B-S/Claisen/Reduction Reaction.
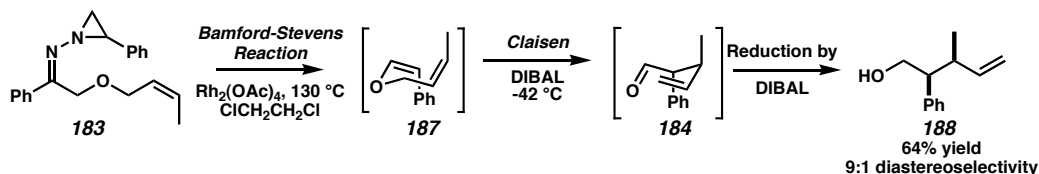
The Bamford-Stevens/Claisen/Reduction reaction also facilitated a study of transition-state fidelity for the tandem reaction. Substrates **189** and **192**, formed from geranyl alcohol and neryl alcohol, respectively, are isomeric about the allyl olefin (Scheme 1.6.2). As the Bamford-Stevens reaction produces identical vinylic substitution,

the products from the reaction would be opposite diastereomers about the newly formed quaternary carbon center. When the reactions were carried out, opposite diastereomers were indeed formed in excellent yield and outstanding selectivity, indicating that the Claisen rearrangement transition state is highly ordered for these reactions. In both cases, the minor diastereomer was undetectable by ^{1}H NMR.

Scheme 1.6.2: Isomeric Allylic Olefins Afford Diastereomeric Products.
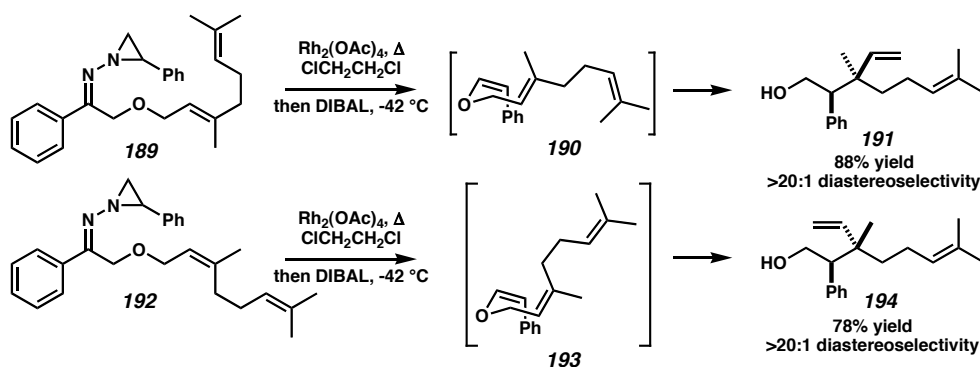
1.6.2 Tandem Bamford-Stevens/Claisen/Carbonyl-Ene Reactions

Substrates **189** and **192** (Scheme 1.6.3) displayed more complex reactivity when exposed to Me₂AlCl as the Lewis acid for the Claisen rearrangement (see section 1.5.2). The Lewis acid again catalyzes the Claisen reaction at low temperature and subsequently promotes a carbonyl-ene addition with the γ-olefin to produce cyclohexanols **197** and **198**, respectively. As in the Claisen rearrangement, carbonyl-ene reactions prefer a chair-like transition state, so only one diastereomer is observed for each product.[18] Again, as a demonstration of the fidelity of all the transformations, the isomeric ethers **189** and **190** lead to the diastereomeric cyclohexanols **197** and **198** with suburb stereospecificity.

Scheme 1.6.3: The Tandem B-S/Claisen/Carbonyl-Ene Reaction.
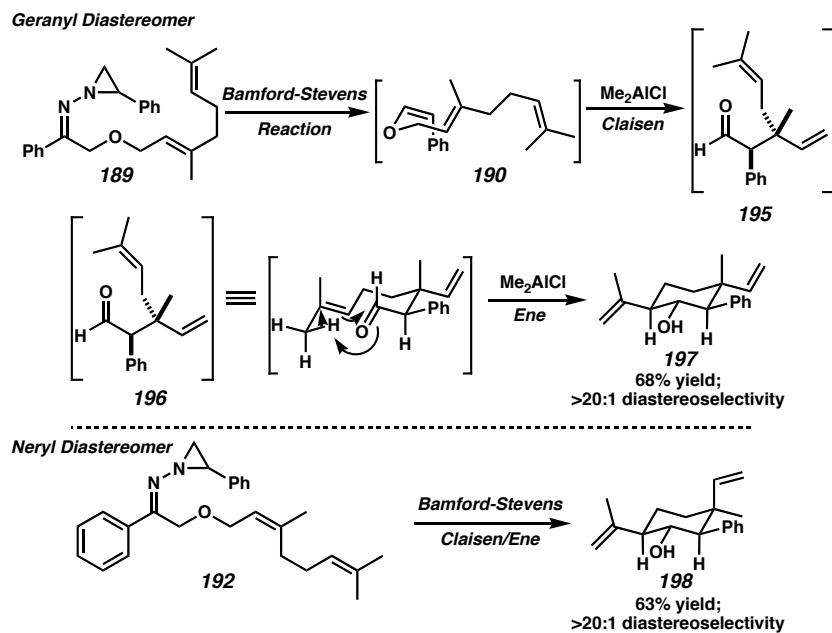
1.6.3 Tandem Bamford-Stevens/Claisen/Cope Reactions

Vinyl hydrazones worked as well in the tandem reaction, though the hydrazones required longer reaction times to thermally decompose, as previously mentioned (section 1.5.1). These reactions proceeded through the Bamford-Stevens and Claisen reactions as above, but the presence of the additional olefin created a 1,5-diene in the product **200** that was capable of thermal Cope [3,3]-sigmatropic rearrangement (Scheme 1.6.4). Thus, the cascade sequence readily occurred to form the α,β-unsaturated aldehyde **201** in good yield and as one isomer. Hydrazone **202** was also transformed to afford only one isomer of α,β-unsaturated aldehyde **203** that contained a trisubstituted olefin and quaternary carbon center. The isolation of only the *E*-isomer of these products suggests that the Cope proceeds through an ordered chair-like transition state as well.[19]

Scheme 1.6.4: The Tandem B-S/Claisen/Cope Reaction.
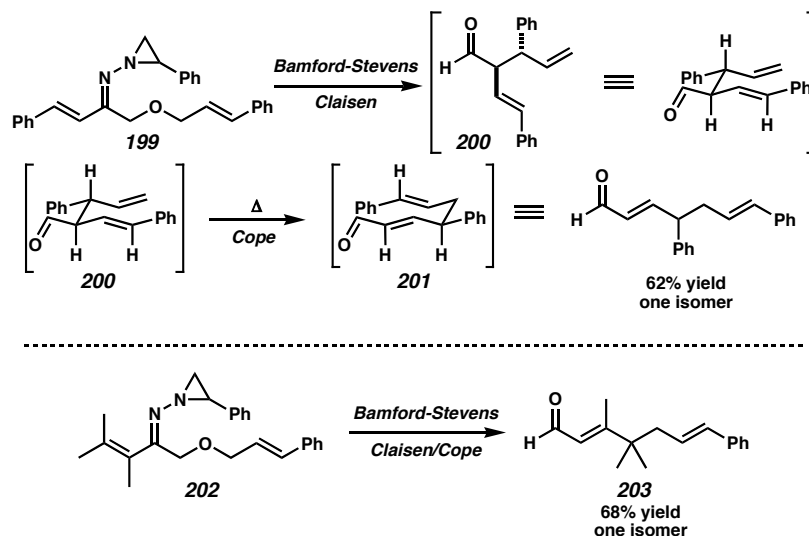
1.7 Confirmation of Product Stereochemistry

1.7.1 Correlations to Known Compounds

The diastereomeric relationship of the products is a direct result of the structure and fidelity of the transition states for these reactions. Therefore, to validate the proposed transition state models, the products were compared with previously characterized compounds reported in the chemical literature to confirm the diastereomeric nature of the products. Bamford-Stevens/Claisen reaction product **164** was similar to ester **204** obtained from the Ireland Claisen reaction, but differed in the carbonyl oxidation state. Thus, oxidation of the aldehyde to the acid and esterification allowed correlation of stereochemistry to that of **204** (Scheme 1.7.1).

Scheme 1.7.1: Transformation to Previously Reported Compounds.

Once the stereochemistry of **164** had been established, similar compounds could be related to it through simple transformations. Ketone **170** was formed through Grignard addition to **164** and oxidation. Similarly, the previously reported ketone **206** was generated from aldehyde **174**. Additionally, both **164** and aldehyde **168** could be transformed to aldehyde **205**. Finally, the *syn*-aldehyde **184** was oxidized and amidated to compare with reported amide **168**. Reduction of aldehyde **184** also linked alcohol **188** to a known compound. These transformations demonstrate the utility of the Bamford-Stevens/Claisen products, as a variety of functionality is available from the aldehydes in Tables 1.5.1 and 1.5.2.

1.7.2 nOe Interactions

For several novel compounds, correlation to previously characterized compounds was not practical. Analysis of nOe interactions between key protons on the molecules, however, provided the necessary stereochemical identification for the assignment of the compounds (Figure 1.7.1). For example, the hydrogens on the same face of the cyclohexanols **197** and **198** exhibited very clear Overhauser effects, allowing relative orientation to be confirmed. In the case of olefins **201** and **203**, the allylic hydrogens demonstrated interactions with the illustrated vinylic hydrogens, substantiating the illustrated stereochemistry. For these appended tandem reactions, the resulting stereochemistry is consistent for a chair-like transition state for both the carbonyl-ene and the Cope reactions as well.

Figure 1.7.1: Important nOe Interactions Observed in Products.
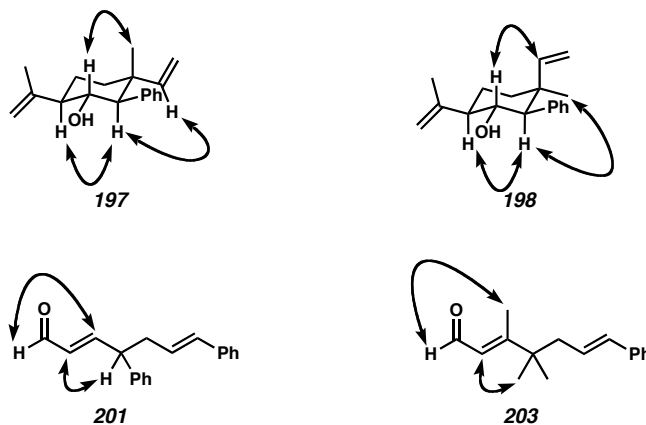
For the product **186**, nOe interactions were insufficient to confidently establish the stereochemistry because of the rotational freedom in the molecule. To provide a better framework for analysis, **186** was oxidized to the carboxylic acid under buffered sodium chlorite conditions, and then iodolactonization provided the fused bicycle **208**

(Scheme 1.7.2). The rigid nature of this bicycle allowed for the characterization of both the major and minor diastereomers through key nOe interactions.

*Scheme 1.7.2: Iodolactonization of **186** to Determine the Relative Stereochemistry.*
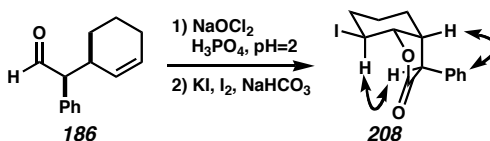
1.7.3 Crystal Structure

The relative stereochemistry of product **186** was further established through the analysis of iodolactone **208** by single-crystal X-ray diffraction of the major diastereomer (Figure 1.7.2). This structure correlated to the relative stereochemistry seen for the other products and to the predicted product from a Z-enol ether proceeding through a chair-like Claisen reaction transition state.

*Figure 1.7.2: Single Crystal Structure for Iodolactone **208**.*
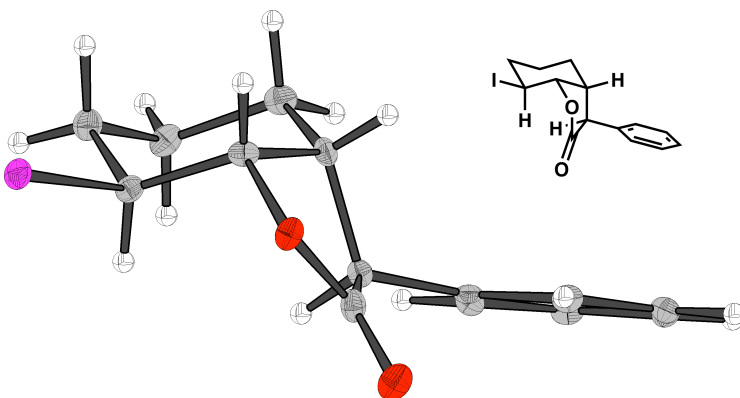
1.7.4 Analogy

For a small number of products, definitive establishment of stereochemistry was not practical (Figure 1.7.3). However, given the reproducibility of the reaction stereoselectivity, assignment of relative stereochemistry was made by analogy to that of

similar products. For example, aldehydes **166** and **172** bear similar substitution to **164**, so similar diastereomeric preference was anticipated. Furthermore, these compounds were similar to **164** spectroscopically and chromatographically. As **191** and **194** are thought to be formed by reduction of aldehydes **195**, the relative stereochemistry of the quaternary and tertiary carbon centers for these molecules is assumed to be the same as that for cyclohexanols **197** and **198**, since the carbonyl-ene reaction would not change that relative stereochemistry.

Figure 1.7.3: Products Where Stereochemistry Was Established via Analogy.

166
analogy to 164

172
analogy to 164

191
analogy to 197

194
analogy to 198
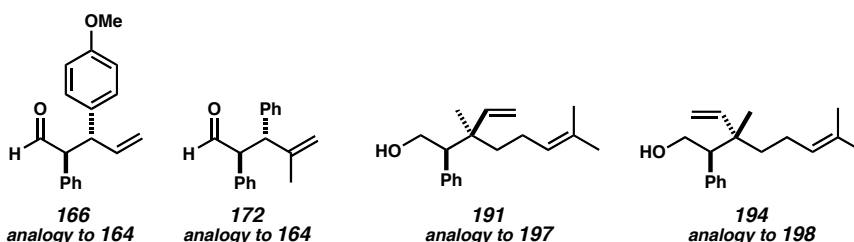
1.8 Future Applications

1.8.1 X-H Insertions

Many studies on NH, OH, and CH insertion have focused on the use of α-diazo carbonyls. Use of the Eschenmoser hydrazones and Rh(II) catalysts for X-H insertions has received no attention, however. A preliminary trial of subjecting hydrazone **209** to the standard reaction conditions generated tetrahydrofuran **210** (Scheme 1.8.1). The identity of **210** was confirmed by comparison to reported data. The overall transformation reductively transformed a γ-hydroxy ketone to a cyclic ether. Many diastereoselective or even enantioselective reactions could be imagined for this chemistry with a variety of substitution patterns.

Scheme 1.8.1: Potential X-H Insertion Reactions.
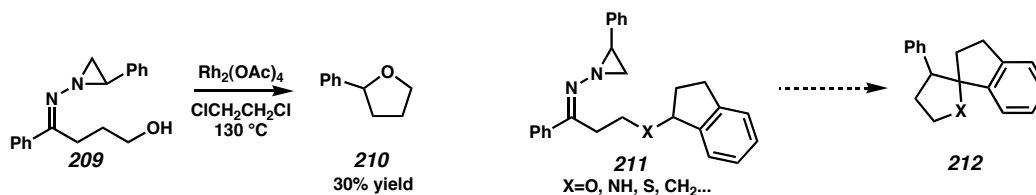
CH insertion offers another method to form new C-C bonds. The overall synthetic transformation of a ketone to a new C-C bond would be attempted by initially mimicking α-diazocarbonyl chemistry. Similar reactivity, such as preference for five-membered rings, insertion into tertiary C-H bonds, and α-heteroatom activation, is expected for the in situ generated diazocompounds. Novel compounds like the polycyclic indene **212** could be accessible from the hydrazone **211**, whereas traditional diazo chemistry would require a greater synthetic effort.

1.8.2 Cyclopropane Formation

As the catalyst and solvent studies (Sections 1.4.1 and 1.4.2) have shown, preferential formation of cyclopropanes for many of these substrates is possible. Such a transformation from these and other hydrazones could lead to synthetically useful compounds with densely substituted carbon frameworks as seen for cyclopropane **213** (Scheme 1.8.2). Here, a reversal of pathway selectivity was accomplished by omission of the Rh(II) catalyst. Thus, either aldehyde **180** or cyclopropane **213** could be obtained selectively. This could be extended to other precursors to generate many structurally important frameworks.

Scheme 1.8.2: Cyclopropane Product Available from Alternate Reaction Conditions.

	BS-Claisen Product		Cyclopropanation
	180		**213**
Thermal, With Rhodium:	10	:	1
Photolytic, Without Rhodium:	1	:	10
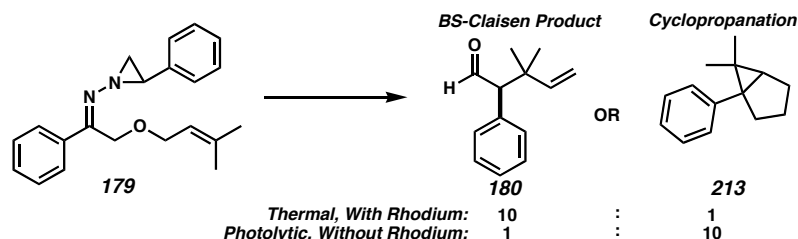
1.8.3 [2,3]-Enol Rearrangement

Judicious use of α,α-disubstituted substrate to avoid the 1,2-hydride shift seen in the Bamford-Stevens reaction could allow the originally proposed [2,3]-rearrangement to take place. The product of such a reaction would be the tetrasubstituted olefin **217**.

Scheme 1.8.4: The Proposed [2,3]-Rearrangement.
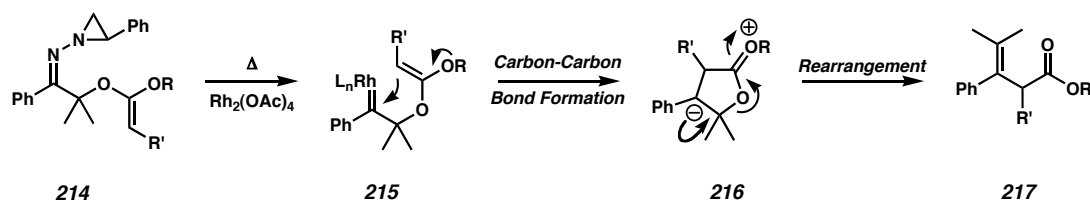
1.8.4 Dipole Cycloadditions

Dipole cycloadditions have been shown to form bridged polycycles, furans, and other ring systems (see section 1.1.2.3). The transformation shown in Scheme 1.8.5 demonstrates how a dicarbonyl system could be used to form a bridged actetal and two new C-C bonds in a single step from hydrazone **218**.

Scheme 1.8.5: A [1,3]-Cycloaddition to Form Polycycles.
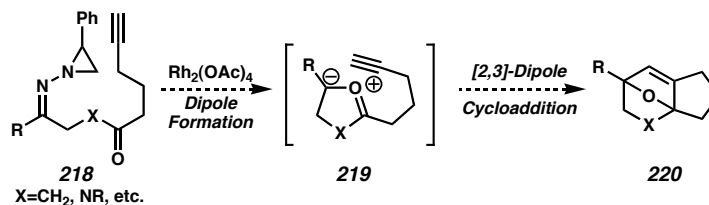
1.8.5 Modular Terpenoids

The tandem Bamford-Stevens/Claisen/Cope reaction offers entry into controlled terpenoid synthesis (Scheme 1.8.6). Reduction of the aldehyde product and formation of an acetic acid ether would then allow formation of weinreb amine **221**. Treatment of this amine with substituted vinyl lithium **222** and then the aminoaziridine acetic acid salt **80** regenerates a tandem reaction substrate. Iterations of these steps would allow the synthesis of polyisoprene products. Importantly, the stepwise addition of two-carbon units would allow for incorporation of selective substitution or isotopic labeling at desired positions. As a proof-of-principle for this cycle, an undergraduate research assistant, Brian Underwood, demonstrated the first iteration of this reaction (i.e., **221** to **224**). Starting with prenyl alcohol, the allyloxy weinreb amide **221** was formed as previously described (see Scheme 1.3.4). Addition of vinyl lithium **222**, followed by aminoaziridinyl salt **80**, created the tandem reaction substrate **223**. Upon exposure to the standard conditions, geranial was formed as demonstrated by comparison to an authentic standard (Aldrich Chemical Co.). Optimization of this process and further iterations could allow incorporation of novel functional groups or isotopic labels into the terpenoid framework.

Scheme 1.8.6: Iterative Terpenoid Synthesis.
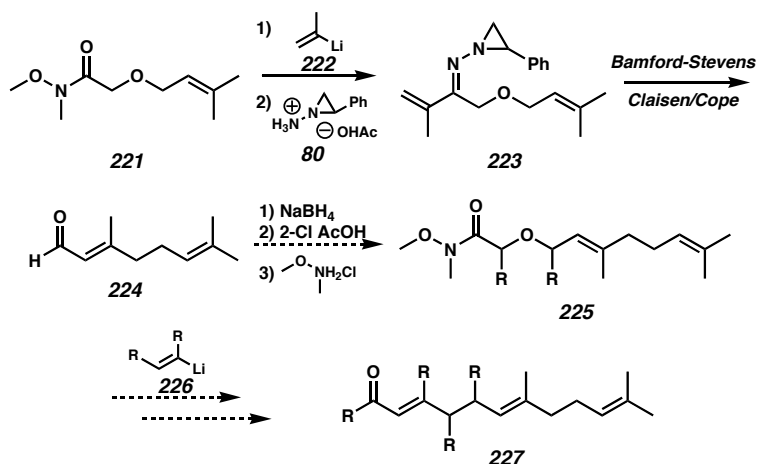
1.8.7 The Ring Expansion Bamford-Stevens/Claisen/Cope Reaction

An unsaturated ring system such as that shown in Scheme 1.8.7 could be a viable substrate for a tandem Bamford-Stevens/Claisen/Cope reaction. As above, selective formation of the *Z*-enolethers **229** and **233** is expected. The Claisen rearrangement, which would likely be highly asynchronous, would form *cis*-1,2-divinylcyclobutane **230** or cyclopentane **234**, which is poised for a ring opening Cope reaction. This would expand the original ring system by two carbons to form unsaturated cyclooctanes **231** or cyclononanes **234**.

Scheme 1.8.7: A B-S/Claisen/Cope Ring Expansion.
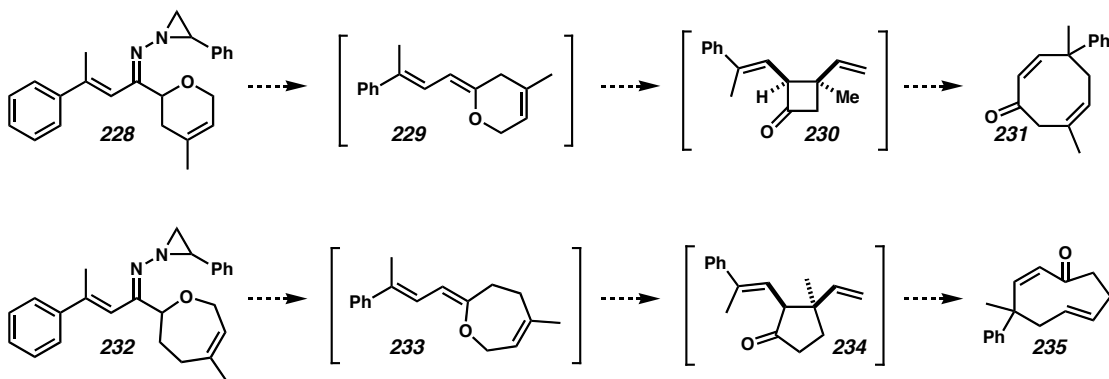
1.8.8 Tandem Electrocyclic Reactions

With appropriate π-systems in the substrate, cycloaddition and electrocyclic chemistry with the Bamford-Stevens product may be possible. As the Bamford-Stevens reaction proceeds at elevated temperatures, thermally allowed cycloadditions and electrocyclic reactions will be analyzed. In the first example (Scheme 1.8.8), the Bamford-Stevens reaction would generate enolether **237**, which could then undergo an inverse-demand Diels-Alder reaction to form the *trans*-decaline-like product **238**. For substrate **239**, the Bamford-Stevens product **240** could undergo a 6-π electrocyclization and then a Diels-Alder reaction to form the bridged polycycle **242**. These reactions would expand the tandem reaction scope for the Eschenmoser hydrazones.

Scheme 1.8.8: Tandem B-S/Diels-Alder and B-S/Electrocyclization Reactions.
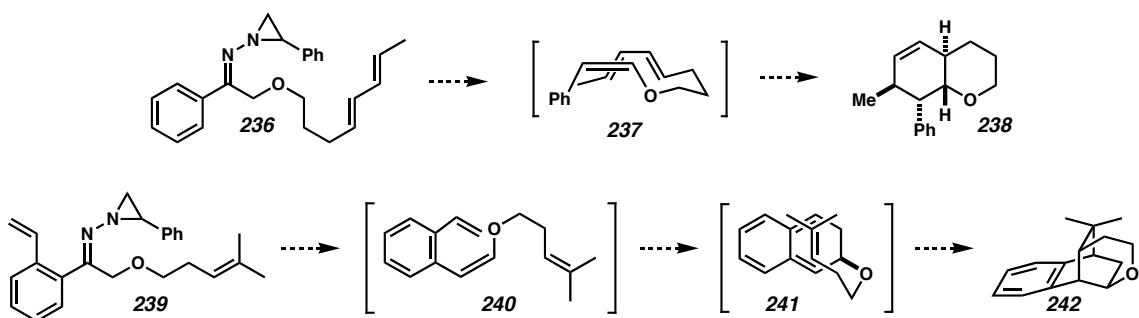
1.8.9 Alternative Precursor Hydrazones

One limitation of the Eschenmoser hydrazones is the thermal threshold for revealing the latent diazo functionality. Conversely, if a chemically triggered protecting group could be designed, the addition of a simple, orthogonal reagent could expose the diazo group and allow the reaction to proceed at a much lower temperature. Possible examples are shown in Figure 1. Several of these provide methods to generate an anionic nitrogen chemically with one protecting group, while the other group mimics the ability

of arylsulfonates to dissociate as sulfinates (see Section 1.1.3.2). An alternative leaving group to sulfinates could be enolates. The resulting diazocompound could then be intercepted by a Rh(II) catalyst as above.

Figure 1.8.1: Potential Chemically Labile Diazo Protecting Groups.

243 **244**
F triggered compounds

245 **246**
Nucleophile triggered compounds

Hydrogenolysis triggered compounds

247 **248**
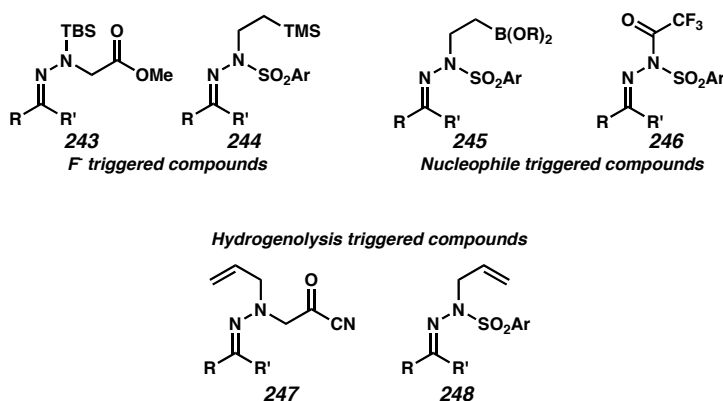
1.9 Conclusion

The use of Eschenmoser hydrazones in conjunction with Rh(II) catalysts has allowed the in situ generation of non-carbonyl stabilized diazo compounds that readily react to form rhodium carbenes. These high-energy species were used for productive, C-C bon-forming reactions with a high degree of control. Expansion of this chemistry to tandem sequences such as the Bamford-Stevens/Claisen reaction was readily made, and further tandem reactions, be they reduction, carbonyl-ene, or Cope, were compiled to generate a reactive cascade.

With the masked diazo compounds demonstrated to function as proposed, many new potential transformations could be made that take advantage of the rhodium carbene reactivity. These reactions would be able to generate novel structures inaccessible to α-diazo carbonyls.

1.10 Experimental Section

1.10.1 Materials and Methods

Unless stated otherwise, reactions were performed in flame-dried glassware under a nitrogen atmosphere. *N*-Methyl 2-pyrrolidinone (NMP) was distilled from P_2O_5, and dichloroethane (DCE) was freshly distilled from CaH_2. Other solvents were dried and purified using activated alumina columns. All other reagents were used as received from commercial sources. Reaction temperatures were controlled by an IKAmag temperature modulator. Photoreactions were performed in a custom photobox lined with aluminum foil and equipped with a Hanova mercury lamp. Thin-layer chromatography (TLC) was performed using E. Merck silica gel 60 F254 precoated plates (0.25mm) and visualized by UV, *p*-anisaldehyde staining, or ceric ammonium molybdate staining (CAM). ICN Silica gel (particle size 0.032-0.063 mm) was used for flash chromatography. ^{1}H and ^{13}C NMR spectra were recorded on a Varian Mercury 300 spectrometer (at 300 MHz and 75 MHz, respectively) in $CDCl_3$ and are internally referenced to the residual chloroform peak (7.27 ppm and 77.23 ppm, respectively) relative to Me_4Si. Data for ^{1}H NMR spectra are reported as follows: chemical shift (δ ppm), multiplicity, coupling constant (Hz), and integration. Data for ^{13}C NMR spectra are reported in terms of chemical shift. IR spectra were recorded on a Perkin Elmer Paragon 1000 spectrometer and are reported in frequency of absorption (cm^{-1}). High resolution mass spectra were obtained from the UC Irvine Mass Spectral Facility.

CAUTION! 1-Amino-2-phenyl-aziridinium acetate is potentially explosive, and proper precautions should be taken whenever it is used (see Müller, Felix, Schreiber, Wintner, and Eschenmoser, *Org. Synth. Coll. Vol.* **1988**, *6*, 56).

1.10.2 Starting Material Preparation

1.10.2.1 General Approach
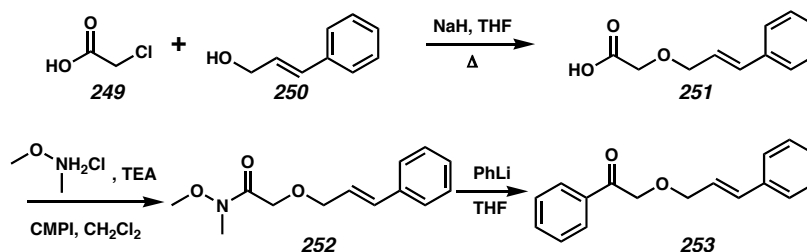
α-Alloxy ketones **253** were obtained via a three-step protocol using established procedures. Treatment of α-chloro acetic acid (**249**) with the appropriate allylic alcohols (i.e., **250**) produced the corresponding α-alloxy acids **251**.[20] Transformation of acids **251** to the Weinreb amide[21] and treatment with either alkyl-lithium or alkyl-magnesium bromides produced the desired keto-ethers **253**.

1.10.2.2 Representative Nucleophilic Addition to a Weinreb Amide
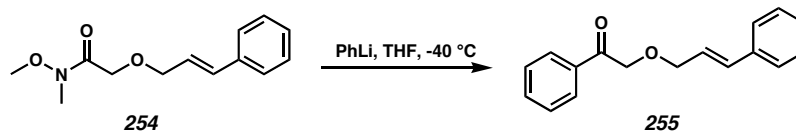
Ketone 255. To a flame-dried flask (100 mL) equipped with a magnetic stirbar was added Weinreb amide **254** (2.85 g, 12.11 mmol) followed by THF (50 mL). This solution was cooled to -40 °C for 5 min, and then a PhLi solution (8.4 mL of a 1.8 M solution in cyclohexane/ether, 15.12 mmol) was added dropwise over 10 min. The mixture was stirred for 10 min and then quenched by the addition of MeOH (8 mL). Et$_2$O (20 mL) and H$_2$O (40 mL) were then added, the layers were separated, and the

aqueous phase was extracted with Et$_2$O (3 x 10 mL). The combined organic layers were dried over MgSO$_4$, and the solvent was removed under reduced pressure. The ketone was purified by flash column chromatography (15:1 hexanes:ethyl acetate eluent) to provide **255** as a white crystalline solid (2.60 g, 10.29 mmol, 85% yield) that was spectroscopically identical to that previously reported.[22] Ketone **255** could be further purified by recrystalization from boiling hexanes. R$_F$ 0.33 (15:1 hexanes:ethyl acetate eluent).

1.10.2.3 Compounds Produced by the General Procedure

256
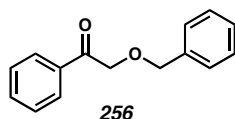
Keto-ether 256. The general procedure outlined above was followed (using 2.87 g, 13.72 mmol of the corresponding Weinreb amide) to provide keto-ether **256** (2.14 g, 9.54 mmol, 70% yield) as a yellow oil. Flash chromatographic purification (15:1 hexanes:ethyl acetate eluent). The spectroscopic data were identical to those previously reported.[23] R$_F$ 0.51 (3:1 hexanes:ethyl acetate eluent).

257
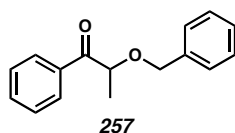
Keto-ether 257. The general procedure outlined above was followed (using 4.01 g, 17.96 mmol of the corresponding Weinreb amide) to provide keto-ether **257** (3.43 g, 14.27 mmol, 79% yield) as a yellow oil. Flash chromatographic purification (9:1

hexanes:ethyl acetate eluent). The spectroscopic data were identical to those previously reported.[24] R$_F$ 0.74 (1:1 hexanes:ethyl acetate eluent).
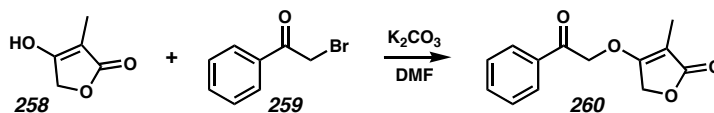
Keto-ether 260. A flame-dried flask (10 mL) equipped with Teflon stirbar was charged with 2-methyltetronic acid (75.2 mg, 0.675 mmol). DMF was added via syringe (2.7 mL), and then K$_2$CO$_3$ (935.0 mg) was added as a solid. Finally, bromoacetophenone (200.2 mg, 1.006 mmol) was added, and the reaction stirred for 10 minutes. TLC analysis (1:1 hexanes : ethyl acetate, p-anisaldehyde stain) showed all the 2-methyltetronic acid to be consumed. After another 20 minutes the reaction was concentrated under reduced pressure, and then the mixture was purified via column chromatography (1:0 → 19:1 → 9:1 → 6:1 → 2:1 → 1:1 hexanes : ethyl acetate eluent) to afford pure **260** (130.5 mg, 0.57 mmol, 84.4% yield). R$_F$ 0.43; ^{1}H NMR (300 MHz, CDCl$_3$) δ 7.90 (t, J =10.16 Hz, 2H), 7.65 (t, J = 7.4 Hz, 1H), 7.51 (t, J = 10.0 Hz, 2H), 6.86 (d, J = 8.2 Hz, 2H), 5.45 (s, 2H), 4.61 (s, 2H), 1.76 (s, 3H); ^{13}C NMR (75 MHz, CDCl3) δ 192.2, 175.0, 170.9, 134.7, 133.3, 129.3, 127.8, 99.9, 71.8, 66.2, 36.6, 7.6.

Keto-ether 261. The general procedure outlined above was followed (using 2.96 g, 11.15 mmol of the corresponding Weinreb amide) to provide keto-ether **261** (1.97 g, 6.98 mmol, 63% yield) as a white solid. Flash chromatographic purification (15:1

hexanes:ethyl acetate eluent).   m.p. 70.0-73.0°; R_F 0.61 (1:1 hexanes:ethyl acetate eluent); ^{1}H NMR (300 MHz, CDCl$_3$) δ 7.94 (d, J = 8.2 Hz, 2H), 7.59 (t, J = 7.4 Hz, 1H), 7.47 (t, J = 8.2 Hz, 2H), 7.34 (d, J = 8.5 Hz, 2H), 6.86 (d, J = 8.2 Hz, 2H), 6.59 (d, J = 15.9 Hz, 1H), 6.20 (dt, J = 6.6, 15.9 Hz, 1H), 4.81 (s, 2H), 4.31 (d, J = 6.6 Hz, 2H), 3.82 (s, 3H); ^{13}C NMR (75 MHz, CDCl$_3$) δ 196.1, 159.2, 134.7, 133.4, 133.2, 129.0, 128.5, 127.7, 127.7, 122.6, 113.8, 72.3, 72.2, 55.3; IR (neat) 2999, 2931, 1700 cm^{-1}.   HRMS (EI) m/z calc'd for 236.1775, found 236.1776. HRMS (EI) m/z calc'd for $[C_{18}H_{18}O_3]^+$ 282.1256, found 282.1256.

262
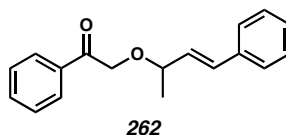
Keto-ether 262. The general procedure outlined above was followed (using 1.81 g, 7.26 mmol of the corresponding Weinreb amide) to provide keto-ether **262** (1.42 g, 5.33 mmol, 73% yield) as a white solid.   Flash chromatographic purification (15:1 hexanes:ethyl acetate eluent). R_F 0.25 (9:1 hexanes:ethyl acetate eluent); ^{1}H NMR (300 MHz, CDCl$_3$) δ 7.92 (d, J = 7.1 Hz, 2H), 7.57 (t, J = 7.4 Hz, 1H), 7.47-7.26 (m, 7H), 6.56 (d, J = 15.9 Hz, 1H), 6.14 (dd, J = 8.0, 15.9 Hz, 1H), 4.83 (d, J = 17.0 Hz, 1H), 4.73 (d, J = 17.0 Hz, 1H), 4.19 (dq, J = 6.3, 8.0 Hz, 1H), 1.47 (d, J = 6.3 Hz, 3H); ^{13}C NMR (75 MHz, CDCl$_3$) δ 196.4, 136.0, 134.9, 133.2, 132.2, 130.4, 128.5, 128.5, 127.8, 127.7, 126.4, 77.5, 70.9, 21.7; IR (neat) 3060, 3028, 2975, 1699 cm^{-1}. HRMS (EI) m/z calc'd for $[C_{18}H_{18}O_2]^+$ 266.1307, found 266.1312.

263

Keto-ether 263. The general procedure outlined above was followed (using 426 mg, 1.71 mmol of the corresponding Weinreb amide) to provide keto-ether **263** (412 mg, 1.55 mmol, 91% yield) as a pale yellow oil. Flash chromatographic purification (15:1 hexanes:ethyl acetate eluent). R_F 0.59 (3:1 hexanes:ethyl acetate eluent); ^{1}H NMR (300 MHz, CDCl$_3$) δ 8.07 (d, J = 7.2 Hz, 2H), 7.59 (t, J = 7.4 Hz, 1H), 7.48 (t, J = 7.7 Hz, 2H), 7.38-7.25 (comp.m, 5H), 6.58 (d, J = 15.9 Hz, 1H), 6.28 (dt, J = 6.1, 15.9 Hz, 1H), 4.84 (q, J = 6.9 Hz, 1H), 4.28 (dd, J = 5.8, 12.4 Hz, 1H), 4.14 (dd, J = 6.6, 12.4 Hz, 1H), 1.55 (d, J = 6.9 Hz, 3H); ^{13}C NMR (75 MHz, CDCl$_3$) δ 200.7, 136.5, 134.9, 133.5, 133.2, 128.9, 128.7, 128.6, 127.9, 126.6, 125.5, 78.2, 70.6, 19.2; IR (neat) 3060, 3027, 2983, 1694 cm^{-1}. HRMS (EI) m/z calc'd for [C$_{18}$H$_{18}$O$_2$]$^+$ 266.1307, found 266.1301.

264
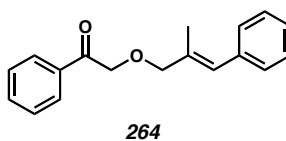
Keto-ether 264. The general procedure outlined above was followed (using 2.28 g, 15.57 mmol of the corresponding Weinreb amide) to provide keto-ether **264** (2.90 g, 10.90 mmol, 70% yield) as a colorless oil. Flash chromatographic purification (15:1 hexanes:ethyl acetate eluent). m.p. 51.5-52.5; R_F 0.32 (3:1 hexanes:ethyl acetate eluent); ^{1}H NMR (500 MHz, CDCl$_3$) δ 7.98 (d, J = 7.3 Hz, 2H), 7.61 (t, J = 7.3 Hz, 1H), 7.50 (t, J = 7.8 Hz, 2H), 7.36 (t, J = 7.8 Hz, 2H), 7.31 (d, J = 7.3 Hz, 2H), 7.25 (t, J = 7.3 Hz, 1H), 6.57 (s, 1H), 4.81 (s, 2H), 4.23 (s, 2H), 1.96 (s, 3H); ^{13}C NMR (125 MHz, CDCl$_3$) δ

196.3, 137.2, 134.9, 134.3, 133.5, 128.9, 128.6, 128.1, 128.0, 127.9, 126.6, 77.6, 72.3; IR

(neat) 3059, 3023, 2908, 1699 cm^{-1}. HRMS (EI) m/z calc'd for $[C_{18}H_{18}O_2]^+$ 266.1307,

found 266.1309.

265
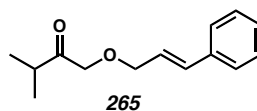
Keto-ether 265. The general procedure outlined above was followed (using 2.00

g, 8.49 mmol of the corresponding Weinreb amide) to provide keto-ether **265** (1.10 g,

5.02 mmol, 59% yield) as a yellow oil. Flash chromatographic purification (15:1

hexanes:ethyl acetate eluent). R_F 0.51 (3:1 hexanes:ethyl acetate eluent); ^{1}H NMR (300

MHz, CDCl$_3$) δ 7.42-7.24 (comp.m, 5H), 6.63 (d, J = 15.9 Hz, 1H), 6.30 (dt, J = 6.0,

15.9 Hz, 1H), 4.23 (d, J = 6.6 Hz, 2H), 4.21 (s, 2H), 2.78 (sept, J = 7.2 Hz, 1H), 1.12 (d,

J = 7.2 Hz, 6H); ^{13}C NMR (75 MHz, CDCl$_3$) δ 211.9, 136.4, 133.5, 128.7, 128.0, 126.7,

125.2, 73.5, 72.2, 37.4, 18.4; IR (neat) 3027, 2971, 1728 cm^{-1}. HRMS (EI) m/z calc'd for

$[C_{14}H_{18}O_2+H]^+$ 218.1307, found 218.1308.

266
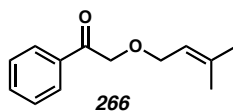
Keto-ether 266. The general procedure outlined above was followed (using 6.23

g, 33.27 mmol of the corresponding Weinreb amide) to provide keto-ether **266** (3.50 g,

17.14 mmol, 52% yield) as a yellow oil. Flash chromatographic purification (15:1

hexanes:ethyl acetate eluent). The spectroscopic data were identical to those previously

reported.[3] R_F 0.34 (9:1 hexanes:ethyl acetate eluent).
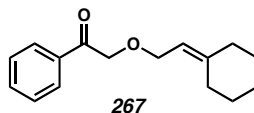
Keto-ether 267. The general procedure outlined above was followed (using 328.0 mg, 1.14 mmol of the corresponding Weinreb amide) to provide keto-ether **267** (295.1 mg, 1.21 mmol, 84% yield) as a pale yellow oil. Flash chromatographic purification (15:1 hexanes:ethyl acetate eluent). R_F 0.38 (3:1 hexanes:ethyl acetate eluent); ^{1}H NMR (300 MHz, CDCl$_3$) δ 7.95 (d, J = 7.1 Hz, 2H), 7.58 (t, J = 7.1 Hz, 1H), 7.47 (t, J = 7.1 Hz, 2H), 5.34 (t, J = 7.1 Hz, 1H), 4.72 (s, 2H), 4.16 (d, J = 7.14 Hz, 2H), 2.19-2.13 (comp.m, 2H), 1.57-1.54 (comp.m, 3H); ^{13}C NMR (75 MHz, CDCl$_3$) δ 196.1, 145.7, 134.5, 132.9, 128.1, 127.4, 116.5, 71.9, 66.3, 36.7, 28.6, 28.1, 27.5, 26.3; IR (neat) 3523, 3385, 2927, 1703, 1699, 1695 cm^{-1}. HRMS (EI) m/z calc'd for $[C_{16}H_{20}O_2-2H]^+$ 214.0994, found 214.1001.
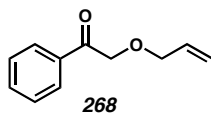
Keto-ether 268. The general procedure outlined above was followed (using 2.39 g, 13.84 mmol of the corresponding Weinreb amide) to provide keto-ether **268** (1.84 g, 9.69 mmol, 70% yield) as a pale yellow oil. Flash chromatographic purification (15:1 hexanes:ethyl acetate eluent). R_F 0.45 (3:1 hexanes:ethyl acetate eluent); ^{1}H NMR (300 MHz, CDCl$_3$) δ 7.95 (d, J = 7.0 Hz, 2H), 7.59 (t, J = 7.3 Hz, 1H), 7.47 (t, J = 7.7 Hz, 2H), 5.81-5.58 (comp.m, 2H), 4.75 (s, 2H), 4.23 (d, J = 7.0 Hz, 2H), 1.68 (d, J = 6.2 Hz, 3H); ^{13}C NMR (75 MHz, CDCl$_3$) δ 196.1, 134.7, 133.2, 128.9, 128.4, 127.6, 125.7, 72.4,

66.3, 13.2; IR (neat) 3063, 3026, 2920, 1701 cm⁻¹. HRMS (EI) m/z calc'd for

[C$_{12}$H$_{14}$O$_2$-20H]⁺ 172.0888, found 172.0888.

269
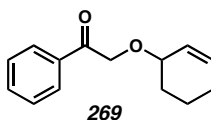
Keto-ether 269. The general procedure outlined above was followed (using 2.65

g, 13.30 mmol of the corresponding Weinreb amide) to provide keto-ether **269** (2.40 g,

11.08 mmol, 83% yield) as a pale yellow oil. Flash chromatographic purification (15:1

hexanes:ethyl acetate eluent). R$_F$ 0.26 (9:1 hexanes:ethyl acetate eluent); ¹H NMR (300

MHz, CDCl$_3$) δ 7.97 (d, J = 7.3 Hz, 2H), 7.59 (t, J = 7.3 Hz, 1H), 7.47 (t, J = 7.7 Hz,

2H), 5.94-5.82 (comp.m, 2H), 4.80 (s, 2H), 4.04 (br.s, 1H,), 2.19-1.51 (comp.m, 6H); ¹³C

NMR (75 MHz, CDCl$_3$) δ 196.5, 134.8, 133.1, 131.4, 128.3, 127.8, 126.8, 73.5, 71.0,

28.1, 25.1, 19.0; IR (neat) 3062, 3028, 2934, 1702 cm⁻¹. HRMS (EI) m/z calc'd for

[C$_{18}$H$_{18}$O$_2$-2H]⁺ 242.1307, found 242.1313.

270
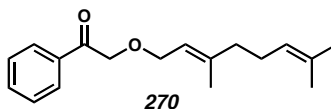
Keto-ether 270. The general procedure outlined above was followed (using 5.10

g, 19.96 mmol of the corresponding Weinreb amide) to provide keto-ether **270** (3.96 g,

14.53 mmol, 73% yield) as a yellow oil. Flash chromatographic purification (15:1

hexanes:ethyl acetate eluent). R$_F$ 0.36 (9:1 hexanes:ethyl acetate eluent); ¹H NMR (300

MHz, CDCl$_3$) δ 7.95 (d, J = 7.0 Hz, 2H), 7.59 (t, J = 7.7 Hz, 1H), 7.47 (t, J = 7.7 Hz,

2H), 5.41 (t, J = 7.0 Hz, 1H), 5.09 (t, J = 4.8 Hz, 1H), 4.73 (s, 2H), 4.17 (d, J = 7.0 Hz,

2H), 2.12-2.02 (comp.m, 4H), 1.68 (s, 6H), 1.60 (s, 3H); ^{13}C NMR (75 MHz, CDCl$_3$) δ

196.3, 141.4, 134.7, 133.2, 131.4, 128.4, 127.6, 123.6, 119.8, 72.2, 67.5, 39.5, 26.2, 25.6,

17.6, 16.4; IR (neat) 2968, 1702 cm^{-1}.   HRMS (EI) m/z calc'd for $[C_{18}H_{24}O_2]^+$

272.1776, found 272.1780.

271
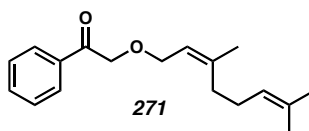
Keto-ether 271. The general procedure outlined above was followed (using 3.82

g, 14.92 mmol of the corresponding Weinreb amide) to provide keto-ether **271** (2.14 g,

7.86 mmol, 53% yield) as a yellow oil.   Flash chromatographic purification (15:1

hexanes:ethyl acetate eluent).   R$_F$ 0.35 (9:1 hexanes:ethyl acetate eluent); ^{1}H NMR (300

MHz, CDCl$_3$) δ 7.95 (d, J = 7.1 Hz, 2H), 7.58 (t, J = 7.2 Hz, 1H), 7.47 (t, J = 7.7 Hz,

2H), 5.42 (t, J = 7.2 Hz, 1H), 5.07 (m, 1H), 4.73 (s, 2H), 4.14 (d, J = 7.1 Hz, 2H), 2.13-

2.02 (comp.m, 4H), 1.77 (s, 3H), 1.67 (s, 3H), 1.59 (s, 3H); ^{13}C NMR (75 MHz, CDCl$_3$)

δ 196.4, 141.5, 134.8, 133.3, 131.9, 128.5, 127.8, 123.5, 120.9, 72.5, 67.4, 32.2, 26.7,

25.7, 23.6, 17.7; IR (neat) 2967, 2917, 1702 cm^{-1}.   HRMS (EI) m/z calc'd for

$[C_{18}H_{24}O_2]^+$ 272.1776, found 272.1785.
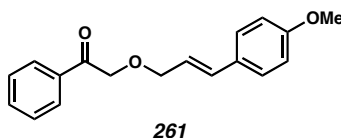

272
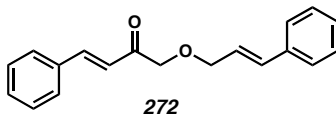
Keto-ether 272. The general procedure outlined above was followed (using 1.29

g, 5.47 mmol of the corresponding Weinreb amide) to provide keto-ether **272** (1.39 g,

5.01 mmol, 92% yield) as a yellow oil. Flash chromatographic purification (15:1 hexanes:ethyl acetate eluent). R_F 0.21 (9:1 hexanes:ethyl acetate eluent); ^{1}H NMR (300 MHz, CDCl$_3$) δ 7.72 (d, J = 16.2 Hz, 1H), 7.59 (dd, J = 3.6, 6.0 Hz, 2H), 7.43-7.24 (comp.m, 8H), 7.00 (d, J = 16.2 Hz, 1H), 6.67 (d, J = 15.9 Hz, 1H), 6.34 (dt, J = 6.0, 15.9 Hz, 1H), 4.37 (s, 2H), 4.30 (d, J = 6.3 Hz, 2H); ^{13}C NMR (75 MHz, CDCl$_3$) δ 197.0, 143.4, 136.2, 134.2, 133.5, 130.7, 128.8, 128.5, 128.4, 127.8, 126.5, 124.9, 121.5, 74.5, 72.1; IR (neat) 3026, 2957, 1695 cm^{-1}.
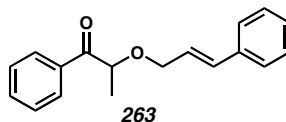

273
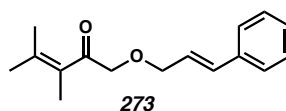
Keto-ether 273. The general procedure outlined above was followed (using 1.58 g, 6.71 mmol of the corresponding Weinreb amide) to provide keto-ether **273** (658.5 mg, 2.70 mmol, 40% yield) as a yellow oil. Flash chromatographic purification (15:1 hexanes:ethyl acetate eluent). R_F 0.29 (9:1 hexanes:ethyl acetate eluent); ^{1}H NMR (300 MHz, CDCl$_3$) δ 7.42-7.27 (comp.m, 5H), 6.63 (d, J = 15.9 Hz, 1H), 6.31 (dt, J = 6.1, 15.9 Hz, 1H), 4.3 (s, 2H), 4.25 (d, J = 6.1 Hz, 2H), 1.88 (s, 3H), 1.84 (s, 3H), 1.77 (s, 3H); ^{13}C NMR (75 MHz, CDCl$_3$) δ 204.0, 140.0, 136.5, 133.4, 128.9, 128.7, 128.0, 126.7, 125.4, 74.3, 72.2, 26.6, 22.8, 21.9; IR (neat) 2922, 1693 cm^{-1}. HRMS (EI) m/z calc'd for [C$_{16}$H$_{20}$O$_2$+H]$^+$ 245.1541, found 245.1544.

1.10.3 Aziridinyl Imine Formation

1.10.3.1 Representative Procedure

CAUTION! 1-Amino-2-phenyl-aziridinium acetate is explosive, and proper precautions should be taken whenever it is used (see Müller, Felix, Schreiber, Wintner, and Eschenmoser, *Org. Synth. Coll. Vol.* **1988**, 6, 56).
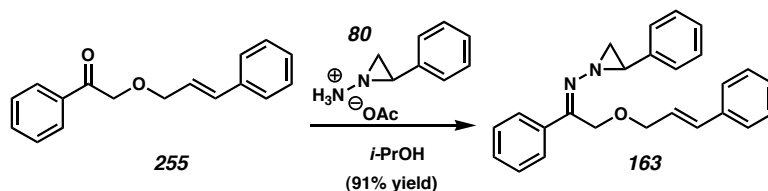
Aziridinyl Imine 163. A flame-dried flask (100 mL) was equipped with a magnetic stirbar and charged with a solution of ketone **255** (1.28 g, 5.09 mmol) in 2-propanol (50 mL). Finally, 1-amino-2-phenyl aziridinium hydrochloride (**80**; 1.52 g, 7.83 mmol) was added, and the reaction was allowed to stir at room temperature until the starting material had been consumed as shown by TLC (3:1 hexanes:ethyl acetate eluent, usually 4-12 h, depending on substrate). The reaction was quenched with powdered $KHCO_3$ and then filtered through celite to remove the base. Removal of solvent under reduced pressure yielded a yellow oil, which was subsequently purified by flash column chromatography (15:1 → 9:1 hexanes:ethyl acetate gradient eluent) to yield α-alloxy aziridinyl imine **163** (1.39 g of the isomer shown (*E*) and 0.321 g of the (*Z*) hydrazone isomer for a total yield of 4.65 mmol, 91%) as a yellow oil. R_F 0.55 (3:1 hexanes:ethyl acetate eluent); ^{1}H NMR (300 MHz, $CDCl_3$) δ 7.81-7.78 (m, 2H), 7.41-7.28 (m, 13H), 6.46 (dt, *J* = 1.5, 15.9 Hz, 1H), 6.12 (dt, *J* = 6.0, 15.6 Hz, 1H), 4.87 (d, *J* = 12.3 Hz, 1H), 4.80 (d, *J* = 12.6 Hz, 1H), 4.01 (dt, *J* = 4.5, 1.8 Hz, 2H), 3.06 (dd, *J* = 7.5, 4.8 Hz, 1H),

2.69 (d, J = 7.8 Hz, 1H), 2.46 (d, J = 4.8 Hz, 1H); ^{13}C NMR (75 MHz, CDCl$_3$) δ 166.2,

138.2, 136.2, 136.3, 135.9, 132.7, 129.4, 128.3, 128.1, 128.0, 127.5, 127.0, 126.3, 126.1,

125.2, 71.3, 64.2, 45.0, 41.6; IR (neat) 3060, 3022, 1604 cm^{-1}. HRMS (EI) m/z calc'd for

[C$_{25}$H$_{24}$N$_2$O+Na]$^+$ 391.1786, found 391.1788.

1.10.3.2 Compounds Synthesized Using General Procedure
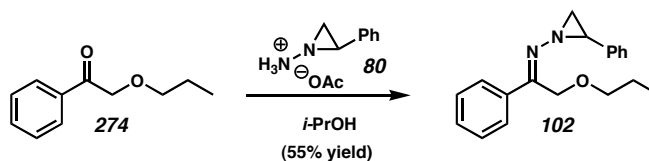
Hydrazone 102. The general procedure outlined above was followed (using

985.3 mg, 5.528 mmol of the corresponding keto-ether **274**) to provide **102** (894.0 mg,

3.037 mmol, 55% yield) as a yellow oil. Flash chromatographic purification (19:1

hexanes : ethyl acetate eluent). R$_F$ 0.57 (3:1 hexanes : ethyl acetate eluent); ^{1}H NMR (300

MHz, CDCl$_3$) δ 7.78-7.75 (m, 2H), 7.39-7.27 (comp.m, 8H), 4.78 (s, 2H), 3.25 (t, J = 6.6

Hz, 2H), 3.04 (dd, J = 4.7, 7.7 Hz, 1H), 2.65 (d, J = 7.4 Hz, 1H), 2.45 (d, J = 4.6 Hz,

1H), 1.45 (dt, J = 6.6, 7.4 Hz, 2H), 0.76 (d, J = 7.4 Hz, 3H).
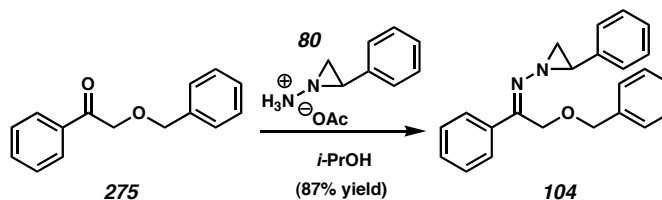
Hydrazone 104. The general procedure outlined above was followed (using 2.14

g, 9.45 mmol of the corresponding keto-ether **275**) to provide **104** (2.81 g, 8.19 mmol,

87% yield) as a yellow oil. Flash chromatographic purification (15:1 → 9:1 hexanes:ethyl acetate gradient eluent). R_F 0.74 (9:1 hexanes:ethyl acetate eluent); ^{1}H NMR (300 MHz, CDCl$_3$) δ 7.79-7.76 (m, 2H), 7.41-7.26 (comp.m, 11H), 7.17-7.14 (m, 2H), 4.88 (d, J = 12.6 Hz, 1H), 4.81 (d, J = 12.6 Hz, 1H), 4.36 (s, 2H), 3.05 (dd, J = 4.9, 7.7 Hz, 1H), 2.65 (d, J = 7.7 Hz, 1H), 2.43 (d, J = 4.7 Hz, 1H); ^{13}C NMR (75 MHz, CDCl$_3$) δ 166.3, 138.2, 137.4, 135.8, 129.4, 128.2, 128.1, 128.0, 127.8, 127.5, 127.1, 127.1, 126.1, 72.7, 64.4, 45.0, 41.6; IR (neat) 3062, 3030, 1605 cm^{-1}. HRMS (EI) m/z calc'd for [C$_{23}$H$_{22}$N$_2$O+Na]$^+$ 365.1630, found 365.1634.

Hydrazone 106. The general procedure outlined above was followed (using 3.04 g, 14.15 mmol of the corresponding keto-ether **257**) to provide **106** (3.28 g, 9.19 mmol, 65% yield) as a yellow oil in a 1:1 mixture of diastereomers. Flash chromatographic purification (15:1 → 9:1 hexanes:ethyl acetate gradient eluent). R_F 0.29 (9:1 hexanes:ethyl acetate eluent); ^{1}H NMR (300 MHz, CDCl$_3$) δ 7.96-7.91 (m, 2H), 7.45-7.06 (comp.m, 13H), 5.69 (q, J = 7.0 Hz, 1H), 4.36 (d, J = 11.4 Hz, 1H), 4.23 (d, J = 11.4 Hz, 1H), 3.19 (dd, J = 4.8, 7.3 Hz, 1H), 2.73 (d, J = 7.7 Hz, 1H), 2.45 (d, J = 4.4 Hz, 1H), 1.62 (d, J = 6.6 Hz, 3H), 1.43 (d, J = 7.0 Hz, 3H); ^{13}C NMR (75 MHz, CDCl$_3$) δ 172.0, 138.0, 135.2, 129.6, 128.5, 128.4, 128.2, 128.1, 128.0, 128.0, 127.7, 127.4, 126.3, 72.2, 71.7, 45.1, 42.3, 19.9; IR (neat) 3087, 3063, 3031, 1698, 1604 cm^{-1}. HRMS (EI) m/z calc'd for [C$_{24}$H$_{24}$N$_2$O+H]$^+$ 357.1967, found 357.1971.

Hydrazone 95. The general procedure outlined above was followed (using 539.4 mg, 2.35 mmol of the corresponding keto-ether **260**) to provide **95** (613.7 g, 1.45 mmol, 61% yield) as a yellow oil. Flash chromatographic purification (9:1 → 1:1 hexanes : ethyl acetate gradient eluent). R_F 0.48 (1:1 hexanes : ethyl acetate eluent); ^{1}H NMR (300 MHz, CDCl$_3$) δ 7.70 (d, 1H), 7.44-7.23 (comp. m, 9H), 5.46 (d, $J = 27.4$ Hz, 1H), 5.43 (d, $J = 27.8$ Hz, 1H), 4.33 (d, $J = 17.9$ Hz, 1H), 4.30 (d, $J = 17.9$ Hz, 1H), 3.00 (t, $J = 4.9$ Hz, 1H), 2.80 (d, $J = 7.8$ Hz, 1H), 2.54 (d, $J = 4.9$ Hz 1H), 1.63 (s, 3H); ^{13}C NMR (75 MHz, CDCl$_3$) δ 187.8, 175.1, 170.7, 130.3, 128.8, 128.8, 128.2, 127.2, 126.3, 66.0, 64.4, 45.7, 42.0, 7.3.

Hydrazone 165. The general procedure outlined above was followed (using 1.50 g, 5.32 mmol of the corresponding keto-ether **261**) to provide **165** (1.68 g, 4.24 mmol, 80% yield) as a yellow oil. Flash chromatographic purification (15:1 → 9:1 hexanes:ethyl acetate gradient eluent). R_F 0.45 (99:1 CH$_2$Cl$_2$:MeOH eluent); ^{1}H NMR (300 MHz, CDCl$_3$) δ 7.80-7.67 (m, 2H), 7.42-7.24 (comp.m, 13H), 6.85 (d, $J = 8.8$ Hz, 2H), 6.40 (d, $J = 15.9$ Hz, 1H), 5.98 (dt, $J = 6.3, 15.9$ Hz, 1H), 4.85 (d, $J = 12.4$ Hz, 1H),

4.79 (d, J = 12.4 Hz, 1H), 3.98 (d, J = 6.3 Hz, 2H), 3.82 (s, 3H), 3.05 (dd, J = 4.7, 7.7

Hz, 1H), 2.67 (d, J = 7.7 Hz, 1H), 2.45 (d, J = 4.4 Hz, 1H); ^{13}C NMR (75 MHz, CDCl$_3$) δ

166.7, 159.3, 138.6, 136.2, 132.9, 129.7, 129.4, 128.5, 128.3, 127.8, 127.4, 127.3, 126.4,

123.2, 114.0, 71.9, 64.5, 55.5, 45.3, 41.9; IR (neat) 3032, 2934, 1607 cm^{-1}. HRMS (EI)

m/z calc'd for [C$_{26}$H$_{26}$N$_2$O$_2$+H]$^+$ 399.2072, found 399.2069.

Hydrazone 13. The general procedure outlined above was followed (using 1.41

g, 5.29 mmol of the corresponding keto-ether **262**) to provide **13** (1.66 g, 4.34 mmol,

82% yield) as a yellow oil in a 1:1 mixture of diastereomers. Flash chromatographic

purification (15:1 → 9:1 hexanes:ethyl acetate gradient eluent).   R$_F$ 0.47 (9:1

hexanes:ethyl acetate eluent); ^{1}H NMR (300 MHz, CDCl$_3$) δ 7.79-7.75 (m, 4H), 7.40-

7.24 (comp.m, 26H), 6.45 (d, J = 15.9 Hz, 1H), 6.40 (d, J = 15.9 Hz, 1H), 6.02 (dd, J =

7.7, 15.9 Hz, 1H), 5.86 (dd, J = 8.0, 15.9 Hz, 1H), 4.87 (d, J = 12.9 Hz, 1H), 4.80 (s,

2H), 4.69 (d, J = 12.9 Hz, 1H), 4.00-3.79 (comp.m, 2H), 3.08 (dd, J = 4.7, 7.4 Hz, 1H),

2.98 (dd, J = 4.7, 7.4 Hz, 1H), 2.68 (d, J = 7.4 Hz, 1H), 2.60 (d, J = 7.4 Hz, 1H), 2.49 (d,

J = 4.7 Hz, 2H), 1.20 (d, J = 6.3 Hz, 3H), 1.16 (d, J = 6.3 Hz, 3H); ^{13}C NMR (75 MHz,

CDCl$_3$) δ 166.9, 166.7, 138.4, 138.3, 136.3, 136.1, 136.0, 131.9, 131.7, 130.6, 130.6,

129.3, 128.4, 128.3, 128.2, 128.0, 127.6, 127.5, 127.2, 127.1, 126.4, 126.4, 126.1, 77.0,

77.0, 62.8, 44.9, 44.9, 41.8, 41.7, 21.5, 21.5; IR (neat) 3060, 3026, 2976, 1605 cm^{-1}.

HRMS (EI) m/z calc'd for [C$_{26}$H$_{26}$N$_2$O+Na]$^+$ 405.1943, found 405.1953.

Hydrazone 169. The general procedure outlined above was followed (using 387.3 mg, 1.45 mmol of the corresponding keto-ether **263**) to provide **169** (495.4 mg, 1.30 mmol, 90% yield) as a yellow oil as a 1:1 mixture of diastereomers. Flash chromatographic purification (15:1 → 9:1 hexanes:ethyl acetate gradient eluent). R_F 0.68 (3:1 hexanes:ethyl acetate eluent); ^{1}H NMR (300 MHz, CDCl$_3$) δ 7.92-7.86 (m, 4H), 7.41-7.23 (comp.m, 26H), 6.51 (d, J = 15.9 Hz, 1H), 6.37 (d, J = 15.9 Hz, 1H), 6.16 (dt, J = 6.0, 15.9 Hz, 1H), 6.07 (dt, J = 6.0, 15.9 Hz, 1H), 5.69 (q, J = 6.6 Hz, 1H), 5.66 (q, J = 6.6 Hz, 1H), 4.08 (d, J = 6.0 Hz, 2H), 3.94 (m, 2H), 3.15 (dd, J = 4.4, 7.1 Hz, 1H), 2.96 (dd, J = 4.4, 7.7 Hz, 1H), 2.71 (d, J = 7.7 Hz, 1H), 2.55 (d, J = 7.7 Hz, 1H), 2.43 (d, J = 4.4 Hz, 1H), 2.40 (d, J = 4.9 Hz, 1H), 1.58 (d, J = 6.6 Hz, 3H), 1.39 (d, J = 6.6 Hz, 3H); ^{13}C NMR (75 MHz, CDCl$_3$) δ 171.8, 138.7, 135.2, 132.9, 132.6, 129.5, 128.6, 128.5, 128.2, 128.0, 127.8, 127.7, 127.4, 127.3, 126.6, 126.4, 126.3, 125.7, 72.0, 71.7, 70.2, 45.3, 44.9, 42.3, 20.0, 19.7; IR (neat) 3027, 2983, 1602 cm^{-1}. HRMS (EI) m/z calc'd for [C$_{26}$H$_{26}$N$_2$O+H]$^+$ 383.2123, found 383.2125.

Hydrazone 171. The general procedure outlined above was followed (using 987.4 mg, 3.71 mmol of the corresponding keto-ether **264**) to provide **171** (1.31 g, 3.41 mmol, 92% yield) as a yellow oil. Flash chromatographic purification (15:1 → 9:1 hexanes:ethyl acetate gradient eluent) as a yellow oil. R_F 0.48 (9:1 hexanes:ethyl acetate eluent); ^{1}H NMR (500 MHz, CDCl$_3$) δ 7.81 (m, 2H), 7.42-7.23 (comp.m, 13H), 6.39 (s, 1H), 4.90 (d, J = 12.5 Hz, 1H), 4.82 (d, J = 12.5 Hz, 1H), 3.91 (s, 2H), 3.08 (dd, J = 4.7, 7.7 Hz, 1H), 2.69 (d, J = 7.7 Hz, 1H), 2.47 (d, J = 4.7 Hz, 1H), 1.76 (s, 3H); ^{13}C NMR (125 MHz, CDCl$_3$) δ 166.9, 138.4, 137.4, 136.1, 134.6, 129.6, 128.9, 128.4, 128.2, 128.0, 127.5, 127.3, 126.5, 126.3, 77.1, 45.0, 41.7, 15.4; IR (neat) 3059, 3026, 2986, 1603 cm^{-1}.

Hydrazone 173. The general procedure outlined above was followed (using 821.1 mg, 3.76 mmol of the corresponding keto-ether **265**) to provide **173** (251.2 mg, 3.54 mmol, 94% yield) as a yellow oil. Flash chromatographic purification (15:1 → 9:1 hexanes:ethyl acetate gradient eluent). R_F 0.35 (9:1 hexanes:ethyl acetate eluent); ^{1}H NMR (300 MHz, CDCl$_3$) δ 7.38-7.22 (comp.m, 10H), 6.53 (d, J = 15.9 Hz, 1H), 6.20 (dt, J = 6.0, 15.9 Hz, 1H), 4.52 (d, J = 14.3 Hz, 1H), 4.39 (d, J = 14.3 Hz, 1H), 4.06 (d, J = 6.0 Hz, 2H), 2.92-2.78 (comp.m, 2H), 2.42 (d, J = 7.7 Hz, 1H), 2.27 (d, J = 5.0 Hz, 1H),

1.15 (d, J = 3.3 Hz, 3H), 1.13 (d, J = 2.8 Hz, 3H); ^{13}C NMR (75 MHz, CDCl$_3$) δ 174.8, 138.9, 136.7, 132.8, 128.6, 128.4, 127.8, 127.2, 126.6, 126.2, 125.7, 72.0, 66.6, 44.4, 41.4, 31.7, 20.6, 20.3; IR (neat) 3028, 2967, 1605 cm^{-1}. HRMS (EI) m/z calc'd for [C$_{22}$H$_{26}$N$_2$O+H]$^+$ 335.2123, found 335.2122.
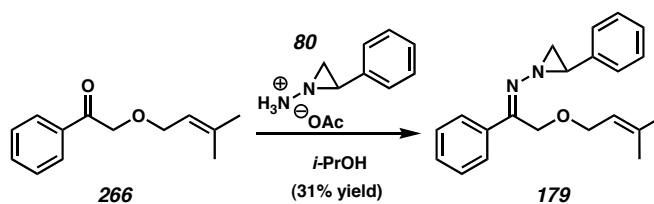
Hydrazone 179. The general procedure outlined above was followed (using 3.50 g, 17.14 mmol of the corresponding keto-ether **266**) to provide **179** (1.71 g, 5.34 mmol, 31% yield) as a yellow oil.   Flash chromatographic purification (15:1 → 9:1 hexanes:ethyl acetate gradient eluent). R$_F$ 0.52 (9:1 hexanes:ethyl acetate eluent); ^{1}H NMR (300 MHz, CDCl$_3$) δ 7.76-7.72 (m, 2H), 7.38-7.24 (m, 8H), 5.20-5.14 (m, 1H), 4.78 (d, J = 22.8 Hz, 1H), 4.72 (d, J = 7.14 Hz, 1H), 3.80 (d, J = 7.1 Hz, 2H), 3.01 (dd, J = 7.7, 4.7 Hz, 1H), 2.64 (d, J = 22.5 Hz, 1H), 2.43 (d, J = 4.6 Hz, 1H), 1.66 (d, J = 0.8 Hz, 3H), 1.46 (d, J = 0.8 Hz, 3H); ^{13}C NMR (75 MHz, CDCl$_3$) δ 166.8, 138.3, 137.7, 135.9, 129.4, 128.2, 128.0, 127.1, 127.1, 126.1, 120.3, 67.0, 64.3, 45.0, 41.7, 25.8, 17.8; IR (neat) 3062, 3030, 2975, 1605 cm^{-1}. HRMS (EI) m/z calc'd for [C$_{21}$H$_{24}$N$_2$O+H]$^+$ 321.1967, found 321.1968.

Hydrazone 181. The general procedure outlined above was followed (using 295 mg, 1.21 mmol of the corresponding keto-ether **267**) to provide **181** (385.7 mg, 1.07 mmol, 89% yield) as a yellow oil. Flash chromatographic purification (15:1 → 9:1 hexanes:ethyl acetate gradient eluent). R_F 0.44 (3:1 hexanes:ethyl acetate eluent); ^{1}H NMR (300 MHz, CDCl$_3$) δ 7.78-7.75 (m, 2H), 7.43-7.27 (comp.m, 8H), 5.15 (t, J = 7.1 Hz, 1H), 4.81 (d, J = 12.6 Hz, 1H), 4.74 (d, J = 12.9 Hz, 1H), 3.83 (d, J = 7.1 Hz, 2H), 3.04 (dd, J = 4.7, 7.4 Hz, 1H), 2.65 (d, J = 7.7 Hz, 1H), 2.45 (d, J = 4.7 Hz, 1H), 2.05 (br.s, 2H), 1.96 (t, J = 5.5 Hz, 2H), 1.53-1.41 (comp.m, 6H); ^{13}C NMR (75 MHz, CDCl$_3$) δ 166.8, 145.6, 138.3, 135.9, 129.4, 128.2, 128.0, 127.1, 127.1, 126.1, 116.9, 66.2, 64.2, 45.0, 41.7, 37.0, 28.8, 28.3, 27.7, 26.6; IR (neat) 3061, 3031, 2927, 1667, 1605 cm^{-1}. HRMS (EI) m/z calc'd for $[C_{24}H_{28}N_2O+Na]^+$ 383.2099, found 383.2082.
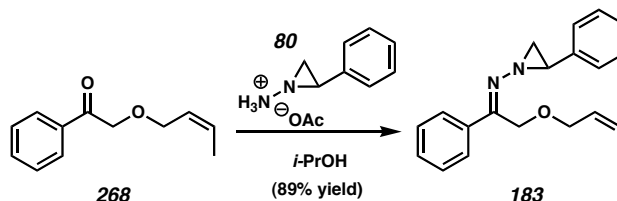
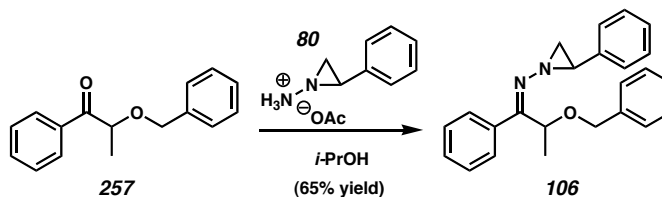**Hydrazone 183.** The general procedure outlined above was followed (using 1.84 g, 9.67 mmol of the corresponding keto-ether **268**) to provide **183** (2.65 g, 8.65 mmol, 89% yield) as a yellow oil. Flash chromatographic purification (15:1 → 9:1 hexanes:ethyl acetate gradient eluent). R_F 0.47 (9:1 hexanes:ethyl acetate eluent); [1]H

NMR (300 MHz, CDCl$_3$) δ 7.78-7.75 (m, 2H), 7.39-7.27 (comp.m, 8H), 5.65-5.55 (m, 1H), 5.46-5.38 (m, 1H), 4.82 (d, J = 12.3 Hz, 1H), 4.75 (d, J = 12.3 Hz, 1H), 3.90 (d, J = 6.6 Hz, 2H), 3.05 (dd, J = 4.8, 7.7 Hz, 1H), 2.67 (d, J = 7.7 Hz, 1H), 2.46 (d, J = 4.8 Hz, 1H), 1.49 (d, J = 6.9 Hz, 3H); ^{13}C NMR (75 MHz, CDCl$_3$) δ 166.3, 138.2, 135.8, 129.3, 128.2, 128.1, 127.9, 127.0, 126.9, 126.0, 126.0, 65.8, 64.3, 44.9, 41.5, 12.9; IR (neat) 3062, 3026, 2986, 1605 cm^{-1}.
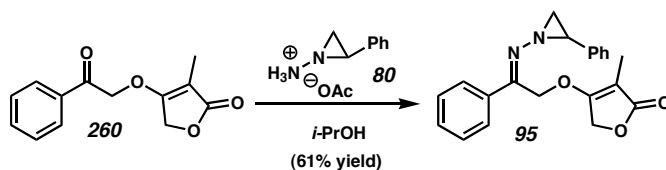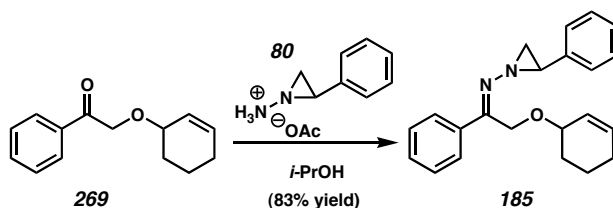

Hydrazone 185. The general procedure outlined above was followed (using 2.40 g, 11.08 mmol of the corresponding keto-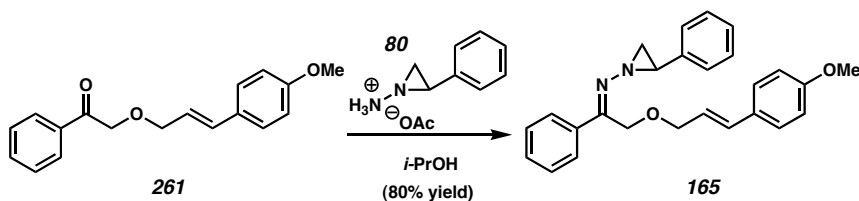ether **269**) to provide **185** (3.06 g, 9.21 mmol, 83% yield) as a yellow oil. Flash chromatographic purification (15:1 → 9:1 hexanes:ethyl acetate gradient eluent). R$_F$ 0.37 (9:1 hexanes:ethyl acetate eluent); ^{1}H NMR (300 MHz, CDCl$_3$) δ 7.85-7.82 (m, 2H), 7.46-7.29 (comp.m, 8H), 5.84-5.77 (m, 1H), 5.64-5.54 (m, 1H), 4.95 (d, J = 12.8 Hz, 1H), 4.84 (d, J = 12.8 Hz, 1H), 3.81 (br.s, 1H), 3.10 (dd, J = 4.8, 7.4 Hz, 1H), 2.69 (d, J = 7.7 Hz, 1H), 2.48 (d, J = 4.8 Hz, 1H), 2.05-1.87 (comp.m, 2H), 1.76-1.41 (comp.m, 4H); ^{13}C NMR (75 MHz, CDCl$_3$) δ 167.2, 138.6, 136.3, 131.2, 129.5, 128.4, 128.2, 127.4, 127.4, 127.4, 126.3, 72.9, 62.6, 45.1, 42.0, 28.1, 25.4, 19.3; IR (neat) 3062, 3028, 2987, 1650, 1605 cm^{-1}. HRMS (EI) m/z calc'd for [C$_{22}$H$_{24}$N$_2$O+H]$^+$ 333.1967, found 333.1968.
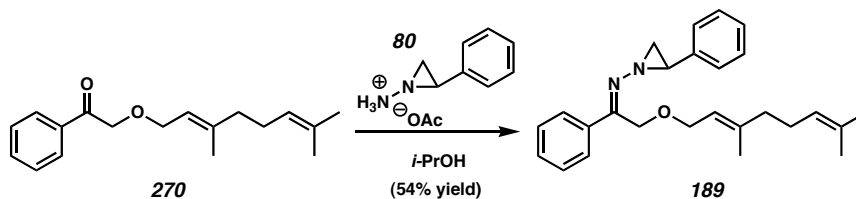
Hydrazone 189. The general procedure outlined above was followed (using 3.96

g, 14.54 mmol of the corresponding keto-ether **270**) to provide **189** (3.06 g, 7.87 mmol,

54% yield) as a yellow oil. Flash chromatographic purification (15:1 → 9:1

hexanes:ethyl acetate gradient eluent). R_F 0.47 (9:1 hexanes:ethyl acetate eluent); [1]H

NMR (300 MHz, CDCl$_3$) δ 7.78-7.75 (m, 2H), 7.44-7.26 (comp.m, 8H), 5.21 (t, J = 6.9

Hz, 1H), 5.07 (t, J = 6.9 Hz, 1H), 4.81 (d, J = 12.6 Hz, 1H), 4.73 (d, J = 12.6 Hz, 1H),

3.84 (d, J = 6.9 Hz, 2H), 3.04 (dd, J = 4.7, 7.4 Hz, 1H), 2.66 (d, J = 7.7 Hz, 1H), 2.45 (d,

J = 4.7 Hz, 1H), 2.06-1.95 (comp.m, 4H), 1.68 (s, 3H), 1.59 (s, 3H), 1.48 (s, 3H); [13]C

NMR (75 MHz, CDCl$_3$) δ 166.8, 141.0, 138.3, 135.9, 131.5, 129.4, 128.3, 128.1, 127.2,

127.1, 126.1, 123.8, 120.0, 67.1, 64.3, 45.0, 41.7, 39.6, 26.4, 25.8, 17.8, 16.3; IR (neat)
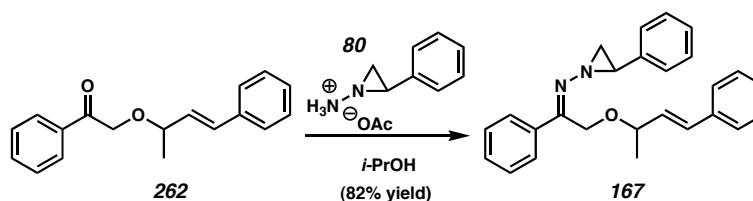
3062, 3031, 2967, 1605 cm^{-1}.
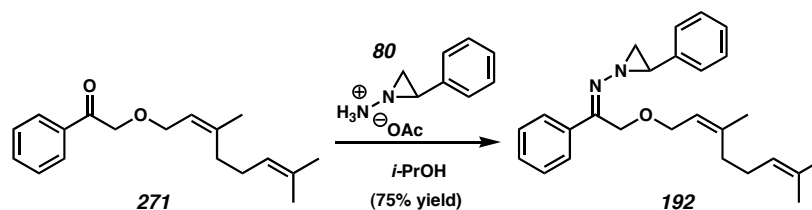
Hydrazone 192. The general procedure outlined above was followed (using 2.14

g, 7.86 mmol of the corresponding keto-ether **271**) to provide **192** (2.30 g, 5.93 mmol,

75% yield) as a yellow oil. Flash chromatographic purification (15:1 → 9:1

hexanes:ethyl acetate gradient eluent). R_F 0.44 (9:1 hexanes:ethyl acetate eluent); [1]H

NMR (300 MHz, CDCl$_3$) δ 7.78-7.75 (m, 2H), 7.49-7.26 (m, 8H), 5.21 (t, J = 6.9 Hz, 1H), 5.01 (t, J = 6.6 Hz, 1H), 4.81 (d, J = 12.6 Hz, 1H), 4.73 (d, J = 12.6 Hz, 1H), 3.83 (d, J = 6.87 Hz, 2H), 3.05 (dd, J = 4.7, 7.7 Hz, 1H), 2.66 (d, J = 7.7 Hz, 1H), 2.45 (d, J = 4.7 Hz, 1H), 1.98-1.88 (m, 4H), 1.69 (s, 3H), 1.68 (s, 3H), 1.58 (s, 3H); ^{13}C NMR (75 MHz, CDCl$_3$) δ 166.2, 140.5, 138.2, 135.7, 131.3, 129.2, 128.0, 127.8, 126.9, 126.8, 125.9, 123.6, 121.0, 66.6, 64.1, 44.8, 41.5, 31.8, 26.5, 25.6, 23.3, 17.5; IR (neat) 2966, 1605 cm^{-1}. HRMS (EI) m/z calc'd for [C$_{26}$H$_{32}$N$_2$O+Na]$^+$ 411.2412, found 411.2395.
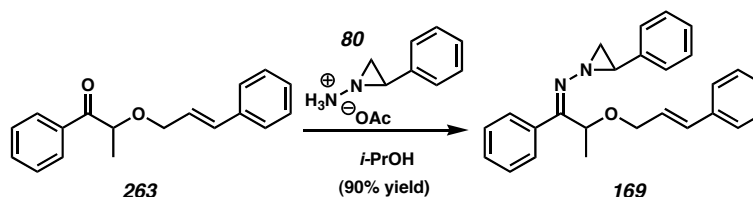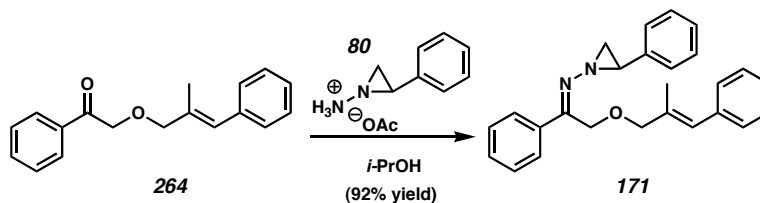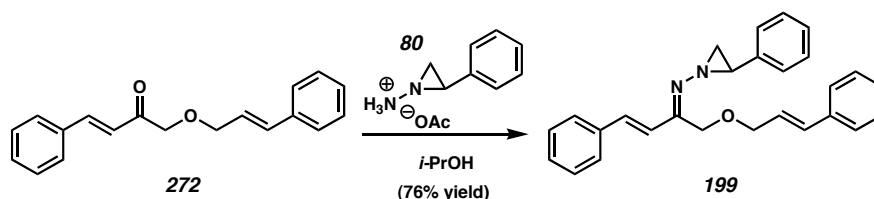

Hydrazone 199. The general procedure outlined above was followed (using 807.8 mg, 2.90 mmol of the corresponding keto-ether **272**) to provide **199** (873.4 mg, 2.21 mmol, 76% yield) as a yellow oil. Flash chromatographic purification (15:1 → 9:1 hexanes:ethyl acetate gradient eluent). R$_F$ 0.29 (9:1 hexanes:ethyl acetate eluent); ^{1}H NMR (300 MHz, CDCl$_3$) δ 7.51 (d, J = 6.9 Hz, 2H), 7.39-7.24 (m, 14H), 6.9 (d, J = 16.5 Hz, 1H), 6.54 (d, J = 15.9 Hz, 1H), 6.20 (dt, J = 6.0, 15.9 Hz, 1H), 4.7 (d, J = 12.6 Hz, 1H), 4.62 (d, J = 12.6 Hz, 1H), 4.07 (d, J = 6.0 Hz, 2H), 5.99 (dd, J = 4.7, 7.4 Hz, 1H), 2.63 (d, J = 7.4 Hz, 1H), 2.46 (d, J = 4.7 Hz, 1H); ^{13}C NMR (75 MHz, CDCl$_3$) δ 166.2, 136.4, 135.5, 133.0, 128.6, 128.5, 128.4, 128.3, 127.6, 127.2, 126.4, 126.1, 125.3, 125.1, 71.5, 64.2, 45.4, 41.9; IR (neat) 3058, 3026, 1622 cm^{-1}. HRMS (EI) m/z calc'd for [C$_{27}$H$_{26}$N$_2$O+Na]$^+$ 417.1943, found 417.1946.
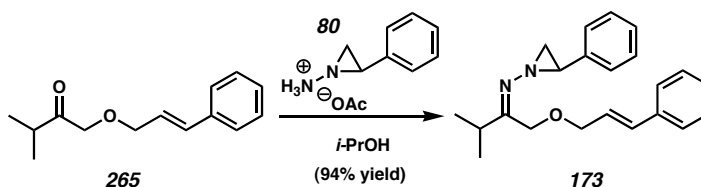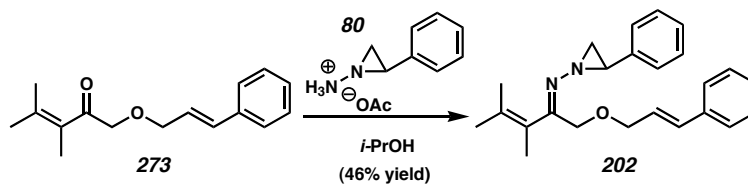
Hydrazone 202. The general procedure outlined above was followed (using

621.2 g, 2.54 mmol of the corresponding keto-ether **273**) to provide **202** (418.4 mg, 1.16

mmol, 46% yield) as a yellow oil. Flash chromatographic purification (15:1 → 9:1

hexanes:ethyl acetate gradient eluent). R_F 0.62 (9:1 hexanes:ethyl acetate eluent); [1]H

NMR (300 MHz, CDCl$_3$) δ 7.38-7.26 (comp.m, 10H), 6.51 (d, J = 15.9, 1H), 6.18 (dt, J

= 6.0, 15.9 Hz, 1H), 4.67 (d, J = 15.4, 1H), 4.52 (d, J = 15.4 Hz, 1H), 4.07 (d, J = 6.0

Hz, 2H), 2.94 (dd, J = 4.4, 7.7 Hz, 1H), 2.52 (d, J = 7.1 Hz, 1H), 2.34 (d, J = 5.0 Hz,

1H), 1.87 (s, 3H), 1.80 (s, 3H), 1.79 (s, 3H); ^{13}C NMR (75 MHz, CDCl$_3$) δ 173.5, 138.6,

136.7, 132.6, 131.6, 128.6, 128.4, 127.8, 127.3, 126.6, 126.2, 126.2, 125.7, 72.0, 67.3,

44.3, 41.2, 22.2, 20.6, 17.7; IR (neat) 3061, 3028, 2987, 1604 cm^{-1}. HRMS (EI) m/z

calc'd for [C$_{24}$H$_{28}$N$_2$O+H][+] 361.2280, found 361.2280.

1.10.4 The Rhodium-Catalyzed Bamford-Stevens Reaction

1.10.4.1 Representative Procedure
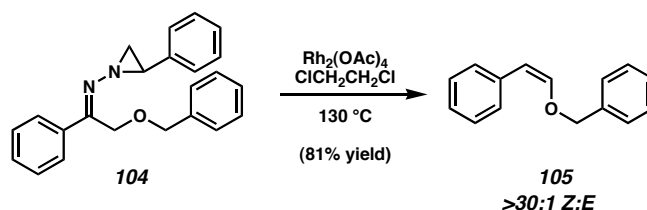
Enolether 105. A flame-dried, sealable schlenk tube (25 mL) was equipped with

magnetic stirbar and charged with Rh$_2$(OAc)$_4$ (2.5 mg, 0.0057 mmol) under stream of

nitrogen. DCE (3 mL) was added via syringe, followed by addition of **104** (101.6 mg,

0.297 mmol). The tube was then sealed under nitrogen and stirred at 130 °C. The

reaction was monitored by TLC (18:1 pentane:ether eluent) and discontinued by removal

from heat after the starting material was consumed (3 h). The crude reaction mixture was

then passed through a pad of silica to remove the catalyst, and the solvent was removed

under reduced pressure. A ¹H NMR spectrum was taken of this crude product to

determine the isomeric ratio, and then the product **105** was purified via flash column

chromatography (25:1 pentane:ether eluent) producing pure Z-enolether (50.2 mg, 0.239

mmol, 81% yield) as a yellow oil. R_F 0.45 (18:1 pentane:Et$_2$O eluent); ¹H NMR (300

MHz, CDCl$_3$) δ 7.72 (d, J = 7.1 Hz, 2H), 7.46-7.35 (comp.m, 7H), 7.24 (q, J = 7.4 Hz,

1H), 6.35 (d, J = 6.9 Hz, 1H), 5.35 (d, J = 6.9 Hz, 1H), 5.05 (s, 2H); ¹³C NMR (75 MHz,

CDCl$_3$) δ 146.1, 137.0, 135.7, 128.1, 128.1, 127.9, 127.1, 125.6, 106.1, 74.8; IR (neat)

3031, 2932, 1651 cm⁻¹. HRMS (EI) m/z calc'd for [C$_{15}$H$_{14}$O]⁺ 210.1045, found

210.1042.

1.10.4.2 Compounds Created by General Procedure
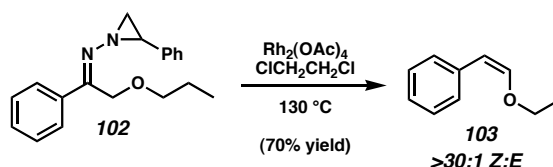
Enolether 103. The general procedure outlined above was followed (using 51.0

mg, 0.173 mmol of the corresponding hydrazone **102**) to provide **103** (19.6 mg, 0.121

mmol, 70% yield) as a yellow oil. Flash chromatographic purification (50:1

pentane:ether eluent). R_F 0.73 (18:1 pentane:ether eluent) to provide the previously reported Z-enolether **103**.[25]
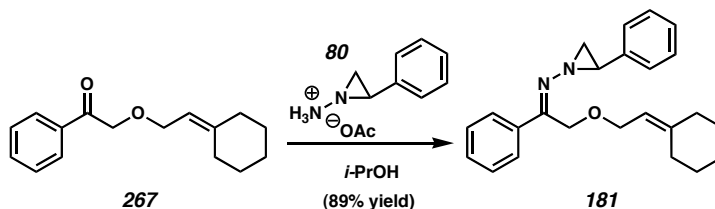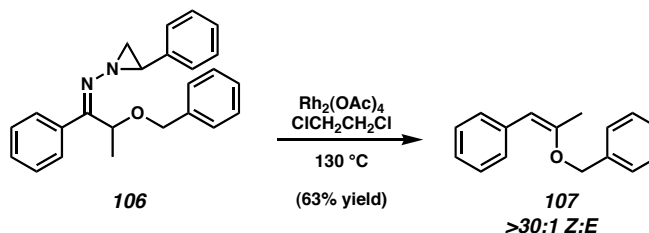

Enolether 107. The general procedure outlined above was followed (using 200.6 mg, 0.561 mmol of the corresponding hydrazone **106**) to provide **107** (83.0 mg, 0.370 mmol, 66% yield) as a yellow oil. Flash chromatographic purification (25:1 pentane:ether eluent). R_F 0.50 (18:1 pentane:ether eluent); ^{1}H NMR (300 MHz, CDCl$_3$) δ 7.66 (d, J = 8.1 Hz, 2H), 7.44-7.27 (comp.m, 6H), 7.16 (t, J = 7.7 Hz, 2H), 5.44 (s, 1H), 5.07 (s, 2H), 2.12 (s, 3H); ^{13}C NMR (75 MHz, CDCl$_3$) δ 152.6, 137.9, 136.7, 128.6, 128.2, 128.1, 127.8, 127.1, 125.4, 107.9, 69.7, 19.7; IR (neat) 3088, 3064, 3029, 2989, 1656 cm^{-1}. HRMS (EI) m/z calc'd for [C$_{16}$H$_{16}$O]+ 224.1201, found 224.1197.
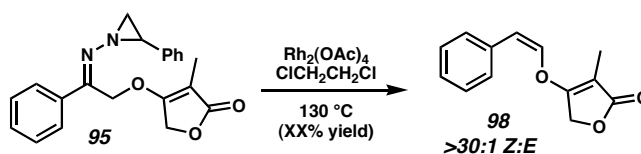
Enolether 98. The general procedure outlined above was followed (using 21.2 mg, 0.0499 mmol of the corresponding hydrazone **95**) to provide **98** (7.6 mg, 0.035 mmol, 70% yield) as a yellow oil. Thin layer chromatographic purification (1% MeOH in CH$_2$Cl$_2$ eluent). R_F 0.30 (1% MeOH in CH$_2$Cl$_2$ eluent); ^{1}H NMR (500 MHz, CDCl$_3$) δ 7.59 (d, J = 7.5 Hz, 2H), 7.39 (t, J = 8.0, 2H), 7.28 (t, J = 7.7 Hz, 1H), 6.62 (d, J = 6.5

Hz, 1H), 5.80 (d, J = 6.5 Hz, 1H), 4.81 (s, 2H), 1.96 (s, 3H); ^{13}C NMR (75 MHz, CDCl$_3$)

δ 174.3, 168.5, 138.0, 133.2, 129.3, 128.8, 128.1, 114.2, 103.0, 65.9, 7.5.

1.10.5 Rhodium-Catalyzed Tandem Bamford-Stevens/Claisen Reaction

1.10.5.1 Representative Procedure for Thermal Conditions
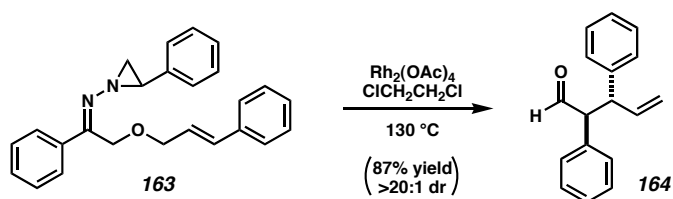
Aldehyde 164. A flame-dried, sealable schlenk tube (25 mL) was equipped with

magnetic stirbar and charged with Rh$_2$(OAc)$_4$ (2.5 mg, 0.0057 mmol) under stream of

nitrogen. DCE (3 mL) was added via syringe, followed by addition of **163** (101.9 mg,

0.277 mmol). The tube was then sealed under nitrogen and stirred at 130 °C. The

reaction was monitored by TLC (18:1 pentane:ether eluent) and discontinued by removal

from heat after the starting material (R$_f$ = 0.15, green by p-anisaldehyde stain) and

Bamford-Stevens intermediate (R$_f$ = 0.2, blue by stain) were consumed (usually 3-5 h).

The crude reaction mixture was then passed through a pad of silica to remove the

catalyst, and the solvent was removed under reduced pressure. A ^{1}H NMR spectrum was

taken of this crude product to determine the diastereomeric ratio, and then the product

was purified via flash column chromatography (25:1 pentane:ether eluent) to give pure

aldehyde **164** (57.1 mg, 0.242 mmol, 87% yield) as a white solid that could be

recrystalized from pentane. mp 101.0-103.5; R$_F$ 0.26 (18:1 pentane:ether eluent); ^{1}H

NMR (300 MHz, CDCl$_3$) δ 9.62 (d, J = 2.4 Hz, 1H), 7.43-7.23 (m, 10H), 5.81 (ddd, J =

2.7, 10.2, 17.1 Hz, 1H), 4.94 (d, J = 9.9 Hz, 1H), 4.87 (d, J = 16.8 Hz, 1H), 4.18 (app.t, J

= 8.1, 1H), 4.04 (dd, J = 3.0, 10.8 Hz, 1H); ^{13}C NMR (75 MHz, CDCl$_3$) δ 198.9, 140.9,

138.1, 134.3, 129.5, 128.9, 128.7, 128.1, 127.7, 126.9, 116.7, 68.9, 50.4; IR (neat) 3060,

3028, 1712 cm^{-1}. HRMS (EI) m/z calc'd for [C$_{17}$H$_{16}$O]$^+$ 236.1201, found 236.1207.

1.10.5.2 Other Examples from the General Thermal Conditions
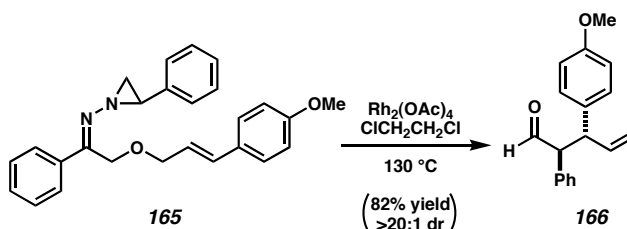
Aldehyde 166. The general procedure outlined above was followed (using 145.9

mg, 0.369 mmol of the corresponding hydrazone **165**) to provide aldehyde **166** (80.6 mg,

0.303 mmol, 82% yield) as a white solid. Flash chromatographic purification (25:1

pentane:ether eluent). R$_F$ 0.15 (18:1 pentane:ether eluent); ^{1}H NMR (300 MHz, CDCl$_3$) δ

9.61 (d, J = 2.8 Hz, 1H), 7.42-7.18 (comp.m, 7H), 6.89 (d, J = 8.2 Hz, 2H), 5.79 (ddd, J

= 7.7, 10.4, 17.0 Hz, 1H), 4.92 (d, J = 10.4 Hz, 1H), 4.85 (d, J = 17.0 Hz, 1H), 4.13 (dd,

J = 7.7, 10.4 Hz, 1H), 3.98 (dd, J = 3.3, 10.4 Hz, 1H), 3.81 (s, 3H); ^{13}C NMR (75 MHz,

CDCl$_3$) δ 199.3, 158.5, 138.6, 138.6, 134.6, 133.1, 129.7, 129.4, 129.1, 127.9, 116.6,

114.3, 64.2, 55.5, 49.8; IR (neat) 2934, 1716 cm^{-1}. HRMS (EI) m/z calc'd for

[C$_{18}$H$_{18}$O$_2$]$^+$ 266.1307, found 266.1312.
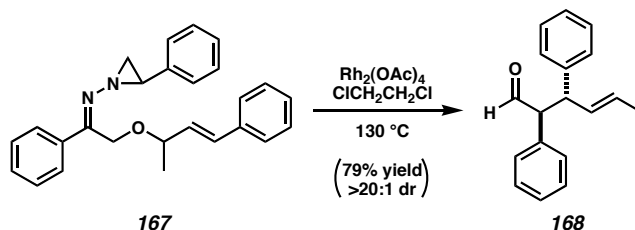
Aldehyde 168. The general procedure outlined above was followed (using 96.9 mg, 0.253 mmol of the corresponding hydrazone **167**) to provide aldehyde **168** (50.1 mg, 0.200 mmol, 79% yield) as a white solid. Flash chromatographic purification (25:1 pentane:ether eluent). Aldehyde **168** could be further purified by recrystalization from pentane. R_F 0.34 (18:1 pentane:ether eluent); ^{1}H NMR (300 MHz, CDCl$_3$) δ 9.60 (d, J = 2.8 Hz, 1H), 7.41-7.20 (comp.m, 10H), 5.46-5.38 (m, 1H), 5.33-5.24 (m, 1H), 4.10 (dd, J = 7.7, 9.9 Hz, 1H), 3.96 (dd, J = 2.9, 9.9 Hz, 1H), 1.49 (d, J = 2.9 Hz, 3H); ^{13}C NMR (75 MHz, CDCl$_3$) δ 199.3, 141.8, 134.5, 130.7, 129.5, 128.7, 128.6, 128.0, 127.5, 126.7, 64.2, 49.5, 18.0; IR (neat) 3062, 3024, 2956, 1711 cm^{-1}. HRMS (EI) m/z calc'd for [C$_{18}$H$_{18}$O]$^+$ 250.1358, found 250.1361.
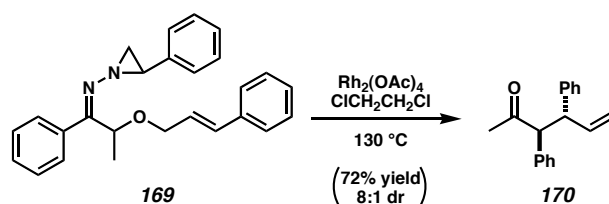
Aldehyde 170. The general procedure outlined above was followed (using 46.9 mg, 0.123 mmol of the corresponding hydrazone **169**) to provide aldehyde **170** (22.2 mg, 0.089 mmol, 72% yield) as a pale yellow oil. Flash chromatographic purification (25:1 pentane:ether eluent). R_F 0.28 (18:1 pentane:ether eluent); ^{1}H NMR (300 MHz, CDCl$_3$) δ 7.40-7.19 (comp.m, 10H), 5.71 (ddd, J = 7.1, 10.3, 17.1 Hz, 1H), 4.83 (d, J = 10.2 Hz,

1H), 4.74 (d, J = 17.3 Hz, 1H), 4.22-4.11 (comp.m, 2H), 1.94 (s, 3H); ^{13}C NMR (75

MHz, CDCl$_3$) δ 206.9, 142.3, 139.1, 136.6, 129.2, 128.9, 128.7, 128.1, 127.7, 126.7,

116.5, 64.5, 52.1, 30.8; IR (neat) 3028, 1707 cm^{-1}. HRMS (EI) m/z calc'd for

[C$_{18}$H$_{18}$O+NH$_4$]$^+$ 268.1702, found 268.1700.

Aldehyde 172. The general procedure outlined above was followed (using 103.4

mg, 0.270 mmol of the corresponding hydrazone **171**) to provide aldehyde **172** (51.5 mg,

0.206 mmol, 76% yield) as a yellow oil. Flash chromatographic purification (25:1

pentane:ether eluent). R$_F$ 0.22 (18:1 pentane:ether eluent); ^{1}H NMR (300 MHz, CDCl$_3$) δ

9.53 (d, J = 3.3 Hz, 1H), 7.42-7.27 (comp.m, 10H), 4.83 (s, 1H), 4.69 (s, 1H), 4.29 (dd, J

= 3.3, 12.1 Hz, 1H), 4.20 (d, J = 12.1 Hz, 1H), 1.54 (s, 3H); ^{13}C NMR (75 MHz, CDCl$_3$)

δ 198.5, 143.9, 140.0, 134.5, 129.0, 128.9, 128.5, 128.0, 127.6, 127.0, 113.3, 61.1, 52.9,

20.6; IR (neat) 3066, 3029, 2959, 1717 cm^{-1}. HRMS (EI) m/z calc'd for [C$_{18}$H$_{18}$O]$^+$

250.1358, found 250.1360.

Aldehyde 180. The general procedure outlined above was followed (using 101.0 mg, 0.315 mmol of the corresponding hydrazone **179**) to provide aldehyde **180** (41.9 mg, 0.223 mmol, 71% yield) as a yellow oil. Flash chromatographic purification (25:1 pentane:ether eluent). R_F 0.35 (18:1 pentane:ether eluent); ^{1}H NMR (300 MHz, CDCl$_3$) δ 9.93 (d, J = 3.3 Hz, 1H), 7.38-7.20 (comp.m, 5H), 6.02 (dd, J = 11.0, 17.6 Hz, 1H), 5.10 (d, J = 10.6 Hz, 1H), 5.00 (d, J = 17.6 Hz, 1H), 3.36 (d, J = 3.7 Hz, 1H), 1.14 (s, 3H), 1.07 (s, 3H); ^{13}C NMR (75 MHz, CDCl$_3$) δ 201.8, 144.5, 134.5, 130.3, 128.1, 127.3, 113.1, 67.6, 40.0, 26.5, 24.8; IR (neat) 3085, 3029, 2966, 1722 cm^{-1}. HRMS (EI) m/z calc'd for [C$_{13}$H$_{16}$O]$^+$ 188.1201, found 188.1197.
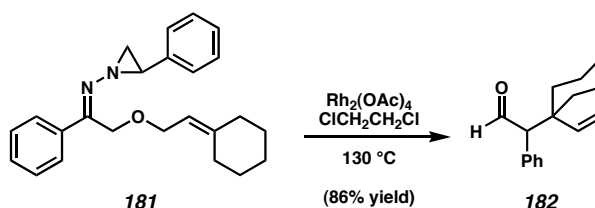
Aldehyde 182. The general procedure outlined above was followed (using 98.9 mg, 0.274 mmol of the corresponding hydrazone **181**) to provide aldehyde **182** (53.9 mg, 0.236 mmol, 86% yield) as a yellow oil. Flash chromatographic purification (25:1 pentane:ether eluent). R_F 0.54 (18:1 pentane:ether eluent); ^{1}H NMR (300 MHz, CDCl$_3$) δ 9.94 (d, J = 4.1 Hz, 1H), 7.34-7.26 (comp.m, 5H), 5.78 (dd, J = 11.0, 17.9 Hz, 1H), 5.37 (d, J = 11.0 Hz, 1H), 5.02 (d, J = 18.1 Hz, 1H), 3.38 (d, J = 3.9 Hz, 1H), 1.91 (s, 1H),

1.59-1.27 (comp.m, 9H); ^{13}C NMR (75 MHz, CDCl$_3$) δ 202.4, 141.7, 134.2, 130.3, 128.0,

127.2, 116.6, 67.8, 43.2, 39.7, 34.3, 26.1, 21.8, 21.7; IR (neat) 3030, 2932, 1720 cm^{-1}.

HRMS (EI) m/z calc'd for [C$_{16}$H$_{20}$O]$^+$ 228.1514, found 228.1514.

1.10.5.3 Representative Procedure for NMP as Solvent (Table 1.5.1, entry 6)
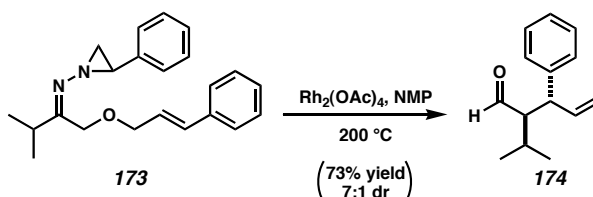
Aldehyde 174. A flame-dried, sealable schlenk tube (25 mL) was equipped with

magnetic stirbar and charged with Rh$_2$(OAc)$_4$ (1.4 mg, 0.0032 mmol) under stream of

nitrogen. NMP (3 mL) was added via syringe and followed by addition of **173** (102.1

mg, 0.305 mmol). The tube was then sealed under nitrogen and stirred at 200 °C. The

reaction was monitored by TLC (18:1 pentane:ether eluent) and discontinued by removal

from heat after the starting material and Bamford-Stevens intermediate were consumed (1

h). The crude reaction mixture was purified by direct flash column chromatography of

the reaction mixture (25:1 pentane:ether eluent) to give pure aldehyde **174** (45.3 mg,

0.224 mmol, 73% yield) as a pale yellow oil. R$_F$ 0.28 (18:1 pentane:ether eluent); ^{1}H

NMR (300 MHz, CDCl$_3$) δ 9.54 (d, *J* = 4.4 Hz, 1H), 7.35-7.17 (comp.m, 5H), 5.90 (ddd,

J = 9.3, 10.2, 17.0 Hz, 1H), 5.17 (d, *J* = 17.0 Hz, 1H), 5.10 (d, *J* = 10.2 Hz, 1H), 3.81

(dd, *J* = 9.9, 9.9 Hz, 1H), 2.65 (ddd, *J* = 4.4, 4.4, 10.7 Hz, 1H), 2.16 (d sept., *J* = 4.1, 7.1

Hz, 1H), 1.11 (d, *J* = 6.9 Hz, 3H), 1.03 (d, *J* = 6.9 Hz, 3H); ^{13}C NMR (75 MHz, CDCl$_3$) δ

205.3, 141.5, 139.5, 128.9, 128.1, 126.9, 116.1, 60.9, 49.1, 28.5, 22.0, 17.2; IR (neat)

3062, 3029, 2962, 1722 cm^{-1}. HRMS (EI) m/z calc'd for the acetal form [C$_{14}$H$_{20}$O$_2$-H]$^+$ 219.1385, found 219.1385.

1.10.5.4 Representative Procedure For Photolytic Conditions
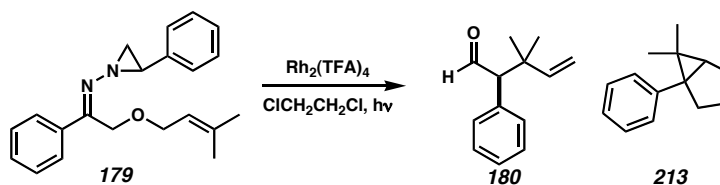
Aldehyde 180. A flame-dried quartz tube (25 mL) was equipped with magnetic stirbar and charged with Rh$_2$(TFA)$_4$ (4.2 mg, 0.0064 mmol). **179** (99.5 mg, 0.311 mmol) was added via syringe, followed by addition of DCE (1.6 mL). The tube was then sealed with a rubber septa, which was wrapped in foil to prevent degradation, and placed in the photoreactor. Note that photobox interior temperature often reached 40 °C during photolysis. The reaction was monitored by TLC (18:1 pentane : ether eluent) and discontinued after the starting material (R$_f$ = .17, green by *p*-anisaldehyde stain) was consumed (usually 6-11 h). The crude reaction mixture was then passed through a pad of silica to remove the catalyst, and the solvent was removed under reduced pressure. A ^{1}H NMR spectrum was taken of this crude product to determine the product ratio, and then the product was purified via flash column chromatography (44:1 pentane:ether eluent) to give aldehyde **180** (12.8 mg, 0.0687 mmol, 22% yield, data presented above) or cyclopropane **213** (16.2 mg, 0.0870 mmol, 28% yield); ^{1}H NMR (300 MHz, CDCl$_3$) δ 7.34-7.19 (comp.m, 5H), 4.17-4.12 (comp.m, 2H), 3.99 (d, *J* = 8.8 Hz, 1H), 3.87 (d, *J* = 8.4 Hz, 1H), 1.72 (d, *J* = 3.7 Hz, 1H), 1.26 (s, 3H), 0.84 (s, 3H); ^{13}C NMR (75 MHz,

CDCl$_3$) δ 139.0, 129.4, 128.3, 126.6, 73.8, 69.2, 43.1, 34.2, 29.7, 24.3, 14.2; IR (neat) 3429, 2917, 2856 cm^{-1}.

1.10.5.5 Representative Procedure for the Me$_2$AlCl-Mediated Claisen Rearrangement (Table 1.5.1, entries 7 and 9)
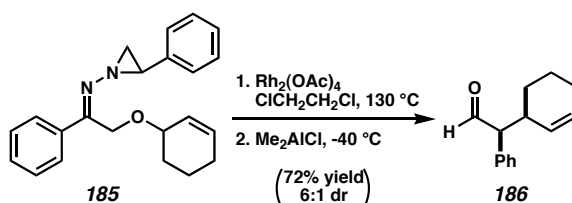
**Aldehyde 186.** A flame-dried, sealable schlenk tube (25 mL) was equipped with magnetic stirbar and charged with Rh$_2$(OAc)$_4$ (1.9 mg, 0.0043 mmol) under stream of nitrogen. DCE (4.5 mL) was added via syringe, followed by addition of **185** (153.1 mg, 0.461 mmol). The tube was then sealed under nitrogen and stirred at 130 °C. The reaction was continued until the starting material had reacted (typically 2-3 h), and then CH$_2$Cl$_2$ (1 mL) was added to suppress freezing, and the mixture was cooled to –40 °C. Me$_2$AlCl in hexanes (480 μl of a 1.0 M solution, 0.480 mmol) was then added over 0.5 min via syringe. TLC analysis (18:1 pentane:ether eluent) usually showed the reaction to be complete within 2 min. 5% HCl (aq) (10 mL) was then added dropwise to quench the excess reagent and dissolve the aluminates. The layers were separated, and the aqueous layer was extracted three times with Et$_2$O (5 mL). The organic layers were combined and dried over MgSO$_4$. After removal of solvent under reduced pressure, the diastereomeric ratio was determined by ^{1}H NMR. Flash column chromatographic purification of the crude mixture (25:1 pentane:ether eluent) provided pure aldehyde **186** (66.5 mg, 0.332

mmol, 72% yield) as a yellow oil. R_F 0.32 (18:1 pentane:ether eluent); ^{1}H NMR (300 MHz, CDCl$_3$) δ 9.77 (d, J = 2.8 Hz, 1H), 7.41-7.18 (comp.m, 5H), 5.83-5.69 (comp.m, 2H), 3.43 (dd, J = 2.8, 9.9 Hz, 1H), 2.97-2.89 (m, 1H), 2.00-1.97 (m, 2H), 1.70-1.44 (comp.m, 3H), 1.18-1.07 (m, 1H); ^{13}C NMR (75 MHz, CDCl$_3$) δ 200.6, 134.9, 129.4, 129.3, 129.1, 128.6, 127.7, 64.8, 35.8, 26.6, 25.5, 21.2; IR (neat) 3426, 3062, 3027, 1723 cm^{-1}. HRMS (EI) m/z calc'd for [C$_{14}$H$_{16}$O]$^+$ 200.1201, found 200.1203.

1.10.5.6 Other Examples of General Me$_2$AlCl Procedure
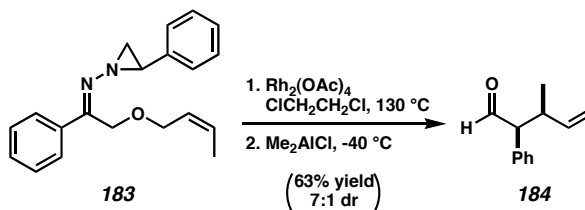
Aldehyde 184. The general procedure outlined above was followed (using 150.3 mg, 0.490 mmol of the corresponding hydrazone **183**) to provide aldehyde **184** (53.8 mg, 0.309 mmol, 63% yield) as a yellow oil. Flash chromatographic purification (25:1 pentane:ether eluent). R_F 0.33 (18:1 pentane:ether eluent); ^{1}H NMR (300 MHz, CDCl$_3$) δ 9.70 (d, J = 2.8 Hz, 1H), 7.41-7.19 (comp.m, 5H), 5.81 (ddd, J = 8.3, 10.4, 17.6 Hz, 1H), 5.13 (d, J = 17.0 Hz, 1H), 5.08 (d, J = 10.1 Hz, 1H), 3.39 (dd, J = 3.3, 9.34 Hz, 1H), 3.00 (m, 1H), 0.89 (d, J = 6.6 Hz, 3H); ^{13}C NMR (75 MHz, CDCl$_3$) δ 200.5, 141.2, 134.9, 129.4, 129.0, 127.7, 115.3, 64.7, 38.9, 17.9; IR (neat) 3082, 3030, 2976, 1725 cm^{-1}. HRMS (EI) m/z calc'd for [C$_{12}$H$_{14}$O+NH$_4$]$^+$ 192.1389, found 192.1395.

1.10.6 Triplet Cascade Reactions

1.10.6.1 Representative Procedure for the DIBAL-Mediated Bamford-Stevens/Claisen Reductive Rearrangement (Scheme 1.6.2)
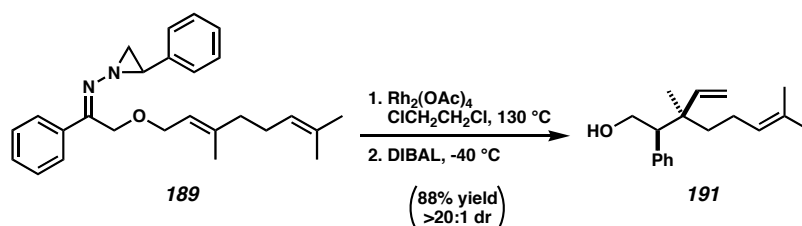
**Alcohol 191.** A flame-dried, sealable schlenk tube (25 mL) was equipped with magnetic stirbar and charged with Rh$_2$(OAc)$_4$ (1.9 mg, 0.0043 mmol) under stream of nitrogen. DCE (4 mL) was added via syringe, followed by addition of **189** (151.9 mg, 0.391 mmol). The tube was then sealed under nitrogen and stirred at 130 °C. The reaction was continued until the starting material had reacted (typically 2 h), and then CH$_2$Cl$_2$ (1 mL) was added to suppress freezing, and the mixture was cooled to –40 °C. DIBAL in hexanes (800 µl of a 1.0 M solution in hexanes, 0.800 mmol) was then added over 0.5 min via syringe. TLC analysis (3:1 hexanes:ethyl acetate eluent) usually showed the reaction to be complete within 20 min for aromatic substituted allyl ethers. Aliphatic substituted allyl ethers were allowed to warm to room temperature in order to completely react. 5% HCl (aq) (15 mL) was then added dropwise to quench the excess reagent and dissolve the aluminates. The layers were separated, and the aqueous layer was extracted three times with Et$_2$O (5 mL). The organic layers were then combined and dried over MgSO$_4$. After removal of solvent under reduced pressure, the diastereomeric ratio was determined by ^{1}H NMR. Flash column chromatographic purification of the crude

mixture (9:1 hexanes:ethyl acetate eluent) furnished pure alcohol **191** (88.4 mg, 0.344

mmol, 88% yield). R_F 0.67 (3:1 hexanes:ethyl acetate eluent); ^{1}H NMR (300 MHz,

CDCl$_3$) δ 7.35-7.21 (comp.m, 5H), 5.79 (dd, J = 11.0, 17.6 Hz, 1H), 5.08 (d, J = 10.7 Hz,

1H), 4.98 (t, J = 7.2 Hz, 1H), 4.90 (d, J = 17.6 Hz, 1H), 4.06-3.91 (comp.m, 2H), 2.81

(dd, J = 5.0, 10.2 Hz, 1H), 1.97-1.73 (m, 2H), 1.64 (s, 3H), 1.54 (s, 3H), 1.35-1.15

(comp.m, 2H), 1.10 (s, 3H); ^{13}C NMR (75 MHz, CDCl$_3$) δ 143.8, 139.1, 131.1, 130.0,

128.0, 126.8, 124.5, 113.3, 62.9, 57.9, 41.9, 39.0, 25.8, 22.6, 21.3, 17.7; IR (neat) 3561,

3377, 3061, 2969 cm^{-1}.

1.10.6.2 Other Examples Using the DIBAL Procedure

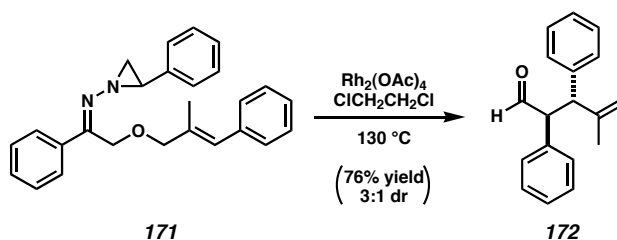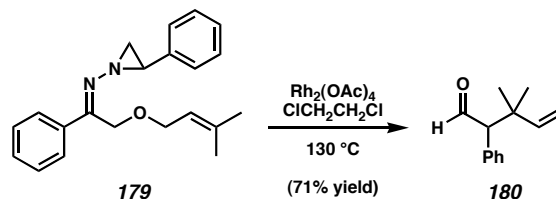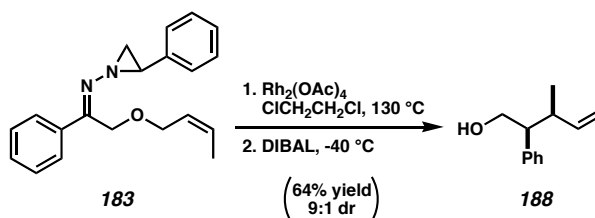**Alcohol 188.** The general procedure outlined above was followed (using 49.6

mg, 0.325 mmol of the corresponding hydrazone **183**) to provide alcohol **188** (36.7 mg,

0.208 mmol, 64% yield) as a pale yellow oil. Flash chromatographic purification (9:1

hexanes:ethyl acetate eluent). R_F 0.15 (9:1 hexanes:ethyl acetate eluent); ^{1}H NMR (300

MHz, CDCl$_3$) δ 7.38-7.19 (comp.m, 5H), 5.79 (ddd, J = 8.5, 9.9, 17.0 Hz, 1H), 5.12 (d, J

= 17.0 Hz, 1H), 5.04 (d, J = 10.2 Hz, 1H), 3.92-3.86 (m, 1H), 3.77-3.71 (m, 1H), 2.64-

2.56 (m, 1H), 2.50-2.44 (m, 1H), 0.82 (d, J = 3.6 Hz, 3H); ^{13}C NMR (75 MHz, CDCl$_3$) δ

142.9, 141.1, 128.5, 128.5, 126.7, 14.3, 66.1, 54.0, 41.3, 19.4; IR (neat) 3559, 3384,

3084, 2970 cm^{-1}. HRMS (EI) m/z calc'd for $[C_{12}H_{16}O]^+$ 176.1201, found 176.1204.
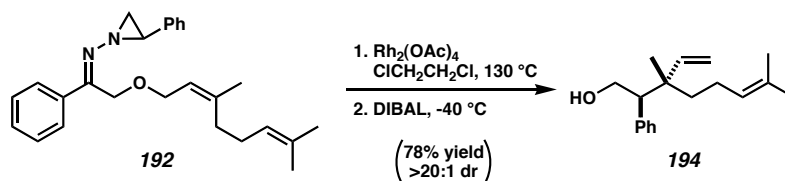
Alcohol 194. The general procedure outlined above was followed (using 99.3

mg, 0.256 mmol of the corresponding hydrazone **192**) to provide alcohol **194** (51.6 mg,

0.200 mmol, 78% yield) as a yellow oil. Flash chromatographic purification (9:1

hexanes:ethyl acetate eluent). R_F 0.14 (9:1 hexanes:ethyl acetate eluent); ^{1}H NMR (300

MHz, CDCl$_3$) δ 7.31-7.23 (m, 5H), 5.82 (dd, J = 11.1, 6.6 Hz, 1H), 5.16 (dd, J = 1.2,

11.1 Hz, 1H), 5.03-4.93 (m, 2H), 4.00-3.89 (m, 2H), 2.81 (dd, J = 5.1, 4.8 Hz, 1H), 1.84

(m, 2H), 1.65 (s, 3H), 1.55 (s, 3H), 0.94 (s, 3H); ^{13}C NMR (75 MHz, CDCl$_3$) δ 145.2,

139.1, 131.1, 129.9, 128.0, 124.5, 113.6, 63.1, 57.1, 42.4, 40.0, 25.7, 22.5, 18.5, 17.7; IR

(neat) 3383, 2969 cm^{-1}.

1.10.6.3 Representative Procedure for the Me₂AlCl-Mediated Bamford-Stevens/Claisen/Carbonyl-ene Rearrangement (Scheme 1.6.3)
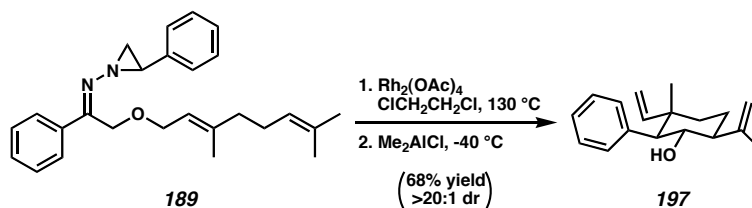
Alcohol 197. A flame-dried, sealable schlenk tube (25 mL) was equipped with magnetic stirbar and charged with $Rh_2(OAc)_4$ (1.9 mg, 0.0043 mmol) under stream of nitrogen. DCE (4 mL) was added via syringe, followed by addition of **189** (150.5 mg, 0.387 mmol). The tube was then sealed under nitrogen and stirred at 130 °C. The reaction was continued until the starting material had reacted (typically 2 h), and then 1 mL of CH_2Cl_2 was added to suppress freezing, and the mixture was cooled to –40 °C. Me_2AlCl in hexanes (400 μl of a 1.0 M solution, 0.400 mmol) was then added at a moderate rate via syringe. TLC analysis (9:1 hexanes:ethyl acetate eluent) usually showed the reaction to be complete within 2 min. 5% HCl (aq) (15 mL) was then added dropwise to quench the excess reagent and dissolve the aluminates. The layers were separated, and the aqueous layer was extracted three times with Et_2O (5 mL). The organic layers were then combined and dried over $MgSO_4$. After removal of solvent under reduced pressure, the diastereomeric ratio was determined by ¹H NMR. Flash column chromatographic purification of **197** (9:1 hexanes:ethyl acetate eluent) yielded pure alcohol (67.5 mg. 0.263 mmol, 68% yield) as a colorless oil. R_F 0.28 (9:1 hexanes:ethyl acetate eluent); ¹H NMR (300 MHz, CDCl₃) δ 7.33-7.18 (comp.m, 5H),

5.69 (dd, J = 11.0, 17.6 Hz, 1H), 4.93 (s, 2H), 4.81 (d, J = 11.0 Hz, 1H), 4.70 (d, J =

18.1 Hz, 1H), 4.15 (t, J = 10.4 Hz, 1H), 2.57 (d, J = 11.0 Hz, 1H), 2.62-2.18 (m, 1H),

1.85-1.54 (comp.m, 4H), 1.84 (s, 3H), 1.02 (s, 3H); ^{13}C NMR (75 MHz, CDCl$_3$) δ 148.2,

146.9, 138.8, 130.1, 127.9, 126.8, 112.8, 111.0, 69.5, 59.6, 54.3, 42.0, 38.6, 26.4, 19.8,

18.3; IR (neat) 3583, 3461, 3082, 3029, 2969 cm^{-1}.   HRMS (EI) m/z calc'd for

[C$_{18}$H$_{24}$O+H]$^+$ 257.1905, found 257.1905.

1.10.6.4 Other Examples Using the General Me$_2$AlCl Procedure
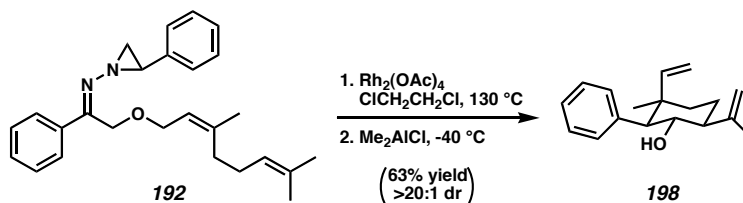
Alcohol 198. The general procedure outlined above was followed (using 102.6

mg, 0.254 mmol of the corresponding hydrazone **192**) to provide **198** (41.0 mg, 0.160

mmol, 63% yield) as a colorless oil.   Flash chromatographic purification (9:1

hexanes:ethyl acetate eluent). R$_F$ 0.27 (9:1 hexanes:ethyl acetate eluent); ^{1}H NMR (300

MHz, CDCl$_3$) δ 7.34-7.21 (comp.m, 5H), 6.18 (dd, J = 11.0, 17.6 Hz, 1H), 5.07 (d, J =

11.0 Hz, 1H), 4.92 (s, 1H), 4.91 (s, 1H), 4.82 (d, J = 17.6 Hz, 1H), 4.05 (t, J = 10.4 Hz,

1H), 2.55 (d, J = 10.7 Hz, 1H), 2.30-2.21 (m, 1H), 1.89-1.79 (m, 1H), 1.82 (s, 3H), 1.68-

1.53 (comp.m, 3H), 0.90 (s, 3H); ^{13}C NMR (75 MHz, CDCl$_3$) δ 147.0, 141.0, 138.5,

130.2, 127.8, 126.8, 114.1, 112.7, 69.7, 61.9, 54.5, 42.0, 39.4, 28.3, 26.3, 19.7; IR (neat)

3564, 3083, 3029 cm^{-1}. HRMS (EI) m/z calc'd for [C$_{18}$H$_{24}$O+H]$^+$ 257.1905, found

257.1907.

1.10.6.5 Representative Procedure for the Rhodium-Catalyzed Bamford-Stevens/Claisen/Cope Rearrangement (Scheme 1.6.4)
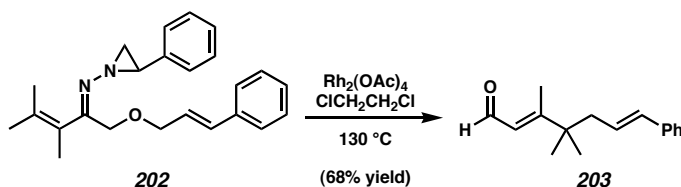
Aldehyde 203. A flame-dried, sealable schlenk tube (25 mL) was equipped with

magnetic stirbar and charged with Rh$_2$(OAc)$_4$ (1.9 mg, 0.0043 mmol) under stream of

nitrogen. DCE (4 mL) was added via syringe, followed by addition of **202** (73.0 mg,

0.203 mmol). The tube was then sealed under nitrogen and stirred at 130 °C. The

reaction was monitored by TLC (9:1 hexanes:ethyl acetate eluent) and discontinued by

removal from heat after the starting material and intermediates were transformed to leave

one product visible by TLC (9:1 hexanes:ethyl acetate eluent, 3-8 h reaction time). The

crude reaction mixture was then passed through a pad of silica to remove the catalyst, and

the solvent was removed under reduced pressure. A ^{1}H NMR spectrum was taken of this

crude product to determine the diastereomeric ratio, and then the crude mixture was

purified via flash column chromatography (9:1 hexanes:ethyl acetate eluent) to yield

aldehyde **203** as an oil (31.5 mg, 0.138 mmol, 68% yield). R$_F$ 0.23 (9:1 hexanes:ethyl

acetate eluent); ^{1}H NMR (300 MHz, CDCl$_3$) δ 10.08 (d, J = 8.0 Hz, 1H), 7.34-7.21

(comp.m, 5H), 6.4 (d, J = 15.7 Hz, 1H), 6.07-5.95 (comp.m, 2H), 2.38 (d, J = 7.4 Hz,

2H), 2.22 (s, 3H), 1.18 (s, 6H); ^{13}C NMR (75 MHz, CDCl$_3$) δ 192.3, 169.2, 137.3, 132.9, 128.6, 127.3, 126.2, 126.1, 125.8, 44.3, 41.7, 26.7, 14.1; IR (neat) 3026, 2969, 1669 cm^{-1}. HRMS (EI) m/z calc'd for [C$_{16}$H$_{20}$O+H]$^+$ 229.1592, found 229.1588.

1.10.6.6 Other Examples Using General Procedure
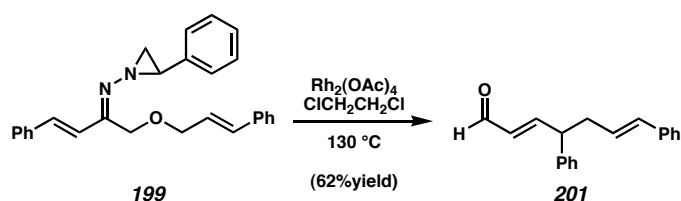
Aldehyde 201. The general procedure outlined above was followed (using 47.8 mg, 0.121 mmol of the corresponding hydrazone **199**) to provide aldehyde **201** (19.7 mg, 0.075 mmol, 62% yield) as a yellow oil. Flash chromatographic purification (9:1 hexanes:ethyl acetate eluent). R$_F$ 0.24 (9:1 hexanes:ethyl acetate eluent); ^{1}H NMR (300 MHz, CDCl$_3$) δ 9.56 (d, J = 7.7 Hz, 1H), 7.41-7.22 (comp.m, 10H), 7.02 (dd, J = 7.2, 15.7 Hz, 1H), 6.46 (d, J = 15.7 Hz, 1H), 6.19-6.05 (comp.m, 2H), 3.74 (dt, J = 7.4, 7.4 Hz, 1H), 2.78 (dd, J = 7.4, 7.4 Hz, 2H); ^{13}C NMR (75 MHz, CDCl$_3$) δ 193.9, 160.0, 140.9, 137.2, 132.6, 132.4, 129.0, 128.6, 127.9, 127.4, 127.4, 126.7, 126.2, 49.2, 28.5; IR (neat) 3082, 3059, 3027, 2924, 1689 cm^{-1}. HRMS (EI) m/z calc'd for [C$_{19}$H$_{18}$O]$^+$ 262.1358, found 262.1359.

1.10.7 Elucidations and Correlations to Confirm Relative Stereochemistry

1.10.7.1 Enolether 105: Coupling Constants

Enolether **105** was assigned the (Z) stereochemistry based on the coupling constants of the vinyl hydrogens.

1.10.7.2 Enolether 103: Coupling Constants

Enolether **103** was assigned the (Z) stereochemistry based on comparison to the reported data for the *E*- and *Z*-isomers.

1.10.7.3 Enolether 107: nOe Interactions

Enolether **107** was assigned the (Z) stereochemistry based on a 1.8% nOe interaction between the vinyl methyl and the vinyl hydrogen.
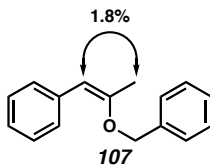
1.10.7.4 Enolether 98: Coupling Constants

Enolether **98** was assigned the (Z) stereochemistry based on the coupling constants of the vinyl hydrogens.

1.10.7.5 Aldehyde 164: Chemical Correlation by Conversion to Ester 204
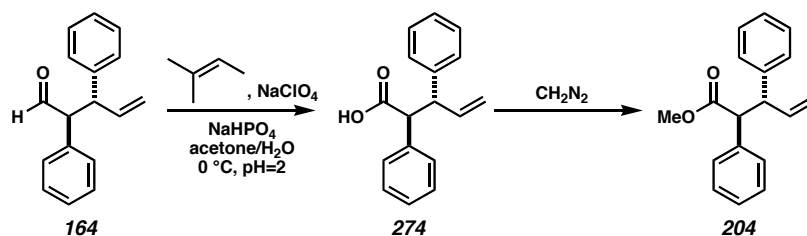
Ester 204. To a flask (100 mL) containing aldehyde **164** (98.4 mg, 0.416 mmol)

and equipped with a magnetic stirbar was added acetone (20 mL) and $NaHPO_4$ buffer (10

mL saturated H_2O solution) adjusted to pH 2 by addition of HCl (concd). This mixture

was cooled to 0 °C, and 2-methyl-2-butene (650 µl, 6.13 mmol) was added.

Immediately, a solution of $NaClO_4$ (93.6 mg, 0.827 mmol) in H_2O (10 mL) was added in

one portion. TLC analysis (R_F 0.29, 3:1 hexanes:ethyl acetate eluent, CAM stain)

showed complete conversion to the acid within 1 min. A 1:1 mixture of $CHCl_3$:H_2O (40

mL) was added, the layers were separated, and the aqueous phase was extracted three

times with $CHCl_3$ (4 mL). The combined organic portions were dried over Na_2SO_4, and

the solvent was removed under reduced pressure to leave an amorphous white solid. This

solid was purified by flash column chromatography (9:1 hexanes:ethyl acetate with 1%

AcOH eluent) to yield the acid **274** (99.8 mg, 0.340 mmol, 95% yield) as a white solid.

Acid **274** (12.1 mg, 0.048 mmol) was then dissolved in Et_2O at 0 °C in a scratch-free

flask (50 mL) equipped with a new, teflon-coated magnetic stirbar, and treated carefully

with a solution of CH_2N_2 in Et_2O (0.2 *M*, 5 mL). Complete conversion was seen by TLC

(3:1 hexanes:ethyl acetate eluent, *p*-anisaldehyde staining), and AcOH was added

dropwise until the yellow color in the reaction mixture was quenched. The solvent was

then removed under reduced pressure to yield pure ester **204** (12.8 mg, 0.048 mmol,

100% yield) as a colorless oil. The spectral data for **204** exactly matched that reported in the literaure.[26] R_F 0.64 (3:1 hexanes:ethyl acetate eluent).

1.10.7.6 Ketone 170: Chemical Correlation by Independent Synthesis from Aldehyde 164
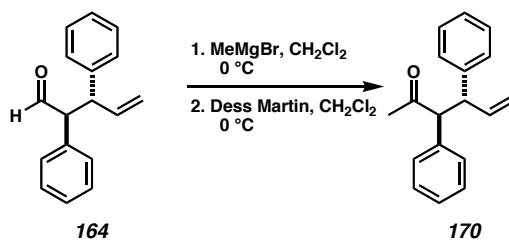
Ketone 170. A flame-dried flask (15 mL) equipped with a magnetic stirbar was charged with aldehyde **164** (52.0 mg, 0.220 mmol) and Et_2O (2 mL). When this solution had been cooled to 0 °C, a solution of MeMgBr (3.0 M in THF, 100 μl, 0.300 mmol) was added via syringe. TLC analysis showed immediate reaction, and H_2O (4 mL) was added in order to quench the reaction mixture. Et_2O (3 mL) was then added, and the layers were separated. The H_2O layer was washed three times with Et_2O (3 mL), the combined organic layers were dried over $MgSO_4$, and the solvent was then removed under reduced pressure to afford the secondary alcohol (R_F 0.23, 3:1 hexanes:ethyl acetate eluent). The secondary alcohol was then dissolved in CH_2Cl_2 (1.5 mL), and Dess Martin periodinane (143.9 mg, 0.339 mmol) was added to the resulting solution. Ketone **170** was immediately formed, so the reaction was quenched by the addition of a 1:1 solution of saturated $NaHCO_3$ (aq) and saturated $Na_2S_2O_3$ (aq) (2 mL). This mixture was extracted three times with CH_2Cl_2 (3 mL), the combined organic layers were dried over $MgSO_4$,

and the solvent was removed under reduced pressure. The ketone was then purified by flash column chromatography (15:1 hexanes:ethyl acetate) to yield pure ketone **170** (47.6 mg, 0.190 mmol, 86% yield for two steps) with spectroscopic data identical to that observed for Bamford-Stevens/Claisen derived ketone. R_F 0.34 (3:1 hexanes:ethyl acetate eluent).

1.10.7.7 Aldehyde 168: Chemical Correlation to Aldehyde 164

Aldehyde 164. A flask (15 mL), equipped with a magnetic stirbar, was charged with diasteroeomerically pure aldehyde **168** (23.7 mg, 0.094 mmol) and a 1:1 mixture of CH_2Cl_2 and MeOH (2 mL). To this solution was added $NaBH_4$ (5.6 mg, 0.147 mmol) in one portion. TLC analysis (R_F 0.26, 3:1 hexanes:ethyl acetate eluent) showed immediate completion. CH_2Cl_2 (2 mL) and H_2O (4 mL) were then added, the layers were separated, and the aqueous phase was extracted three times with CH_2Cl_2 (2 mL). The combined organic layers were dried over $MgSO_4$, and the solvent was removed under reduced pressure. The crude alcohol product (23.5 mg, 0.093 mmol) was then dissolved in THF in a flask (15 mL), which was subsequently charged with imidazole (24.3 mg, 0.357 mmol) and *tert*-butyl-dimethylsilyl chloride (48.8 mg, 0.324 mmol). This solution was heated to reflux for 6.5 hr, then cooled when TLC analysis (R_F 0.56, 15:1 hexanes:ethyl acetate eluent) showed completion. After addition of H_2O (5 mL) and Et_2O (3 mL), the

layers were separated, and the aqueous phase was extracted with Et_2O (3 x 3 mL). The combined organic phases were dried over $MgSO_4$, and the solvent was removed under reduced pressure. This crude product was subjected to flash chromatographic purification (50:1 hexanes:ethyl acetate eluent) to furnish the silyl ether as a clear oil. This oil (33.4 mg, 0.091 mmol) was transferred to a vial (20 mL) equipped with magnetic stirbar and diluted with THF (1.5 mL) and H_2O (0.5 mL). NMO (35.0 mg, 0.299 mmol) was added, followed by OsO_4 (5 mg, 0.020 mmol). The solution was stirred at room temperature for 7 hr, when complete conversion was observed by TLC analysis (R_F 0.66, 1:1 hexanes:ethyl acetate eluent). The reaction mixture was quenched by addition of saturated aq $Na_2S_2O_4$ (4 mL) and Et_2O (2 mL). The layers were separated, and the aqueous phase was extracted with Et_2O (5 x 2 mL). The combined organic phases were dried over $MgSO_4$, and the solvent was removed under reduced pressure. This crude product was subjected to flash chromatographic purification (5:1 hexanes:ethyl acetate eluent) to furnish the diol as a clear oil. This diol (17.0 mg, 0.0440 mmol), dissolved in CH_2Cl_2 (1 mL), was added in a dropwise fashion to a stirred, 0 °C solution of $Pb(OAc)_4$ (37.3 mg, 0.084 mmol) in CH_2Cl_2 (1 mL). TLC analysis showed immediate conversion to the aldehyde (R_F 0.41, 9:1 hexanes:ethyl acetate eluent). Heptane (2 mL) was added, and the hetergeneous mixture was filtered through celite, which was washed three times with heptane (1 mL). The resulting clear solution was concentrated to an oil under reduced pressure and then diluted with ethyl acetate (3 mL). This solution was filtered through a small plug of silica, which was washed five times with ethyl acetate (1 mL). The solvent was removed under reduced pressure to produce the crude product. This product was purified by flash column chromatography (15:1 hexanes:ethyl acetate eluent)

to furnish pure aldehyde **205** as a clear oil (10.2 mg, 0.029 mmol, 31% overall yield). R_F 0.41 (9:1 hexanes:ethyl acetate eluent); ^{1}H NMR (300 MHz, CDCl$_3$) δ 9.68 (d, *J* = 2.8 Hz, 1H), 7.42-7.24 (comp.m, 10H), 4.16 (dd, *J* = 2.2, 9.3 Hz, 1H), 3.66-3.49 (comp.m, 3H), 0.84 (s, 9H), -0.17 (s, 3H), -0.19 (s, 3H); ^{13}C NMR (75 MHz, CDCl$_3$) δ 200.1, 140.7, 134.8, 129.9, 129.0, 129.0, 128.4, 127.8, 64.4, 60.7, 49.3, 26.1, 18.5, -5.5, -5.5; IR (neat) 3063, 3030, 2954, 1727 cm^{-1}. HRMS (EI) m/z calc'd for [C$_{22}$H$_{30}$O$_2$Si+H]$^+$ 355.2093, found 355.2095. The identical procedure commencing with aldehyde **164** (19.0 mg, 0.080 mmol) also furnished aldehyde **205** (11.9 mg, 0.34 mmol, 43% overall yield), demonstrating identical relative stereochemistries between aldehyde **168** and aldehyde **164**.

1.10.7.8 Aldehyde 174: Chemical Correlation by Conversion to Ketone 206.
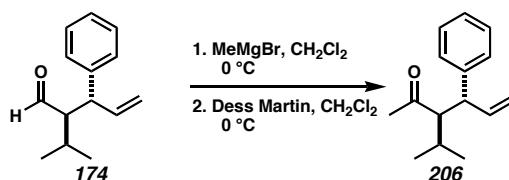
Ketone 206. A flame-dried flask (15 mL) equipped with a magnetic stirbar was charged with aldehyde **174** (27.0 mg, 0.133 mmol) and Et$_2$O (1.5 mL). When this solution had been cooled to 0 °C, a solution of MeMgBr (3.0 *M* in THF, 60 μl, 0.180 mmol) was added via syringe. TLC analysis showed immediate reaction, and H$_2$O (4 mL) was added in order to quench the crude reaction mixture. Et$_2$O (3 mL) was then added, and the layers were separated. The H$_2$O layer was washed three times with Et$_2$O (3 mL), the combined organic layers were dried over MgSO$_4$, and the solvent was then

removed under reduced pressure to afford the secondary alcohol (R_F 0.23, 9:1 hexanes:ethyl acetate eluent). The secondary alcohol was then dissolved in CH_2Cl_2 (1.5 mL), and Dess Martin periodinane (143.9 mg, 0.339 mmol) was added to the resulting solution. Ketone **206** was immediately formed, and the reaction was quenched by the addition of a 1:1 solution of saturated aq $NaHCO_3$ and saturated aq $Na_2S_2O_3$ (2 mL). This mixture was extracted three times with CH_2Cl_2 (3 mL), the combined organic layers were dried over $MgSO_4$, and the solvent was removed under reduced pressure. The ketone was then purified by flash column chromatography (15:1 hexanes:ethyl acetate) to yield pure compound **206** (19.5 mg, 0.090 mmol, 68% yield for two steps) as a colorless foam. The spectral data for this compound correspond to those reported previously for the *anti* product.[27] R_F 0.44 (2:1 hexanes:ethyl acetate eluent).

1.10.7.9 Aldehyde 184: Chemical Correlation by Conversion to Amide 207.
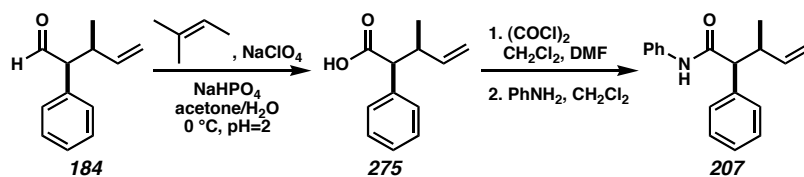
Amide 207. To a flask (50 mL) containing aldehyde **184** (56.0 mg, 0.321 mmol) and equipped with a magnetic stirbar was added acetone (8 mL) and $NaHPO_4$ buffer (4 mL saturated H_2O solution) adjusted to pH 2 by addition of HCl (concd). This mixture was cooled to 0 °C, and 2-methyl-2-butene (500 µl, 4.72 mmol) was added. Immediately, a solution of $NaClO_4$ (73.3 mg, 0.757 mmol) in H_2O (4 mL) was added in one portion. TLC analysis (R_F 0.34, 3:1 hexanes:ethyl acetate eluent, CAM stain) showed complete conversion to the acid within 1 min. A 1:1 mixture of $CHCl_3$:H_2O (16

mL) was added, the layers were separated, and the aqueous phase was extracted three times with $CHCl_3$ (8 mL). The combined organic portions were dried over Na_2SO_4, and the solvent was removed under reduced pressure to leave an amorphous white solid. This solid was purified by flash column chromatography (9:1 hexanes:ethyl acetate with 1% AcOH) to yield the acid **275** in quantitative yield.

Acid **275** (61.1 mg, 0.321 mmol) was dissolved in CH_2Cl_2 (2 mL) in a flask (15 mL) equipped with magnetic stirbar and cooled to 0 °C. Oxalyl chloride (100 µL) was added via syringe, as was a catalytic amount of DMF (3 µl). Once gas generation ceased, the temperature was allowed to rise to 23 °C, and the reaction was stirred for 2 h until TLC analysis showed completion (treatment of a sample with MeOH produced the corresponding methyl ester; R_F 0.71, 3:1 hexanes ethyl acetate eluent). The reaction solvent was removed under reduced pressure, and then benzene was added and removed under reduced pressure twice to displace any excess oxalyl chloride. This acid chloride was then dissolved in CH_2Cl_2 (2 mL) and added to a 0 °C solution of aniline (1 mL) in CH_2Cl_2 (2 mL). TLC analysis showed immediate completion of the reaction. The mixture was diluted with Et_2O (8 mL) and washed with 5% HCl (aq, 4 mL), $NaHCO_3$ (saturated aq, 4 mL), and water (4 mL). The Et_2O phase was then dried over Na_2SO_4, the solvent was removed under reduced pressure, and the product was subjected to flash chromatographic purification (15:1→ 9:1 hexanes:ethyl acetate gradient eluent) to furnish amide **207** as a yellow oil (67.2 mg, 0.253 mmol, 79% yield for two steps). The spectral data for **207** exactly matched that reported in the literature.[28] R_F 0.60 (9:1 hexanes:ethyl acetate eluent).

1.10.7.10 Alcohol 188: Independent Synthesis from Aldehyde 184

184   *188*
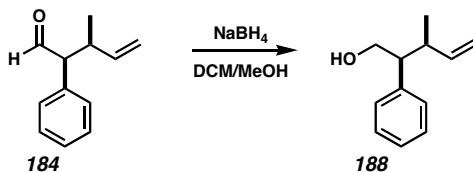
A flame-dried vial (20 mL) equipped with a Teflon-coated stirbar was charged with aldehyde **184** (174.6 mg, 1.00 mmol). DCM (5 mL) and MeOH (5 mL) were added, and then $NaBH_4$ was added in one portion. Gas evolution was observed, and after 0.5 h water (5mL) and Et_2O (10 mL) were added. The layers were separated, and the ether was washed with brine (10 mL), dried over $MgSO_4$, and passed through a filter. Solvent was removed under reduced pressure, and the residue was purified via flash column chromatography (9:1 hexanes : ethyl acetate eluent) to afford pure alcohol **188** (102.2 mg, 0.580 mmol, 58% yield).

1.10.7.11 Alcohol 197: nOe Interactions

The stereochemistry was assigned based on the shown nOe interactions between the axial substituents.

197
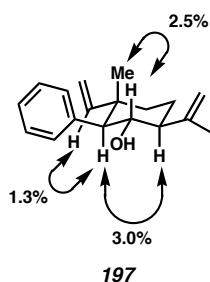
1.10.7.12 Alcohol 198: nOe Interactions

The stereochemistry was assigned based on the shown NOE interactions between the axial substituents.

198
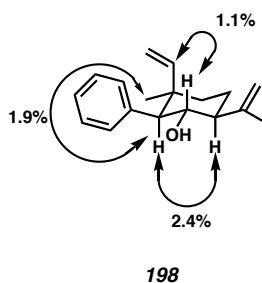
1.10.7.13 Aldehyde 201: nOe Interactions

The stereochemistry was assigned as the (*E*) stereochemistry based on the shown NOE interactions between the vinyl hydrogens and their respective *cis*-allylic hydrogens.
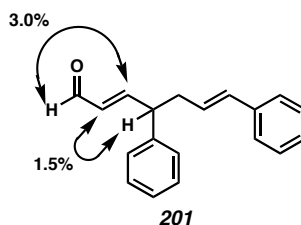
201

The other olefinic stereochemistry was assigned based on the vinyl protons' coupling constants.

1.10.7.14 Aldehyde 203

The stereochemistry was assigned as the (*E*) stereochemistry based on the shown NOE interactions between the respective *cis*-allylic groups.
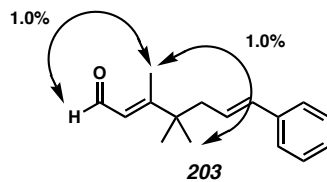
203

The other olefinic stereochemistry was assigned based on the vinyl protons' coupling constants.

1.10.7.15 Aldehyde 186: nOe Interactions and X-Ray Diffraction

1.10.7.15.1 Chemical Conversion to Crystalline Iodolactone 208.

186   **276**   **208**
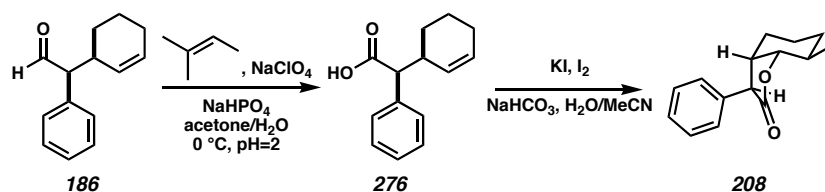
Lactone 208. To a flask (50 mL) containing aldehyde **186** (74.2 mg, 0.426 mmol) and equipped with a magnetic stirbar was added acetone (8 mL) and $NaHPO_4$ buffer (4 mL saturated H_2O solution) adjusted to pH 2 by addition of HCl (concd). This mixture was cooled to 0 °C, and 2-methyl-2-butene (500 μl, 4.72 mmol) was added. Immediately, a solution of $NaClO_4$ (85.6 mg, 0.757 mmol) in H_2O (4 mL) was added in one portion. TLC analysis (R_F 0.35, 3:1 hexanes:ethyl acetate eluent, CAM stain) showed complete conversion to the acid within 1 min. A 1:1 mixture of $CHCl_3:H_2O$ (16 mL) was added, the layers were separated, and the aqueous phase was extracted three times with $CHCl_3$ (8 mL). The combined organic portions were dried over Na_2SO_4, and the solvent was removed under reduced pressure to leave an amorphous white solid. This solid was purified by flash column chromatography (9:1 hexanes:ethyl acetate with 1%

AcOH) to yield the acid **276** in quantitative yield. A flask (25 mL) containing acid **276** (76.0 mg, 0.351 mmol, 5:1 diastereomeric ratio) was equipped with a magnetic stirbar and charged with MeCN (4 mL), and the mixture was cooled to 0 °C. A solution of NaHCO$_3$ (41.7 mg, 0.497 mmol) in H$_2$O (4 mL total volume) was then added, and the mixture was stirred for 5 min. KI (76.6 mg, 0.461 mmol) and I$_2$ (118.0 mg, 0.464 mmol) were then added simultaneously. The reaction was allowed to warm to room temperature over 45 min and was then stirred for 2 h. The addition of 10% Na$_2$S$_2$O$_3$ (aq) (4 mL) quenched the reaction, and the addition of brine (10 mL) and EtOAc (20 mL) followed. The resulting layers were separated, and the aqueous phase was extracted three times with EtOAc (5 mL). The organic layers were dried over Na$_2$SO$_4$, and then the solvent was removed under reduced pressure. The crude white solid was purified by flash column chromatography (15:1 → 9:1 hexanes:ethyl acetate gradient eluent) to furnish **208** (85.2 mg, 0.249 mmol, 71% yield) as a white solid. Crystals suitable for X-ray diffraction were grown from an EtOAc/heptane mixture. mp 158.0-159.1 (dec); R$_F$ 0.53 (3:1 hexanes:ethyl acetate eluent); ^{1}H NMR (300 MHz, CDCl$_3$) δ 7.42-7.20 (comp.m, 5H), 4.82 (dd, J = 6.6, 7.7 Hz, 1H), 4.25 (ddd, J = 3.9, 7.7, 9.9 Hz, 1H), 3.68 (d, J = 9.9 Hz, 1H), 2.83 (ddd, J = 5.5, 10.4, 10.4 Hz, 1H), 2.35-2.26 (m, 1H), 2.06-1.94 (m, 1H), 1.80-1.56 (comp.m, 4H); ^{13}C NMR (75 MHz, CDCl$_3$) δ 176.0, 134.8, 129.1, 128.3, 128.0, 83.3, 49.7, 43.8, 35.0, 27.7, 24.8, 22.2; IR (neat) 3030, 2935, 2860, 1776 cm^{-1}. HRMS (EI) m/z calc'd for [C$_{14}$H$_{15}$IO$_2$+H]$^+$ 343.0195, found 343.0189. The minor diastereomer was also isolated (18.7 mg, 0.053 mmol, 15% yield).

1.10.7.15.2 nOe Interactions

NOE values were determined for this product between the lactone hydrogen and the hydrogen geminal to the iodide, as well as between the bridgehead hydrogens as shown below.

208
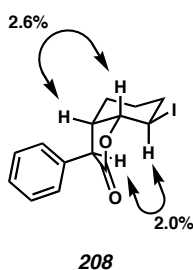
1.10.7.15.3 Single Crystal X-ray Diffraction

SM23
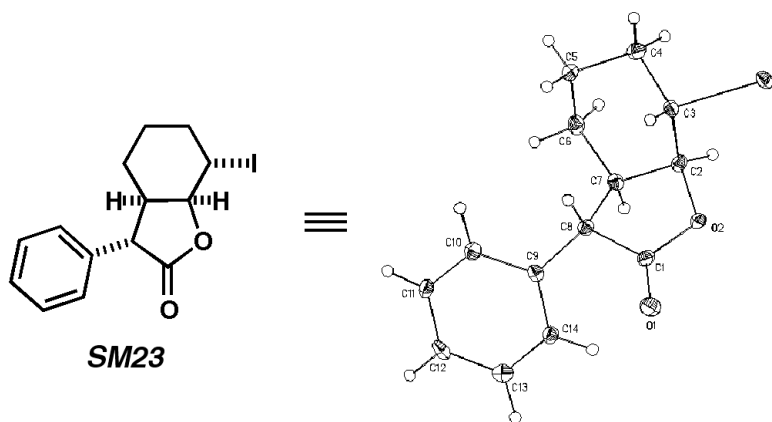
Table 1. Crystal data and structure refinement for 208 (CCDC 186889). <u>Note:</u> The crystallographic data has been deposited in the Cambridge Database (CCDC). The deposition number is 186889.

Empirical Formula	$C_{14}H_{15}IO_2$
Formula Weight	342.16
Crystallization Solvent	Heptane/Chloroform
Crystal Habit	Lozenge
Crystal size	0.12 x 0.12 x 0.10 mm^3
Crystal color	Colorless

Data Collection

Preliminary Photos	Rotation
Type of diffractometer	Bruker SMART 1000
Wavelength	0.71073 Å MoKa
Data Collection Temperature	98(2) K
q range for 13809 reflections used in lattice determination	2.56 to 28.45°
Unit cell dimensions	a = 8.7729(6) Å
	b = 8.8307(6) Å
	c = 15.9057(11) Å
Volume	1232.23(15) Å^3
Z	4
Crystal system	Orthorhombic
Space group	$P2_12_12_1$
Density (calculated)	1.844 Mg/m^3
F(000)	672
Data collection program	Bruker SMART v5.054
q range for data collection	2.56 to 28.30°
Completeness to q = 28.30°	97.1%
Index ranges	$-11 \leq h \leq 11, -11 \leq k \leq 11, -20 \leq l \leq 21$
Data collection scan type	w scans at 7 f settings
Data reduction program	Bruker SAINT v6.022
Reflections collected	18248
Independent reflections	2922 [R_{int}= 0.0576]
Absorption coefficient	2.586 mm^{-1}
Absorption correction	None
Max. and min. transmission	0.7820 and 0.7467

Structure Solution and Refinement

Structure solution program	SHELXS-97 (Sheldrick, 1990)
Primary solution method	Direct methods
Secondary solution method	Difference Fourier map
Hydrogen placement	Difference Fourier map
Structure refinement program	SHELXL-97 (Sheldrick, 1997)
Refinement method	Full matrix least-squares on F^2
Data / restraints / parameters	2922 / 0 / 214
Treatment of hydrogen atoms	Unrestrained
Goodness-of-fit on F^2	1.358
Final R indices [I>2s(I), 2781 reflections]	R1 = 0.0194, wR2 = 0.0381
R indices (all data)	R1 = 0.0214, wR2 = 0.0385
Type of weighting scheme used	Sigma
Weighting scheme used	$w=1/s^2(Fo^2)$
Max shift/error	0.002
Average shift/error	0.000
Absolute structure parameter	-0.017(17)
Largest diff. peak and hole	0.801 and -0.495 e.Å^{-3}

Special Refinement Details

Refinement of F^2 against ALL reflections. The weighted R-factor (wR) and goodness of fit (S) are based on F^2, conventional R-factors (R) are based on F, with F set to zero for negative F^2. The threshold expression of $F^2 > 2s(F^2)$ is used only for calculating R-factors(gt) etc. and is not relevant to the choice of reflections for refinement. R-factors based on F^2 are statistically about twice as large as those based on F, and R-factors based on ALL data will be even larger.

All esds (except the esd in the dihedral angle between two l.s. planes) are estimated using the full covariance matrix. The cell esds are taken into account individually in the estimation of esds in distances, angles, and torsion angles; correlations between esds in cell parameters are only used when they are defined by crystal symmetry. An approximate (isotropic) treatment of cell esds is used for estimating esds involving l.s. planes.

1.11 Preliminary Experiments for Future Directions

1.11.1 O-H Insertion
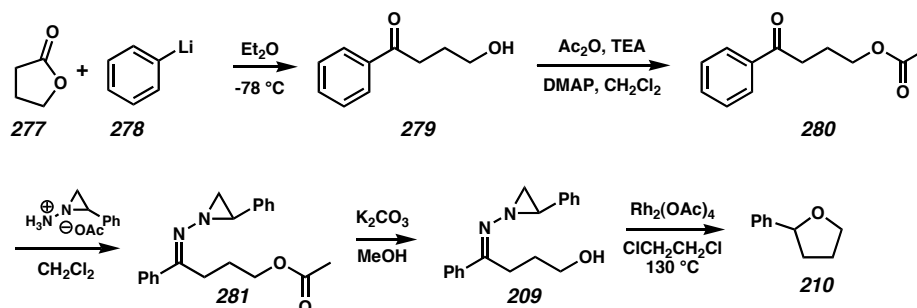
Hydroxy ketone 279: A flame-dried flask (50 mL) equipped with a teflon stirbar was charged with lactone **277** (895 μL, 11.6 mmol) and then ether (24 mL, should use more in the future). The solution was cooled to –78 °C, and then phenyllithium (1.8 M in cyclohexane/ether, 3.25 mL, 5.8 mmol) was added to the mixture slowly. The reaction was stirred for 3 hours, and then it was quenched with saturated NH$_4$Cl$_{(aq)}$ (5 mL). The mixture was extracted three times with ether (10 mL), and the organic layer was dried

over MgSO$_4$, filtered, and concentrated under vacuum. The residue was purified via flash column chromatography (19:1 → 9:1 → 1:1 hexanes : ethyl acetate) to afford hydroxy ketone **279** (441.7 mg, 2.69 mmol, 46% yield); R$_F$ 0.07 (3:1 pentane : ether eluent).

Acetate ketone 280: A flame-dried flask (100 mL) equipped with a teflon stirbar was charged with hydroxy ketone **279** (142.0 mg, 0.865 mmol) and then CH$_2$CH$_2$ (20 mL). Triethylamine (200 μL, 1.43 mmol), acetic anhydride (150 μL, 1.58 mmol), and dimethylaminopyridine (15 mg, 0.12 mmol) were added in that order. The reaction was stirred for 30 min, and then it was diluted with ether (50 mL). The mixture was washed with sat. NaHCO$_3$(aq) (25 mL) and brine (25 mL), and the organic layer was dried over MgSO$_4$, filtered, and concentrated under vacuum. The residue was purified via flash column chromatography (9:1 hexanes : ethyl acetate) to afford acetate ketone **280** (177.7 mg, 0.862 mmol, 99% yield); R$_F$ 0.35 (3:1 pentane : ether eluent).

Hydrazone 281: A flame-dried flask (25 mL) equipped with a teflon stirbar was charged with acetate ketone **280** (177.7 mg, 0.862 mmol) and then CH$_2$CH$_2$ (9 mL). Aziridinyl amine salt **80** (337.2 mg, 1.736 mmol) was added. The reaction was stirred for 24 h, and then K$_2$CO$_3$ (300 mg) was added to quench. The suspension was filtered and concentrated under vacuum. The residue was purified via flash column chromatography (9:1 hexanes : ethyl acetate) to afford hydrazone **281** (186.2 mg, 0.578 mmol, 67% yield); R$_F$ 0.46 (3:1 pentane : ether eluent).

Hydroxy hydrazone 209: A vial (20 mL) equipped with a teflon stirbar was charged with hydrazone **281** (186.2 mg, 0.578 mmol) and then MeOH (10 mL). K$_2$CO$_3$ (45.8 mg, 0.58 mmol) was added to the solution. The reaction was stirred for 90 min, and then it was diluted with CH$_2$CH$_2$ (10 mL), filtered, and concentrated under vacuum. The

residue was purified via flash column chromatography (5:1 hexanes : ethyl acetate) to afford hydroxy hydrazone **209** (160.1 mg, 0.571 mmol, 99% yield); R_F 0.24 (3:1 pentane : ether eluent).

Tetrahydrofuran 210: A flame-dried vial (20 mL) equipped with a teflon stirbar was charged with hydrazone **209** (18.8 mg, 0.0671 mmol), then dichloroethane (1 mL), and then Rh$_2$(OAc)$_4$ (0.7 mg, 0.0016 mmol). The reaction was stirred for 36 h and changed color from pink to orange to red-orange to brown. It was passed through a plug of silica and concentrated under vacuum. The residue was purified via flash column chromatography (9:1 → 4:1 → 1:1 pentane : ether) to afford tetrahydrofuran **210** (3.4 mg, 0.023 mmol, 34% yield); R_F 0.59 (3:1 pentane : ether eluent), which was spectroscopically identical to the reported data.

1.11.2 Cyclopropane Formation

See section 1.10.5.4 for photolytic conditions. When rhodium was omitted, the aldehyde:cyclopropane ration was 1:10.

1.11.3 Iterative Terpenoid Synthesis
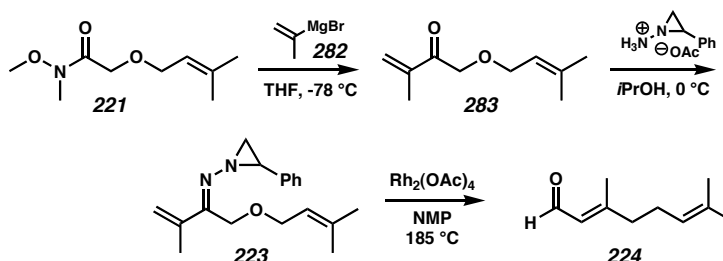
Enone 224: A flame-dried vial (20 mL) equipped with a teflon stirbar was charged with Weinreb amide **221** (267.4 mg, 1.40 mmol) and then THF (11 mL). The solution was cooled to –78 °C, and the Grignard reagent **282** (0.3 *M* in THF, 650 μL, 1.75 mmol) was added dropwise. After 15 min of stirring, MeOH was added to quench any excess reagent. Et$_2$O (9 mL) was added, and the solution was washed with water (20 mL). The organic layer was dried over MgSO$_4$, filtered, and concentrated under vacuum. The residue was purified via flash column chromatography (15:1 hexanes : ethyl acetate) to afford enone **221** (110.7 mg, 0.658 mmol, 47% yield); R$_F$ 0.72 (1:1 pentane : ether eluent).

Hydrazone 223: A flame-dried vial (20 mL) equipped with a teflon stirbar was charged with enone **283** (299.3 mg, 1.78 mmol) and then *i*PrOH (9 mL). The solution was cooled to 0 °C, and the aziridinyl amine salt **80** (422.8 mg, 2.18 mmol) was added. The reaction was stirred for 2 h, and then K$_2$CO$_3$ (300 mg) was added to quench. The suspension was filtered and concentrated under vacuum. The residue was purified via flash column chromatography (15:1 hexanes : ethyl acetate) to afford hydrazone **223** (387.7 mg, 1.35 mmol, 77% yield); R$_F$ 0.66 (3:1 pentane : ether eluent).

Geranial (224): A flame-dried vial (20 mL) equipped with a teflon stirbar was charged with hydrazone **223** (23.4 mg, 0.0814 mmol) and then *N*-methylpyrrolidinone (2 mL). Rh$_2$(OAc)$_4$ was added, and the solution was heated to 185 °C. The reaction was stirred for 3 h, and then it was passed through a small plug of silica gell and concentrated under vacuum. The residue was purified via flash column chromatography (9:1 pentane : ether) to afford geranial (**224**) (2.9 mg, 0.019 mmol, 24% yield); R$_F$ 0.48 (9:1 pentane : ether eluent), which was identical to an authentic sample (Aldrich Chemical Co.).

1.12 Notes and References

(1) Previously reported in May, J. A.; Stoltz, B. M. *J. Am. Chem. Soc.* **2002**, *124*, 12426.

(2) Denmark, S. E.; Thorarensen, A. *Chem. Rev.* **1996**, *96*, 137-165.

(3) Ethyl diazoacetate: Regitz, M.; Hocker, J.; Liedhegener, A. *Org. Synth. Coll. Bol. 5*, Baumgarten, J. E., Ed.; John Wiley & Sons: New York, 1973, 179-83.

(4) de Boer, T. J.; Backer, H. J. *Org. Synth. Coll. Vol. 4*, Rabjohn, N., Ed.; John Wiley & Sons: New York, 1963, 250-53.

(5) For an excellent monograph on the preparation and use of diazo carbonyl compounds, see: Doyle, M. P.; McKervey, M. A.; Ye, T. *Modern Catalytic Methods for Organic Synthesis with Diazo Compounds: From Cyclopropanes to Ylides*; Wiley & Sons: New York, **1998**.

(6) Wood, J. L.; Moniz, G. A.; Pflum, D. A.; Stoltz, B. M.; Holubec, A. A.; Dietrich, H.-J. *J. Am. Chem. Soc.* **1999**, *121*, 1748.

(7) Davies, J. M. L.; McAfee, M. J.; Oldenburg, C. E. M. *J. Org. Chem.* **1989**, *54*, 930-936.

(8) Padwa, A.; Straub, C. S. *J. Org. Chem.* **2003**, *68*(2), 227-239.

(9) For alternative approaches, see: (a) Aggarwal, V. K.; Vicente, J.; Bonnert, R. V. *Org. Lett.* **2001**, *3*, 2785. (b) Doyle, M. P.; High, K. G.; Su-Min, O.; Osborn, A. K. *Tetrahedron Lett.* **1989**, *30*, 3049.

(10) Eschenmoser, *Helv. Chim. Acta*, **1970**, *53*, 1479.

(11) (a) Felix, D.; Müller, R. K.; Horn, U.; Joos, R.; Schreiber, J.; Eschenmoser, A. *Helv. Chim. Acta* **1972**, *55*, 1276. For a recent review, see: (b) Kirmse, W. *Eur. J. Org. Chem.* **1998**, *2*, 201.

(12) Fang, F. G.; Maier, M. E.; Danishefsky, S. J.; Schulte, G. *J. Org. Chem.* **1990**, *55*, 831.

(13) Namamura; Chi; Yan; Nakasugi; Yoshizawa; Irino; Hashimoto; Kinjo; Nohara; and Sakurada *J. Nat. Prod.* **1999**, *62*, 1293.

(14) Confirmation of this product was achieved by comparison with reported data and by aminolysis with NH_3/MeOH to form acetamide and acetophenone.

(15) Burgstahler and Nordin *J. Am. Chem. Soc.* **1961**, *83*, 198 Takai; Mori; Oshima; and Nozaki *Bull. Chem. Soc. Jpn.* **1984**, *57*, 446.

(16) (a) Wipf, P. In *Comprehensive Organic Synthesis*; Trost, B. M., Fleming, I., Eds.; Pergamon Press: Oxford, 1991; Vol. 5, Chapter 7.2; p 827. (b) Ziegler, F. E. *Chem. Rev.* **1988**, *88*, 1423.

(17) Santelli, M.; Pons, J.-M. *Lewis Acids and Selectivity in Organic Synthesis*; CRC Press: New York, 1996.

(18) For a similar ene reaction, see: Corey, E. J.; Roberts, B. E.; Dixon, B. R. *J. Am. Chem. Soc.* **1995**, *117*, 193.

(19) For the Tandem Claisen Cope reaction, see: Ziegler, F. E.; Piwinski, J. J. *J. Am. Chem. Soc.* **1982**, *104*, 7181.

(20) Sibi, M. P.; Stessman, C. C.; Schultz, J. A.; Christensen, J. W.; Lu, J; Marvin, M. *Synth. Comm.* 1995, **25**, 1255.

(21) Oh, T.; Wrobel, Z.; Rubenstein, S. M. *Tetrahedron Lett.* **1991**, 32, 4647.

(22) Kachinski, J. L. C.; Salomon, R. G. *J. Org. Chem.* 1986, **51**, 1393.

(23) Aitken, R. A.; Thomas, A. W. *Synlett* 1998, **1**, 102.

(24) Sarko, C. R.; Guch, I. C.; Dimare, M. *J. Org. Chem.* 1994, **59**, 705.

(25) Sigmund, U. *Monatsh. Chem.* **1929**, *51,* 245.

(26) Corey, E. J.; Lee, D.-H. *J. Am. Chem. Soc.* 1991, **113**, 4026.

(27) Daub, G. W.; Sanchez, M. G.; Cromer, R. A.; Gibson, L. L. *J. Org. Chem.* 1982, **47**, 745.

(28) Ban, E. M.; Gil, S.; Mestres, R.; Parra, M. *Tetrahedron* **1998**, *54*, 15305.

APPENDIX ONE

Spectra Relevant to Chapter 1:

Non-Carbonyl Stabilized Diazo Compounds in the Tandem Bamford-Stevens/Claisen Reaction
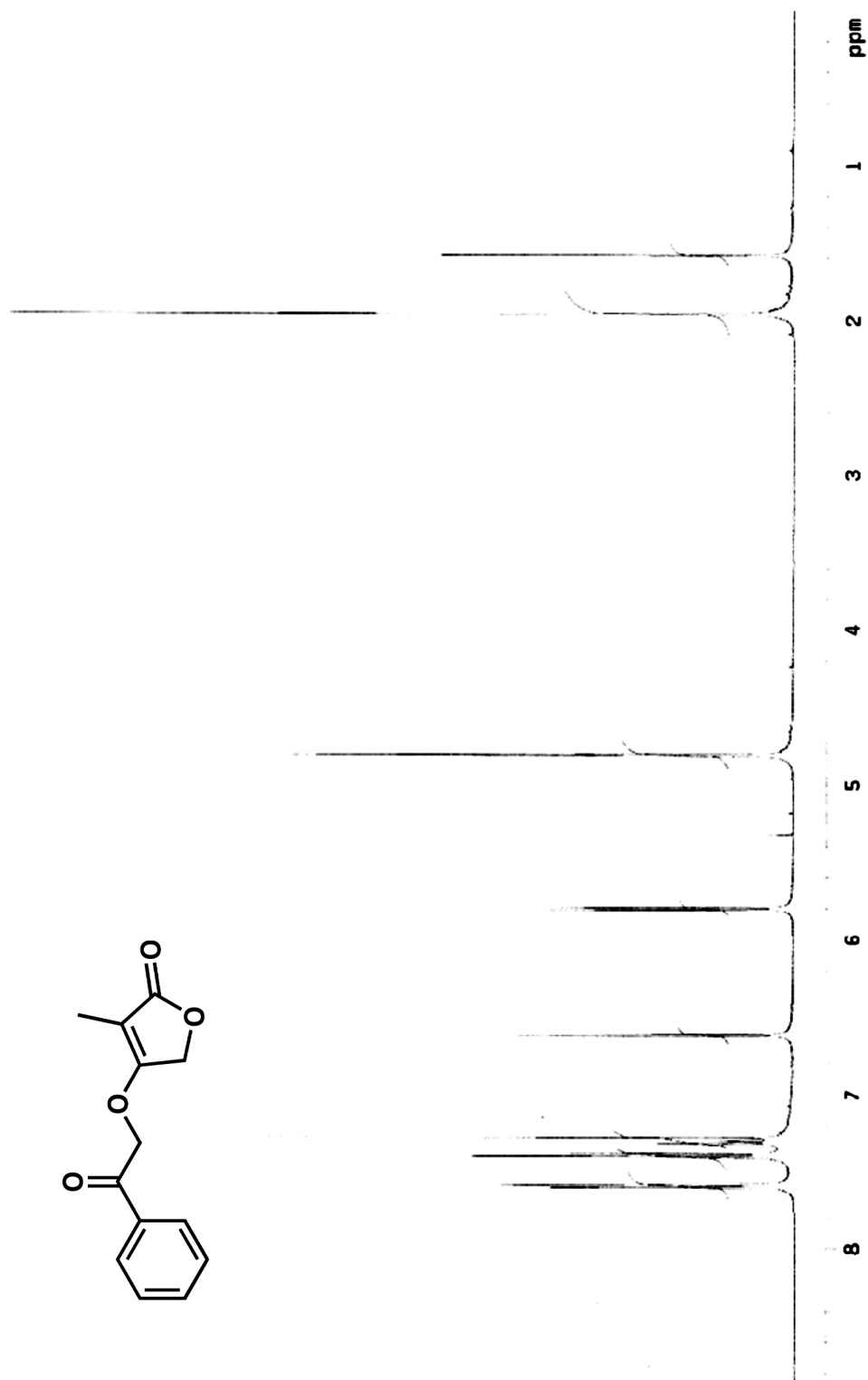
Figure A.1.1 ¹HNMR (300 MHz, CDCL₃) of compound **260**.

Figure A.1.2 Infrared spectrum (thin film/NaCl) of compound **260**.

Figure A.1.3 ^{13}CNMR (75 Mhz, CDCl$_3$) of compound **260**.

Figure A.1.4 ¹HNMR (300 MHz, CDCL₃) of compound **261**.
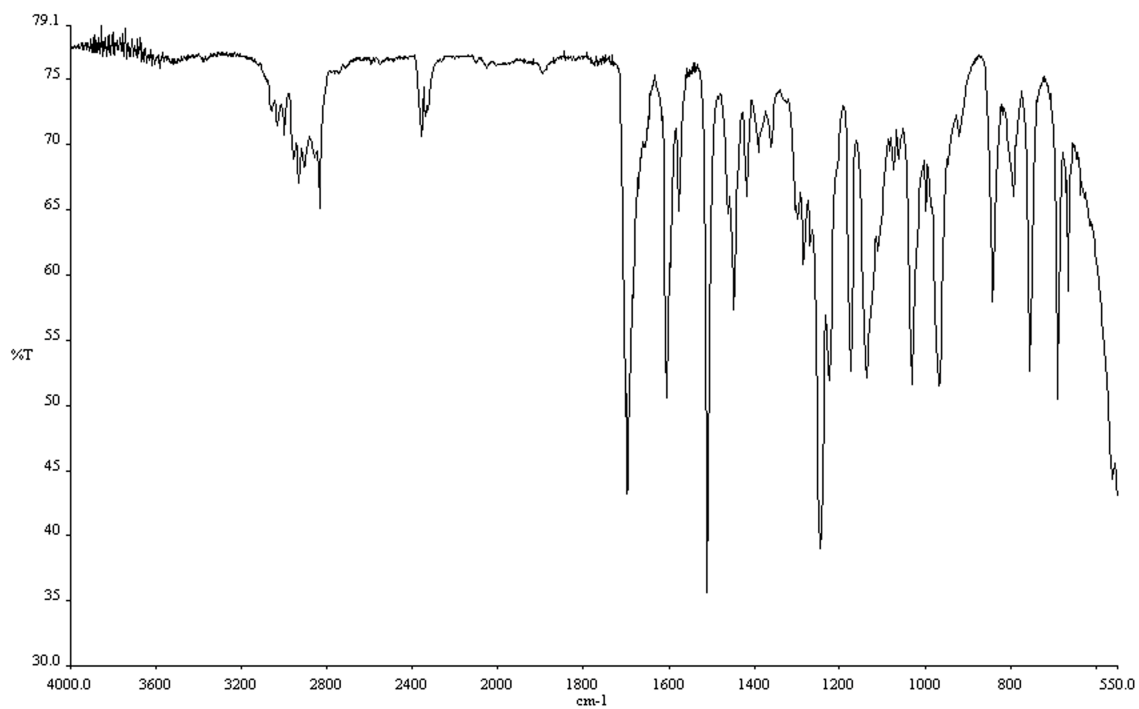
Figure A.1.5 Infrared spectrum (thin film/NaCl) of compound **261**.
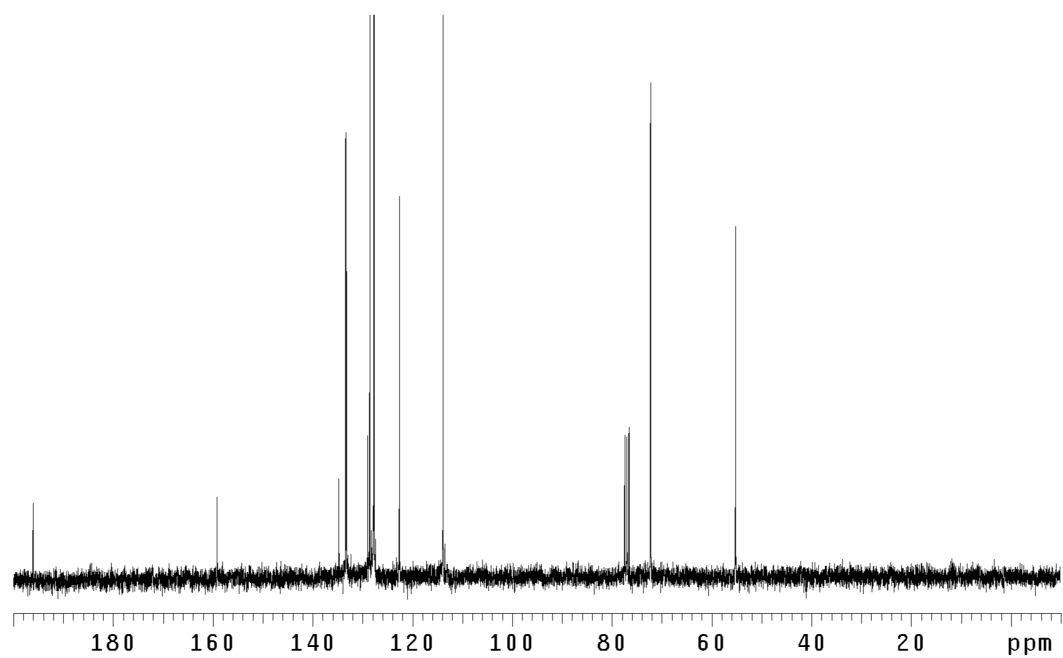
Figure A.1.6 ^{13}CNMR (75 Mhz, CDCl$_3$) of compound **261**.

Figure A.1.7 ¹HNMR (300 MHz, CDCL₃) of compound **262**.

Figure A.1.8 Infrared spectrum (thin film/NaCl) of compound **262**.

Figure A.1.9 ^{13}CNMR (75 Mhz, CDCl$_3$) of compound **262**.

Figure A.1.10 ¹HNMR (300 MHz, CDCL₃) of compound **263**.

Figure A.1.11 Infrared spectrum (thin film/NaCl) of compound **263**.

Figure A.1.12 ^{13}CNMR (75 Mhz, CDCl$_3$) of compound **263**.

Figure A.1.13 ¹HNMR (300 MHz, CDCL₃) of compound **264**.

Figure A.1.14 Infrared spectrum (thin film/NaCl) of compound **264**.

Figure A.1.15 ^{13}CNMR (75 Mhz, CDCl$_3$) of compound **264**.
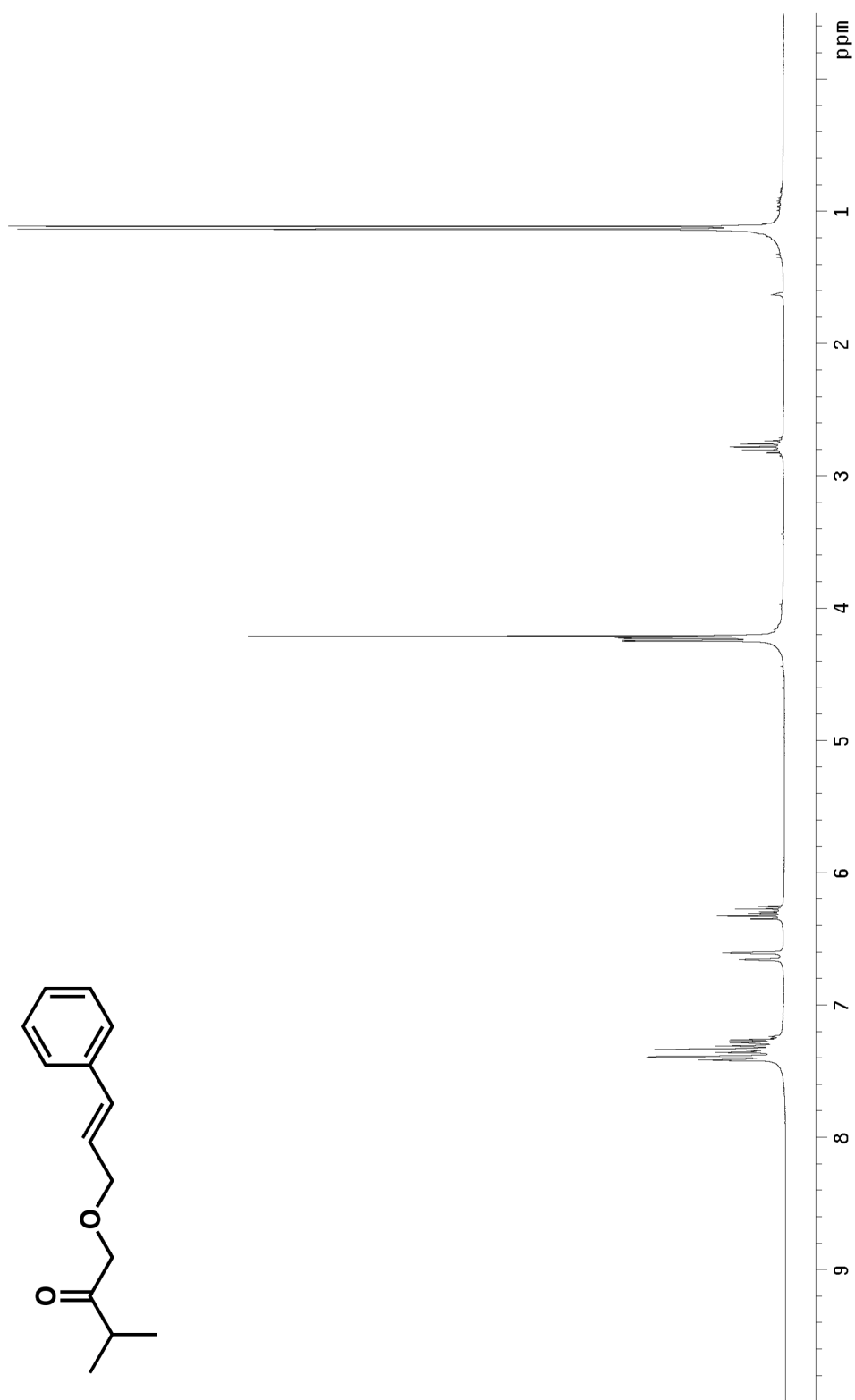
Figure A.1.16 ¹HNMR (300 MHz, CDCL₃) of compound **265**.
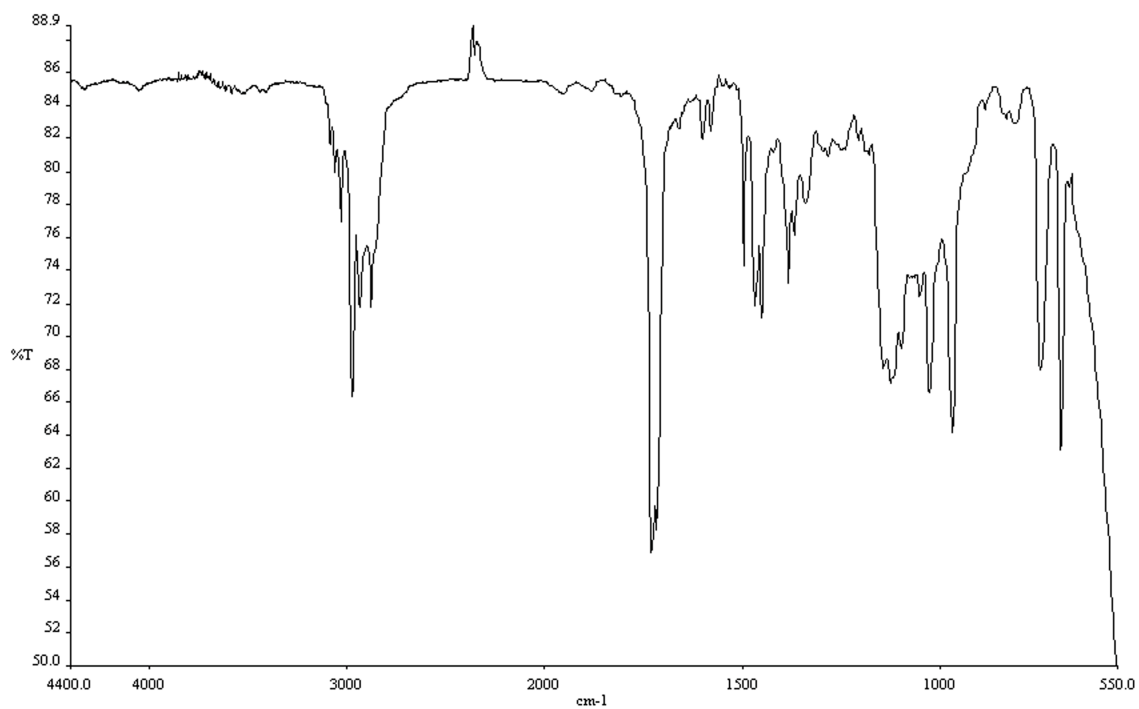
Figure A.1.17 Infrared spectrum (thin film/NaCl) of compound **265**.
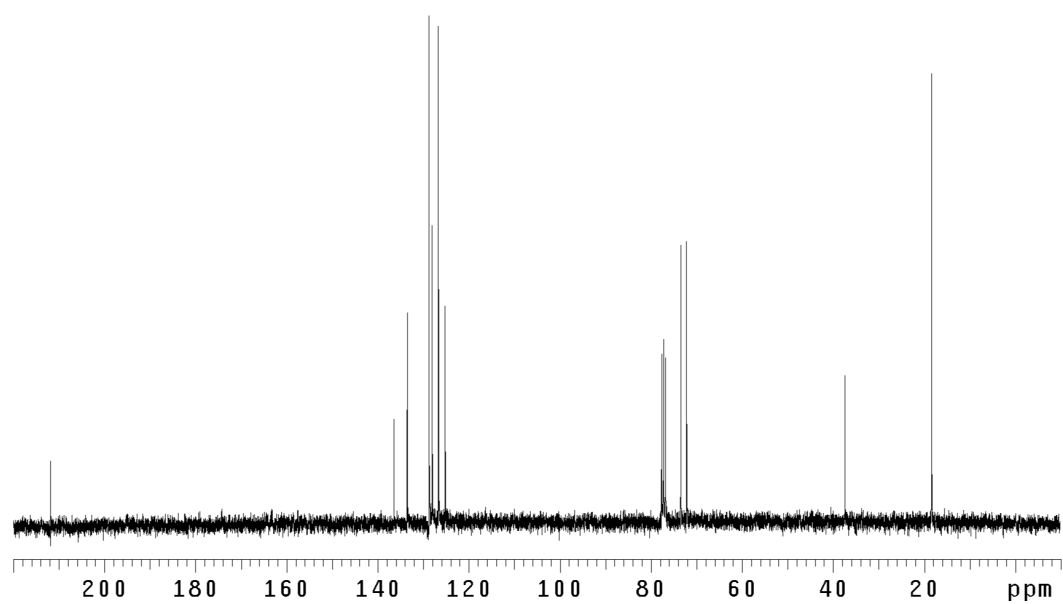
Figure A.118 ^{13}CNMR (75 Mhz, CDCl$_3$) of compound **265**.

Figure A.1.19 ¹HNMR (300 MHz, CDCL₃) of compound **267**.
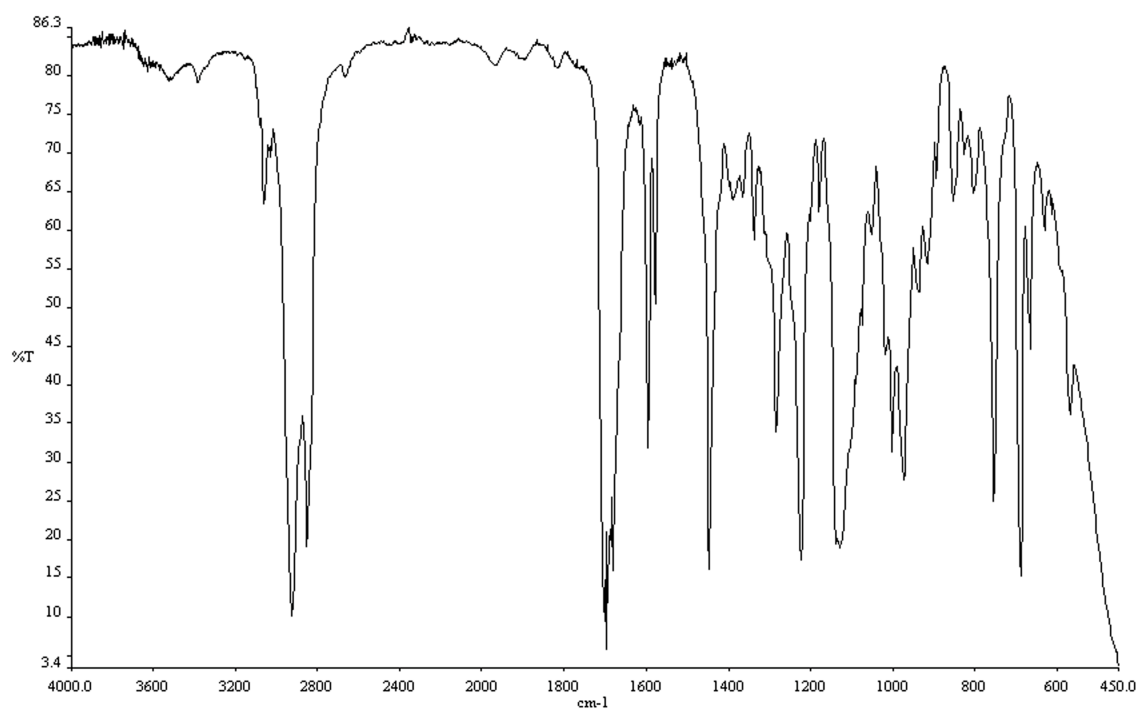
Figure A.1.20 Infrared spectrum (thin film/NaCl) of compound **267**.
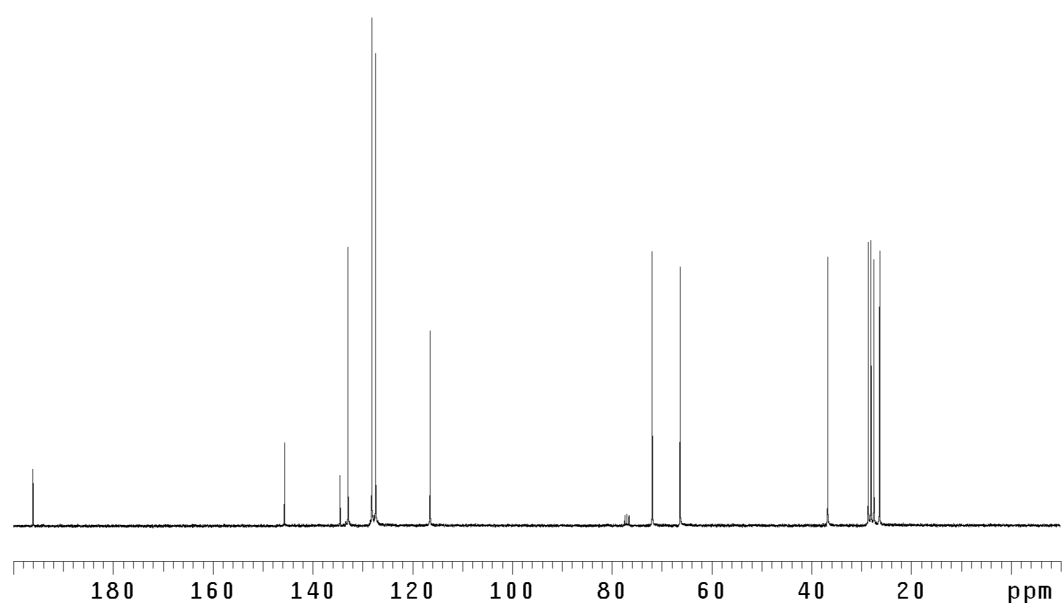
Figure A.1.21 ^{13}CNMR (75 Mhz, CDCl$_3$) of compound **267**.

Figure A.1.22 ¹HNMR (300 MHz, CDCL₃) of compound **268**.
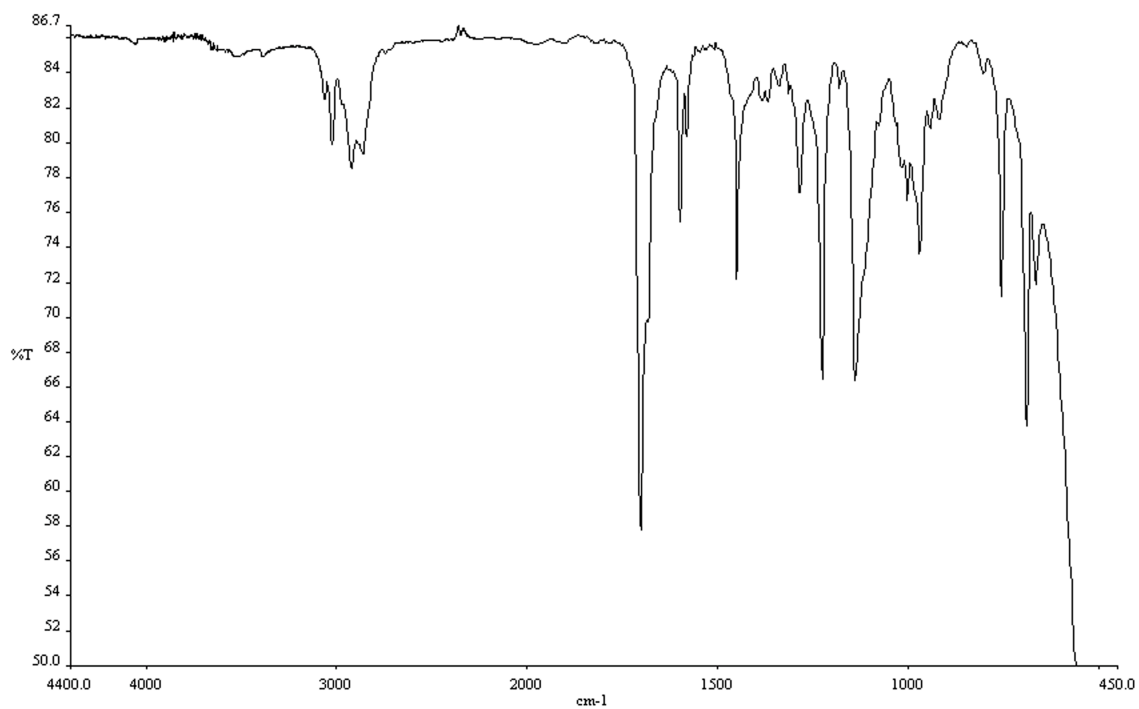
Figure A.1.23 Infrared spectrum (thin film/NaCl) of compound **268**.
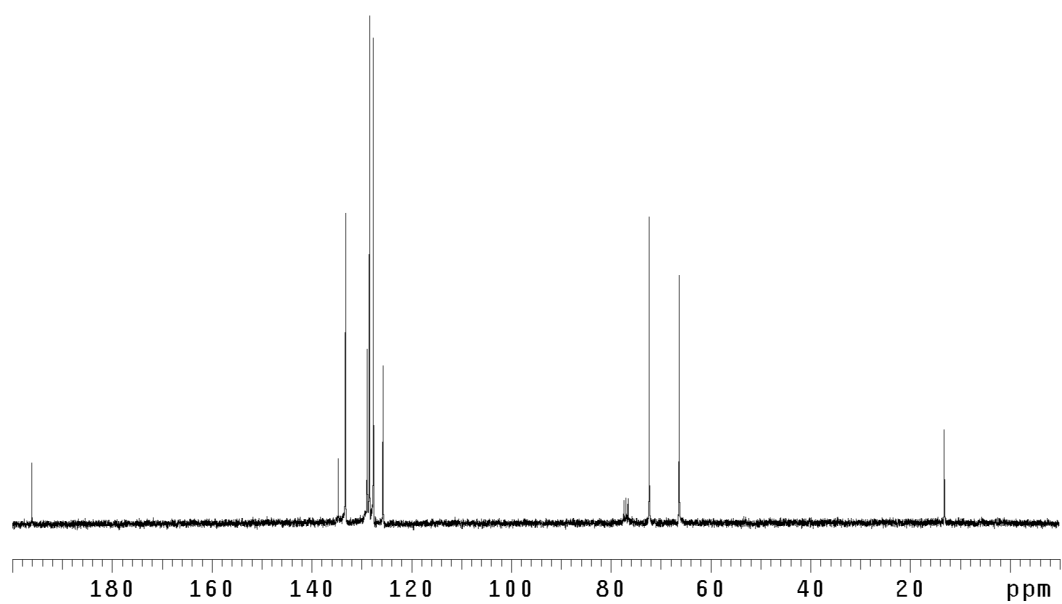
Figure A.1.24 ¹³CNMR (75 Mhz, CDCl₃) of compound **268**.
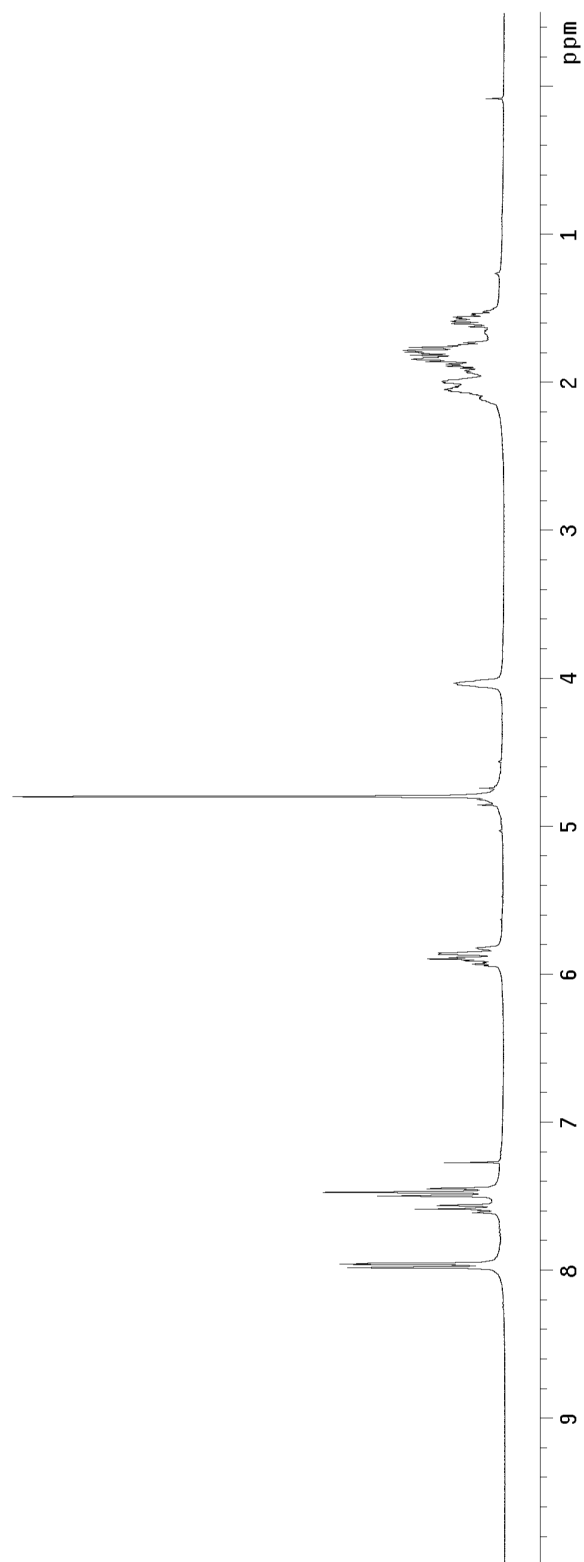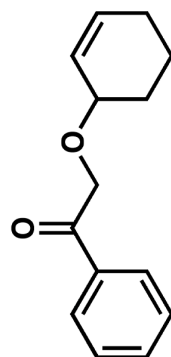
Figure A.1.25 ^{1}HNMR (300 MHz, CDCL$_3$) of compound **269**.
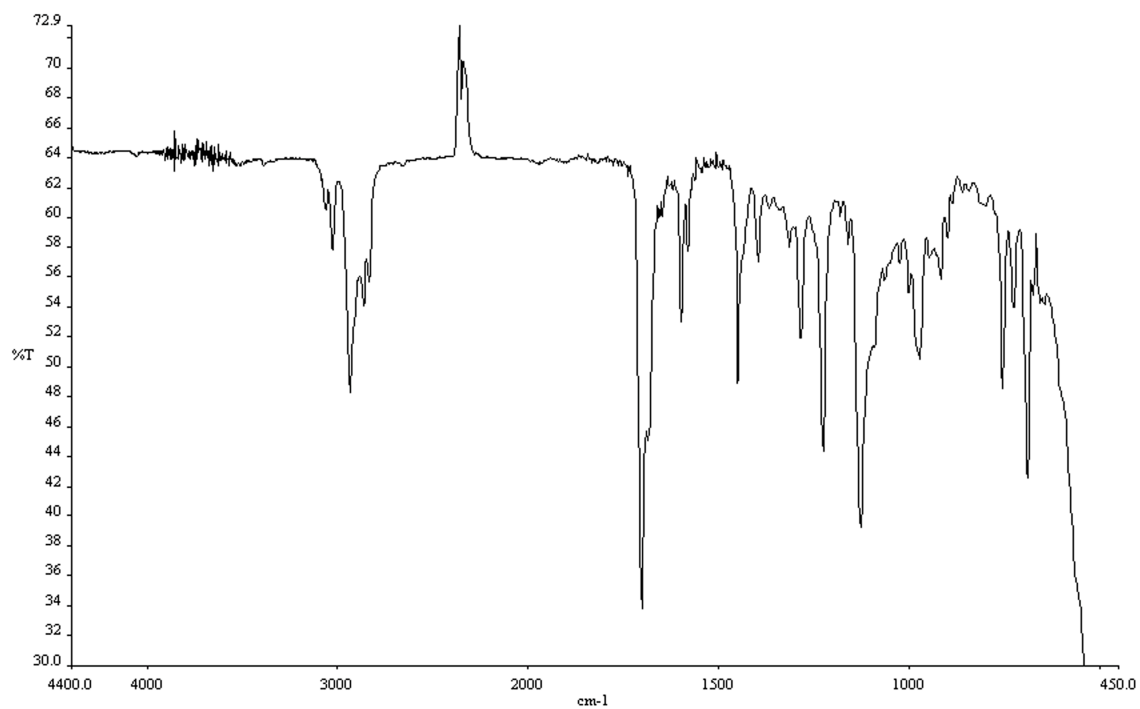
Figure A.1.26 Infrared spectrum (thin film/NaCl) of compound **269**.
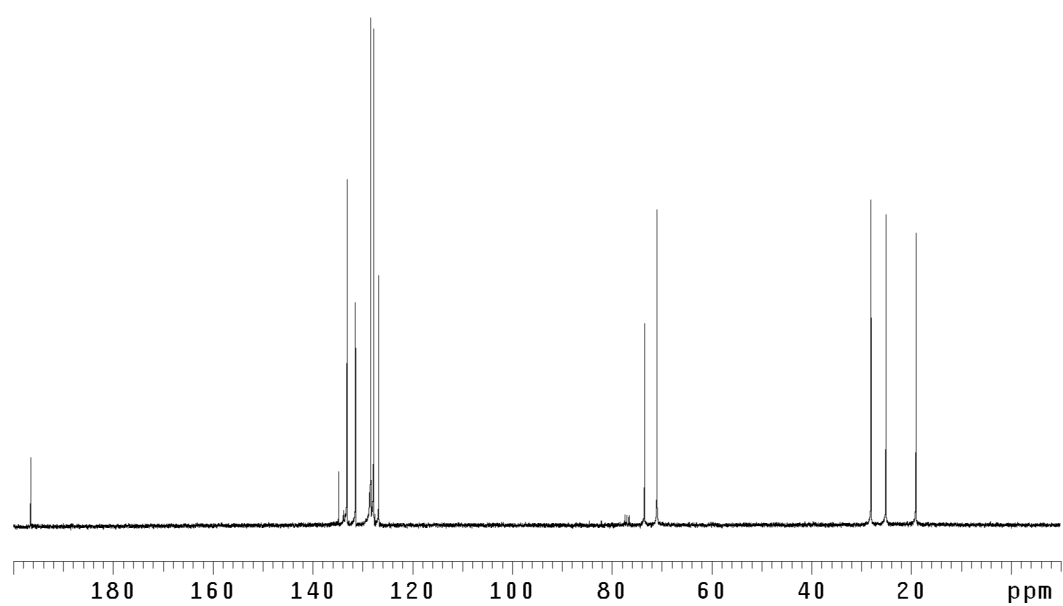
Figure A.1.27 ^{13}CNMR (75 Mhz, CDCl$_3$) of compound **269**.
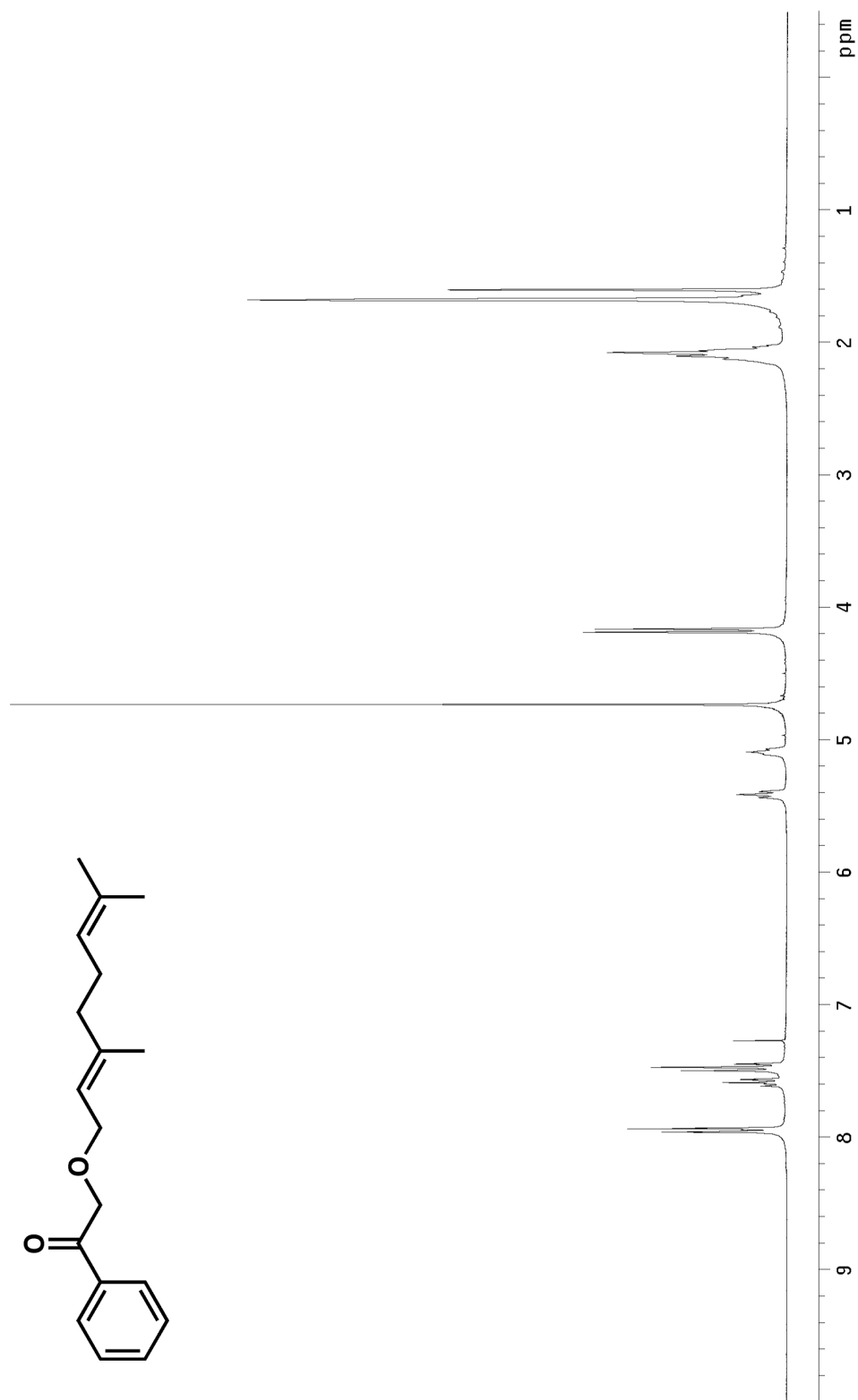
Figure A.1.28 ¹HNMR (300 MHz, CDCL₃) of compound **270**.
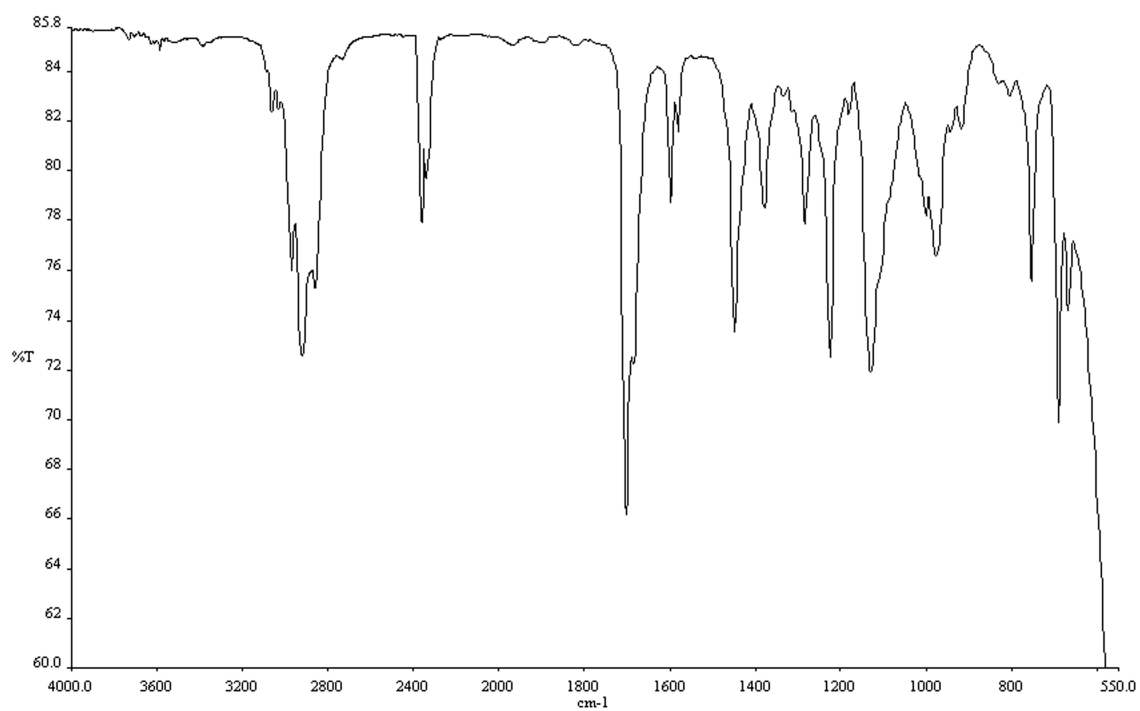
Figure A.1.29 Infrared spectrum (thin film/NaCl) of compound **270**.
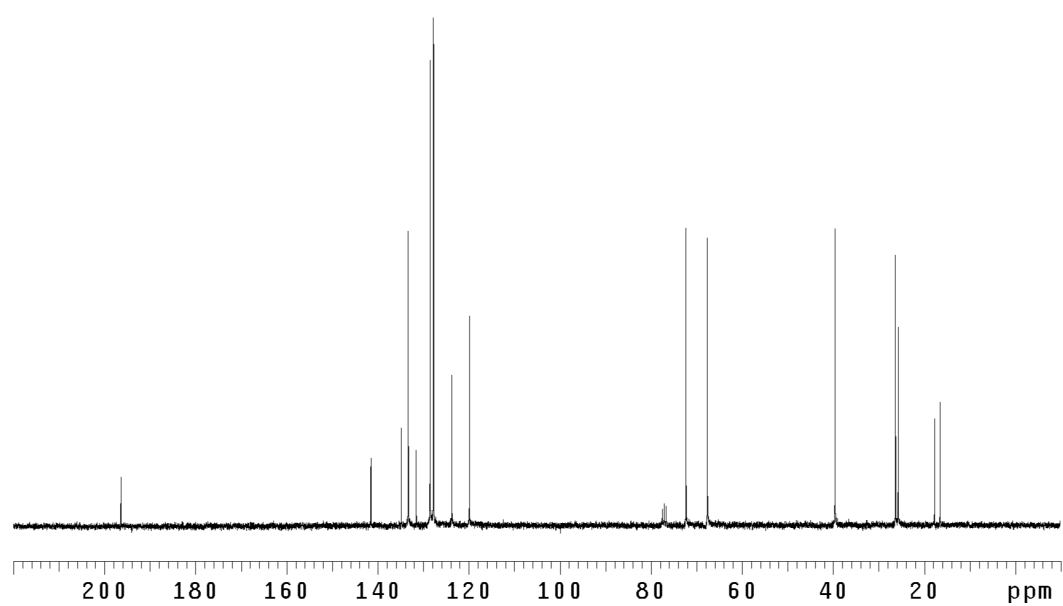
Figure A.1.30 ^{13}CNMR (75 Mhz, CDCl$_3$) of compound **270**.
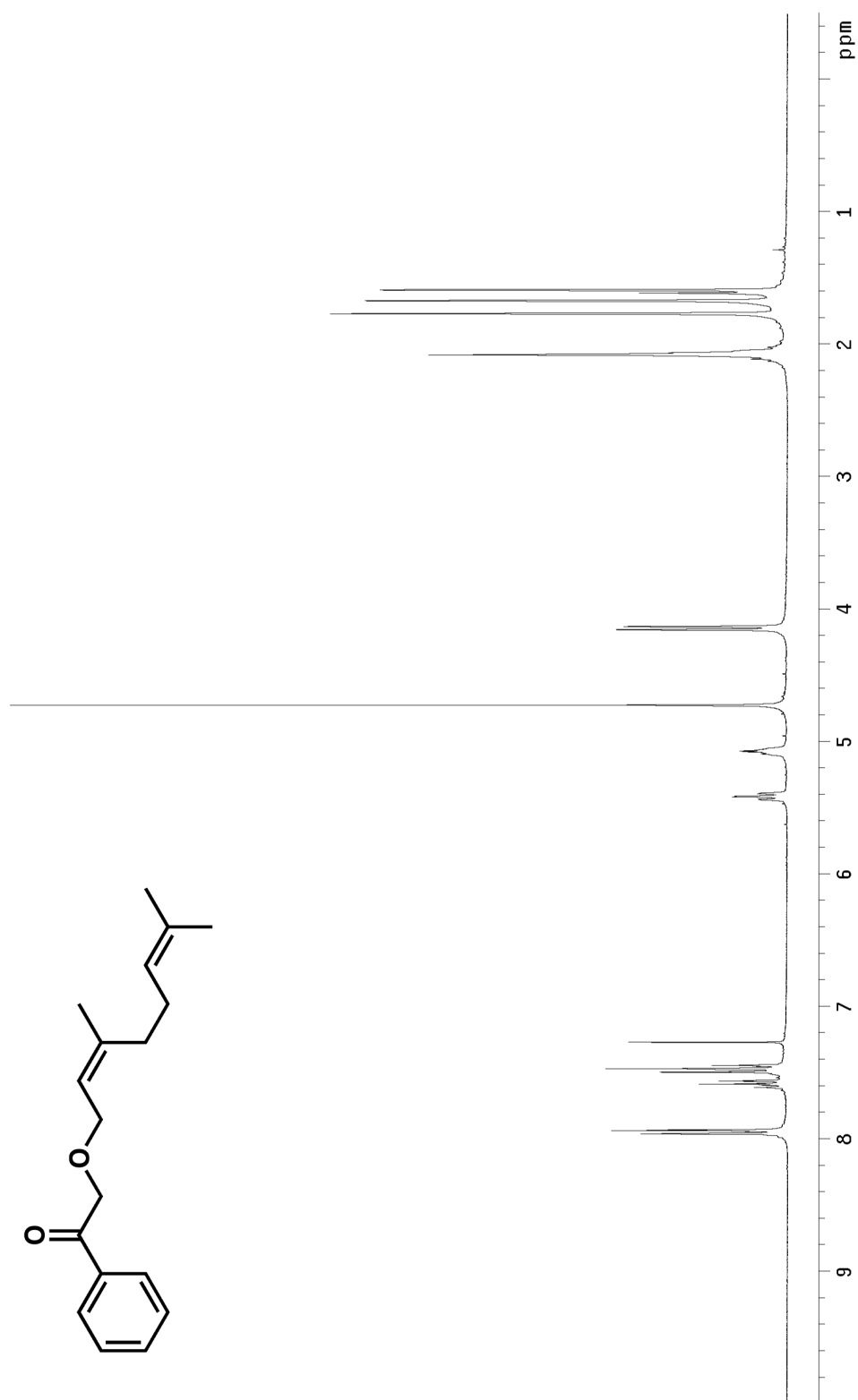
Figure A.1.31 ¹HNMR (300 MHz, CDCL₃) of compound **271**.
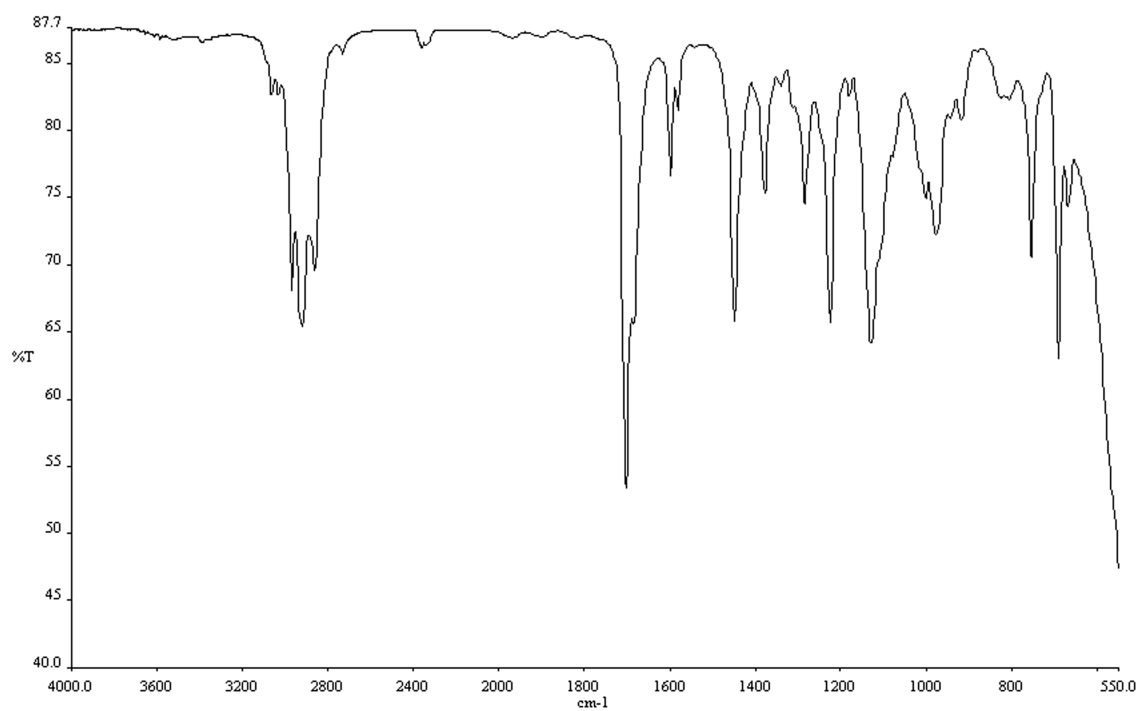
Figure A.1.32 Infrared spectrum (thin film/NaCl) of compound **271**.
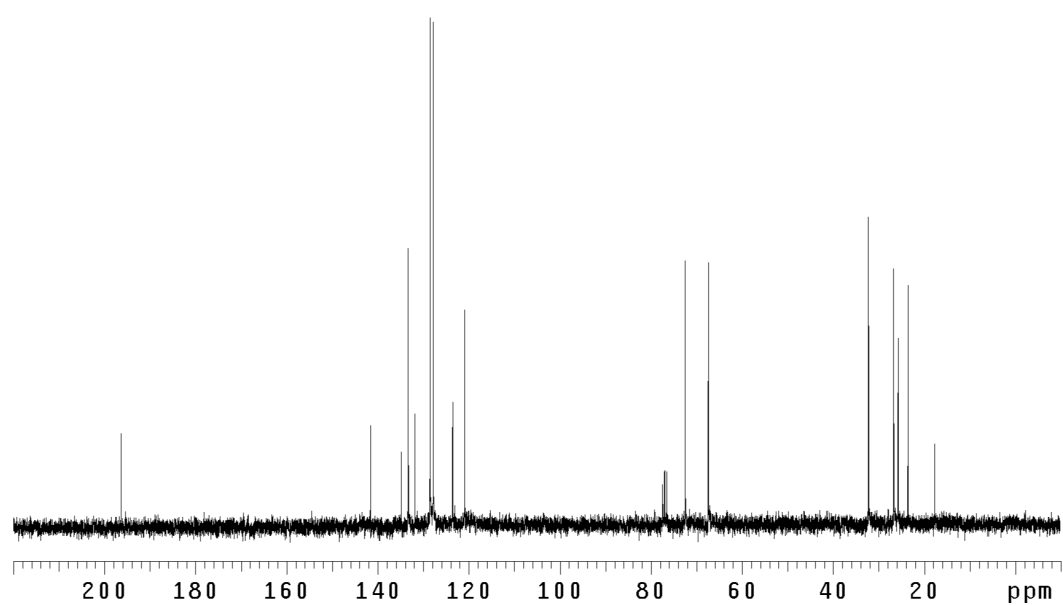
Figure A.1.33 ^{13}CNMR (75 Mhz, CDCl$_3$) of compound **271**.
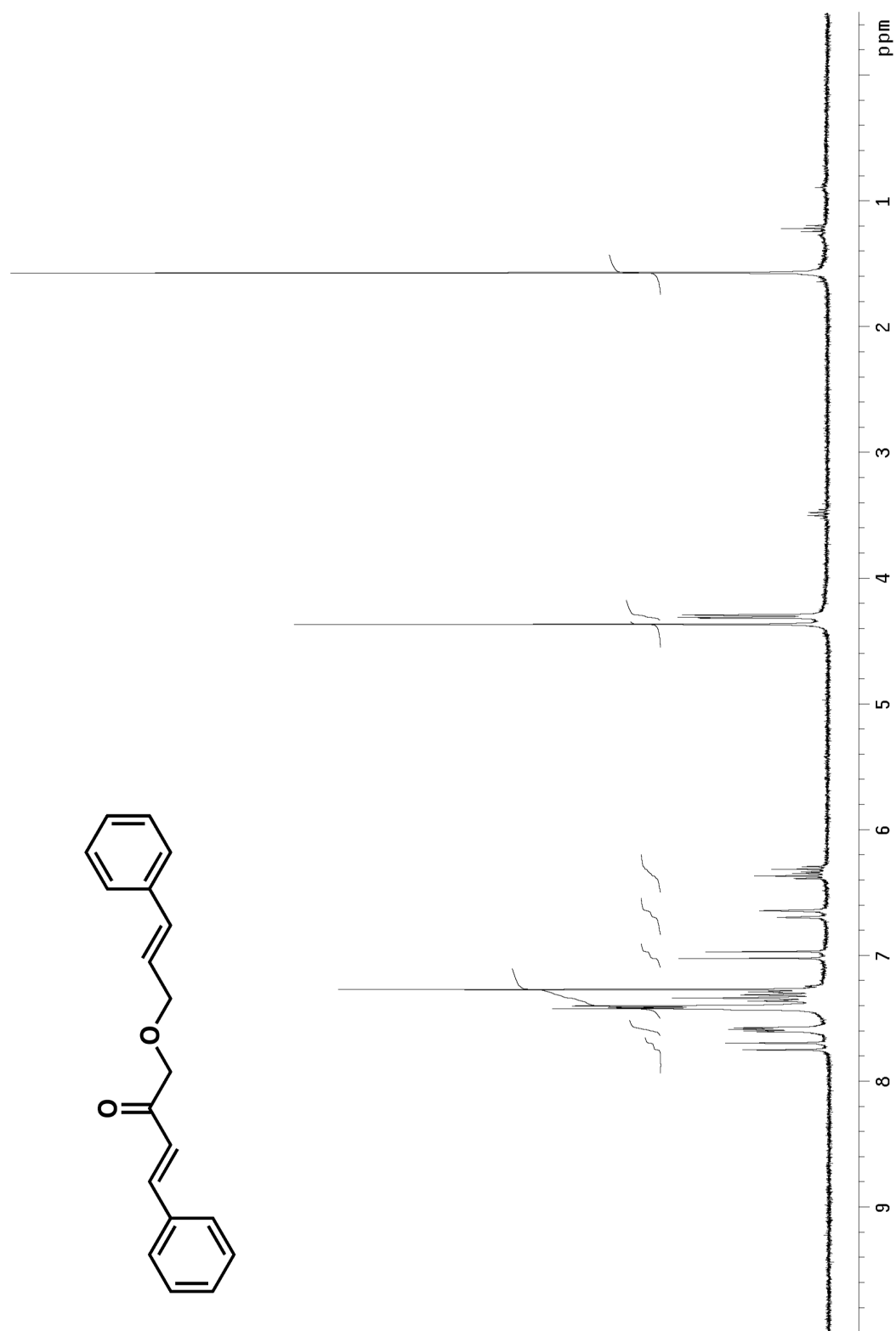
Figure A.1.34 ¹HNMR (300 MHz, CDCL₃) of compound **272**.
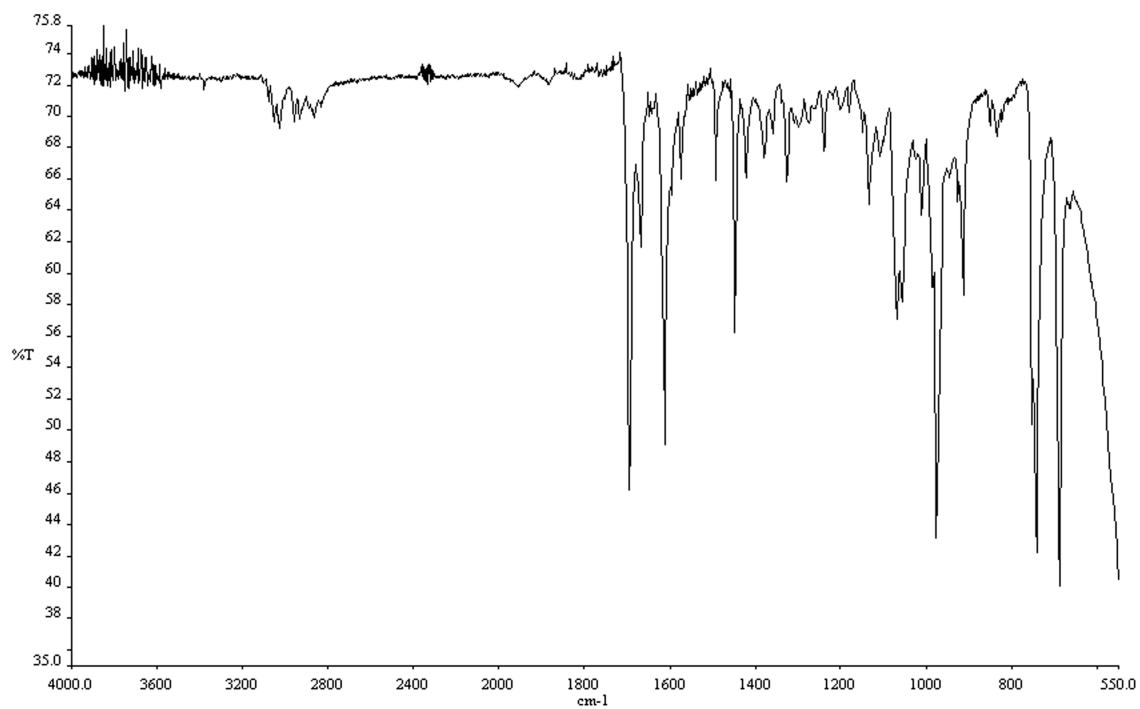
Figure A.1.35 Infrared spectrum (thin film/NaCl) of compound **272**.
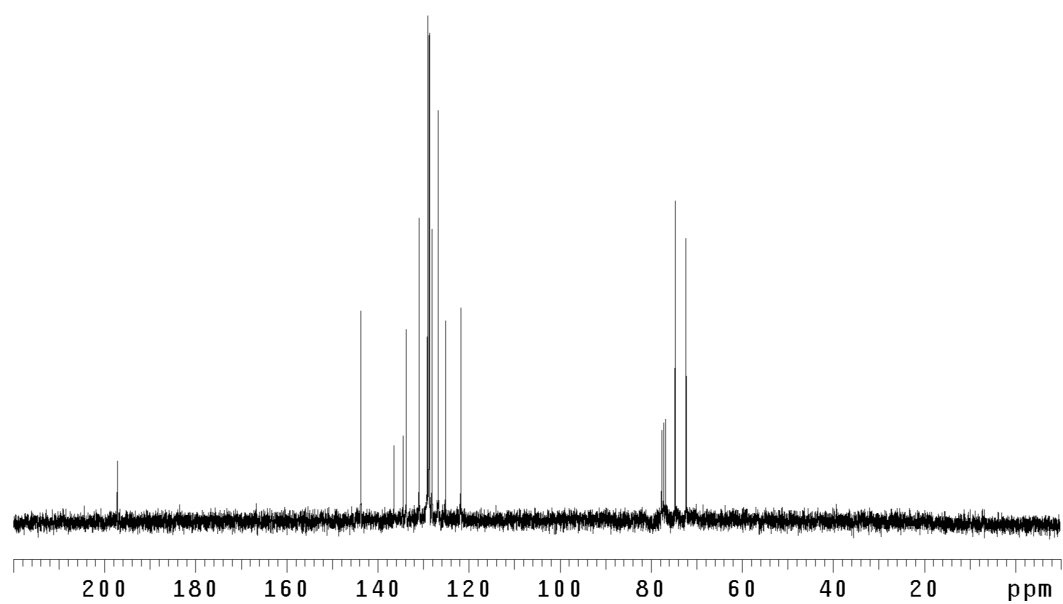
Figure A.1.36 ^{13}CNMR (75 Mhz, CDCl$_3$) of compound **272**.
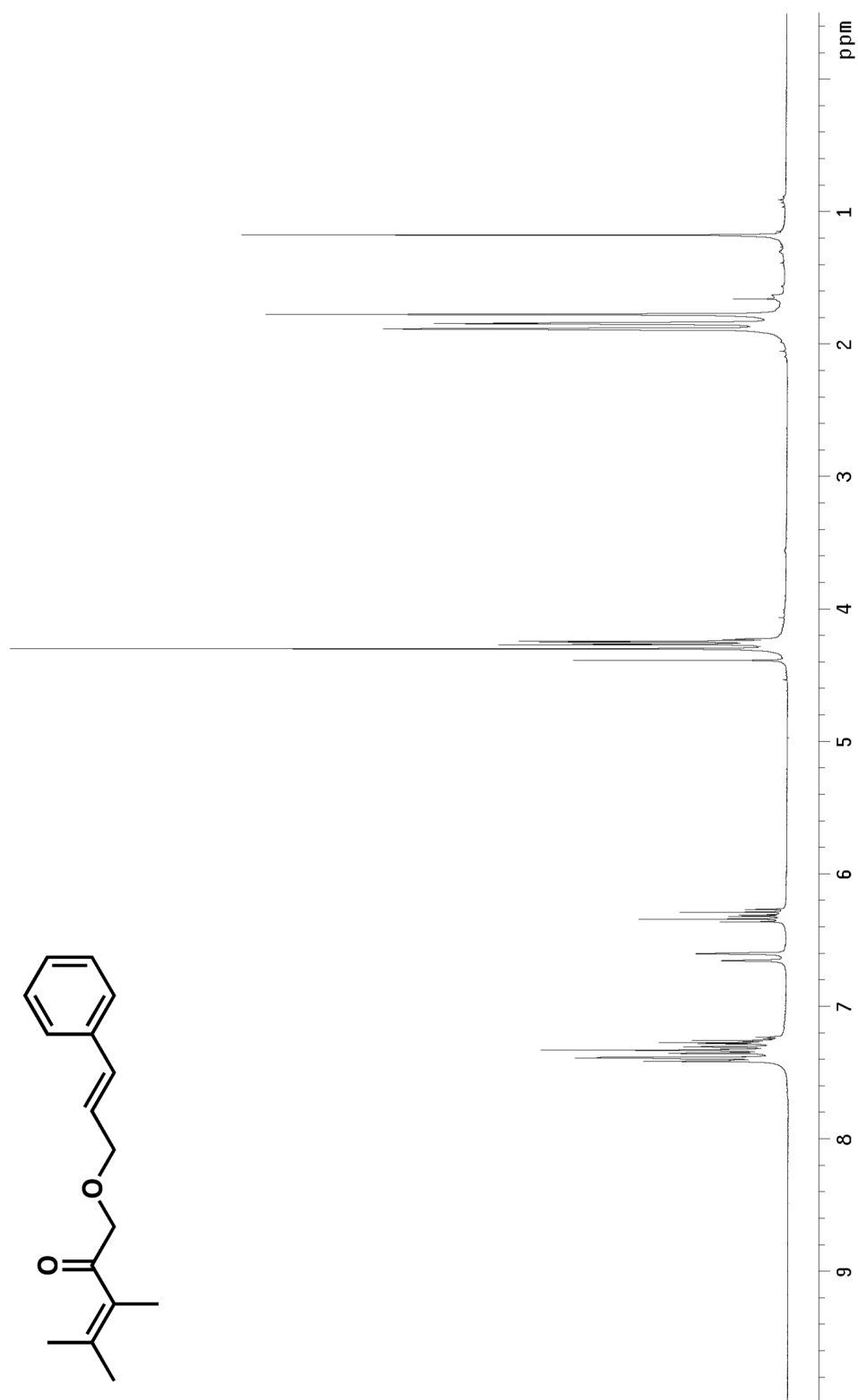
Figure A.1.37 ¹HNMR (300 MHz, CDCL₃) of compound **273**.
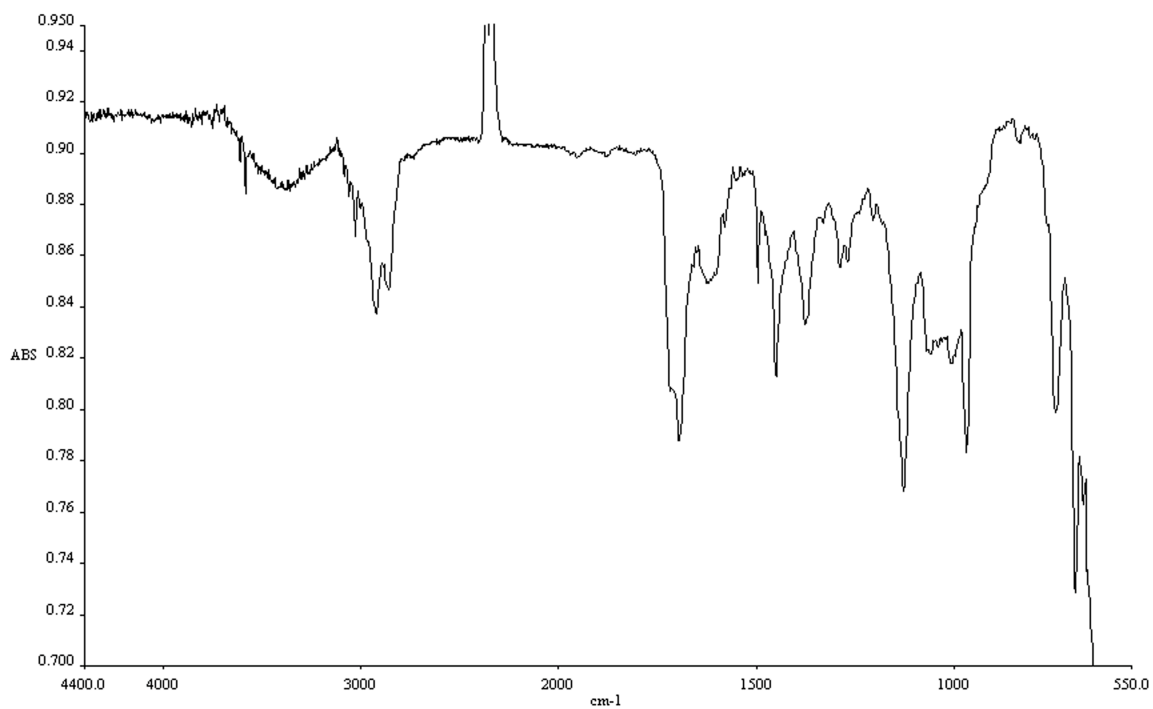
Figure A.1.38 Infrared spectrum (thin film/NaCl) of compound **273**.
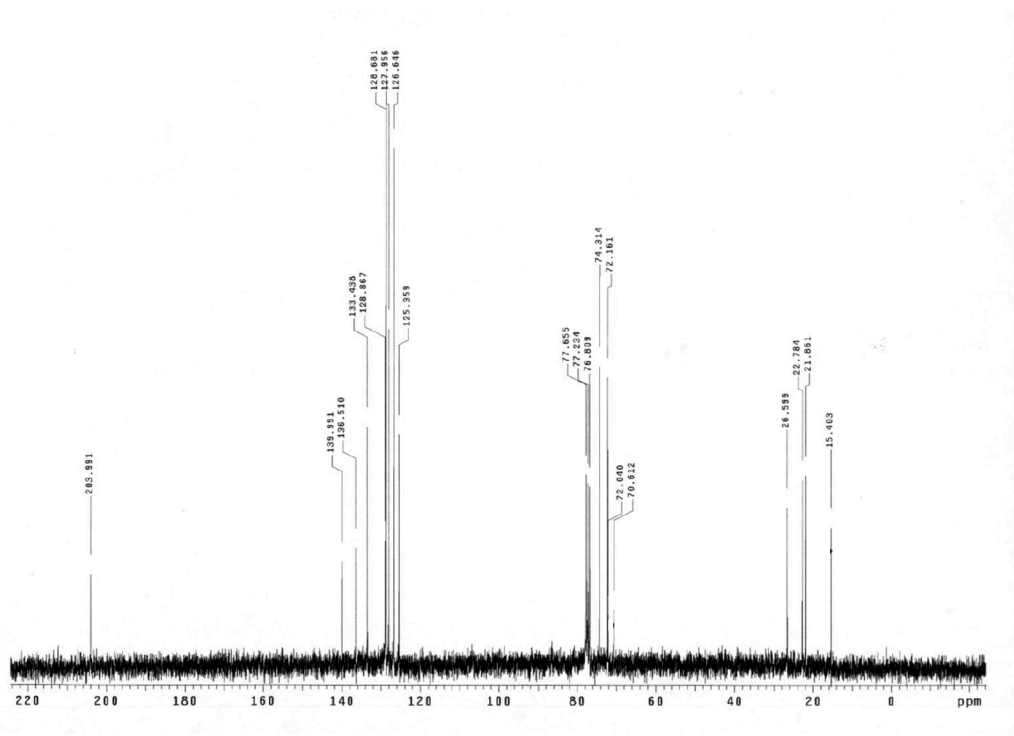
Figure A.1.39 ^{13}CNMR (75 Mhz, CDCl$_3$) of compound **273**.
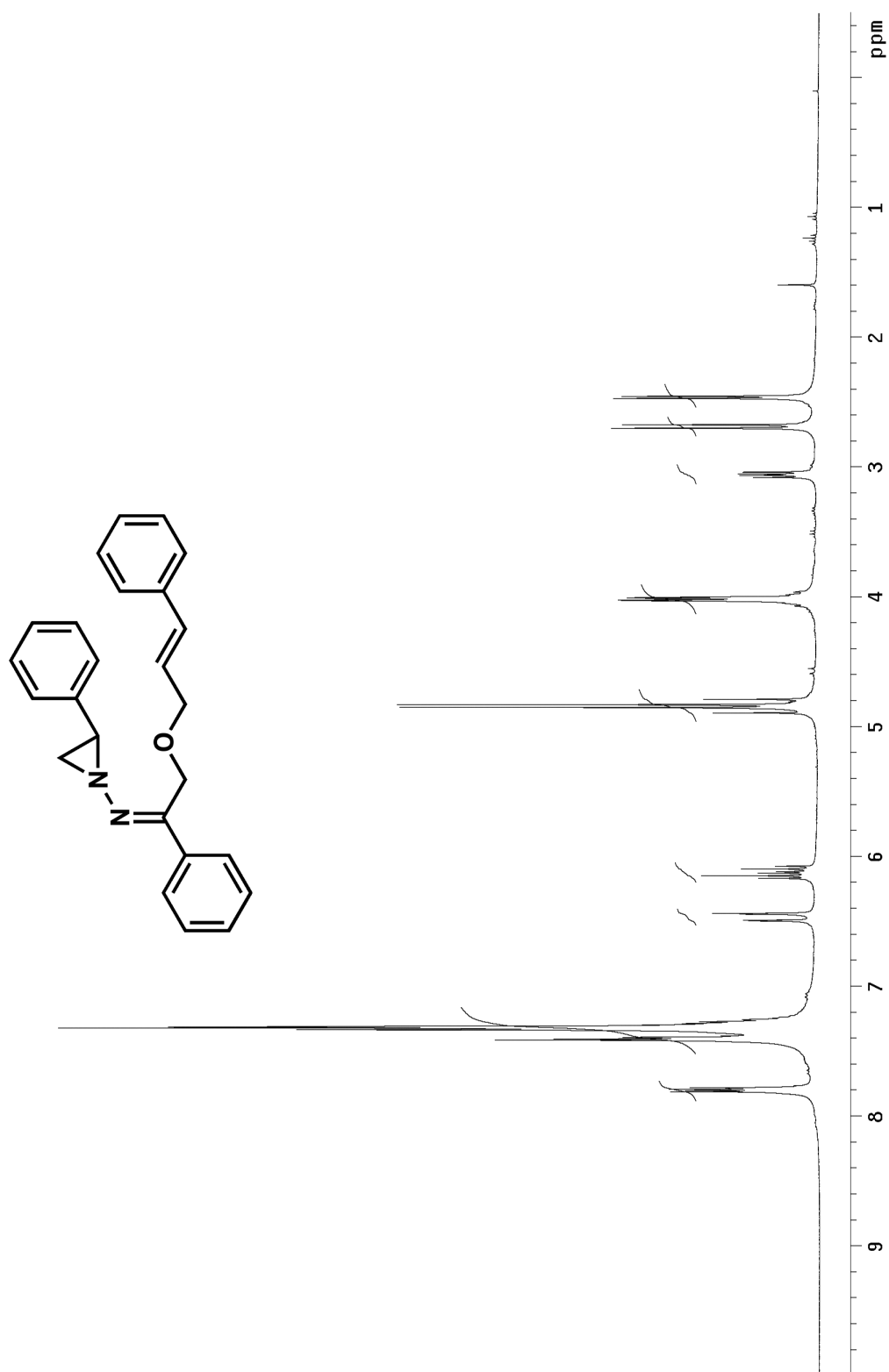
Figure A.1.40 ¹HNMR (300 MHz, CDCL₃) of compound **163**.
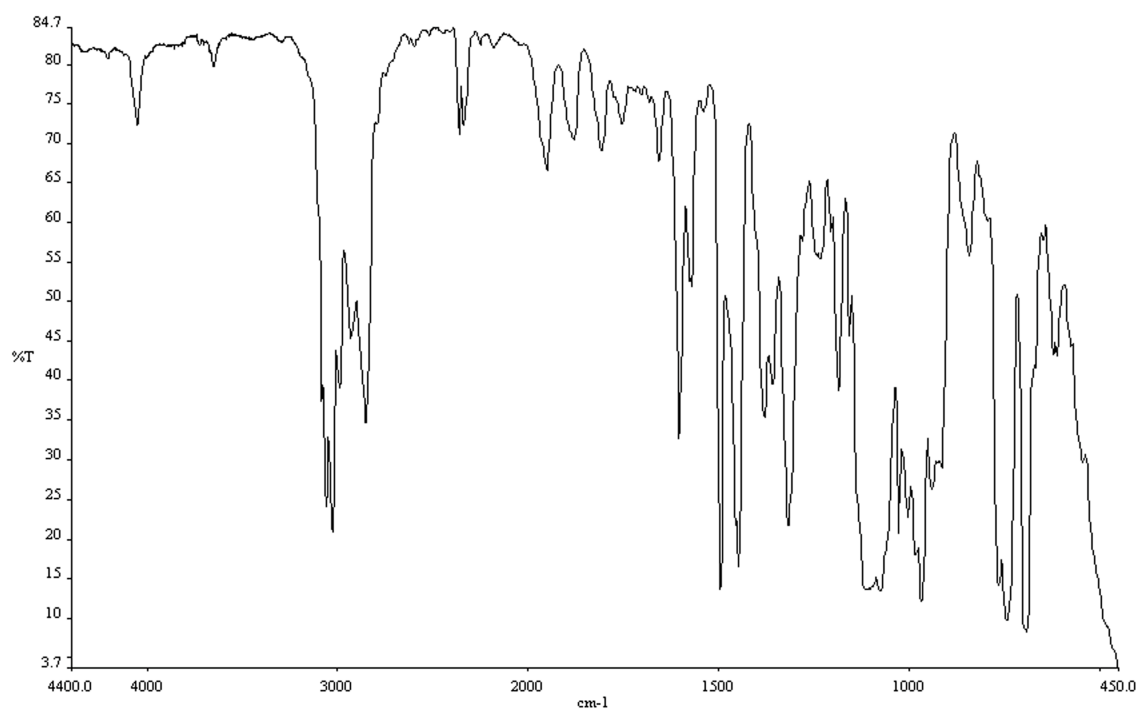
Figure A.1.41 Infrared spectrum (thin film/NaCl) of compound **163**.
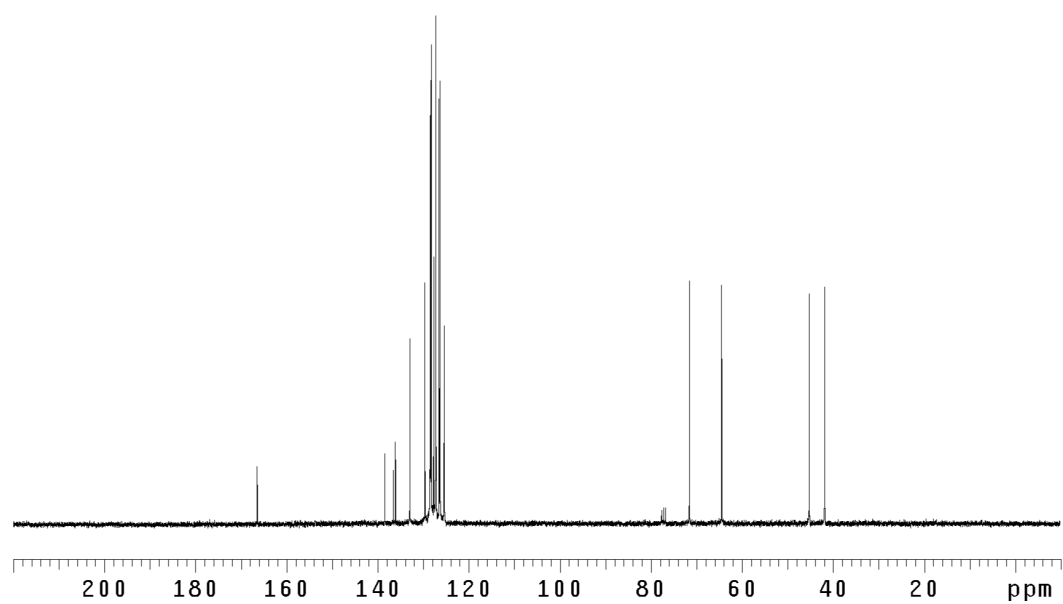
Figure A.1.42 ^{13}CNMR (75 Mhz, CDCl$_3$) of compound **163**.
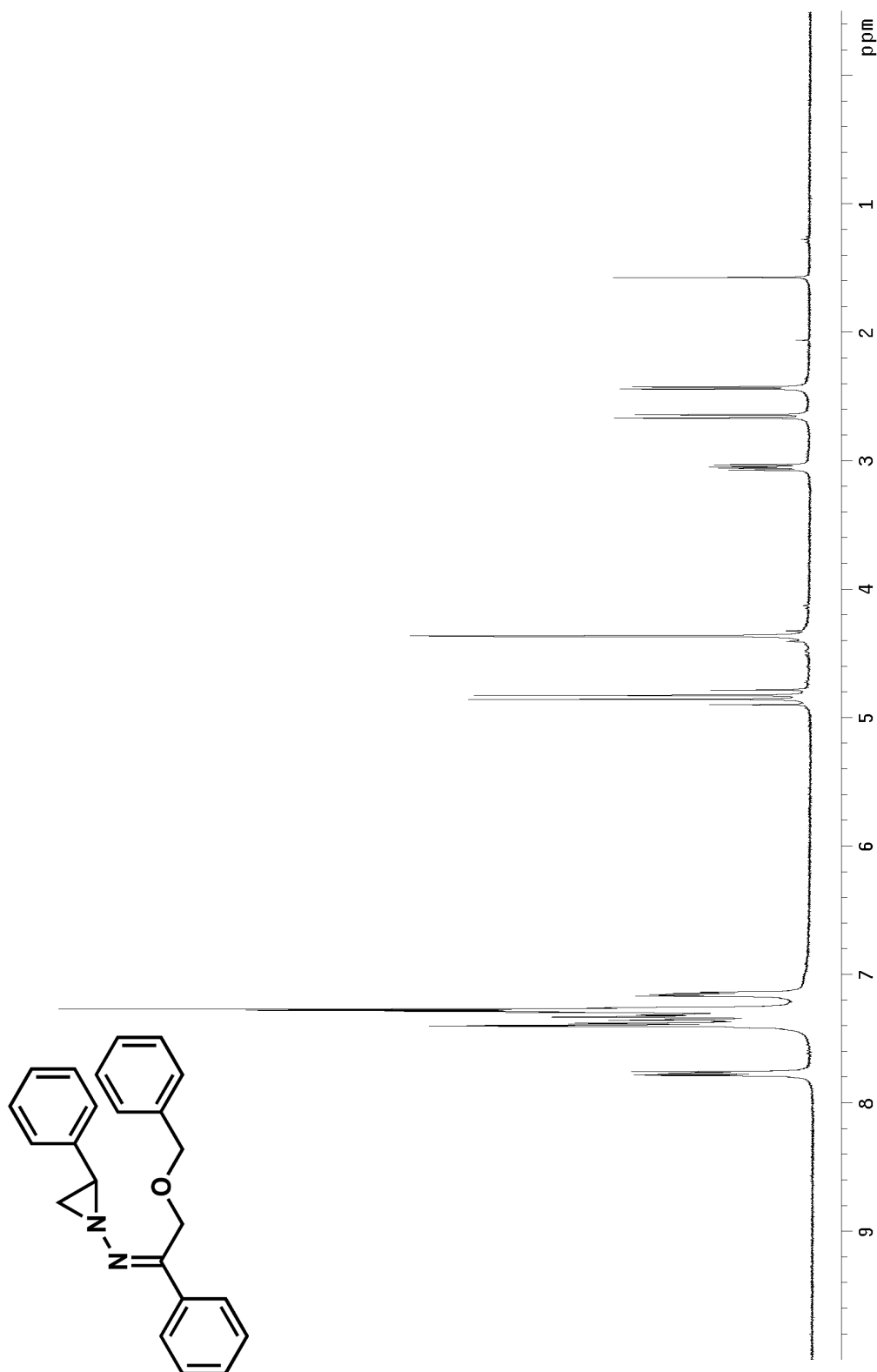
Figure A.1.43 ¹HNMR (300 MHz, CDCL₃) of compound **104.**
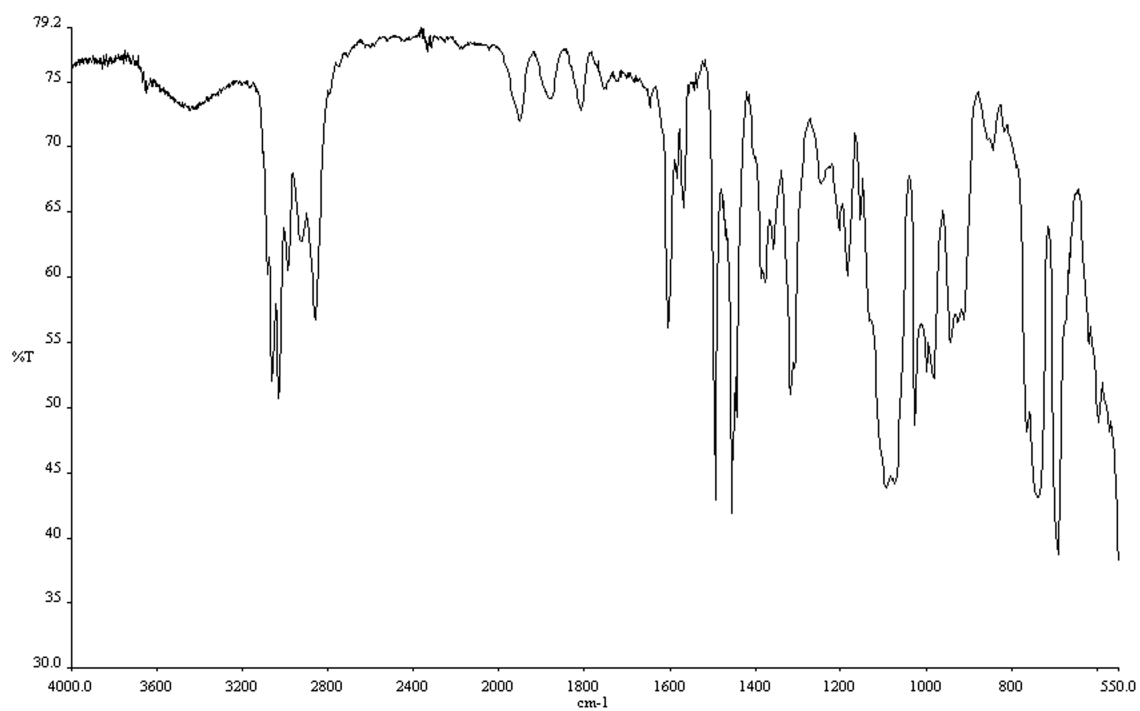
Figure A.1.44 Infrared spectrum (thin film/NaCl) of compound **104**.
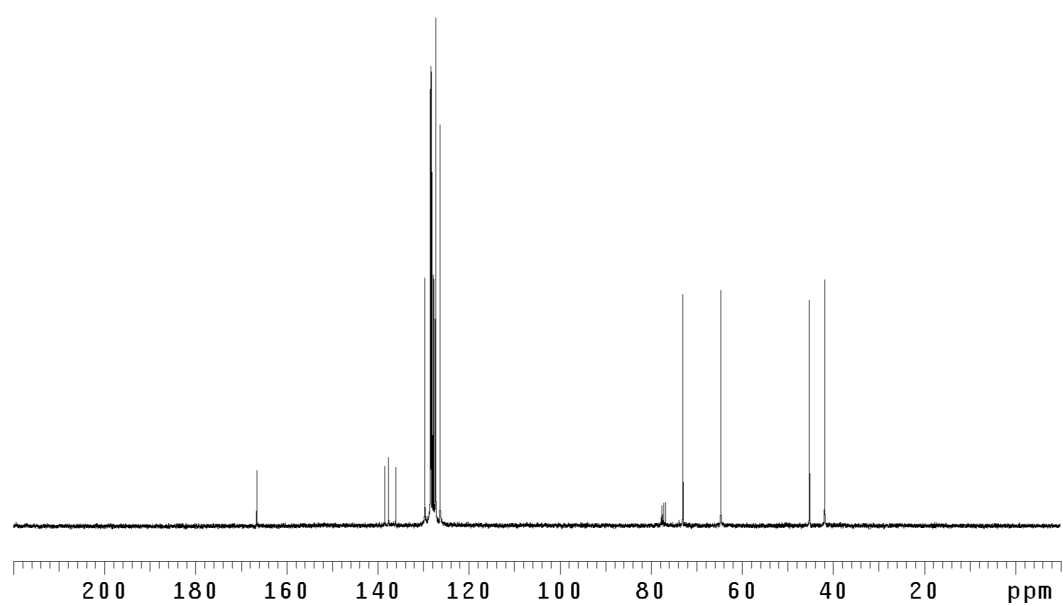
Figure A.1.45 ¹³CNMR (75 Mhz, CDCl₃) of compound **104**.
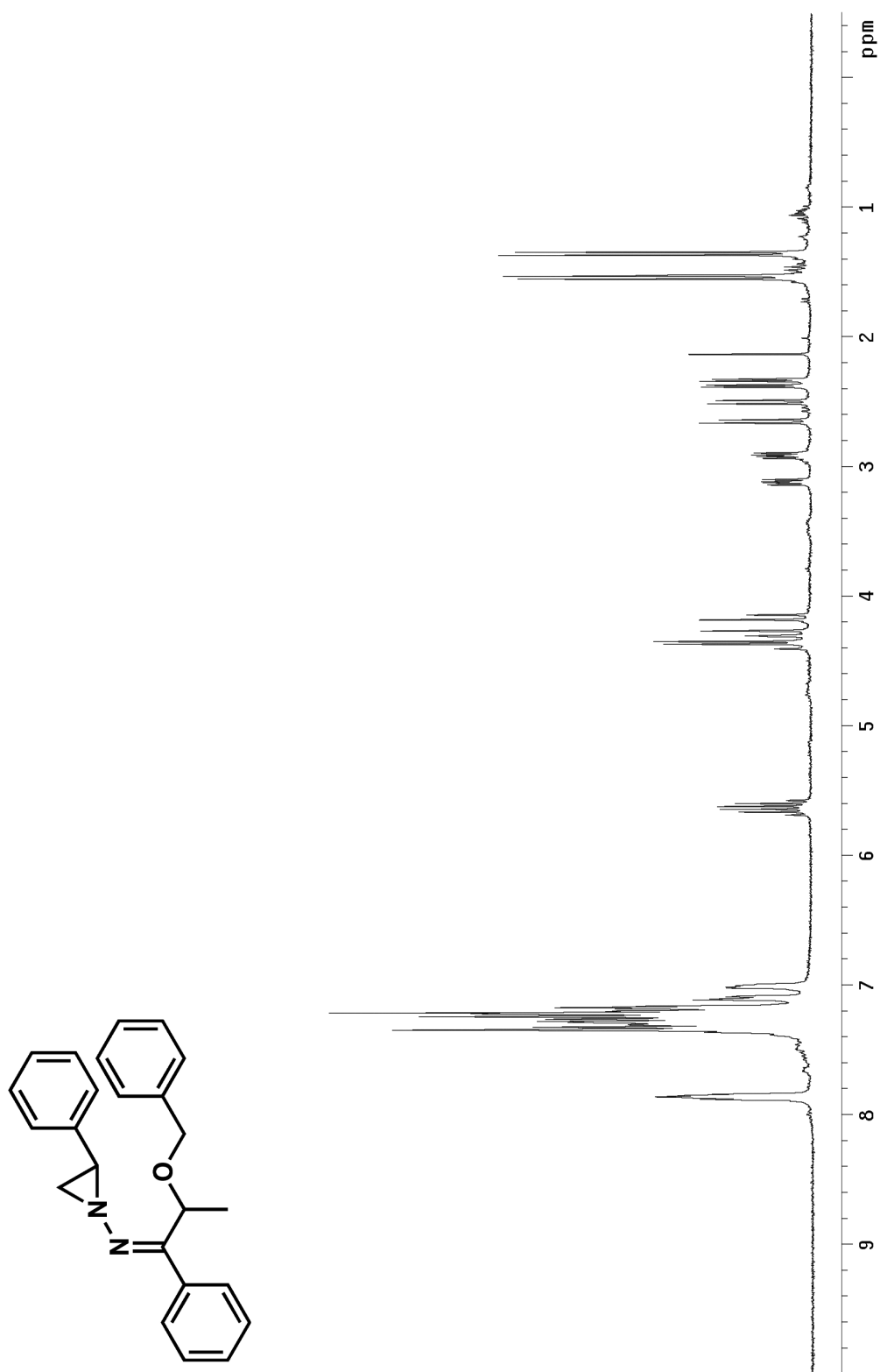
Figure A.1.46 ^{1}HNMR (300 MHz, CDCL$_3$) of compound **106**.
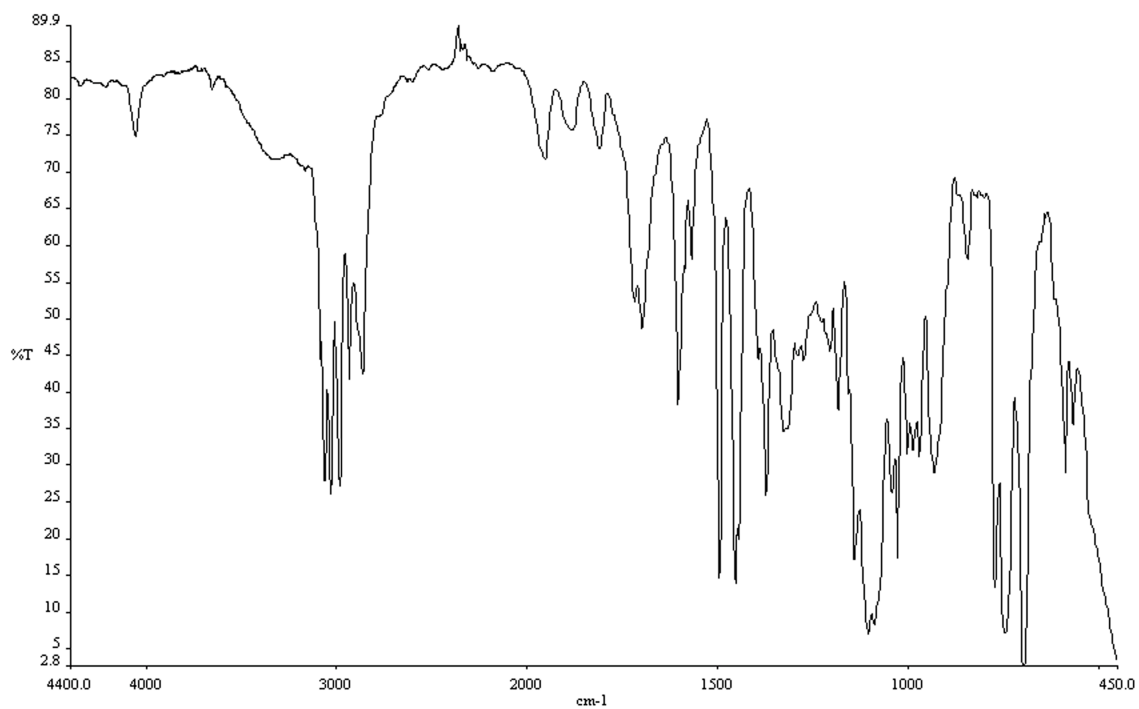
Figure A.1.47 Infrared spectrum (thin film/NaCl) of compound **106**.
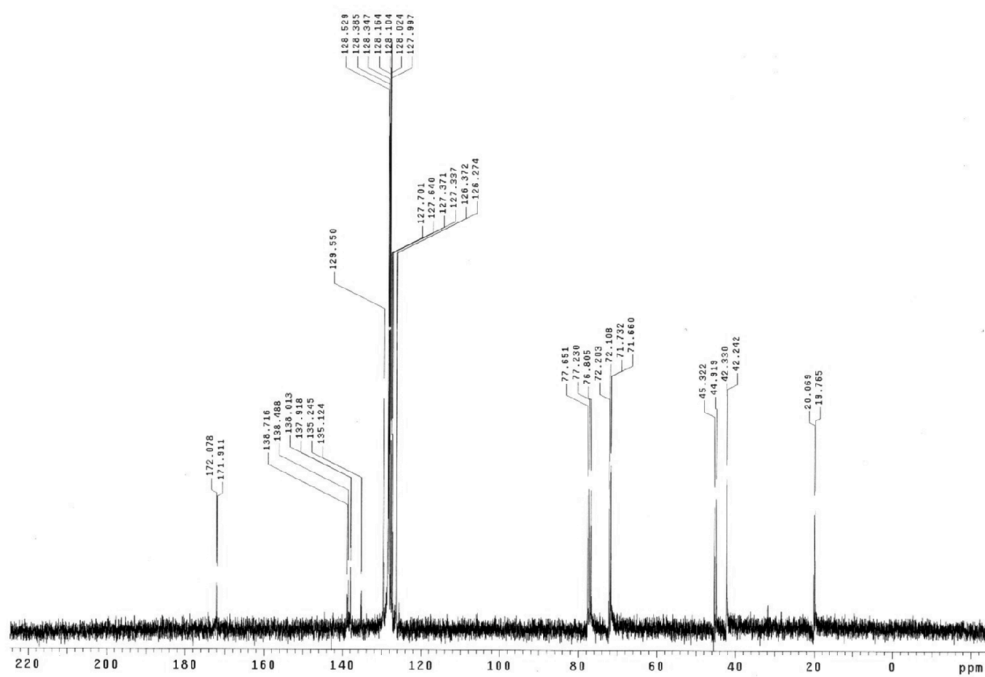
Figure A.1.48 ^{13}CNMR (75 Mhz, CDCl$_3$) of compound **106**.
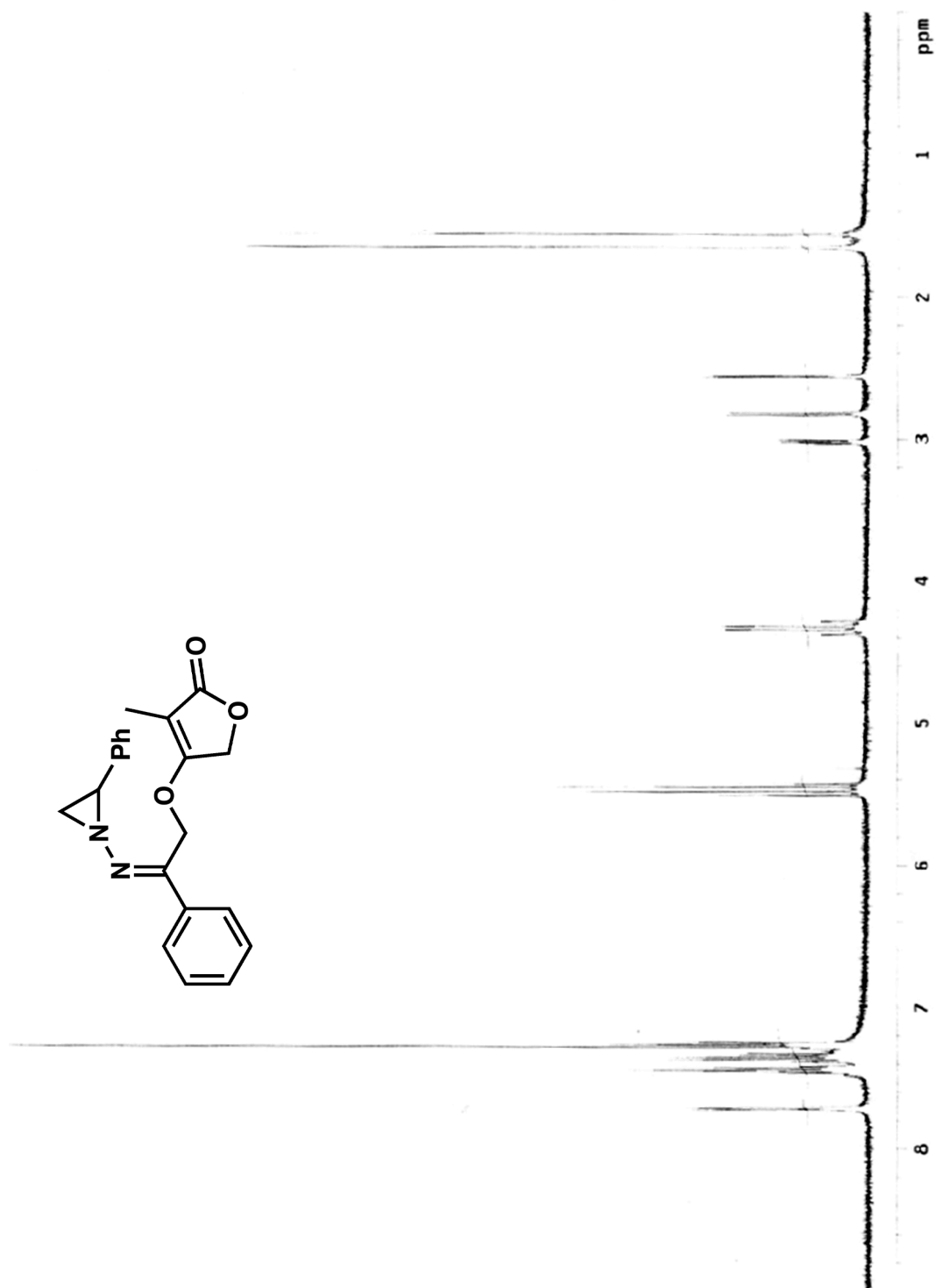
Figure A.1.49 ¹HNMR (300 MHz, CDCL₃) of compound **95**.

Figure A.1.50 Infrared spectrum (thin film/NaCl) of compound **95**.
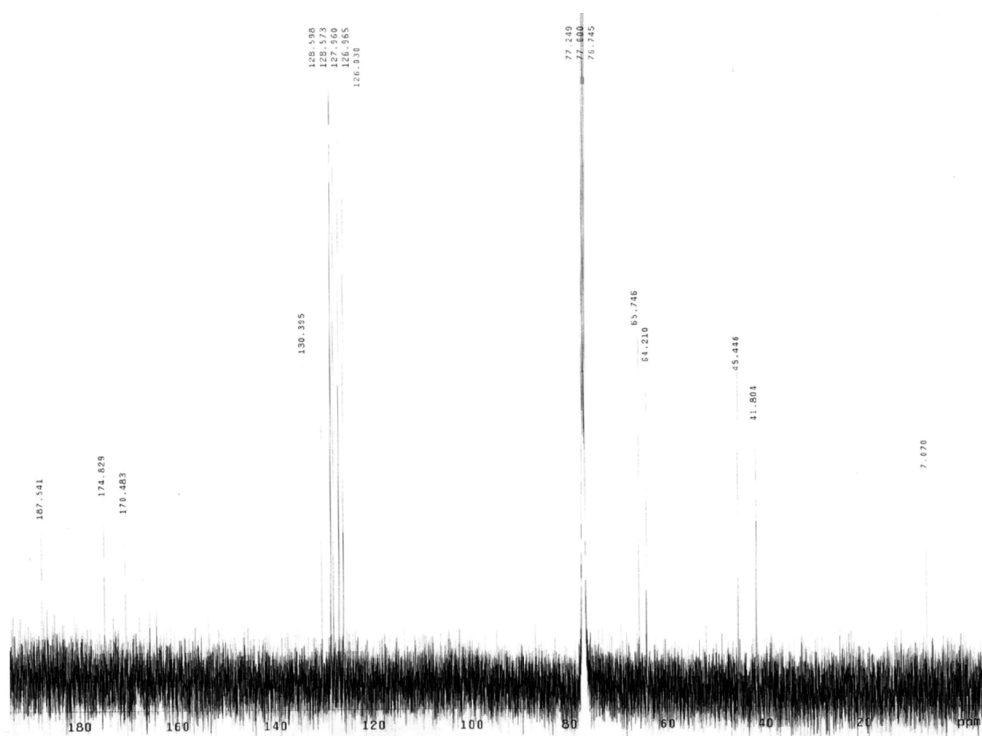
Figure A.1.51 ¹³CNMR (75 Mhz, CDCl₃) of compound **95**.
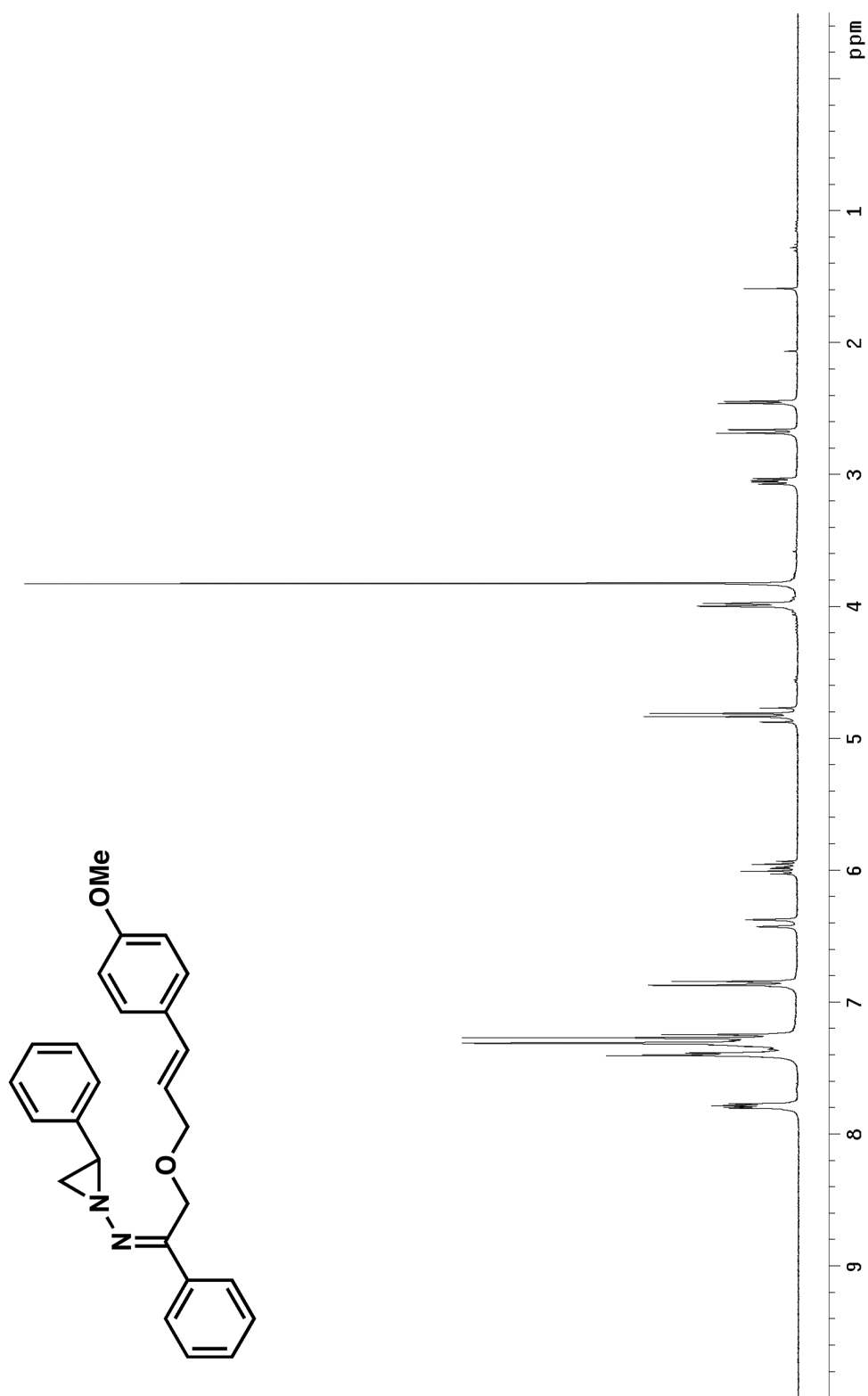
Figure A.1.52 ¹HNMR (300 MHz, CDCL₃) of compound **165**.
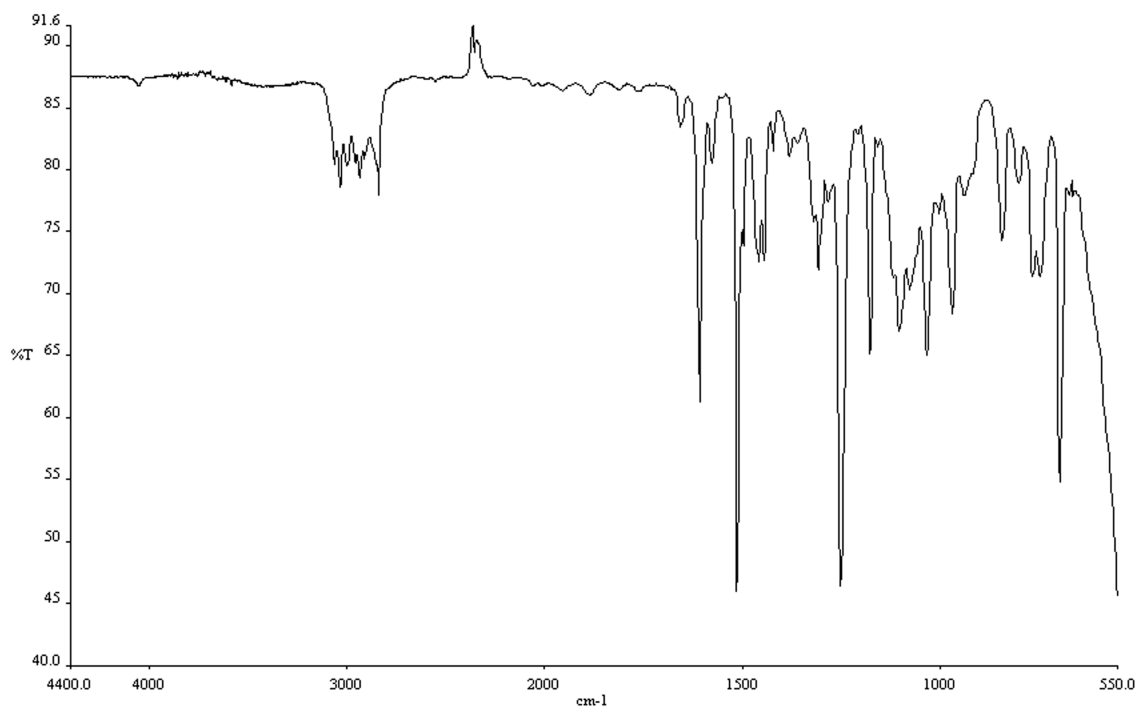
Figure A.1.53 Infrared spectrum (thin film/NaCl) of compound **165**.
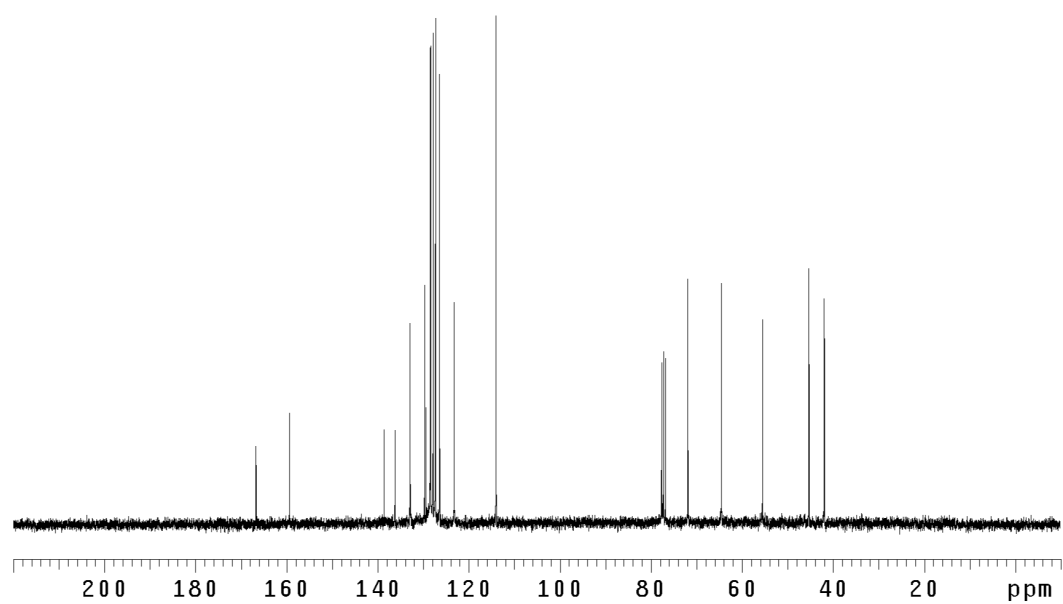
Figure A.1.54 ^{13}CNMR (75 Mhz, CDCl$_3$) of compound **165**.
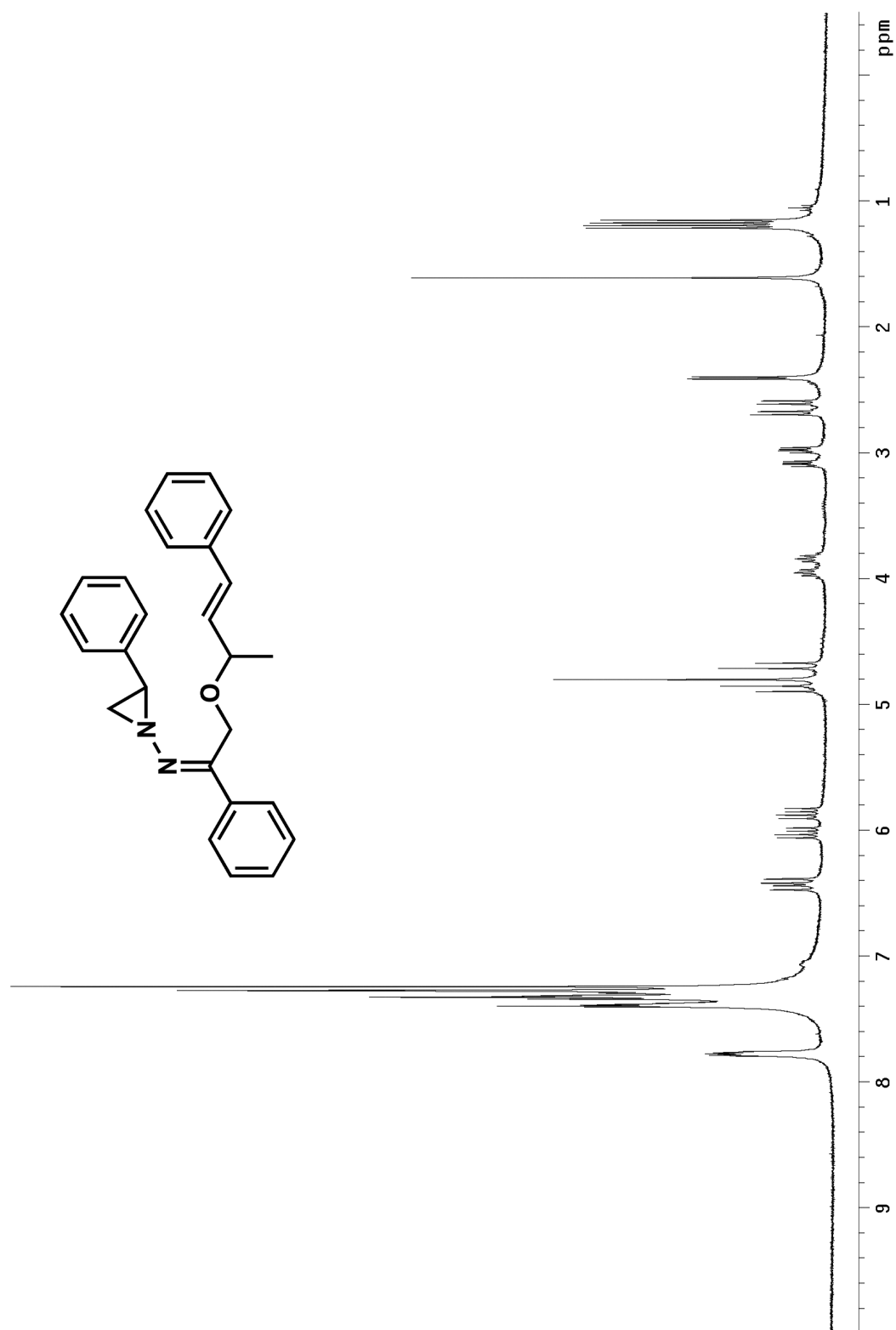
Figure A.1.55 ¹HNMR (300 MHz, CDCL₃) of compound **167**.
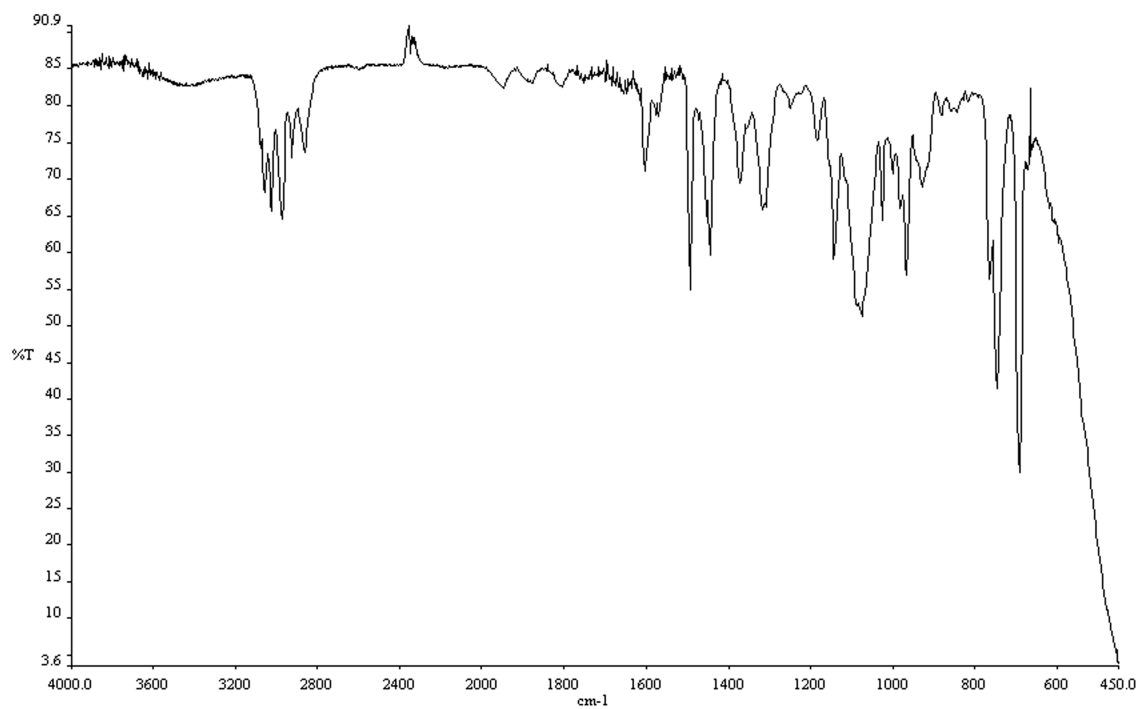
Figure A.1.56 Infrared spectrum (thin film/NaCl) of compound **167**.
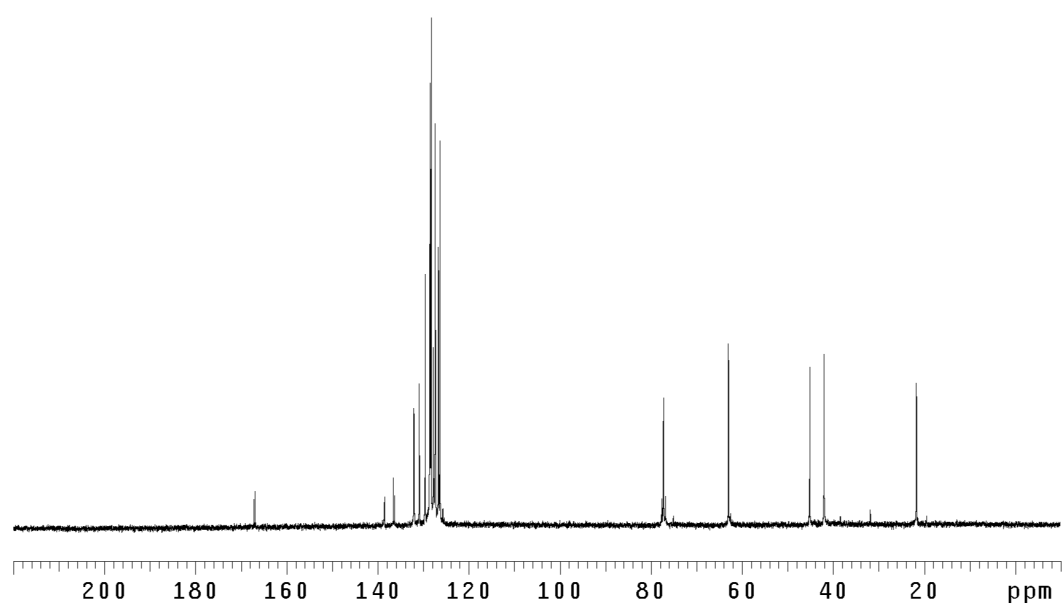
Figure A.1.57 ¹³CNMR (75 Mhz, CDCl₃) of compound **167**.
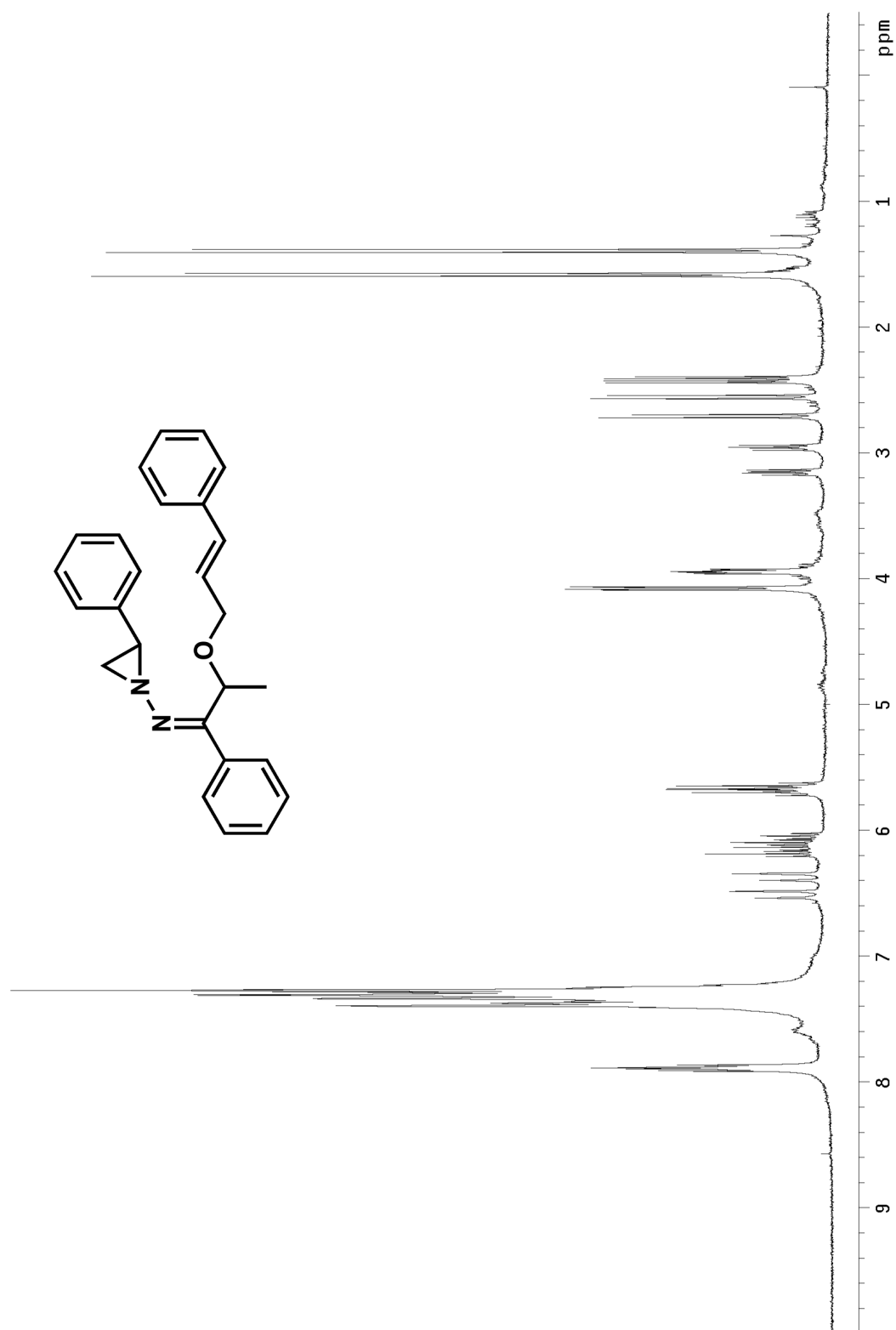
Figure A.1.58 ^{1}HNMR (300 MHz, CDCL$_3$) of compound **169**.
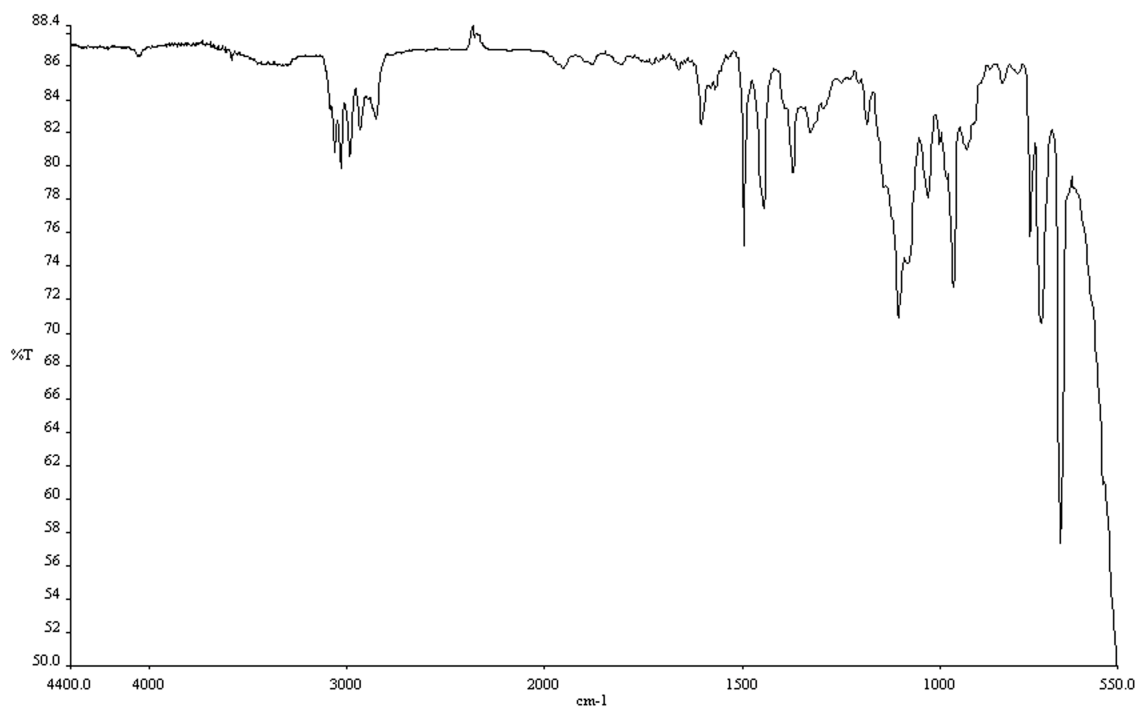
Figure A.1.59 Infrared spectrum (thin film/NaCl) of compound **169**.
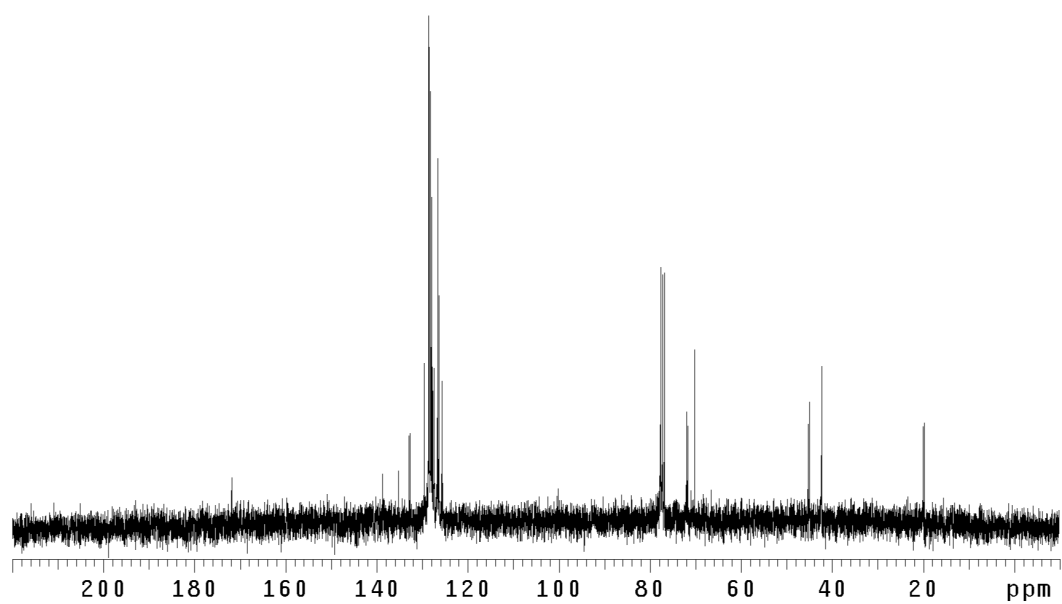
Figure A.1.60 ^{13}CNMR (75 Mhz, CDCl$_3$) of compound **169**.
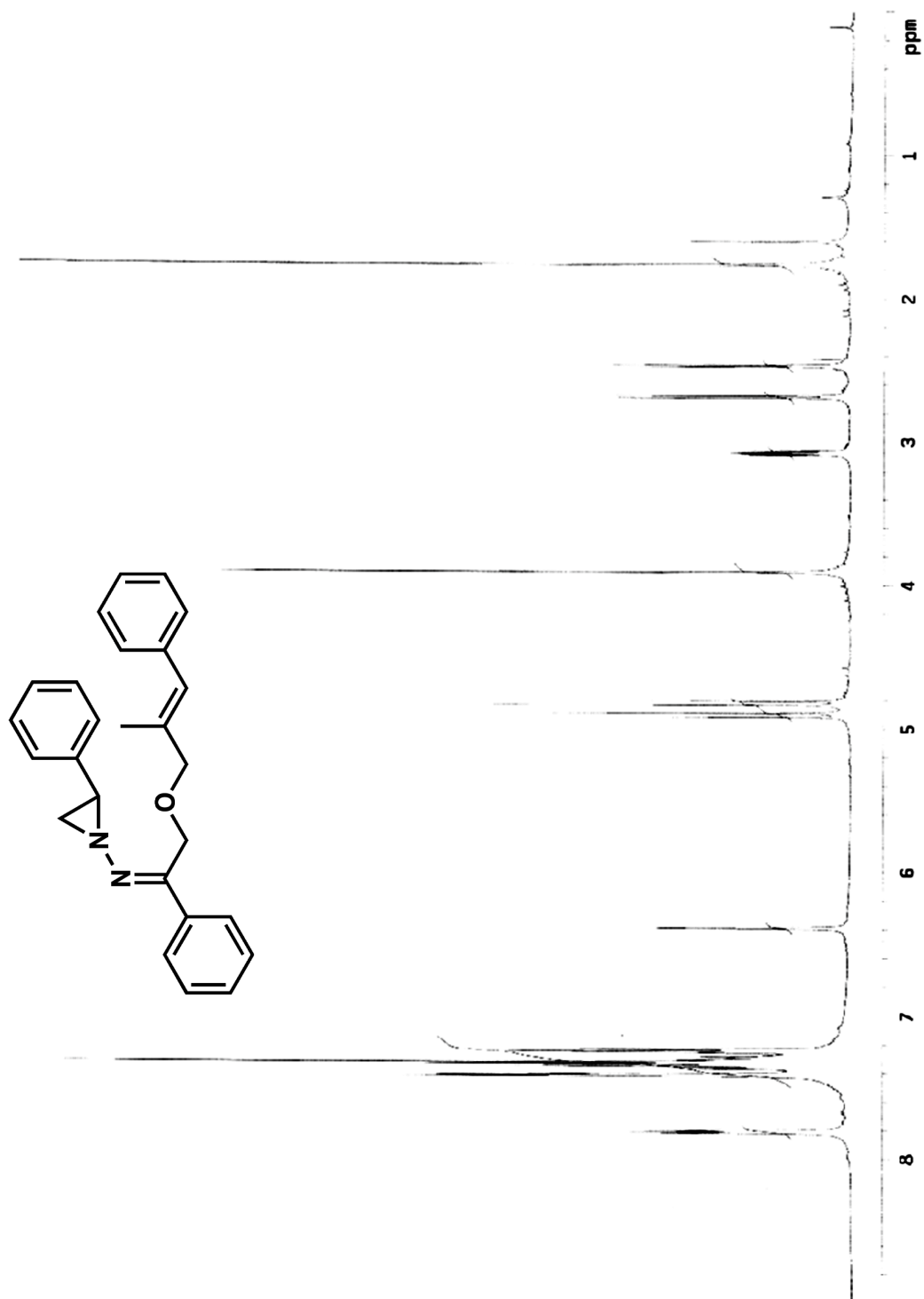
Figure A.1.61 ¹HNMR (300 MHz, CDCL₃) of compound **171**.

Figure A.1.62 Infrared spectrum (thin film/NaCl) of compound **171**.

Figure A.1.63 ^{13}CNMR (75 Mhz, CDCl$_3$) of compound **171**.
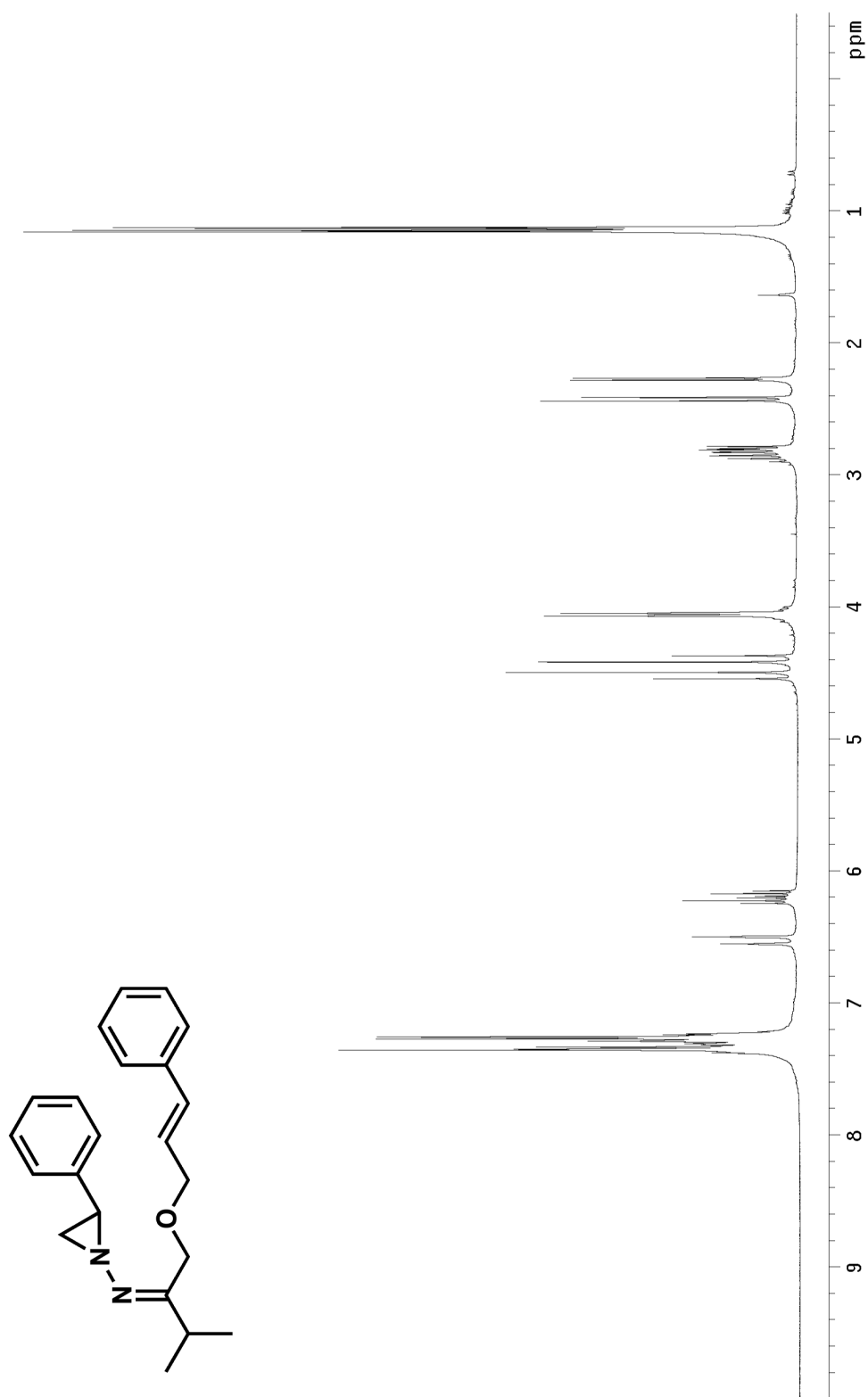
Figure A.1.64 ¹HNMR (300 MHz, CDCL₃) of compound **173**.
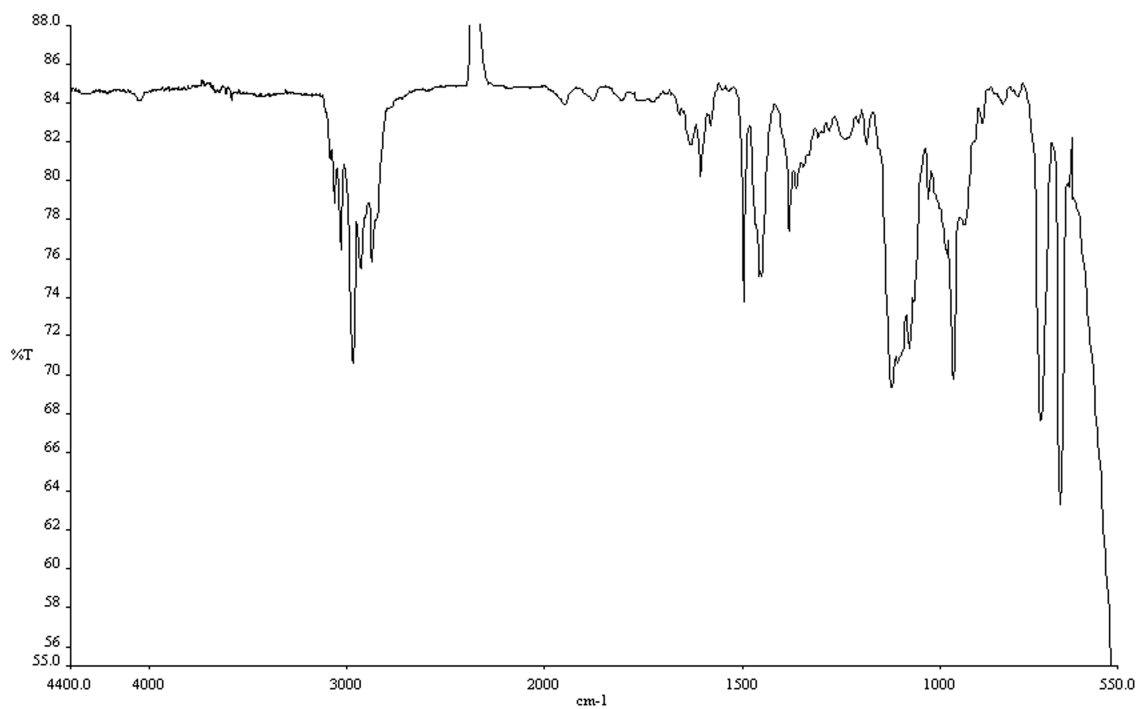
Figure A.1.65 Infrared spectrum (thin film/NaCl) of compound **173**.
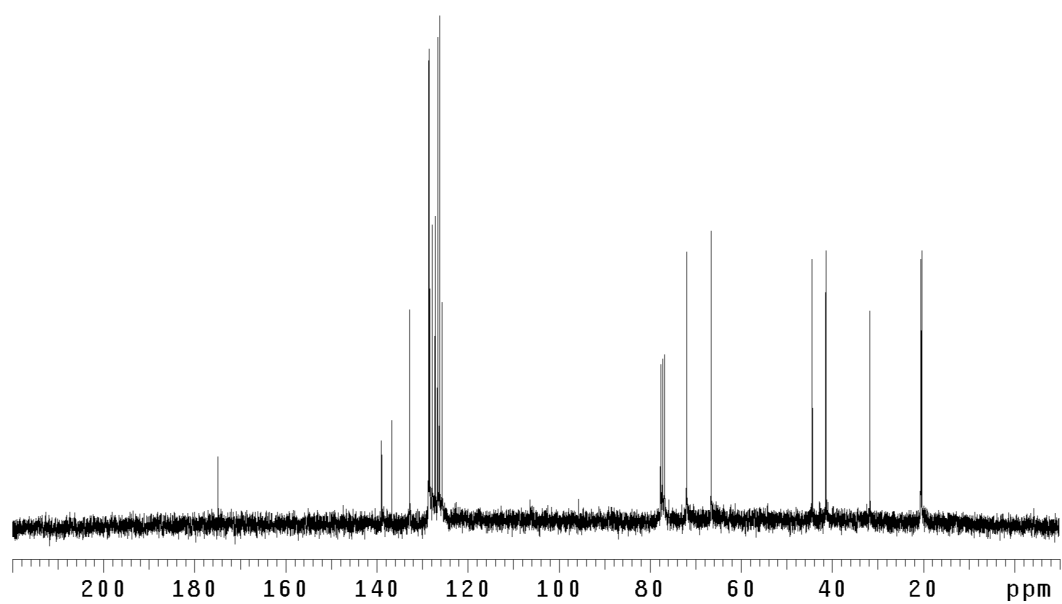
Figure A.1.66 ^{13}CNMR (75 Mhz, CDCl$_3$) of compound **173**.
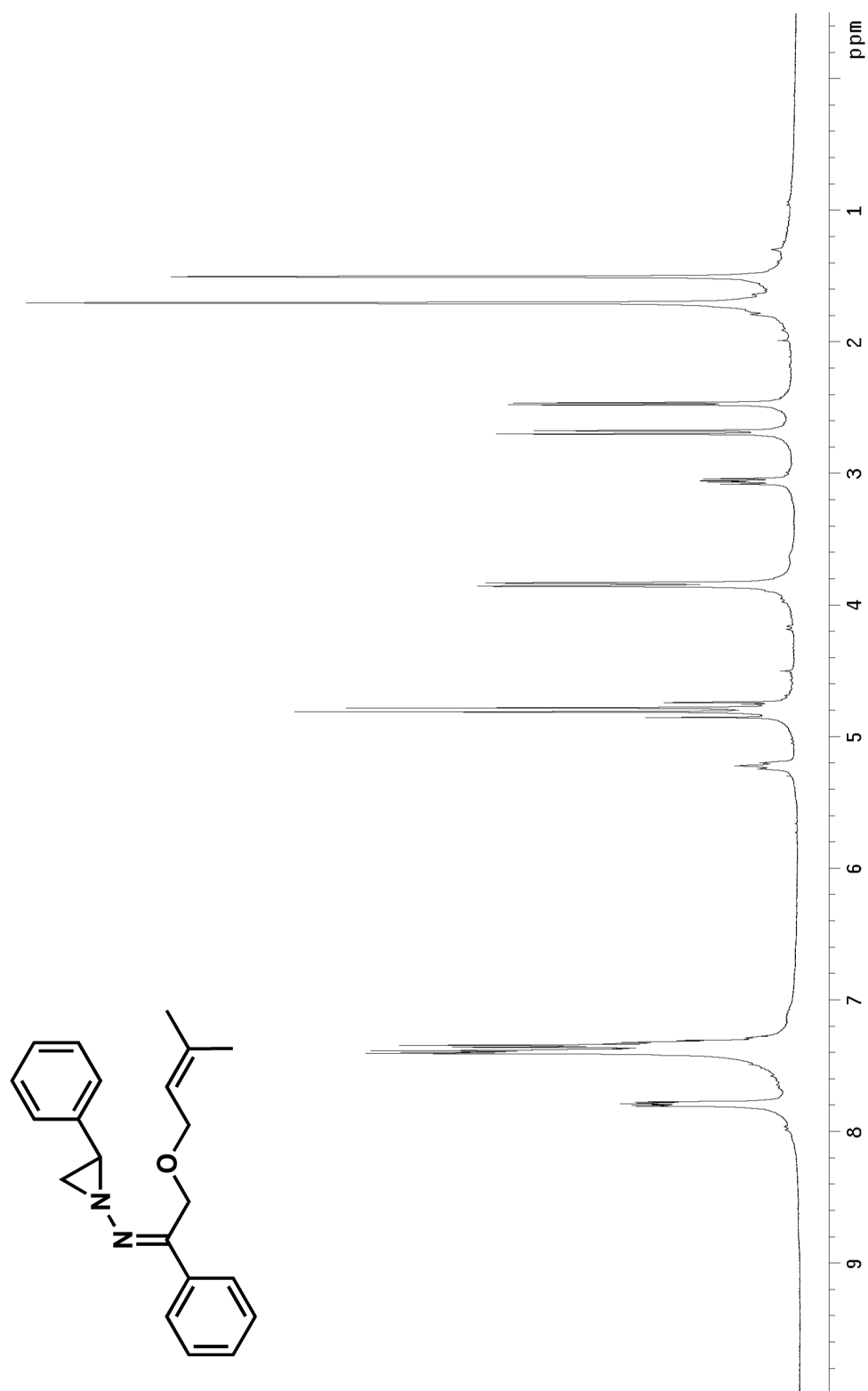
Figure A.1.67 ¹HNMR (300 MHz, CDCL₃) of compound **179**.
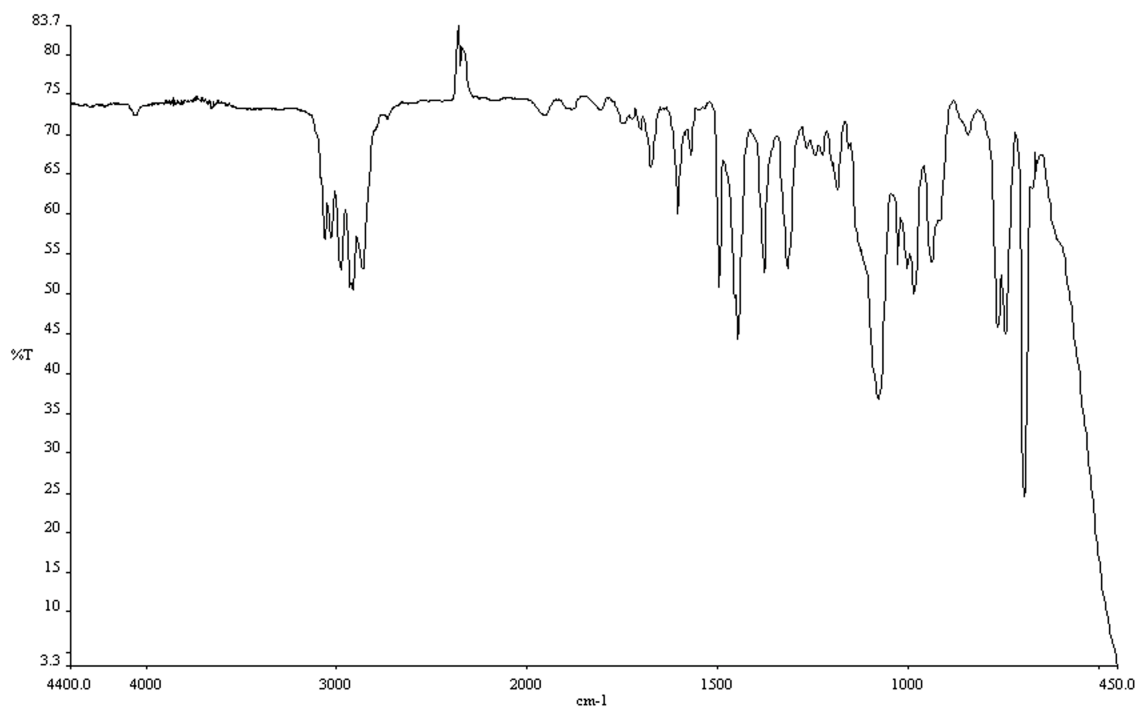
Figure A.1.68 Infrared spectrum (thin film/NaCl) of compound **179**.
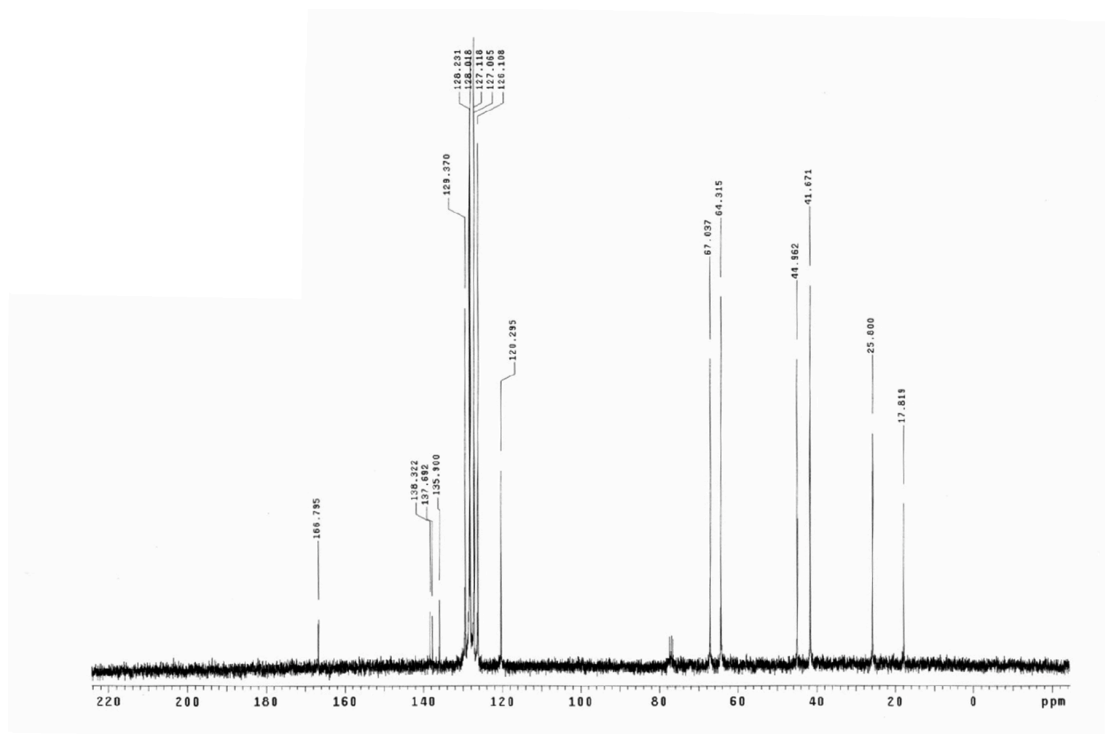
Figure A.1.69 ^{13}CNMR (75 Mhz, CDCl$_3$) of compound **179**.
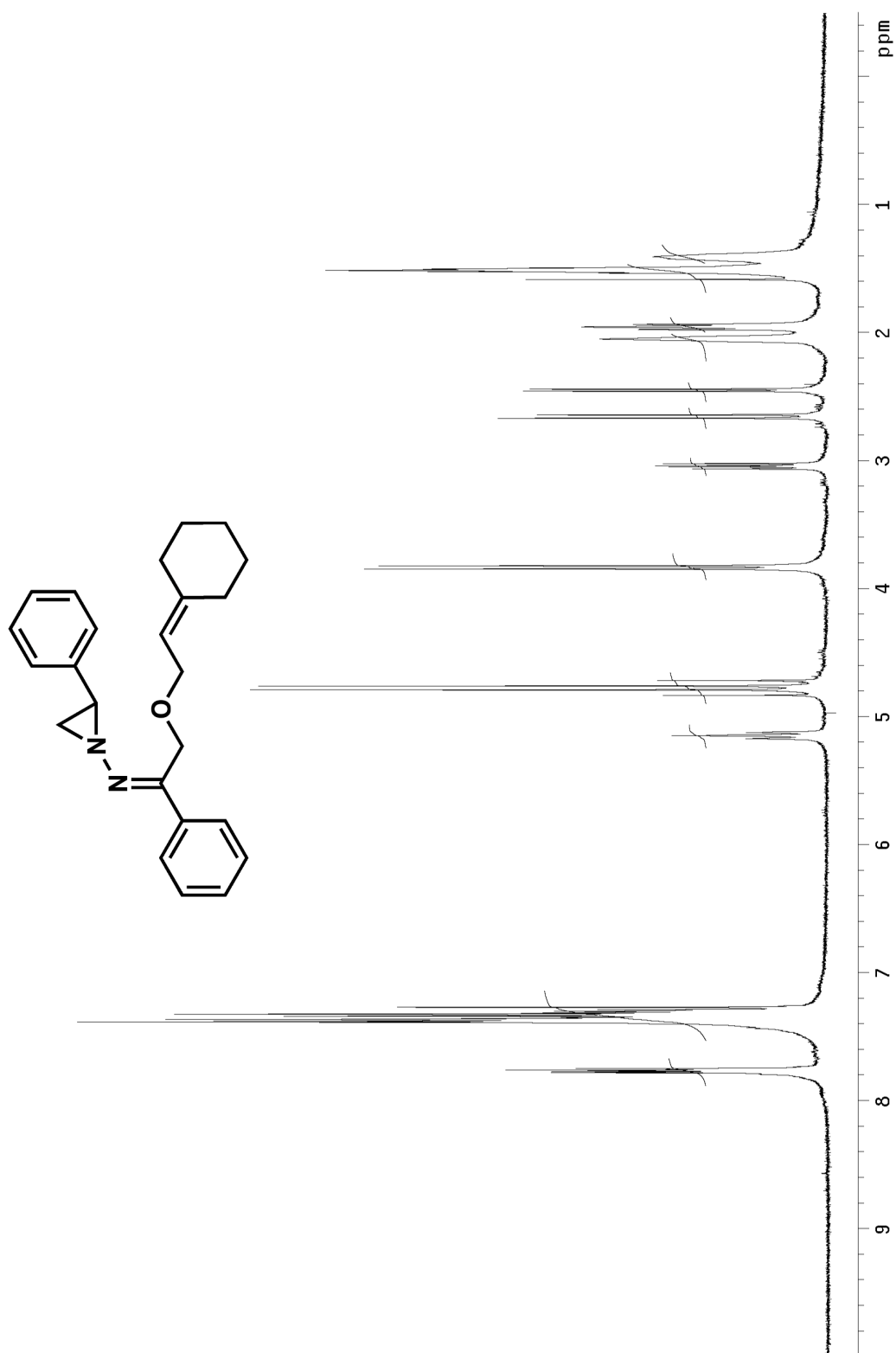
Figure A.1.70 ¹HNMR (300 MHz, CDCL₃) of compound **181**.
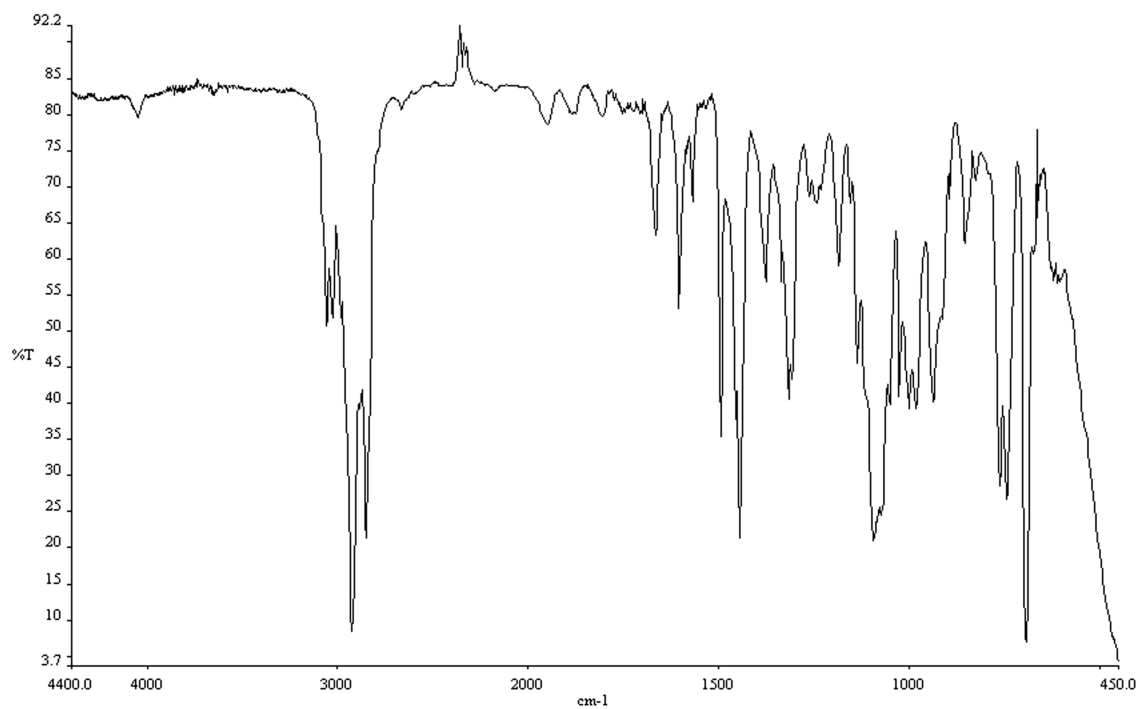
Figure A.1.71 Infrared spectrum (thin film/NaCl) of compound **181**.
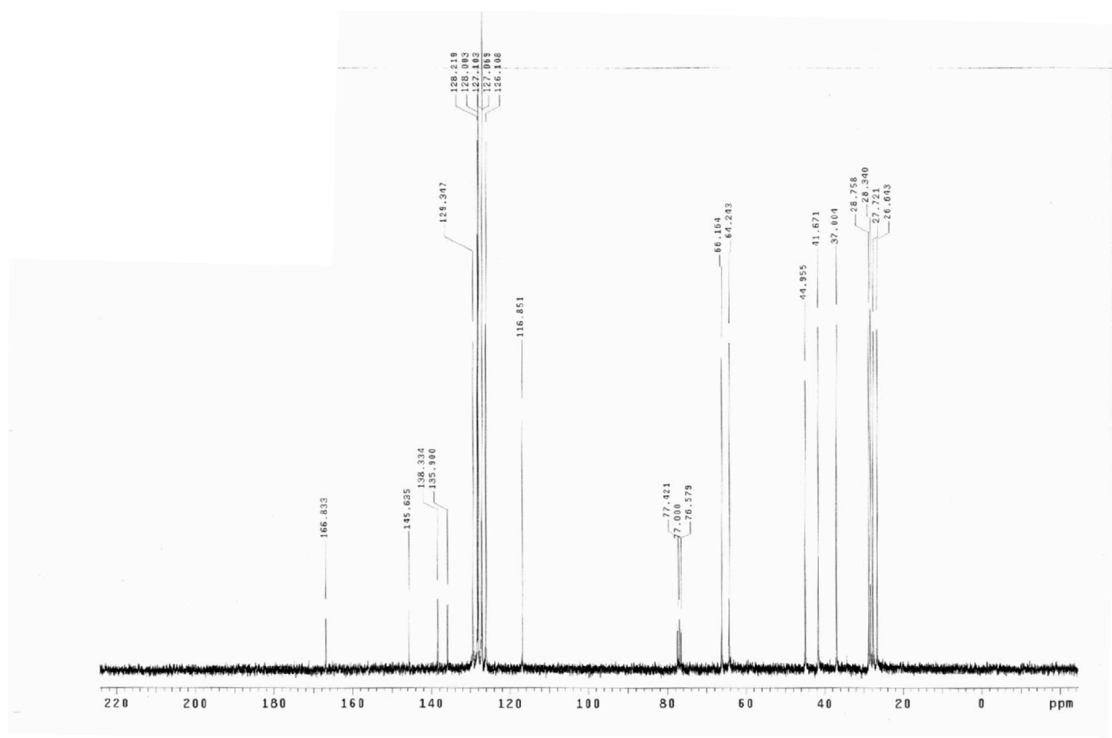
Figure A.1.72 ^{13}CNMR (75 Mhz, CDCl$_3$) of compound **181**.
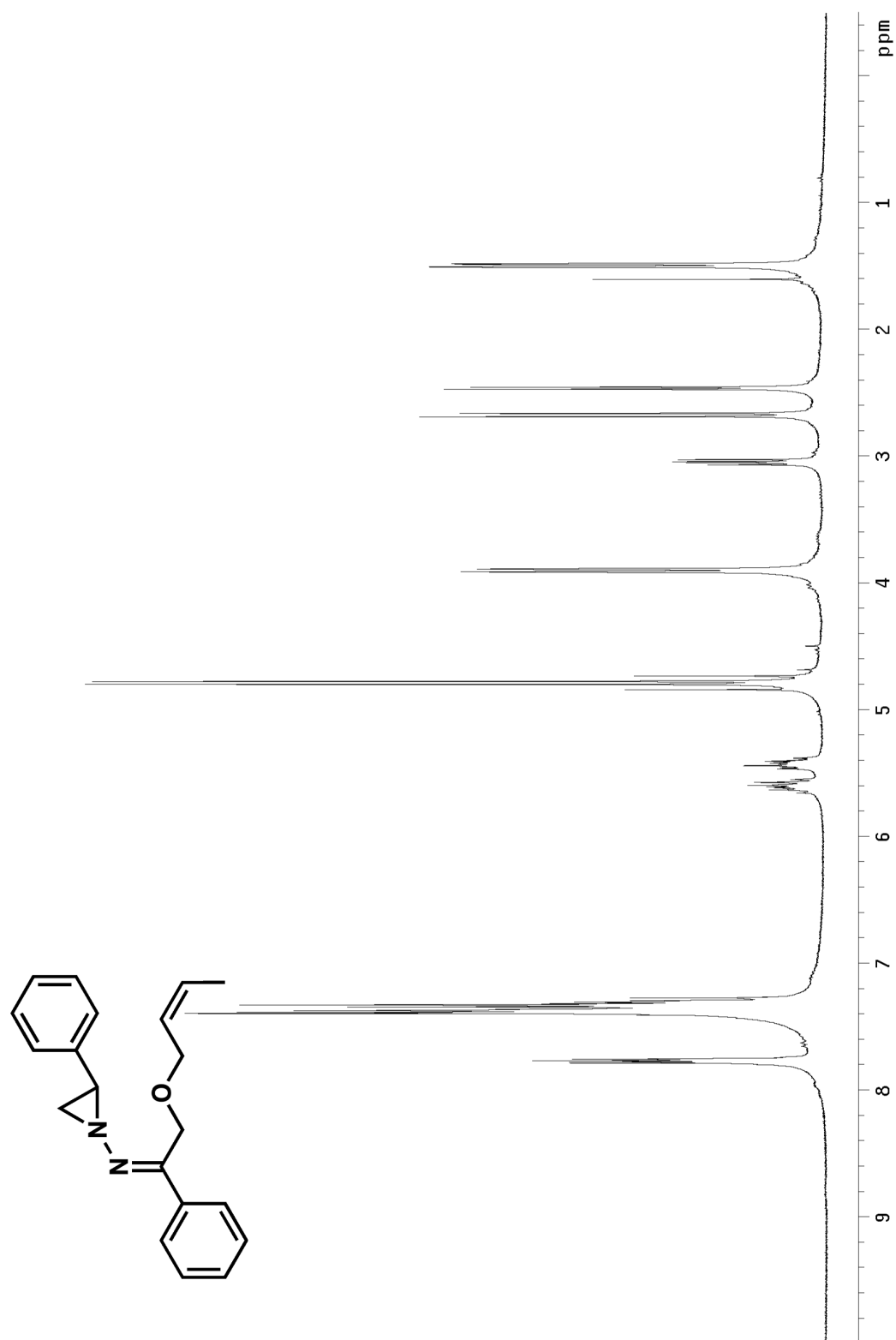
Figure A.1.73 ¹HNMR (300 MHz, CDCL₃) of compound **183**.
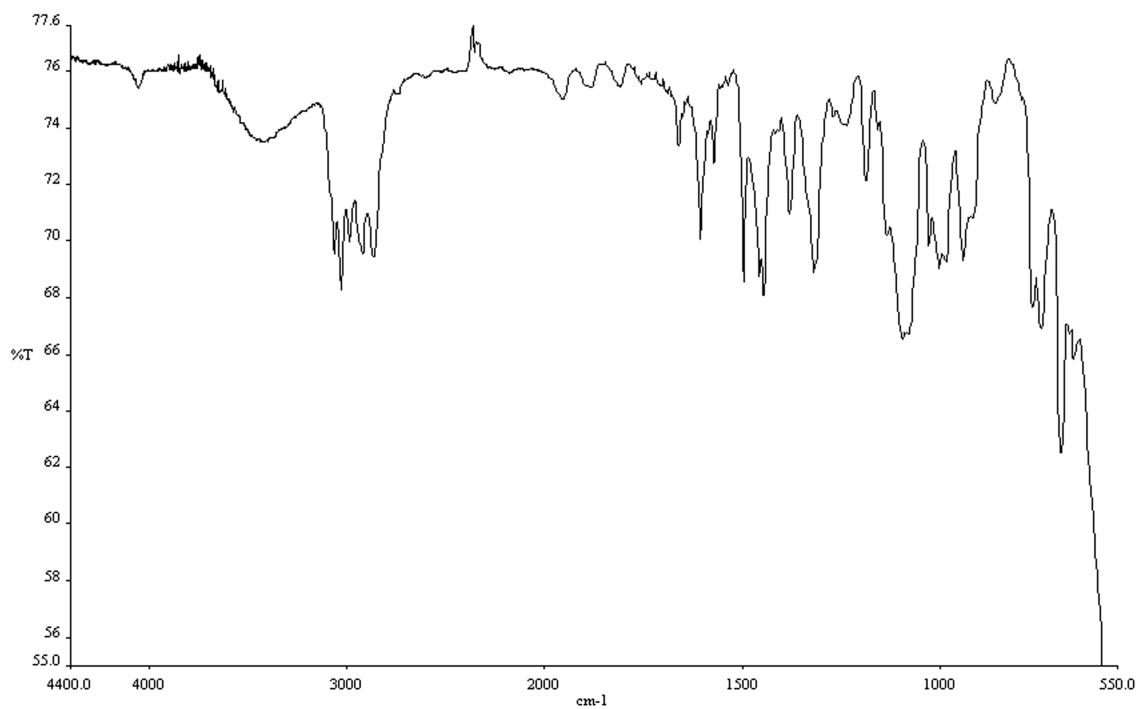
Figure A.1.74 Infrared spectrum (thin film/NaCl) of compound **183**.
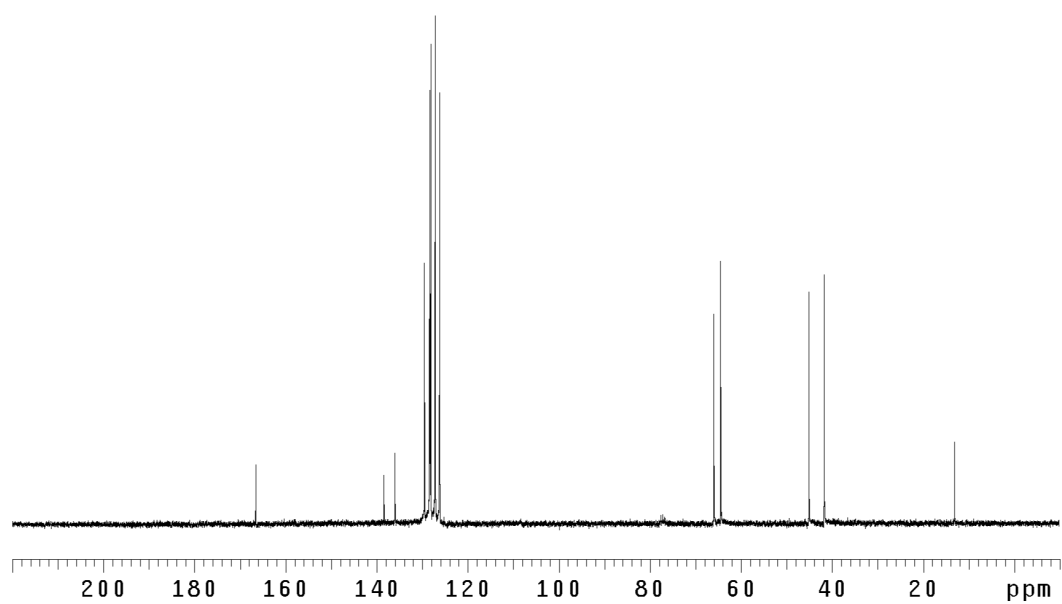
Figure A.1.75 ^{13}CNMR (75 Mhz, CDCl$_3$) of compound **183**.
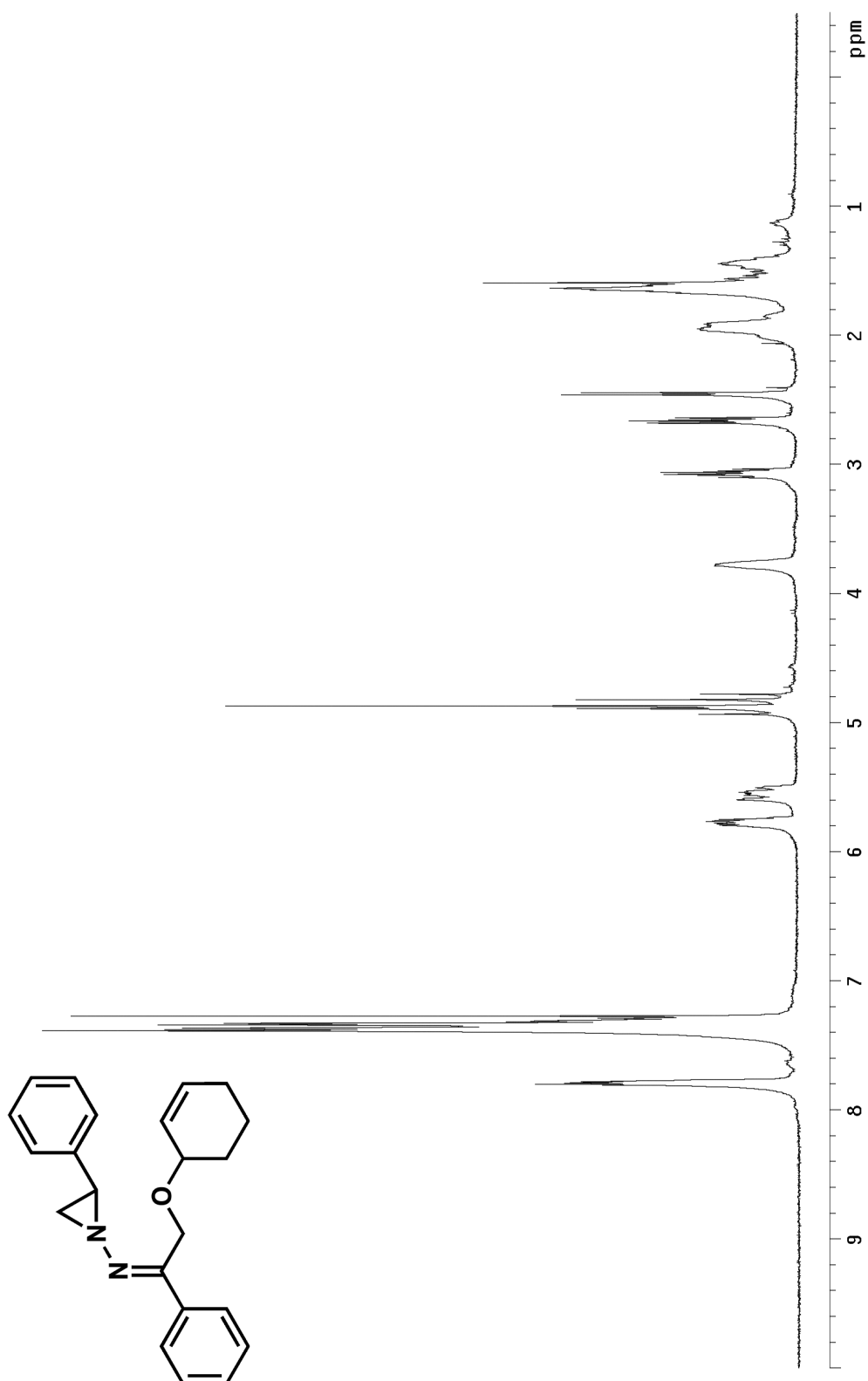
Figure A.1.76 ¹HNMR (300 MHz, CDCL₃) of compound **185**.
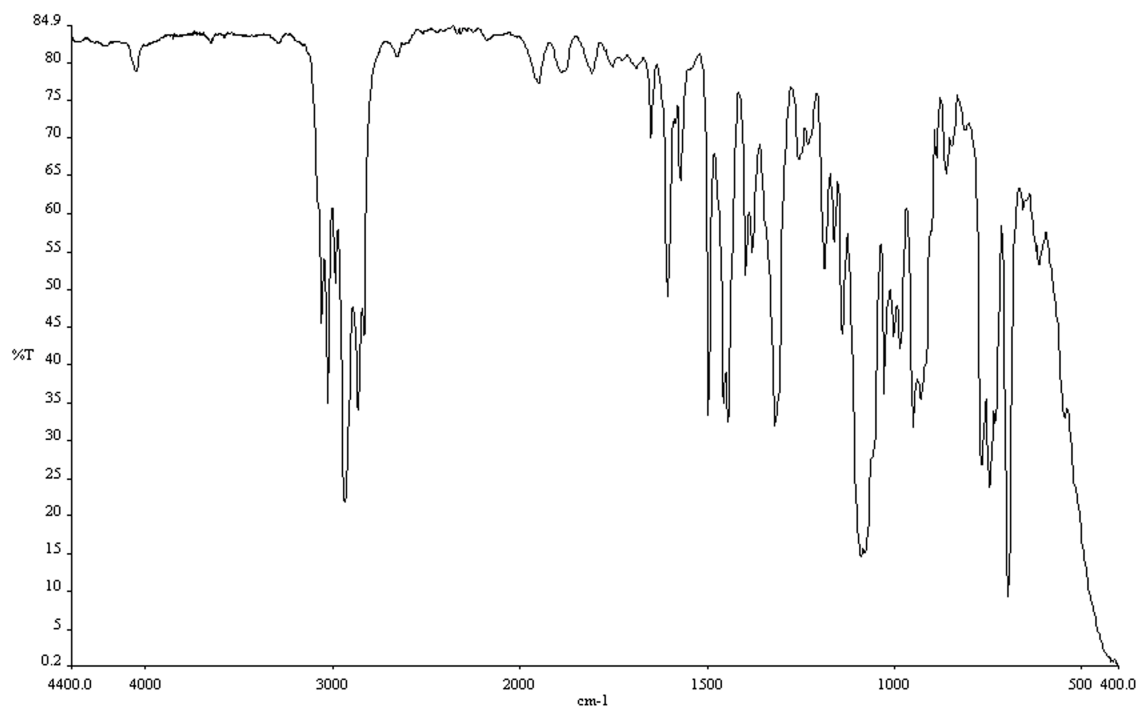
Figure A.1.77 Infrared spectrum (thin film/NaCl) of compound **185**.
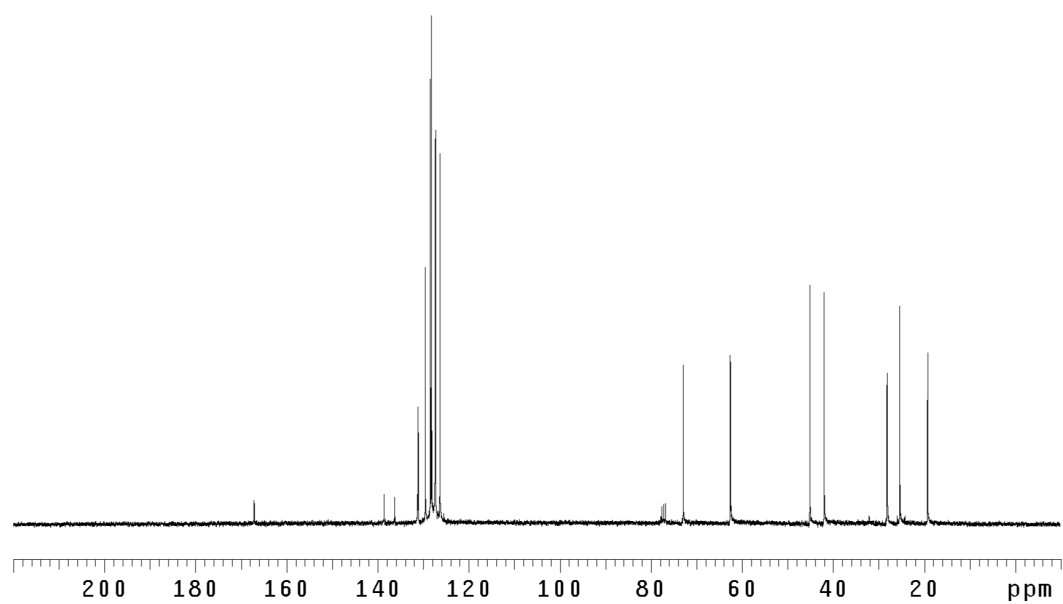
Figure A.1.78 ^{13}CNMR (75 Mhz, CDCl$_3$) of compound **185**.
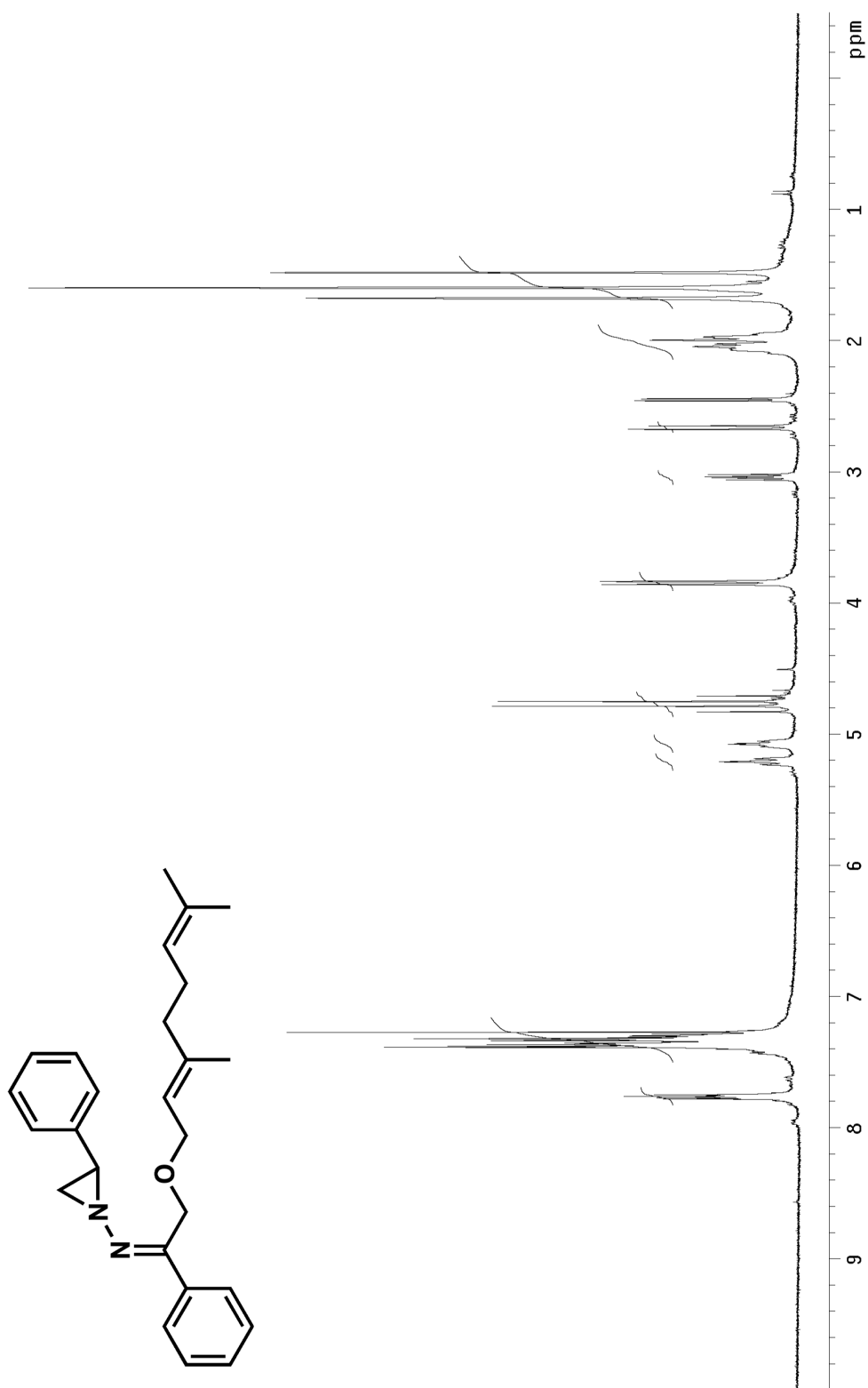
Figure A.1.79 ^{1}HNMR (300 MHz, CDCL$_3$) of compound **189**.
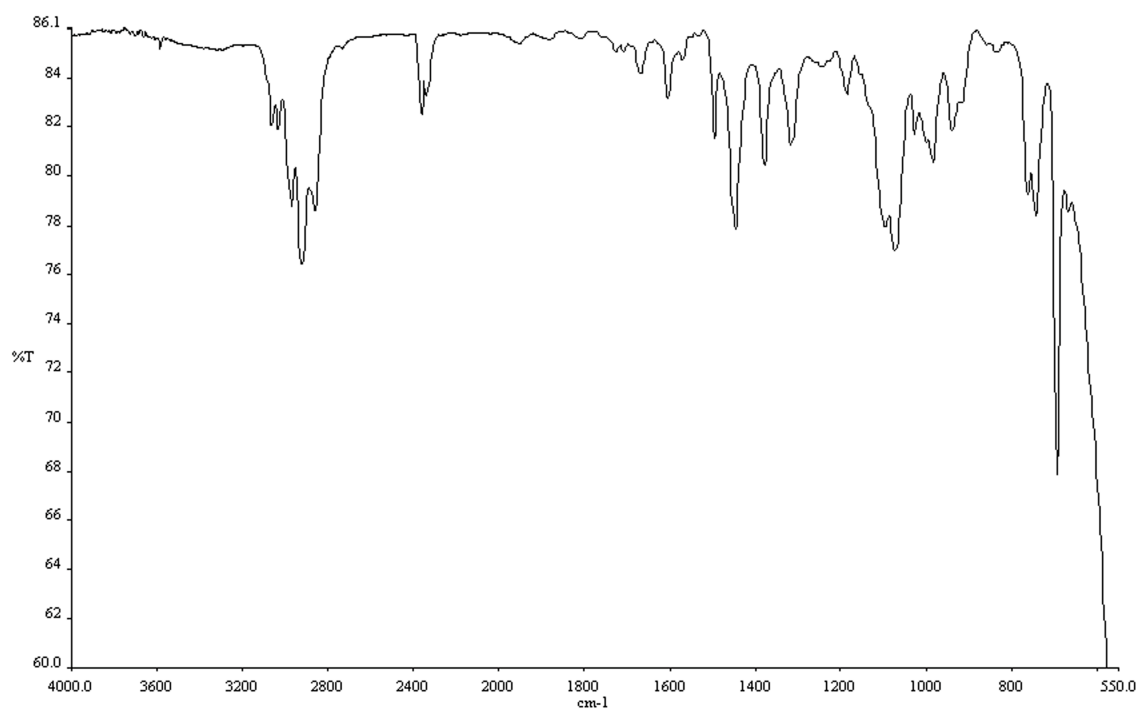
Figure A.1.80 Infrared spectrum (thin film/NaCl) of compound **189**.
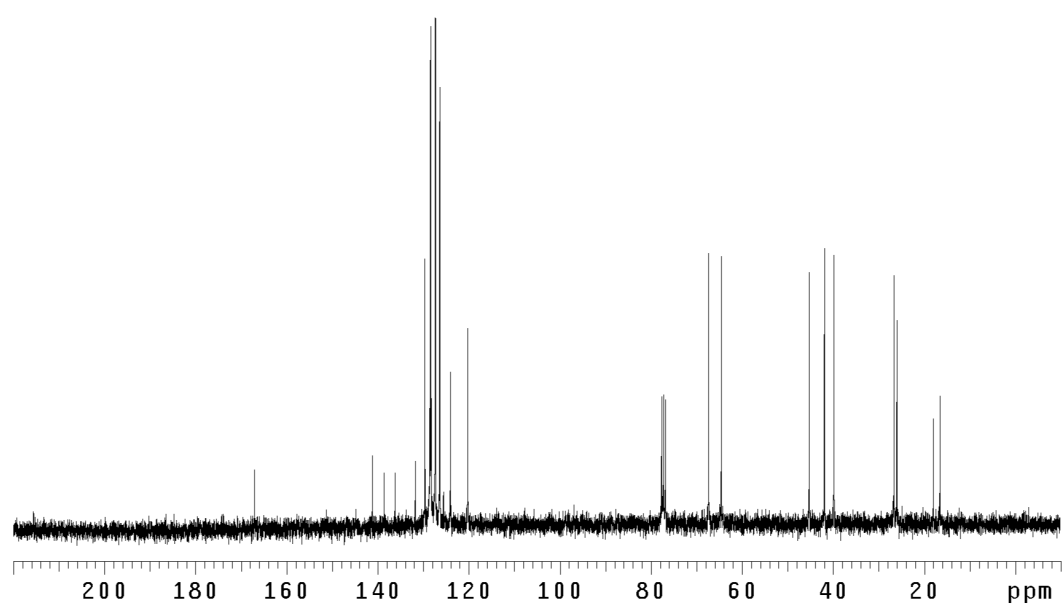
Figure A.1.81 ¹³CNMR (75 Mhz, CDCl₃) of compound **189**.
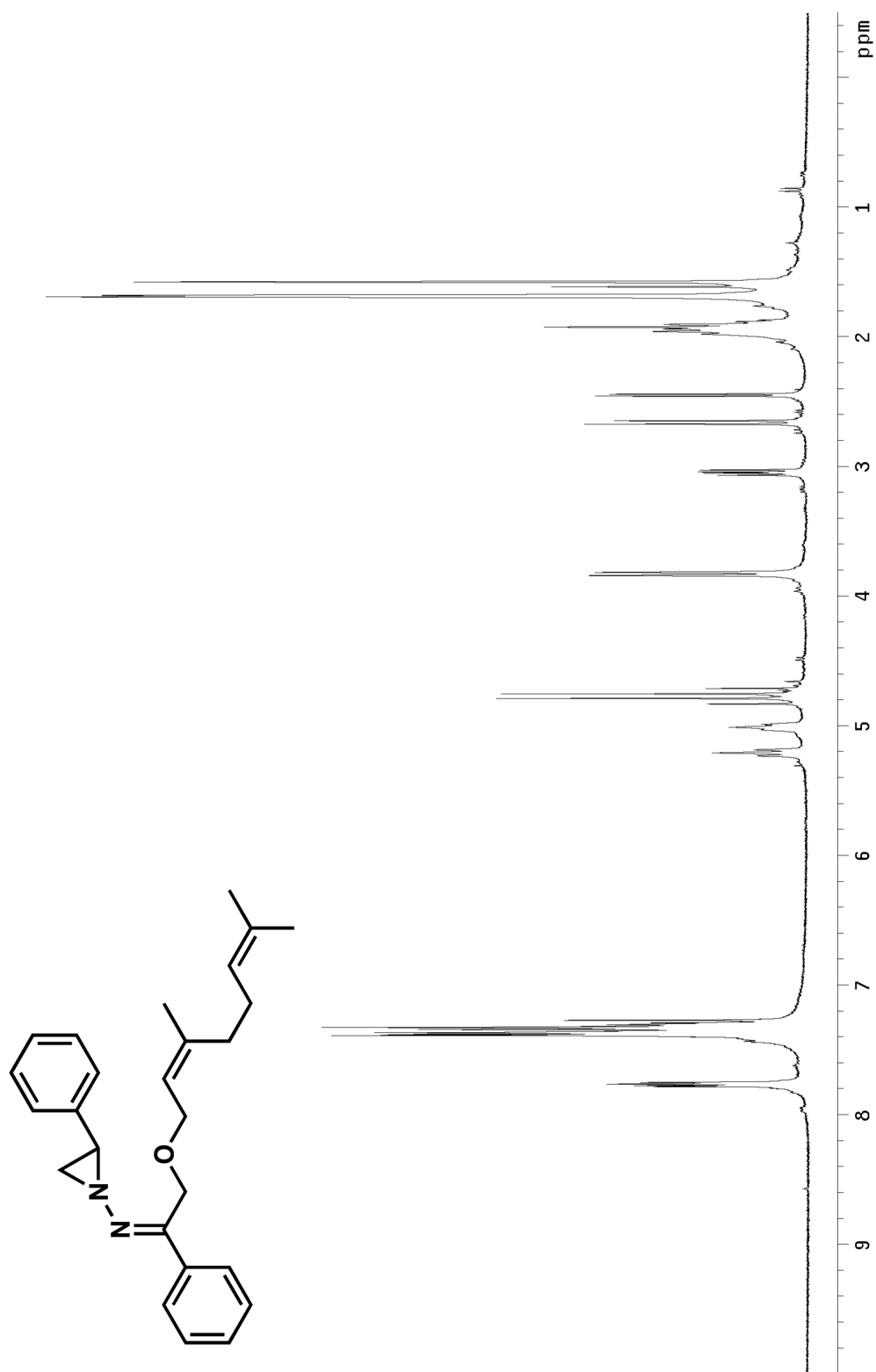
Figure A.1.82 ¹HNMR (300 MHz, CDCL₃) of compound **192**.
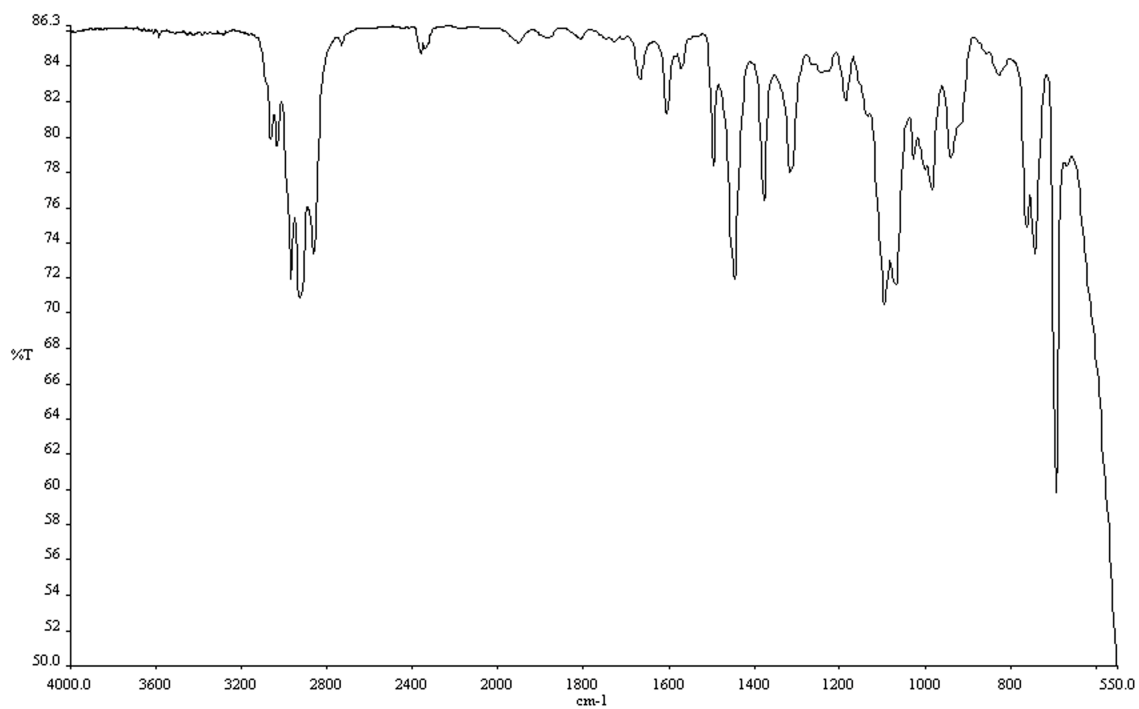
Figure A.1.83 Infrared spectrum (thin film/NaCl) of compound **192**.
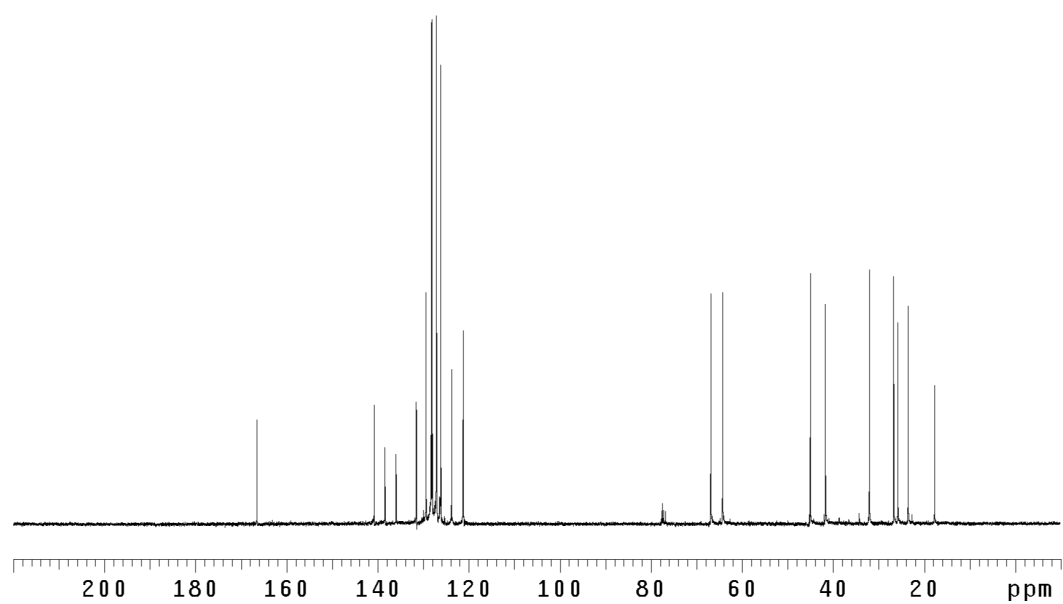
Figure A.1.84 ¹³CNMR (75 Mhz, CDCl₃) of compound **192**.
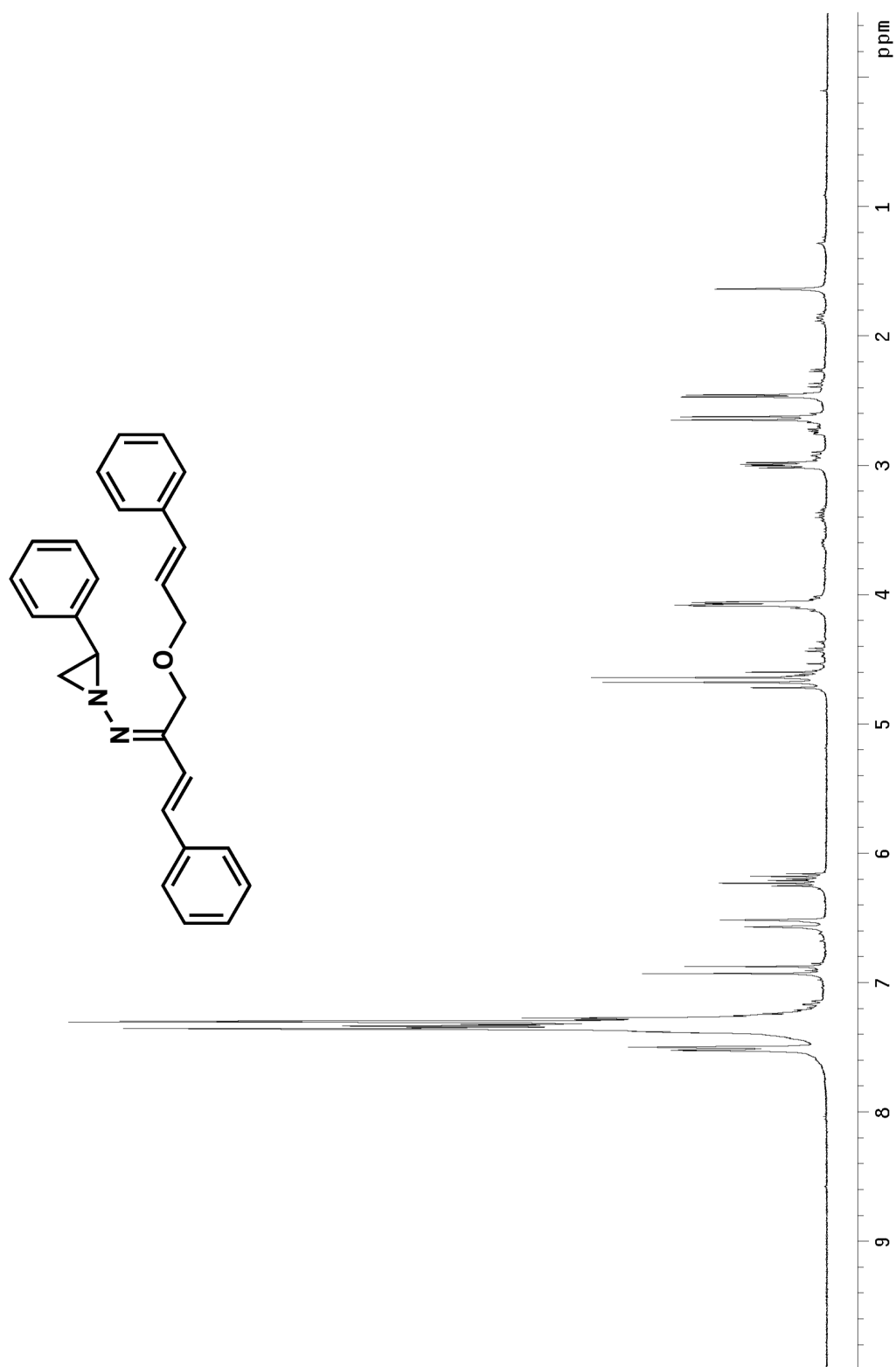
Figure A.1.85 ¹HNMR (300 MHz, CDCL₃) of compound **199**.
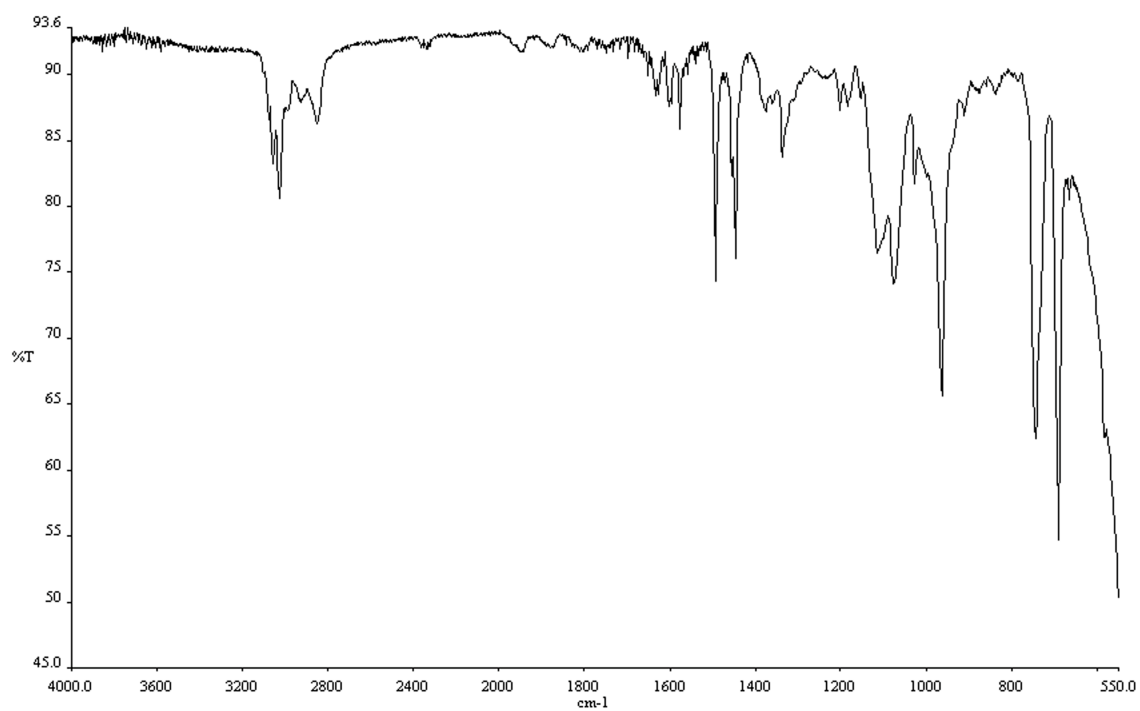
Figure A.1.86 Infrared spectrum (thin film/NaCl) of compound **199**.
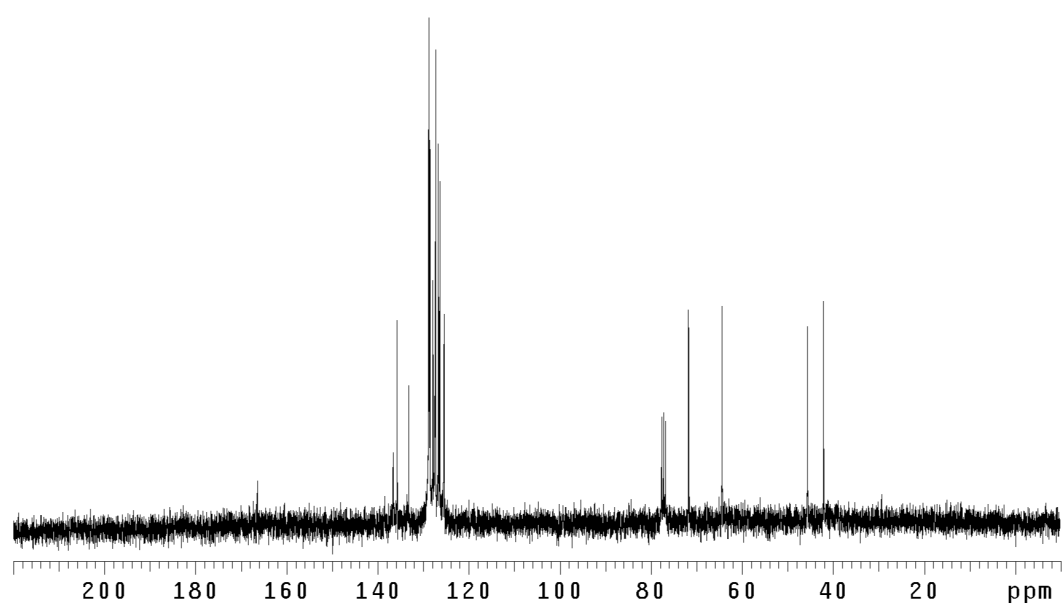
Figure A.1.87 ^{13}CNMR (75 Mhz, CDCl$_3$) of compound **199**.
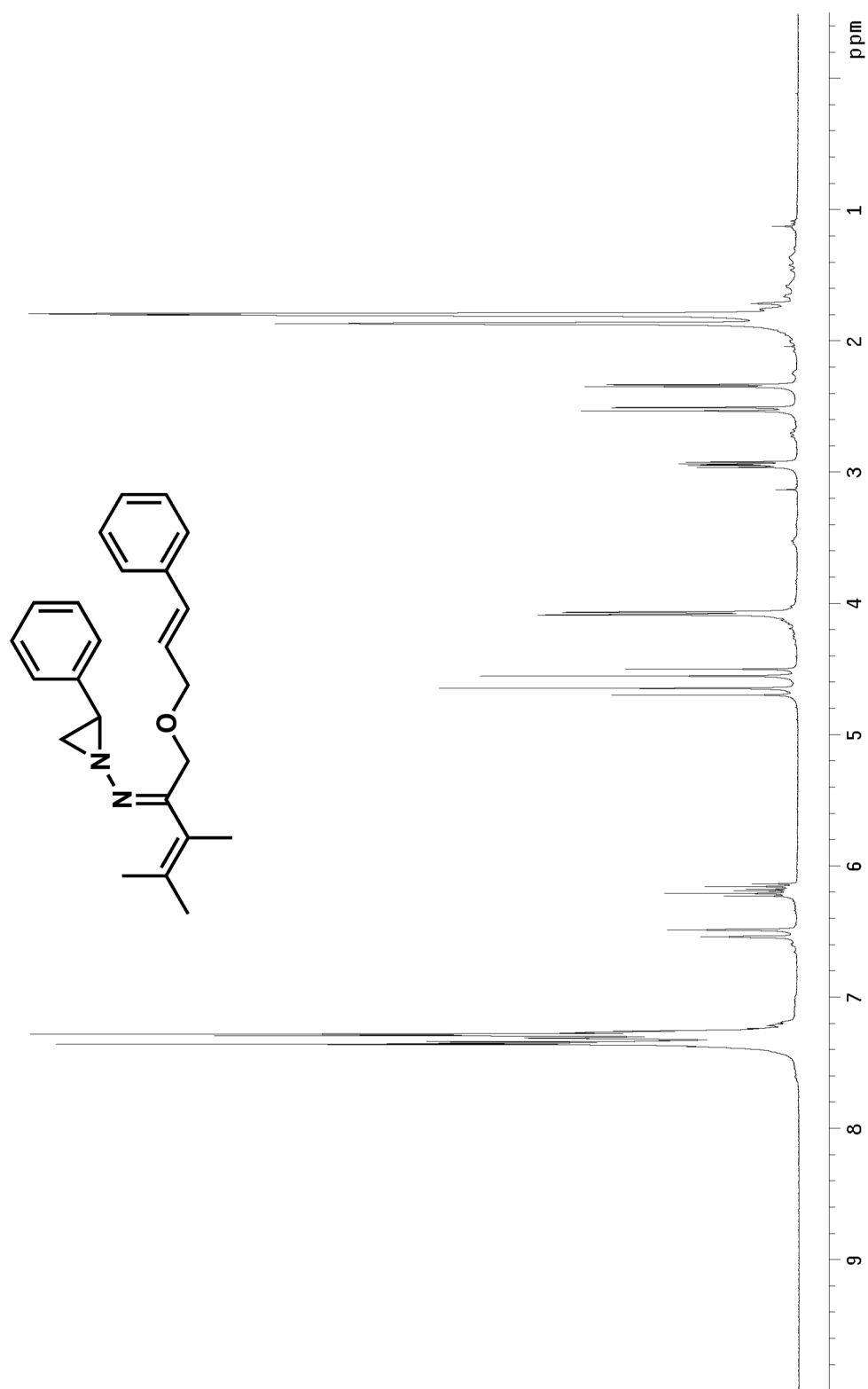
Figure A.1.88 ¹HNMR (300 MHz, CDCL₃) of compound **202**.
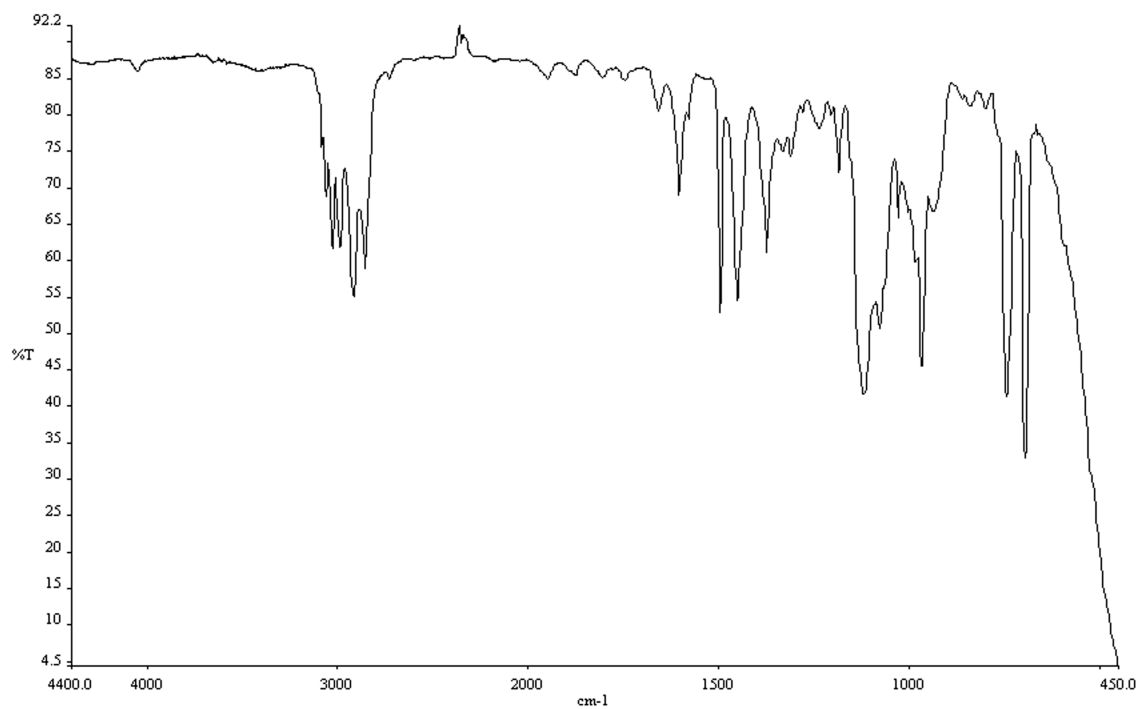
Figure A.1.89 Infrared spectrum (thin film/NaCl) of compound **202**.
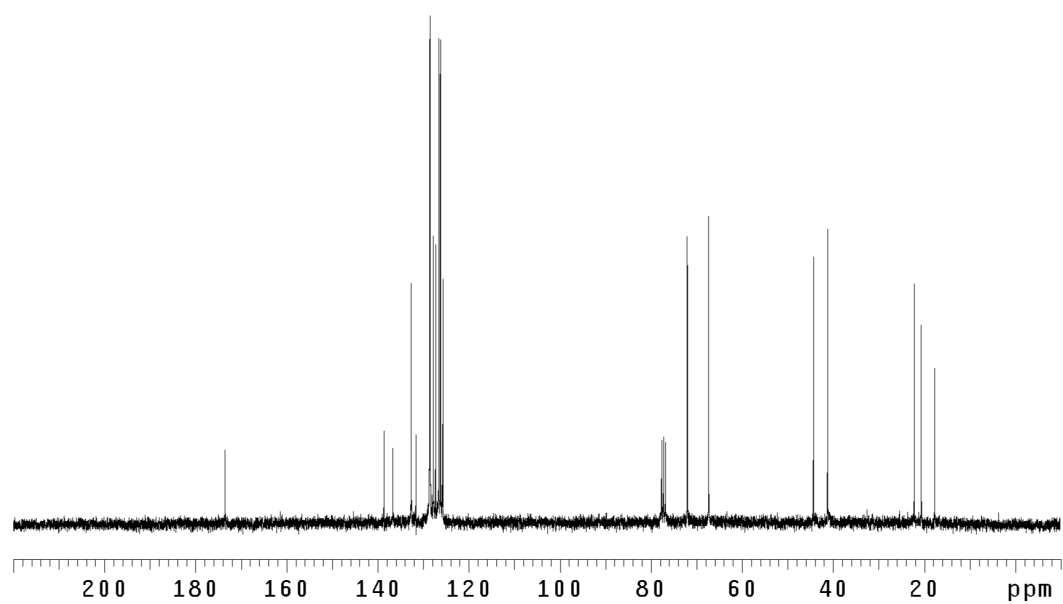
Figure A.1.90 ^{13}CNMR (75 Mhz, CDCl$_3$) of compound **202**.
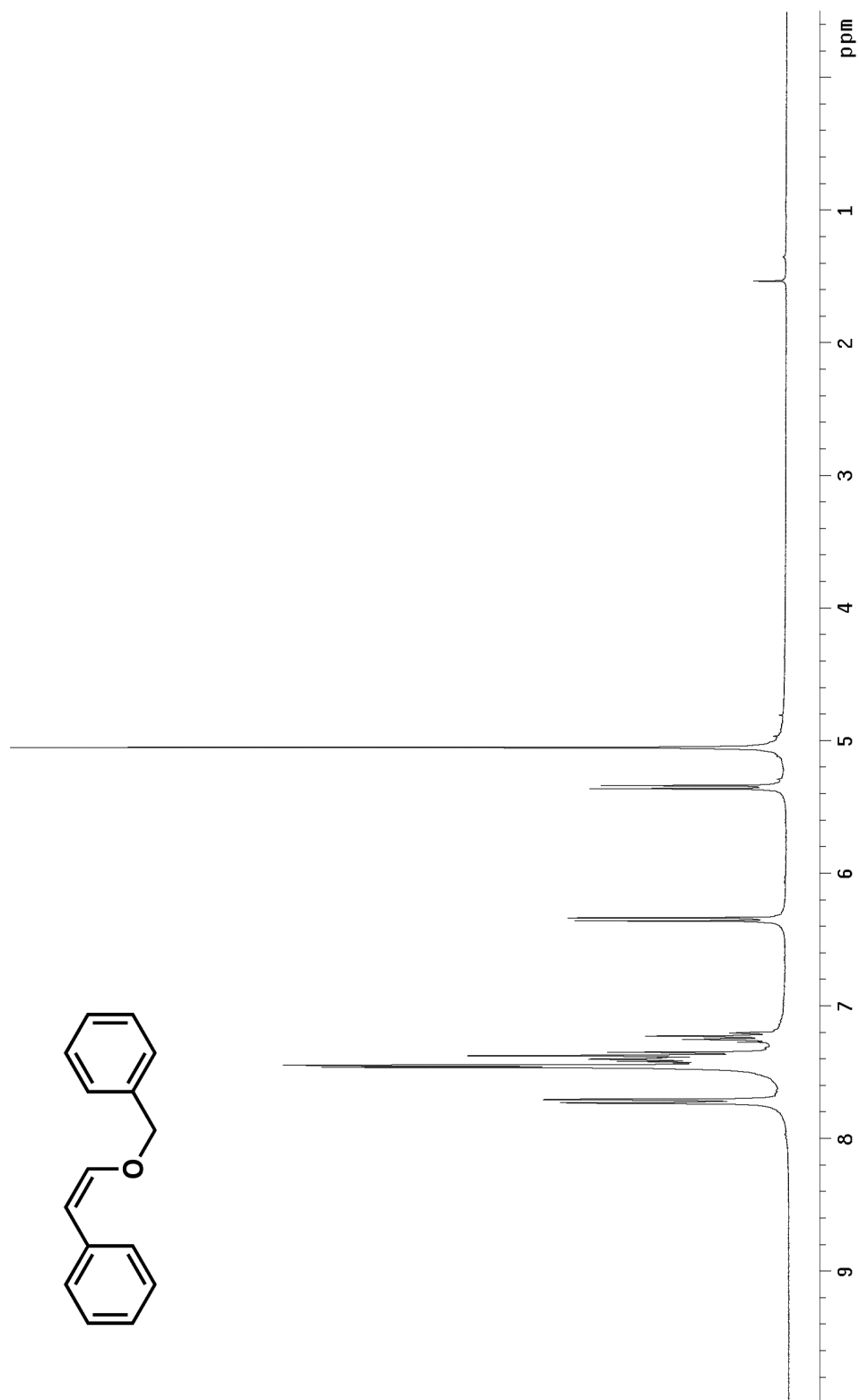
Figure A.1.91 ¹HNMR (300 MHz, CDCL₃) of compound **105**.
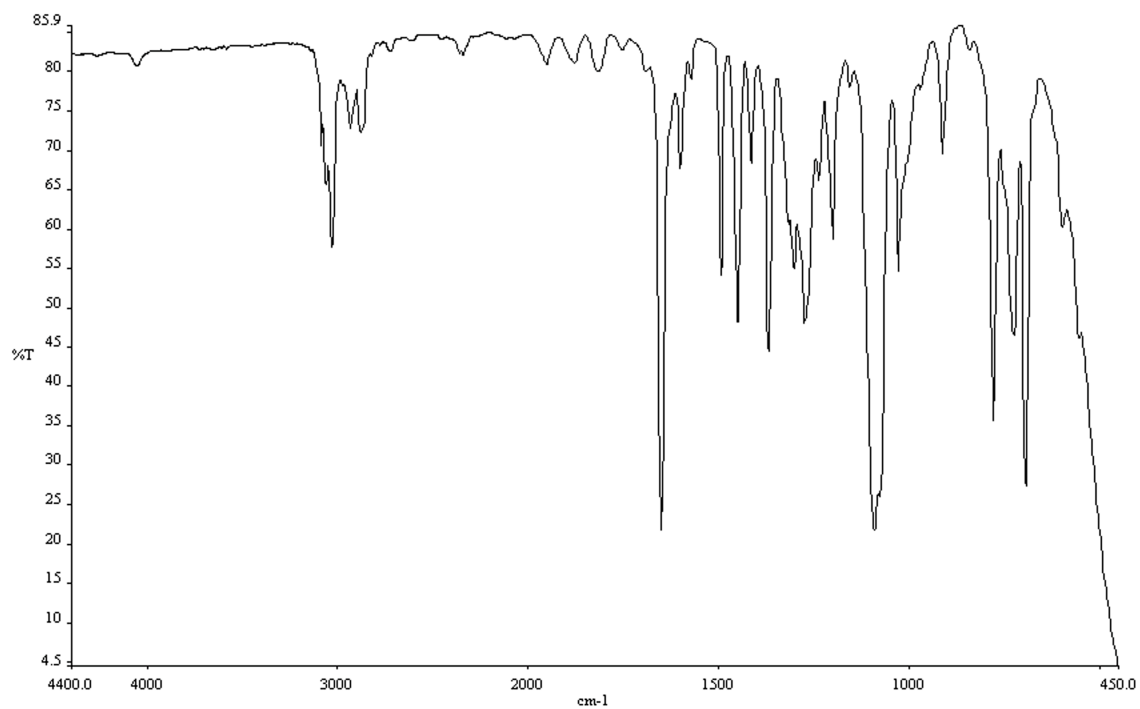
Figure A.1.92 Infrared spectrum (thin film/NaCl) of compound **105**.
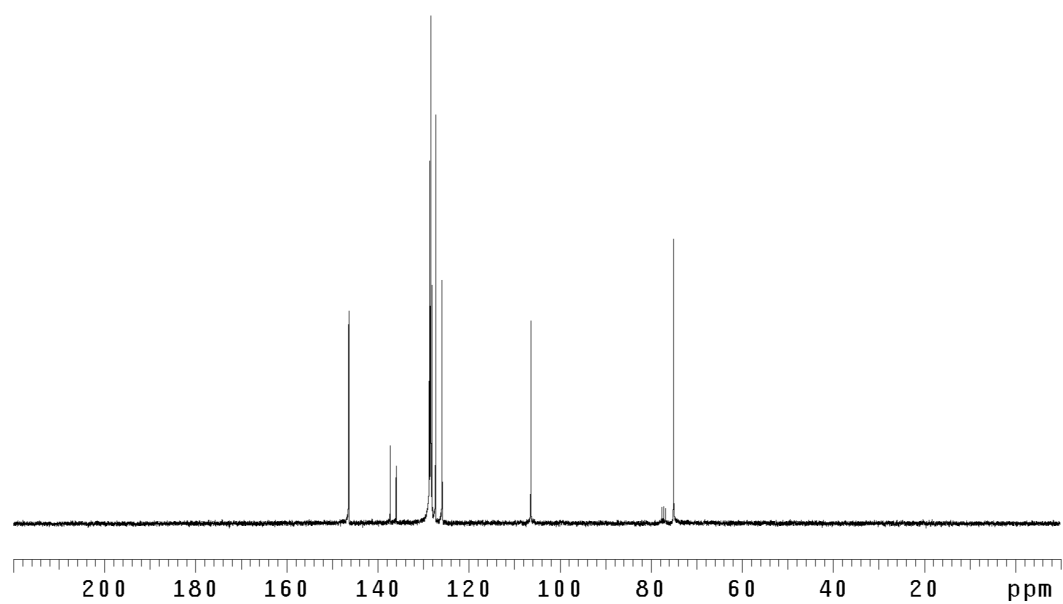
Figure A.1.93 ^{13}CNMR (75 Mhz, CDCl$_3$) of compound **105**.
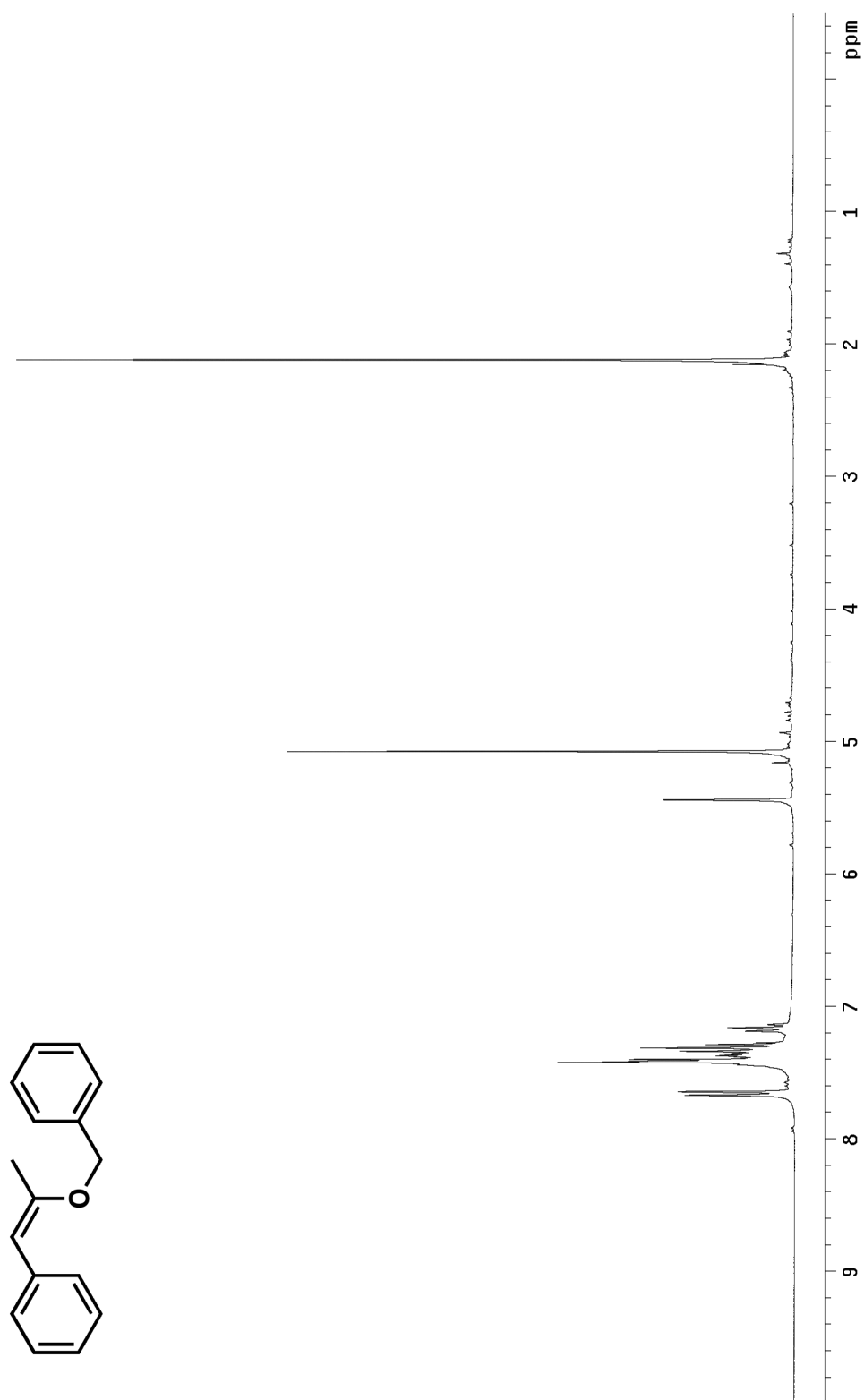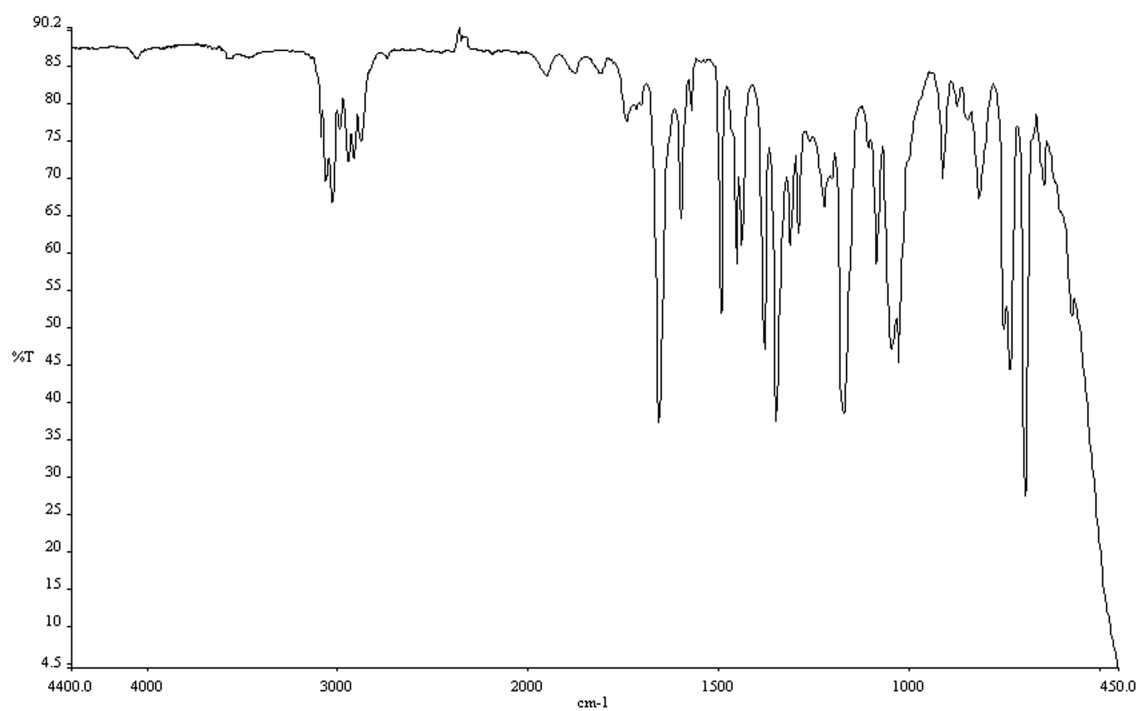
Figure A.1.95 Infrared spectrum (thin film/NaCl) of compound **107**.
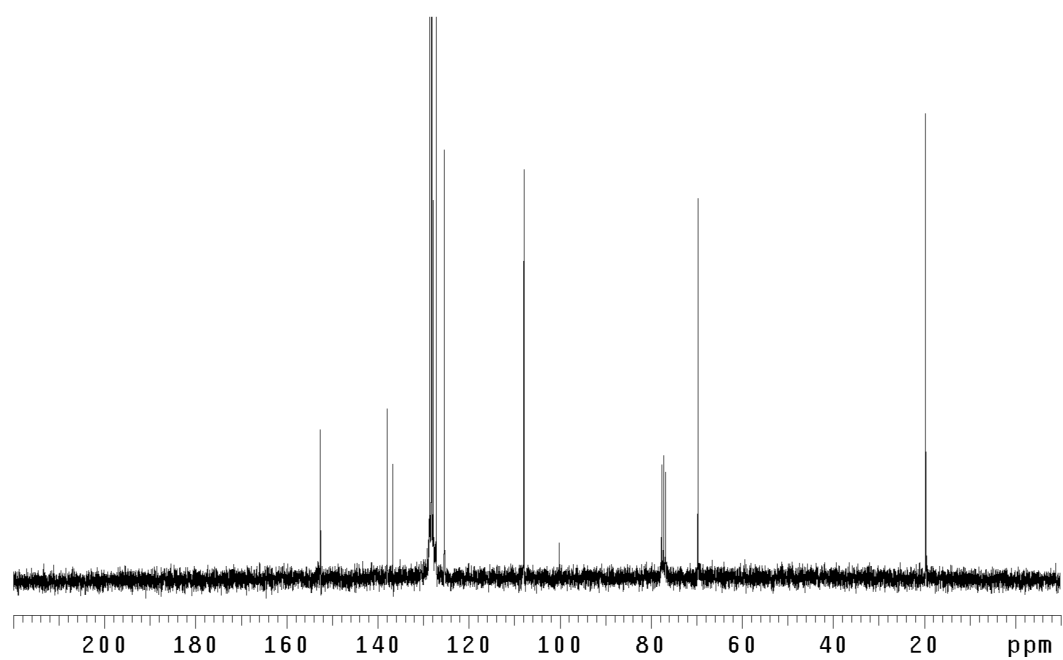
Figure A.1.96 ^{13}CNMR (75 Mhz, CDCl$_3$) of compound **107**.
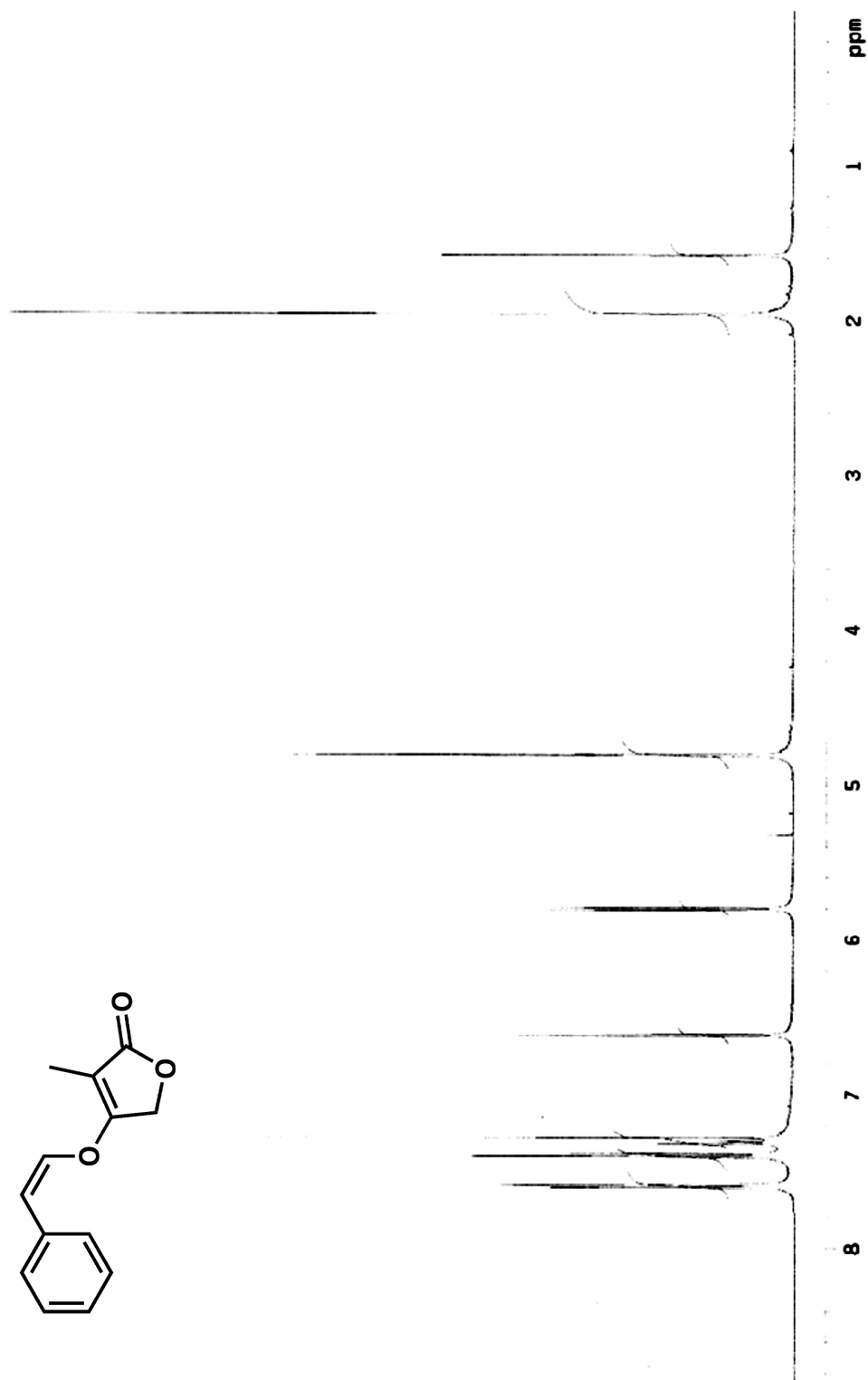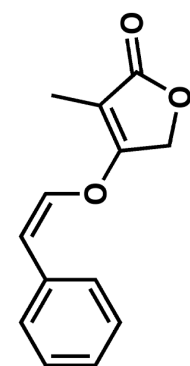
Figure A.1.97 ¹HNMR (300 MHz, CDCL₃) of compound **98**.

Figure A.1.98 Infrared spectrum (thin film/NaCl) of compound **98**.
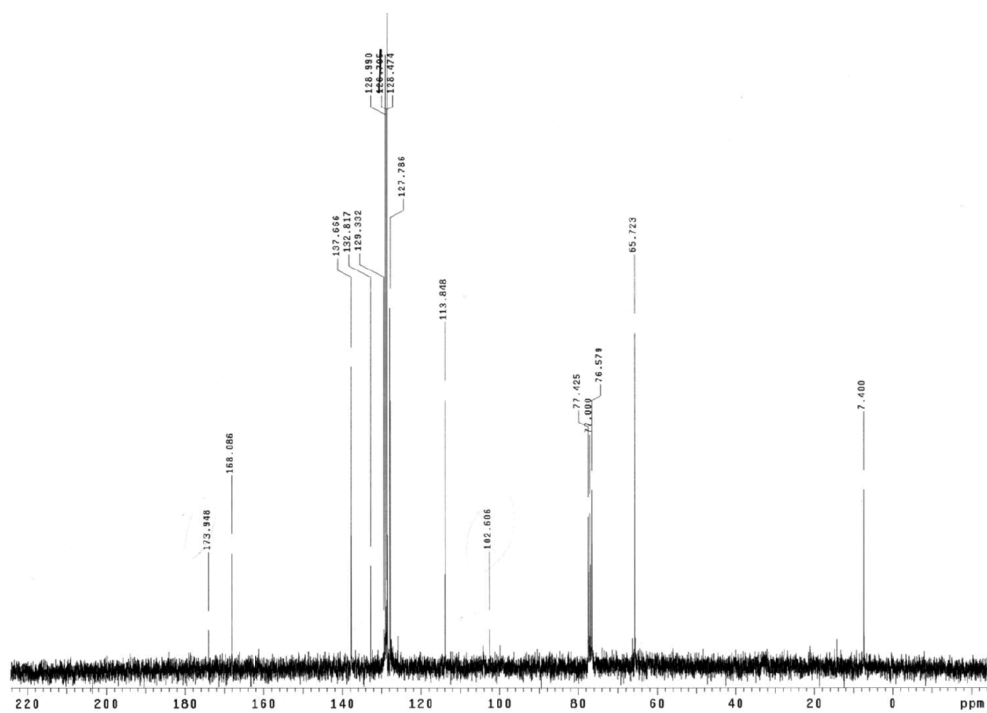
Figure A.1.99 ^{13}CNMR (75 Mhz, CDCl$_3$) of compound **98**.
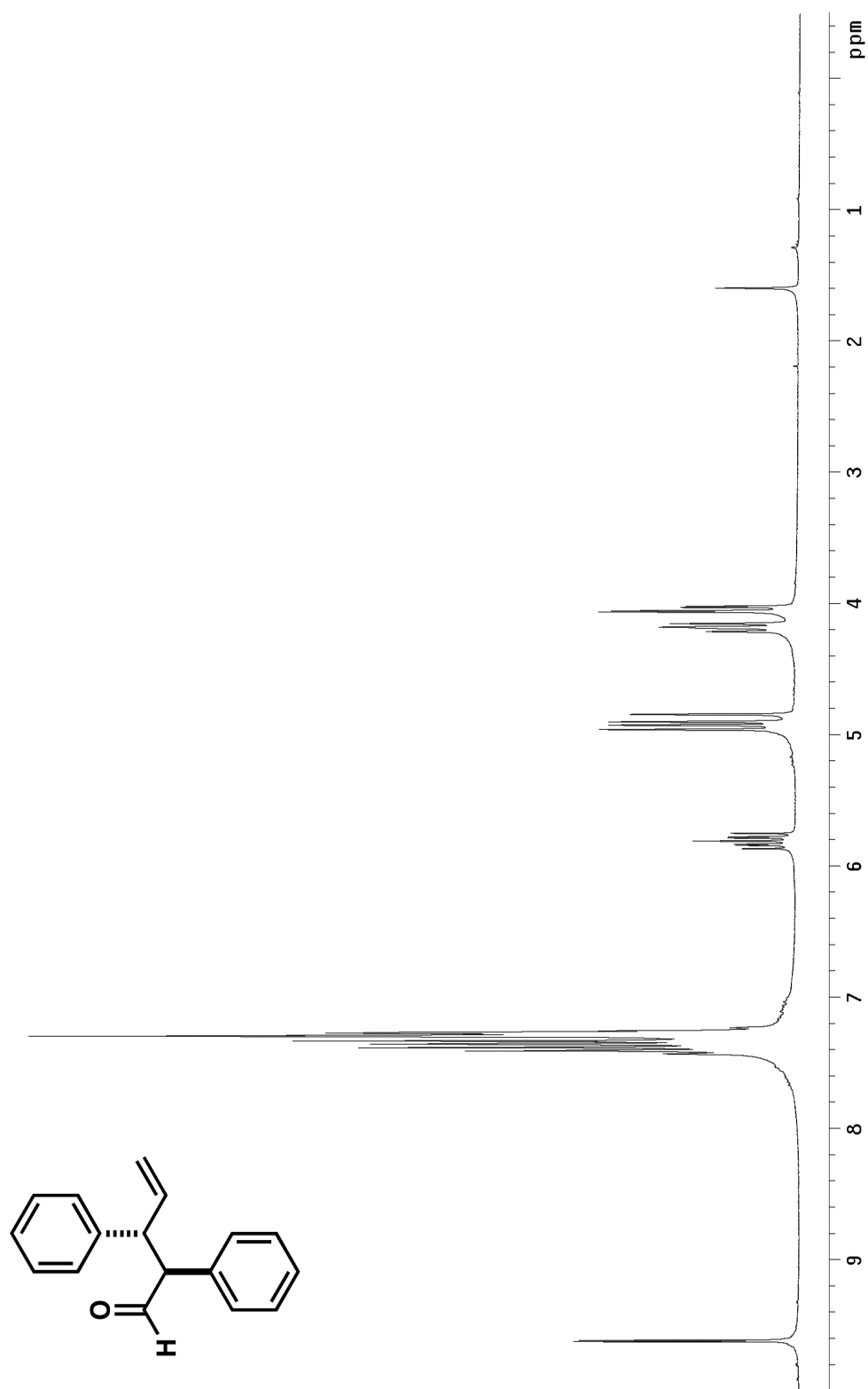
Figure A.1.100 ^{1}HNMR (300 MHz, CDCL$_3$) of compound **164**.
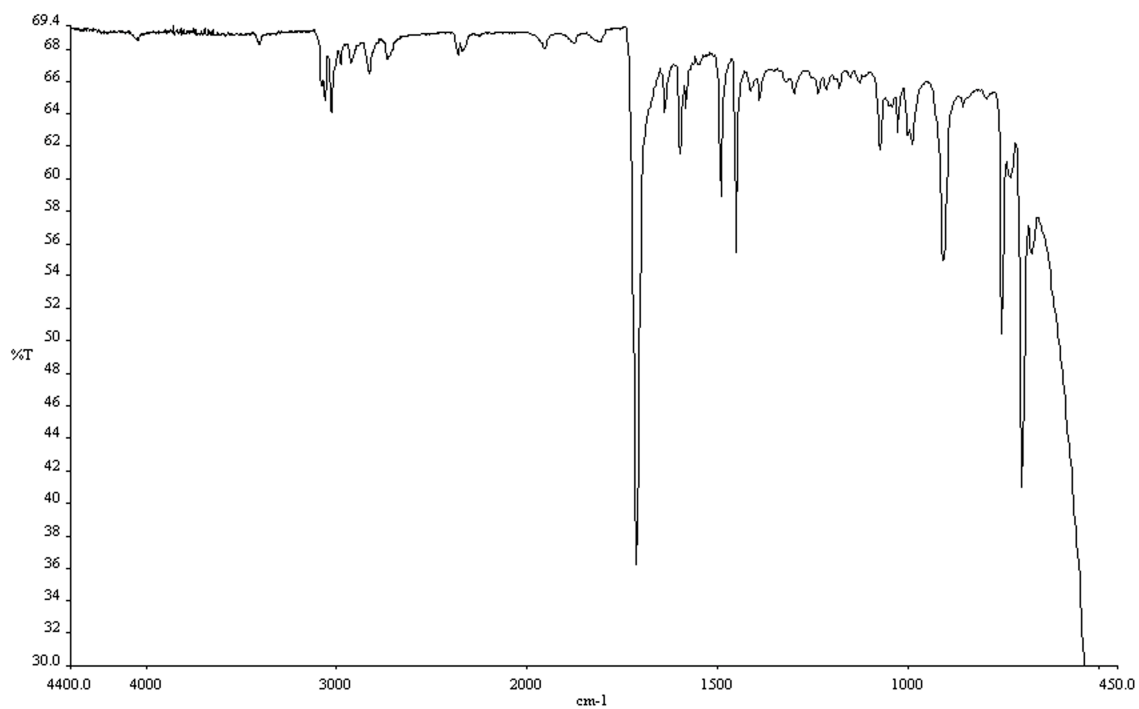
Figure A.1.101 Infrared spectrum (thin film/NaCl) of compound **164**.
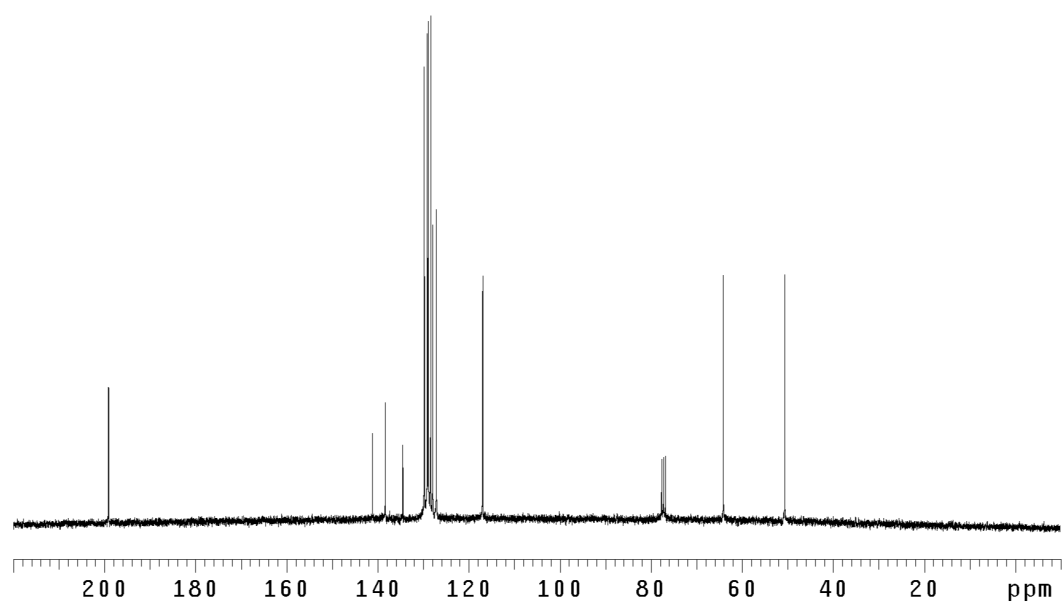
Figure A.1.102 ¹³CNMR (75 Mhz, CDCl₃) of compound **164**.

174
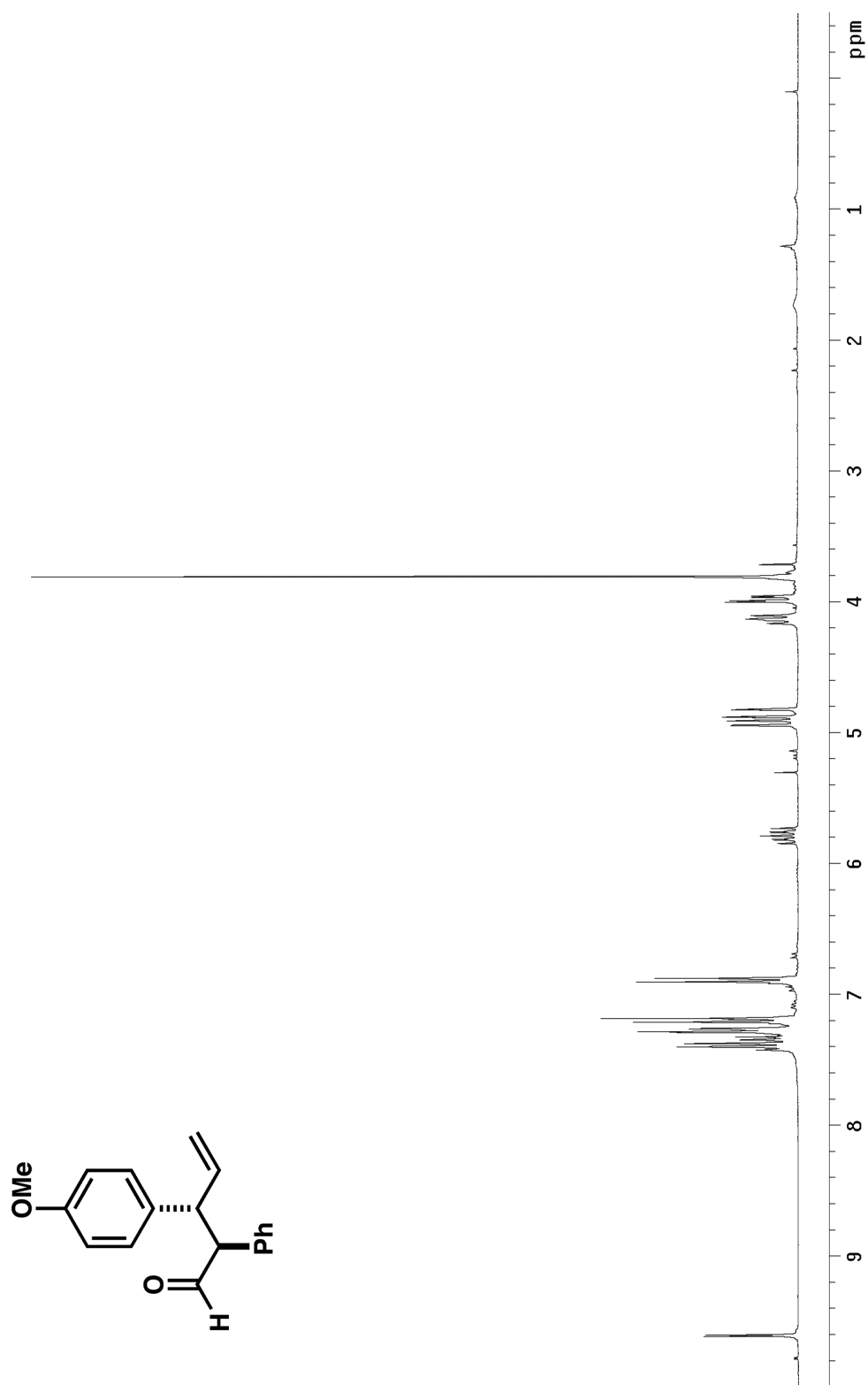
Figure A.1.103 ¹HNMR (300 MHz, CDCL₃) of compound **166**.
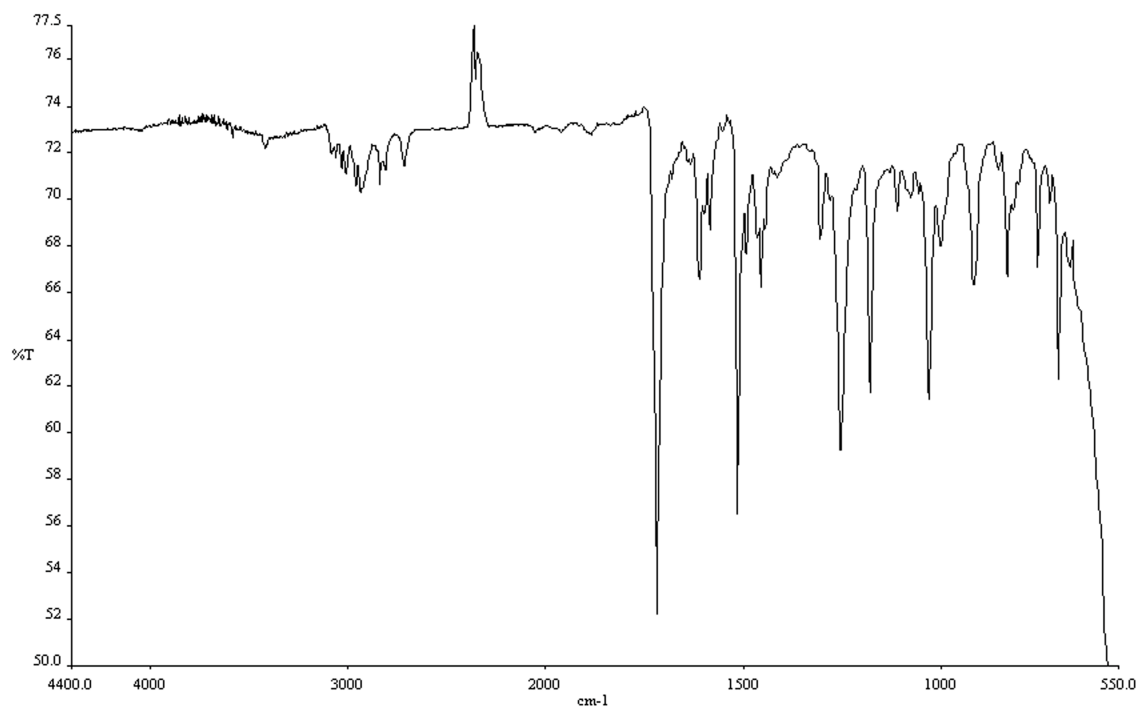
Figure A.1.104 Infrared spectrum (thin film/NaCl) of compound **166**.
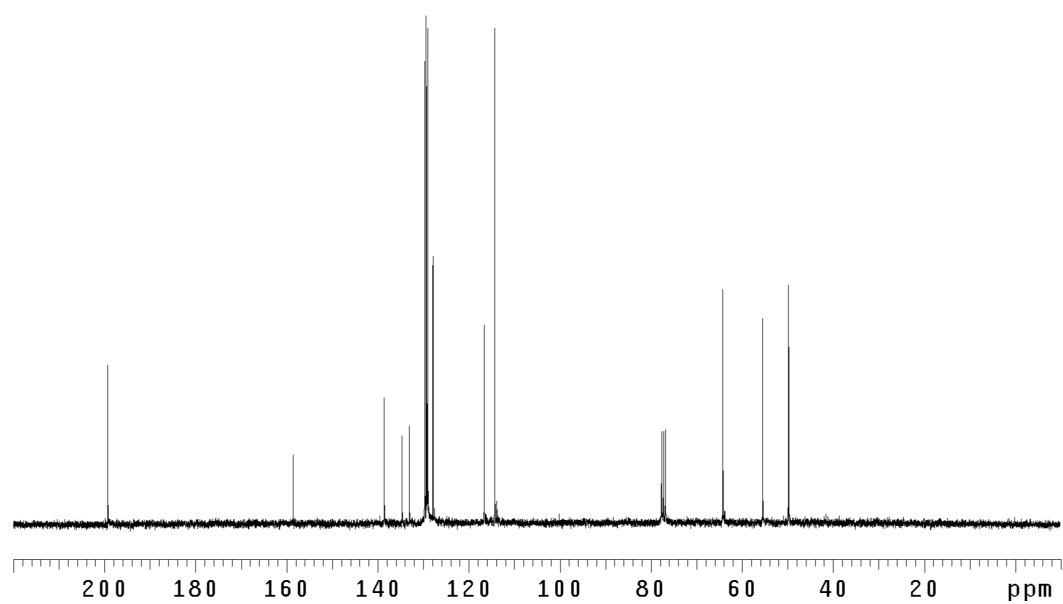
Figure A.1.105 ¹³CNMR (75 Mhz, CDCl₃) of compound **166**.
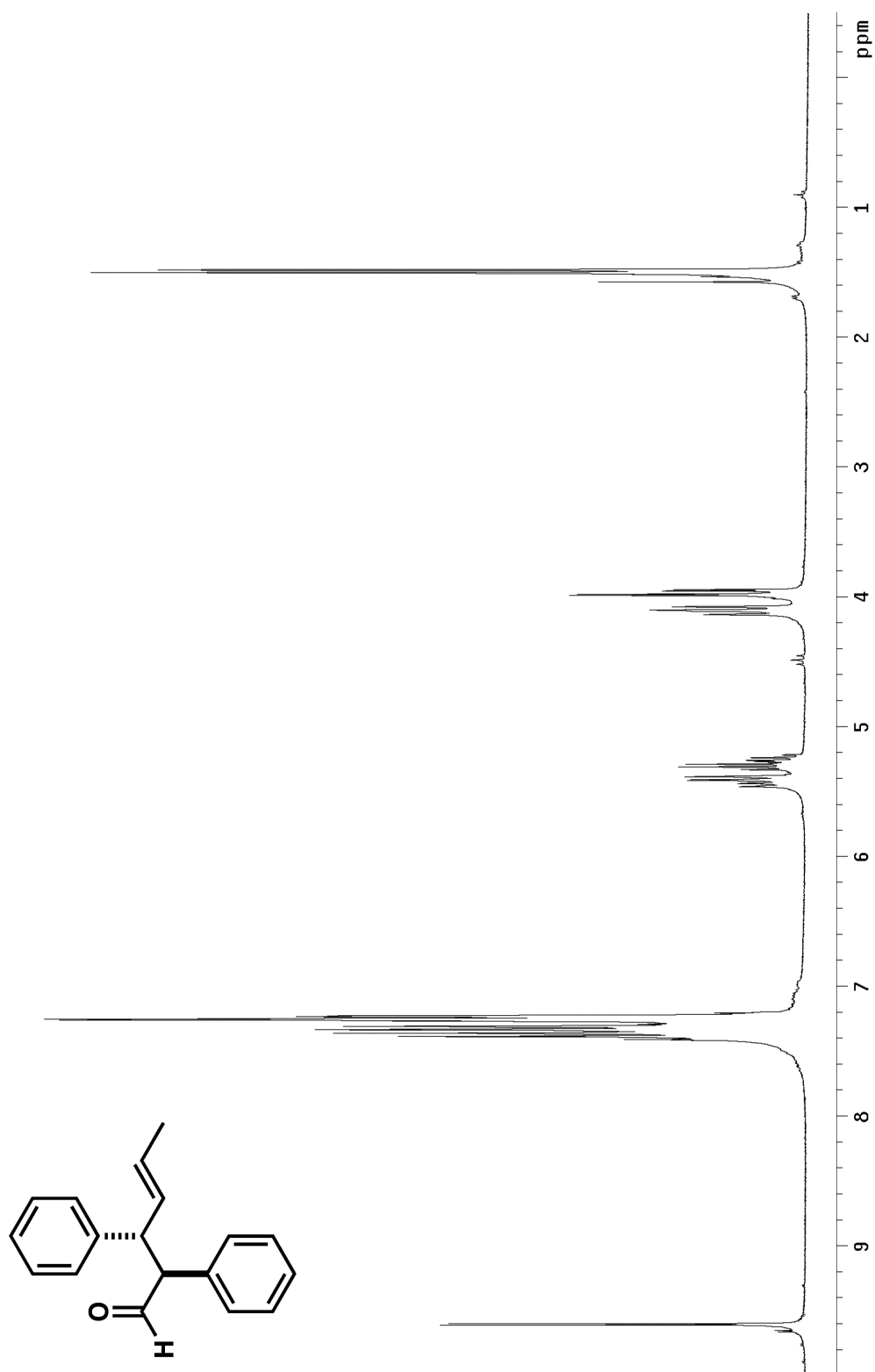
Figure A.1.106 ^{1}HNMR (300 MHz, CDCL$_3$) of compound **168**.
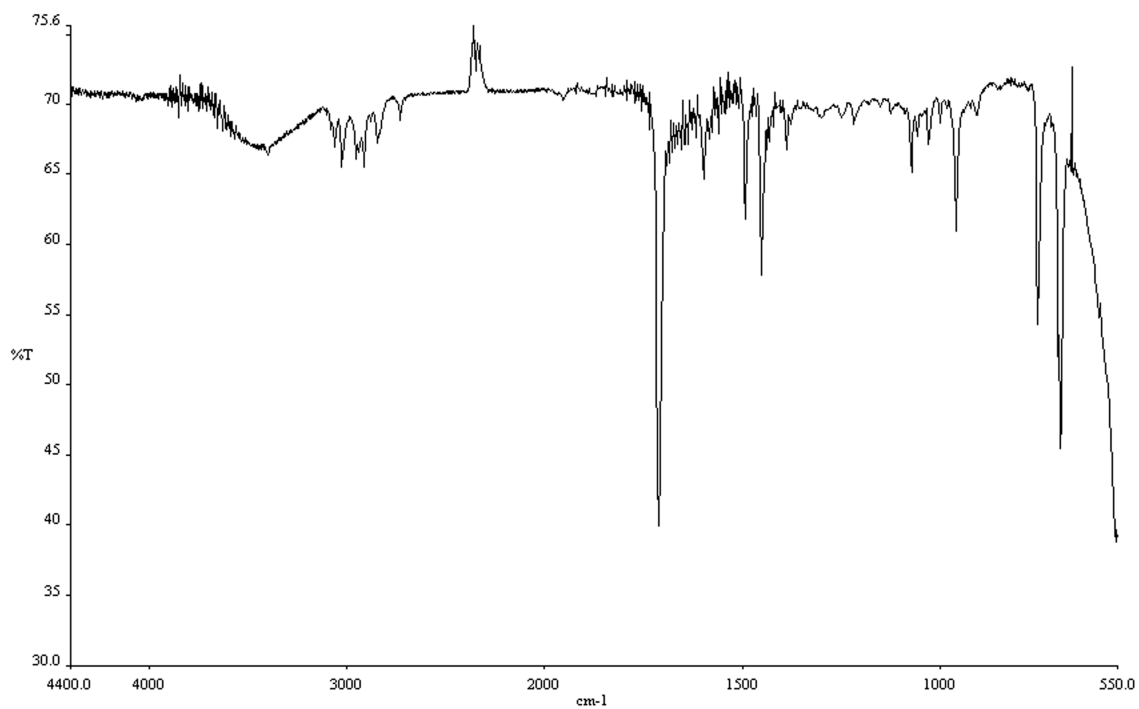
Figure A.1.107 Infrared spectrum (thin film/NaCl) of compound **168**.
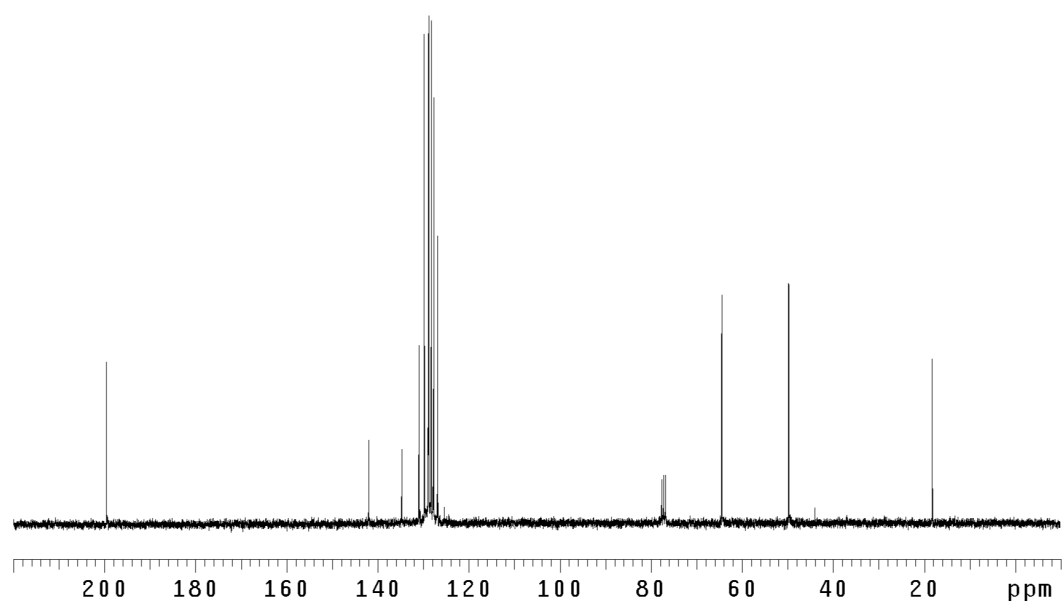
Figure A.1.108 ¹³CNMR (75 Mhz, CDCl₃) of compound **168**.
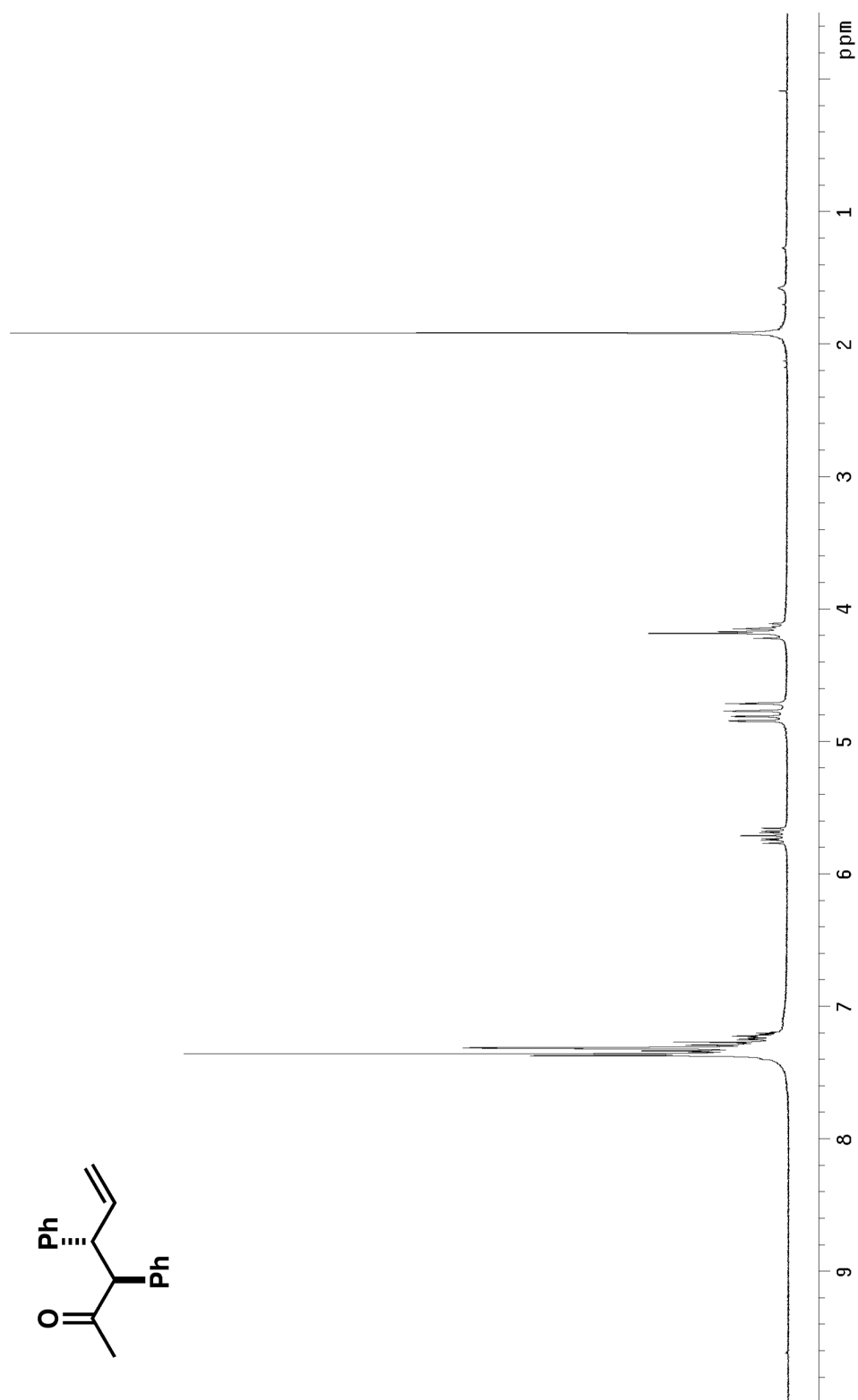
Figure A.1.109 ¹HNMR (300 MHz, CDCL₃) of compound **170**.
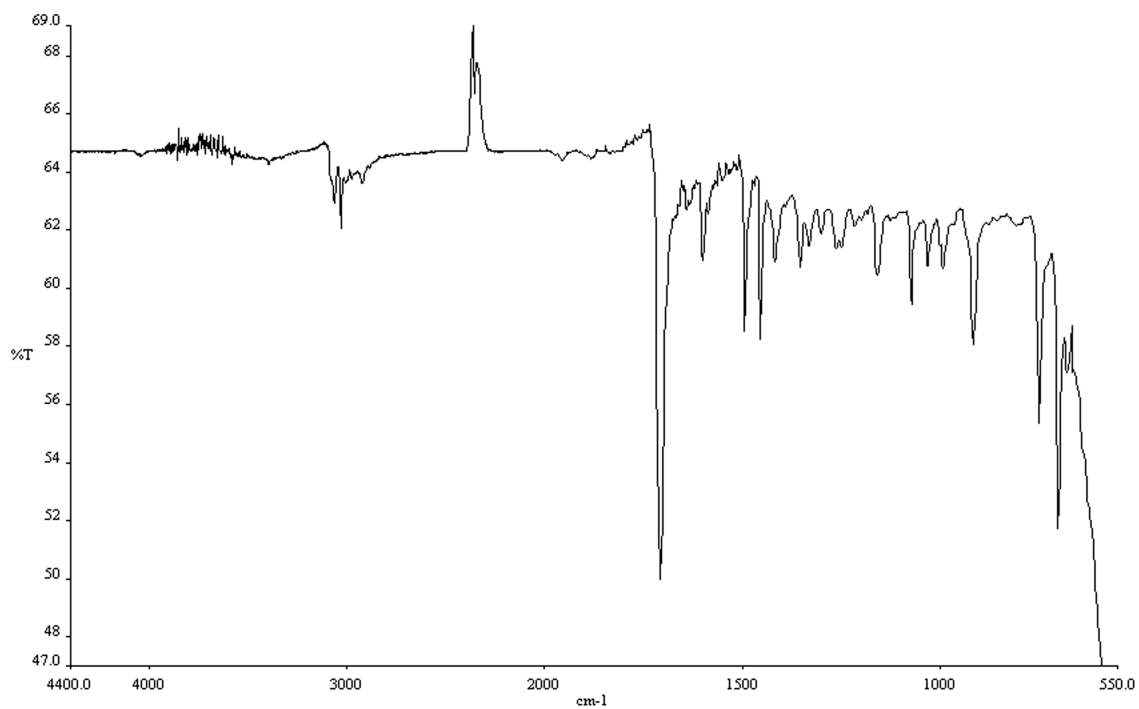
Figure A.1.110 Infrared spectrum (thin film/NaCl) of compound **170**.
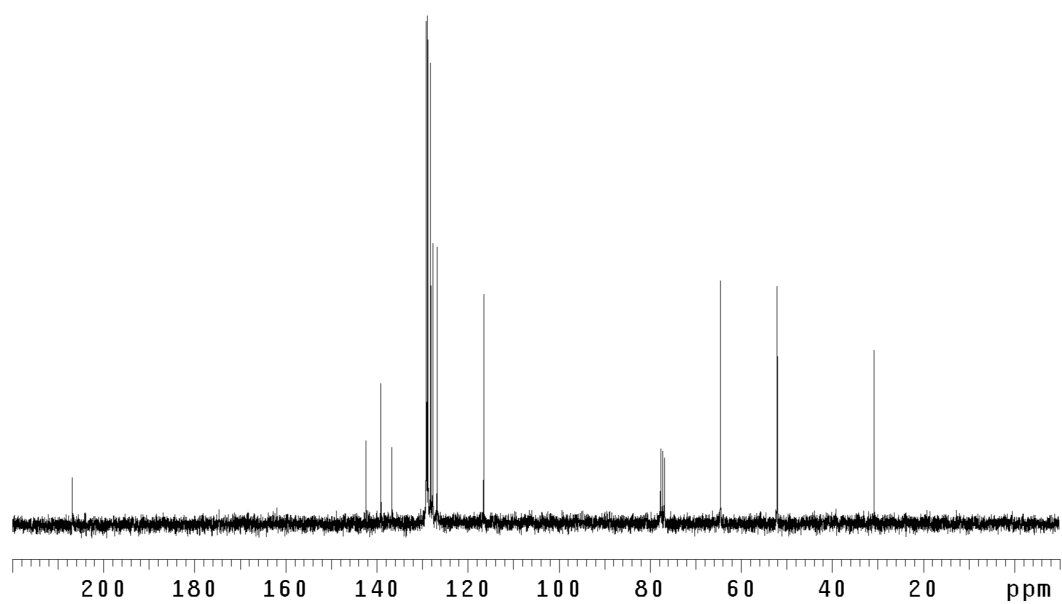
Figure A.1.111 ^{13}CNMR (75 Mhz, CDCl$_3$) of compound **170**.
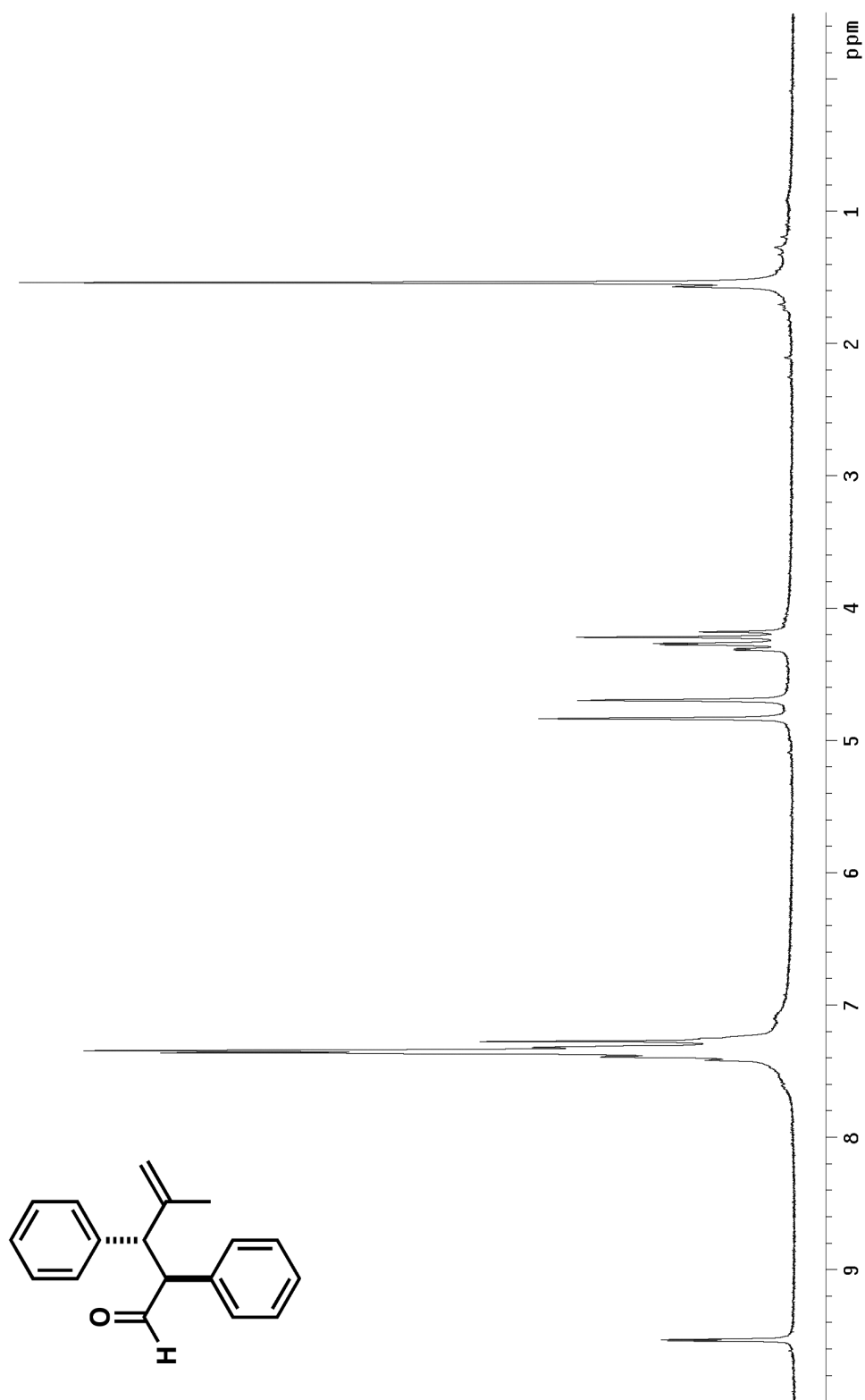
Figure A.1.112 ¹HNMR (300 MHz, CDCL₃) of compound **172**.
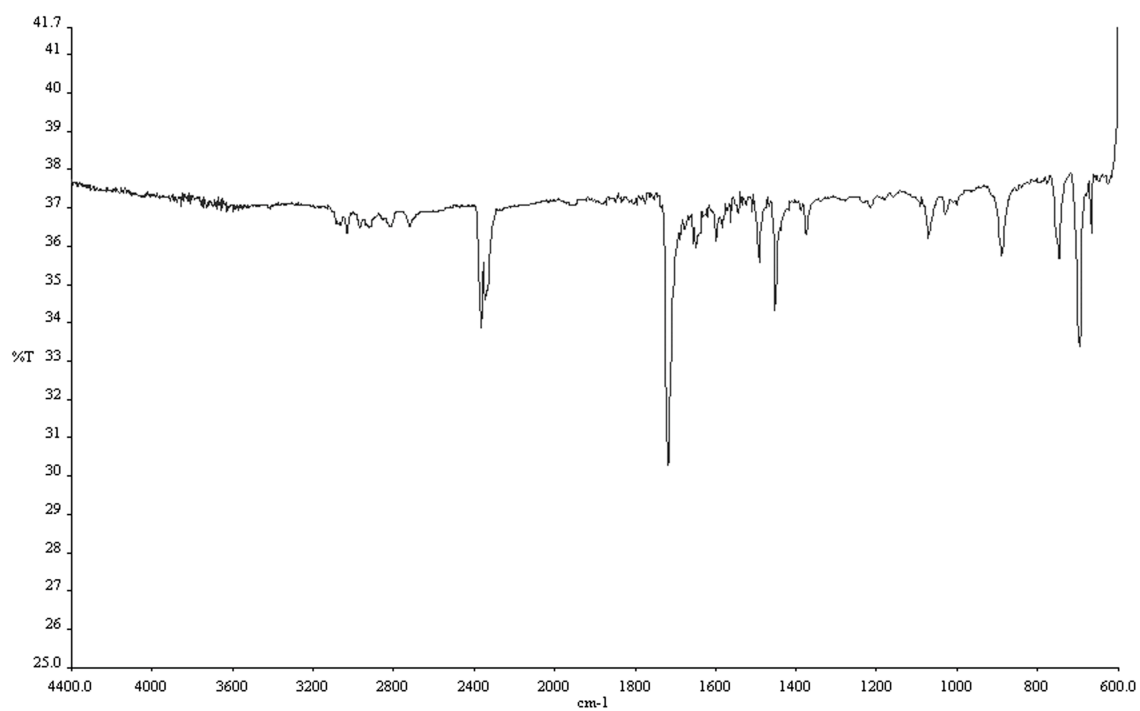
Figure A.1.13 Infrared spectrum (thin film/NaCl) of compound **172**.
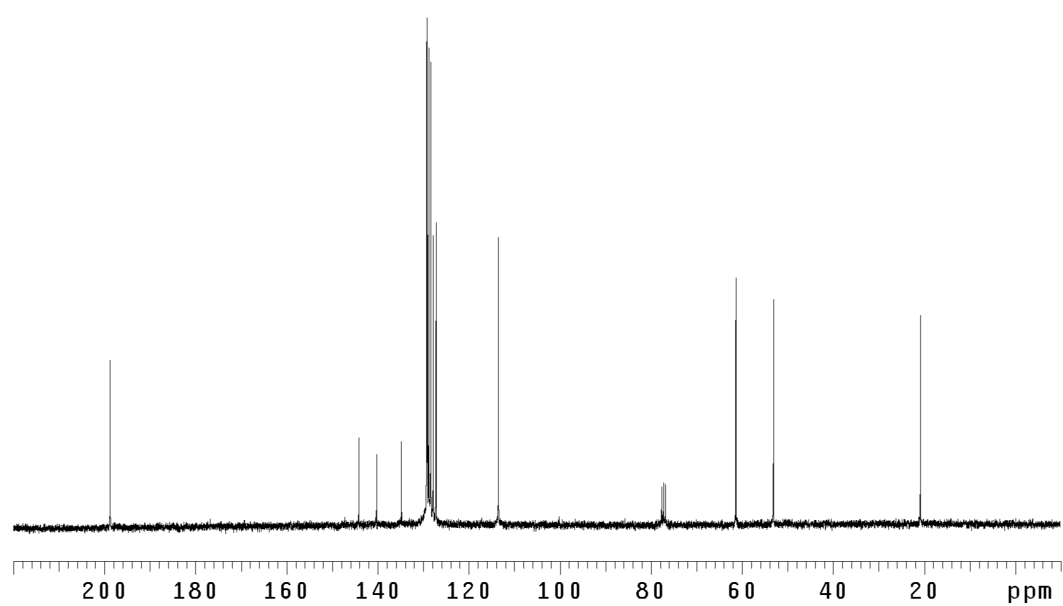
Figure A.1.14 ^{13}CNMR (75 Mhz, CDCl$_3$) of compound **172**.
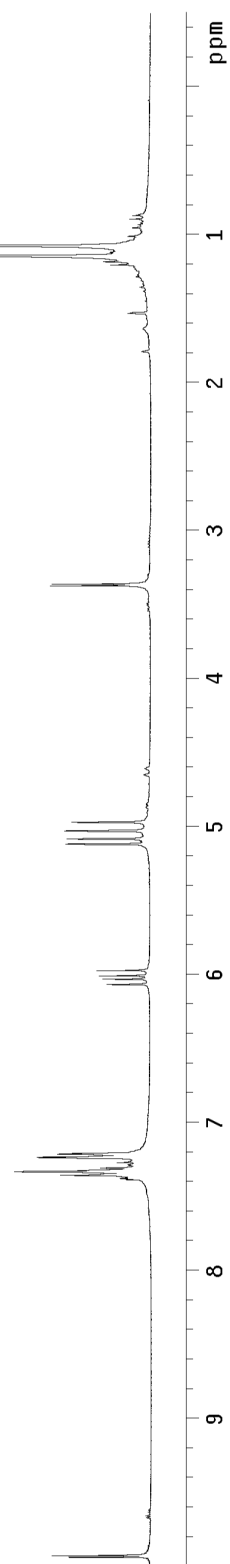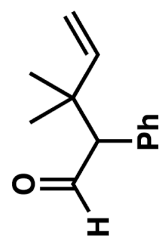
Figure A.1.115 ¹HNMR (300 MHz, CDCL₃) of compound **180**.
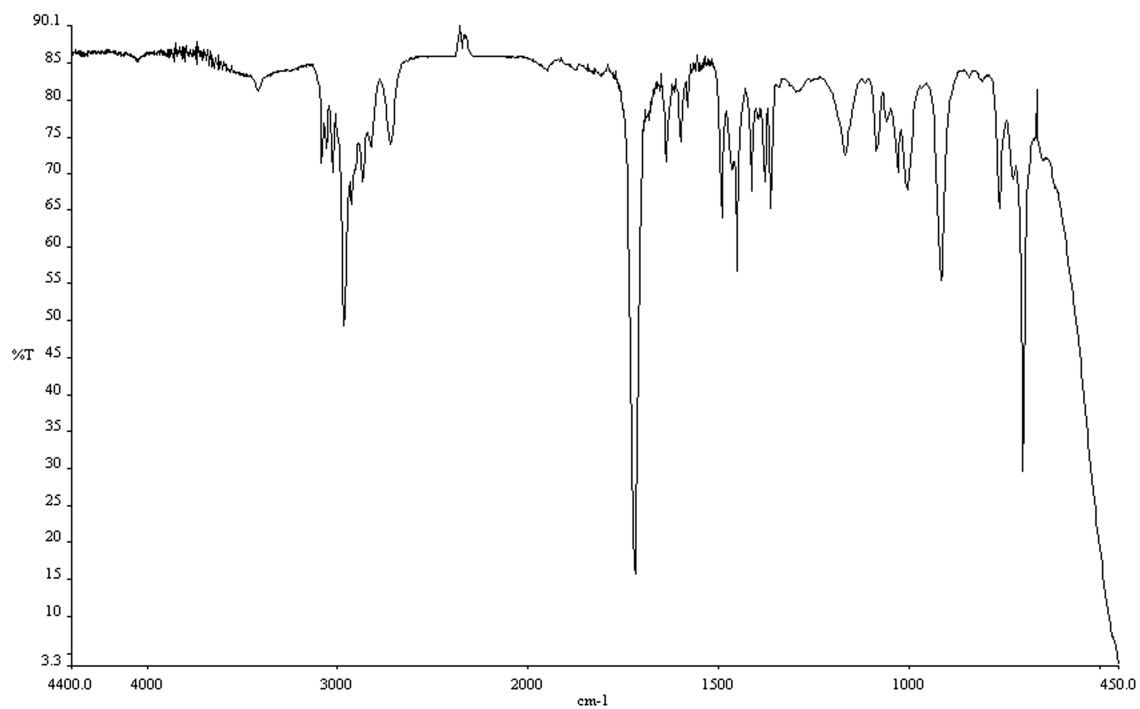
Figure A.1.116 Infrared spectrum (thin film/NaCl) of compound **180**.
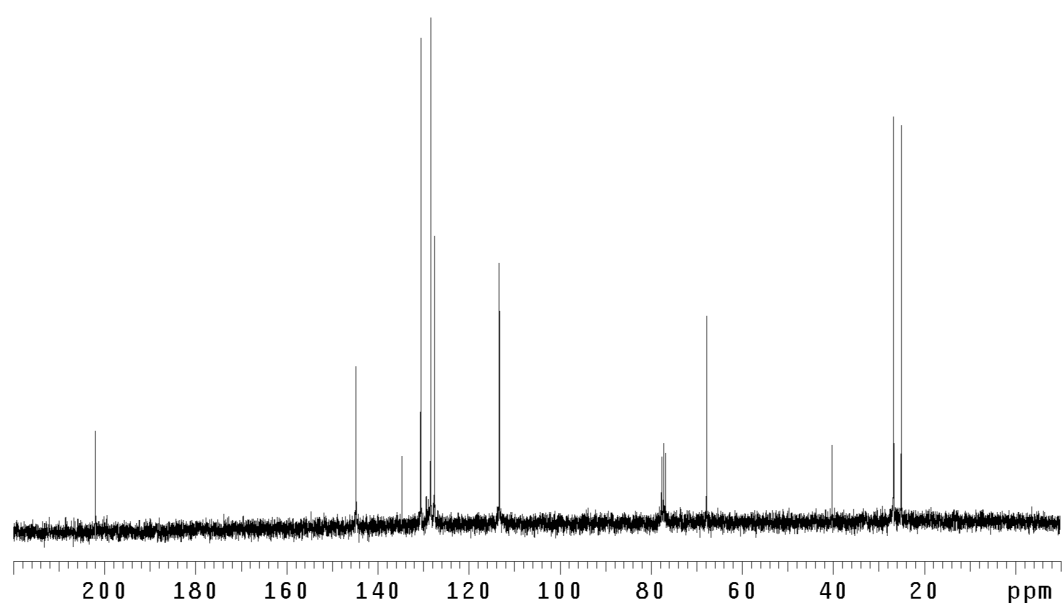
Figure A.1.117 ^{13}CNMR (75 Mhz, CDCl$_3$) of compound **180**.
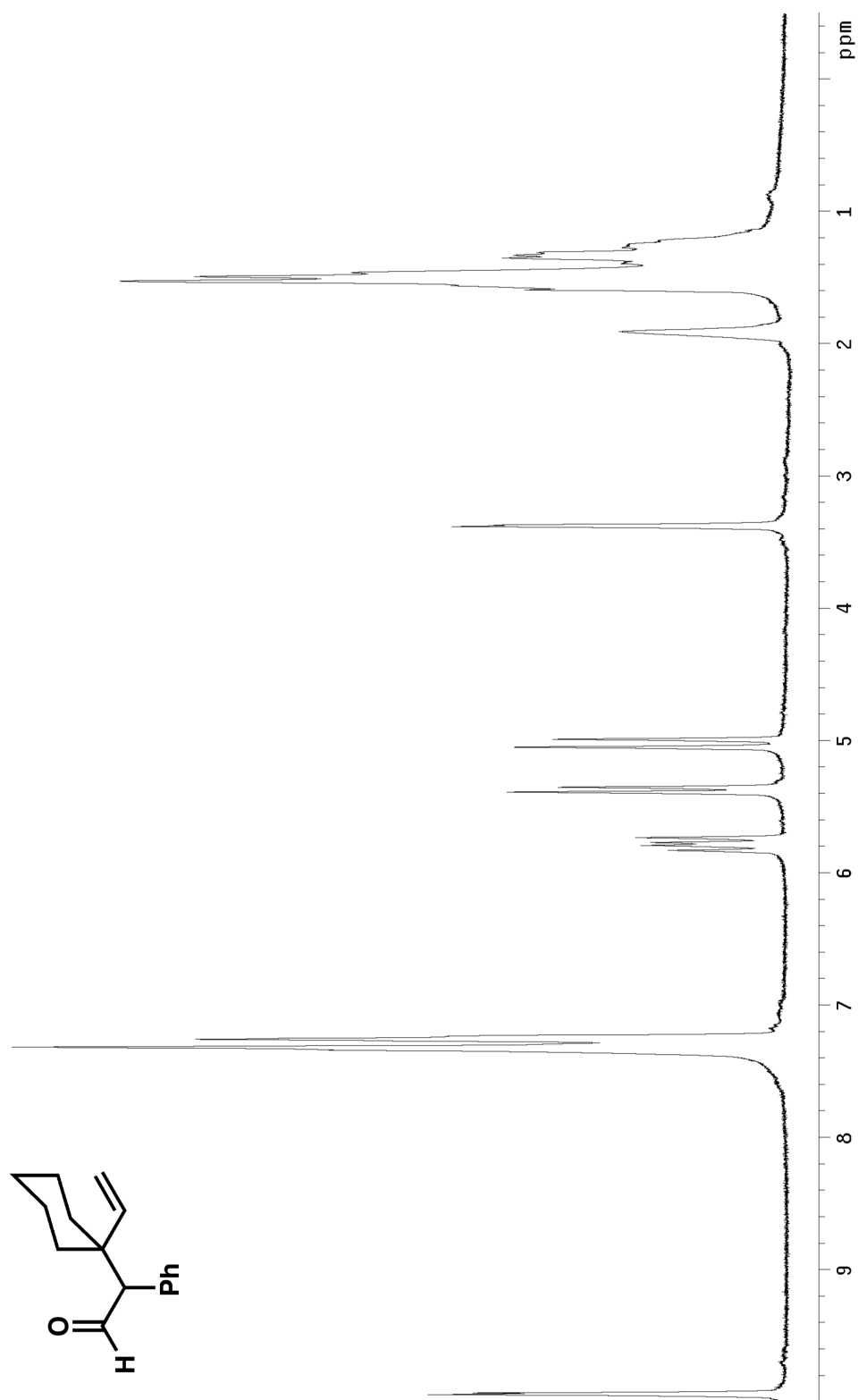
Figure A.1.118 ^{1}HNMR (300 MHz, CDCL$_3$) of compound **182**.
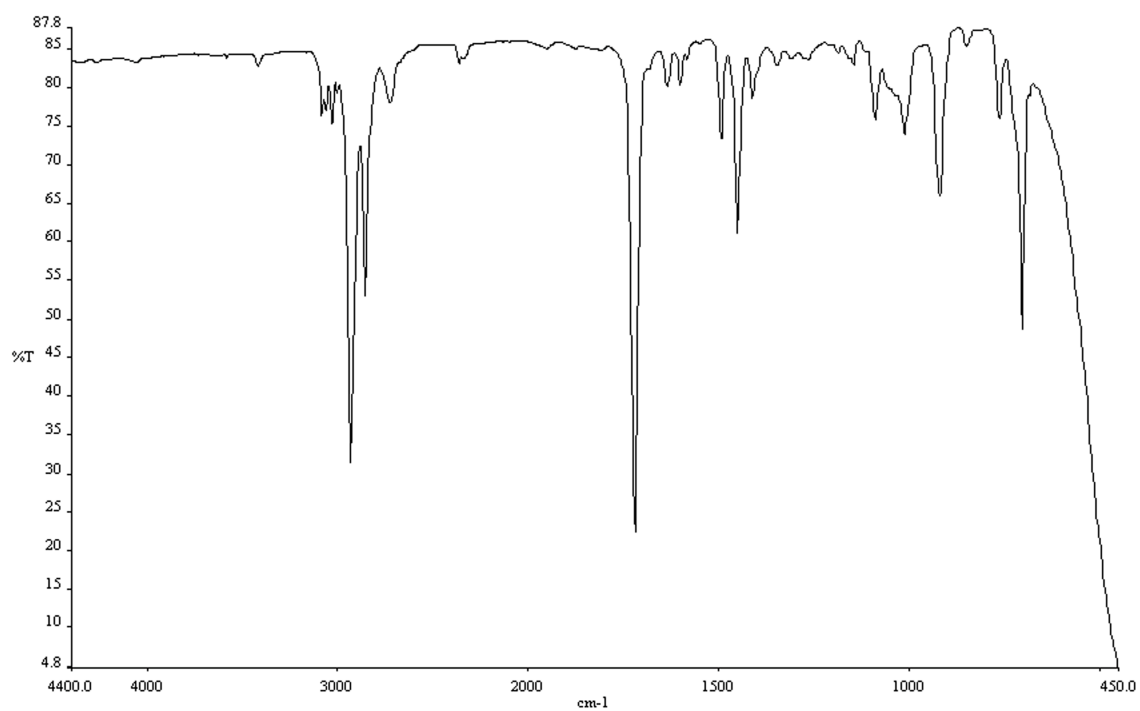
Figure A.1.119 Infrared spectrum (thin film/NaCl) of compound **182**.
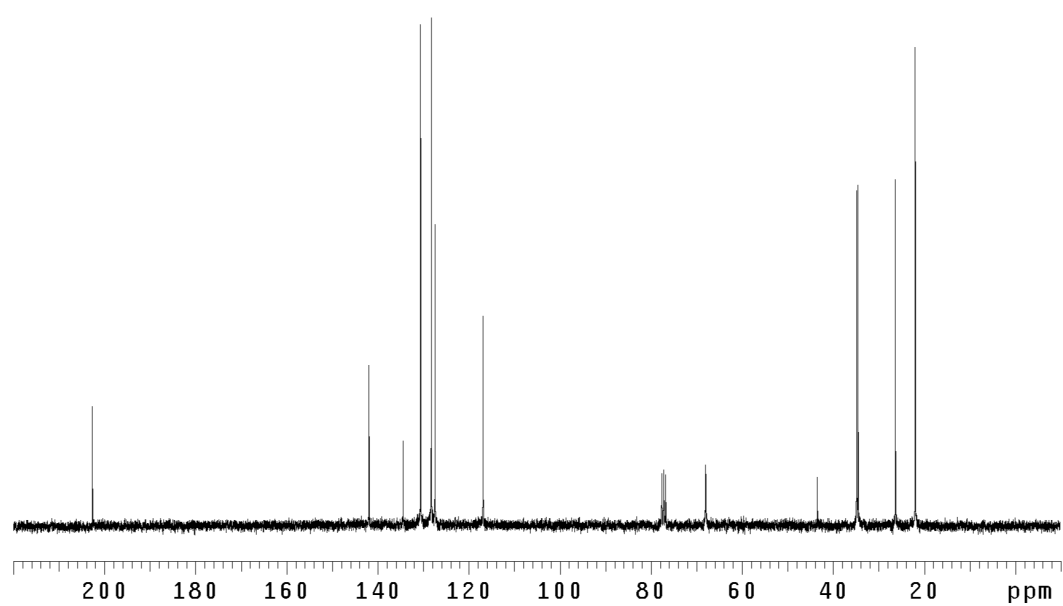
Figure A.1.120 ¹³CNMR (75 Mhz, CDCl₃) of compound **182**.
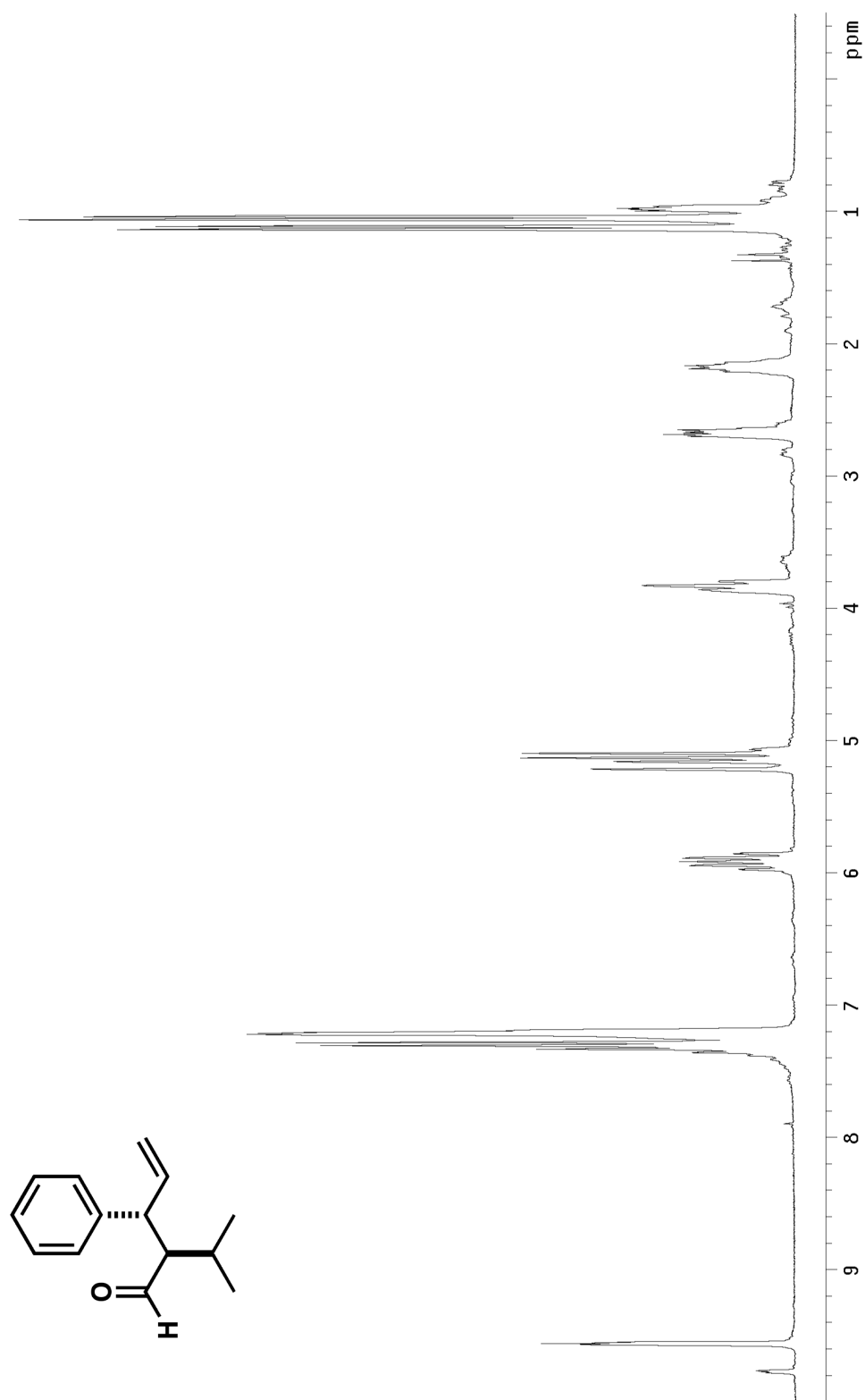
Figure A.1.121 ^{1}HNMR (300 MHz, CDCL$_3$) of compound **174**.
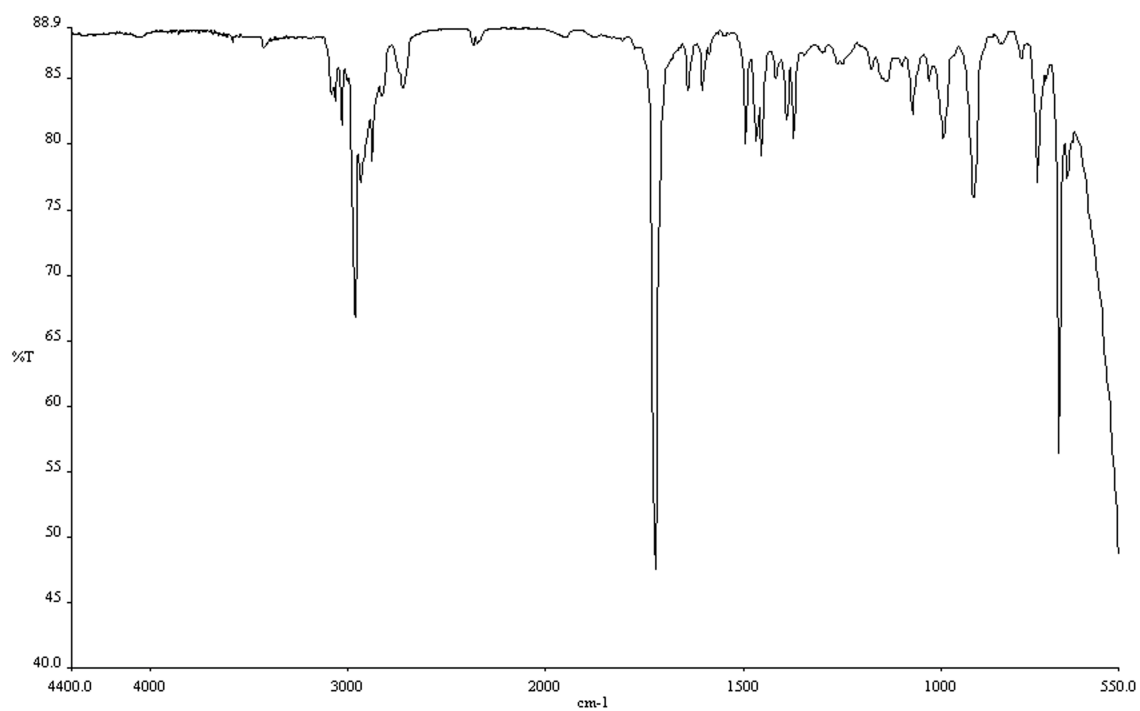
Figure A.1.122 Infrared spectrum (thin film/NaCl) of compound **174**.
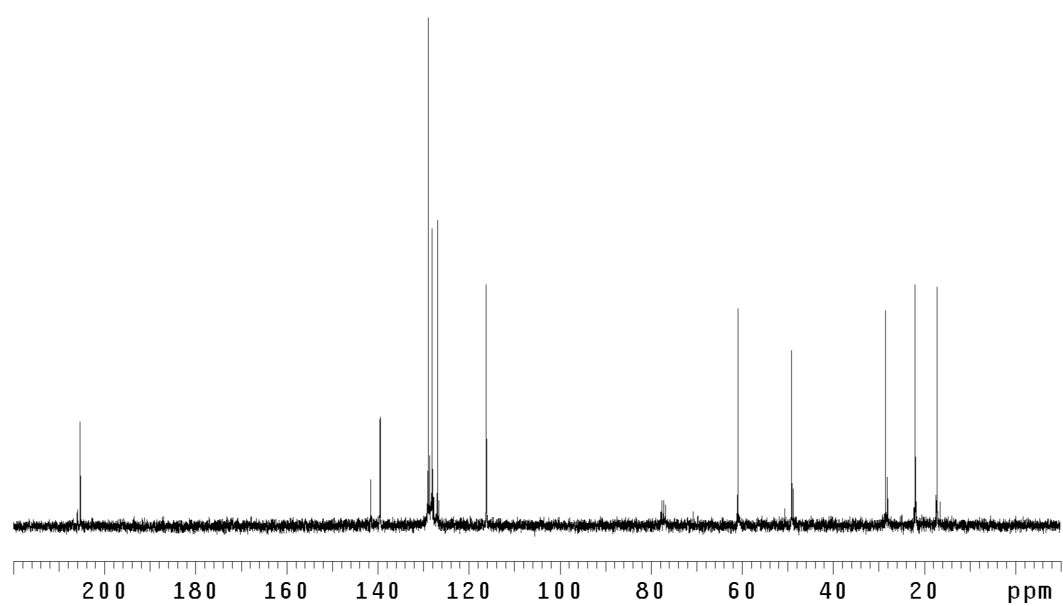
Figure A.1.123 ^{13}CNMR (75 Mhz, CDCl$_3$) of compound **174**.
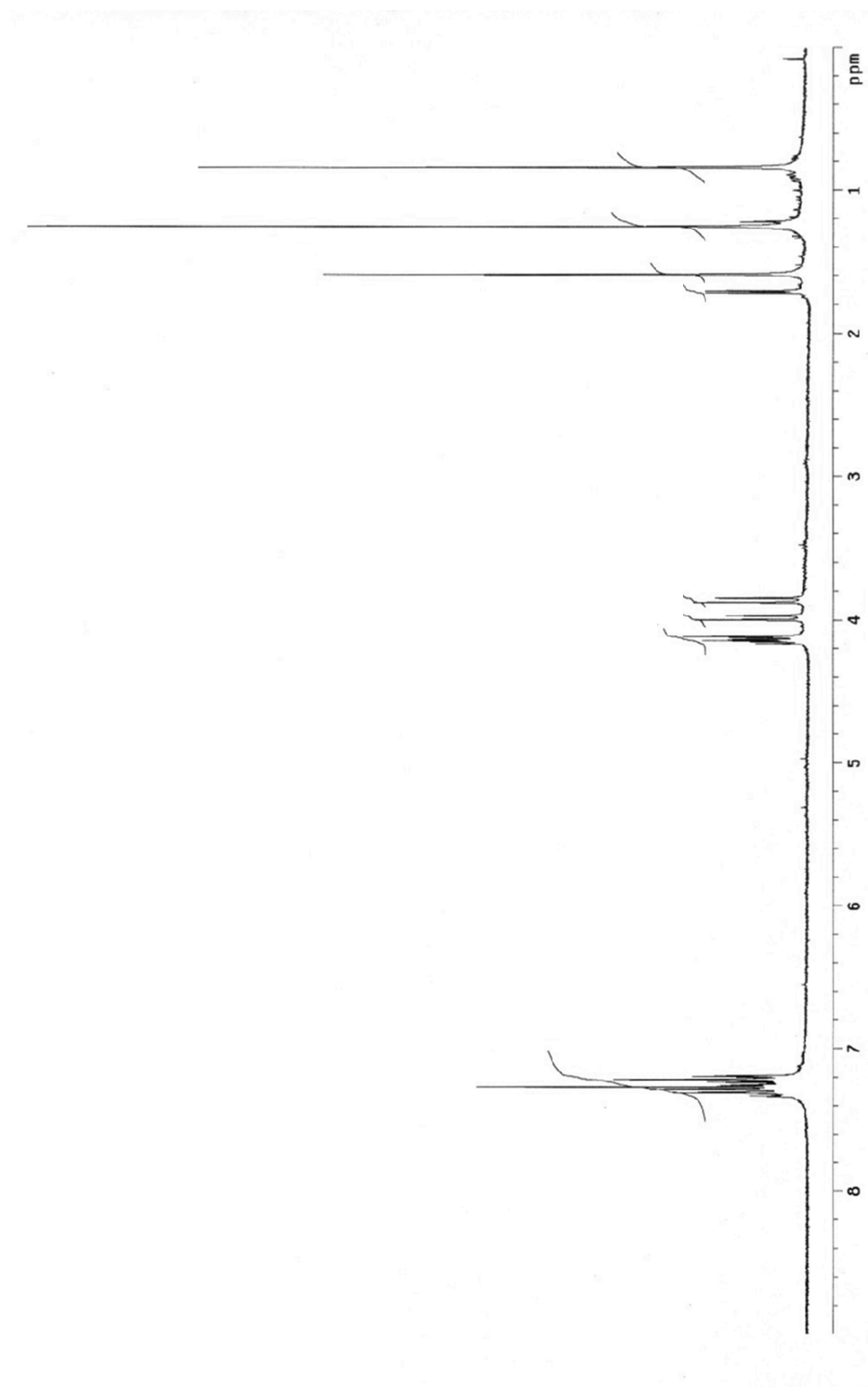
Figure A.1.124 ^{1}HNMR (300 MHz, CDCL$_3$) of compound **213**.
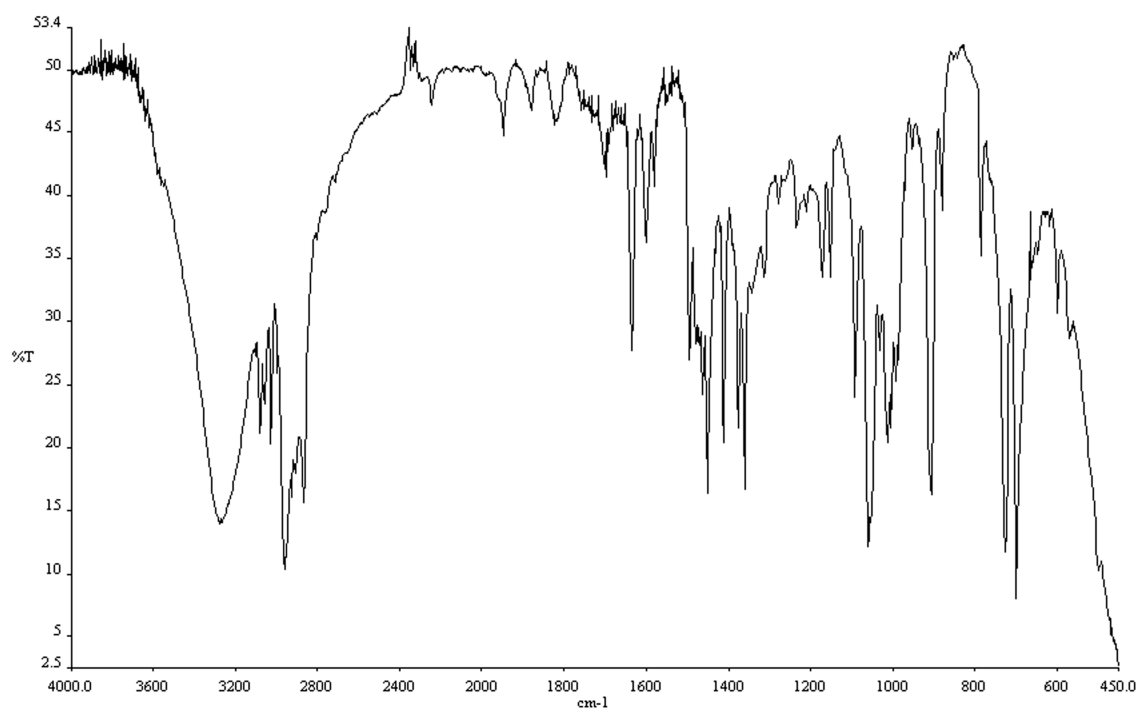
Figure A.1.125 Infrared spectrum (thin film/NaCl) of compound **213**.

Figure A.1.126 ^{13}CNMR (75 Mhz, CDCl$_3$) of compound **213**.
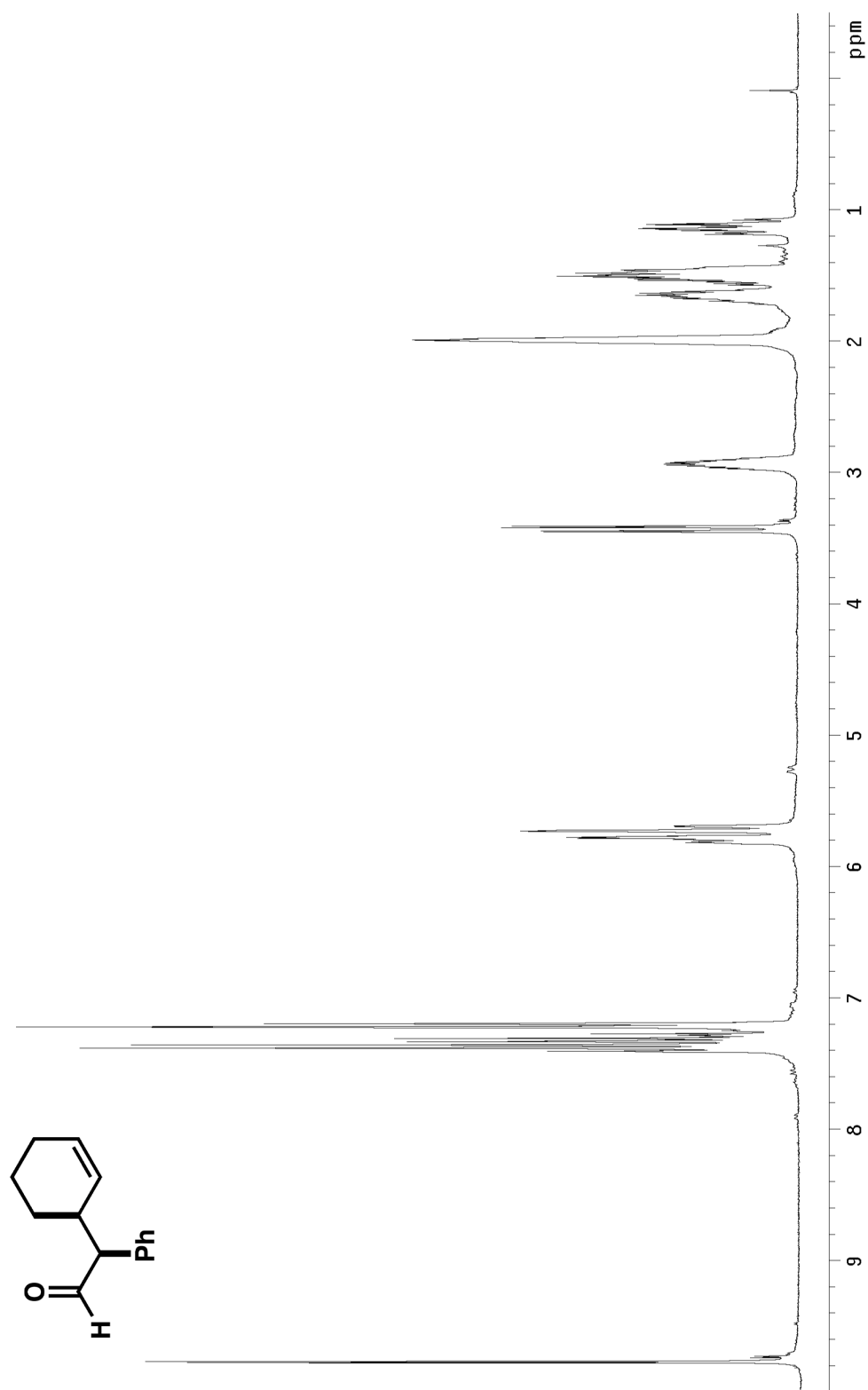
Figure A.1.127 ^{1}HNMR (300 MHz, CDCL$_3$) of compound **186**.
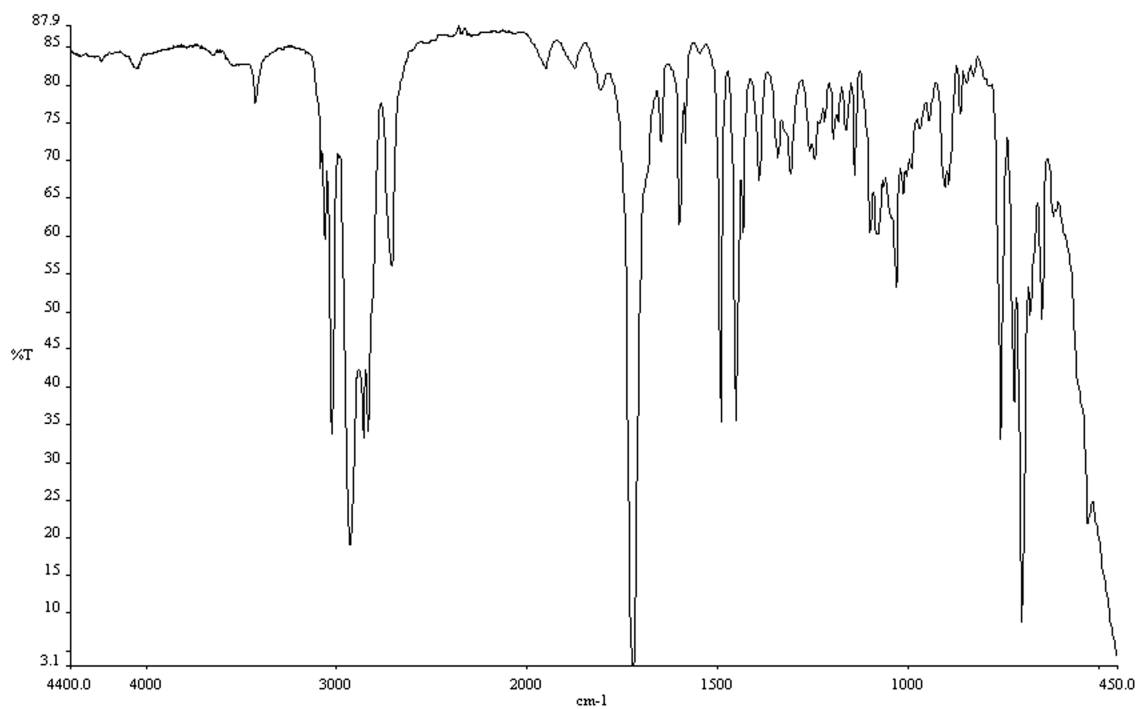
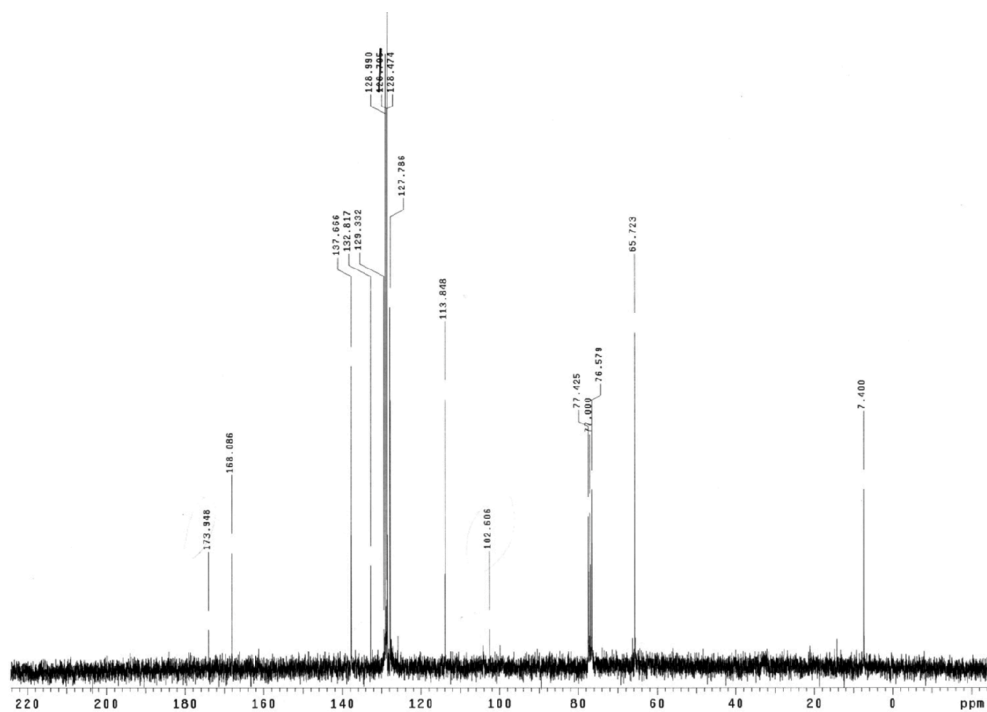*Figure A.1.128* Infrared spectrum (thin film/NaCl) of compound **186**.
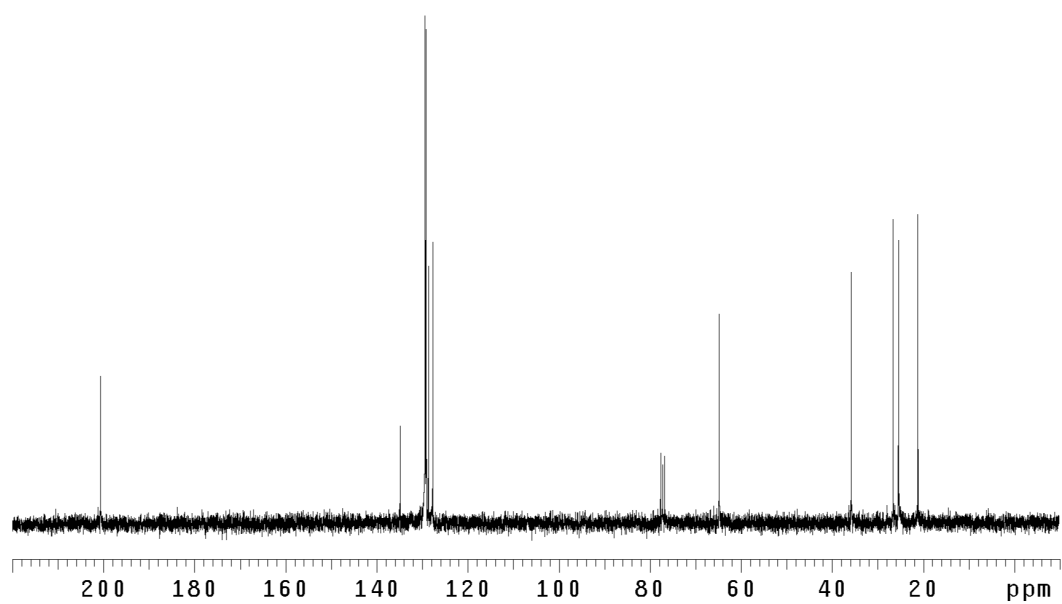
Figure A.1.129 ^{13}CNMR (75 Mhz, CDCl$_3$) of compound **186**.
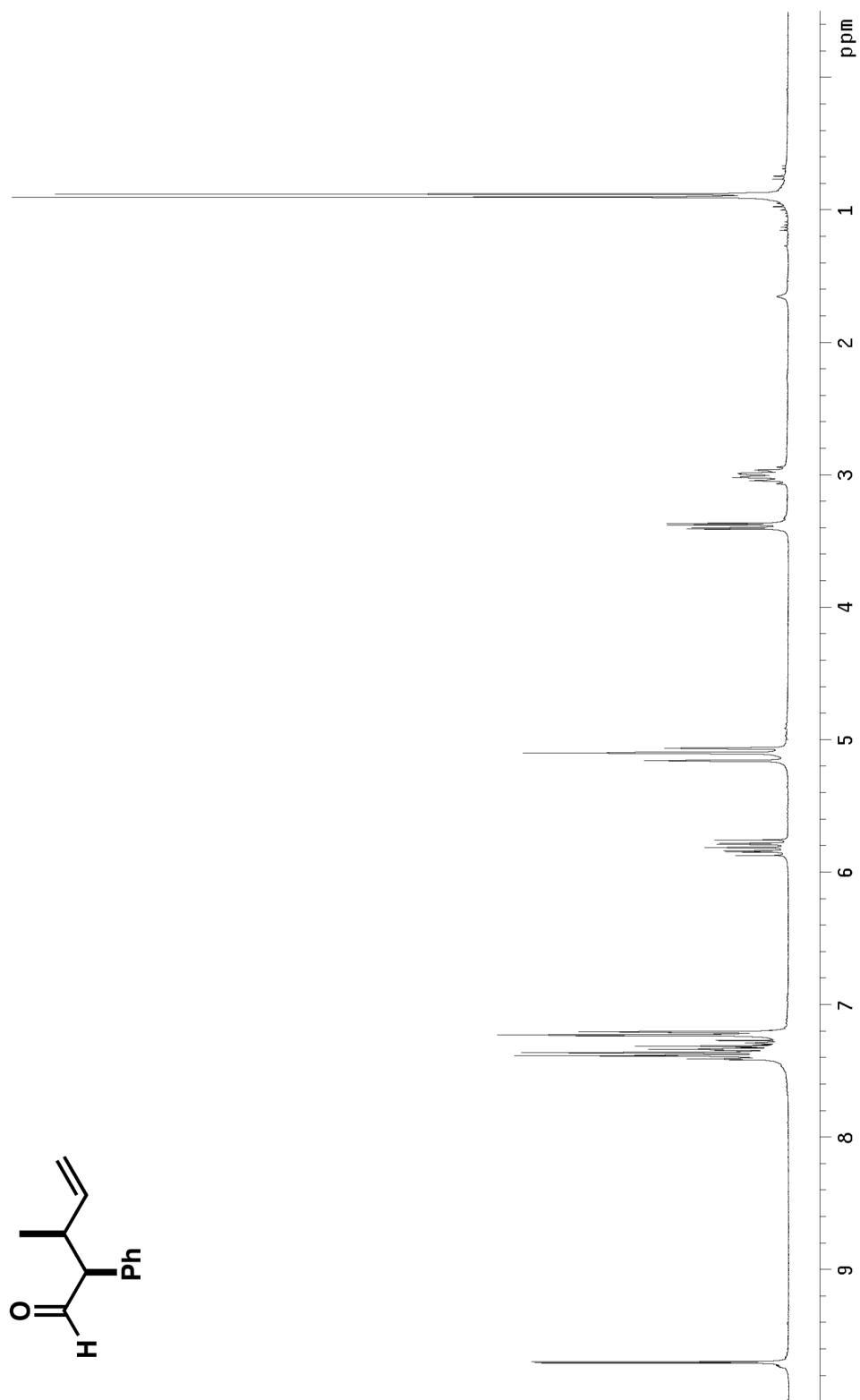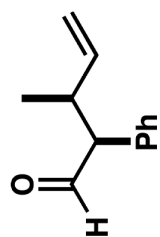
Figure A.1.130 ¹HNMR (300 MHz, CDCL₃) of compound **184**.
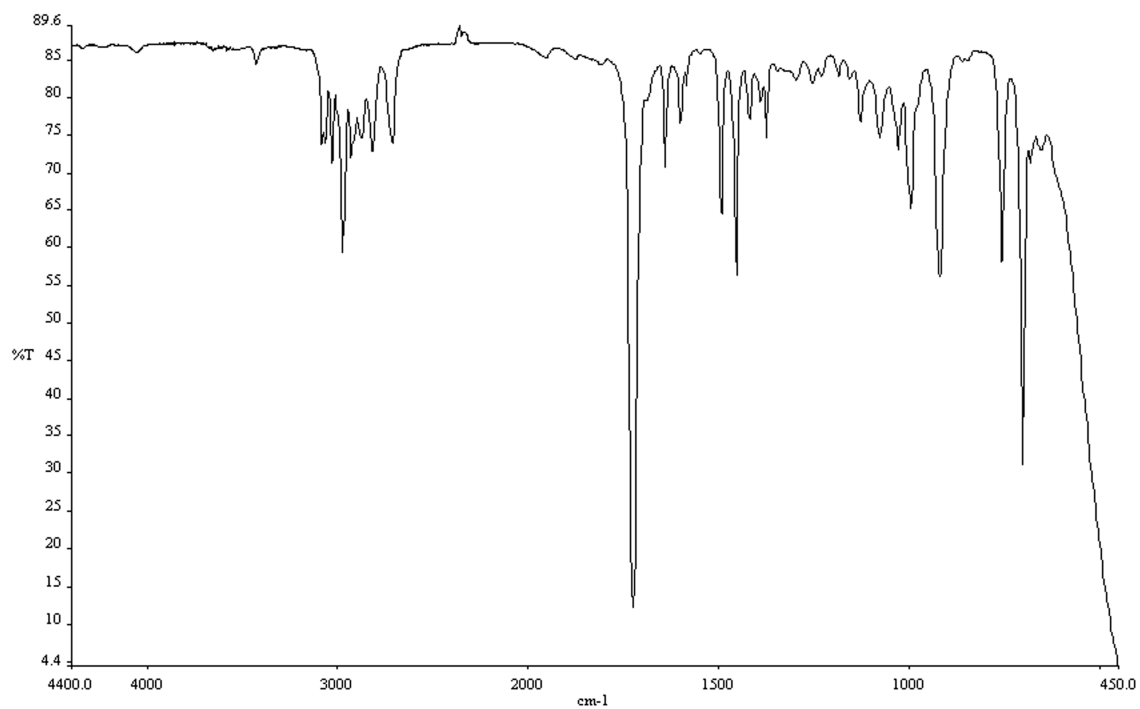
Figure A.1.131 Infrared spectrum (thin film/NaCl) of compound **184**.
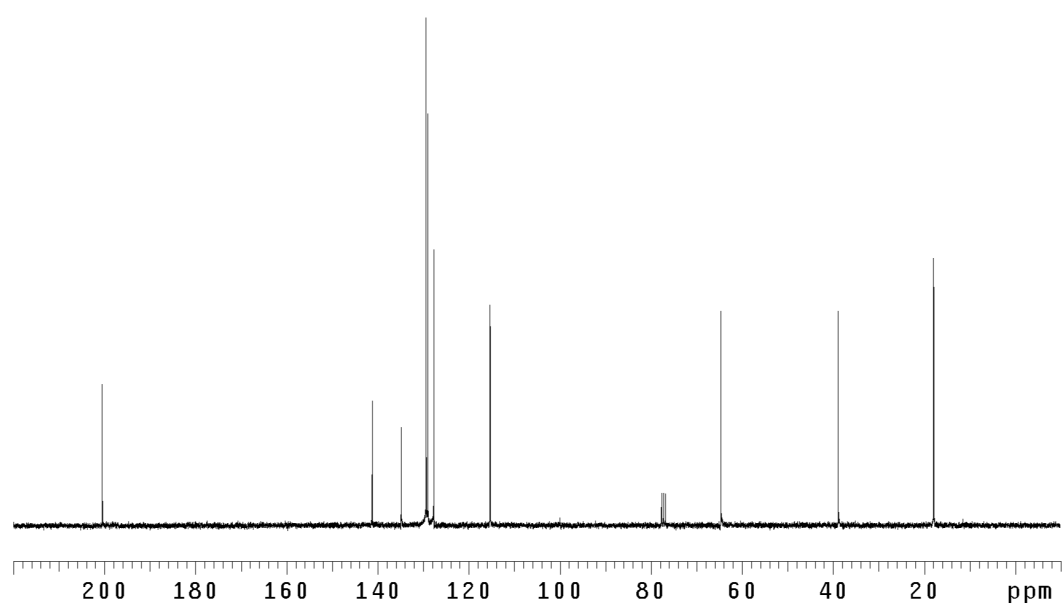
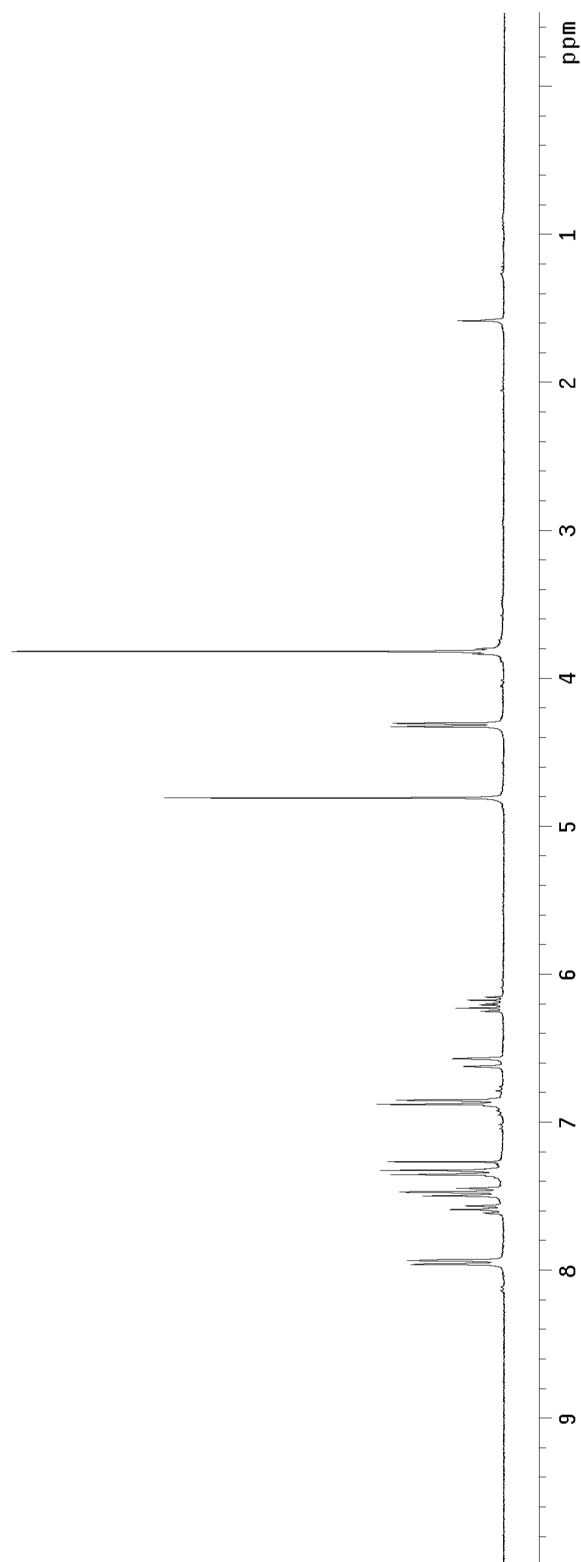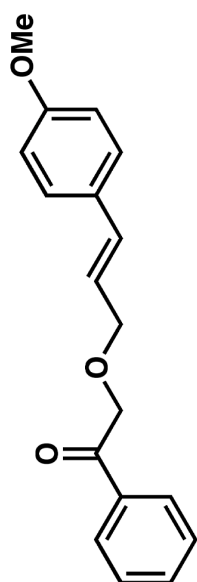*Figure A.1.132* ^{13}CNMR (75 Mhz, CDCl$_3$) of compound **184**.
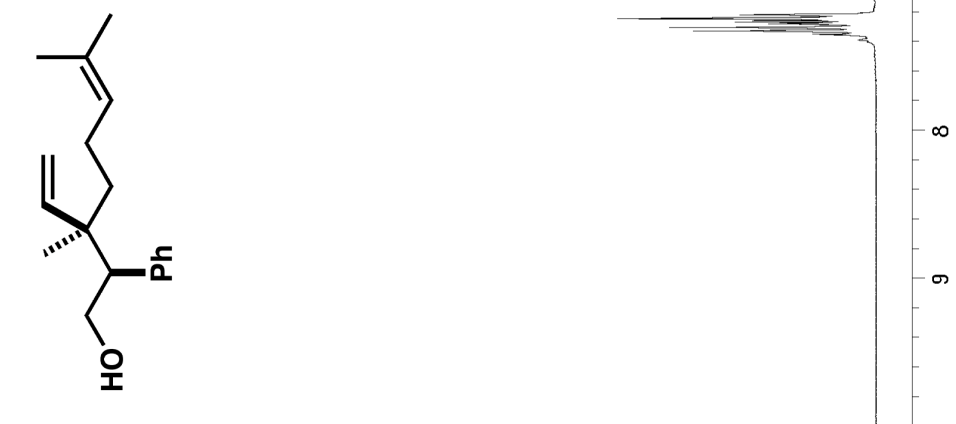
Figure A.1.133 ¹HNMR (300 MHz, CDCL₃) of compound **191**.
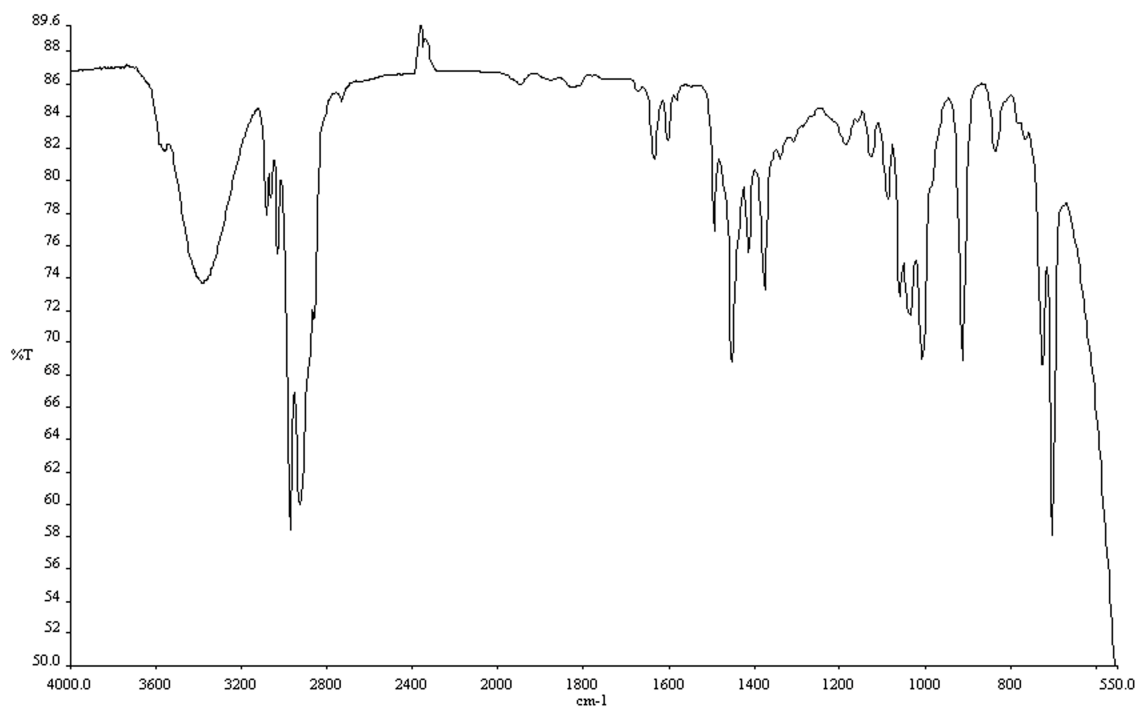
Figure A.1.134 Infrared spectrum (thin film/NaCl) of compound **191**.
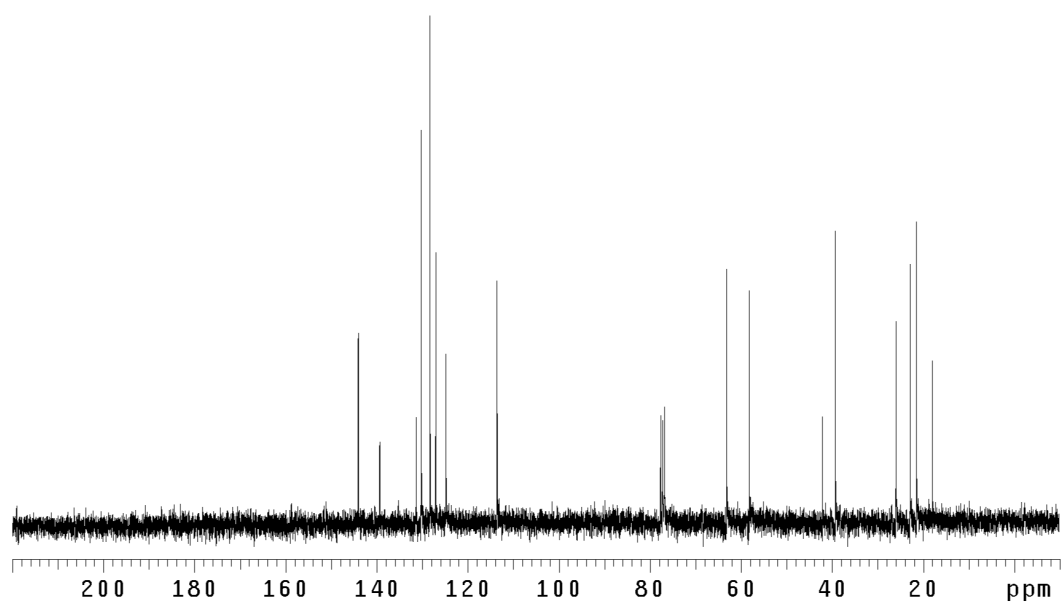
Figure A.1.135 ^{13}CNMR (75 Mhz, CDCl$_3$) of compound **191**.
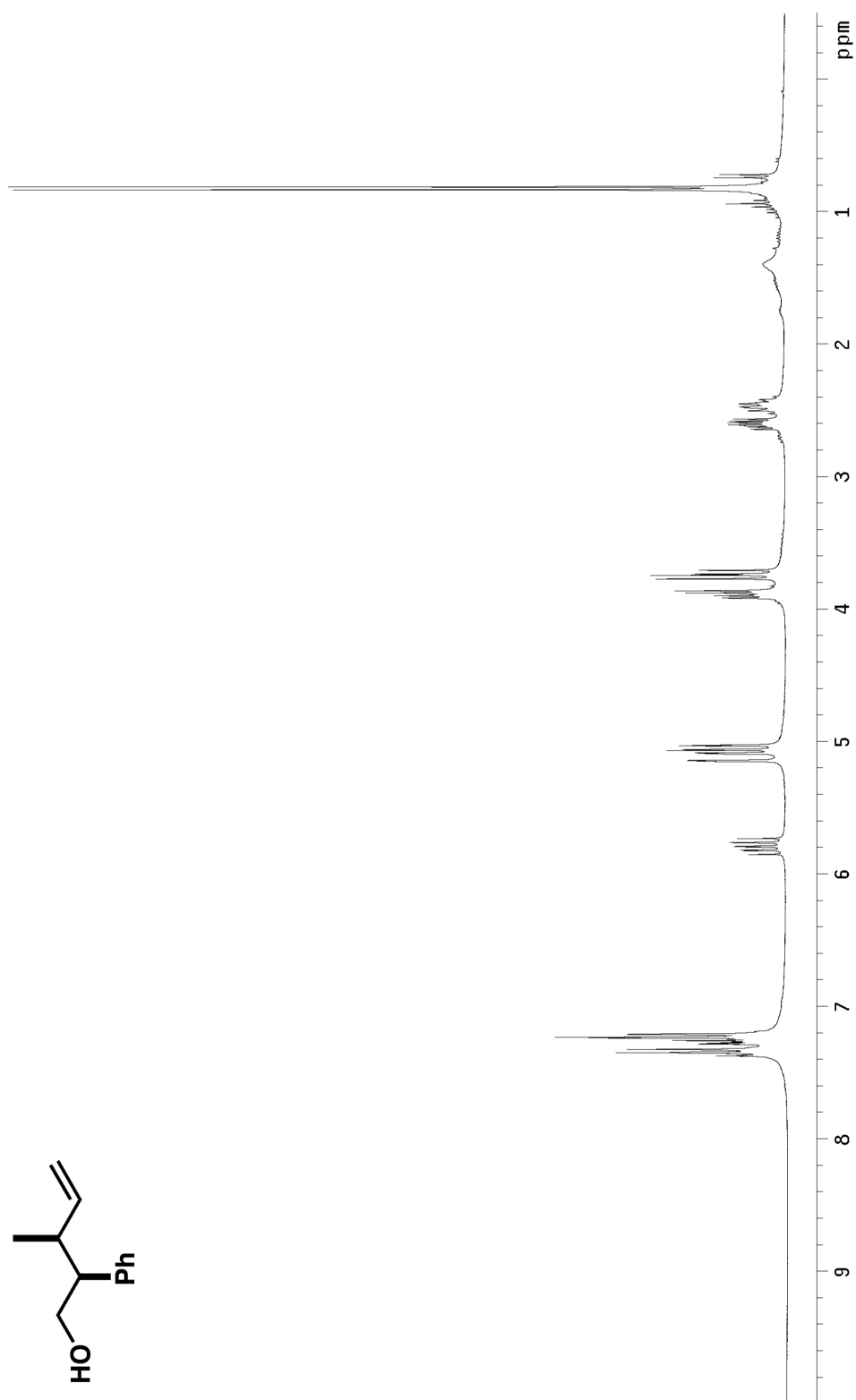
Figure A.1.136 ^{1}HNMR (300 MHz, CDCL$_3$) of compound **188**.
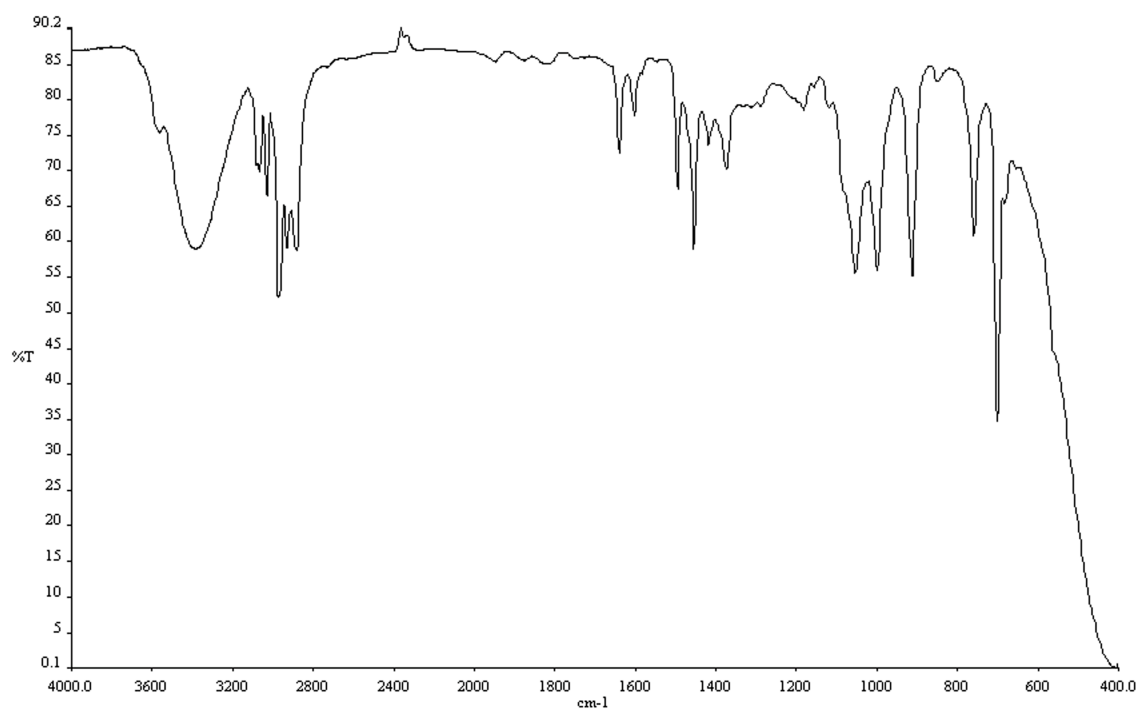
Figure A.1.137 Infrared spectrum (thin film/NaCl) of compound **188**.
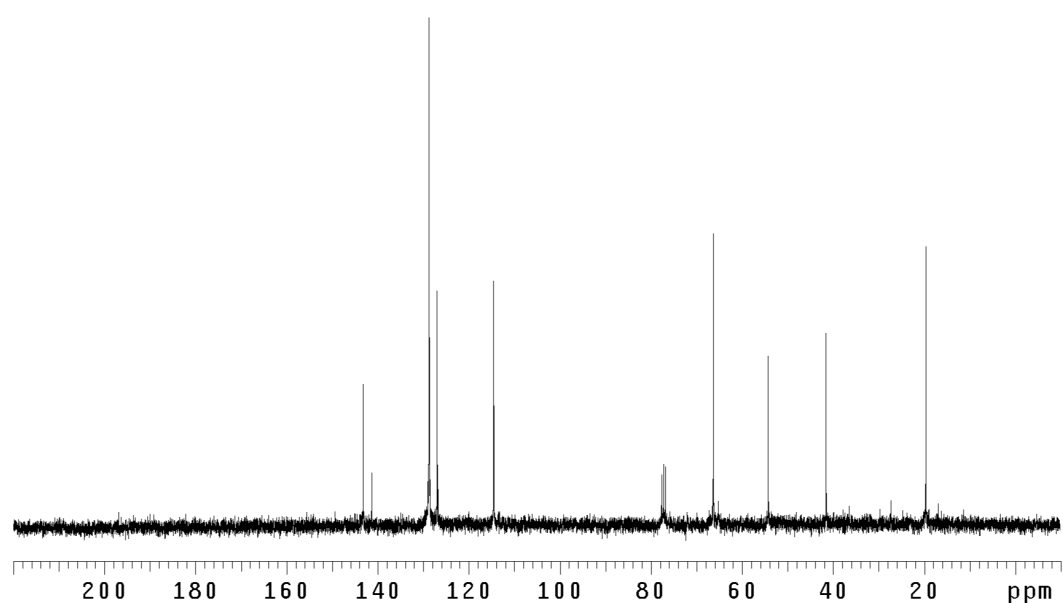
Figure A.1.138 ^{13}CNMR (75 Mhz, CDCl$_3$) of compound **188**.
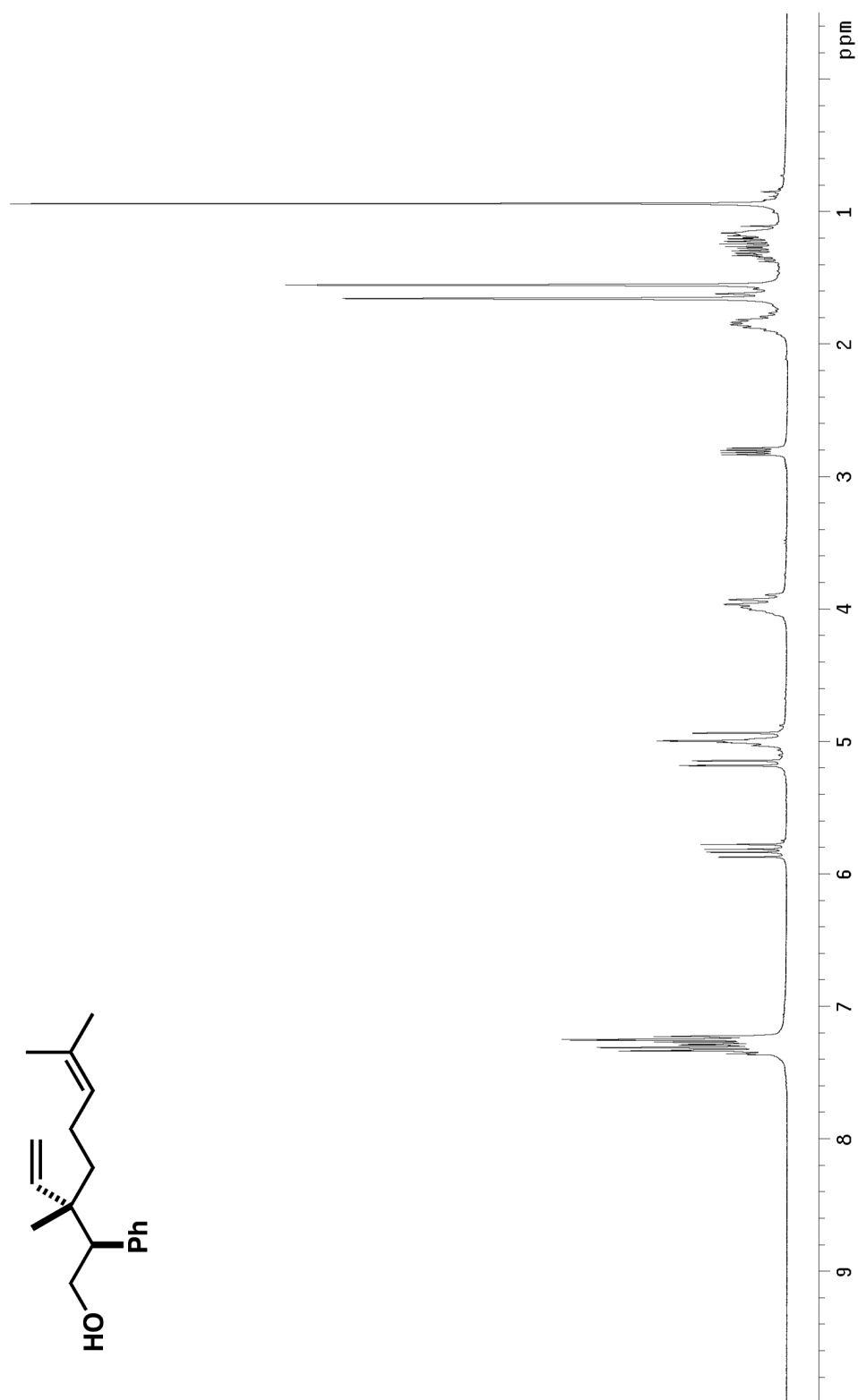
Figure A.1.139 ^{1}HNMR (300 MHz, CDCL$_3$) of compound **194**.

Figure A.1.140 Infrared spectrum (thin film/NaCl) of compound **194**.
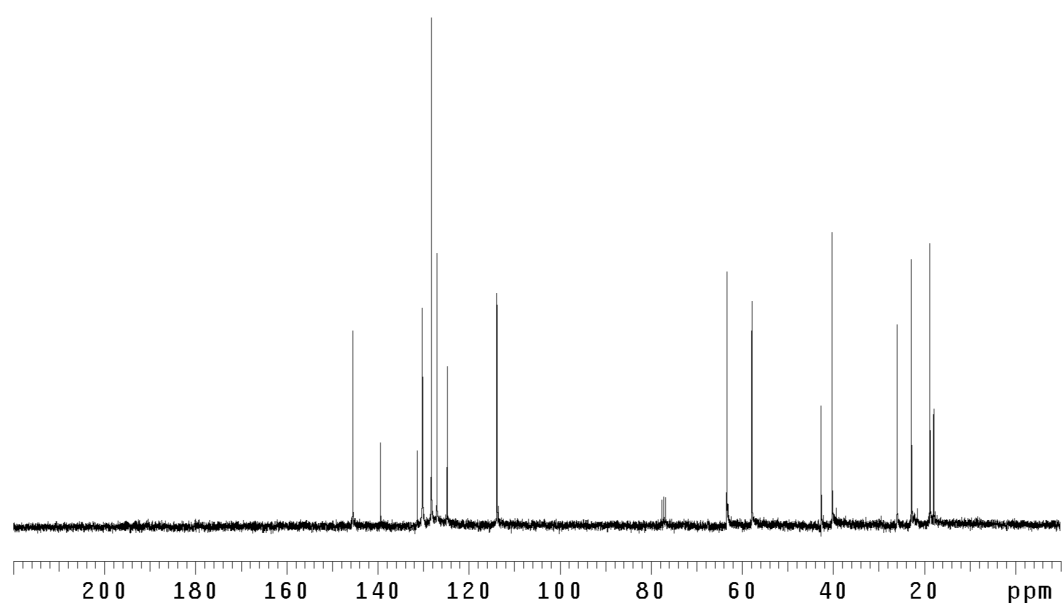
Figure A.1.141 ^{13}CNMR (75 Mhz, CDCl$_3$) of compound **194**.
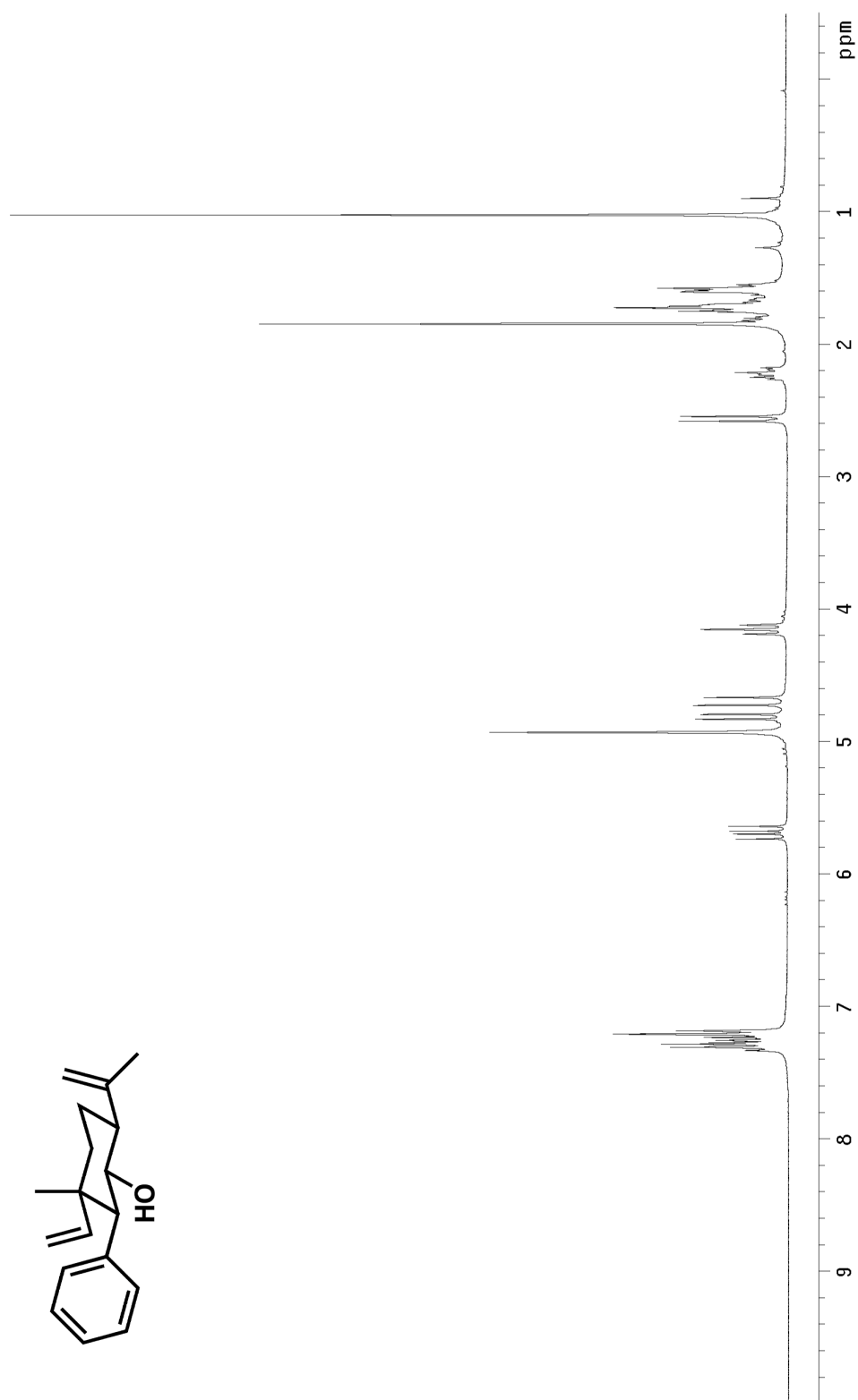
Figure A.1.142 ^{1}HNMR (300 MHz, CDCL$_3$) of compound **197**.
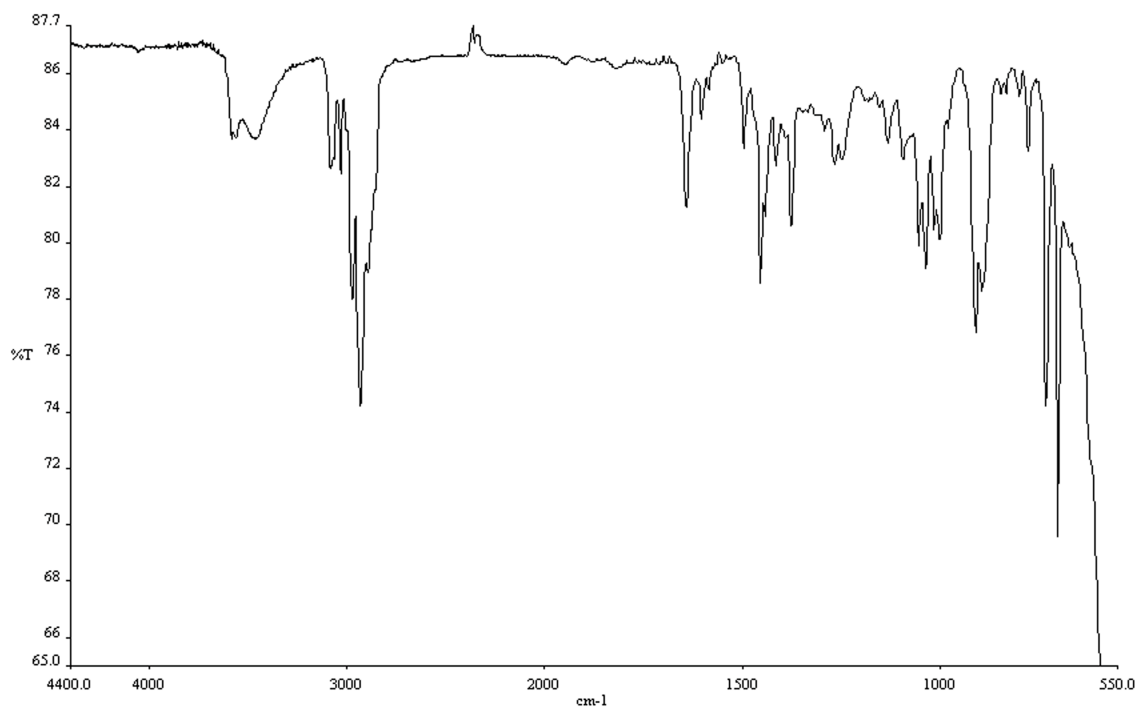
Figure A.1.143 Infrared spectrum (thin film/NaCl) of compound **197**.
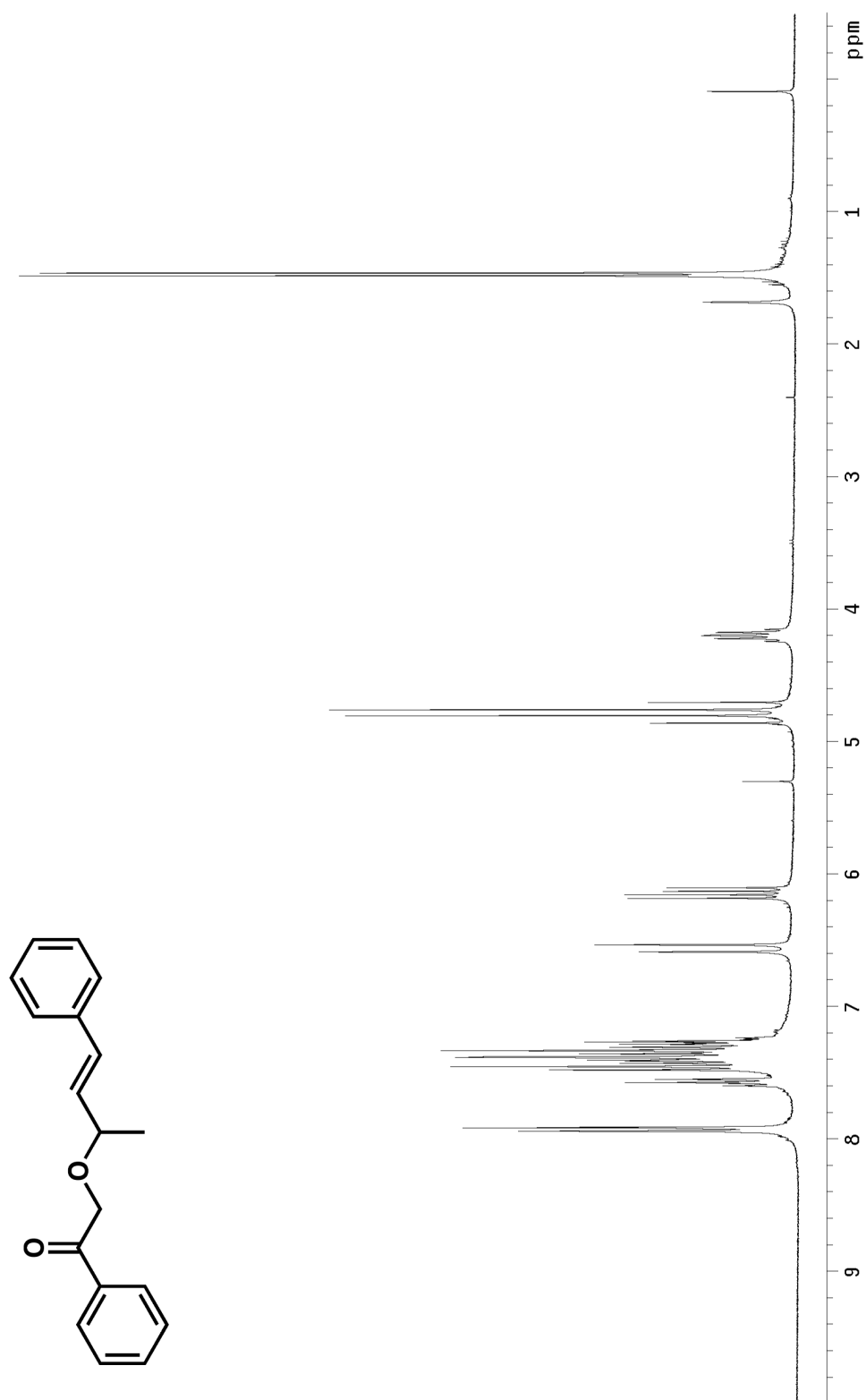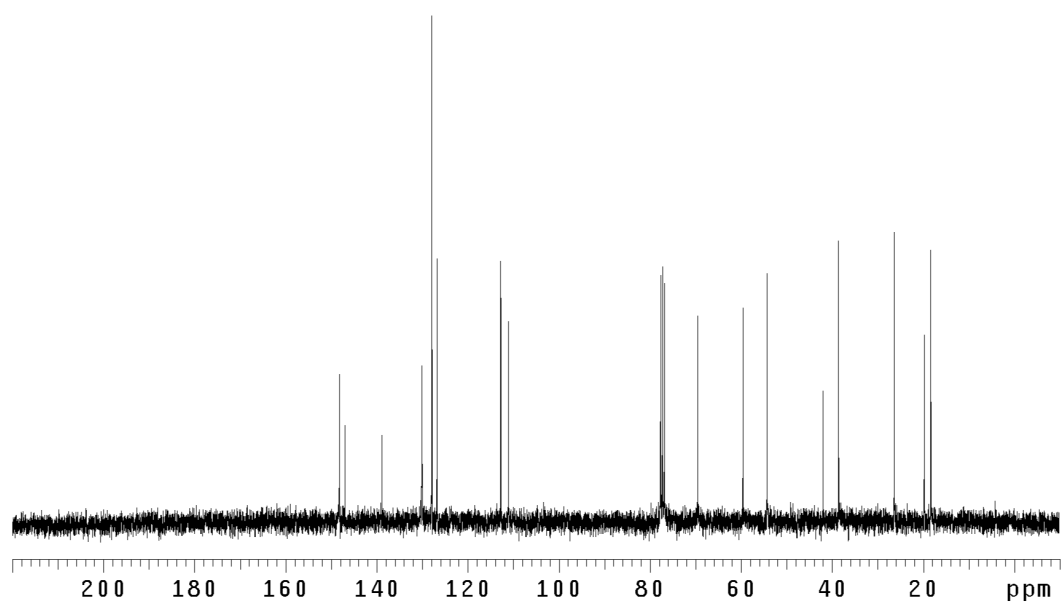

Figure A.1.144 ¹³CNMR (75 Mhz, CDCl₃) of compound **197**.
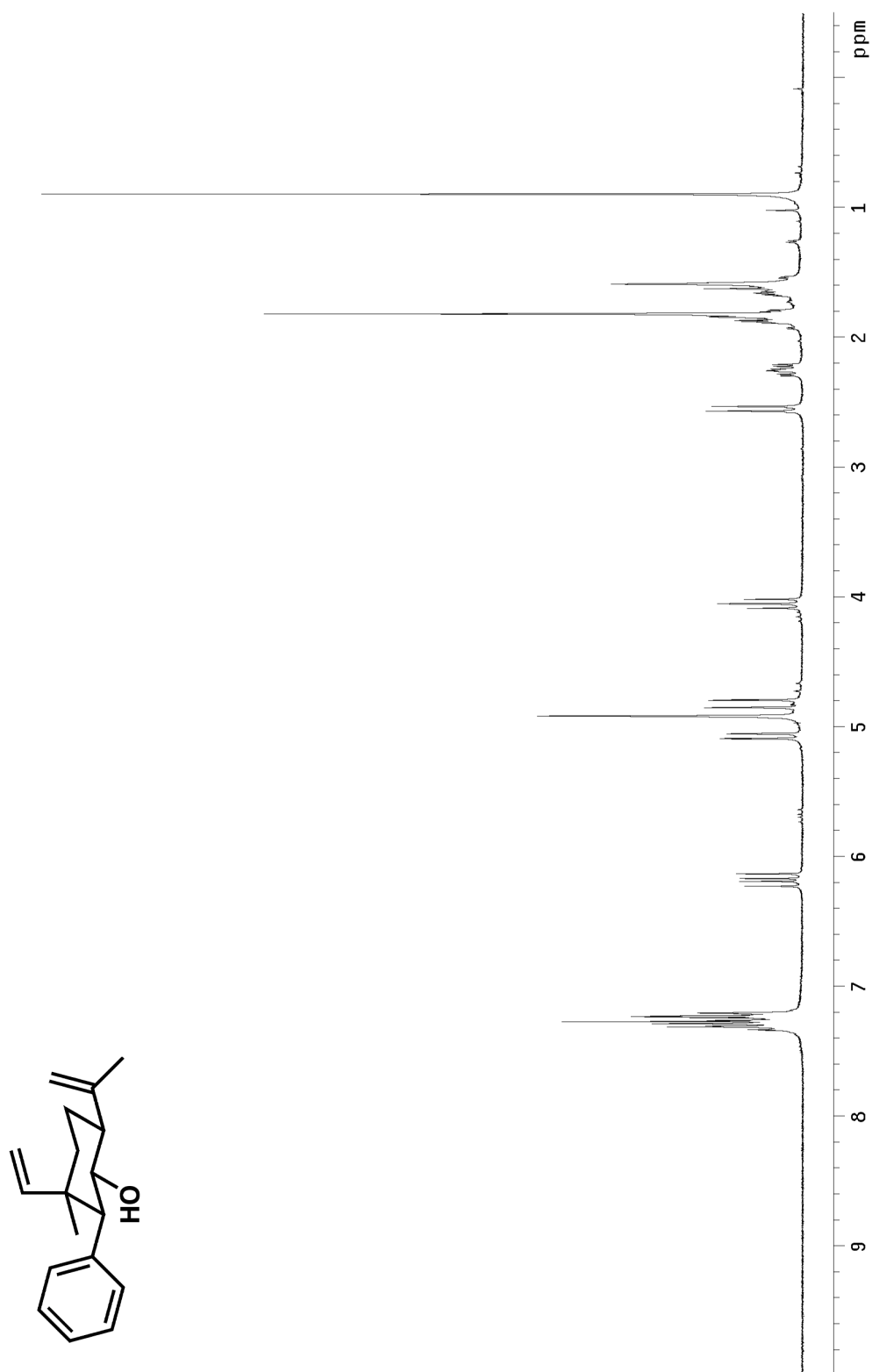
Figure A.1.145 ¹HNMR (300 MHz, CDCL₃) of compound **198**.
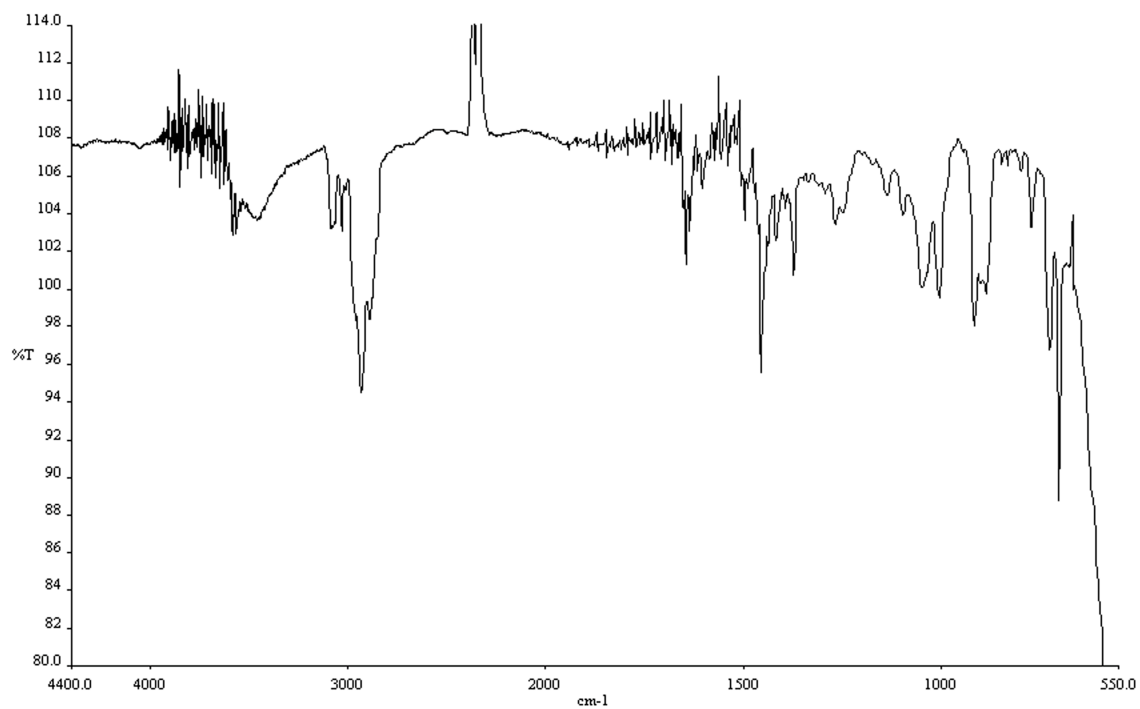
Figure A.1.146 Infrared spectrum (thin film/NaCl) of compound **198**.
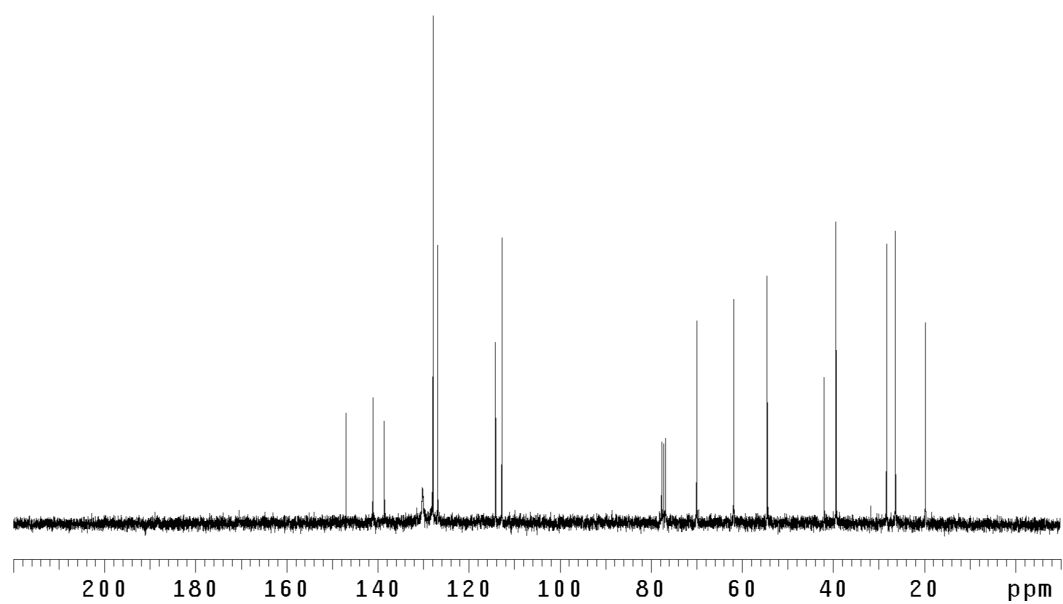
Figure A.1.147 ¹³CNMR (75 Mhz, CDCl₃) of compound **198**.
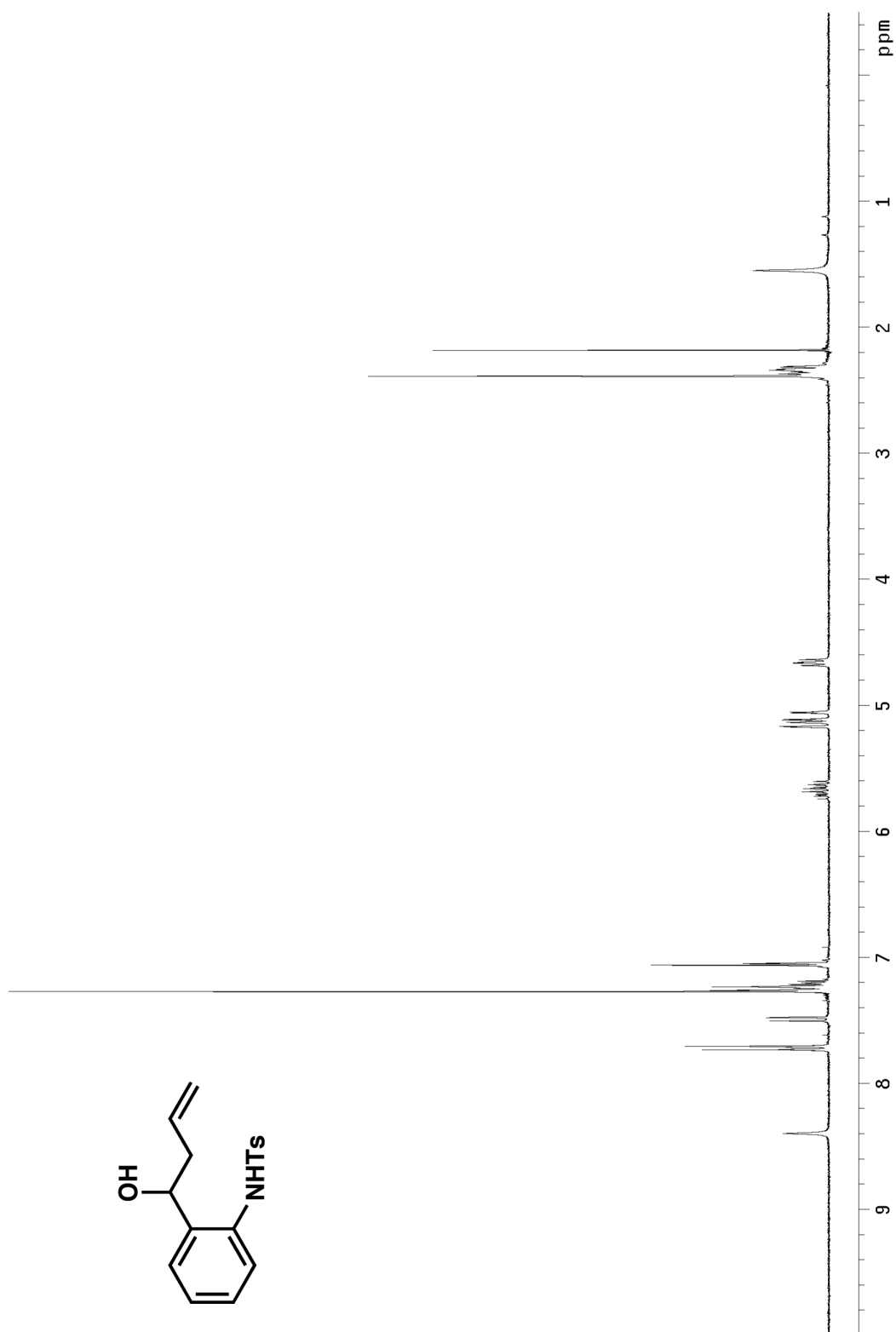
Figure A.1.148 ¹HNMR (300 MHz, CDCL₃) of compound **507**.
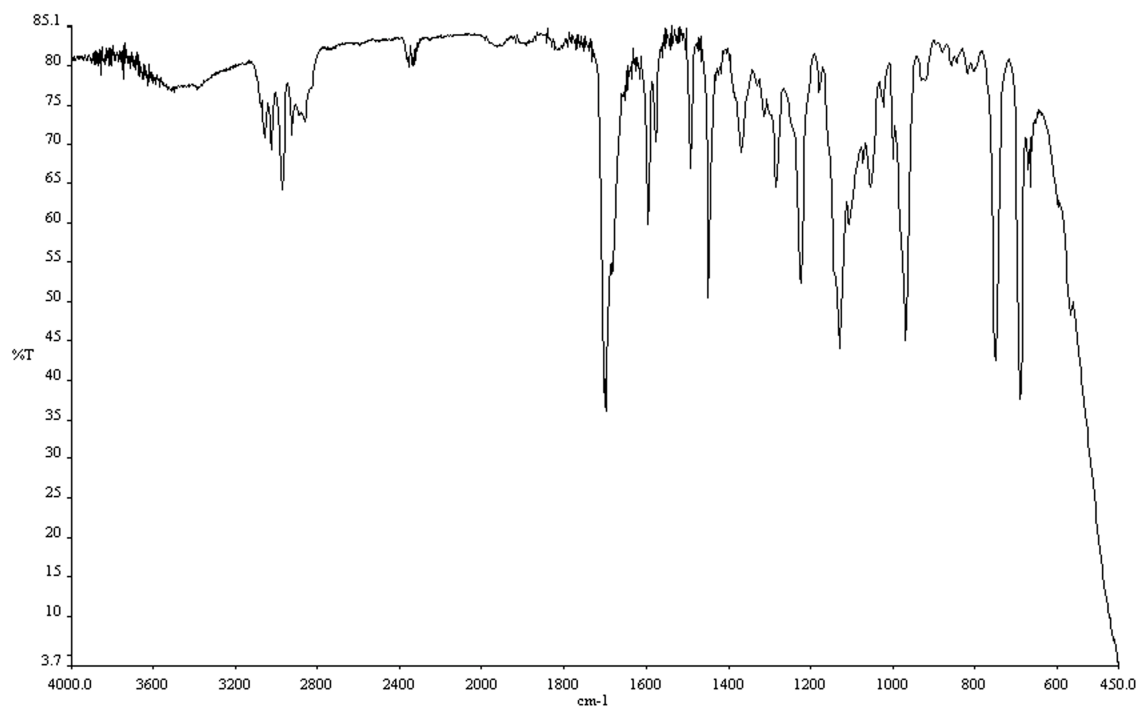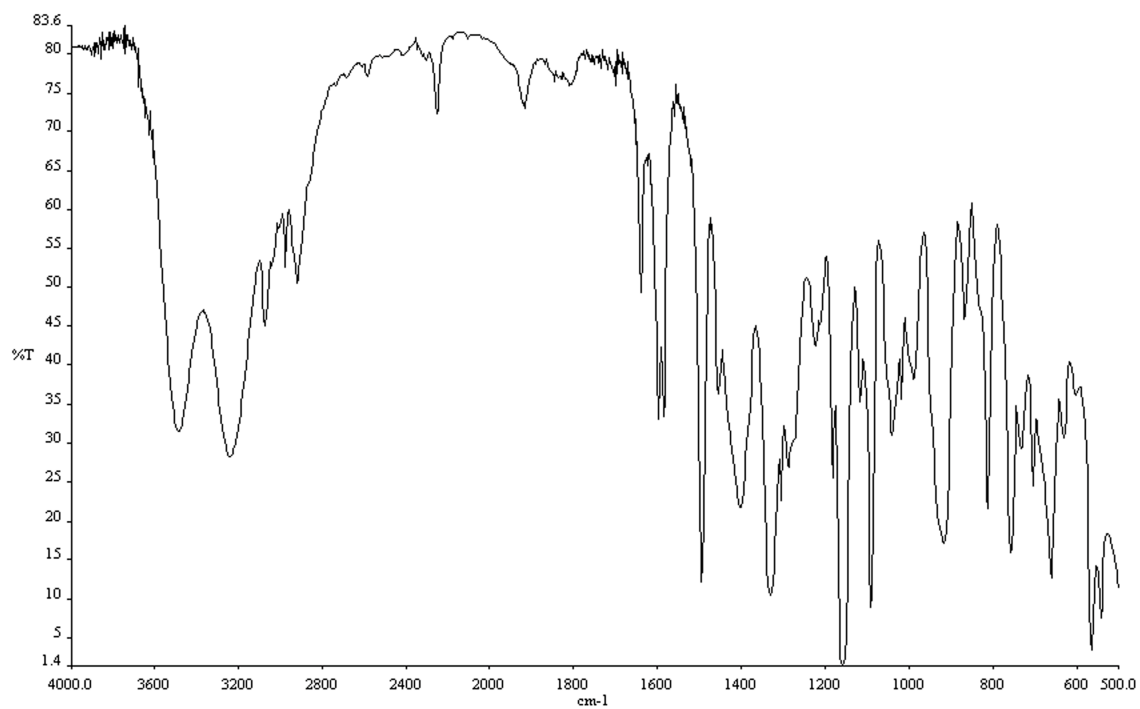
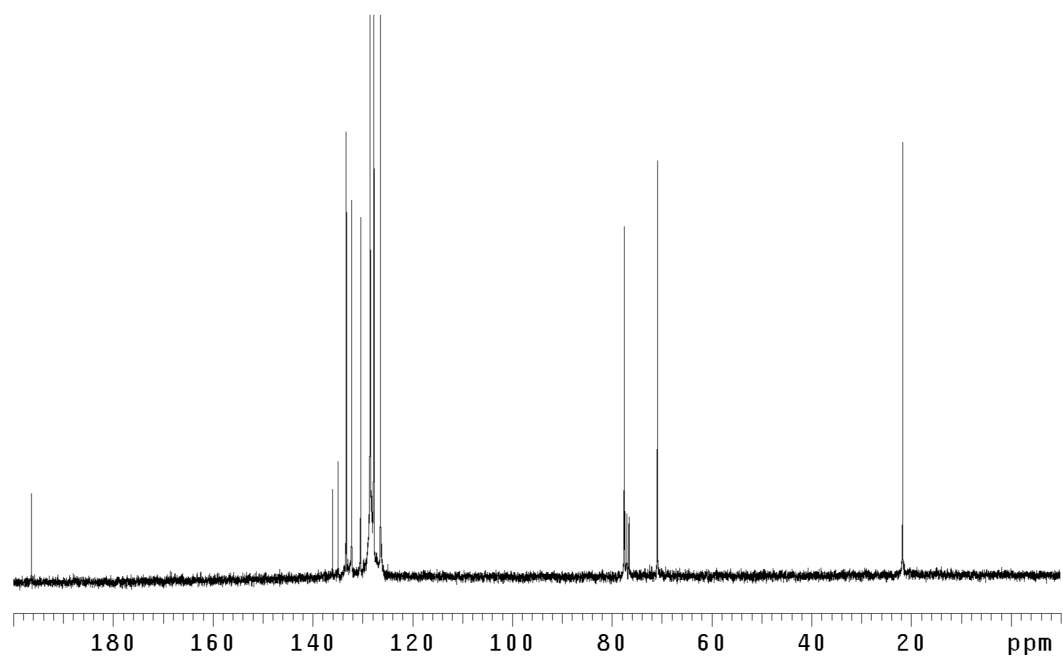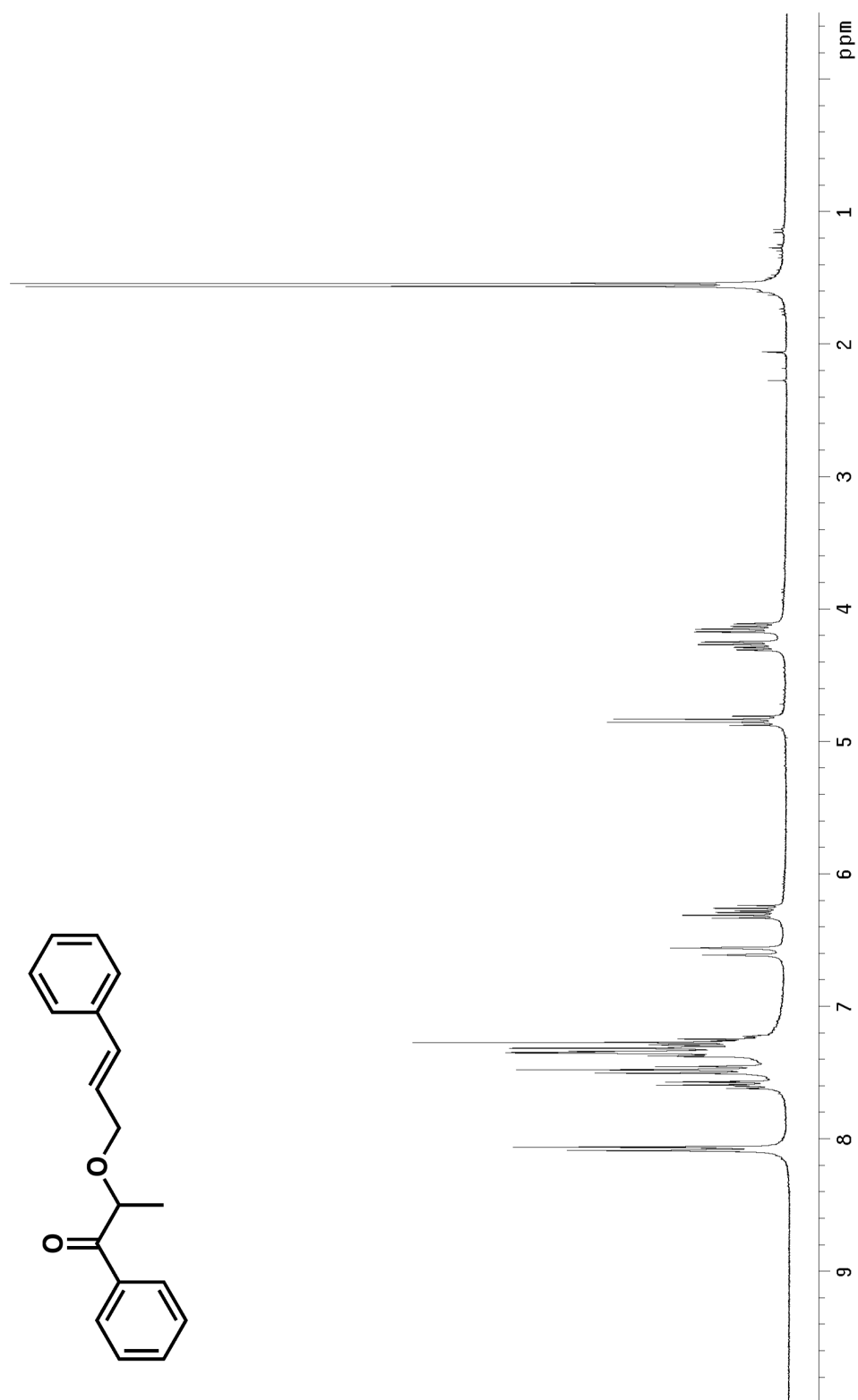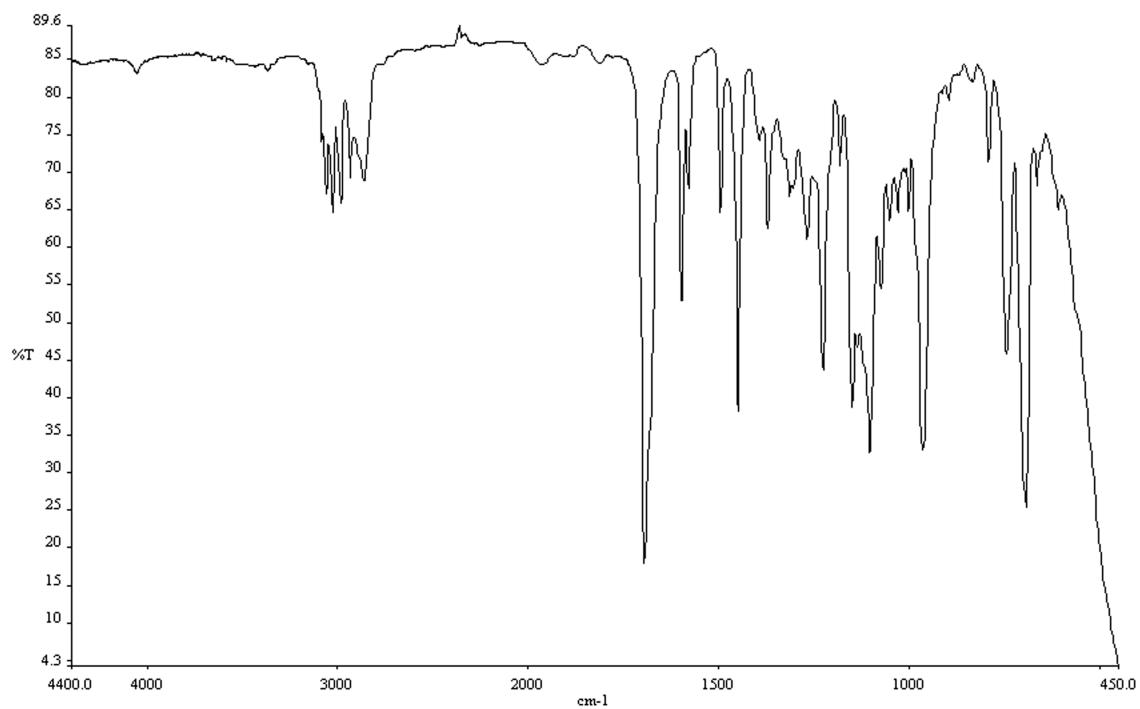*Figure A.1.149* Infrared spectrum (thin film/NaCl) of compound **507**.
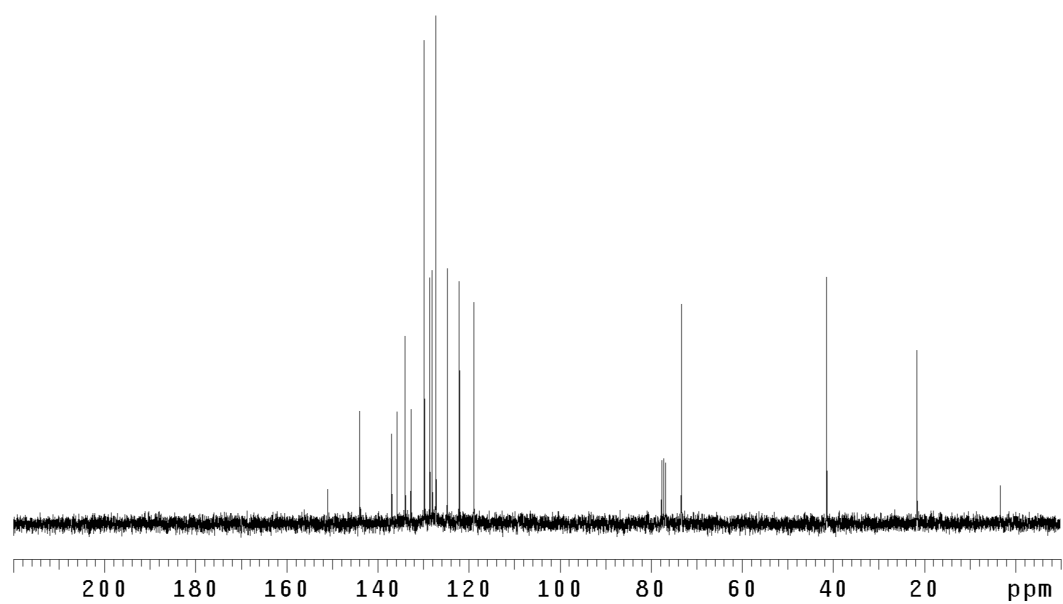
Figure A.1.150 ^{13}CNMR (75 Mhz, CDCl$_3$) of compound **507**.
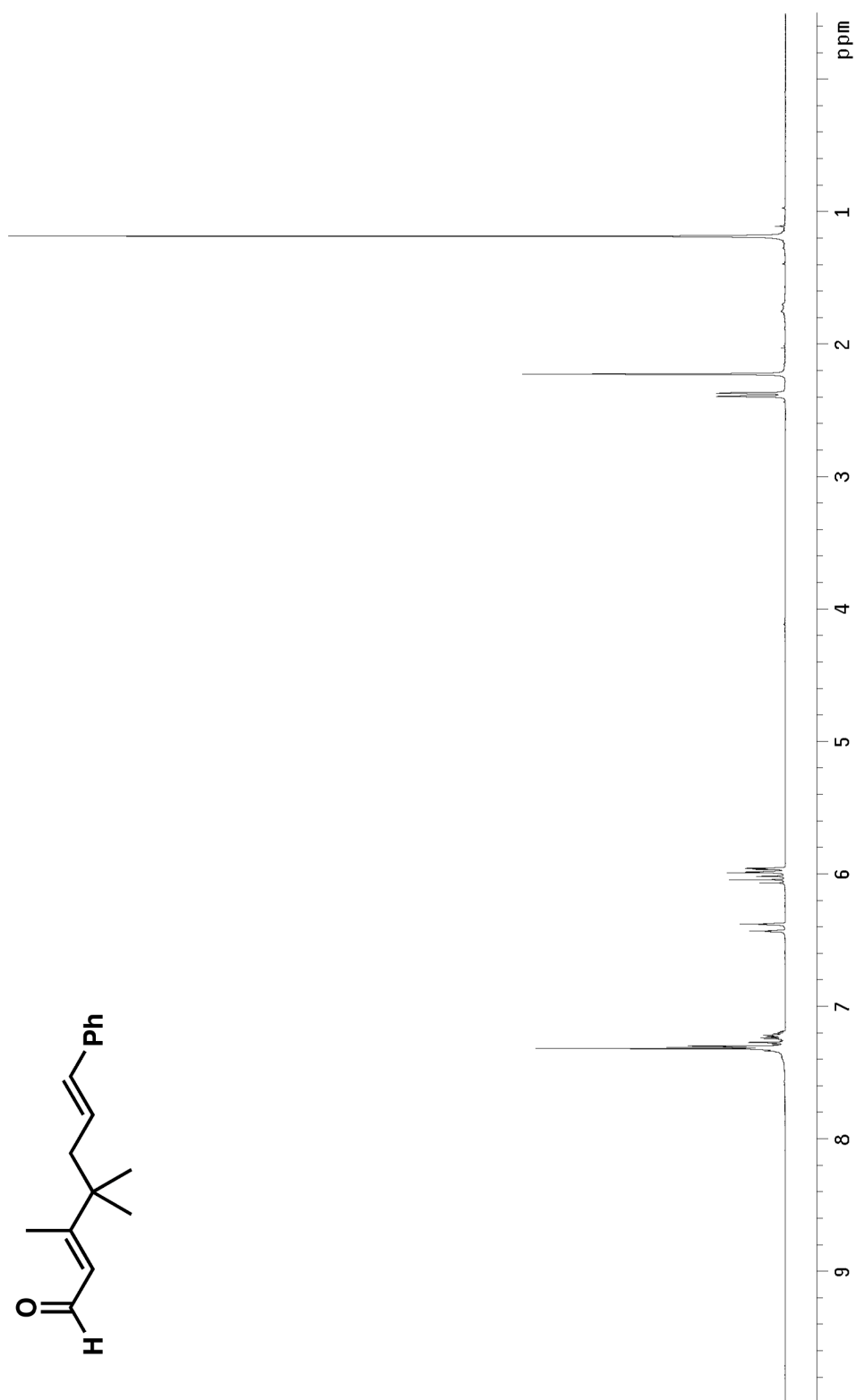
Figure A.1.151 ¹HNMR (300 MHz, CDCL₃) of compound **203**.
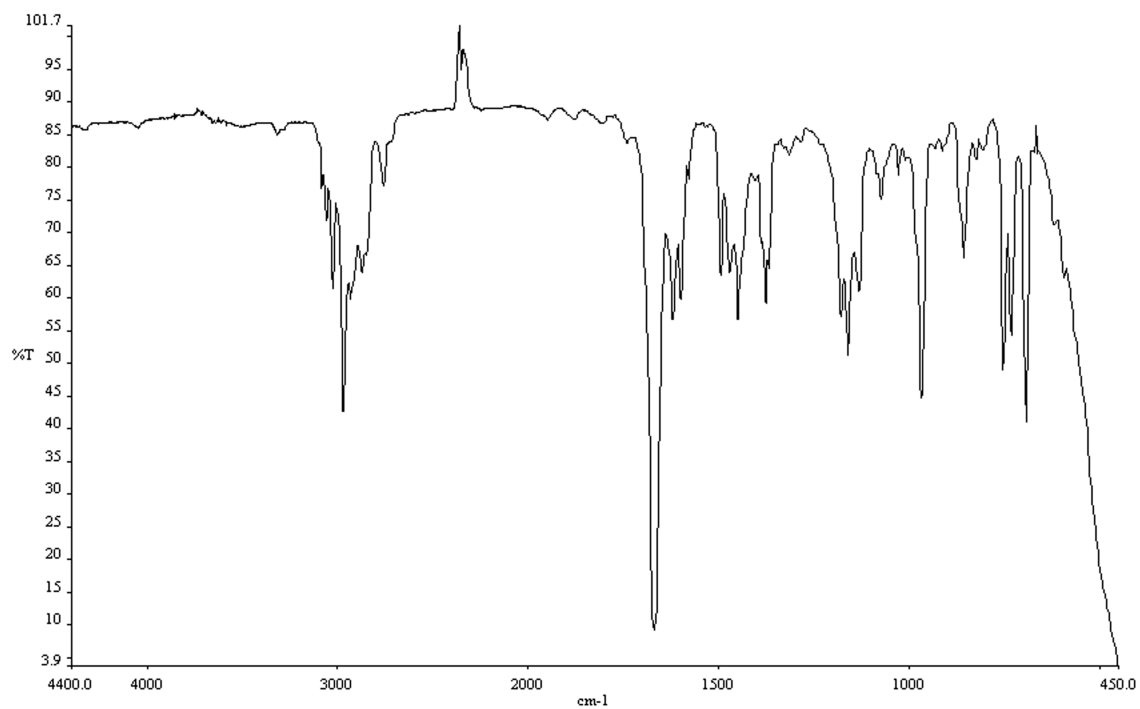
Figure A.1.152 Infrared spectrum (thin film/NaCl) of compound **203**.
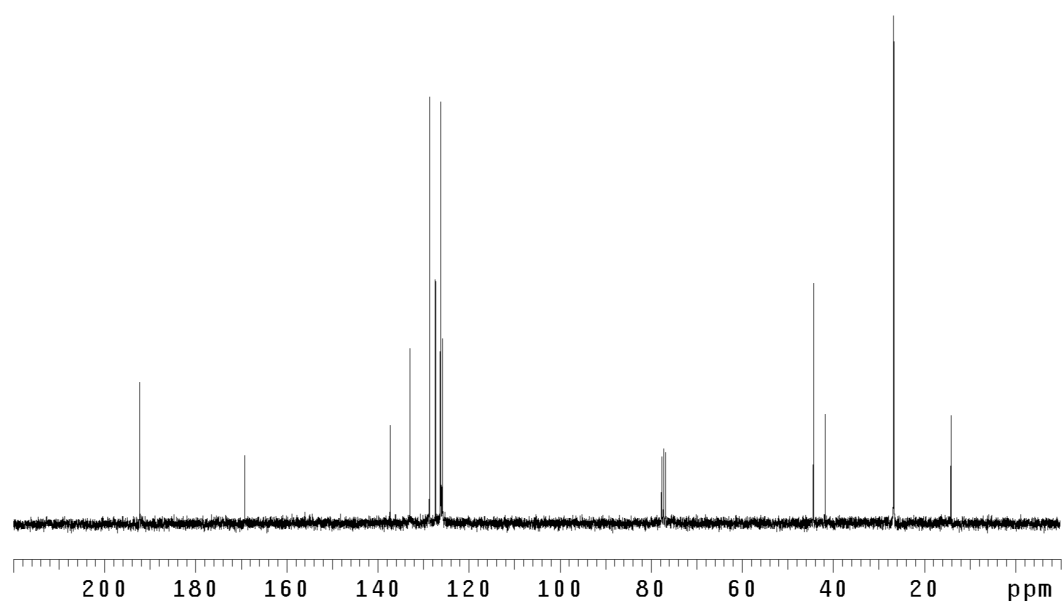
Figure A.1.153 ^{13}CNMR (75 Mhz, CDCl$_3$) of compound **203**.
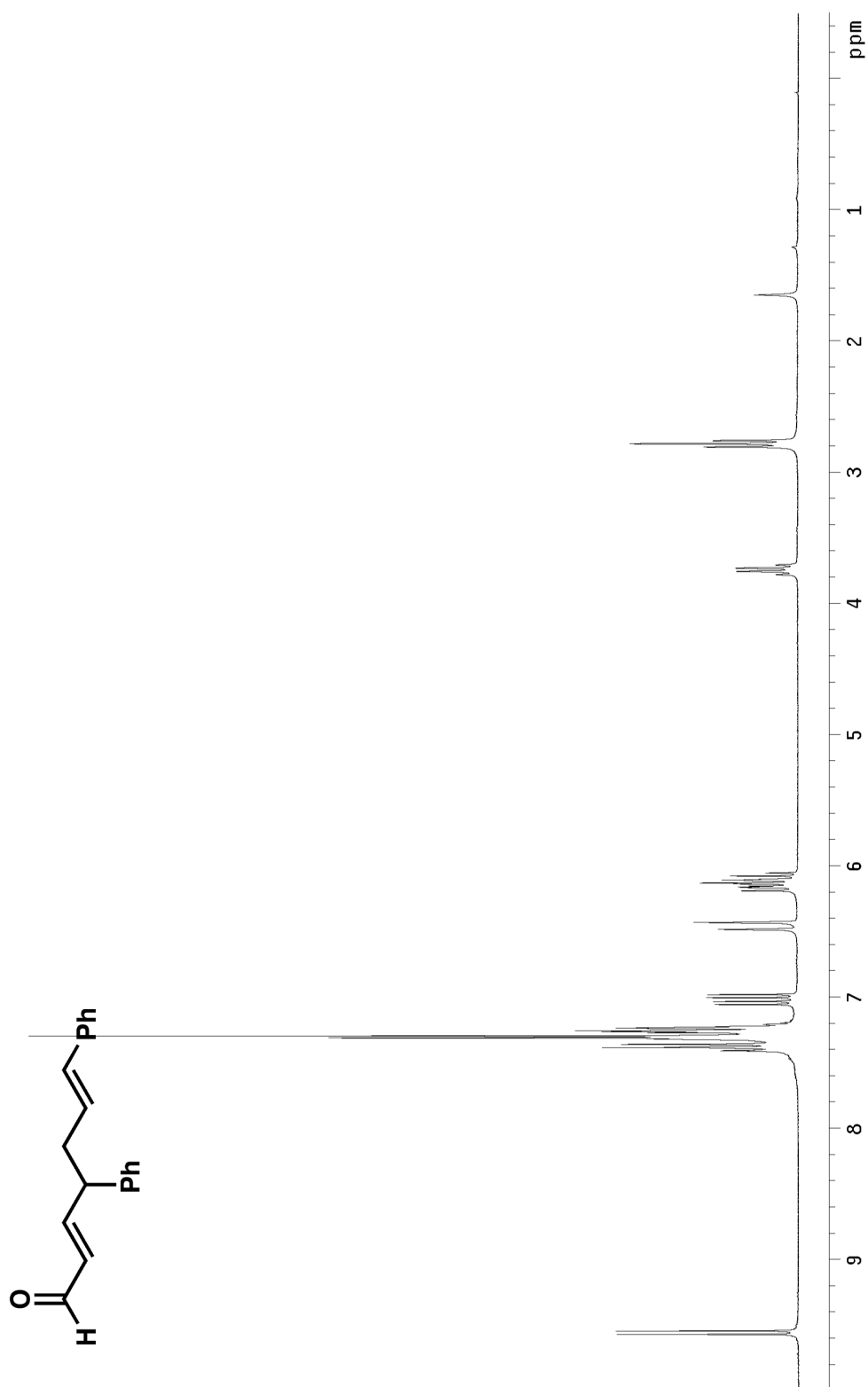
Figure A.1.154 ¹HNMR (300 MHz, CDCL₃) of compound **201**.
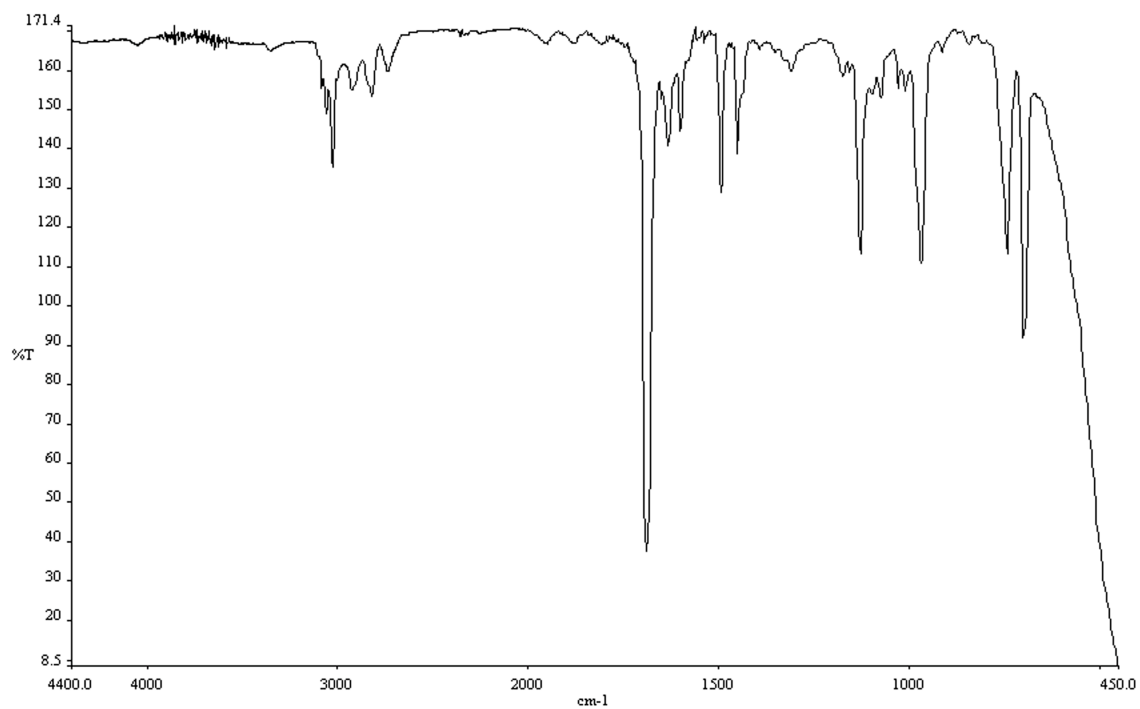
Figure A.1.155 Infrared spectrum (thin film/NaCl) of compound **201**.
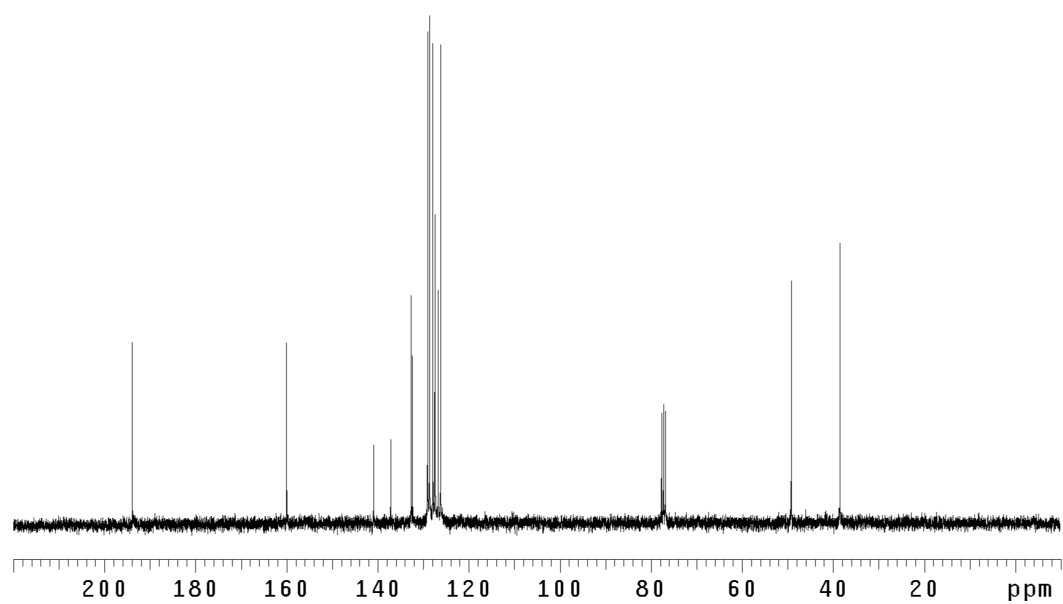
Figure A.1.156 ^{13}CNMR (75 Mhz, CDCl$_3$) of compound **201**.
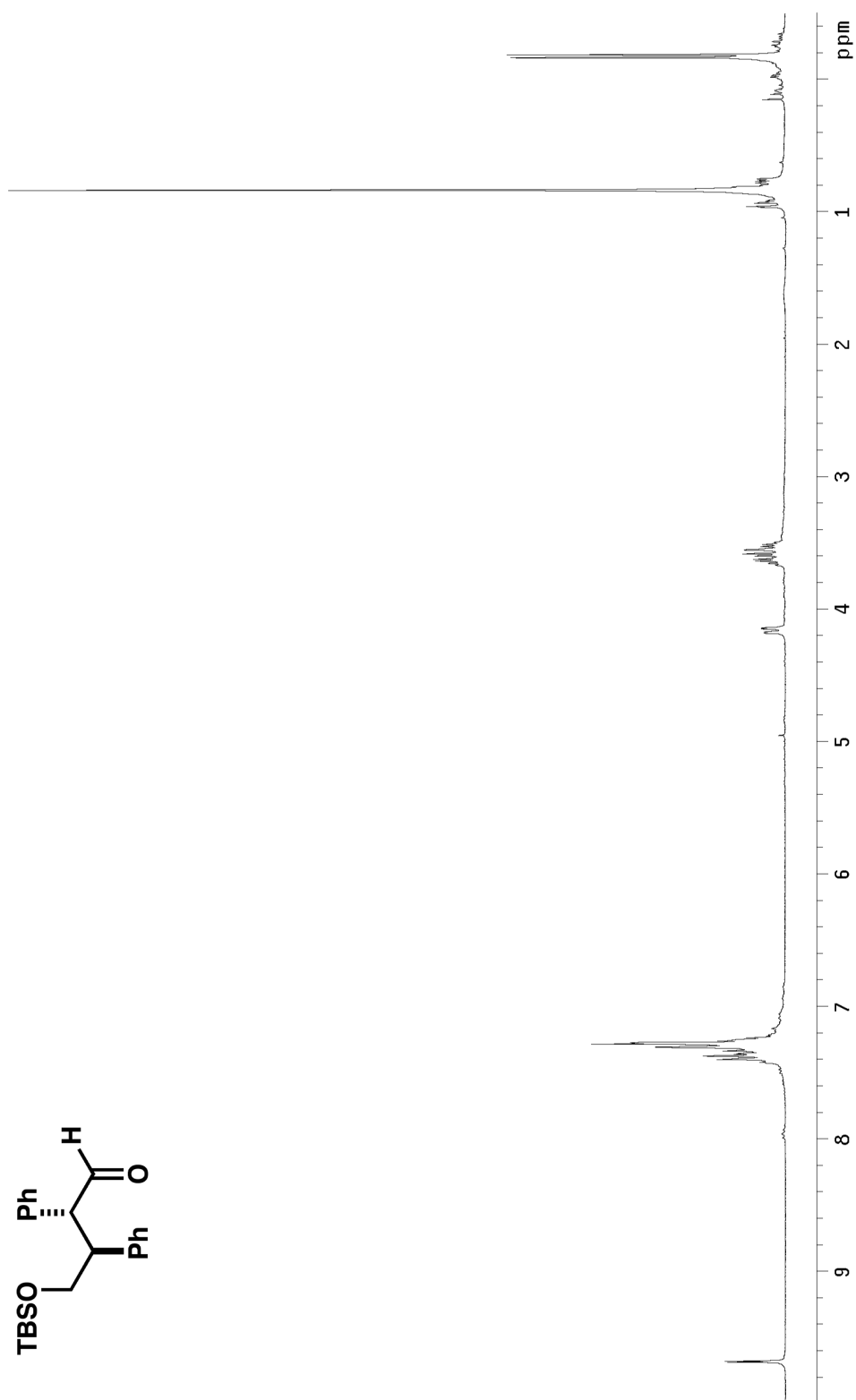
Figure A.1.157 ¹HNMR (300 MHz, CDCL₃) of compound **205**.
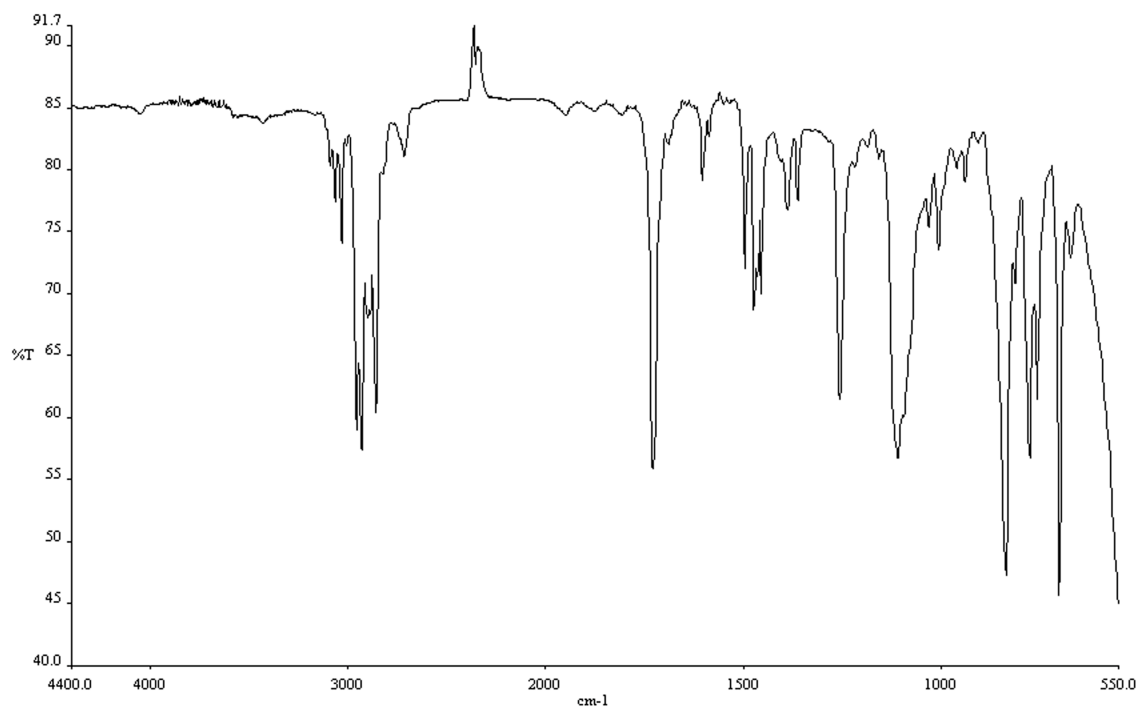
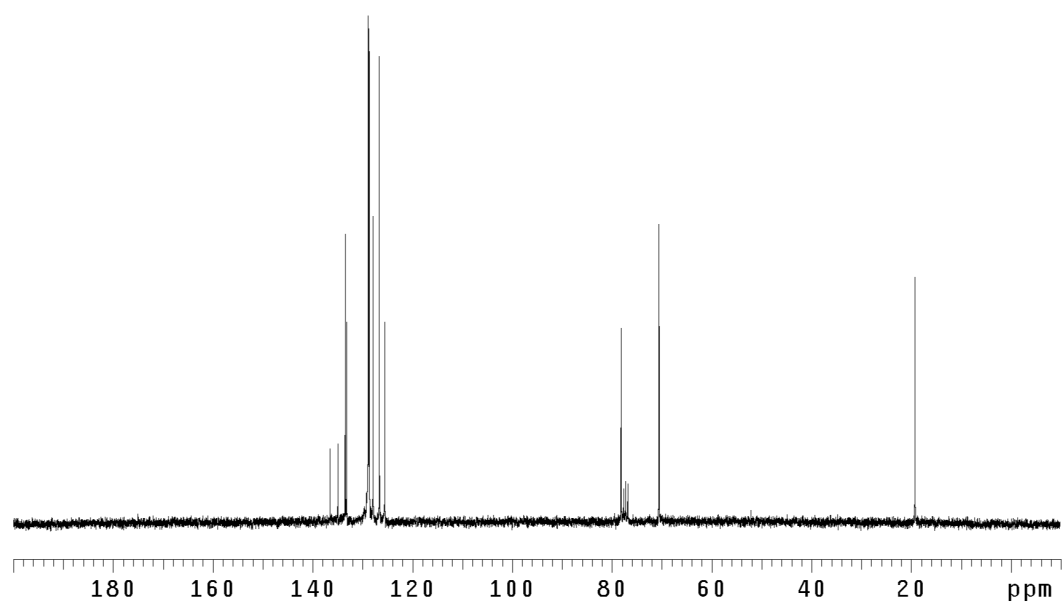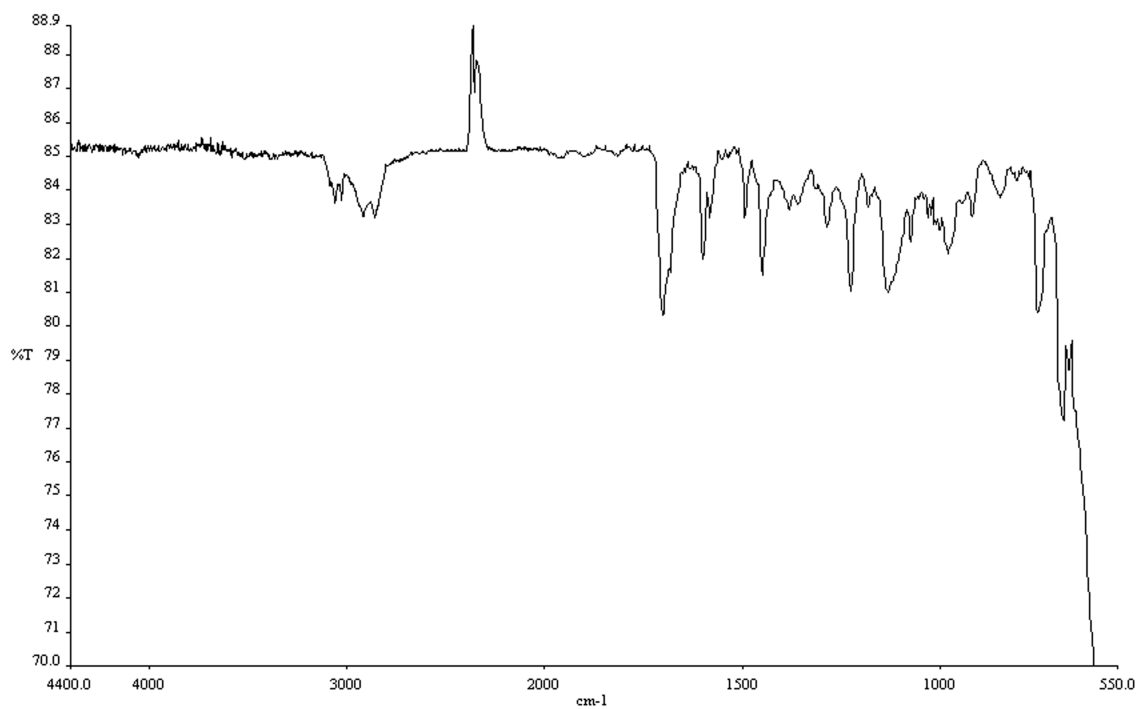*Figure A.1.158* Infrared spectrum (thin film/NaCl) of compound **205**.
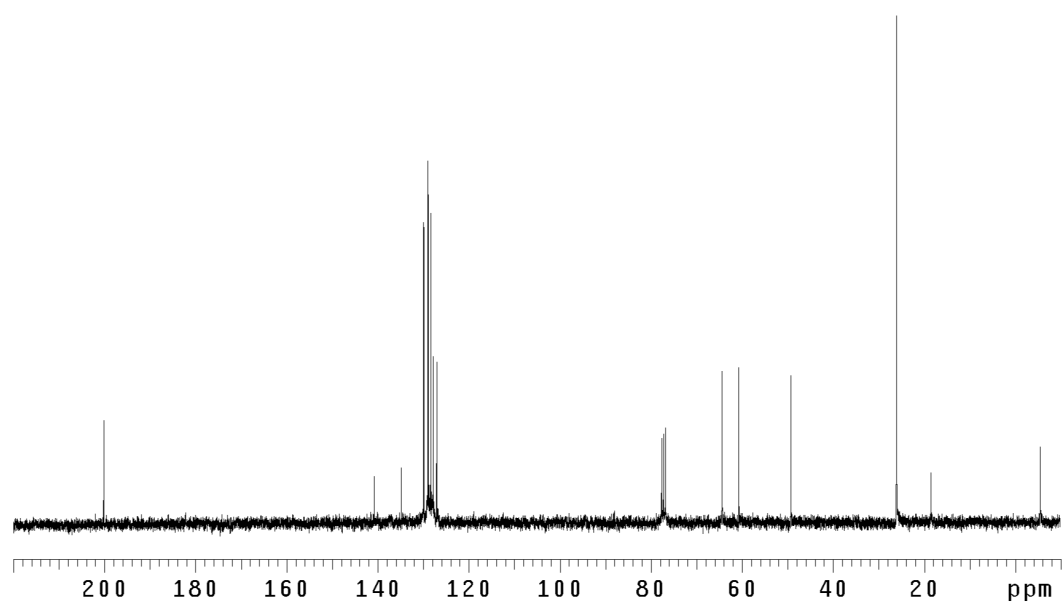
Figure A.1.159 ^{13}CNMR (75 Mhz, CDCl$_3$) of compound **205**.
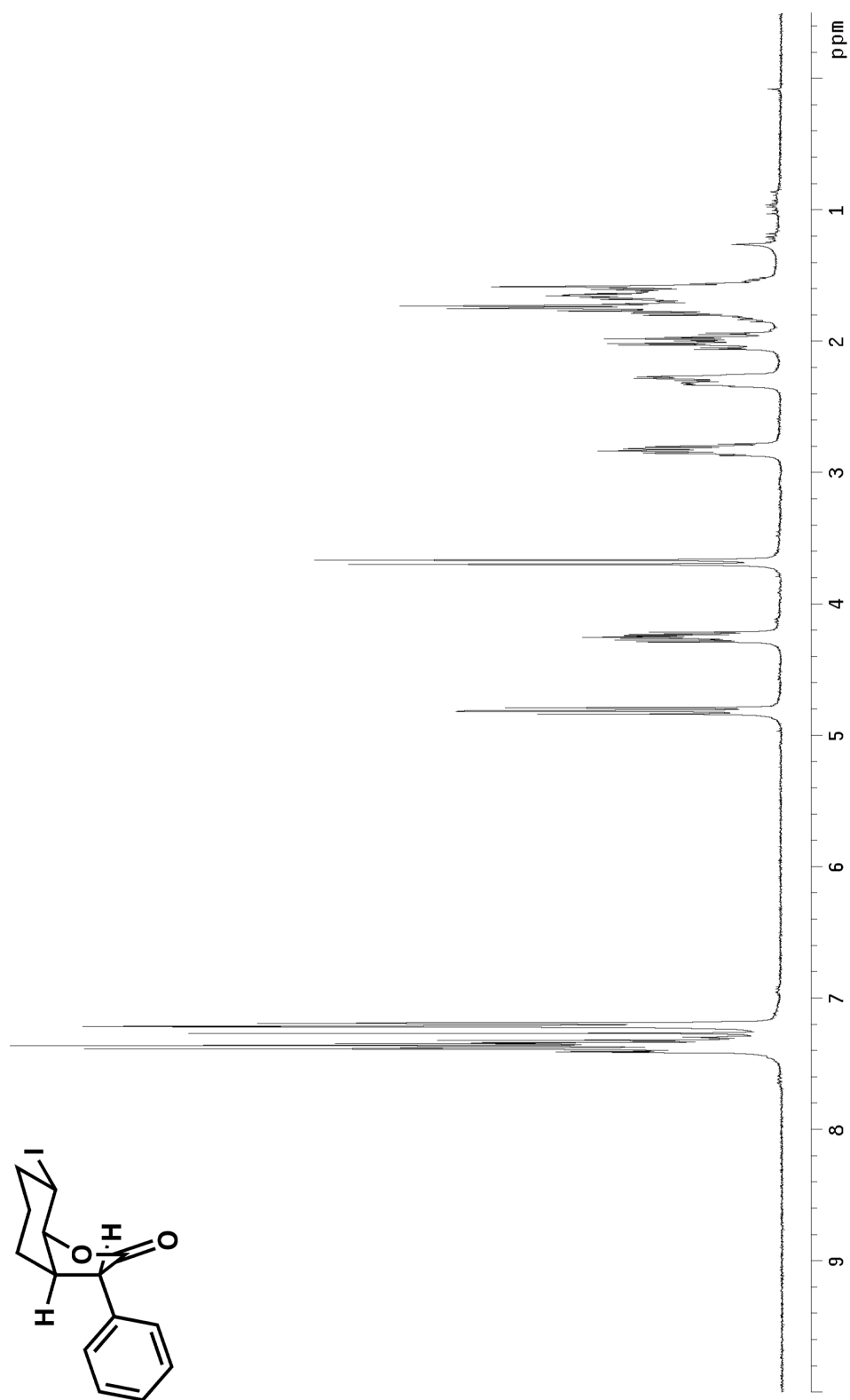
Figure A.1.160 ^{1}HNMR (300 MHz, CDCL$_3$) of compound **208**.

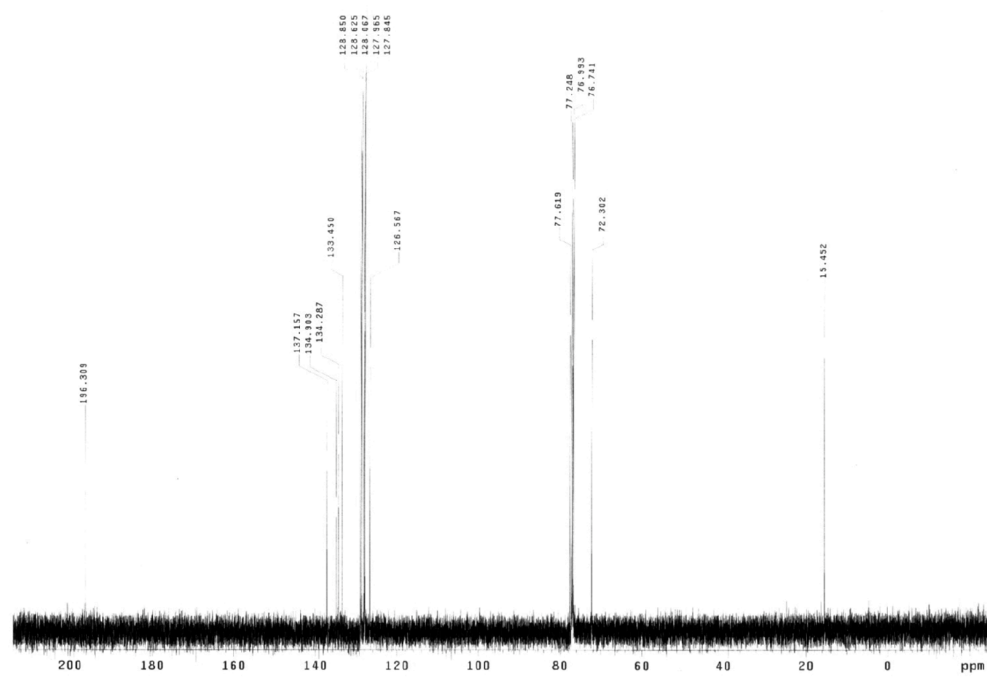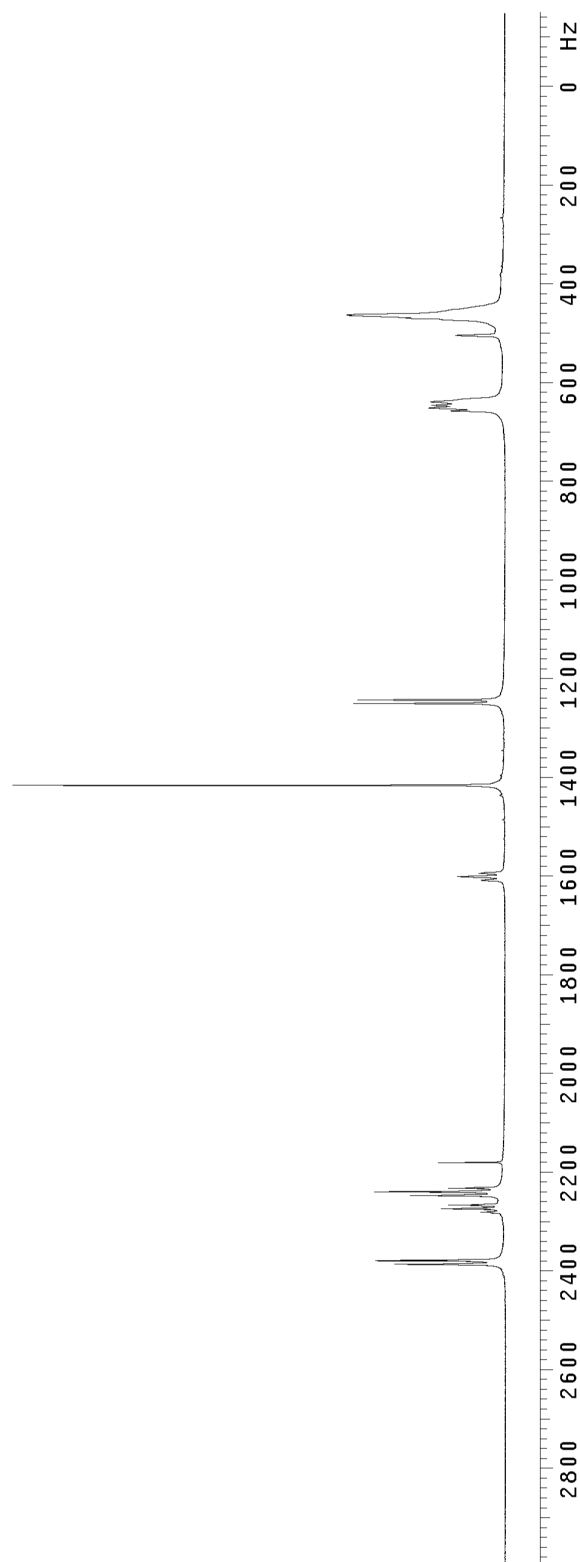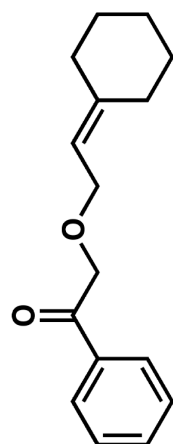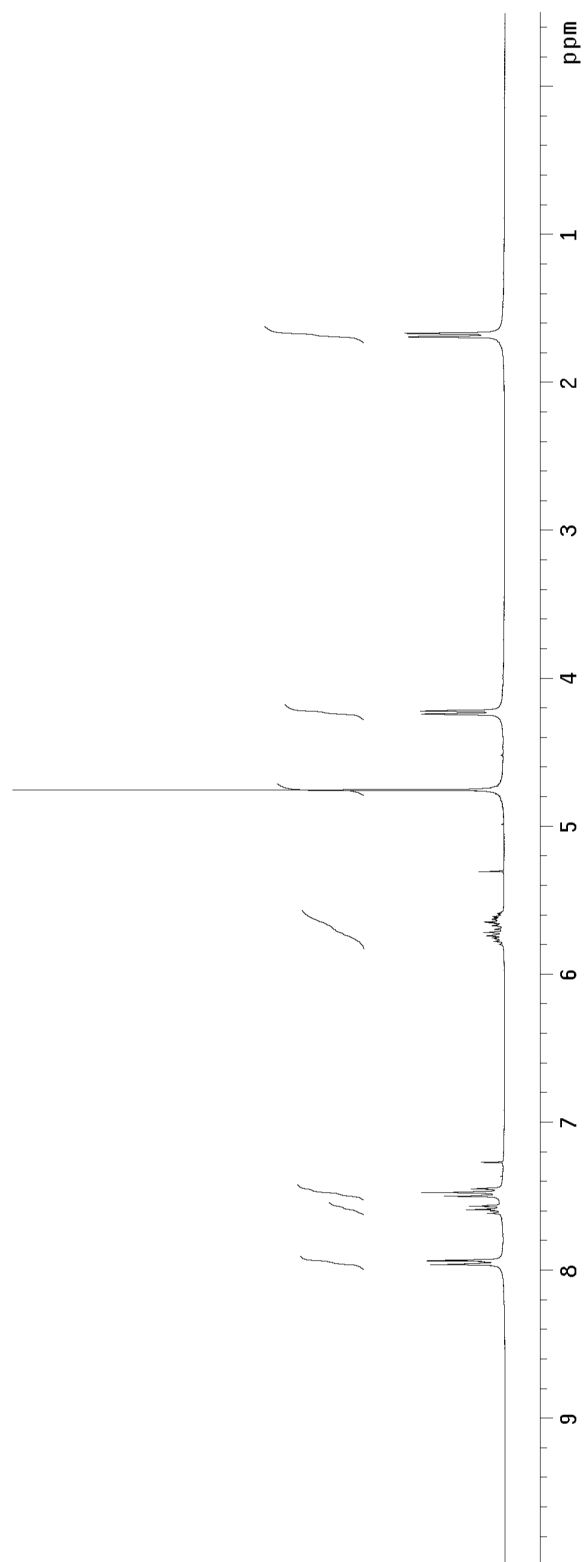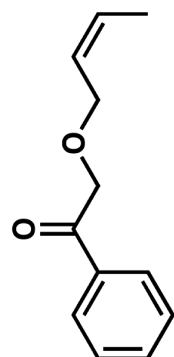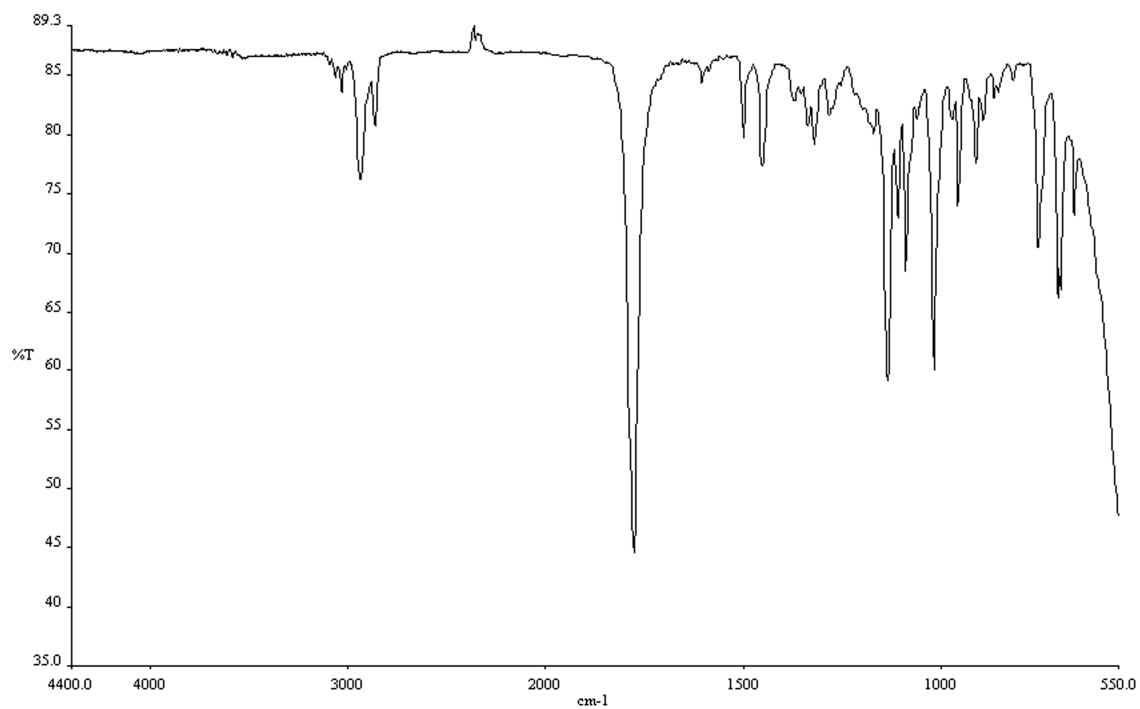*Figure A.1.161* Infrared spectrum (thin film/NaCl) of compound **208**.
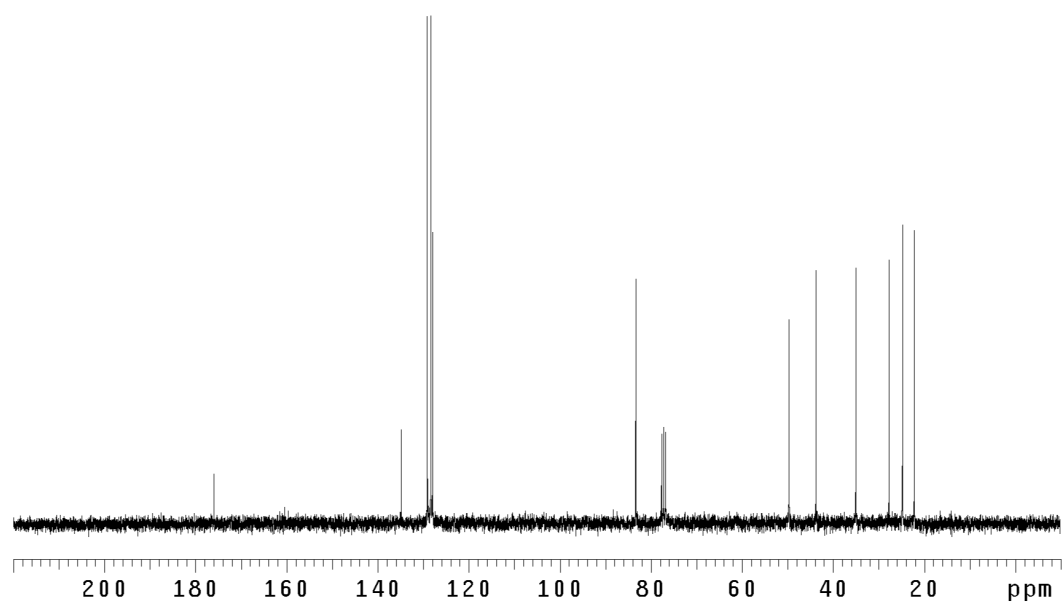
Figure A.1.162 ^{13}CNMR (75 Mhz, CDCl$_3$) of compound **208**.

Chapter 2

Molecular Mousetraps: Gas-Phase Studies of the Covalent Coupling of Noncovalent Complexes Initiated by Reactive Carbenes Formed by Controlled Activation of Diazo Precursors[1]

2.1 Background

2.1.1 Supramolecular Chemistry and Molecular Recognition

The field of supramolecular chemistry is devoted in part to the study of noncovalent molecular interactions.[2] Among the myriad applications of supramolecular chemistry, one focus is the discovery and development of specific receptors designed to recognize biologically relevant species. Recent efforts have produced substantial progress in this endeavor utilizing a variety of hosts including crown ethers,[3] lariat crown ethers,[4] cyclodextrins,[5] calixarenes,[6] cyclophanes,[7] cyclofructans,[8] sulfonate dyes,[9] and monosaccharides[10] among others. Although the majority of these studies have been performed in solution, the number of gas-phase studies of supramolecular chemistry has been increasing.[11]

2.1.2 Amino-Acid Side Chains as Targets

For the molecular recognition of a specific side chain in a peptide or protein, the charged amino acids arginine, histidine, lysine, glutamic acid, and aspartic acid offer the most easily distinguished targets, as they are the most basic and most acidic of the twenty amino acids. The acidic side chains are difficult to distinguish because both terminate with a carboxylic acid and differ only in the number of methylene units joining the acidic functionality to the backbone. The different chemical functionalities of the basic side chains enhance the possibility of achieving specificity; consequently, lysine and arginine have received the most attention with regard to molecular recognition.

2.1.3 Beauchamp Group Contributions

2.1.3.1 Lysine recognition

The Beauchamp Group has demonstrated the excellent molecular recognition capabilities of 18-crown-6 (18C6) as a specific host for the side chain of lysine in the gas phase.[3] In these experiments, 18C6 is mixed into a solution with a lysine-containing peptide, which is then electrosprayed into the gas phase. The 18C6 forms a specific complex with the alkyl-ammonium group on the protonated side chain of lysine, stabilized by three hydrogen bonds. This complex forms in solution and is transferred intact to the gas phase using electrospray ionization. The quantification of lysine residues in small peptides is possible with this technique through the formation of multiple adducts.[3]

2.1.3.2 Arginine Recognition

In other work, experiments were conducted with various macrocycles to determine which was ideally suited to host the side chain of arginine. The molecular recognition capabilities of 18C6 were utilized in combination with larger macrocycles, yielding additional information about the amino acid composition of peptides.

The protonated alkyl-guanidinium side chain of arginine formed a stable noncovalently bound complex with dibenzo-30-crown-10 (DB30C10) in the gas phase. The supramolecular complex is stabilized by extensive hydrogen bonding and ion–dipole interactions between the protonated guanidinium group and the 10 oxygen atoms present in DB30C10. Competitive collision induced dissociations (CID) experiments demonstrated that DB30C10 possesses a higher affinity for alkyl-guanidinium ions than the related compound 27-crown-9 (27C9). That affinity was attributed to the smaller size of 27C9, which does not afford extra space to accommodate the alkyl portion of the side chain of arginine.

2.1.3.3 Simultaneous Lysine and Arginine Recognition

The molecular recognition capabilities of 18C6 and DB30C10 were mutually compatible and could be utilized to determine whether a peptide contains arginine or lysine (or both) without any prior knowledge of the peptide sequence. Competitive CID experiments demonstrated that the DB30C10/arginine interaction is stronger than the 18C6/lysine interaction when they are attached to the same peptide. In contrast to the behavior observed for 18C6 interacting with lysine-containing peptides, multiple adducts of DB30C10 with a peptide containing multiple arginine residues were not observed in great abundance, limiting the utility of DB30C10 for the quantification of arginine residues.[12]

2.1.4 Experimental Approach

Attempts to effect intermolecular reactions between the cluster components described above are often frustrated by the lability of the noncovalent complexes, which results from the relatively weak interactions (compared to covalent bonds) that hold them together. In the present work, we planned to initiate intermolecular reactions in noncovalent clusters. First, a strongly bound host–guest complex would form in solution and be transferred to the gas phase by ESI. Second, a diazo group that was incorporated into the host would be efficiently converted into a highly reactive carbene[13] by low-energy collision-activated dissociation (CAD).[14] This carbene[15,16] could then react in an intermolecular fashion, covalently binding the host–guest complex. Key to the success of this approach is that the dissociation energy of N_2 from the diazo compound be less than the binding energy between the host and guest. The reagents designed for these characteristics are herein referred to as "molecular mousetraps."

2.2 Design of the Mousetraps

We have synthesized and examined the chemistry of the prototypical molecular mousetraps **300** and **301** (Figure 2.2.1). 18-Crown-6 (18C6) is a well-known host for protonated primary amines, both in solution and in the gas phase,[17] and has been shown to selectively bind to lysine residues in small peptides.[3a] Mousetrap **300** is designed to bind molecules with either one or, preferentially, two protonated primary amines. Mousetrap **301**, with a single 18C6 unit, binds to a single protonated primary amine. Thus, the 18C6 component of **300** and **301** acts as the bait to the trap. The ensnarement is provided by the diazo functionality. When activated, nitrogen gas is released to generate a reactive carbene that is capable of forming a covalent bond with any nearby molecule. As the bait was designed to bring the prey into close proximity, the carbene is more likely to react with the desired target.

Figure 2.2.1: Molecular Mousetraps.
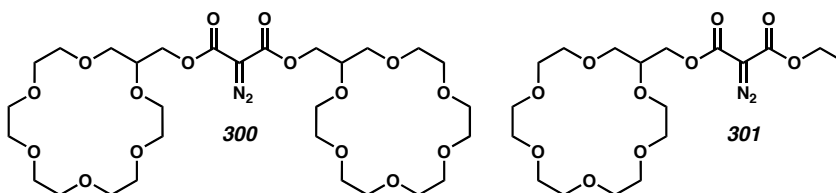
2.3 Proof of Principle: Trapping Host/Guest Interactions

2.3.1 Modeling of Doubly Charged DAH and 300

A possible interaction between **300** and doubly protonated 1,6-diaminohexane (DAH) is shown in Figure 2.3.1. This structure presents a noncovalent adduct in the gas phase, as determined by PM3 semiempirical calculations. As previously demonstrated,[3a] the proximal charges are stabilized by the crown ethers, so doubly charged DAH is preferred.

*Figure 2.3.1: **300** and Doubly Protonated DAH (Apparent Mass of 400 Da).*
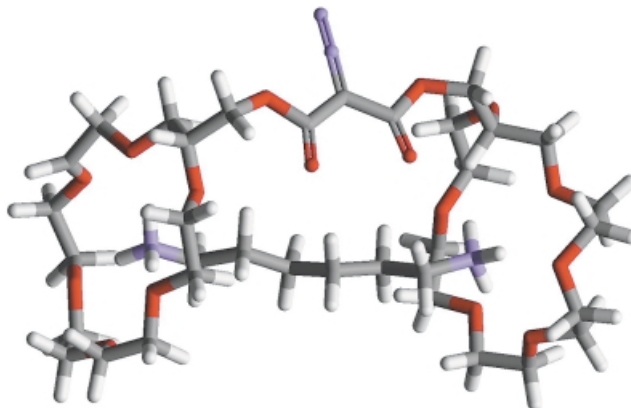
2.3.2 Results for Doubly Charged DAH and 300

2.3.2.1 Formation of a Carbene through Diazo Fragmentation

The DAH complex with **300** forms in solution and can be transferred intact to the gas phase by ESI, as seen in Figure 2.3.2a. This complex can be isolated from other adducts and subjected to CAD, as shown in Figure 2.3.2b. The sole product results from a neutral loss of 28 Da, which is interpreted to be the loss of the diazo group in the form of N_2 while the DAH remains associated. Significantly, this fragmentation demonstrates covalent-bond cleavage in preference to dissociation of the non-covalently bound complex. Therefore, the barrier for diazo fragmentation must be lower than the coordination energy of a protonated primary amine to 18C6. The loss of N_2 would yield the corresponding carbene (**:300**) as a highly reactive, short-lived intermediate, which can then undergo either an intermolecular or intramolecular reaction as described below.

*Figure 2.3.2: a) Mass spectrum of 1 with DAH; b) CAD spectrum of [300+DAH+2H]²⁺; c) MS/MS/MS analysis of [:300+DAH+2H]²⁺. I=relative intensity, *=300 + alkali-metal adduct peaks.*
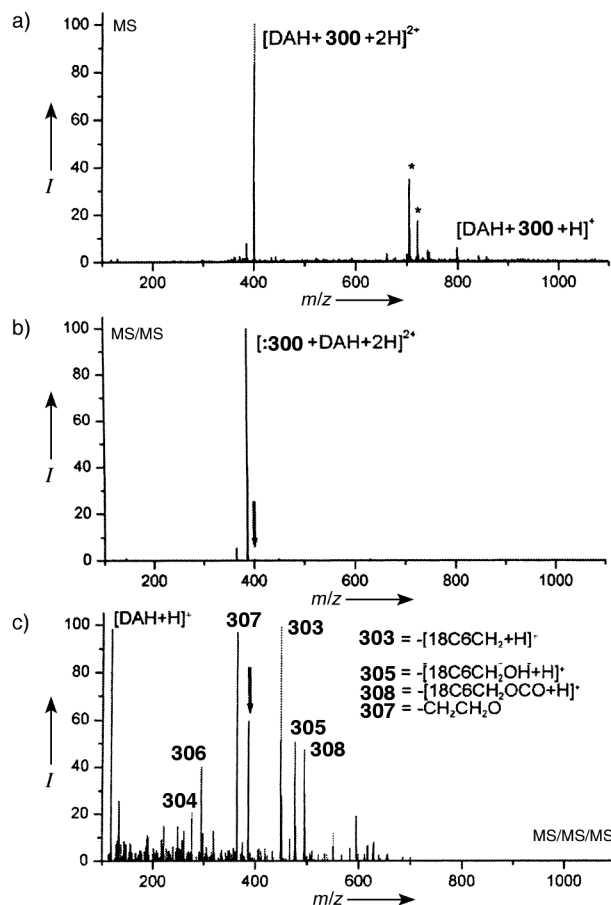
2.3.2.2 The Reactivity of the Malonate Carbene

When the carbene product described in Figure 2.3.2b is subjected to further collisional activation, as shown in Figure 2.3.2c, the majority of the product-ion intensity results from covalent-bond cleavage with loss of a crown (**303**, **305**, and **308**) or part of a crown (**307**, Scheme 2.3.1). Importantly, DAH is retained in spite of the fragmentation of the relatively strong C-O bonds. The fragmentation of the host without the accompanying loss of the guest provides evidence that an intermolecular reaction involving covalent coupling between the host and guest occurs by C-H insertion of the

carbene to form a construct similar to **302**.

Scheme 2.3.1 Fragmentations Observed in Figure 2.3.2c.

302
apparent mass of 386 Da

303
apparent mass of 495 Da

304
apparent mass of 277 Da

-44 Da per fragment

305
apparent mass of 477 Da

306
apparent mass of 295 Da

307

-CO

308
apparent mass of 449 Da
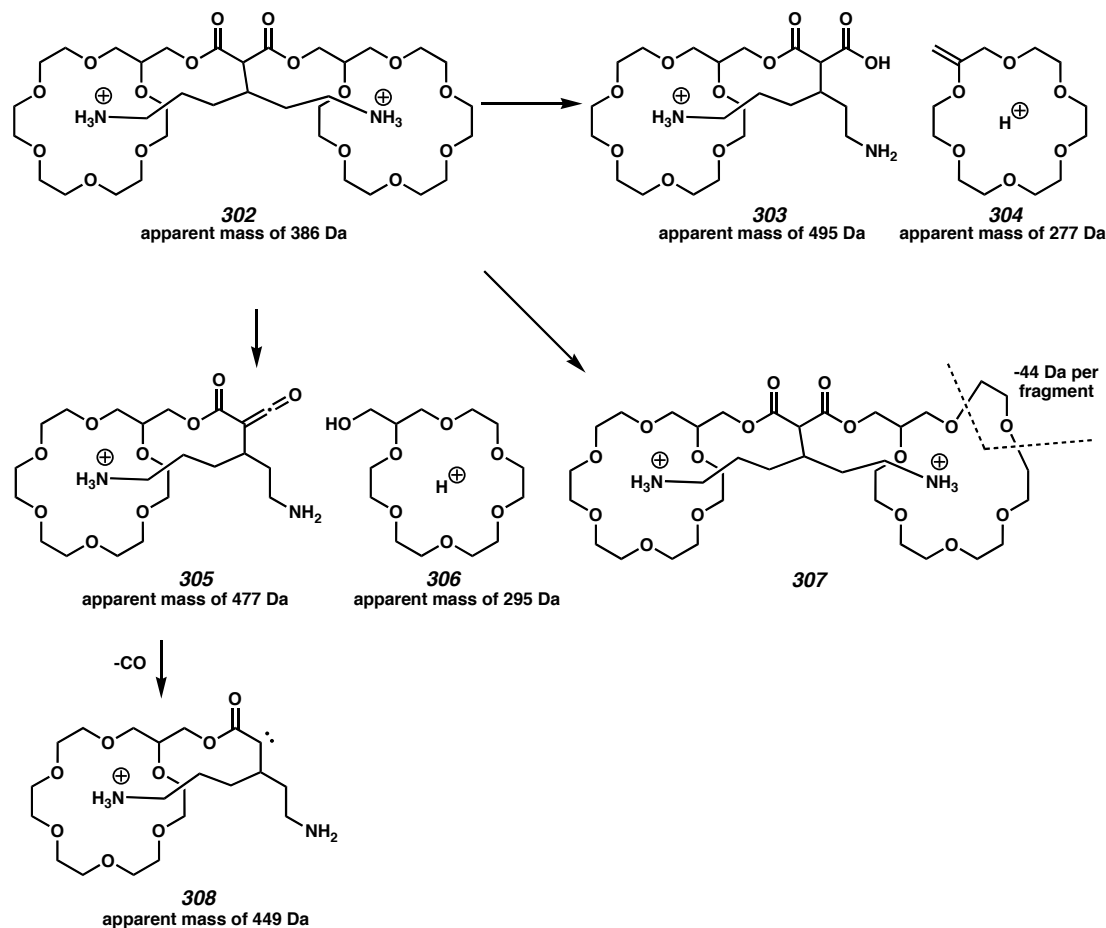
A C-H insertion to produce **302** is likely because the complexation of the protonated primary amines of the doubly protonated DAH by the crown ethers reduces the likelihood of an N-H insertion reaction by the carbene.[18] Figure 2.2.2c also shows that some of the DAH appears to dissociate from the complex, which suggests that an intramolecular reaction by the carbene is competitive in this case. Specifically, a Wolff rearrangement from the malonate carbene is likely (see Chapter 4 for more detailed study).[19]

2.3.3 Results for Singly Charged DAH and 301

2.3.3.1 Initial Loss of N$_2$ and 18C6-Methanol

Singly charged DAH has a lower binding energy to **300** than the doubly charged species, yet [**:300**+DAH+H]$^+$ (seen in Figure 2.3.2a) is generated with high efficiency from the [**300**+DAH+H]$^+$ complex as illustrated in Figure 2.3.3a. The loss of nitrogen is accompanied by an additional loss of 294 Da, which can be accounted for by the loss of 18-crown-6 methanol. This additional loss is observed for all complexes of both **300** and **301** in which there is a neutral primary amine or alcohol available (in experiments with **301**, the loss of ethanol is also observed[20]). As no loss of DAH is seen for this or subsequent fragmentations (*vide infra*), **:300** appears to undergo intermolecular reactions with the DAH without any competing intramolecular reactions (i.e., Wolff rearrangements).

Figure 2.3.3: a) CAD of [300+DAH+H]⁺; b) MS/MS/MS analysis of [:300+DAH+H]⁺;
c) MS/MS/MS analysis of [:300+DAH+H-294]⁺. A bold downward arrow indicates the
peak being subjected to CAD. I=relative intensity.
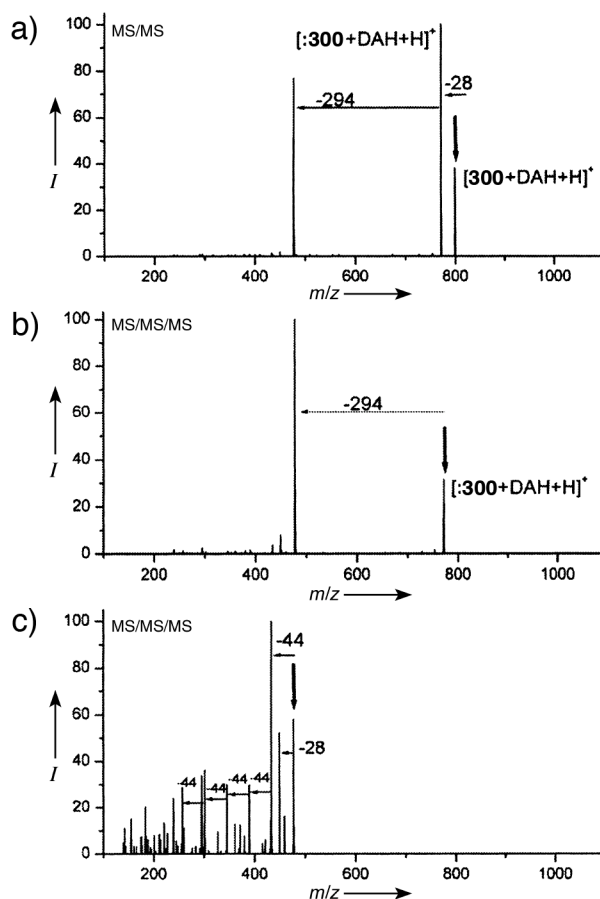
2.3.3.2 Calculations on a Model Compound

Diazodimethylmalonate (**3**) was used as a model compound in computations to understand the reactions of **300** that could lead to alcohol extrusion upon loss of N_2. DFT calculations at the B3LYP/CCPVTZ(-F)⁺ level on **3** (Scheme 2.3.2) describe a singlet ground state, with a singlet/triplet splitting of 3 ± 1 kcal mol⁻¹. This result suggests that the singlet state is certainly accessible and perhaps favorable, which is in agreement with experimental results.[21] DFT calculations at the B3LYP/6-31G** level on **309** and methylamine lead to the formation of an ammonium ylide **310** without a barrier. The

ammonium ylide **310** is a local minimum on the potential energy surface, and previous reports have suggested that all carbenes will initially react with amines by the formation of an intermediate ylide.[22]

Scheme 2.3.2 Reaction Pathway Used for DFT Calculations.
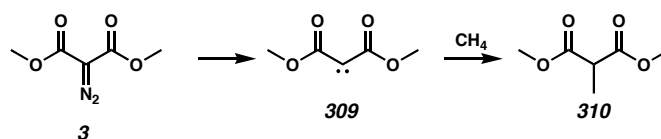
2.3.3.3 Mechanisms for Alcohol Extrusion from DFT Calculations

From this ammonium ylide, two reaction pathways with minimal barriers are possible, as shown in Scheme 2.2.3. It should be pointed out that both pathways lead to covalent attachment of the host–guest complex through intermolecular reactions; one route leads to formal N-H insertion by proton transfer, and the other proceeds through elimination of an alcohol group and the generation of a ketene.

Scheme 2.3.3: Mechanisms for observed CAD products.
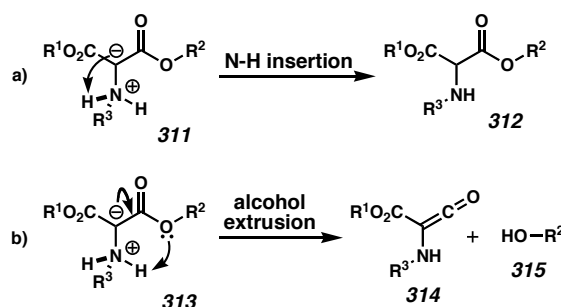
2.3.3.4 Results from Continued Analysis of 300 and Singly Charged DAH.

Further excitation of the isolated [**:300**+DAH+H]$^+$ species, after the loss of nitrogen, exclusively leads to the loss of 294 Da, as shown in Figure 2.3.3b. Since the N-H insertion product **312** shown in Scheme 2.3.3a is protonated at the secondary amine, transfer of this proton to the ester and elimination of the 18C6 methanol can lead to the

loss observed in Figure 2.3.3b. It is also possible, though unlikely, that the ammonium ylide **311**, represented by the data in Figure 2.3.3a, could be sufficiently long-lived in Figure 2.3.3a to yield this product directly upon subsequent activation in Figure 2.3.3b. More likely is that the loss of 294 Da in Figure 2.3.3a represents pathway b in Scheme 2.3.3, and that the loss of 294 Da in Figure 2.3.3b represents elimination of alcohol from the product of N-H insertion.

2.3.3.5 Demonstration of Covalent Bond Formation

Figure 2.3.3c presents several critical results. First, the loss of 28 Da is probably from loss of CO from the ketene **314** shown in Scheme 2.3.3b. Second, the fragment being subjected to further collisional activation in Figure 2.3.3c contains only a single remaining crown. The primary losses are multiple $\{CH_2CH_2O\}$ fragments from this remaining crown. The data reveal the sequential removal of almost the entire remaining crown ether without the loss of the guest molecule. In the absence of both crowns, retention of the guest can only be explained by a newly formed covalent bond.

2.4 Conclusion

These studies demonstrate reagents that have been designed to bind specific functional groups in complex molecules and that have been derivatized to introduce the means to covalently couple to target molecules with convenient methods of activation. We have combined 18C6, which binds strongly to protonated primary amines,[3a] and a diazo precursor to a reactive carbene to form a potent "molecular mousetrap" that can be used to target lysines in peptides or proteins. Full details of the chemistry and applications of these and related molecular mousetraps will be described in further publications.

2.5 Experimental

2.5.1 Methods for ESI•MS

All spectra were obtained using a Finnigan LCQ ion-trap quadrupole mass spectrometer without modification. Sample concentrations were typically kept in the 10 to 100 μm range for all species of interest. All samples were electrosprayed in an 80:20 mixture of methanol/water. The appropriate host was added to the sample and electrosprayed with the guest in order to observe adduct formation. Semiempirical calculations for Figure 2.3.1 were performed on HyperChem 5.1 Professional Suite using the PM3 parameter set.

2.5.2 Methods for Calculations

Calculations to determine the singlet/triplet splittings were performed on structures fully optimized at the B3LYP/CCPVTZ(-F)$^+$ level of theory. Comparison of this methodology with previous computational and experimental results for the following carbenes: CH_2, $HCCl$, HCF, CCl_2, CF_2, and $HCCHO$ yielded results within (on average) ±0.6 kcal mol^{-1} of the best experimental or theoretical value.[23] Zero-point energy corrections were not included. Reactions were modeled at the B3LYP/6-31G** level of theory by minimizing structures containing both reactants, with several different starting geometries. Initial geometries included likely starting points for the most probable reaction mechanisms, that is, hydrogen abstraction, concerted insertion, and ylide formation. The DFT calculations were carried out using Jaguar 4.1 (Schrödinger, Inc., Portland, Oregon).

2.5.3 General Synthetic Information

Due caution should always be used when handling diazo compounds. Reactions

were performed in flame-dried glassware under a nitrogen atmosphere using freshly

distilled solvents. All other reagents were used as received from commercial sources.

Reaction temperatures were controlled by an IKAmag temperature modulator. ^{1}H NMR

spectra were recorded on a Varian Mercury 300 spectrometer (at 300 MHz) and are

internally referenced to the chloroform peak (7.27 ppm) relative to Me$_4$Si. Data for ^{1}H

NMR spectra are reported as follows: chemical shift (δ ppm), multiplicity, coupling

constant (Hz), and integration. IR spectra were recorded on a Perkin Elmer Paragon 1000

spectrometer and are reported in frequency of absorption (cm^{-1}). Preparatory reversed

phase HPLC was performed on a Beckman HPLC with a Waters DeltaPak 25 x 100 mm,

100 μm C18 column equipped with a guard.

2.5.4 Synthetic Procedures
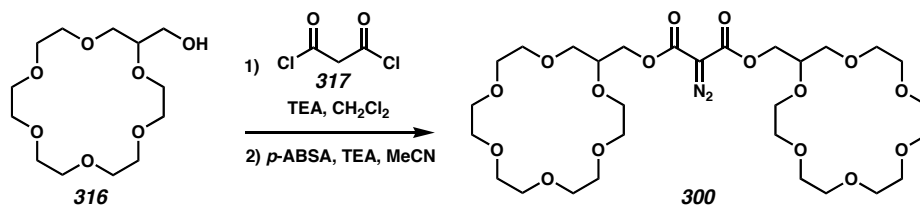
Compound 300: To a stirred, dry solution of 18-crown-6-methanol (50.0 μl, 0.16

mmol), dichloromethane (1.5 ml), and triethylamine (25 μl, 0.18 mmol) was added

malonyl dichloride (9.0 μl, 0.09 mmol). The mixture was heated to reflux for eight

hours, cooled, and then evaporated *in vacuo*. The residue was dissolved in acetonitrile

(1.2 ml) and treated with triethylamine (220 μl, 1.58 mmol). To this solution was added

p-acetamidobenzenesulfonyl azide (*p*-ABSA) (31.9 mg, 0.13 mmol), and the mixture was

stirred for ten hours. The solvent was removed *in vacuo*, the residue dissolved in a

minimal amount of dichloromethane (500 μl), and the undesired salts were precipitated

out of solution with the addition of ether (5 ml). Filtration through Celite and removal of

solvent *in vacuo* yielded **300** (41.8 mg, 81% yield). A small sample (~15 mg) was

chromatographed to analytical purity by HPLC, (0.1% (wt/v) TFA in water, 8.0 ml/min,

0.30% acetonitrile/min, 83-85 min). FTIR (thin film) 3429, 2918, 2143, 1743, 1691,

1595, 1454, 1356, 1251, 1108 cm^{-1}; ^{1}H NMR (300 MHz, CDCl$_3$) δ 4.44 (dd, J = 3.85,

11.5 Hz, 1H), 4.26 (dd, J = 5.49, 11.0 Hz, 1H), 3.87-3.58 (m, 23H); ESI-MS *m/z* 683.3

(H$^+$).
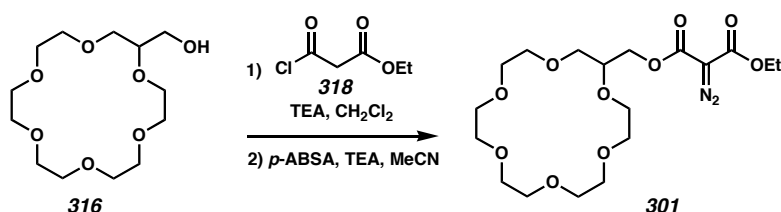
Compound 301: To a stirred, dry solution of 18-crown-6-methanol (50.0 μl, 0.16

mmol), dichloromethane (1.5 ml), and triethylamine (33 μl, 0.24 mmol) was added ethyl

malonyl chloride (28 μl, 0.22 mmol). The mixture was heated to reflux for eight hours,

cooled, and then evaporated *in vacuo*. The residue was dissolved in acetonitrile (750 μl)

and treated with triethylamine (30 μl, 0.22 mmol). To this solution was added *p*-ABSA

(53.1 mg, 0.22 mmol), and the mixture was stirred for ten hours. The solvent was

removed *in vacuo*, the residue was dissolved in a minimal amount of dichloromethane

(500 μl), and the undesired salts were precipitated out of solution with the addition of

ether (5 ml). Filtration through Celite and removal of solvent *in vacuo* yielded **301** (59.8

mg, 87% yield). A small sample (~15 mg) was chromatographed to analytical purity by

HPLC (0.1% (wt/v) TFA in water, 8.0 ml/min, 0.30% acetonitrile/min, 82-85 min). FTIR

(thin film) 2879, 2142, 1755, 1689, 1457, 1326, 1102, 762; ^{1}H NMR (300 MHz, CDCl3)

δ 4.45 (dd, J = 3.85, 12.1 Hz, 1H), 4.31 (q, J = 7.14 Hz, 2H), 4.27 (m, 1H), 3.85 (t, J =

4.95), 3.80 (s, broad, 1H), 3.67 (s, broad, 21H), 1.32 (t, j = 7.14 Hz, 3H); ESI-MS *m/z*

435.2 (H⁺).

3
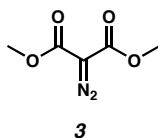
Compound 3: 3 was prepared according to previously established methods.[24]

The product was isolated as a yellow oil (2.58 g, 16.29 mmol, 93% yield) with the same

physical properties as previously reported.

2.6 Notes and References

(1) Note that this research was performed in collaboration with Ryan Julian and previously reported in Julian, R. R.; May, J. A.; Stoltz, B. M.; Beauchamp, J. L. *Angew. Chem. Int. Ed.* **2003**, *42*, 1012.

(2) Beer, P.D.; Gale, P.A.; Smith, D.K. Supramolecular Chemistry, Oxford University Press, New York, 1999.

(3) Julian, R.R.; Beauchamp, J.L. *Int. J. Mass Spectrom.* **2001**, *210*, 613.

(4) Galan, A.; Andreu, D.; Echavarren, A.M.; Prados, P.; de Mendoza, J. *J. Am. Chem. Soc.* **1992**, *114*, 1511.

(5) (a) Hauser, S.L.; Johanson, E.W.; Green, H.P.; Smith, P.J. *Org. Lett.* **2000**, *2*(23), 3575; (b) Ramirez, J.; He, F.; Lebrilla, C.B. *J. Am. Chem. Soc.* **1998**, *120*, 7387.

(6) Ludwig, R.; Fresen, J. *Anal. Chem.* **2000**, *367*, 103.

(7) Ngola, S.M.; Kearney, P.C.; Mecozzi, S.; Russell, K.; Dougherty, D.A. *J. Am. Chem. Soc.* **1999**, *121*, 1192.

(8) Sawada, M.; Shizuma, M.; Takai, Y.; Adachi, H.; Takeda, T.; Uchiyama, T. *Chem. Commun.* **1998**, 1453.

(9) Salih, B.; Zenobi, R. *Anal. Chem.* **1998**, *70*, 1536.

(10) Krishna, P.; Prabhakar, S.; Manoharan, M.; Jemmis, E.D Vairamani, M. *Chem. Commun.* **1999**, 1215.

(11) Schalley, C.A. *Int. J. Mass Spectrom.* **2000**, 194, 11.

(12) Julian, R. R.; Akin, M.; May, J. A.; Stoltz, B. M.; Beauchamp, J. L. *Int. J. Mass Spectrom.* **2002**, *220*, 87-96.

(13) A neutral, two-electron carbene is formed. Other studies have focused on carbene radical cations such as $[CH_2]^+$, see for example: Flammang, R.; Nguyen, M. T.; Bouschoux, G.; Gerbaux, P. *Int. J. Mass Spectrom.* **2002**, *202*, A8 –A25.

(14) a) Marzluff, E. M.; Beauchamp J. L. in Large Ions: Their Vaporization, Detection, and Structural Analysis; (Eds.: T. Baer, C. Y. Ng, I. Powis), Wiley, New York, 1996, pp. 115 – 143; b) McLuckey, S. A. *J. Am. Soc. Mass Spectrom.* **1992**, *3*, 599–614; c) Hayes, R. N.; Gross, M. L. *Methods Enzymol.* **1990**, *193*, 237–263.

(15) a) Rice, F. O.; Glasebrook, A. L. *J. Am. Chem. Soc.* **1934**, *56*, 2381–2383; b) Herzberg, G. *Proc. R. Soc. London Ser. A* **1961**, *262*, 291–317; c) Carbenes, Vols. 1 and 2 (Eds.: R. A. Moss, M. Jones, Jr.), Wiley, New York, **1973**, 1975; d) Rynbrandt, J. D.; Rabinovitch, B. S. *J. Phys. Chem.* **1970**, *74*, 4175–4176; e) Rynbrandt, J. D.; Rabinovitch, B. S. *J. Chem. Phys.* **1971**, *54*, 2275–2276; f) J. C. Poutsma, J. J. Nash, J. A. Paulino, R. R. Squires, *J. Am. Chem. Soc.* **1997**, *119*, 4686–4697; g) J. A. Paulino, R. R. Squires, *J. Am. Chem. Soc.* **1991**, *113*, 5573–5580; h) D. G. Leopold, K. K. Murray, A. E. S. Miller, W. C. Lineberger, *J. Chem. Phys.* **1985**, *83*, 4849–4865, and references therein; i) R. Bertani, R. A. Michelin, M. Mozzon, P. Traldi, R. Seraglia, L. Busetto, M. C. Cassani, P. Tagleatesta, G. D'Arcangelo, *Organometallics* **1997**, *16*, 3229–3233.

(16) a) M. P. Doyle, M. A. McKervey, T. Ye, Modern Catalytic Methods for Organic Synthesis with Diazo Compounds, Wiley-Interscience, New York, 1998; b) C. J. Moody, Whitham, G. H. Reactive Intermediates, Oxford University Press, New York, 1992, pp. 26 – 50.

(17) a) J. S. Bradshaw, R. M. Izatt, A. V. Borkunov, C. Y. Zhu, J. K. Hathaway, Comprehensive Supramolecular Chemistry, Vol. 1 (Ed.: G. W. Gokel), Pergamon/Elsevier, Oxford, 1996, pp. 35–95; b) S. Maleknia, J. Brodbelt, *J. Am. Chem. Soc.* **1993**, *115*, 2837–2843; c) D. V. Dearden, C. Dejsupa, Y. Liang, J. S. Bradshaw, R. M. Izatt, *J. Am. Chem. Soc.* **1997**, *119*, 353–359; d) C. A. Schalley, *Mass Spectrom. Rev.* **2001**, *20*, 253–309; e) J. A. Loo, *Int. J. Mass Spectrom.* **2000**, *200*, 175–186.

(18) 18C6 locks protons onto primary amines, see ref. [3a] and: S.-W. Lee, H.-N. Lee, H. S. Kim, J. L. Beauchamp, *J. Am. Chem. Soc.* **1998**, *120*, 5800–5805.

(19) See, for example, a) I. Likhotvorik, Z. Zhendong, E. L. Tae, E. Tippmann, B. T. Hill, M. S. Platz, *J. Am. Chem. Soc.* **2001**, *123*, 6061–6068; b) ref. (23).

(20) For more detailed experiments, see Chapter 3.

(21) Both results obtained in the current work and in: a) D. C. Richardson, M. E. Hendrick, M. Jones, *J. Am. Chem. Soc.* **1971**, *93*, 3790–3791, where Wolff rearrangement is observed, must proceed through the singlet state. b) See also Chapter 4.

(22) J. R. Pliego, W. B. Almeida, *J. Phys. Chem. A* **1999**, *103*, 3904–3909.

(23) A. P. Scott, M. S. Platz, L. Radom, *J. Am. Chem. Soc.* **2001**, *123*, 6069–6076.

(24) Falorni, M.; Dettori, G.; Giacomelli, G. *Tetrahedron: Asymmetry* **1998**, *9*, 1419

Chapter 3

Biomimetic Approaches to Gas-Phase Peptide Chemistry: Combining Selective Binding Motifs with Reactive Carbene Precursors to Form Molecular Mousetraps[1]

3.1 Background

3.1.1 Gas-Phase Peptide Sequencing in Proteomics Using Innate Functionality

In the post-genomic world of proteomics,[2] many substantial advances in sequence characterization will be made through gas-phase experiments. Therefore, understanding and ultimately controlling gas-phase peptide chemistry is of paramount importance. For example, such study has revealed that selective cleavage of the peptide backbone will occur at aspartic acid residues.[3,4] The cleavage occurs by a displacement reaction to yield a stable five-membered ring. This understanding allows for the accurate prediction of peptide cleavages in aspartic acid containing peptides. Furthermore, C-terminal peptide sequencing in the gas phase, where the C-terminal amino acids are sequentially removed via a similar mechanism, has also yielded promising results.[5] Unfortunately, this C-terminal sequencing is limited to peptides with eight amino acids or less, severely limiting the utility of this technique for sequencing proteins in the gas phase.

3.1.2 Gas-Phase Peptide Sequencing in Proteomics Using Metal Addition

The addition of transition metals can also mediate peptide chemistry in the gas phase.[6,7] Preliminary studies have shown that Zn^{2+}, Ni^{2+}, and Co^{2+} will attach to histidine and promote peptide fragmentation at this residue.[6] These experiments were carried out on a very limited sampling of peptides, but the resulting cleavages were highly specific. Similarly, Fe^{2+} complexes with cysteine-containing peptides enhanced the number of

cleavages observed at the cysteine residues when the peptide was collisionally activated. These important initial results illustrate that peptide chemistry can be influenced by the addition of appropriate reagents.

3.2 Experimental Approach

In an effort to develop experimental methodologies for the controlled gas-phase manipulation of peptides, we have undertaken a systematic study to develop biomimetic reagents capable of selectively attaching to and reacting with peptides. These reagents are envisioned to be capable of initiating a wide range of chemical reactions, such as peptide backbone cleavage at specific residues. With appropriate modifications, the type of reagents proposed herein could serve as fluorescent probes, chemical cross-linkers, and sequence-specific binding agents. In the present work, two reagents, **319** and **320** (Figure 3.2.1), are designed to initiate selective cleavage of the peptide backbone near lysine residues. In addition, diazocarbonyl reagents **300** and **301** were designed to covalently attach to lysine-containing peptides following appropriate activation to generate a reactive carbene center. This chapter expands upon Chapter 2, which presented initial experiments with this class of reagents that we have termed molecular mousetraps.[8] Considerations that led to the design of these reagents will be discussed initially.

Figure 3.2.1: Molecules Developed to Study Gas Phase Reactions.

319

320 R=H
321 R=Me

300

301
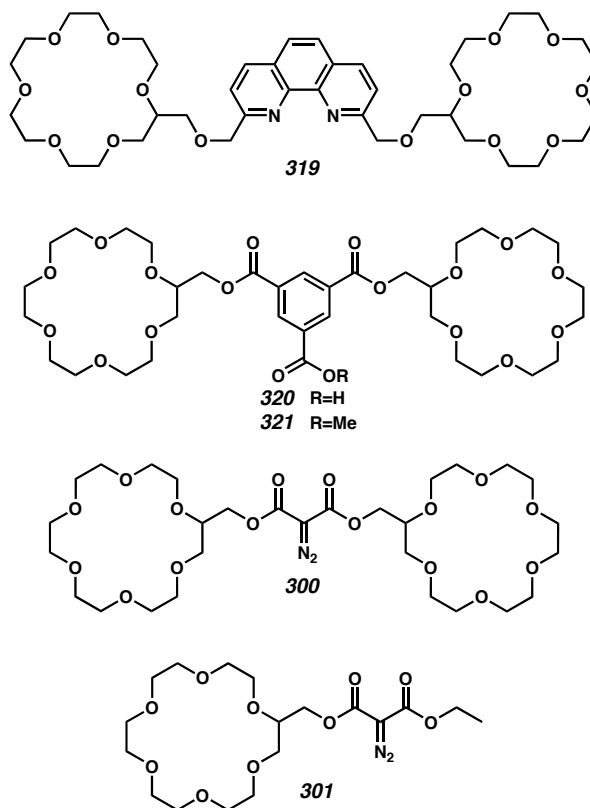
3.3 Reagent Design

3.3.1 The Recognition Element

Reagents **319–301** all rely on molecular recognition of an amino acid side chain to form specific non-covalent complexes in the gas phase. Fortunately, a significant amount of work developing reagents that selectively recognize and non-covalently attach to specific amino acid side chains has already been reported.[9,10,11] These side chain hosts represent the first and simplest form of a biomimetic reagent, one that is only capable of recognition. Importantly, the facile formation of non-covalent complexes with strong binding interactions is critical to the success of this type of experiment, and proper conditions for enhancing non-covalent complex formation have been studied extensively.[12,13]

3.3.2 Use of 18-Crown-6 to Recognize Lysine

18-Crown-6 ether (18C6) was chosen as the recognition and binding motif because it is both synthetically flexible and amenable to non-covalent complexation. It is well known for its ability to bind both metal cations and protonated primary amines in solution and in the gas phase.[14] This ability is particularly useful for the recognition of lysine, because the side chain of this amino acid terminates in a primary amine. 18C6 complexes to protonated primary amines through a combination of three hydrogen bonds and ion–dipole interactions. Non-covalent complexes with 18C6 bound to protonated primary amines can be transferred into the gas phase by electrospray ionization mass spectrometry (ESI-MS). When added to a solution containing a peptide, the 18C6 complex with the peptide is typically the most abundant peak in the spectrum.[10] Appropriately modified lariat crown ethers (i.e., crown ethers with an appended chain), such as those in Figure 3.2.1 behave similarly, forming non-covalent complexes that can be transferred to the gas phase as shown previously[15] and in the present work.

3.3.3 Adding Functionality to the Recognition Element

3.3.3.1 Reagents for Peptide Cleavage

3.3.3.1.1 Synthesis of the 18C6/Phenanthroline Macromolecule

Lariat crown ether **319** was synthesized and tested to determine its ability to selectively cleave various peptides (Scheme 3.3.1). The 18C6 was anticipated to coordinate the lysine side chain, and the phenanthroline was anticipated to form a complex with a metal and catalyze peptide bond cleavage as was seen for the histidine-coordinated metals (*vide supra*). The synthesis of the 18C6-appended phenanthroline **319** commenced from 18C6methanol (**316**). Unfortunately, the neutral alcohol **316** was

not reactive enough to displace the benzylic bromide from the phenanthroline dibromide **324**. By first treating the alcohol with lithium diethylamide to generate the lithium alkoxide, however, the alkylation proceeded smoothly to generate the bis-18C6-appended phenanthroline. At the completion of the reaction the product needed purification from the various byproducts in the reaction. These crown ethers presented several special purification problems. Neither silica gel chromatography nor aqueous/organic solvent extractions were viable purification methods, as 18C6 is quite polar and soluble in almost any solvent. Fortunately, the desired reactions could be made specific enough that the only byproducts were inorganic salts. Dilution of a concentrated reaction solution with Et_2O, though, caused all the inorganic contaminants to precipitate out of solution, and filtration afforded nearly pure product in solution, which could be concentrated in vacuo. This method of purification was utilized for all the described 18C6-appended reagents. When synthesized, **319** was introduced into various solutions with a lysine-containing peptide and several different metals.

*Scheme 3.3.1: Synthesis and Mechanism of 18C6-Phenanthroline **319**.*
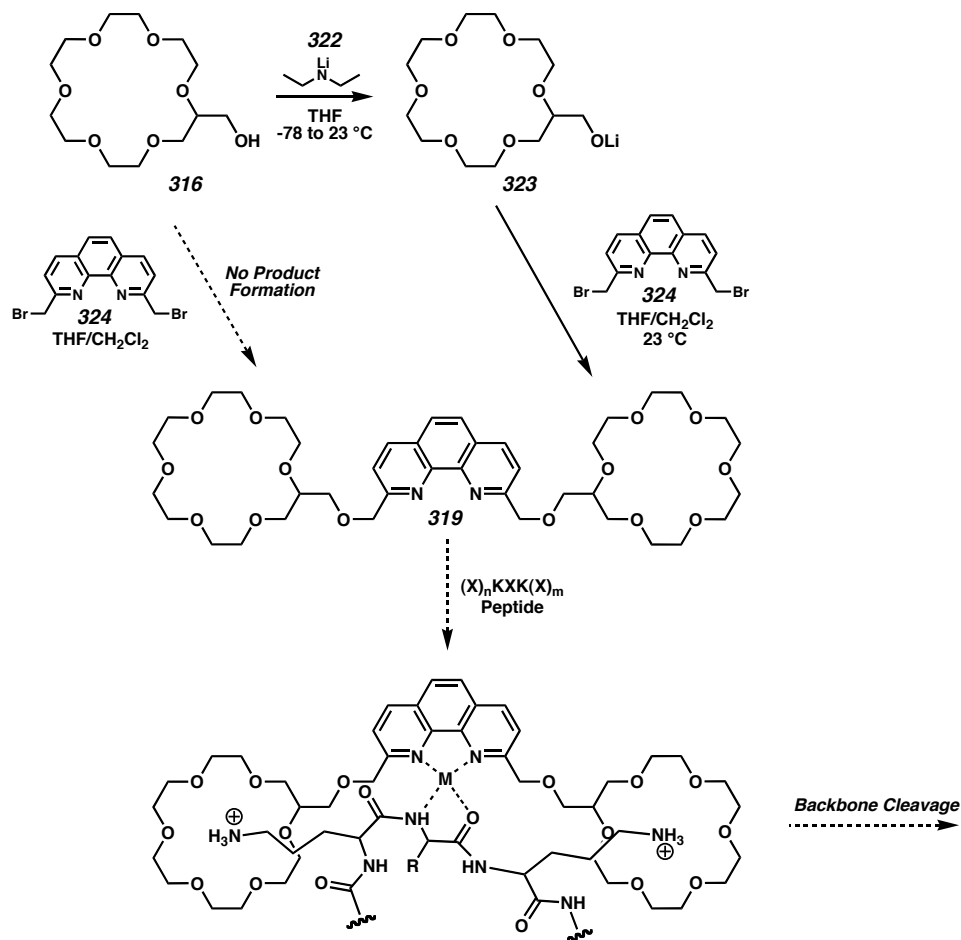
3.3.3.1.2 Synthesis of the 18C6/Benzoic Acid Macromolecule

The carboxylic acid **320** was anticipated to mimic the aspartic acid and C-terminal displacements described in Section 3.1.1. Fortunately, 1,3,5-benzenetricarbonyl trichloride (**325**) provided easy access to both the 18C6-appended benzoic acid **320** and ester **321** (Scheme 3.3.2). The modified crown ether **316** reacted with **325** directly with a 2:1 stoichiomeric ratio. The triply substituted benzoic ester was not observed. The product of bis-substitution, **326**, could be subjected to a water or methanol quench to provide the acid or ester, respectively. Purification as described for the phenanthroline reagent provided the products ready to use in gas-phase studies. If **320** could bind to

adjacent lysines and advantageously position the carboxylic acid, acid-catalyzed amide bond cleaveage could occur.

*Scheme 3.3.2: Synthesis and Proposed Mechanism for 18C6-Benzoic Acid **320***.
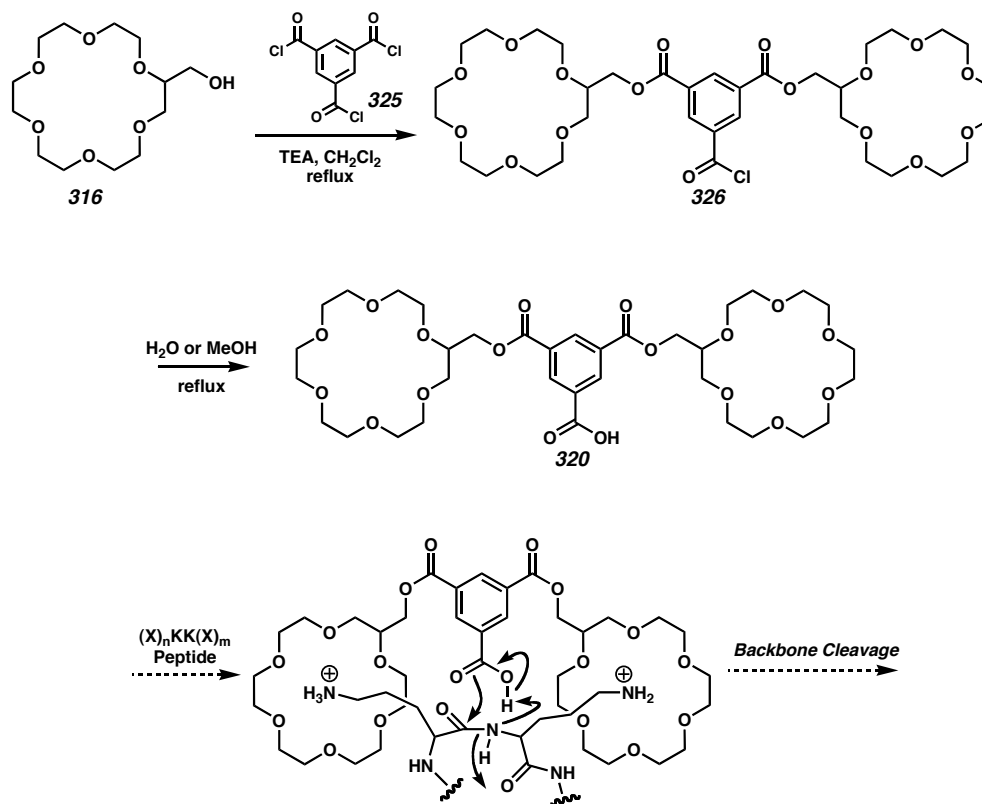
While these gas-phase reagents did not demonstrate optimal reactivity, only producing limited results with regards to peptide cleavage, they serve to illustrate important factors in biomimetic reagent design.

3.3.3.2 Reagents for Covalent Attachment

Greater success for achieving reactivity in the gas phase was achieved with reagents **300** and **301**, which are designed to covalently attach to peptides. The malonate esters are readily synthesized in a similar manner to the benzoic acid **320**. Both malonyl dichloride and ethylmalonyl chloride are commercially available and readily react with the 18C6 methanol **316** in the presence of base. Diazotization is accomplished with

para-acetamidobenzenesulfonyl azide (*p*-ABSA) in the presence of base. Purification as described for the phenanthroline reagent then provided the desired diazomalonate esters.

Scheme 3.2.3: Synthesis and Proposed Mechanism for the 18C6-Diazomalonates.
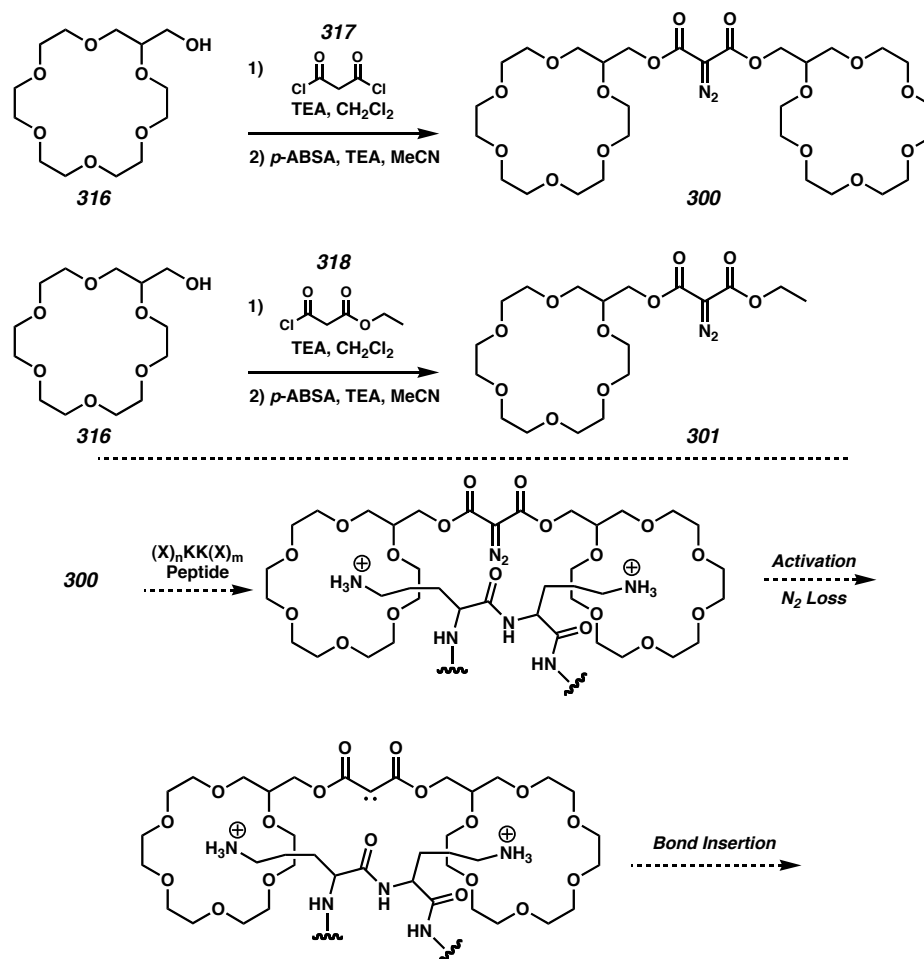
When synthesized, these malonate esters were complexed with a series of small molecules and peptides. Collisional activation was utilized to generate a carbene from the diazo functionality without dissociation of the complex. The intermolecular reactions were studied with ESI-MS and density functional theory (DFT). Sequential MS^n spectra revealed covalent bond attachment between the constituents of the complex subsequent to the generation of the carbene. The data demonstrate that the insertion reactions are sensitive to the presence or absence of N–H and O–H functional groups.

3.4 Results and Discussion

3.4.1 Use of Transition Metals for Peptide Cleavage

3.4.1.1 Doubly Charged Complex

Transition metals have been observed to influence peptide dissociation in previous gas-phase experiments.[6,7] In an attempt to utilize the reactivity of transition metals for the selective cleavage of peptide bonds, reagent **319** was developed. **319** consists of two 18C6 ethers linked by a phenanthroline moiety, which can bind a variety of transition metals. Figure 3.4.1a shows that **319** forms an abundant non-covalent complex with the peptide KK and copper (I). Collisional activation of the base peak [**319** + KK + Cu + H]$^{2+}$ results primarily in dissociation of the complex into [**319** + Cu]$^{+}$ and [KK + H]$^{+}$, with an additional prominent peak corresponding to the loss of 44 Da from [KK + H]$^{+}$. This loss is most likely explained as elimination of CO_2 from the C-terminus.

*Figure 3.4.1: (a) ESI-MS of **319**, copper (I), and KK; (b) MS^2 on the doubly charged complex results in simple dissociation. (c) MS^2 on the triply charged complex results in the loss of CO^2 from the C-terminus of the peptide. Bold downward arrow indicates the peak being subjected to collisional activation.*
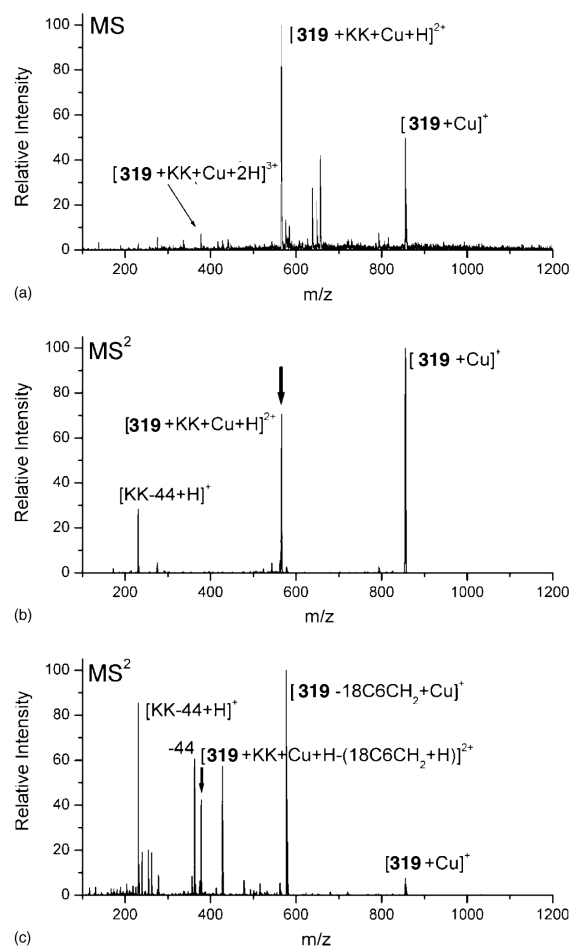
3.4.1.2 Triply Charged Complex

In Figure 3.4.1c, collisional activation of the much less abundant complex [**319** + KK + Cu + 2H]$^{3+}$ yields the loss of CO_2 directly. In the absence of the copper (I) ion, no loss of 44 Da is observed for either charge state, suggesting that copper (I) effectively initiates this reaction. Unfortunately, this chemistry only occurs with very short peptides that end with KK or RK, and reagent **319** did not initiate any other cleavages.

3.4.1.3 Other Complexed Metals

A wide variety of peptides and different transition metals including Ag(I), Fe(III), Co(II), Zn(I), Zn(II), Mn(II), Ni(II), Pd(II), and Cu(II) were tested. Many of these experiments failed to produce an abundant non-covalent complex, and, when the complex could be formed and isolated with a peptide that contained an internal KK sequence, simple dissociation of the associated molecules occurred in every case.

3.4.1.4 Explanation of Results

These results can be rationalized by insufficient binding energy of the non-covalent complex in the gas phase. The presence of a cationic transition metal trapped between two positively charged lysine residues results in unfavorable coulombic interactions that effectively reduce the binding energy of the complex. The binding energy is reduced by $\sim 80 \pm 10$ kcal/mol for inserting a singly charged transition metal ion as determined by PM5 calculations. This repulsion explains why only minimal complexation (or none) occurs for internal KK sequences, and the reduced binding energy leads to the exclusive dissociation of these complexes upon collisional activation. A deprotonated C-terminus effectively mitigates the unfavorable interactions and increases the binding energy by neutralizing the central positive charge. Therefore, reagent **319** is suitable for selectively attaching near the C-terminus of peptides that end in KK or RK/KR; however it did not prove effective at cleaving peptides in the gas phase.

3.4.2 Carboxylic Acid Promoted Cleavage

As mentioned in Section 3.1.1, selective gas-phase cleavage at aspartic acid residues has been observed previously, indicating that acid/base chemistry may provide

an alternate route for cleaving peptides.[3,4] Reagent **320** was designed with this premise as a goal, so it contains two 18C6 ethers linked through esters to a benzoic acid. Deprotonation of the acid is assisted by favorable electrostatic interactions upon complexation with two protonated lysine residues. The ESI mass spectrum for a solution of **320** and KKKK is shown in Figure 3.4.2a. The doubly charged adduct [**320** + KKKK+2H]$^{2+}$ forms the base peak in the spectrum. Collisional activation of this peak results primarily in dissociation of the complex. However, there are additionally two peaks corresponding to the loss of water and the *N*-terminal lysine. To verify that this reactivity was initiated by the benzoic acid, an additional experiment was conducted where the acid was converted to a methyl ester (**321**). The results are shown in Figure 3.4.2c and are nearly identical to those shown in Figure 3.4.2b.

*Figure 3.4.2: (a) ESI-MS of KKKK with **320**, demonstrating excellent recognition; (b) MS^2 on the base peak leads to the loss of the N-terminal lysine; (c) Control experiment with **321** yields same results as in (b), suggesting that **320** is merely a spectator adduct and does not initiate the cleavage of the N-terminal lysine. *=**320** + alkali-metal adducts. Bold downward arrow indicates the peak being subjected to collisional activation.*
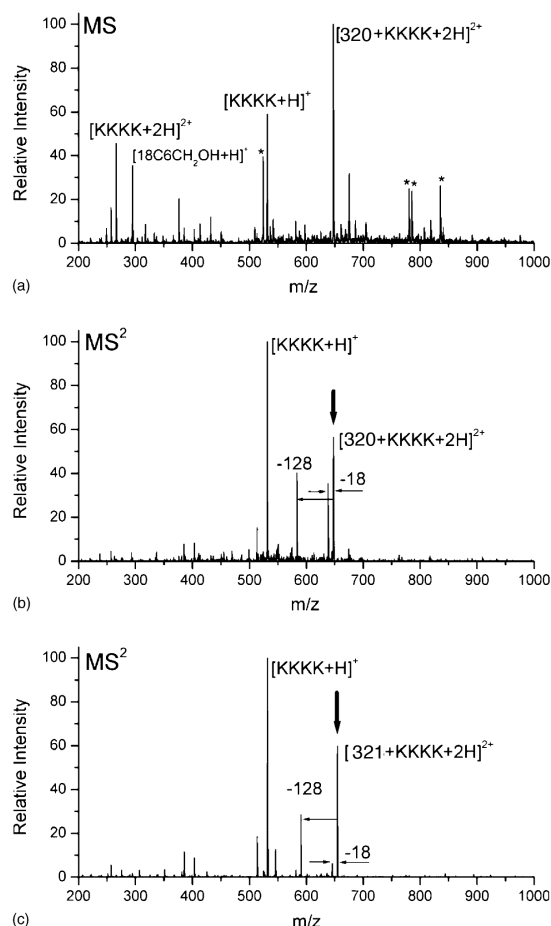
Thus, **320** is likely merely a spectator adduct, which is bound sufficiently to remain attached after a covalent bond cleavage has occurred but does not directly affect the cleavage process. Earlier studies of selective cleavages at aspartic acid residues suggest that process is favored due to the proximity of the aspartic acid side chain to the peptide backbone, with acidity enhanced by a proximal positive charge.[3] The observation that the reactivity of glutamic acid (with the addition of a single methylene) is greatly

reduced in comparison to aspartic acid suggests that the reaction has very special geometrical constraints. It may be that the acidic group in **320** cannot exploit the same reaction pathway as inferred for aspartic acid cleavages because it is not held in close proximity to the peptide backbone. Nevertheless, the results from **320** are important because they demonstrate that biomimetic reagents with multiple crown ethers have sufficient binding energy to mitigate dissociation relative to peptide cleavage processes.

3.4.3 Covalent Bond Formation

3.4.3.1 Introduction

Although cleaving peptide bonds remains an important goal, covalent attachment to peptides is another important reaction that is often used for labeling or for cross-linking peptides and proteins.[16] Molecular mousetraps **300** and **301** are designed to covalently attach to peptides containing lysine residues or any other molecule that contains a protonated primary amine. Both **300** and **301** contain a reactive diazo group, which yields a highly reactive carbene upon collisional activation. Experimental and theoretical results for the interactions of **300** with 1,6-diaminohexane have been reported previously.[8] In order to understand the underlying chemistry, we have performed several experiments with simple small molecules **327**-**330** (Figure 3.4.3) to further elucidate the reaction pathways.

Figure 3.4.3: Guest Molecules.
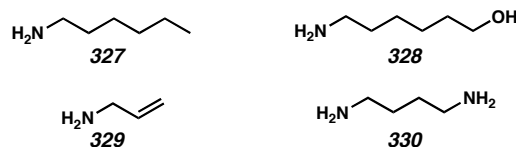
3.4.3.2 Reactions with small molecules

3.4.3.2.1 1-Aminohexane and 300

In Figure 3.4.4a, the ESI spectrum for a solution of 1-aminohexane (**327**) and **300** is shown. The complex corresponding to [**327** + **300** + H]$^+$ clearly forms the base peak in the spectrum, demonstrating the excellent recognition of **300** for protonated primary amines. This complex is subjected to collisional activation in Figure 3.4.4b. The loss of N$_2$ is the only major product observed, yielding the reactive carbene (denoted by **:300**) in nearly 100% yield.

*Figure 3.4.4: (a) ESI-MS of 1-aminohexane (**327**) and **300** demonstrating excellent recognition; (b) MS² on the base peak leads primarily to the loss of N₂ and the generation of the corresponding carbene; (c) Further excitation does not result in loss of **327**, suggesting that an intermolecular insertion reaction has occurred. Bold downward arrow indicates the peak being subjected to collisional activation.*
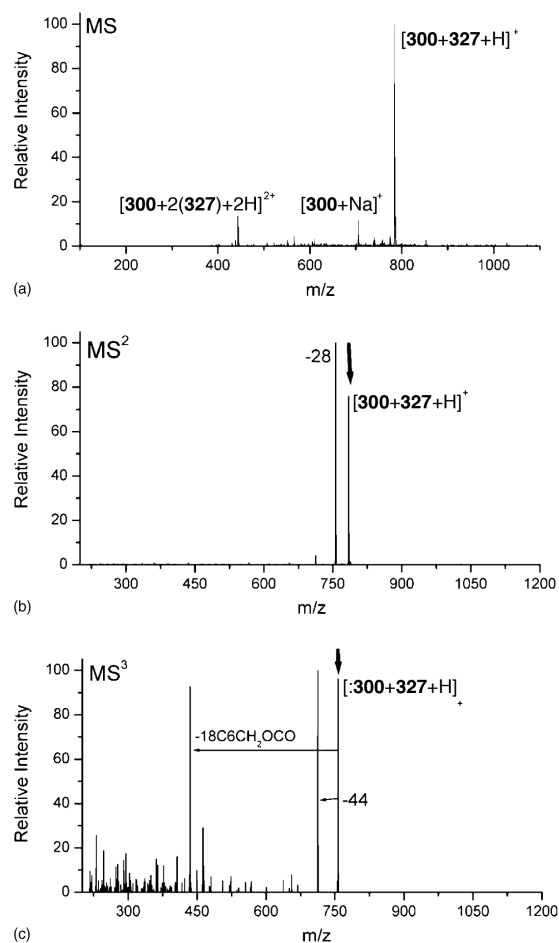
Theoretical results at the B3LYP/6-31G** level with methane and a similar carbene, **309**, suggest that C–H insertion occurs with little or no barrier in a concerted fashion.[17] In Figure 3.4.4b, the carbene **:300** can react with **327** by C–H insertion at various points along the hydrocarbon chain. This insertion is confirmed in Figure 3.4.4c, where no dissociation of **327** is observed after further collisional activation. Instead, several covalent bond cleavages are observed, with one of the two largest corresponding to the loss of a CH₂CH₂O link (MW = 44 Da) from 18C6 and the other corresponding to

the loss of an entire crown. This suggests that C–H insertion does in fact occur and leads to the covalent attachment of the host/guest complex.

Scheme 3.4.1 The Theoretical Reaction Used as a Model.

| 3 | 309 | 331 |
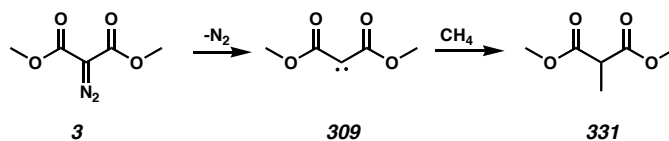
3.4.3.2.2 1,6-Aminohexanol and 300

3.4.3.2.2.1 Experimental Results

Hydroxyl groups are found in three amino acid side chains and can exhibit enhanced reactivity towards carbenes. Figure 3.4.5 shows the results for CAD experiments with **300** and 1,6-aminohexanol (**328**), which is used as a model compound. In Figure 3.4.5a, the CAD of [**300** + **328** + H]$^+$ leads to similar results to those obtained previously for 1,6-diaminohexane.[8] The initial loss of N_2 is accompanied by an additional loss of 18C6CH$_2$OH. The MS^3 spectrum is shown in Figure 3.4.5b for the CAD of [**:300** + **328** +H]$^+$. The loss of CH$_2$CH$_2$O leads to the base peak, while the loss of 18C6CH$_2$OH is secondary. The loss of CH$_2$CH$_2$O is not present in the MS^2 spectrum in Figure 3.4.5a. This suggests that the loss of 18C6CH$_2$OH in Figure 3.4.5a and b proceed by two different reaction mechanisms and that the two products produced in Figure 3.4.5a are generated competitively rather than consecutively (see Section 3.4.3.2.2.2 for more detailed explanation).

In Figure 3.4.5c, further excitation of the complex following the loss of one 18C6 results primarily in the loss of the other 18C6 without the accompanying loss of any **328**. In the absence of both crowns, the retention of the **328** can only be explained by an

insertion reaction, which has transformed the non-covalent complex into a covalent molecule.

*Figure 3.4.5: (a) MS² on [**300** + **328** + H]⁺ yields similar results to those for 1,6-diaminohexane; (b) MS³ spectrum is notably different, suggesting that peaks produced in (a) occur competitively; (c) Further excitation of the complex does not result in any dissociation of **328**. Bold downward arrows indicate peaks being subjected to CAD.*

(a)

(b)

(c)
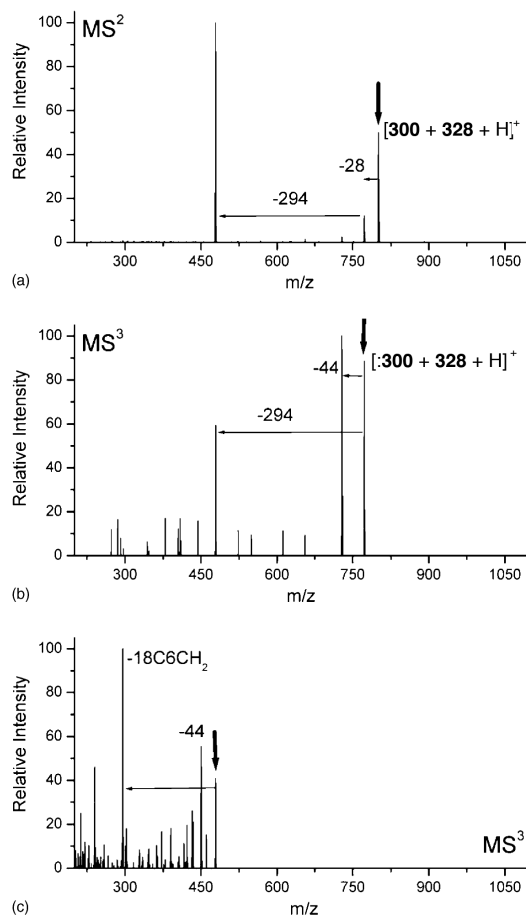
3.4.3.2.2.2 Mechanistic Analysis

The two proposed reaction pathways for the reactions seen in Figure 3.4.5 are shown in Scheme 3.4.2 and are similar to those proposed for the comparable 1,6-diaminohexane system.[8] DFT calculations on **309** and H_2O at the B3LYP/6-31G** level support the formation of an intermediate oxonium ylide **332**. The formation of the ylide proceeds without barrier from several different starting geometries. Precedence for this

mechanism can be found in previous studies, which have revealed oxonium ylide

formation in reactions of various alcohols with carboethoxycarbene, a closely related

molecule.[18] All of the experimental and theoretical data support the reaction mechanisms

shown in Scheme 3.4.2 for any system with a free hydroxyl or unprotonated amines (as

shown previously[8]). In fact, the additional loss of 294 in the MS^2 spectrum is indicative of

the presence of alcohols and amines.

Scheme 3.4.2: Possible Mechanistic Pathways.
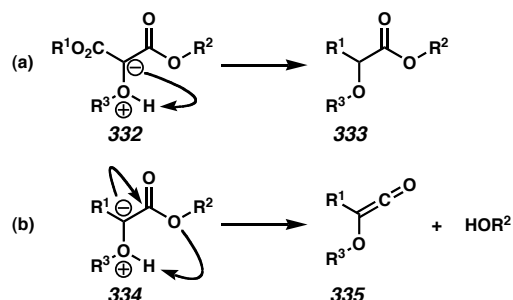
3.4.3.2.3 Allylamine and 301

Reagent **301** contains only a single crown ether connected to a diazo malonate

opposite an ethyl ester. The results for complexing allylamine (**329**) with reagent **301** are

given in Figure 3.4.6. Collisional activation of the complex [**301** + **329** + H]⁺ results

primarily in the loss of N_2 (Figure 3.4.6a). Further excitation of the product peak yields

the loss of neutral EtOH and a multitude of other peaks in Figure 3.4.6b. However,

dissociation of **329** is not observed, suggesting that covalent attachment has been

achieved. Carbene cycloaddition to double bonds is a well-documented phenomenon in

solution and is the most likely explanation for the results observed here.[19]

*Figure 3.4.6: (a) MS² on complex with host **301** and allylamine (**329**) results in the loss of N₂; (b) MS³ spectrum reveals many fragmentation pathways, none of which lead to dissociation of the guest. Bold downward arrows indicate peaks being subjected to CAD.*
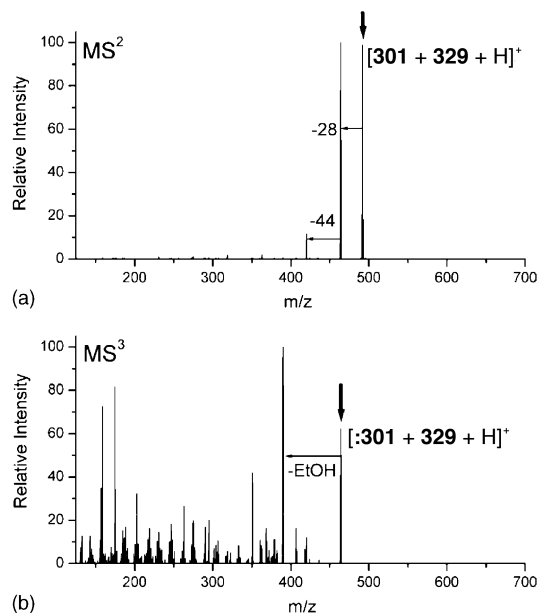
3.4.3.2.4 1,4-Diaminobutane and 301

Experiments with **301** and 1,4-diaminobutane (**330**) yield results similar to those obtained with host **300** and protonated 1,6-aminohexanol or 1,6-diaminohexane,[8] except that loss of EtOH is observed in addition to the loss of 18C6CH$_2$OH. In Figure 3.4.7a it is shown that the loss of EtOH is approximately twice as abundant as the loss of 18C6CH$_2$OH. This is consistent with the proposed reaction mechanisms. In Figure 3.4.7b, a fragment that contains no 18C6 is subjected to CAD. **330** (mass 88 Da) does not dissociate from the complex. Since there is no crown ether present to bind to a primary amine, this data offers compelling evidence that what was once a non-covalent complex is now a single molecule.

Figure 3.4.7: (a) CAD spectrum of 1,4-diaminobutane (330) and 301 loses N₂, EtOH, and 18C6CH₂OH; (b) MS³ spectrum on peak containing no 18C6 ring fragments rather than dissociating, offering compelling evidence for covalent attachment between the host and guest. Bold downward arrows indicate peaks being subjected to CAD.

(c)

(d)
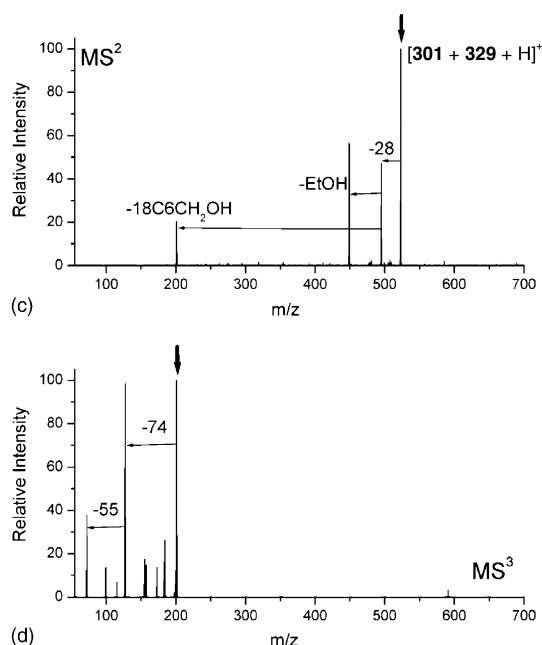
3.4.3.2.5 Summary of Small Molecule Reactions

All of the data obtained by reactions with small molecules suggests that covalent attachment occurs rapidly and almost exclusively when the complex containing **300** or **301** is subjected to CAD. The corresponding carbenes (**:300** and **:301**) can undergo insertion reactions with a wide variety of functional groups. The appropriate next step is to see whether these reagents can covalently attach to peptides themselves.

3.4.3.3 Reactions with Peptides

3.4.3.3.1 KGK and 300

Reagent **300** is designed to bind peptides containing two lysines. The ESI spectrum for **300** with the simple peptide KGK is shown in Figure 3.4.8a. Abundant adduct peaks are observed, indicating excellent recognition. In Figure 3.4.8b, the [**300** +

KGK + 2H]$^{2+}$ peak is subjected to CAD. The loss of N$_2$ leads to the base peak in the

spectrum; an additional loss of 294 Da is observed also. No KGK dissociation appears,

suggesting that the appropriate combination of high binding energy and low activation

barriers has been achieved for reagent **300**. Further collisional activation in Figure 3.4.8c

does not lead to any dissociation of KGK, again confirming that an intermolecular

reaction has occurred. Very similar results are obtained for other peptides containing two

lysines in close proximity, such as INLKAIAALVKKVL, AAKRKAA, and KK.

*Figure 3.4.8: (a) ESI-MS of KGK and **300** shows abundant non-covalent complex formation. (b) MS^2 on [**300** + KGK + 2H]$^{2+}$ yields the expected loss of N$_2$. (c) Further CAD reveals that the peptide has been trapped by the molecular mousetrap and the two are now covalently attached. Downward arrows indicate peaks being subjected to CAD.*
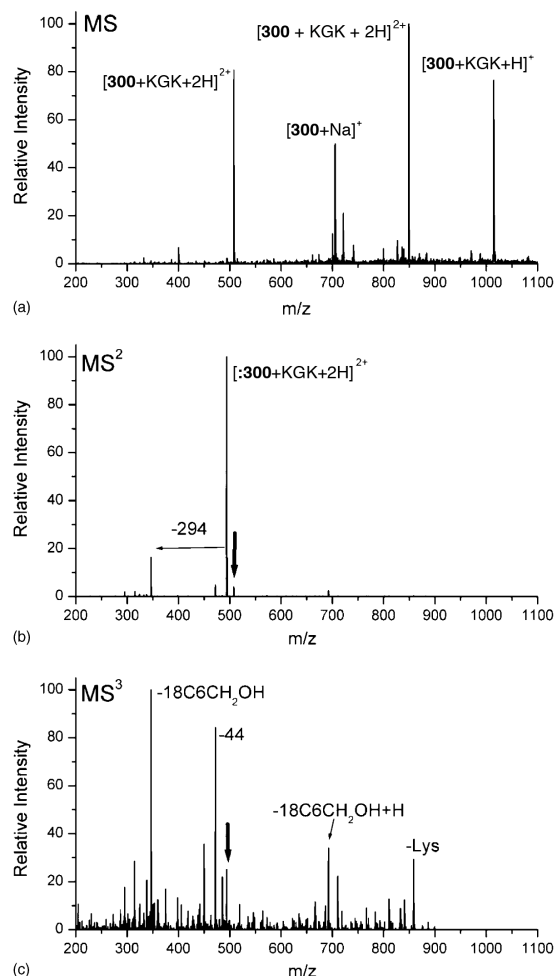
If the singly charged [**300** + KGK + H]⁺ complex is subjected to CAD, then a neutral loss of **300** yields the only observed product. This would appear to suggest that two crown ethers are necessary to achieve sufficient binding energy for the intermolecular reaction to occur. However, it will be demonstrated below that this is not the case and that the dissociation mechanism results from the presence of a neutral primary amine and a lower charge overall for the complex.

3.4.3.3.2 KGK and 301

Reagent **301** only contains a single 18C6 and therefore can only bind to a single lysine, reducing the overall binding energy relative to **300**. Even so, the spectrum in Figure 3.4.9a shows that **301** forms abundant non-covalent complexes with KGK. Isolation and collisional activation of the doubly charged complex [**301** + KGK + 2H]²⁺ results exclusively in the loss of N_2, generating a reactive carbene (Figure 3.4.9b). Re-isolation and further activation of this peak in Figure 3.4.9c yield fragments corresponding to the loss of the charged C-terminal (-147 Da) or N-terminal (-129 Da) lysine residues and the loss of 17 Da (presumably NH_3). Simple dissociation is not observed, indicating covalent attachment through an intermolecular reaction occurred. The loss of lysine from both termini of the peptide suggests that either attachment of the crown is not selective for one lysine over another, that the insertion reaction is not selective, or both. In very similar reactions to those shown in Figure 3.4.9b and c, reagent **301** has been covalently attached to many peptides including: INLKAIAALVKKVL, AAKRKAA, KPPGFSPFR, GGK, and GGKAA.

Figure 3.4.9: (a) ESI-MS of KGK and 301; (b) MS² on [301 + KGK + 2H]² yields the expected loss of N₂; (c) Further CAD reveals that the two molecules are now covalently attached; (d) MS² on the singly charged complex results in simple dissociation. *=301 + alkali-metal adducts. Bold downward arrows indicate peaks being subjected to CAD.
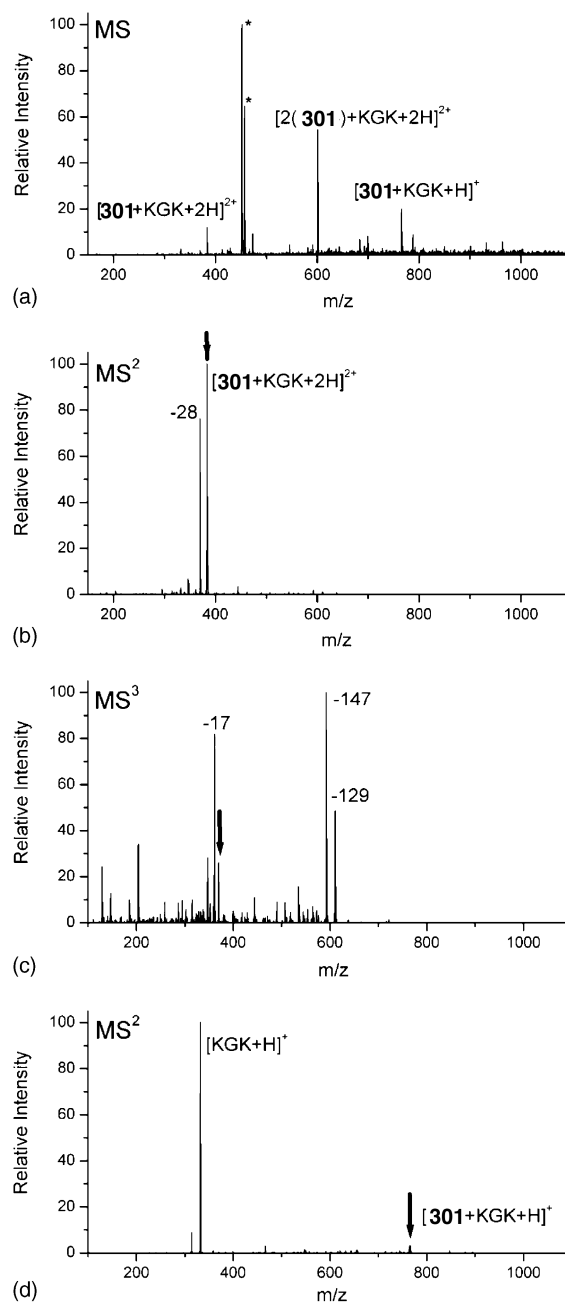
CAD of the singly charged [**301** + KGK + H]⁺ complex results in loss of the

neutral mousetrap **301** exclusively (Figure 3.4.9d) in a similar manner to activation of the

[**300** + KGK + H]$^+$ complex. The exact cause for this interesting behavior is not known, but the results can be explained by at least two possibilities. Either the binding energy of the complex is enhanced by the addition of a second proton, or the absence of the second proton enables a lower energy dissociation pathway. Regardless of the cause, complexes with higher charge states generally tend to favor intermolecular reactions, while lower charge states tend to favor simple dissociation.

3.5 Conclusion

These experiments demonstrate that development of biomimetic reagents capable of directing gas-phase peptide chemistry is possible, and the first successful examples of such reagents have been given. The search for a reagent that selectively cleaves peptides in the gas phase is still ongoing, but we have shown that with the proper combination of high binding energy and low reaction barriers, it is possible to initiate intermolecular reactions in non-covalent complexes with peptides. Furthermore, it is shown that sufficient binding energy to favor peptide cleavage over complex dissociation can be achieved with two 18C6 ethers attached to two lysines. Molecular mousetraps capable of covalently attaching to any lysine-containing peptide are presented herein. This type of molecule represents the first step towards the development of gas-phase cross-linking reagents. The knowledge acquired from these initial results is anticipated to aid the development of other reagents capable of initiating controlled peptide chemistry in the gas phase. Although in the present study only gas-phase activation of these adducts to initiate covalent attachment has been considered, similar chemistry should be possible to effect in solution, with carbene formation initiated by either photochemical or metal catalyzed processes.[20]

3.6 Experimental

3.6.1 Mass Spectrometry

All spectra were obtained using a Finnigan LCQ quadrupole ion trap mass spectrometer without modification. The critical instrument settings that yield adduct formation include capillary voltage 5–15V, capillary temperature 200 °C, and tube lens offset -30 to -50V. Higher capillary temperatures can dissociate the non-covalent complexes. The tube lens offset controls the acceleration of ions as they leave the capillary region. The tube lens voltage is minimized to avoid collisions with the He buffer gas. Soft sampling is crucial for the detection of these non-covalent complexes.

Sample concentrations were typically kept in the ~10 to 100 μM range for all species of interest. All samples were electrosprayed in a mixture of 80:20 methanol/water. The appropriate host was added to the sample and electrosprayed with the guest in order to observe adducts. Collision activated dissociation (CAD) was performed by isolating and then exciting the isolated peak by colliding it with He buffer gas. Samples were electrosprayed with a flow of 3–5 μL/min from a 500 μL Hamilton syringe for optimal signal. Silica tubing with an inner diameter of 0.005 in. was used as the electrospray tip.

3.6.2 Calculations

The energetics of the carbene insertion reactions were quantitatively evaluated by carrying out reactions with the model compound **3**. The structures of all reactants were fully minimized, and several different reaction mechanisms were tested. Initial structures included likely starting points for hydrogen abstraction, concerted insertion, and ylide formation. The starting structures for each of these possibilities corresponded

respectively to: one hydrogen directed at the carbene, symmetrical presentation of the H–C–H or O–H bonds, and one lone pair directed at the carbene. The DFT calculations were carried out using Jaguar 4.1 (Schrödinger, Inc., Portland, Oregon). PM5 semi-empirical calculations were carried out using CACHe Worksystem Pro 5.04 (Fujitsu, Inc., Beaverton, Oregon).

3.6.3 Experimental Details for Syntheses

Due caution should always be used when handling diazo compounds. Reactions were performed in flame-dried glassware under a nitrogen atmosphere. Solvents were dried and purified using activated alumina columns. Diethylamine was distilled from CaH_2. 18-Crown-6-methanol was dried prior to use by heating (~100 °C) under vacuum. All other reagents were used as received from commercial sources. Reaction temperatures were controlled by an IKAmag temperature modulator.
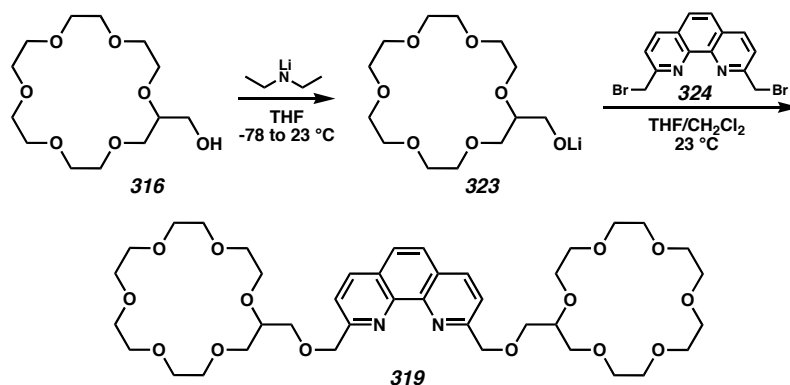
Compound 319: To a stirred solution of diethylamine (13 μL, 0.123 mmol) in THF (500 μL) at 0 °C was added *n*BuLi (60 μL, 2.1 M, 0.126 mmol) dropwise. The mixture was stirred for 10 min and then transferred via syringe to a solution of 18-crown-6-methanol (30 μL, 0.109 mmol) in THF (500 μL) stirred at -78 °C. The solvent was

removed under reduced pressure as the reaction warmed to room temperature. Excess

diethylamine was removed by two consecutive additions of THF (1 mL) and removal

under reduced pressure. The residue was then redissolved in THF (1 mL), and 2,9-

bis(bromomethyl)-1,10-phenanthroline[21] (324) (19 mg, 0.052 mmol) in CH_2Cl_2 (4 mL)

was added. The resulting solution was stirred for 24 h, and then ether (10 mL) was added

to precipitate the salt byproduct, which was removed by filtration through celite. The

removal of solvent under reduced pressure yielded 319 (37.5 mg, 0.047 mmol, 91%

yield) in sufficient purity for experimental use.
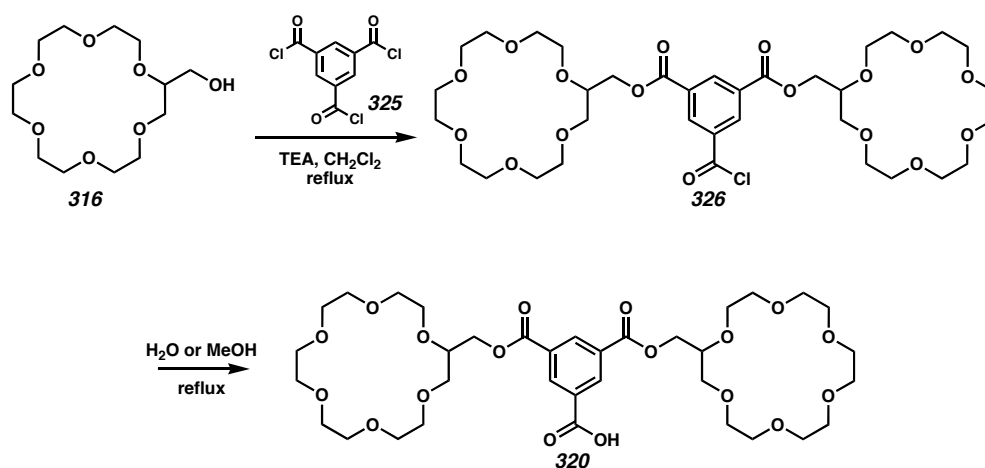
Compound 320: To a stirred solution of 18-crown-6-methanol (47 μL, 0.150

mmol), triethylamine (25 μL, 0.179 mmol), and dichloromethane (4.5 mL) was added

1,3,5-benzenetricarbonyl trichloride (325) (20.4 mg, 0.077 mmol). The mixture was

heated to reflux for 12 h, and then H_2O (1.5 mL) was added, and the mixture was again

heated to reflux for 1 h. The solvent was removed under reduced pressure, the residue

dissolved in a minimal amount of dichloromethane (500 mL), and the undesired salts

were precipitated out of solution with the addition of ether (5 mL). Filtration through

Celite and removal of solvent under reduced pressure yielded **320** (54.2 mg, 0.071 mmol, 95% yield) in sufficient purity for experimental use.
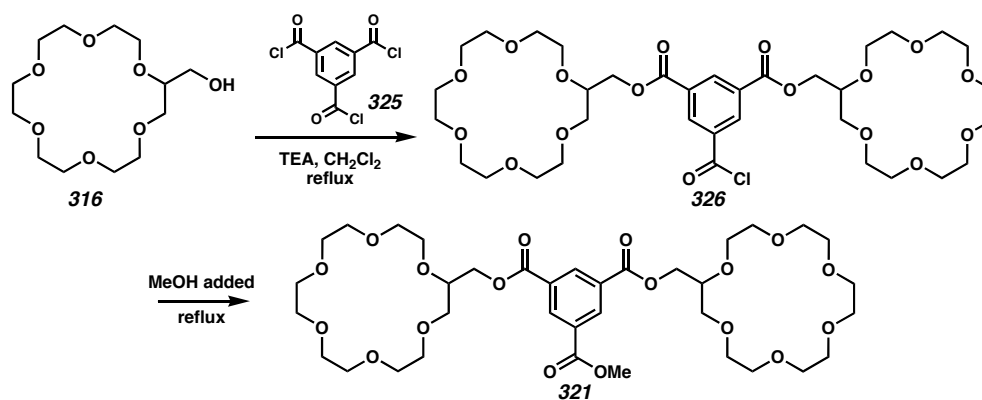
Compound 321: An identical procedure as that for the formation of **320** was followed with the exception that the reaction was quenched with MeOH (500 μL) instead of H$_2$O to yield 3 (49.1 mg, 0.063 mmol, 82% yield) in sufficient purity for experimental use.

Compounds 300, 301, and 3: Compounds **300**, **301**, and **3** were prepared according to established techniques.[8]

3.7 Notes and References

(1) Note that this research was performed in collaboration with Ryan Julian and previously reported in Julian, R. R.; May, J. A.; Stoltz, B. M.; Beauchamp. J. L. *Int. J. Mass Spectrom.* **2003**, *228*(2-3), 851-64.

(2) Vihinen, M. *Biomol. Eng.* **2001**, *18*, 241.

(3) (a) Tsaprailis, G.; Arpad, S.; Nikolaev, E.N.; Wysocki, V.H. *Int. J. Mass Spectrom.* **2000,** *195/196*, 467; (b) Tsaprailis, G.; Nair, H.; Somogyi, A.; Wysocki, V.H.; Zhong, W.; Futrell, J.H.; Summerfield, S.G.; Gaskell, S.J. *J. Am. Chem. Soc.* **1999**, *121*, 5142.

(4) Lee, S.-W.; Kim, S.K.; Beauchamp, J.L. *J. Am. Chem. Soc.* **1998**, *120,* 3188.

(5) Lin, T.; Glish, G.L. *Anal. Chem.* **1998**, *70,* 5162.

(6) Hu, P.; Loo, J.A. *J. Am. Chem. Soc.* **1995**, *117,* 11314.

(7) Nemirovskiy, O.V.; Gross, M.L. *J. Am. Soc. Mass Spectrom.* **1998**, *9,* 1285.

(8) (a) Julian, R.R.; May, J.A.; Stoltz, B.M.; Beauchamp, J.L. *Angew. Chem. Int. Ed.* **2003**, *42,* 1012. (b) See Chapter 2, this thesis.

(9) Some reagents have been developed specifically for the gas phase: (a) Friess, S.D.; Zenobi, R. *J. Am. Soc. Mass Spectrom.* **2001**, *12*(7), 810; (b) Julian, R.R.; Akin, M.; May, J.A.; Stoltz, B.M.; Beauchamp, J.L. *Int. J. Mass Spectrom.* **2002**, *220*, 87.

(10) Julian, R.R.; Beauchamp, J.L. *Int. J. Mass. Spectrom.* **2001**, *210*, 613.

(11) For solution phase reagents, please see: (a) Bell, T.W.; Khasanov, A.B.; Drew, M.G.B.; Filikov, A.; James, T.L. *Angew. Chem. Int. Ed.* **1999**, *38*, 2543; (b) Galan, A.; Andreu, D.; Echavarren, A.M.; Prados, P.; de Mendoza, J. *J. Am. Chem. Soc.* **1992**, *114*, 1511; (c) Ludwig, R.; Fresen, J. *Anal. Chem.* **2000**, *367*, 103; (d) Ngola, S.M.; Kearney, P.C.; Mecozzi, S.; Russell, K.; Dougherty, D.A. *J. Am. Chem. Soc.* **1999**, *121*, 1192; (e)

Rensing, S.; Arendt, A.; Springer, A.; Grawe, T.; Schrader, T. *J. Org. Chem.* **2001**, *66*, 5814; (f) Schrader, T.H. *Tetrahedron Lett.* **1998**, *39*, 517.

(12) (a) Schalley, C.A. *Mass Spectrom. Rev.* **2001**, *20*, 253; (b) Smith, R.D.; Bruce, J.E.; Wu, Q.Y.; Lei, Q.P. *Chem. Soc. Rev.* **1997**, *26*, 191; (c) Veenstra, T.D. *Biophys. Chem.* **1999**, *79*, 63; (d) Loo, J.A. *Int. J. Mass Spectrom.* **2000**, *200*, 175.

(13) (a) Schwartz, B.L.; Light-Wahl, K.J.; Smith, R.D. *J. Am. Soc. Mass Spectrom.* **1994**, *5*, 201; (b) Nemirovskiy, O.V.; Ramanathan, R.; Gross, M.L. *J. Am. Soc. Mass Spectrom.* **1997**, *8*, 809; (c) Brodbelt, J.S. *Int. J. Mass Spectrom.* **2000**, *200*, 57; (d) Eckart, K. Spiess, J. *J. Am. Soc. Mass Spectrom.* **1995**, *6*, 912.

(14) (a) Bradshaw, J.S.; Izatt, R.M.; Borkunov, A.V.; Zhu, C.Y.; Hathaway, J.K. in: Gokel, G.W. (Ed.), Comprehensive Supramolecular Chemistry, vol. 1, Pergamon/Elsevier, Oxford, **1996**, p. 35; (b) Maleknia, S.; Brodbelt, J. *J. Am. Chem. Soc.* **1993**, *115*, 2837.

(15) Julian, R.R.; Beauchamp, J.L. *J. Am. Soc. Mass Spectrom.* **2002**, *13*, 493.

(16) Steen, H.; Jensen, O.N. *Mass Spectrom. Rev.* **2002**, *21*, 163.

(17) The insertion reaction only occurs when the H–C–H bond is presented symmetrically to the carbene, suggesting a minimal barrier may exist. Higher level DFT calculations at the B3LYP/CCPVTZ(-F)[+] level on :6 yield a singlet ground state with a singlet/triplet splitting of 3 ± 1 kcal/mol suggesting that these reactions may proceed through the singlet state.

(18) Toscano, J.P.; Platz, M.S.; Nikolaev, V.; Popic, V. *J. Am. Chem. Soc.* **1994**, *116*, 8146.

(19) Moss, R.A.; Jones Jr., M. (Eds.), Carbenes, vols. 1 and 2, Wiley, New York, 1973, 1975.

(20) (a) Doyle, M.P.; McKervey, M.A.; Ye, T. Modern Catalytic Methods for Organic Synthesis with Diazo Compounds, Wiley-Interscience, New York, 1998; (b) Moody, C.J.; Whitham, G.H.; Reactive Intermediates, Oxford University Press, New York, 1992, p. 26.

(21) (a) Chandler, C.J.; Deady, L.W.; Reiss, J.A.; *J. Heterocycl. Chem.* **1981**, *18*, 599; (b) Weijnen, J.G.J.; Koudijs, A.; Schellekens, G.A.; Engbersen, J.F.J. *J. Chem. Soc. Perkin Trans*. **1992**, *2*, 830.

Chapter 4

The Gas-Phase Synthesis of Charged Copper and Silver Fischer Carbenes from Diazomalonates: Mechanistic and Conformational Considerations in Metal-Mediated Wolff Rearrangements[1]

4.1 Background

4.1.1 Mechanistic Study of Metallocarbenes in the Gas Phase

The gas-phase synthesis of metallocarbene compounds has a surprisingly long history.[2] In early studies, metallocarbenes were created by high-energy methods using electron impact ionization. The resulting ions were then used in bimolecular reactions with various neutral molecules to study the chemistry of charged Fischer carbenes and determine the metal-carbon bond strengths. The importance of studying gas-phase species in determining mechanistic pathways for carbene intermediates in olefin metathesis was also realized early.[2b] Recently, studies have taken advantage of electrospray ionization (ESI) to continue this work.[3] Extending this approach, gas-phase experiments have also enabled mechanistic studies with other highly reactive metallocarbene species.[4]

4.1.2 Diazo Compounds as Carbene Precursors

The utility of diazo compounds as carbene and metallocarbene precursors has been heavily exploited in solution-phase chemistry.[5] The use of diazo compounds as precursors in gas-phase studies involving mass spectrometry (MS) remains less explored.[6] We have recently reported that diazo compounds are excellent carbene precursors for gas-phase studies.[7] In these experiments, a carbene is produced through the low-energy collision-activated dissociation (CAD)[8] of a diazo compound. The

resulting loss of N_2 and generation of the carbene are achieved under conditions sufficiently mild that noncovalently bound complexes are not fragmented in the process. The highly reactive carbene then inserts into the guest and converts the noncovalent complex into a covalently bound molecule. All of the molecules in our recent study were based on the diazomalonate core with at least one 18-crown-6 ether attached. These reagents have been appropriately named "molecular mousetraps."[7] In these mousetrap experiments, covalent bond formation was observed as demonstrated by covalent bond cleavage. To better understand the bond cleavage events that resulted in the loss of crown ethers from the ester intermediates, we have pursued mechanistic studies with malonate carbene intermediates.

4.1.3 The Wolff Rearrangement

Diazomalonates,[9] e.g., **3** and **336** (Figure 4.1.1), and related diazo ketones[10] are known to undergo Wolff rearrangement in the gas phase. As shown in Scheme 4.1.1, the Wolff reaction proceeds with loss of N_2 from an α-diazo carbonyl compound (**337**), a reactive carbene (**338**) is formed. This carbene causes a carbon-carbon bond rearrangement to ketene **339**. In solution, this Wolff product can react with a nucleophile, but in the gas phase the ketene often fragments to produce CO and carbene **340**. Since its discovery in 1902, the Wolff rearrangement[11] has been the subject of numerous studies.[12]

Figure 4.1.1: Diazomalonates.
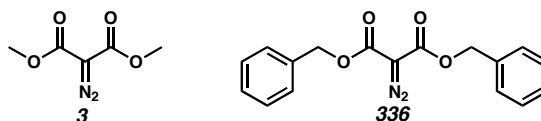
Scheme 4.1.1: Wolff Reaction Mechanism.
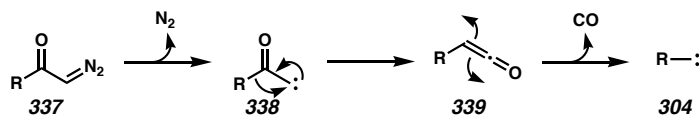
4.1.4 Experimental Approach

In the present work, we use the solvent-free environment of gas-phase experiments to study the mechanism of multiple, consecutive Wolff rearrangements observed in diazomalonates.[9] The effects that various coordinated metal ions and other charged groups have on Wolff rearrangements are discerned from gas-phase MS experiments. Theory is used to quantitatively assess each intermediate for the proposed mechanism. Although the solution-phase synthesis of stable copper(I) and silver(I) Fischer carbenes has been known for some time,[13] here we report the first gas-phase synthesis of copper(I) and silver(I) Fischer carbenes. Results for several intermolecular reactions of these carbenes with molecules coordinated to the metal ion are presented.

4.2 Copper(I) Complexes

4.2.1 Sequential Reaction of Copper(I) and Diazodimethylmalonate (3)

The ESI-MS spectrum for a mixture of copper(I) and **3** is shown in Figure 4.2.1a (for clarity, the corresponding structures of the complexes are provided to the right of the mass spectra). The base peak corresponds to $[3 + MeCN + Cu]^+$, or **341**. It can also be seen from Figure 4.2.1a that **3** has a high affinity for Na^+ (present as an impurity) and that Cu(I) has a high affinity for acetonitrile. As seen in Figure 4.2.1b, isolation of **341** followed by CAD leads to two sequential losses of 28 Da. The first loss of 28 Da corresponds to the loss of N_2 from the diazo functionality leading to structure **342**. The second loss of 28 Da results from Wolff rearrangement of **342** accompanied by a loss of

CO yielding **343**. In Figure 4.2.1c, structure **343** is isolated and subjected to further CAD

resulting in another loss of 28 Da. This loss is attributed to Wolff rearrangement of **343**,

followed by the loss of a second CO fragment, yielding the stable copper Fischer carbene

344. Figure 4.2.1d shows the results of CAD of **344**. Here, the associated acetonitrile is

lost, followed by the addition of either water or methanol. This recruitment is not

surprising given the vacant copper(I) coordination site and the fact that the spectra were

acquired from a water/methanol solution, which would provide for ambient solvent

molecules.

*Figure 4.2.1: (a) MS of a mixture of **3** and Cu(I) in a 20:80 (v/v) water/methanol solution with ~0.1% MeCN. (b) MS² on complex **341**. N₂ and CO are lost sequentially. (c) MS³ on complex **343** resulting in the loss of an additional CO. (d) MS⁴ on **344** resulting in the exchange of the MeCN ligand for either water or methanol.*
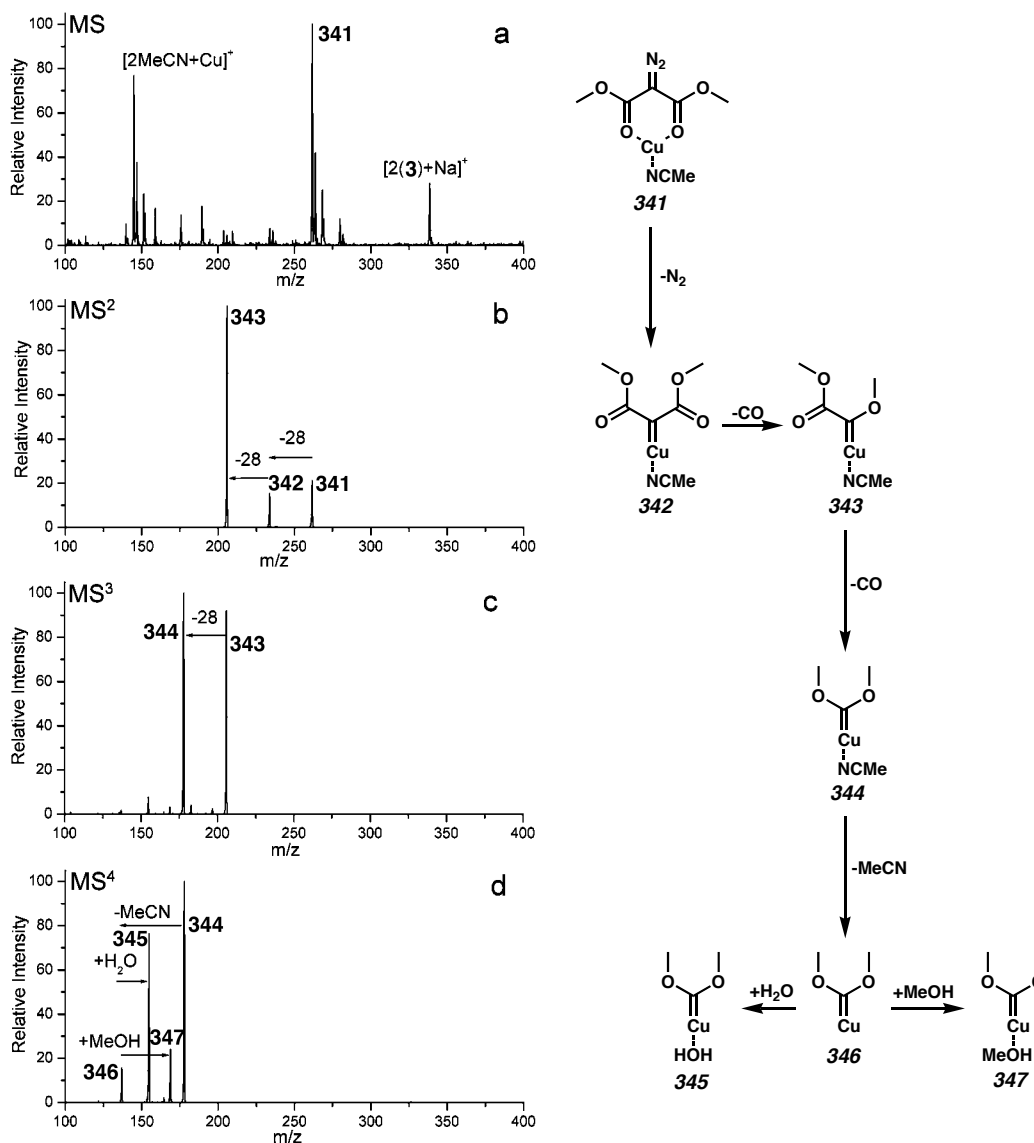
4.2.2 The Mechanism of Initial Carbene Formation

DFT calculations at the B3LYP level using the LACVP** basis set were performed to determine structures and relative energetics for the products and probable intermediates in Figure 4.2.1. The structures and energetics are presented in the reaction

coordinate diagram in Figure 4.2.2. When a group such as N_2 or CO is lost, the energy of the minimized separated molecule is added to compare with the complex prior to dissociation. The initial complex, **341**, is found to be the global minimum, with crystal structure data supporting this binding mode.[14] Direct dissociation of N_2 from **341** is unlikely because the copper(I) ligand restrains the geometry of the molecule in a triplet-like conformation, whereas the thermal dissociation of N_2 must yield the singlet state.[15] Furthermore, **349** has a singlet ground state,[7] and attempts to minimize structure **341** with the N_2 removed were unsuccessful. Matrix isolation studies on similar systems suggest that copper(I) insertion into the C-N bond of intermediate **348** is a more likely alternative.[16]

*Figure 4.2.2: Diagram illustrating the energetics of reaction intermediates in Figure 4.2.1. The energetics are calculated relative to structure **341** and are given in parentheses (in kcal/mol).*
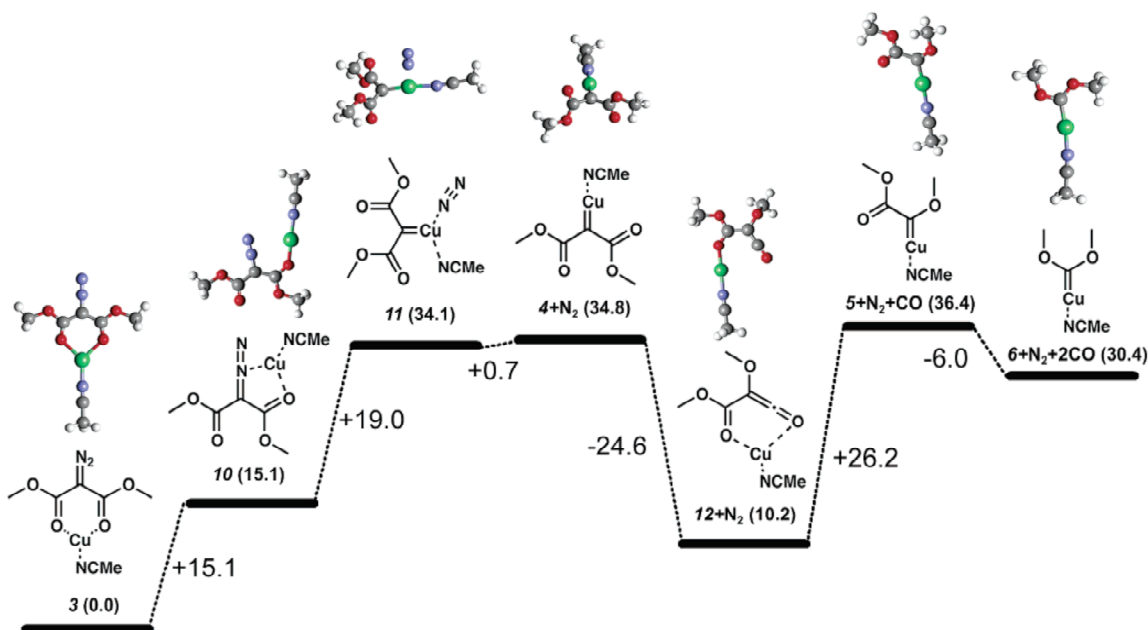
4.2.3 Subsequent Mechanistic Steps

The reaction shown in Figure 4.2.2 proceeds by rearrangement of structure **341** to structure **348** followed by Cu^{+} insertion as shown in **349**. Crystal structures of copper(I) Fischer carbenes have C-Cu bond lengths similar to those in **349** and, in some cases, demonstrate a high affinity for MeCN ligands.[17] Copper insertion is postulated as a prelude to the Wolff rearrangement from **342** to **350**, which must proceed through a singlet state. There is poor agreement between theoretically and experimentally determined barriers to Wolff rearrangement, with theory predicting higher values than those observed experimentally.[18] Theory would predict a large barrier for the conversion of **342** to **350** because of the exothermicity of the reaction.[18b] The experimental evidence in Figure 4.2.1b suggests that both rearrangement of **342** to **350** and subsequent loss of CO to produce **343** proceed with minimal barriers. It should be pointed out that, given a low barrier to rearrangement, the structure for the observed peak in Figure 4.2.1b may be the rearranged product **350** rather than carbene **342**.[19] In either case, the observed products suggest that the presence of copper lowers the barrier to Wolff rearrangement in addition to facilitating the generation of the initial carbene.

The Wolff rearrangement product of **343** undergoes copper insertion without barrier upon energy minimization, suggesting that the transition state may occur prior to rearrangement. Therefore, theory suggests the loss of the second CO likely occurs in a concerted fashion without a true ketene intermediate. The data in Figure 4.2.1b and c show that the initial two losses occur simultaneously, but more activation is needed for the other CO loss, suggesting a higher barrier to the loss of the second CO. However, the noncovalently bound MeCN is retained throughout the process, limiting the reaction

barriers to the bond dissociation energy of Cu-NCMe (or ~43 kcal/mol). Finally, a stable Fischer carbene (**344**) is produced upon loss of the second CO. Subsequent excitation of this complex results in the loss of the MeCN ligand followed by attachment of either H_2O or MeOH from the residual solvent vapor present in the ion trap (Figure 4.2.1d).

4.2.4 Energy Constraints on the Coppercarbene System

Further experimental and theoretical evidence suggests that the copper(I) ion mediates the generation of the carbene from **3**. CAD experiments on [**3** + Na]$^+$ (Figure 4.2.1a) result in the complete loss of signal without producing observable peaks, suggesting dissociation of the sodium ion (which has an m/z ratio too small to detect). Similar experiments with rubidium exclusively afford a peak corresponding to Rb$^+$ from the collisional activation of [**3** + Rb]$^+$. The calculated ΔH for reaction 1 (Figure 4.2.3) is -59 kcal/mol, which can be regarded as the binding energy of the sodium ion to **3**. Similarly, calculations reveal a ΔH of -43 kcal/mol for reaction 2, which is the binding energy of MeCN to the **3**•Cu complex. This value is in reasonable agreement with similar reports.[20] The MeCN ligand is retained throughout the reactions shown in Figure 4.2.2. Thus, though the barriers at each step were not calculated, they must be below 43 kcal/mol, otherwise MeCN would simply dissociate. Furthermore, the binding energy of the sodium ion is much greater at 59 kcal/mol, yet the ion dissociates prior to loss of N_2 and generation of the carbene, demonstrating that copper(I) lowers the activation barrier for carbene generation by at least 16 kcal/mol relative to sodium complexation.

Figure 4.2.3: Calculations for Adduct Formation.

$$\textbf{3} + Na^+ \rightarrow \textbf{3}\bullet Na^+ \qquad \Delta H \approx -59 \text{ kcal/mol} \qquad (1)$$

$$\textbf{3}\bullet Cu + MeCN \rightarrow \textbf{3} \qquad \Delta H \approx -43 \text{ kcal/mol} \qquad (2)$$

4.3 Silver(I) Complexes

4.3.1 Sequential Reaction of Silver(I) and Diazodimethylmalonate (3)

In the presence of silver(I), structure **351** (Figure 4.3.1a) is formed in high abundance. However, unlike the initial loss of N_2 from the parallel copper(I) complex, **341**, collisional activation causes immediate loss of the MeCN ligand from silver (Figure 4.3.1b). This difference is due to the weak binding of the monodentate ligand to the silver(I) cation.[21] Loss of MeCN is followed by collisional cooling of the product **352**, which leads to complexes formed by the association of residual methanol (**353**) or water (**354**) from the ion trap in a similar manner to Figure 4.2.1b. Further CAD of reisolated **352** leads to the exclusive loss of 56 Da in the form of N_2 and CO fragments, with no observable intermediate from the loss of only N_2. Again, these losses are followed by association of methanol or water to form **356** or **357**, respectively. The absence of an observable intermediate from the loss of N_2 suggests that silver(I) is more efficient at facilitating the Wolff rearrangement and subsequent loss of CO than is copper(I). This conclusion is consistent with the greater synthetic utility of silver(I) as an efficient Wolff rearrangement catalyst relative to copper.[5a,b] Isolation and activation of **355** leads to the expected loss of a second equivalent of CO, yielding structure **358** and adducts **359** and **360** from the ensuing association of water or methanol. The silver Fischer carbenes **358**, **359**, and **360** are the final observable carbene products in this sequence. Further CAD of **358** leads to the loss of the Ag^+ cation, presumably generating the neutral dimethoxycarbene in the process.

Figure 4.3.1: (a) MS spectrum showing complexation with a mixture of silver(I) and 3. (b) MS² spectrum of 351, where the loss of MeCN generates the most abundant product ion peak. (c) MS³ spectrum of 352 showing the facile loss of N₂ and CO. (d) MS⁴ spectrum of 355 showing loss of second CO and generation of final silver Fischer carbenes. (e) MS⁵ spectrum of 358, where further CAD results in the cleavage of the metal-carbon bond.
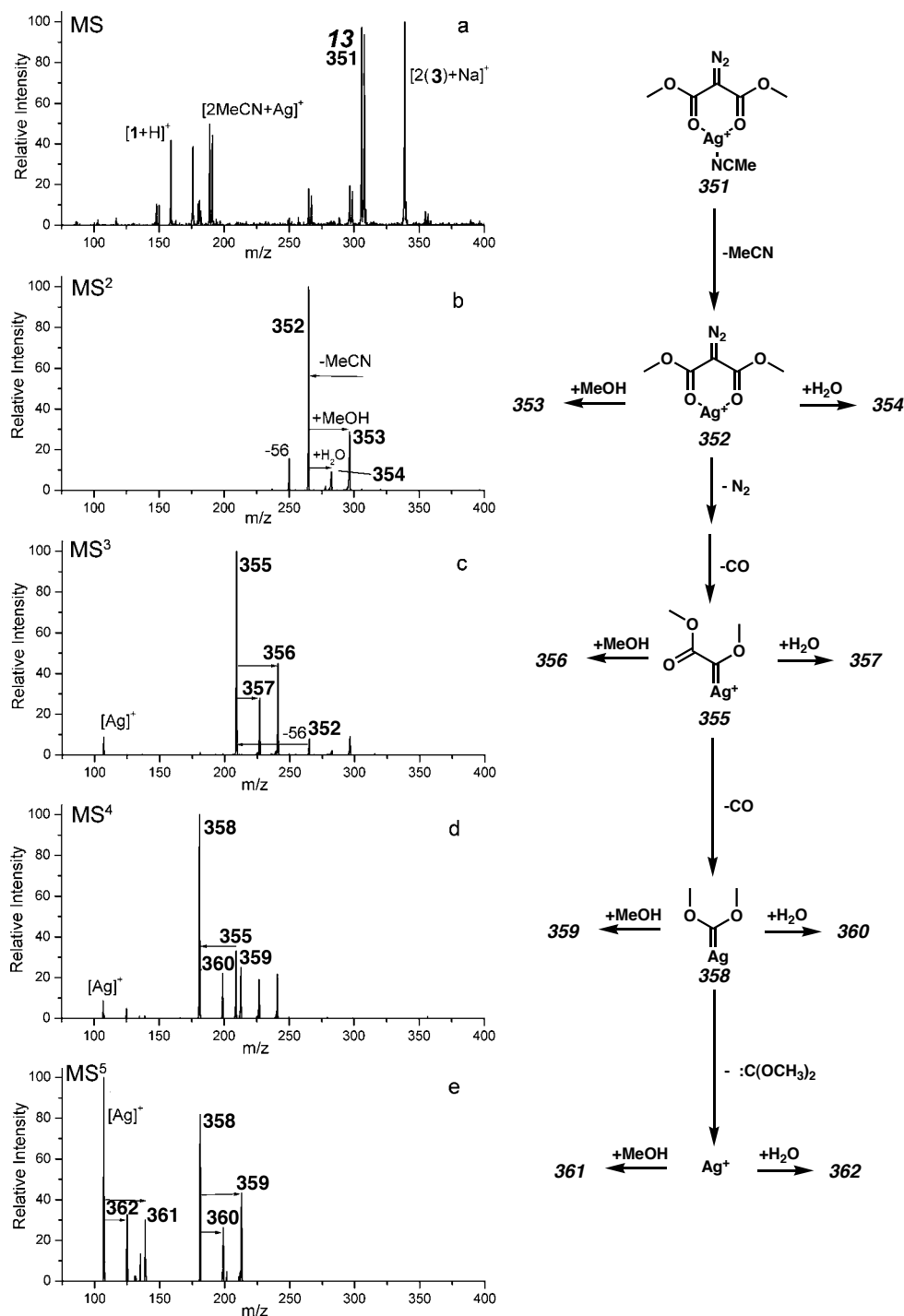
4.4 Labeling Experiments

4.4.1 Deuterium Labeling

Isotopic labeling experiments were performed to confirm the proposed reaction pathways. The results for the labeled compound, **363**, are given in Table 4.4.1. Diazomalonate **363** is deuterium labeled on each of the terminal methyl groups. Comparison of the data in Table 4.4.1 with that shown in Figure 4.2.1 reveals that **363** reacts identically to **3** and that the six deuteriums are retained throughout the entire experiment. This retention suggests that only interior carbons are lost in the reaction sequence and that no detectable MeOH scrambling occurs in the ion trap.

Table 4.4.1: Important Signals in Deuterium-Labeled Diazomalonate Studies.

peaks from MS^2	% intensity	mass change	fragment lost
268	21	0	none
240	15	-28	N_2
212	100	-56	N_2, CO
193	12	-75	

peaks from MS^3	% intensity	mass change	fragment lost/added
212	80	0	none
184	100	-28	CO
161	11	-51	-MeCN, +H_2O

peaks from MS^4	% intensity	mass change	fragment lost/added
184	100	0	none
175	8	-9	-MeCN, +MeOH
161	43	-23	-MeCN, +H_2O
143	5	-41	-MeCN

4.4.2 ^{13}C Labeling

To confirm which carbons are lost and to determine the extent to which rearrangement of the carbene occurs, structure **364** was synthesized with ^{13}C at the 1,3 positions. Experiments with **364** confirm that the two interior ^{13}C-labeled carbons are sequencially lost, as shown in Table 4.4.2. No apparent rearrangement of the carbene via

an oxirene intermediate as depicted in Scheme 4.4.2 is observed.[12] This intermediate

forms by association of the oxygen from the adjacent carbonyl. The oxirene thus formed

can open to a new carbene **369**. Fortunately, this does not occur in this system.

Furthermore, the experiments with **363** and **364** serve to confirm that N_2 is lost first, as

expected, and that the carbon atoms in the 1 and 3 positions, specifically, are lost as CO.

Table 4.4.2: Important Peaks for the 1,3-^{13}C-labeled Diazomalonate Studies.

peaks from MS^2	% intensity	mass change	fragment lost
264	2	0	none
236	11	-28	N_2
207	100	-57	N_2, ^{13}CO

peaks from MS^3	% intensity	mass change	fragment lost
207	98	0	none
178	100	-29	^{13}CO

Scheme 4.4.1: Potential Carbene Scrambling via Oxirene (Not Observed).
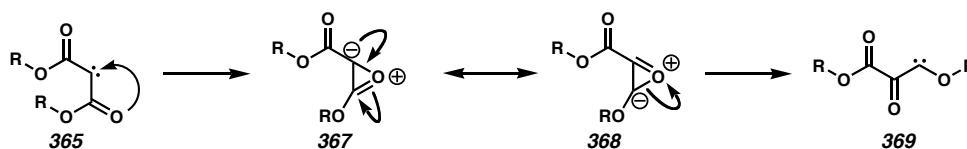
4.5 The Effect of Charge versus Metal Presence in the Wolff Rearrangement

4.5.1 Copper(II) and Nickel(II) Complexes

The experimental MS data for several experiments on **3** with doubly charged

metals are summarized in Table 4.5.1. For both copper(II) and nickel(II), the metal is

primarily complexed with three molecules of **3**, or [3(**3**) + M]$^{2+}$ (where M = Ni or Cu),

with the ligands most likely coordinating the metal in a pseudooctahedral fashion. CAD

of these complexes does not lead to the loss of N_2 but instead yields only the loss of an

entire coordinating molecule. A small amount of [**3** + Cu + 2MeCN]$^{2+}$ is also formed

from the copper solution. However, as the data show in Table 4.5.1, this complex simply loses one of the MeCN ligands upon CAD. These results illustrate that copper(II) and nickel(II) are not as efficient at mediating dinitrogen liberation, Wolff rearrangements, or the subsequent formation of Fischer carbenes. Protonated **3** does not lose N_2 upon CAD either, but it instead yields the assortment of fragments shown in Table 4.5.1.

Table 4.5.1: Key Peaks in the Doubly Charged Metal Studies.

peaks from MS²	% intensity	mass change	fragment lost
268.4	<1	0	none
189.5	100	-79	XX

peaks from MS²	% intensity	mass change	fragment lost
266	<1	0	none
203	72	-63	-XX + MeOH
196	100	-70	-XX + H₂O
187	30	-79	XX
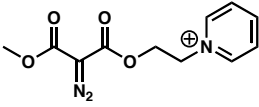
peaks from MS²	% intensity	mass change	fragment lost/added
151	0	0	none
147	50	-4	-MeCN + MeOH
140	100	-11	-MeCN + H₂O

peaks from MS²	% intensity	mass change	fragment lost
159	<1	0	none
145	28	-14	N or CH₂
127	93	-32	MeOH
101	8	-58	unknown
87	100	-72	unknown
69	6	-90	unknown
55	80	-104	unknown

4.5.2 Reaction without a Coordinating Metal

The results presented thus far suggest that the charge on the coordinating metal can dictate the resulting chemistry upon collisional activation in diazo compounds. Structure **370** was designed to investigate the energetics of N_2 loss and Wolff rearrangements in the absence of a coordinating metal. In **370**, the charge is provided by a fixed quaternary nitrogen from a pyridinium group. As seen in Table 4.5.2, the most

abundant product in the MS^2 spectrum from CAD is formed by loss of N$_2$. Further

collisional activation of the resulting molecule demonstrates Wolff rearrangement with

loss of multiple CO molecules. However, this process is accompanied by other

fragmentations not related to Wolff rearrangement. In fact, the loss of pyridine yields the

base peak in the MS^3 spectrum. Consequently, the energetics associated with Wolff

rearrangement and loss of CO for this reaction must be similar to those for the loss of

pyridine.[22]

Table 4.5.2: Key Signals from Pyridinium Diazomalonate Fragmentation.

370

peaks from MS^2	% intensity	mass change	fragment lost
264	22	0	none
236	100	-28	N$_2$
157	13	-107	N$_2$, pyridine
113	8	-151	N$_2$, pyridine(CH$_2$)$_2$O$^-$

peaks from MS^3	% intensity	mass change	fragment lost
236	57	0	none
208	61	-28	CO
192	40	-44	CO$_2$?
180	42	-56	CO
157	100	-79	pyridine

4.5.3 The Importance of the Metal Catalyst and Charge

The pattern of losses for molecule **370** contrasts sharply with the results obtained

for all of the copper(I) and silver(I) adducts. Wolff rearrangement products are no longer

favored in the absence of a coordinated metal. Metal adducts of **3** lose N$_2$ and the first

CO in one step without the addition of further excitation energy. The loss of the second

CO occurs upon further activation, but no other competitive products are produced in

significant abundance at any stage of the experiment. In the case of **370**, N$_2$ loss occurs

without any accompanying loss of CO. Upon further excitation of [**370** - N$_2$]$^+$, Wolff rearrangement, followed by the loss of the first and second CO molecules, occurs with the appearance of several other competitive products. These results suggest that copper(I) and silver(I) facilitate the Wolff rearrangement and loss of CO as shown in Figures 4.2.1 and 4.3.1. By facilitating the Wolff rearrangement, the metals offer more control and specificity.

4.6 Effect of Benzyl Groups

In the diazomalonate **336**, the methyl groups of **3** are replaced by benzyl groups. For the addition of copper(I) to a solution of **336**, the ESI-MS contains a prominent [**336** + Cu + MeCN]$^+$ peak. As shown in Table 4.6.1 CAD dissociation of this peak leads primarily to the loss of the MeCN ligand. No appreciable pickup of water or methanol is observed following the loss of MeCN, which suggests that the benzyl groups are able to coordinate the metal ion sufficiently so that the lost ligand is not replaced. Crystal structure studies provide precedence for this type of coordination.[23] Interestingly, further CAD of [**336** + Cu]$^+$ leads to the sequential loss of N$_2$, CO, and CO, with each intermediate being observed. Once loss of N$_2$ occurs, no further collisional activation is necessary to observe the other two fragmentations. Similar experiments with silver(I) and **336** yield very similar results (Table 4.6.1), but in this case, the [**336** + Ag]$^+$ peak is formed directly from solution in high abundance. Because the metal ion is coordinated to **336** by the benzyl groups, the relative conformation of the diazo functionality to the esters is different for the copper(I) and silver(I) adducts of **3** and **336**. DFT calculations suggest the silver(I) adduct structure shown in **371**. The fact that Wolff rearrangement proceeds more easily for [**336** + Cu]$^+$ than for **341** suggests that the conformational

energy minimum is similar to the preferred conformational orientation that leads to Wolff rearrangement for [**336** + Cu]$^+$. Conformational effects have been observed to influence Wolff rearrangements.[12]

Table 4.6.1: Key Signals from the Diazodibenzylmalonate Fragmentation.

peaks from MS^2	% intensity	mass change	fragment lost
414	10	0	none
373	100	-41	MeCN
345	8	-69	MeCN, N$_2$

peaks from MS^3	% intensity	mass change	fragment lost
373	100	0	none
345	42	-28	N$_2$
317	37	-56	N$_2$, CO
289	55	-84	N$_2$, CO

peaks from MS^2	% intensity	mass change	fragment lost
417	16	0	none
389	100	-28	N$_2$
361	96	-56	N$_2$, CO
345	25	-72	
333	39	-84	N$_2$, CO
317	17	-100	
289	12	-128	

peaks from MS^3	% intensity	mass change	fragment lost
389	100	0	none
361	69	-28	CO
333	26	-56	CO, CO
317	10	-72	

*Figure 4.6.1: Complex of Diazodibenzylmalonate (**336**) with Ag$^+$.*

371
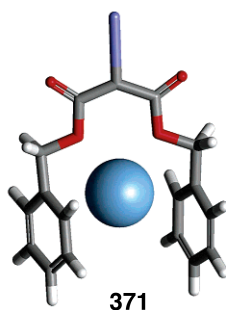
4.7 Macrocycles

4.7.1 Crown Ether Incorporation

Crown ethers and other related macrocycles are well suited to coordinate a variety of metal ions and charged functional groups[24] and often mitigate the association of other solvent adducts once in the gas phase. Therefore, structures **372** and **301** are well suited

to study the proximal effects of various cations and different coordination motifs on the Wolff rearrangement in the absence of weakly bound ligands. The diazo group for **372** is included in the ring, bringing the charge in close proximity to the diazo group. However, it should be noted that the coordination geometry between the charge and the diazo is significantly different for **3** and **372** due to conformational constraints imposed by the macrocycle. Structure **301** is more flexible, allowing for either coordination or separation of the metal and the diazo group.

Figure 4.7.1: Crown Ether Diazomalonates.
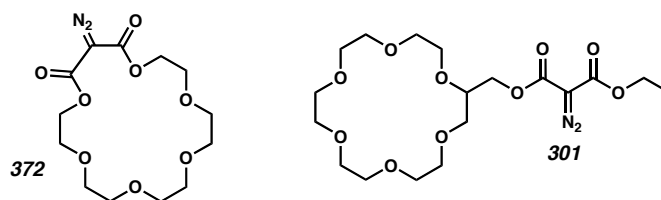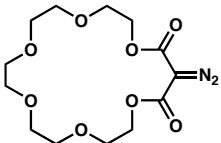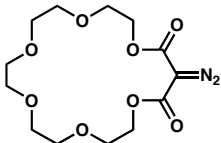
4.7.2 Reaction of Macrocycle 372 and Copper(I) or Sodium

The CAD results for **372** coordinated to copper(I) and sodium are presented in Table 4.7.1. In both cases, the loss of N_2, CO, and CO occurs predominantly one step at a time, requiring the acquisition of an MS^4 scan to induce the loss of the second CO. This suggests that the more conformationally restrained macrocycle requires additional activation energy to induce Wolff rearrangement, but it does not necessarily exclude participation of the cation in the reaction. The resonance excitation rf voltages applied at each step of the experiment for sodium and for copper(I) are 0.67, 0.83, and 0.99 V and 0.69, 0.82, and 0.71 V, respectively. The excitation voltages are very similar for the first two steps of the experiment for both cations, but copper(I) clearly promotes the loss of the second CO more efficiently than sodium (DV ~0.3 V). This is additionally confirmed

by the absence of competitive fragments in the copper(I) experiment, whereas for sodium the base peak in the MS^4 spectrum is not the product of Wolff rearrangement.

Table 4.7.1: Important Results for a Macrocycle Diazomalonate with Na$^+$ and Cu$^+$.
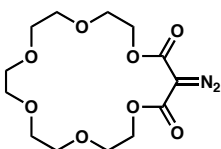
372 (with Na$^+$)

peaks from MS^2	% intensity	mass change	fragment lost
355	6	0	none
327	100	-28	N$_2$

peaks from MS^3	% intensity	mass change	fragment lost
327	5	0	none
299	100	-28	CO
271	6	-56	CO, CO
255	13	-72	CO, CH$_2$CH$_2$O

peaks from MS^4	% intensity	mass change	fragment lost
299	18	0	none
271	73	-28	CO
255	40	-44	CH$_2$CH$_2$O
225	100	-74	CH$_2$OCH$_2$CH$_2$O

372 (with Cu$^+$)

peaks from MS^2	% intensity	mass change	fragment lost
395	18	0	none
367	100	-28	N$_2$
339	26	-56	N$_2$, CO

peaks from MS^3	% intensity	mass change	fragment lost
367	100	0	none
339	94	-28	CO

peaks from MS^4	% intensity	mass change	fragment lost
339	38	0	none
311	100	-28	CO
265	16	-74	CH$_2$OCH$_2$CH$_2$O

4.7.3 Reaction of Macrocycle 372 and Copper(II) or Ammonium

The copper(II) adduct of **372** can also be prepared in small abundance, and the results for the CAD are found in Table 4.7.2. Copper(II) catalyzes the loss of 44 *m/z*, which is presumably the loss of ethylene oxide from the crown ether portion of the molecule.[25] The loss of N$_2$ is not detected, furthur suggesting that copper(II) does not catalyze N$_2$ loss, the Wolff rearrangement, or the subsequent formation of Fischer carbenes as observed with other cations.

Table 4.7.2: Important Results for a Macrocycle Diazomalonate with Cu²⁺.
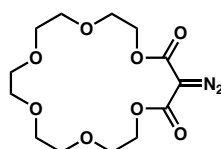
372
with Cu²⁺

peaks from MS²	% intensity	mass change	fragment lost/added
197.5	5	0	none
191.2	21	-6.3	$-CH_2CH_2O, +MeOH$
184.3	6	-13.2	$-CH_2CH_2O, +H_2O$
175.5	100	-22	CH_2CH_2O

CAD of the ammonium adduct of **372** is presented in Table 4.7.3. In this case, the loss of NH_3, followed by subsequent cleavage of protonated **372**, is the only process observed. This suggests that close proximity of a labile proton can prevent the loss of N_2 and subsequent reactions from occurring. However, it should be noted that this problem is easily corrected by complexation with a more basic amine such as 1-hexylamine. CAD of the hexylamine adduct leads primarily to the loss of N_2 (data not shown). Alternatively, weaker binding by ammonium versus 1-hexylamine may explain the dissociation in the case of ammonium. These experiments confirm the notion that the cation can greatly influence the subsequent chemistry upon excitation of these molecules.

Table 4.7.3: Important Results for a Macrocycle Diazomalonate with NH_4^+.

372
with NH₄⁺

peaks from MS²	% intensity	mass change	fragment lost
350	72	0	none
333	33	-17	NH_3
261	100	-89	N_2, CH_2CH_2O
217	12	-133	$N_2, (CH_2CH_2O)_2$
173	11	-177	$N_2, (CH_2CH_2O)_3$
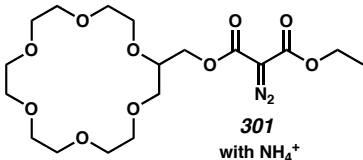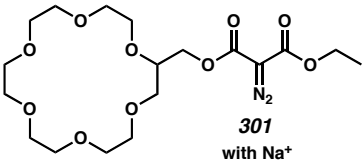
4.7.4 Charge Proximity Effects
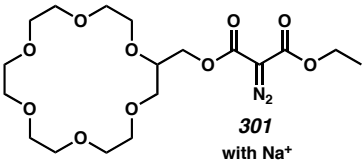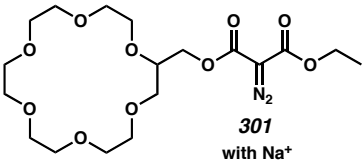
In the copper(I) and silver(I) adducts of **336**, the metal ion is coordinated to the benzyl groups and is not in close proximity to the diazo group. It is not surprising that the resulting CAD spectra are very similar for both metals. In general, charges that are not in close proximity to the diazo group have less influence on the resulting CAD patterns. This is well illustrated by comparing **372** and **301**. Molecular dynamic simulations suggest that the collisional heating of **301** leads to extended structures where the lariat sidearm extends away from the charge in the macrocycle. This leads to a large separation between the charge and the diazo group. In contrast, heating of the quasimolecular complex **372** does not lead to significant structural changes, leaving the charge in close proximity to the diazo group. The net effect is that the diazo group is ~2 Å further from the charge in **301** when compared to **372**.

CAD of $[\mathbf{372} + NH_4]^+$ does not lead to the loss of N_2 or subsequent Wolff rearrangement products. However, when **301** is complexed with ammonium, CAD leads to the loss of N_2 and formation of a carbene (Table 4.7.3). This implies that the ammonium ion does not interact with the diazo group in **301**, but this does not rule out subsequent interactions between the newly generated carbene and the cation. Interestingly, subsequent CAD of $[\mathbf{301} - N_2 + NH_4]^+$ only leads to Wolff rearrangement products with concomitant loss of ammonia or crown fragments. The high proton affinity of the carbene,[26] which reacts with the ammonium, and the higher activation energy for the Wolff rearrangement of $[\mathbf{301} - N_2 + NH_4]^+$ are the likely causes for the observation of the covalent bond cleavage. CAD of **301** complexed with sodium leads to the expected loss of N_2 and the formation of both Wolff rearrangement products in the MS^3 spectrum.

Weaker binding of ammonium by **372** relative to **301** may explain the difference in experimental results.

Table 4.7.4: *Results for a Macrocycle Diazomalonate with NH₄⁺.*

301 with NH₄⁺			**301** with Na⁺			

peaks from MS²	% intensity	mass change	fragment lost	peaks from MS²	% intensity	mass change	fragment lost
452	61	0	none	457	9	0	none
424	100	-28	N₂	429	100	-28	N₂
380	12	-172		385	3	-72	N₂, CH₂CH₂O

peaks from MS³	% intensity	mass change	fragment lost	peaks from MS³	% intensity	mass change	fragment lost
424	100	0	none	429	30	0	none
351	44	-73	NH₃, CO, CO	401	20	-28	CO
291	19	-133	NH₃, CO, (CH₂CH₂O)₂	385	10	-44	CH₂CH₂O
247	19	-177	NH₃, CO, (CH₂CH₂O)₃	373	100	-56	CO, CO
203	21	-221	NH₃, CO, (CH₂CH₂O)₄	357	29	-72	CO, CH₂CH₂O
175	26	-249	NH₃, 2X CO, (CH₂CH₂O)₄	299	10	-130	2X CO, CH₂O(CH₂)₂O

4.7.5 Conformational Effects

The degree of conformational restraint present in a molecule can favor or disfavor subsequent Wolff rearrangement. The previous section established that copper(I) and silver(I) adducts of **336** behave very similarly with the simultaneous creation of all products, but it should be noted that the CAD spectra of these two complexes are not similar to any others obtained in the course of this study. We attribute this to a conformational effect where the metal restrains the molecule in a conformation that favors Wolff rearrangement. The opposite effect is observed in [**372** + Na]⁺, which is also conformationally restrained. In this case, Wolff rearrangement is not favored, and additional activation energy must be added at each step. Interestingly, the barrier becomes much larger when the diameter of the macrocycle is reduced. This supports the proposition that conformational constraints lead to the larger activation barriers required

for the CAD of **372** bound to various ions. Unconstrained systems with a remote charge that do not react with the carbene, such as **370** and $[\mathbf{301} + Na]^+$, demonstrate similar behavior to each other upon CAD.

4.8 Intermolecular Reactions

4.8.1 Hexynenitrile

Given the spectator MeCN ligand present in **341**, a suitably elaborated nitrile ligand could be introduced to the noncovalent complex that might undergo intermolecular reactions in the presence of the intermediate Fischer carbene. The results for attaching three types of modified ligands are summarized in Table 4.8.1. In each of these experiments, activation is continued until the ligand is either exclusively lost or competitively lost (i.e., loss of another fragment is seen concomitantly with the ligand). Facile ligand loss for these complexes suggests that the binding energy of the ligand to the copper(I) cation is not greatly increased by the presence of the additional functional groups. In particular, 5-hexynenitrile is weakly bound to copper(I).

Table 4.8.1: Intermolecular Reactions with Fischer Carbenes.

molecule	attached cation	initial ligand	point of covalent bond cleavage^a
3	Cu^+	5-hexynenitrile	MS^3 (after N_2 loss)
336	Cu^+	5-hexynenitrile	none
3	Cu^+	5-hexenenitrile	none
3	Cu^+	4-phenylbutyronitrile	MS^3 (after N_2 loss)

If the loss of the weakly bound ligand is not observed, and a covalent bond cleavage occurs in lieu of an established sequential rearrangement process (i.e., loss of N_2, CO, and CO), then an intermolecular reaction is assumed to have occurred, and therefore the reactive carbene is unavailable to continue the Wolff sequence. The

reactions that lead to subsequent covalent bond cleavages are complicated and will not be fully described here, as the demonstration of covalent bond formation sufficiently establishes the reactivity of the gas-phase Fischer carbenes. In addition, the results confirm that alkynes are more reactive than analogous alkenes toward carbenes, which is a reasonable result given the greater reactivity of alkynes in general.

4.8.2 Phenylbutyronitrile

The observed reactivity of the phenyl group of 4-phenylbutyronitrile was unexpected, but, like 5-hexynenitrile, it underwent intermolecular reaction. In contrast, the two appended phenyl rings of **336** merely displaced the metal ligand and prevented other reactions from occurring. The aromatic rings of that complex showed no reactivity to the intermediate carbenes.

4.8.3 Loss of Methyl Radical

It is also interesting to note that CAD of [**3** + hexynenitrile + Cu]$^+$ yielded the loss of a neutral methyl radical from the methyl ester in the MS^3 spectrum. This unusual loss was confirmed by experiments with **374** in which the loss of CD_3 was observed. The loss of methyl radical is accompanied by the association of water or methanol. It is unlikely that the methyl group was a metal ligand prior to dissociation, so an alternative explanation is required to explain the acquisition of water or methanol. One possibility involves the oxidation of copper(I) to copper(II) accompanied by the reduction of the newly formed terminal CO_2. The oxidation to copper(II) would create a new vacant ligand site and lead to the observed additions. The exact role of the alkyne in this process remains unclear, but it may serve to stabilize the higher oxidation state of the copper.

4.9 Conclusion

In summary, the synthesis of copper(I) and silver(I) Fischer carbenes from various diazomalonates in the gas phase is demonstrated for the first time. The carbenes are generated by the facile loss of N_2 and undergo multiple Wolff rearrangements in the gas phase, leading sequentially to multiple losses of carbon monoxide. Surprisingly, up to six different carbenes or metallocarbenes can be produced in a single experiment. A series of control experiments that elucidate the effects of metal mediation and conformation on Wolff rearrangements are detailed. Although the data have been gathered from gas-phase experiments, the results reveal general trends that should be applicable for either enhancing or deterring Wolff rearrangements in solution. Coordinated metal ions profoundly affect the energetics of these reactions. Silver(I) is most efficient at initiating Wolff rearrangements, followed by copper(I); in general, associated metal catalysts lower the barriers to the Wolff process, providing for a cleaner reaction. However, no direct metal mediation is required for the Wolff rearrangement, so molecules labeled with nonparticipating charges undergo similar chemistry, though at higher energies. Conformational effects are also found to be important in determining the requisite energy for Wolff rearrangement. Divalent metal ions and protons interfere with the loss of N_2 and do not promote the formation of carbenes.

4.10 Experimental

4.10.1 Materials and Methods

All mass spectra were acquired on a Finnigan LCQ Classic quadrupole ion trap instrument utilizing a standard electrospray source. Solutions of the reagents in the 30-80 μM range were electrosprayed from a 80/20 (v/v) solution of methanol/water with a

minimum of 0.1% MeCN added. Soft ionization settings that minimize energetic collisions during sample collection were used to maximize the intensity of noncovalently bound complexes.[27] Ions of interest were isolated and subjected to collisional activation until product peaks were observed. Helium was used as the collision gas for all experiments. For each MS^n step, the peak of interest was reisolated prior to further dissociation. All chemicals were purchased from Sigma-Aldrich and used without further purification unless otherwise noted. Metal ion complexes were formed by adding an appropriate salt to the solution. No counterion effects were noted. For studies of intermolecular reactions, the desired ligand (such as 5-hexynenitrile) was added directly to the solution in several-fold excess.

4.10.2 Calculations

Candidate structures were evaluated initially at the PM3 semiempirical level. Following minimization at the lower level of theory, structures were optimized using density functional theory (DFT). The DFT calculations were carried out using Jaguar 4.1 (Schrödinger, Inc., Portland, OR). Full geometry optimization was performed at the B3LYP/LACVP** level of theory. Semiempirical PM3 MNDO-type calculations were carried out using the HyperChem 5.1 Professional Suite (Hypercube, Inc., Gainesville, FL). Molecular dynamics simulations were carried out using CACHe Worksystem Pro 5.04 (Fujitsu, Inc., Beaverton, OR). Structures were heated to 300 K for 10 ps with a 0.001-ps time interval utilizing the augmented MM3 parameters.

4.10.3 Synthesis

Reactions were performed in flame-dried glassware under a nitrogen atmosphere. Solvents were dried and purified using activated alumina columns. All other reagents

were used as received from commercial sources. Reaction temperatures were controlled by an IKAmag temperature modulator. Thin-layer chromatography (TLC) was performed using E. Merck silica gel 60 F254 precoated plates (0.25 mm) and visualized by UV and p-anisaldehyde staining. ICN silica gel (particle size 0.032-0.063 mm) was used for flash chromatography. ^{1}H NMR spectra were recorded on a Varian Mercury 300 spectrometer (at 300 MHz) in $CDCl_3$ and are internally referenced to the residual chloroform peak (7.27 ppm) relative to Me_4Si. Data for ^{1}H NMR spectra are reported as follows: chemical shift (δ ppm), multiplicity, coupling constant (Hz), and integration. IR spectra were recorded on a Perkin-Elmer Paragon 1000 spectrometer and are reported in frequency of absorption (cm^{-1}). Preparatory reversed-phase HPLC was performed on a Beckman HPLC with a Waters DeltaPak 25 X 100 mm, 100-μm C18 column equipped with a guard.

3

2-Diazodimethyl Malonate (3). **3** was prepared according to previously established methods.[28] The product was isolated as a yellow oil (2.58 g, 16.29 mmol, 93% yield) with the same physical properties as previously reported.

2-Diazodibenzyl Malonate (336). A round-bottomed flask (10 mL) was charged with dibenzylmalonate (77 μL, 0.308 mmol), MeCN (3 mL), and p-acetamidobenzylsulfonyl azide (116 mg, 0.485 mmol). Et_3N (150 μL, 1.08 mmol) was

then added, and the reaction was stirred at room temperature for 10 h. TLC analysis (3:1

hexanes/EtOAc eluent, $R_F = 0.46$) showed the reaction to be complete. The solvent was

removed by evaporation under reduced pressure, and the crude mixture was subjected to

flash chromatographic purification (5:1 hexanes : EtOAc eluent) to afford **336** as a

yellow oil (75 mg, 0.242 mmol, 78% yield) with the same physical properties as

previously reported.[29]

Diazomalonate 363. A round-bottomed flask (5 mL) was charged with CH_2Cl_2

(1 mL), CD_3OD (500 μL, 11.3 mmol), and Et_3N (100 μL, 0.717 mmol). This mixture

was stirred rapidly while malonyl dichloride (20 μL, 0.206 mmol) was added dropwise at

room temperature. TLC analysis (3:1 hexanes : EtOAc eluent, $R_F = 0.45$) showed

complete conversion to the malonate ester within 2 h. The solvent and excess reagents

were removed by evaporation under reduced pressure, and then MeCN (2 mL) and *p*-

acetamidobenzylsulfonyl azide (103.5 mg, 0.431 mmol) were added to the flask. Et_3N

(100 μL, 0.717 mmol) was added, and the solution was stirred for 24 h. The solvent was

then removed by evaporation under reduced pressure. The product was purified by

dissolving the residue in a minimal amount of CH_2Cl_2 (500 μL) and then precipitating the

salts by addition of Et_2O (5 mL). Filtration through Celite removed the salts, and the

solvent was removed by evaporation under reduced pressure to afford **363** as a yellow oil

(11.9 mg, 0.073 mmol, 35% yield). **363** was identical to **3** spectroscopically except for

the absence of methyl proton peak in the ^1H NMR spectrum and additional product mass.

Diazomalonate 364. To a stirred solution of H₂C(¹³CO₂H)₂ (19.7 mg, 0.179 mmol) in Et₂O (2 mL) in a scratch-free flask (25 mL) was added ethereal diazomethane solution (0.2 M, 4.0 mL, 0.800 mmol). TLC analysis (3:1 hexanes : EtOAc eluent, R_F = 0.45) showed the reaction to be complete. The solvent and excess reagents were removed by evaporation under reduced pressure, and then MeCN (1 mL) and *p*-acetamidobenzylsulfonyl azide (25.9 mg, 0.108 mmol) were added to the flask. Et₃N (41 µL, 0.294 mmol) was added, and the solution was stirred for 24 h. The solvent was then removed by evaporation under reduced pressure. The product was purified by dissolving the residue in a minimal amount of CH₂Cl₂ (500 µL) and then precipitating the salts by addition of Et₂O (5 mL). Filtration through Celite removed the salts, and the solvent was eliminated by evaporation under reduced pressure to afford **364** as a yellow oil (17.4 mg, 0.108 mmol, 60% yield). **364** was identical to **3** spectroscopically except for the enriched ¹³C peak in the NMR spectrum and the additional product mass.

Diazomalonate 370. A round-bottomed flask (10 mL) was charged with CH₂Cl₂ (2 mL), EtOH (25 µL, 0.687 mmol), and 2-bromoethanol (30 µL, 0.421 mmol). This mixture was stirred rapidly while malonyl dichloride (20 µL, 0.206 mmol) was added

dropwise at room temperature. The reaction yielded a statistical mixture of esters within 2 h as determined by ESI-MS. The primary product was 2-bromoethyl ethylmalonate. The solvent and excess reagents were removed by evaporation under reduced pressure, and then MeCN (2 mL) and pyridine (50 μL) were added to the flask. After 24 h, p-acetamidobenzylsulfonyl azide (94.1 mg, 0.392 mmol) and then Et$_3$N (150 μL, 1.076 mmol) were added. The solution was stirred for another 12 h. The solvent was removed by evaporation under reduced pressure to afford **370**; the yield was qualitatively estimated to be 50% by MS (m/z 264.3).
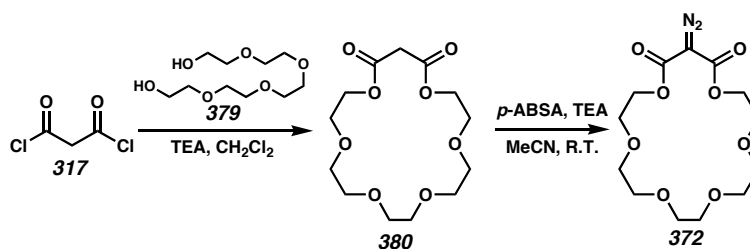
Diazomalonate 372. To a stirred, dry solution of penta(ethylene glycol) (44.4 μL, 0.210 mmol), CH$_2$Cl$_2$ (20 mL), and Et$_3$N (150 μL, 1.076 mmol) was added malonyl dichloride (24 μL, 0.247 mmol). The mixture was heated to reflux for 5.5 h and cooled, and then the solvent was removed by evaporation under reduced pressure. The product was recovered by extraction of the crude residue with refluxing hexanes (20 mL). The solvent was then removed by evaporation under reduced pressure to leave the malonate crown ether. This malonate ester[30] was then dissolved in MeCN (3 mL). Stepwise addition of p-acetamidobenzenesulfonyl azide (151.0 mg, 0.629 mmol) and Et$_3$N (200 μL, 1.435 mmol) provided **372** after stirring for 10 h. The solvent was removed in vacuo, the residue was dissolved in a minimal amount of CH$_2$Cl$_2$ (500 μL), and the undesired

salts precipitated out of solution with the addition of Et$_2$O (5 mL). Filtration through Celite and removal of solvent by evaporation under reduced pressure yielded **372** (59.3 mg, 0.179 mmol, 85% yield).
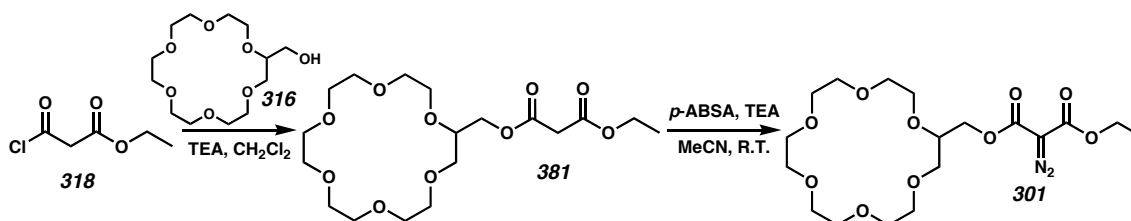
Diazomalonate 301. To a stirred, dry solution of 18-crown-6-methanol (50.0 μL, 0.159 mmol), CH$_2$Cl$_2$ (1.5 mL), and Et$_3$N (33 μL, 0.237 mmol) was added ethylmalonyl chloride (28 μL, 0.219 mmol). The mixture was heated to reflux for 8 h, the solution was cooled, and then the solvent was removed by evaporation under reduced pressure. The residue was dissolved in MeCN (750 μL) and treated with Et$_3$N (30 μL, 0.215 mmol). To this solution was added p-acetamidobenzenesulfonyl azide (53.1 mg, 0.221 mmol), and the mixture was stirred for 10 h. The solvent was removed by evaporation under reduced pressure, the residue was dissolved in a minimal amount of CH$_2$Cl$_2$ (500 μL), and the undesired salts were precipitated out of solution with the addition of Et$_2$O (5 mL). Filtration through Celite and removal of solvent by evaporation under reduced pressure yielded **301** (59.8 mg, 0.138 mmol, 87% yield) as a light yellow oil. A small sample (15 mg) was chromatographed to analytical purity by HPLC (0.1% (wt/v) TFA in water, 8.0 mL/min, 0.30% acetonitrile/min, 82-85 min). FTIR (thin film) 2879, 2142, 1755, 1689; ^{1}H NMR (300 MHz, CDCl$_3$) 4.45 (dd, J = 3.85, 12.1 Hz, 1H), 4.31 (q, J = 7.14 Hz, 2H), 4.27 (m, 1H), 3.85 (t, J = 4.95, 1H), 3.80 (br s, 1H), 3.67 (br s, 21H), 1.32 (t, J = 7.14 Hz, 3H); MS m/z 435.2 (H$^+$).

4.11 Notes and References

(1) Note that this research was performed in collaboration with Ryan Julian and previously reported in Julian, R. R.; May, J. A.; Stoltz, B. M.; Beauchamp. J. L. *J. Am. Chem. Soc.* **2003**, *125*, 4478.

(2) Stevens, A. E.; Beauchamp, J. L. *J. Am. Chem. Soc.* **1978**, *100*, 2584-2585. (b) Stevens, A. E.; Beauchamp, J. L. *J. Am. Chem. Soc.* **1979**, *101*, 6449-6450. (c) Halle, L. F.; Armentrout, P. B.; Beauchamp, J. L. *J. Am. Chem. Soc.* **1981**, *103*, 962-963.

(3) Adlhart, C.; Hinderling, C.; Baumann, H.; Chen, P. *J. Am. Chem. Soc.* **2000**, *122*, 8204-8214.

(4) Bertani, R.; Michelin, R. A.; Mozzon, M.; Traldi, P.; Seraglia, R.; Busetto, L.; Cassani, M. C.; Tagliatesta, P.; D'Arcangelo, G. *Organometallics* **1997**, *16*, 3229-3233.

(5) Doyle, M. P.; McKervey, M. A.; Ye, T. *Modern Catalytic Methods for Organic Synthesis with Diazo Compounds*; Wiley-Interscience: New York, 1998. (b) Sarpong, R.; Su, J. T.; Stoltz, B. M. *J. Am. Chem. Soc.* **2003**, *125*, 13624. (c) Moody, C. J.; Whitham, G. H. *Reactive Intermediates*; Oxford University Press: New York, 1992; pp 26-50. (d) Straub, B. F.; Hofmann, P. *Angew. Chem., Int. Ed.* **2001**, *40*, 1288-1290.

(6) Lebedev, A. T.; Bakulev, V. A.; Hayes, R. N.; Bowie, J. H. *Rapid Commun. Mass. Spectrom.* **1991**, *5*, 234-237. (b) Lebedev, A. T. *Rev. Mass Spectrom.* **1991**, *10*, 91-132. (c) Armentrout, P. B.; Sunderlin, L. S.; Fisher, E. R. *Inorg. Chem.* **1989**, *28*, 4436-4437.

(7) Julian, R. R.; May, J. A.; Stoltz, B. M.; Beauchamp, J. L. *Angew. Chem., Int. Ed.* **2003**, *42*(9), 1012-1015. See also Chapters 2 and 3 of this thesis.

(8) Marzluff, E. M.; Beauchamp, J. L. In *Large Ions: Their Vaporization, Detection, and Structural Analysis*; Baer, T., Ng, C. Y., Powis, I.; Eds.; John Wiley & Sons Ltd.: New

York, 1996; pp 115-143. (b) McLuckey, S. A. *J. Am. Soc. Mass Spectrom.* **1992**, *3*, 599-614. (c) Hayes, R. N.; Gross, M. L. *Methods Enzymol.* **1990**, *193*, 237-263.

(9) Richardson, D. C.; Hendrick, M. E.; Jones, M. *J. Am. Chem. Soc.* **1971**, *93*, 3790-3791.

(10) Marfisi, C.; Verlaque, P.; Davidovics, G.; Pourcin, J.; Pizzala, L.; Aycard, J.-P.; Bodot, H. *J. Org Chem.* **1983**, *48*, 533-537.

(11) Wolff, L. *Justus Liebigs Ann. Chem.* **1902**, *325*, 129.

(12) Sudrik, S. G.; Chavan, S. P.; Chandrakumar, K. R. S.; Pal, S.; Date, S. K.; Chavan, S. P.; Sonawane, H. R. *J. Org. Chem.* **2002**, *67*, 1574-1579 and references therein. (b) McMahon, R. J.; Chapman, O. L.; Hayes, R. A.; Hess, T. C.; Krimmer, H. P. *J. Am. Chem. Soc.* **1985**, *107*, 7597-7606. (c) Fenwick, J.; Frater, G.; Ogi, K.; Strausz, O. P. *J. Am. Chem. Soc.* **1973**, *95*, 124-132. (d) Pomerantz, M.; Levanon, M. *Tetrahedron Lett.* **1991**, *32*, 995-998. Also see ref 4a Chapter 9.

(13) Arduengo, A. J.; Dias, H. V. R.; Calabrese, J. C.; Davidson, F. *Organometallics* **1993**, *12*, 3405.

(14) Dias, H. V. R.; Polach, S. A. *Inorg. Chem.* **2000**, *39*, 4676-4677.

(15) Wentrup, C. *Reactive Molecules: The Neutral Reactive Intermediates in Organic Chemistry*; John Wiley & Sons: New York, 1984; pp 177-264.

(16) Chang, S.-C.; Kafafi, Z. H.; Hauge, R. H.; Billups, W. E.; Margrave, J. L. *J. Am. Chem. Soc.* **1987**, *109*, 4508-4513.

(17) Barluenga, J.; Lopez, L. A.; Lober, O.; Tomas, M.; Garcia-Granda, S.; Alvarez-Rua, C.; Borge, J. *Angew. Chem., Int. Ed.* **2001**, *40*, 3392-3394. (b) Tulloch, A. A. D.;

Danopoulos, A. A.; Kleinhenz, S.; Light, M. E.; Hursthouse, M. B.; Eastham, G. *Organometallics* **2001**, *20*, 2027-2031.

(18) Likhotvorik, I.; Zhu, Z.; Tae, E. L.; Tippmann, E.; Hill, B. T.; Platz, M. S. *J. Am. Chem. Soc.* **2001**, *123*, 6061-6068. (b) Scott, A. P.; Platz, M. S.; Radom, L. *J. Am. Chem. Soc.* **2001**, *123*, 6069-6076.

(19) Similarly, it is impossible to distinguish experimentally whether structures **359** and **343** have already undergone Wolff rearrangement prior to experimental observation.

(20) Vitale, G.; Valina, A. B.; Huang, H.; Amunugama, R.; Rodgers, M. T. *J. Phys. Chem. A* **2001**, *105*, 11351-11364. (b) Chu, Y.; Yang, Z.; Rodgers, M. T. *J. Am. Mass Spectrom.* **2002**, *13*, 453-468.

(21) Shoeib, T.; Aribi, H. E.; Siu, K. W. M.; Hopkinson, A. C. *J. Phys. Chem. A* **2001**, *105*, 710-719.

(22) Katritzky, A. R.; Watson, C. H.; Dega-Szafran, Z.; Eyler, J. R. *J. Am. Chem. Soc.* **1990**, *112*, 2471-2478.

(23) Dattelbaum, A. M.; Martin, J. D. *Inorg. Chem.* **1999**, *38*, 6200-6205. (b) Wen, M.; Munakata, M.; Suenaga, Y.; Kuroda-Sowa, T.; Maekawa, M. *Inorg. Chim. Acta* **2002**, *332*, 18-24.

(24) Bradshaw, J. S.; Izatt, R. M.; Bordunov, A. V.; Zhu, C. Y.; Hathaway, J. K. *Comprehensive Supramolecular Chemistry*; Gokel, G. W., Ed., Pergamon/Elsevier: Oxford, U.K., 1996; Vol. 1, pp 35-95.

(25) Maleknia, S.; Brodbelt, J. *J. Am. Chem. Soc.* **1993,** *115*, 2837-2843.

(26) Vogt, J.; Beauchamp, J. L. *J. Am. Chem. Soc*. **1975,** *97*, 6682-6685. (b) Pliego J. R.; De Almeida, W. B. *J. Chem. Soc., Faraday Trans*. **1997**, *93*, 1881-1883.

(27) Julian, R. R.; Beauchamp, J. L. *Int. J. Mass. Spectrom.* **2001**, *210*, 613-623.

(28) Falorni, M.; Dettori, G.; Giacomelli, G. *Tetrahedron: Asymmetry* **1998**, *9*, 1419.

(29) Kametani, T.; Yukawa, H.; Honda, T. *J. Chem Soc., Perkin Trans. 1* **1990**, *3*, 571-577.

(30) Lamb, J. D.; Izatt, R. M.; Swain, C. S.; Bradshaw, J. S.; Christensen, J. J. *J. Am. Chem. Soc*. **1980**, *102*, 479-482.

Chapter 5

Structural Implications of Biosynthesis for the Calycanthaceous Alkaloids,[1] the Communesins, and Nomofungin

5.1 Background

Natural product synthesis and biosynthetic studies are often used synergistically to illuminate problems and to further understanding in each discipline. Transformations, purifications, conformations, and characterizations are all shared aspects of the two approaches to understanding natural products. This overlap is most prominent when dealing with classes of natural products that are targets of synthetic efforts for structural elucidation, activity studies, and biogeneration.

5.1.1 Calycanthaceous Alkaloids

Organic chemists are well acquainted with the Calycanthaceous alkaloids, which were first isolated from the plant genus Calycanthus. Early isolations of individual members showed a closely related skeleton that differed only in the aminal connectivity for the various natural products.[2] No less than five structural isomers are possible by formation of aminal linkages from the hypothetical intermediate **400** (see Figure 5.1.1), though only three arrangements (**401**, **402**, and **403**) are represented by natural products. The subtle differences in possible structures required substantial effort to establish the relative and absolute stereochemistry of these compounds. Chemical degradation studies, nuclear magnetic resonance (NMR) techniques, X-ray diffraction analysis, and total synthesis techniques were required to elucidate unambiguously the structures of these alkaloids.

Figure 5.1.1: Possible Topologies for the Calycanthaceous Alkaloids.
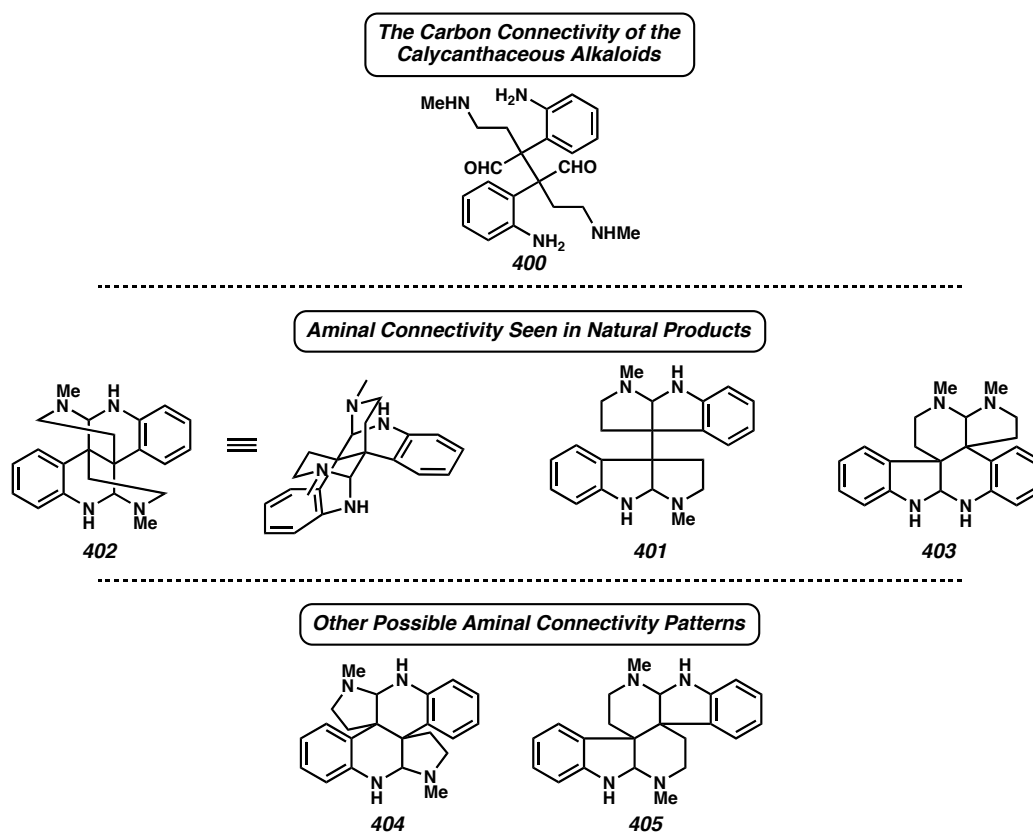
5.2 Natural Product Examples of the Scaffolds in Figure 5.1.1

5.2.1 Calycanthine

The first calycanthoid to be characterized was (+)-calycanthine (**402**, Figure 5.2.1). The structure was established chemically by Robinson[3] and Woodward[4] and crystallographically by Hamor and Robertson using the dihydrobromide dihydrate salt.[5] Two appended bridged bicycles comprise this C_2-symmetric structure, the most intricate of the five regioisomers. The absolute stereochemistry of calycanthine was determined using circular dichroism analysis by Mason soon after the publication of the crystal structure.[6]

Figure 5.2.1: Calycanthine.

402
(+)-Calycanthine
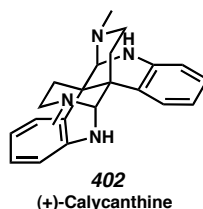
5.2.2 The Chimonanthines

The structure of (–)-chimonanthine (**407**, Figure 5.2.2), isolated from *Chimonanthus fragrans* (Hodsen et al.[7]), was shortly thereafter elucidated by Hamor and Robertson through X-ray analysis of the dihydrobromide salt.[8] Chimonanthine contains two indoline units, each with an annulated pyrrolidine, that are 3,3'-connected. Interestingly, both the C_2-symmetric isomers and the *meso* isomer exist naturally. The absolute stereochemistry of the vicinal quaternary carbon centers is identical to that of calycanthine, as the two isomers equilibrate under acidic conditions. Two other ambiguous structures, those of calycanthidine[9] (**408**) and folicanthine[10] (**409**), were also confirmed by the chimonanthine crystal structure, as these compounds had been shown to be the successive methylation products of chimonanthine.[11]

*Figure 5.2.2: Compounds Representative of Scaffold **401**.*

406
meso-**Chimonanthine**

407 R=R'=H   (–)-Chimonanthine
408 R=H, R'=Me (–)-Calycanthidine
409 R=R'=Me   (–)-Folicanthine

402
(+) Calycanthine
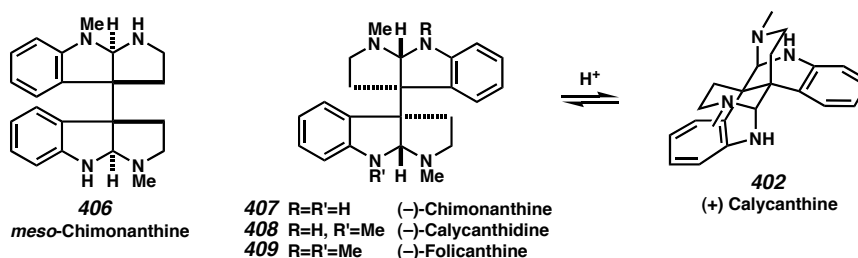
Many closely related compounds have been isolated from the animal kingdom. In fact, the antipodes for the Calycanthus-derived structures, (–)-calycanthine (**403**) and (+)-chimonanthine (**404**), were isolated from the Colombian poison-dart frog, *Phyllobates terribilis* (Figure 5.2.3).[12]

Figure 5.2.3: Products from the Colombian Poison-Dart Frog.

403
(–) Calycanthine

404
(+) Chimonanthine
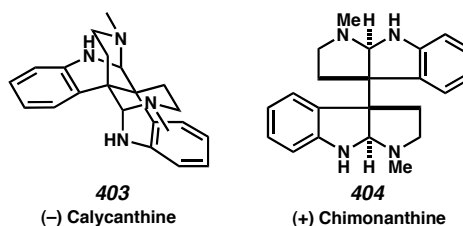
5.2.3 Perophoramidine

Skeleton **405** (Figure 5.1.1) appeared in a recently isolated fungal (*Perophora namei* ascidia) alkaloid as perophoramidine (**405**, Figure 5.2.4).[13] This compound demonstrated cytotoxicity with the HCT116 colon carcinoma cell line with an IC_{50} of 60 μM and induced apoptosis via PARP cleavage within 24 h.

The apparently convergent development of the calycanthaceous alkaloids by such disparate natural sources indicates they are a highly effective family of compounds for many organisms and thus are likely to be important as research targets. An understanding of the plant biosynthesis of these compounds is likely to aid in the study of related compounds and synthetic efforts toward the bis-tryptophan derived skeletons.

Figure 5.2.4: Perophoramidine.

405
Perophoramidine
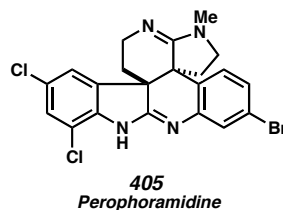
5.3 Biosynthesis of the Calycanthaceous Alkaloids

5.3.1 General Biosynthetic Pathway

Both biosynthetic labeling and biomimetic synthesis have established a mechanism for calycanthoid construction. The widely accepted biosynthesis of the calycanthaceous alkaloids is predicated on an oxidative dimerization of *N*-methyl tryptamine (**406**, Scheme 5.3.1). The newly formed bis-indolenine can undergo hydrolysis to access hypothetical intermediate **400**, or it can easily form the chimonanthine scaffold **401** or scaffold **405** by attack of the free amines on the indolenine imines. As scaffold **405** remains unrepresented by isolated natural products, the chimonanthine scaffold is likely the favored product of aminal closure. This scaffold can then be modified to provide the various chimonanthine derivatives. Two more scaffolds, **404** and **402**, are accessible from intermediate **400**. Again, only one possibility, **402**, is represented in natural products and is presumed to be the

favored isomer. Thus, the calycanthine and chimonanthine skeletons are shaped by aminal formation through a controlled equilibrium from **407**.

Scheme 5.3.1: Biosynthetic Pathway to the Calycanthaceous Alkaloids.
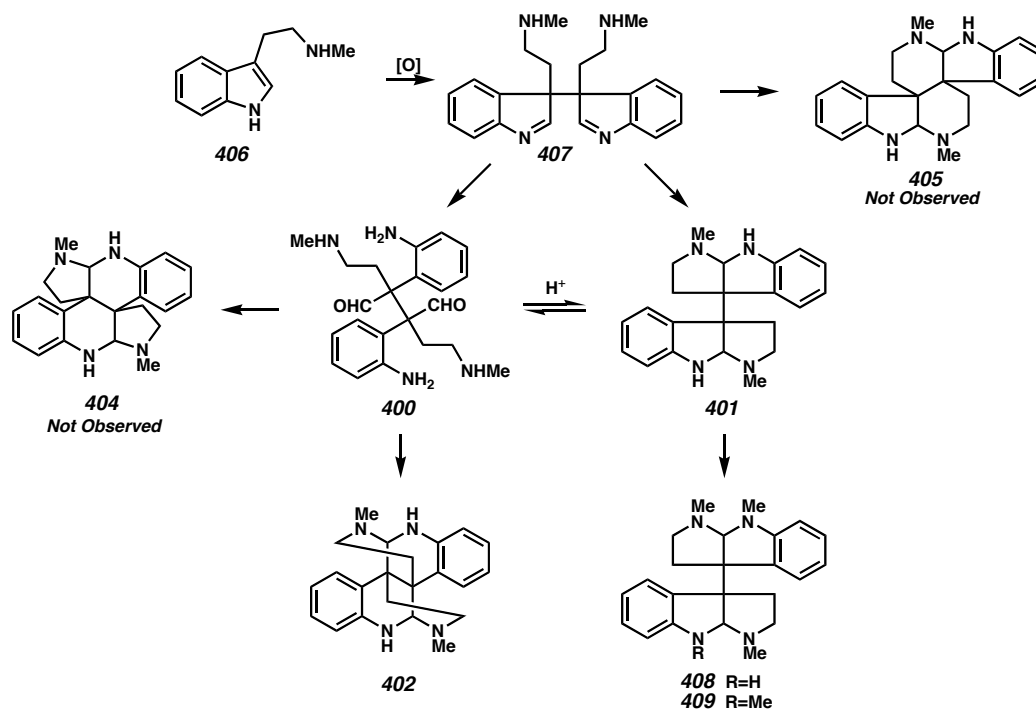
5.3.2 Hendrickson's Study

The oxidative coupling of tryptamine equivalents has been replicated in the laboratory using several oxidants. In an early study, Hendrickson et al. performed the coupling using sodium hydride and iodine to afford the bis-oxindole **409** as a 1:1 mixture of diastereomers (C_2-symmetric and *meso*, Scheme 5.3.2). The C_2-symmetric isomer can be reductively cyclized with LAH in refluxing THF to form (±)-chimonanthine (**402/403**, Scheme 5.3.2).[2]

Scheme 5.3.2: Biomimetic Synthesis Studies by Hendrickson.
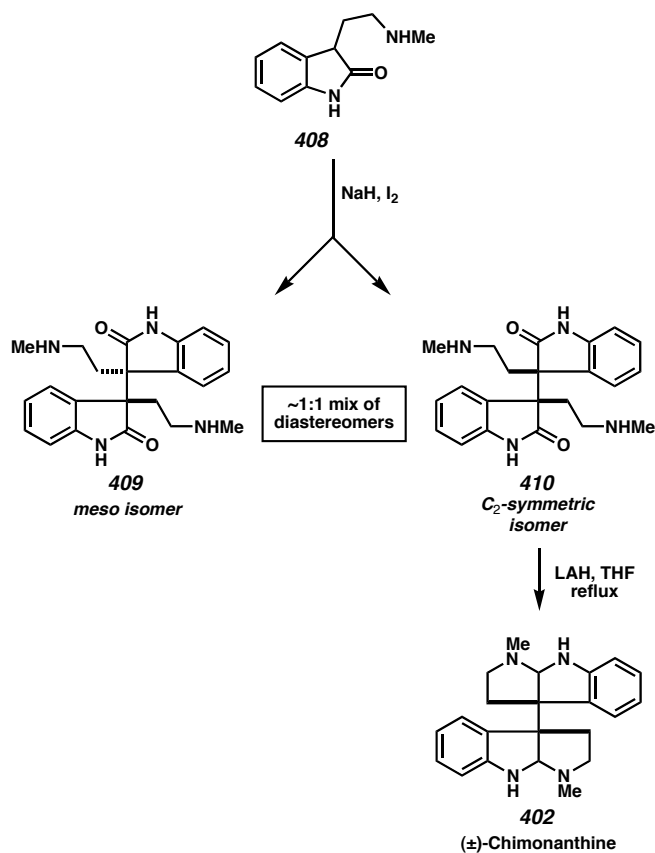
5.3.3 Scott's Study

In a later study, Scott et al. prepared the magnesium salt of methyl tryptamine and oxidatively dimerized it using iron (III) chloride to produce the indolenine dimer **407** (Scheme 5.3.3).[14] Subsequent aminal formation by the tryptamine sidechains under the reaction conditions afforded *meso-* and (±)-chimonanthine (**401**) in one step. Moreover, (±)-calycanthine is accessible from treating (±)-chimonanthine with aqueous acid, demonstrating that scaffold **402** is thermodynamically preferred to scaffold **401**. [2,13]

Scheme 5.3.3: Scott's Direct Biomimetic Synthesis of Chimonanthine and Calycanthine.

meso- and (±)-Chimonanthine
20% yield

402
Calycanthine
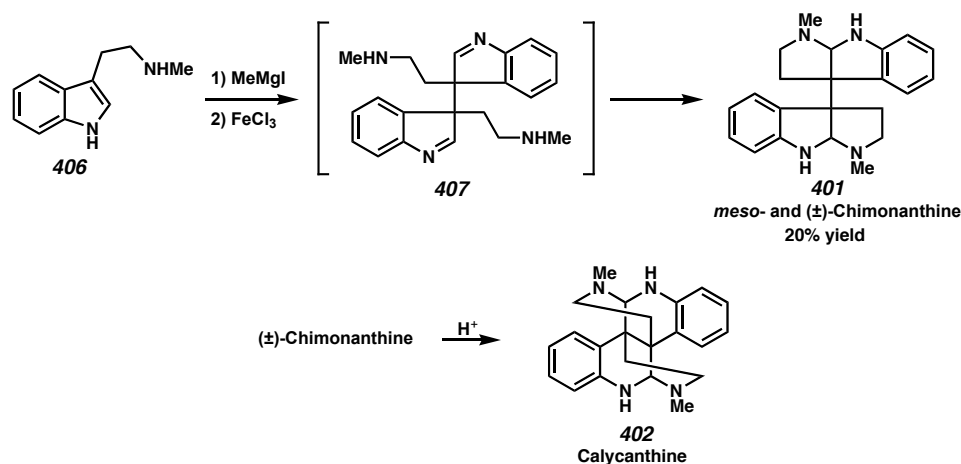
5.3.4 Kirby's Study

Both of these sequences, though characterized by low yields of the desired product,[15] demonstrate the feasibility of the proposed biosynthesis. The model by Scott et al., however, better approximates the actual biosynthetic pathway; Kirby has shown that 2-tritio-tryptophan and 2-tritio-tryptamine retain their label when processed by *Calycanthus floridus* into chimonanthine (Figure 5.3.1).[16] The retention of the 2-tritio label excludes the possibility of oxindole intermediates.

Figure 5.3.1: Label Studies with Chimonanthine.
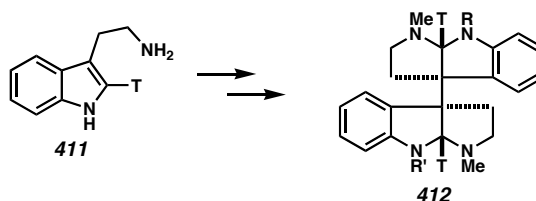
5.3.5 Production of an Alternate Core Structure

An interesting side-note emerges from the oxidative indole coupling reported by Hendrickson. As stated above, the C_2-symmetric isomer of the oxindole dimer produces (±)-chimonanthine when subjected to a hydride reduction; however, the *meso*-dimer does not produce *meso*-chimonanthine upon treatment with LAH. The *meso*-dimer **409** affords the isomeric hexacycle **403** (Scheme 5.3.4) under the LAH reductive conditions instead of *meso*-chimonanthine (**406**). Presumably, reduction occurs similarly to the C_2-symmetric

adduct, but the Lewis acidic nature of LAH promotes an aminal rearrangement to a preferred geometry. This study suggests that a biosynthetis c pathway optimized to produce a *meso*-tryptamine or tryptophan adduct could produce indole alkaloids with framework **403**.

*Scheme 5.3.4: Formation of the Framework **403**.*
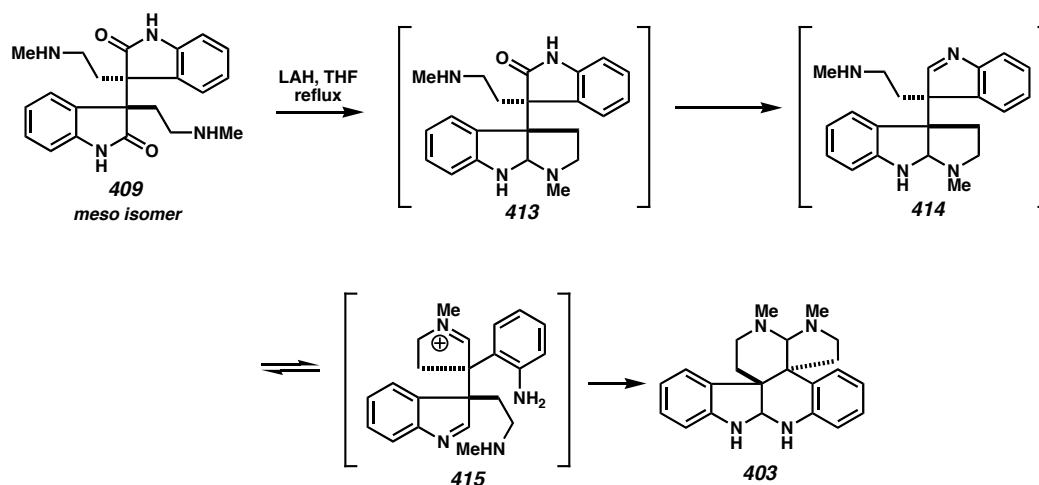
5.3.6 Non-Biomimetic Synthetic Efforts toward the Chimonanthenes

5.3.6.1 Overman's Approach

Overman has synthesized many calycanthine alkaloids.[17] A strategy his lab has fully utilized is to direct the formation of the viscinal quaternary carbon centers with an enatiopure C2-symmetric chiral electrophile **417**. Forming a bisenolate from the bisoxindole **416** and addition of the electrophile forms the *meso*-product under the conditions shown, or forms the C2-symmetric product if HMPA is added. These products can then be advanced to the chimonanthines.

Scheme 5.3.5: Overman's Approach.
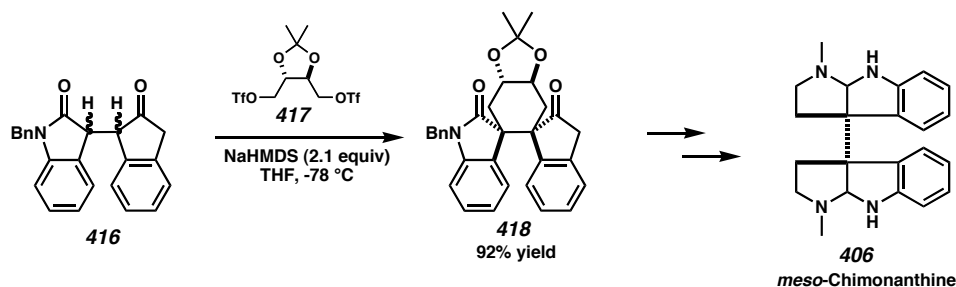
5.3.6.2 MacMillan's Approach

The MacMillan lab has developed an enantioselective, organocatalytic Michael addition of indoles into α,β-unsaturated aldehydes.[18] This addition forms one of the key quaternary carbon centers, and using this framework MacMillan and coworkers have developed routes to chimonanthenes and other indole alkaloids

Scheme 5.3.6: MacMillan's Approach.
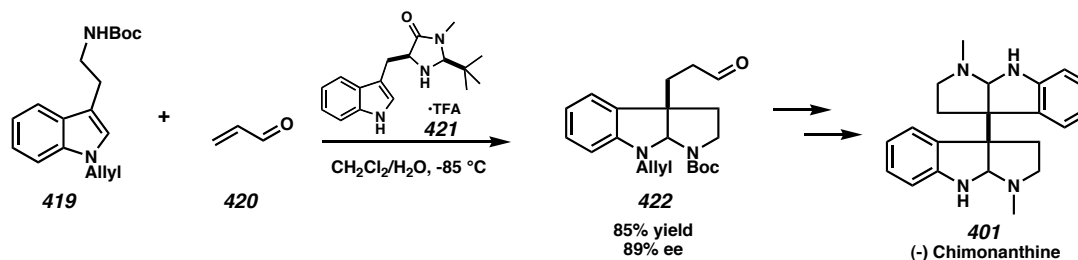
5.3.7 Biosynthesis of Perophoramidine

The defining feature of construct **403** is the unique presence of non-equivalent *N*-methyl groups, a trait easily recognized by proton NMR. This skeletal arrangement was unknown for naturally occurring alkaloids until the recent isolation of perophoramidine (**425**),[13] where the core is an oxidized form of geometry **403**. Hendrickson's findings suggest perophoramidine could arise from a tryptamine dimerization in a similar fashion to the calycanthus alkaloids, but with dissimilar diastereoselectivity (Scheme 5.3.7).[2] The product of aminal formation would then be the tetrahydroperophoramidine core **403** instead of chimonanthine, and subsequent oxidation and halogenation would yield perophoramidine.

Scheme 5.3.7: Perophoramidine Biosynthesis.
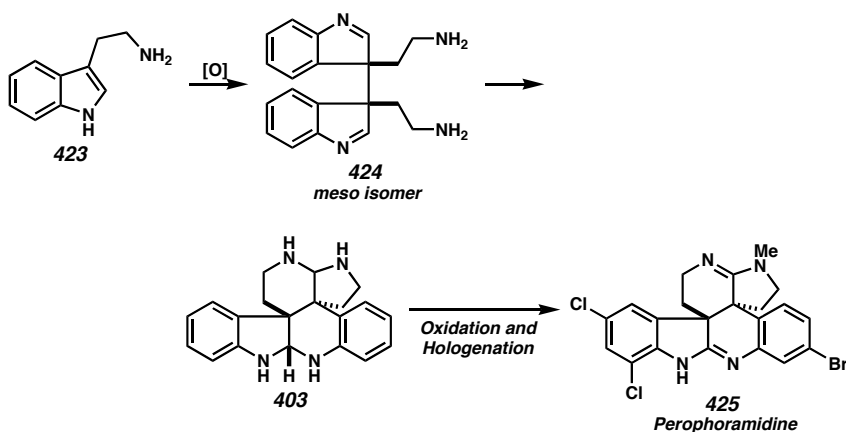
5.4 Nomofungin and the Communesins

5.4.1 Isolation and Characterization

Other intriguing fungal natural products, apparently from the same family as perophoramidine, were identified as containing the core scaffold **403**. Recently characterized was the alkaloid nomofungin (**434**, Figure 5.4.1).[19] Nomofungin was found to disrupt microtubule formation in cultured mammalian cells. It is somewhat cytotoxic and demonstrates minimum inhibitory concentrations of 2 and 4.5 μg/mL with LoVo and KB cells, respectively.

Figure 5.4.1: The Communesins and Nomofungin.

Communesin		R	R'
426	A	CH$_3$	CH$_3$
427	B	CH$_3$	
428	C	H	
429	D	CHO	
430	E	H	CH$_3$
432	G	CH$_3$	CH$_2$CH$_3$
433	H	CH$_3$	CH$_2$CH$_2$CH$_3$
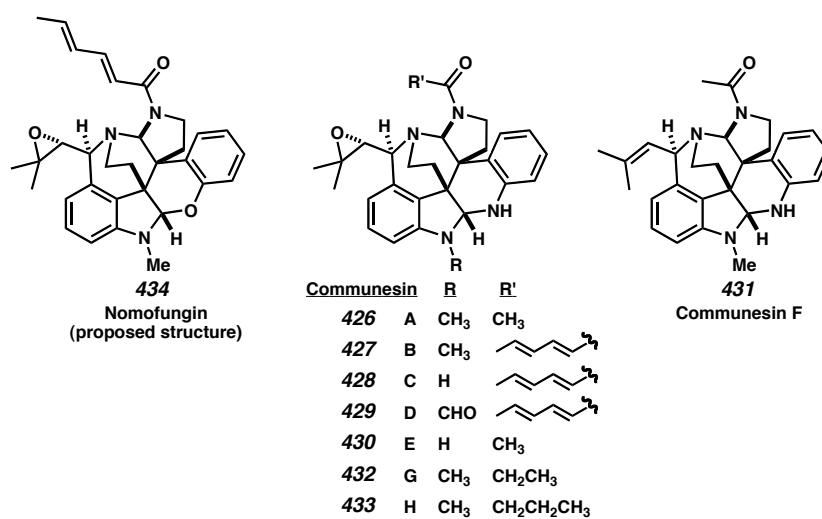
Interestingly, this structure is nearly identical to communesin B (**427**), which was isolated from a strain of *Penicillum sp.* marine fungus in 1993.[20] Communesin B had cytotoxic effects on P-388 lymphocytic leukemia cells with an effective dose of 0.45 μg/mL. Communesin A (**426**), isolated at the same time as communesin B, had an effective dose of 3.5 μg/mL. Later isolations of Communesins C-H have shown varied substitution on the nitrogens and pendant isobutene.[21] Communesins C-F also showed antiproliferative and insecticidal activity, but G and H did not.[21c]

The similarities between nomofungin and communesin B extend beyond their proposed structures; spectroscopically, the structures are identical as well (see Table 6.3.1, Chapter 6), indicating that they are, in fact, the same compound isolated from distinct fungi.[22]

5.4.2 Communesin Biosynthesis

In attempting to determine which proposed structure is correct, a clue presents itself in a comparison of this core structure to the calycanthaceous alkaloids. The structural isomer **403** is present in communesin, though with an additional carbocycle formed from an *N*-prenyl group. This carbocycle is present in the *Penicillum* fungal alkaloid aurantioclavine (**435**), a natural product synthesized from tryptamine or tryptophan.[23] A possible biosynthesis that follows the pattern of the calycanthaceous alkaloids appears in Scheme 5.4.1. The most notable adaptation to the pathway is the oxidative coupling of tryptamine (**423**) with the aurantioclavine instead of another tryptamine. Subsequent formation of the requisite aminal bonds, functionalization of the appropriate nitrogens, and oxidation of the butenyl group to generate the epoxide yields communesin B. Importantly, nomofungin has no such biosynthetic pathway for its generation from biogenic compounds. The precedent of Calycanthus biosynthesis and synthetic efforts with model systems[22] indicate that **438** represents the correct structure for both communesin B and nomofungin.

Scheme 5.4.1: Nomofungin/Communesin Biosynthesis.
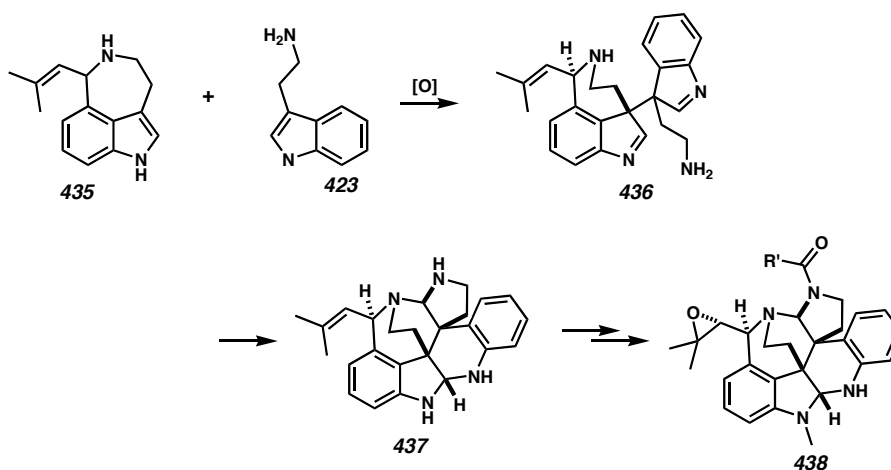
5.4.3 Alternate Biosynthesis of the Communesins

5.4.3.1 The Stoltz Proposal

An alternate biosynthetic pathway was proposed for the communesin family in 2003.[22] In Scheme 5.4.2, tryptophan or tryptamine is transformed into the oxidized oxindole **441**, which contains an activated *ortho*-methide imine. This electron deficient diene can then react with aurantioclavine (**435**) through an inverse-demand Diels-Alder reaction to generate the bridged lactam **442**. As lactam **442** is highly reactive due to the poor alignment of the nitrogen lone pair with the carbonyl, the pendant amino group can easily open the lactam, thus forming spirocycle **443**. Further functionalization generates communesin B.

Scheme 5.4.2: Alternate Communesin Biosynthesis.
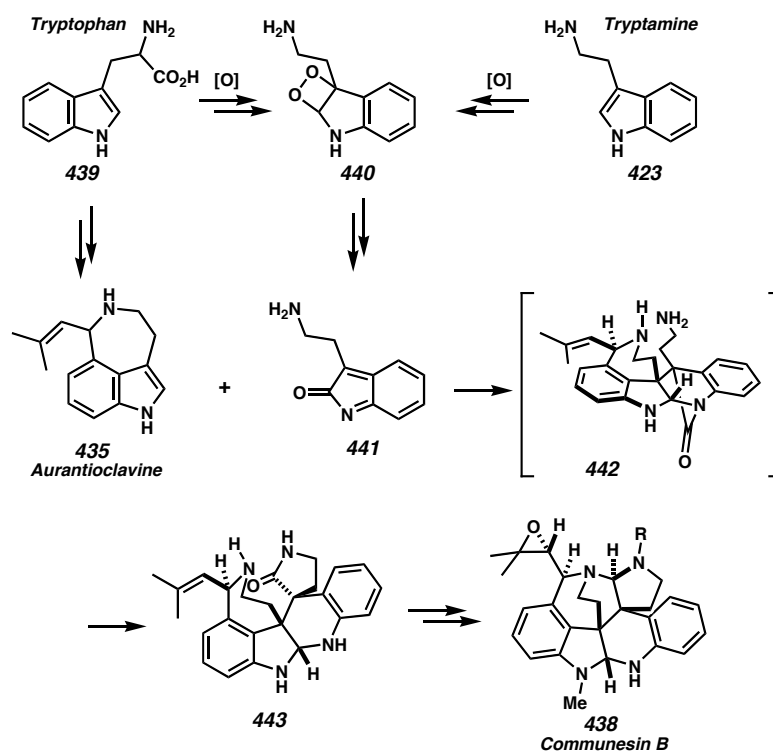
5.4.3.2 The Funk Proposal

A year after the Stoltz proposal for communesin biosynthesis, the Funk lab proposed a similar biosynthesis in a report on synthetic efforts toward perophoramidine (see Section 5.4.3).[24] The only differences in this sequence are that 4-prenyltryptamine is used in place of aurantioclavine and a late-stage oxidative amino cyclization onto the prenyl group is proposed.

Scheme 5.4.3: Funk's Biosynthesis.
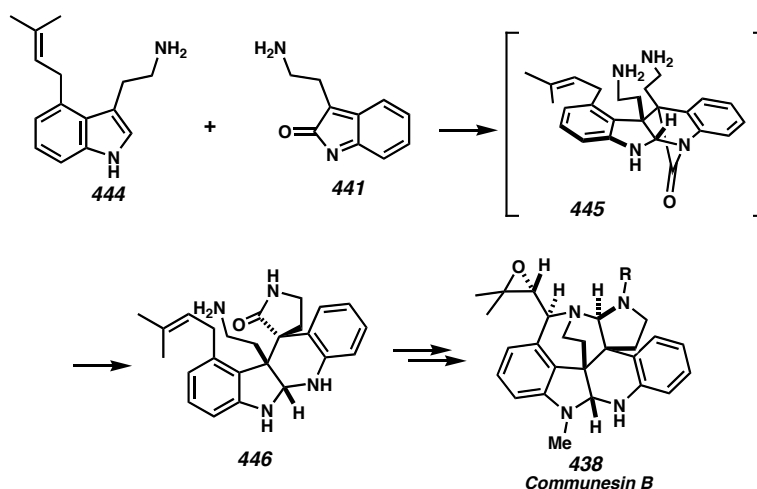
5.5 Synthetic Work toward Perophoramidine

5.5.1 Work in the Stoltz Lab

See Chapter 7 for discussion of preliminary work toward perophoramidine in the Stoltz lab.

5.5.2 Weinreb's Approach

The Weinreb lab has begun a synthetic strategy toward perophoramidine[25] using an oxindole-forming carbonylative Heck reaction developed by Overman[26] (Scheme 5.5.1). Thus, aryliodide **449** undergoes a Pd(0) catalyzed cyclization to form oxindole **450** and build one of the quaternary carbon centers found in perophoramidine. Acidic cyclization to the lactone and subsequent stereoselective alkylation of that lactone form the other quaternary carbon center with the desired relative stereochemistry.

Scheme 5.5.1 Weinreb's Preliminary Work toward Perophoramidine.
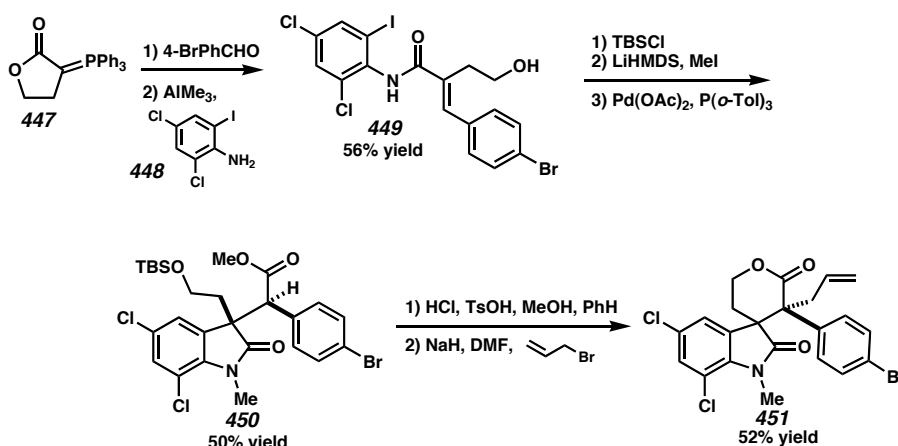
5.5.3 Synthesis by Funk

A successful synthesis of perophoramidine was reported by Funk in 2004 that utilized chemistry proposed in the Stoltz and Funk biosyntheses (Scheme 5.5.2).[24] Bromooxindole **453** is mixed with base to generate the *ortho*-methide imine **453b**. In the presence of modified indole **452** these reactants combine to provide adduct **454**. **454** has both of the vicinal quaternary carbons installed and was isolated with >20:1 dr. Further manipulations allowed formation of the hexacycle, and a final oxidation gave perophoramidine.

Scheme 5.5.2: Funk's Synthesis of Perophoramidine.
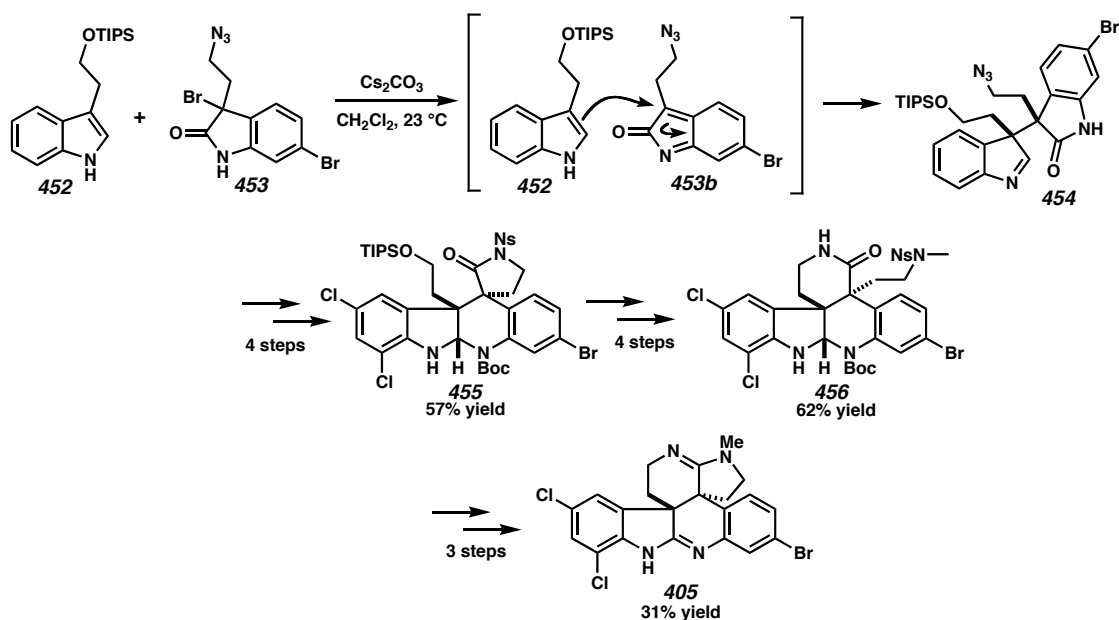
5.6 Synthetic Work toward the Communesin Family

5.6.1 Work by the Stoltz Group

Chapters 6 and 7 of this thesis describe the synthetic efforts toward the communesins in the Stoltz lab. Chapter 6 sets forth the structural comparison of nomofungin and communesin B, along with model systems that aided the assignment of **438** to be representative of communesin B and nomofungin.[22] Chapter 7 outlines the development of approaches to perophoramidine and the communesins.

5.6.2 Work by the Funk Group

To confirm the Stoltz findings that communesin B represented the actual structure of nomofungin as well, the Funk lab generated the alkaloid **461** (Scheme 5.6.1).[27] The synthesis started from a stripped down aurantioclavine analogue, **457**. Alkylation with epoxide **458** and treatment with phenylchloroformate generated the carbonate **459**. Heating in dichlorobenzene generated an *ortho*-methide imine that reacted through an intramolecular Diels-Alder reaction to provide a carbon framework similar to that of the communesins. NMR data from this study further confirmed the structure of communesin B to be **458**.

Scheme 5.6.1: Funk's Model Study.

PhO₂C, O   NHCO₂Et

NHCO₂Et   1) *i*-PrOH, 25 °C

2) ClCO₂Ph,
pyr, CH₂Cl₂

459

160 °C

457   *458*

64% yield

KOH, H₂NNH₂
HOCH₂CH₂OH

460 R=CO₂Et

461 R=H

47% yield
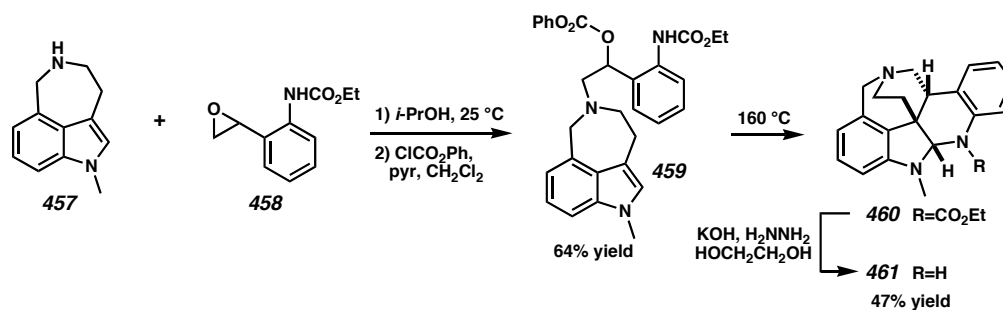
5.7 Conclusion

The interrelations between the calycanthaceous family of alkaloids have relevance to synthetic efforts that generate such architectures. New methods that build dimeric tryptamines with vicinal quaternary centers in a highly controlled fashion can thus lead to many of these compounds through the simple transformations established by early studies. Overman's recent syntheses of (+)-calycanthine and *meso*-, (+)-, and (—)-chimonanthine exemplify the merging of novel synthetic approaches with biosynthetic knowledge and an understanding of the kinetics and thermodynamics for formation of the various skeletal arrangements.[28]

The presence of underrepresented structures, such as **404** and **405**, suggests that new natural products may await isolation and require novel strategies for synthesis. While synthesizing bis-tryptophan alkaloids, the diverse possibilities of structural isomers also require thorough characterization to assure the correct stereochemistry of synthetic intermediates. Awareness of this past work will continue to aid synthetic progress in the alkaloid arena. Specifically, these lessons will be applied toward the synthetic effort for the total synthesis of the communesin family of natural products described in the next two chapters.

5.8 Notes and References

(1) Note that a mini-review on the characterization and biosynthesis for the calycanthaceous alkaloids was previously published on the world wide web by the Organic Division of the American Chemical Society in 2003 in association with a graduate student fellowship. See: http://organicdivision.org/fellowship_awardee_bios_03.html#May

(2) Hendrickson, J. B.; Rees, R.; Goschke *Proc. Chem. Soc.* **1962**, 383.

(3) Robinson, R.; Teuber, H. *J. Chem. Ind.* **1954**, 783.

(4) Woodward, R. B.; Yand, N.; Katz, T. *J. Proc. Chem. Soc.* **1960**, 76.

(5) (a) Hamor, T. A.; Robertson, J. M.; Shrivastave, H. N.; Silverton, J. V. *Proc. Chem. Soc.* **1960**, 78. (b) Hamor, T. A.; Robertson, J. M. *J. Chem. Soc.* **1962**, 194.

(6) Mason, S. F. *Proc. Chem. Soc.* **1962**, 362.

(7) Hodson, H. F.; Robinson, B.; Smith, G. F. *Proc. Chem. Soc.* **1961**, 465.

(8) (a) Grant, I. J.; Hamor, T. A.; Robertson, J. M.; Sim, G. A. *Proc. Chem. Soc.* **1962**, 148. (b) Grant, I. J.; Hamor, T. A.; Robertson, J. M.; Sim, G. A. *J. Chem. Soc.* **1965**, 5678.

(9) Saxton, J. E.; Bardsley, W. G.; Smith, G. F. *Proc. Chem. Soc.* **1962**, 148.

(10) Eiter, K.; Svierak, O. *Monatsh. Chem.* **1951**, *82*, 186.

(11) Byhlmann; Mannhardt *Prog. Chem. Org. Nat. Prod.*, **1957**, *14*, 1.

(12) Tokuyama, T.; Daly, J. W. *Tetrahedron* **1983**, *39*, 41.

(13) Verbitski, S. M.; Mayne, C. L.; Davis, R. A.; Concepcion, G. P; Ireland, C. M. *J. Org. Chem.* **2002**, *67*, 7124.

(14) Scott, A. I.; McCapra, F.; Hall, E. S. *J. Am. Chem. Soc.* **1964**, *86*, 302.

(15) Fang, C-L; Horne, S.; Taylor, N.; Rodrigo, R. *J. Am. Chem. Soc.* **1994**, *116*, 9480.

(16) Kirby, G. W.; Shah, S. W.; Herbert, E. J. *J. Chem. Soc. C* **1969**, 1916.

(17) Overmann, L. E.; Paone, D. V.; Stearns, B. A *J. Am. Chem. Soc.* **1999**, *121*, 7702-7703. (b) Overmann, L. E.; Larrow, J. F.; Stearns, B. A.; Vance, J. M. *Angew. Chem. Int. Ed.* **2000**, *39*(1) 213.

(18) Austin, J. F.; Kim, S.-G.; Sinz, C. J.; Xiao, W.-J.; MacMillan, D. W. C. *Proc. Nat.*

Acad. Sci, **2004**, *101*, 5482-5487.

(19) Ratnayake, A. S.; Yoshida, W. Y.; Mooberry, S. L.; Hemscheidt, T. K. *J. Org. Chem.* **2001**, *66*, 8717. Note that this publication has since been withdrawn.

(20) Numata, A.; Takahashi, C.; Ito, Y.; Takaka, T.; Kawai, K.; Usami, Y.; Matsumura, E.; Imachi, M.; Ito, T.; Hasegawa, T. *Terahedron. Lett.* **1993**, *34*, 2355.

(21) (a) Communesins B, C, D: Jadulco, R.; Edrada, R. A.; Ebel, R.; Berg, A.; Schaumann, K.; Wray, V.; Steube, K; Proksch, P. *J. Nat. Prod.* 2004, *67*, 78-81. (b) Communesins D, E, F: Hayashi, H.; Matsumoto, H.; Akiyama, K. *Biosci. Biotechnol. Biochem.* **2004**, *68*(3), 753-756. (c) Communesins G, H: Dalsgaard, P. W.; Blunt, J. W.; Munro, M. H. G.; Frisvad, J. C.; Christophersen, C. *J. Nat. Prod.* **2005**, *68*, 258-261.

(22) May, J. A.; Zeidan, R. K.; Stoltz, B. M. *Tetrahedron Lett.* **2003**, *44*,1203.

(23) (a) Kozlovskii, A. G.; Soloveva, T. F.; Sakharovskii, V. G.; Adanin, V. M. *Dokl. Akad. Nauk SSSR* **1981**, *260*, 230. (b) Sakharovskii, V. G.; Aripovskii, A. V.; Baru, M. B.; Kozlovskii, A. G. *Khim. Prir. Soedin.* **1983**, 656.

(24) Fuchs, J. R.; Funk, R. L. *J. Am. Chem. Soc.* **2004**, *126*, 5068.

(25) Artman III, G. D.; Weinreb, S. M. *Org. Lett.* **2003**, *5*(9), 1523-1526.

(26) (a) Oestrich, M.; Dennison, P. R.; Kodanko, J. J.; Overman, L. E. *Angew. Chem., Int. Ed.* **2001**, *48*, 1439. (b) Ashimori, A.; Overman, L. E. *J. Synth. Org. Chem. Jpn.* **2000**, *58*, 718. (c) Asimori, A.; Bachand, B.; Overman, L. E.; Poon, D. J. *J. Am. Chem. Soc.* **2000**, *122*, 192. (d) Link, J. T.; Overman, L. E. *CHEMTECH* **1998**, *28*, 19. (e) Ashimori, A.; Bachand, B.; Overman, L. E.; Poon, D. J. *J. Am. Chem. Soc.* **1998**, *120*, 6477. (f) Ashimori, A.; Bachand, B.; Calter, M. A.; Govek, S. P.; Overman, L. E.; Poon, D. J. *J. Am. Chem. Soc.* **1998**, *120*, 6488. (g) Overman, L. E. *Pure Appl. Chem.* **1994**, *66*, 1423.

(27) Crawley, S. L.; Funk, R. L. *Org. Lett.* **2003**, *5*(18), 3169-3171.

(28) (a) Overman, L. E.; Larrow, J. F.; Stearns, B. A.; Vance, J. M. *Angew. Chem. Int. Ed.* **2000**, *39*, 213. (b) Overman, L. E.; Paone, D. V.; Stearns, B. A. *J. Am. Chem. Soc.* **1999**, *121*, 7702.

Chapter 6

Evaluating the Structure of and Proposing a Biomimetic Approach to Communesin B (a.k.a. Nomofungin)

6.1 Background

Indole alkaloids and related indoline-containing natural products are among the most intensely studied and interesting classes of molecules available for synthetic chemists. We have recently initiated synthetic studies directed toward the indoline alkaloids communesins A (**426**) and B (**427**).[1] Interestingly, the structure of communesin B is nearly identical to that of nomofungin (**434**), a natural product that was recently reported (Figure 6.1.1).[2] Herein, we report our preliminary studies directed toward the synthesis of the communesins and attempt to clarify the structure of nomofungin based on a biosynthetic hypothesis and ^{1}H and ^{13}C NMR chemical shift data of synthetic intermediates.[3]

Figure 6.1.1: Communesin A and B Compared with Nomofungin.

426 Communesin A R = Ac
427 Communesin B R =

434
Nomofungin
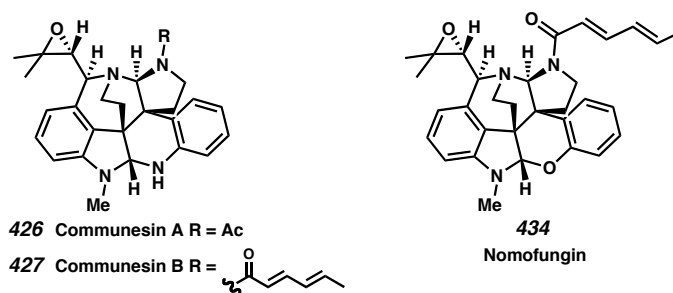
6.2 Communesin Biosynthesis

Biogenetically, the communesins can be thought of as arising via an oxidative union of tryptamine (**439**) with the related natural product, aurantioclavine (**435**, Scheme

6.2.1).[3,4] Perhaps more provocative is the notion that an oxidation of tryptamine leads to the quinone methide imine **441**, which undergoes an exo inverse-demand Diels–Alder reaction with aurantioclavine derivative **435** to form polycyclic intermediate **442**. This intermediate, possessing a highly twisted lactam (analogous to the strained quinuclidone ring system) should readily undergo transamidation with the residual primary amine to produce the spiro lactam **443**. Biosynthetic reduction of the lactam, aminal closure, epoxidation, and acylation affords communesins A and B. In contrast, a reasonable, equivalent biosynthetic pathway that would lead to the proposed structure for nomofungin cannot be formulated. In light of this comparison, we began our investigations with the hypothesis that communesin B was assigned the correct structure, and nomofungin was incorrect.

Scheme 6.2.1: Proposed Biogenesis for Communesin B.
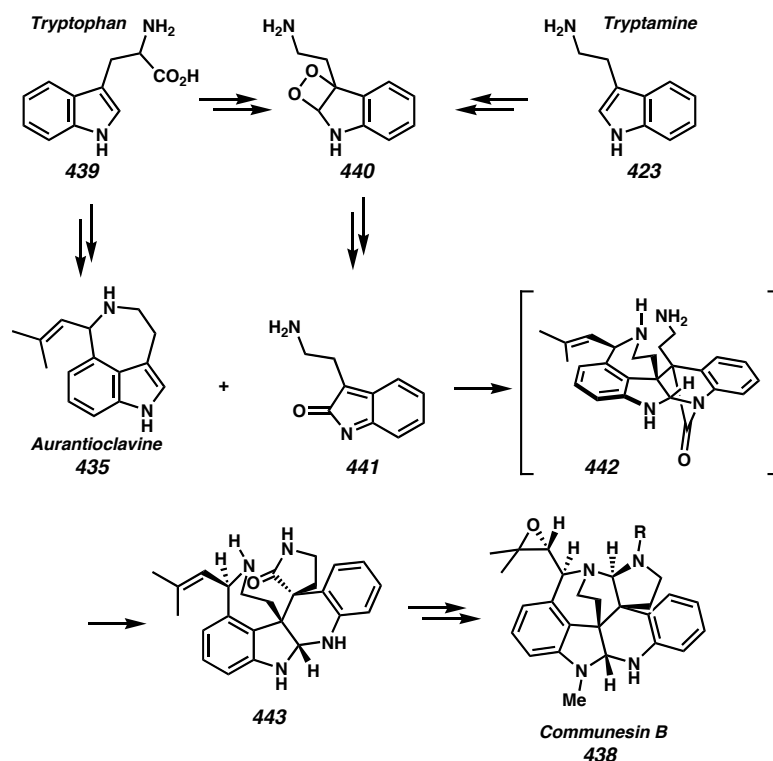
6.3 Comparison of Data for Nomofungin and Communesin B

6.3.1 Comparison to Each Other

The similarity of nomofungin and communesin B prompted us to examine the reported ^{1}H and ^{13}C NMR data for the two more closely. Interestingly, the chemical shifts and coupling constants are essentially identical in all respects (Table 6.3.1). In particular, the chemical shift of the C(6) proton is reported to be 4.70 ppm for communesin B and 4.69 ppm for nomofungin. Analogously, the ^{13}C NMR chemical shift for C(6) is 82.4 ppm for both compounds. From these data, and the similarity of the full NMR data set, we conclude that communesin B and nomofungin must be the same molecule.

Table 6.3.1: A Full Comparison of NMR Data for Communesin B and Nomofungin.

X=O   Nomofungin:
X=NH   Communesin B:
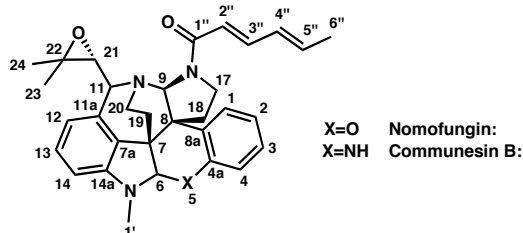
	Communesin B[1]			Nomofungin[2]			Communesin B[1]		Nomofungin[2]
	^{1}H			^{1}H			^{13}C		^{13}C
	ppm		J(Hz)	ppm		J(Hz)	ppm	DEPT	ppm
1	6.66	d	3.5	6.65	m		123.41	(t)	123.4
2	6.67	d	7.8	6.66	m		120.52	(t)	120.5
3	6.98	ddd	7.8, 5.2, 3.5	6.88	ddd	7.0, 7.0, 2.4	127.38	(t)	127.4
4	6.66	d	5.2	6.67	m		116.82	(t)	116.8
4a							142.65	(q)	142.6
5	4.60	brs							
6	4.70	s		4.69	s		82.39	(t)	82.4
7							51.40	(q)	51.4
7a							132.25	(q)	132.2
8							52.14	(q)	52.1
8a							132.32	(q)	132.3
9	5.11	s		5.10	s		79.00	(t)	79.0
11	4.18	d	9.0	4.17	d	9.0	65.55	(t)	65.5
11a							136.57	(q)	136.6
12	6.08	d	7.8	6.08	d	7.7	113.23	(t)	113.2
13	6.87	t	7.8	6.88	dd	7.7, 7.7	128.87	(t)	128.9
14	5.95	d	7.8	5.95	d	7.7	101.85	(t)	101.9
14a							150.53	(q)	150.5
17A	3.07	td	12.5, 7.0	3.07	ddd	12.0, 12.0, 7.0	44.21	(s)	44.2
17B	3.87	dd	12.5, 8.4	3.87	dd	12.0, 8.4			
18A	2.00	dd	12.5, 7.0	2.00	dd	13.2, 7.0	30.46	(s)	30.4
18B	2.71	td	12.5, 8.4	2.72	m				
19A	2.25	dd	12.8, 8.5	2.27	m		37.82	(s)	37.8
19B	2.34	ddd	12.8, 9.2, 8.5	2.35	m				
20A	3.40	dt	16.0, 8.5	3.40	m		36.03	(s)	36.0
20B	3.48	dd	16.0, 9.2	3.45	m				
21	2.90	d	9.0	2.90	d	9.0	63.95	(t)	63.9
22							59.75	(q)	59.7
23	1.65	s		1.64	s		20.54	(p)	20.5
24	1.42	s		1.42	s		24.89	(p)	24.8
1'	2.85	s		2.84	s		29.60	(p)	29.2
1''							168.43	(q)	168.4
2''	6.55	d	15.2	6.54	d	15.1	121.27	(t)	121.3
3''	7.32	dd	15.2, 10.1	7.31	dd	15.1, 10.7	141.83	(t)	141.8
4''	6.18	dd	15.5, 10.1	6.19	dd(br)	15.1, 10.7	130.72	(t)	130.7
5''	6.12	dq	15.5, 5.8	6.10	dq	15.1, 6.5	137.13	(t)	137.1
6''	1.85	d	5.8	1.85	d	6.5	18.71	(p)	18.6

6.3.2 Comparison to Shifts in Other Natural Products

Furthermore, comparison to known chemical shift values for aminal and hemi-aminal functionalities confirms the tendency for the ^{1}H NMR chemical shifts of the former to reside upfield relative to the latter. For example, the aminal protons in isochimonanthine (**463**) and calycanthine (**402**) are 4.32 ppm and 4.42 ppm, respectively, whereas the shifts for hemi-aminals **464**, **465**, and **467** are 5.0 ppm, 5.4 ppm, and 6.3 ppm (Figure 6.3.1).[5] The nomofungin and communesin B value of 4.7 ppm resides closer to that for an aminal. Similarly, ^{13}C chemical shifts for aminal carbons are typically in the range of 71.0 to 84.0 ppm, while those for hemi-aminal carbons are shifted downfield to between 97.0 and 106.0 ppm.[6] The case of the proposed and actual structures for Diazonamide A, **466** and **467**, respectively, shows a general trend that additional oxygenation shifts the signals further downfield. The nomofungin and communesin shift, 82 ppm, is clearly in the range for aminal carbons. Given the ^{1}H and ^{13}C NMR chemical shift data and the biogenetic proposal outlined in Scheme 6.2.1, we have determined that communesin B represents the true structure and have undertaken the synthesis of the structure proposed for communesin B (**438**).[7,8]

Figure 6.3.1: Peak Frequencies of Known Compounds.[5,6]

	Nomo/Comm XX	(+)-Isochimonanthine XX	(+)-Calycanthine XX
^{13}C NMR	82.4	83.7	71.0
^{1}H NMR	4.7	4.32	4.42

	XX	XX	Diazonamide A
^{13}C NMR	97.2	-------	X=O 104.0 / X=NH 106.1
^{1}H NMR	5.0	5.44	X=O 6.93 / X=NH 6.34

XX X=O Diazonamide A (proposed)
XX X=NH Diazonamide A (authentic)
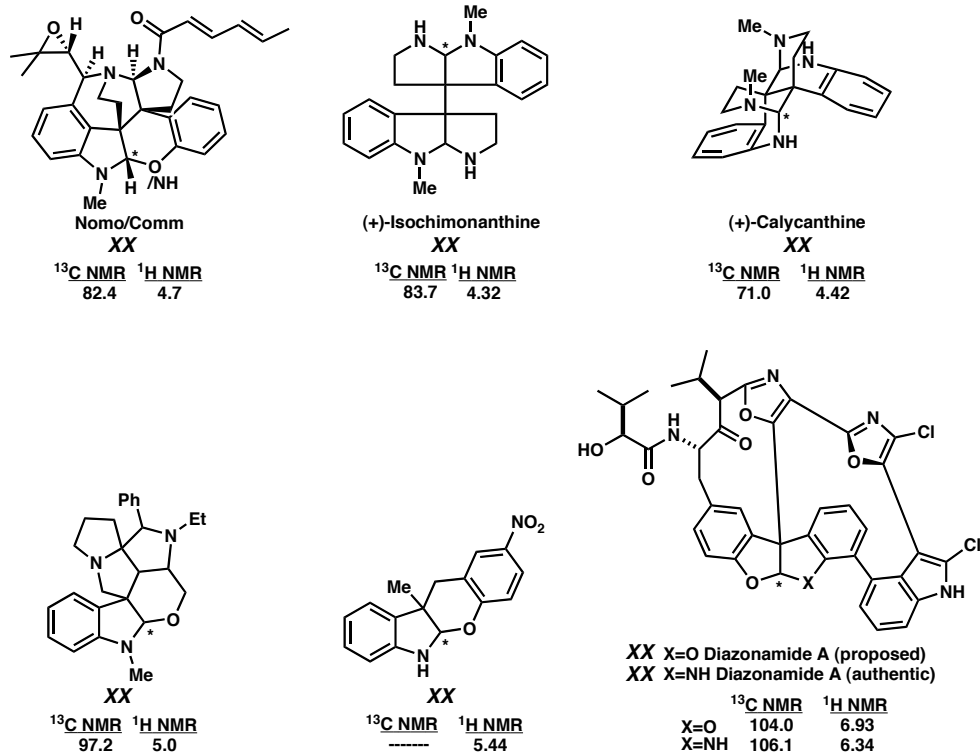
6.4 The Synthesis of Model Compounds

6.4.1 A Simple 6,5,6,6 Ring System

As a model system for the proposed Diels–Alder type cycloaddition of **435** and **441**, we investigated the cyclization of 1,3-dimethylindole (**468**) and chloroaniline **469** (Scheme 6.4.1) using conditions previously developed by Corey for the cycloaddition of **469** with electron-rich olefins[9]. To our delight, upon slow addition of chloride **469** to a mixture of indole **468** and Cs_2CO_3 in CH_2Cl_2 at -78 °C, a reaction immediately occurred to provide a single diastereomer of adduct **470** in 86% yield. Cleavage of the sulfonamide group by exposure of tetracycle **470** to Mg, MeOH, and NH_4Cl produced aminal **471**. Interestingly, the ^{1}H NMR chemical shift of the proton at C(6) is at 4.14 ppm, and the ^{13}C resonance is at 83.9 ppm. These shifts are in good accord with the values of 4.69–4.70 ppm (^{1}H) and 82.4 ppm (^{13}C) reported for both communesin B and

nomofungin, strongly suggesting that the communesin structure is the appropriate representation for the natural product.

Scheme 6.4.1: The Corey Inverse-Demand Diels-Alder Reaction with Indole.
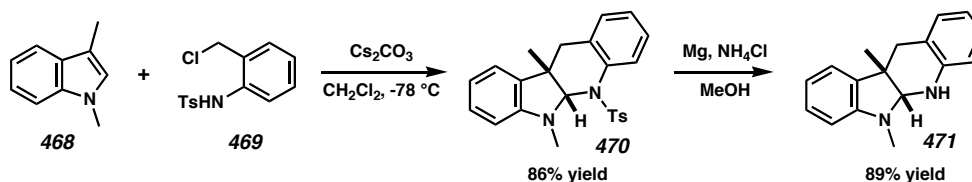
6.4.2 A Model System with Aurantioclavine

More recently, we have prepared (±)-aurantioclavine (**435**) by known methods[10] and utilized the *N*-Boc-1-methyl derivative **472** in the cycloaddition reaction with **469** (Scheme 6.4.2). Cycloaddition again proceeded smoothly upon treatment with Cs_2CO_3 to produce the adducts that we have assigned as **472** and **473**. Unfortunately, the putative cycloadduct was produced as a 2:1 mixture of diastereomers with respect to the methylpropenyl side chain at C(11). Following cleavage of the sulfonyl group with Mg and NH_4Cl in MeOH, separation of the diastereomers was possible by preparative thin-layer silica-gel chromatography. Importantly, the ^{13}C NMR residues for C(6) of diastereomers **474** and **475** were at 84.8 and 83.9 ppm, again in full accord with the data for the communesins and nomofungin.

Scheme 6.4.2: The Inverse-Demand Diels-Alder Reaction with Aurantioclavine.
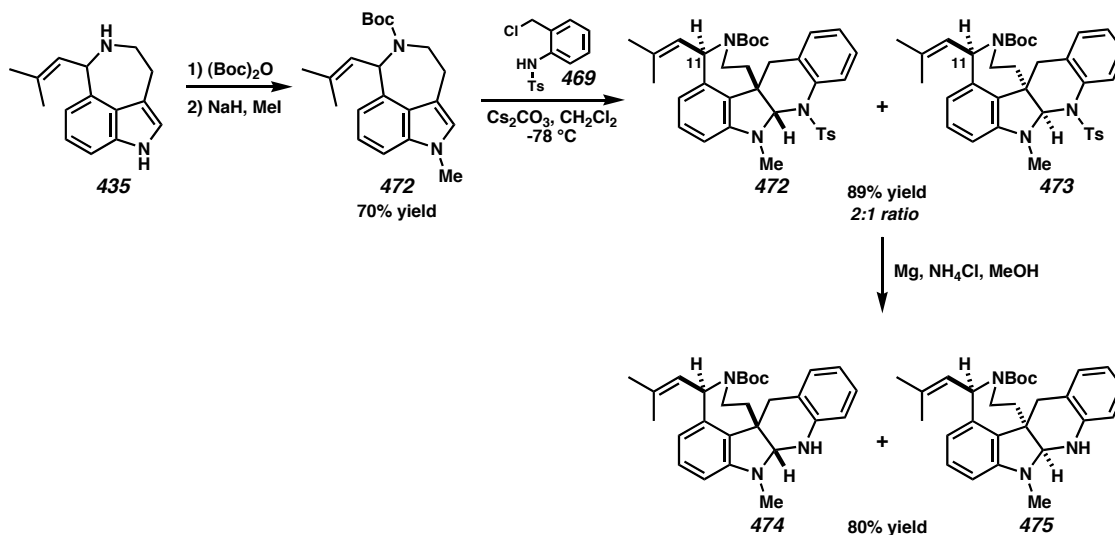
Fortunately, the minor diastereomer, **475**, could be recrystallized by slow cooling from refluxing heptane to provide crystals suitable for single-crystal X-ray diffraction studies. The structure thus obtained is shown in Figure 6.4.1. Here, the isobutenyl group is on the same face as electrophile addition. Thus, the major isomer was generated by addition of the electrophile to the aurantioclavine face opposite the pendant olefin, indicating a small capacity for the olefin to direct the reaction. One possible reason for the low selectivity is also seen in the crystal structure; the Boc group resides on the face opposite the olefin and thus competes for directional control. A smaller protecting group is likely to improve the selectivity of the reaction.

Figure 6.4.1: Structure Confirmation by Single-Crystal X-Ray Diffraction.
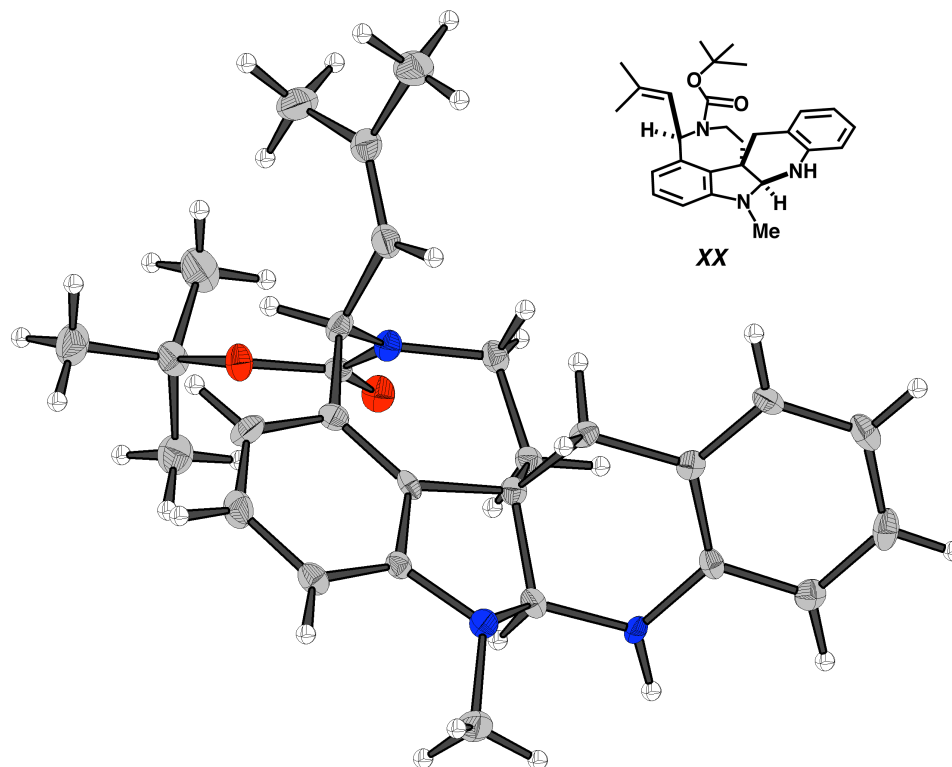
6.5 Conclusion

In conclusion, we propose that the natural products nomofungin and communesin B are, in fact, identical molecules and that the structure of communesin B more correctly represents the actual structure. We initially came to this conclusion based on biosynthetic hypotheses. More recently, ^{1}H NMR chemical shift data of synthetic analogs to the communesin structure have bolstered this argument. Finally, a potential intermediate (**474**) in our synthesis of communesin B has been prepared by a [4+2] cycloaddition route (Scheme 6.4.2) that is similar to the biosynthetic proposal outlined in Scheme 6.2.1.[11] Efforts to complete the total synthesis of communesin B (a.k.a. nomofungin) by such biomimetic routes are ongoing.

6.6 Experimental

6.6.1 Materials and Methods

Reactions were performed in flame-dried glassware under a nitrogen atmosphere using freshly purified solvents. Solvents were purified by passing through an activated alumina column. All other reagents were used as received from commercial sources. Reaction temperatures were controlled by an IKAmag temperature modulator. Thin-layer chromatography (TLC) was performed using E. Merck silica gel 60 F254 precoated plates (0.25mm) and visualized by UV, *p*-anisaldehyde staining, or ceric ammonium molybdate staining (CAM). ICN Silica gel (particle size 0.032-0.063 mm) was used for flash chromatography. ^{1}H and ^{13}C NMR spectra were recorded on a Varian Mercury 300 spectrometer (at 300 MHz and 75 MHz, respectively) in $CDCl_3$ and are internally referenced to the residual chloroform peak (7.27 ppm and 77.23 ppm, respectively) relative to Me_4Si. Data for ^{1}H NMR spectra are reported as follows: chemical shift (δ ppm), multiplicity, coupling constant (Hz), and integration. Data for ^{13}C NMR spectra are reported in terms of chemical shift. IR spectra were recorded on a Perkin Elmer Paragon 1000 spectrometer and are reported in frequency of absorption (cm^{-1}). High resolution mass spectra were obtained from the California Institute of Technology Mass Spectrometry Facility.

6.6.2 Synthetic Details
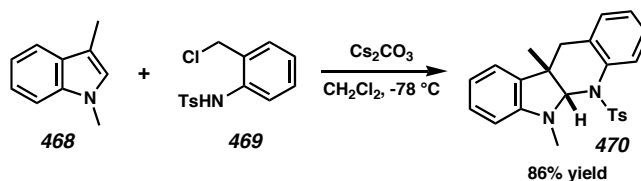
Indoline 470: To a cooled solution of 1,3-dimethyl indole (**468**, 23 mg, 0.16 mmol) and Cs_2CO_3 (168 mg, 0.360 mmol) in 0.2 mL anhydrous CH_2Cl_2 at -78°C was added chloroaniline **469** (53 mg, 0.179 mmol) in anhydrous CH_2Cl_2 (0.8 ml) via syringe pump over 4 h. The solution was then warmed to 23°C for 30 min, immediately filtered over a Celite plug, rinsing with CH_2Cl_2 (3x 10 mL), concentrated under reduced pressure, and subjected to flash column chromatography (6:1 hexane/ethyl acetate eluent) to provide the Diels–Alder adduct **470** (54.7 mg, 86% yield) as a white solid. **470**: ^{1}H NMR (300 MHz, $CDCl_3$) 7.55 (dd, J=7.9, 1.2 Hz, 1H), 7.48 (d, J=8.5 Hz, 2H), 7.22 (d, J=8.2 Hz, 2H), 7.11 (t, J=7.6 Hz, 1H), 6.98 (td, J=7.6, 4.4 Hz, 1H), 6.88 (dd, J=7.6, 7.6 Hz, 1H), 6.76 (dd, J=7.6, 7.6 Hz, 2H), 6.45 (dd, J=7.3, 7.3 Hz, 1H), 6.14 (d, J=7.9 Hz, 1H), 5.66 (s, 1H), 2.99 (s, 3H), 2.52 (d, J=14.1 Hz, 1H), 2.42 (s, 3H), 1.62 (s, J=14.1 Hz, 1H), 1.34 (s, 3H); ^{13}C NMR (75 MHz, $CDCl_3$) 150.0, 143.8, 137.9, 135.3, 135.1, 132.8, 129.8, 128.4, 128.2, 128.0, 127.3, 127.2, 126.8, 121.6, 117.0, 104.5, 86.5, 51.0, 38.1, 29.9, 29.2, 21.8; IR (neat) 3052, 3028, 2951, 2920, 1608, 1494 cm^{-1}; MS m/z calcd for $[C_{24}H_{24}N_2O_2S+H]^+$: 405.1637, found 405.1634.
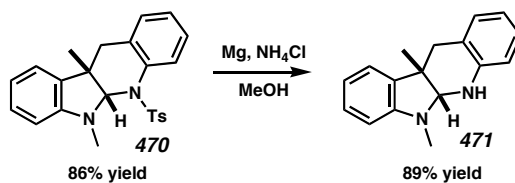
Indoline 471: A vial (20 mL) equipped with a teflon stirbar was charged with tosylamine **470** (28 mg, 0.069 mmol), which was subsequently dissolved in MeOH (2.7 mL). To this solution was added solid NH$_4$Cl (131 mg, 2.45 mmol) and Mg (131 mg, 5.39 mmol). Equal masses of NH$_4$Cl and Mg were added every few hours (usually to hundreds of equivalents) until all the starting material was converted to product as visualized by TLC. The solution was then filtered over a Celite plug, rinsing with CH$_2$Cl$_2$ (3x 10 mL), and concentrated under reduced pressure. Purification was performed via flash column chromatography (9:1 hexanes/ethyl acetate eluent) to afford **471** (21.2 mg, 0.0847 mmol, 89% yield) as a white solid. R_F 0.44 (3:1 hexane/ethyl acetate eluent); ^{1}H NMR (300 MHz, CDCl$_3$) 7.17–7.12 (comp. m, 2H), 7.06 (dd, J=7.3, 7.9 Hz, 1H), 7.00 (d, J=7.3 Hz, 1H), 6.79 (dd, J=7.0, 7.6 Hz, 1H), 6.69 (dd, J=7.3, 7.3 Hz, 1H), 6.64 (d, J=7.9 Hz, 1H), 6.54 (d, J=7.6 Hz, 1H), 4.65 (br. s, 1H), 4.14 (s, 1H), 2.81 (d, J=15.2 Hz, 1H), 2.78 (s, 3H), 2.51 (d, J=15.2 Hz, 1H), 1.24 (s, 3H); ^{13}C NMR (75 MHz, CDCl$_3$) 149.2, 141.1, 137.2, 129.2, 127.9, 127.1, 121.5, 121.4, 118.8, 118.0, 113.5, 108.1, 83.9, 39.1, 37.7, 32.5, 21.7; IR (neat) 3404, 2956, 2851, 1609 cm^{-1}; MS m/z calcd for [C$_{17}$H$_{18}$N$_2$+H]$^+$: 250.1470, found 250.1461.
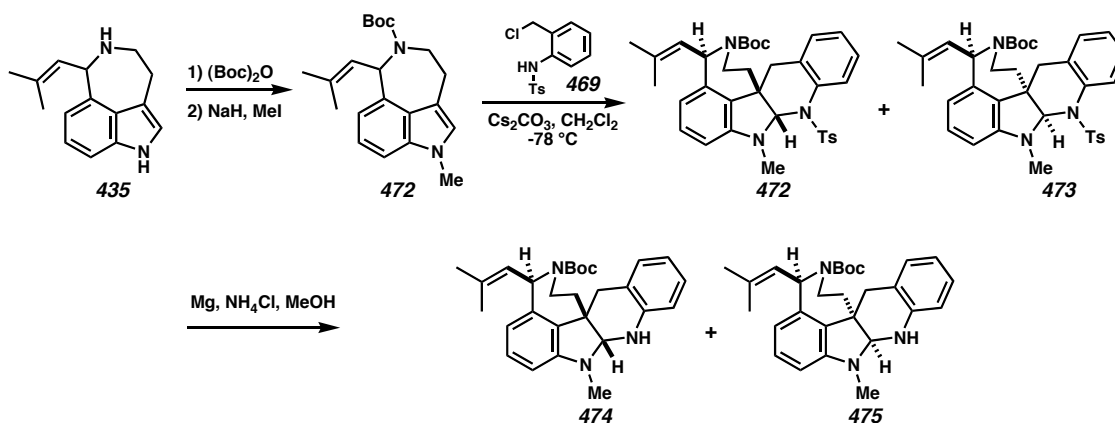
N-Boc-1-methylaurantioclavine (472): A flame-dried flask (10 mL) equipped

with a teflon stirbar was charged with aurantioclavine (**435**, 100 mg, 0.442 mmol).

Dioxane (4.5 mL) was then added, and the solution was cooled to 10 °C. (Boc)$_2$O (164.2

mg, 0.752 mmol) was then added, and the solution was warmed to room temperature.

After 30 min water (100 μL) was added to quench any excess reagent, then brine was

added. The mixture was extracted three times with ethyl acetate, the combined organic

layers were dried over Na$_2$SO$_4$, and the solution was filtered and concentrated under

vacuum. Purification by flash column chromatography (3:1 hexanes/ethyl acetate eluent)

yielded N-Boc-aurantioclavine (127.4 mg, 0.390 mmol, 88% yield) as a light yellow oil;

R_F 0.23 (3:1 hexanes/ethyl acetate eluent). A flame-dried flask (25 mL), equipped with a

teflon stirbar, was charged with NaH (35.7 mg, 0.893 mmol) and THF (1 mL), and the

mixture was cooled to 0 °C. Boc-aurantioclavine (125.2 mg, 0.384 mmol) was then

added in a solution of THF (2 mL) dropwise. MeI (119 μL, 1.90 mmol) was added, and

the solution was warmed to room temperature. After 30 min water (100 μL) was added

to quench any excess reagent, then brine was added. The mixture was extracted three

times with ethyl acetate, the combined organic layers were dried over Na$_2$SO$_4$, and the

solution was filtered and concentrated under vacuum. Purification by flash column

chromatography (9:1 hexanes/ethyl acetate eluent) yielded **472** (102.9 mg, 0.302 mmol, 79% yield) as a yellow oil; R_F 0.40 (3:1 hexanes/ethyl acetate eluent).

Diels-Alder adducts 472 and 473: A flame-dried flask (5 mL) equipped with a teflon stirbar was charged with Cs_2CO_3 (62.1 mg, 0.191 mmol) and *N*-Boc-*N*-methylaurantioclavine (**472**, 19.3 mg, 0.0567 mmol). Dichloromethane was then added, and the mixture was cooled to –78 °C. 2-Chloromethyltosylaniline (**469**, 24.5 mg, 0.0828 mmol) was added dropwise in a solution of dichloromethane (400 μL). The combined solution was stirred for one hour and then allowed to warm to room temperature slowly (30 min) before quenching with water (500 μL). The mixture was extracted three times with ethyl acetate, the combined organic layers were dried over Na_2SO_4, and the solution was filtered and concentrated under vacuum. Purification by flash column chromatography (15:1 to 9:1 hexanes/ethyl acetate eluent) gave an inseparable mixture of **472** and **473** (30.1 mg, 0.0502 mmol, 89 % yield) as a white solid.

Indoline alkaloids 474 and 475: A vial (20 mL) equipped with a teflon stirbar was charged with the mixture of tosylamines **472** and **473** (30 mg, 0.05 mmol), which were subsequently dissolved in MeOH (5 mL). To this solution was added solid NH_4Cl (137 mg, 2.56 mmol) and Mg (137 mg, 5.64 mmol). Equal masses of NH_4Cl and Mg were added every few hours (usually to hundreds of equivalents) until all the starting material was converted to product as visualized by TLC with stain. Purification was performed via preparative thin-layer chromatography (4:1 hexanes/ethyl acetate eluent run four times) to afford **474** (13.4 mg, 0.0301 mmol, 60% yield) and **475** (4.8 mg, 0.0108 mmol, 22% yield) as white solids.

Indoline 474: R_F 0.33 (3:1 hexane/ethyl acetate eluent); ^{1}H NMR (300 MHz,

CDCl$_3$, 50°C) 7.10–7.05 (comp. m, 3H), 6.79 (dd, J=7.1, 7.7 Hz, 1H), 6.63 (d, J=8.2 Hz, 1H), 6.54 (br. s, 1H), 6.42 (d, J=7.7 Hz, 1H), 6.15 (br. d, J=6.5 Hz, 1H), 5.34 (br. s, 1H), 4.59 (br. s, 1H), 4.01 (br. s, 2H), 3.20–3.12 (m, 1H), 2.77 (app. s, 2H), 2.73 (s, 3H), 1.82 (s, 3H), 1.77 (s, 3H), 1.69–1.62 (comp. m, 3H), 1.53 (s, 9H); ^{13}C NMR (75 MHz, CDCl$_3$, 50°C) 155.1, 141.2, 139.6, 132.6, 129.8, 129.4, 128.0, 127.2, 124.4, 121.0, 118.0, 113.2, 106.7, 84.8, 80.0, 57.6, 56.4, 40.0, 33.2, 32.1, 29.0, 25.9, 18.7; IR (neat) 3371, 2975, 2245, 1672, 1600 cm^{-1}; MS m/z calcd for [C$_{28}$H$_{35}$N$_3$O$_2$-H]$^+$: 444.2651, found 444.2640.

Indoline 475: Crystals suitable for X-ray diffraction studies could be grown from heptane. R_F 0.32 (3:1 hexane/ethyl acetate eluent); ^{1}H NMR (300 MHz, CDCl$_3$, 50°C) 7.25 (d, J=4.0 Hz, 1H), 7.09-7.01 (comp. m, 2H), 6.69 (dd, J=6.0, 7.7 Hz, 1H), 6.63 (d, J=7.1 Hz, 1H), 6.52 (br. s, 1H), 6.45 (d, J=7.7 Hz, 1H), 6.0 (d, J=57.7 Hz, 1H), 5.43 (br. s, 1H), 4.58 (br. s, 1H), 3.96 (s, 1H), 3.91–3.70 (m, 1H), 3.50–3.35 (m, 1H), 3.09–2.80 (comp. m, 2H), 2.74 (s, 3H), 1.84 (s, 3H), 1.77 (s, 3H), 1.57–1.29 (comp. m, 2H), 1.42 (s, 9H); ^{13}C NMR (75 MHz, CDCl$_3$, 23°C) 154.9, 150.3, 141.4, 141.2, 140.6, 138.5, 138.3, 132.6, 132.2, 129.8, 128.1, 127.8, 127.5, 124.3, 120.1, 119.9, 118.8, 117.9, 113.6, 113.5, 107.5, 83.9, 79.9, 79.5, 59.0, 57.7, 41.7, 41.5, 38.7, 38.1, 33.2, 33.1, 32.5, 32.4, 31.2, 28.7, 26.1, 18.6, 18.5; IR (neat) 3363, 2973, 2242, 1672, 1594 cm^{-1}; MS m/z calcd for [C$_{28}$H$_{35}$N$_2$O$_2$]$^+$: 445.2729, found 445.2731.

6.6.3 Crystallographic Data

CALIFORNIA INSTITUTE OF TECHNOLOGY
BECKMAN INSTITUTE
X-RAY CRYSTALLOGRAPHY LABORATORY

Date 25 July 2005

Crystal Structure Analysis of:

475

Note: The crystallographic data has been deposited in the Cambridge Database (CCDC) and has been placed on hold pending further instructions from me. The deposition number is 220259. Ideally the CCDC would like the publication to contain a footnote of the type: "Crystallographic data have been deposited at the CCDC, 12 Union Road, Cambridge CB2 1EZ, UK and copies can be obtained on request, free of charge, by quoting the publication citation and the deposition number 220259."

Table 1. Crystal data and structure refinement for 475 (CCDC 220259).

Empirical formula	$C_{28}H_{35}N_3O_2 \cdot \_(C_7H_{16})$
Formula weight	470.64
Crystallization Solvent	Heptane
Crystal Habit	Columns
Crystal size	0.30 x 0.15 x 0.15 mm^3
Crystal color	Colorless

Data Collection

Preliminary Photos	Rotation
Type of diffractometer	Bruker SMART 1000
Wavelength	0.71073 Å MoKα
Data Collection Temperature	100(2) K
θ range for 16251 reflections used in lattice determination	2.19 to 27.68°
Unit cell dimensions	a = 31.9247(17) Å
	b = 8.8438(5) Å β= 90.2510(10)°
	c = 37.912(2) Å
Volume	10703.7(10) Å^3
Z	16
Crystal system	Monoclinic
Space group	C2/c
Density (calculated)	1.168 Mg/m^3
F(000)	4072
θ range for data collection	1.67 to 28.78°
Completeness to θ = 28.78°	91.9 %
Index ranges	-40 ≤ h ≤ 42, -11 ≤ k ≤ 11, -49 ≤ l ≤ 49
Data collection scan type	ω scans at 5 φ settings
Reflections collected	78166
Independent reflections	12801 [R$_{int}$= 0.0822]
Absorption coefficient	0.073 mm^{-1}
Absorption correction	None
Max. and min. transmission	0.9891 and 0.9783

Table 1 (cont.)

Structure Solution and Refinement

Structure solution program	SHELXS-97 (Sheldrick, 1990)
Primary solution method	Direct methods
Secondary solution method	Difference Fourier map
Hydrogen placement	Difference Fourier map
Structure refinement program	SHELXL-97 (Sheldrick, 1997)
Refinement method	Full matrix least-squares on F^2
Data / restraints / parameters	12801 / 11 / 938
Treatment of hydrogen atoms	Unrestrained
Goodness-of-fit on F^2	1.418
Final R indices [I>2σ(I), 7679 reflections]	R1 = 0.0518, wR2 = 0.0700
R indices (all data)	R1 = 0.0980, wR2 = 0.0746
Type of weighting scheme used	Sigma
Weighting scheme used	$w=1/\sigma^2(\text{Fo}^2)$
Max shift/error	0.025
Average shift/error	0.001
Largest diff. peak and hole	0.634 and -0.575 e.Å^{-3}

Special Refinement Details

Refinement of F^2 against ALL reflections. The weighted R-factor (wR) and goodness of fit (S) are based on F^2, conventional R-factors (R) are based on F, with F set to zero for negative F^2. The threshold expression of $F^2 > 2\sigma(F^2)$ is used only for calculating R-factors(gt) etc. and is not relevant to the choice of reflections for refinement. R-factors based on F^2 are statistically about twice as large as those based on F, and R-factors based on ALL data will be even larger.

All esds (except the esd in the dihedral angle between two l.s. planes) are estimated using the full covariance matrix. The cell esds are taken into account individually in the estimation of esds in distances, angles and torsion angles; correlations between esds in cell parameters are only used when they are defined by crystal symmetry. An approximate (isotropic) treatment of cell esds is used for estimating esds involving l.s. planes.

Table 2. **Atomic coordinates (x 10⁴) and equivalent isotropic displacement parameters (Å²x 10³) for 475 (CCDC 220259). U(eq) is defined as the trace of the orthogonalized U^{ij} tensor.**

	x	y	z	U$_{eq}$	Occ
O(1A)	2248(1)	-664(1)	562(1)	24(1)	1
O(2A)	1703(1)	-1947(1)	807(1)	23(1)	1
N(1A)	2941(1)	2961(1)	1848(1)	19(1)	1
N(2A)	2437(1)	1408(1)	2170(1)	19(1)	1
N(3A)	1806(1)	489(1)	945(1)	19(1)	1
C(1A)	2840(1)	4435(2)	1760(1)	17(1)	1
C(2A)	3145(1)	5568(2)	1778(1)	21(1)	1
C(3A)	3039(1)	7045(2)	1699(1)	25(1)	1
C(4A)	2639(1)	7419(2)	1593(1)	24(1)	1
C(5A)	2339(1)	6292(2)	1569(1)	20(1)	1
C(6A)	2432(1)	4803(2)	1654(1)	17(1)	1
C(7A)	2101(1)	3598(2)	1659(1)	19(1)	1
C(8A)	2277(1)	2010(2)	1580(1)	17(1)	1
C(9A)	2416(1)	1874(2)	1196(1)	18(1)	1
C(10A)	2058(1)	1869(2)	930(1)	20(1)	1
C(11A)	1465(1)	388(2)	1205(1)	20(1)	1
C(12A)	1624(1)	126(2)	1579(1)	19(1)	1
C(13A)	1392(1)	-835(2)	1798(1)	24(1)	1
C(14A)	1505(1)	-1083(2)	2145(1)	24(1)	1
C(15A)	1856(1)	-394(2)	2288(1)	22(1)	1
C(16A)	2083(1)	569(2)	2076(1)	18(1)	1
C(17A)	2693(1)	873(2)	2463(1)	26(1)	1
C(18A)	2649(1)	1740(2)	1833(1)	17(1)	1
C(19A)	1972(1)	837(2)	1721(1)	16(1)	1
C(20A)	1945(1)	-715(2)	757(1)	20(1)	1
C(21A)	1726(1)	-3240(2)	556(1)	24(1)	1
C(22A)	1391(1)	-4276(2)	698(1)	33(1)	1
C(23A)	2152(1)	-3990(2)	570(1)	31(1)	1
C(24A)	1614(1)	-2677(2)	190(1)	36(1)	1
C(25A)	1177(1)	1746(2)	1197(1)	23(1)	1
C(26A)	851(1)	1942(2)	983(1)	24(1)	1
C(27A)	571(1)	3291(2)	1016(1)	32(1)	1
C(28A)	729(1)	873(2)	695(1)	32(1)	1
O(1B)	3691(1)	11330(1)	2166(1)	26(1)	1
O(2B)	4255(1)	9828(1)	2286(1)	27(1)	1
N(1B)	3183(1)	9693(2)	638(1)	24(1)	1
N(2B)	3594(1)	7494(1)	819(1)	24(1)	1
N(3B)	4209(1)	10983(1)	1762(1)	21(1)	1
C(1B)	3330(1)	10953(2)	460(1)	23(1)	1
C(2B)	3058(1)	11781(2)	243(1)	28(1)	1
C(3B)	3202(1)	13031(2)	64(1)	32(1)	1
C(4B)	3615(1)	13481(2)	98(1)	34(1)	1
C(5B)	3883(1)	12667(2)	315(1)	29(1)	1
C(6B)	3745(1)	11404(2)	497(1)	23(1)	1
C(7B)	4028(1)	10496(2)	733(1)	23(1)	1
C(8B)	3793(1)	9865(2)	1057(1)	20(1)	1

C(9B)	3647(1)	11115(2)	1306(1)	21(1)	1
C(10B)	3990(1)	11942(2)	1506(1)	21(1)	1
C(11B)	4550(1)	9994(2)	1634(1)	23(1)	1
C(12B)	4381(1)	8581(2)	1457(1)	22(1)	1
C(13B)	4567(1)	7188(2)	1540(1)	27(1)	1
C(14B)	4431(1)	5866(2)	1384(1)	31(1)	1
C(15B)	4101(1)	5861(2)	1145(1)	28(1)	1
C(16B)	3914(1)	7229(2)	1062(1)	23(1)	1
C(17B)	3296(1)	6290(2)	742(1)	30(1)	1
C(18B)	3410(1)	8970(2)	919(1)	21(1)	1
C(19B)	4050(1)	8587(2)	1220(1)	20(1)	1
C(20B)	4021(1)	10744(2)	2079(1)	23(1)	1
C(21B)	4065(1)	8973(2)	2580(1)	27(1)	1
C(22B)	3916(1)	10014(2)	2870(1)	34(1)	1
C(23B)	3718(1)	7993(2)	2436(1)	36(1)	1
C(24B)	4432(1)	8019(3)	2704(1)	39(1)	1
C(25B)	4852(1)	10860(2)	1404(1)	24(1)	1
C(26B)	5102(1)	11965(2)	1510(1)	26(1)	1
C(27B)	5107(1)	12556(2)	1883(1)	35(1)	1
C(28B)	5394(1)	12729(3)	1257(1)	37(1)	1
C(31)	5440(1)	13698(4)	-185(1)	42(1)	0.50
C(32)	5386(1)	12256(4)	43(1)	95(3)	0.50
C(33)	5056(1)	11242(3)	-140(1)	45(1)	0.50
C(34)	5043(2)	9710(3)	57(1)	53(1)	0.50
C(35)	4696(2)	8736(4)	-116(2)	130(3)	0.50
C(36)	4777(2)	7065(3)	-20(1)	81(2)	0.50
C(37)	4569(2)	6747(5)	340(1)	95(3)	0.50

Table 3. Bond lengths [Å] and angles [°] for 475 (CCDC 220259).

O(1A)-C(20A)	1.2209(18)	C(21A)-C(24A)	1.517(2)
O(2A)-C(20A)	1.3500(17)	C(21A)-C(22A)	1.511(2)
O(2A)-C(21A)	1.4888(17)	C(22A)-H(22A)	1.025(16)
N(1A)-C(1A)	1.3840(18)	C(22A)-H(22B)	1.020(15)
N(1A)-C(18A)	1.4280(18)	C(22A)-H(22C)	1.013(17)
N(1A)-H(1A)	0.898(16)	C(23A)-H(23A)	1.003(16)
N(2A)-C(16A)	1.3951(18)	C(23A)-H(23B)	1.050(16)
N(2A)-C(17A)	1.4552(19)	C(23A)-H(23C)	1.008(16)
N(2A)-C(18A)	1.4777(18)	C(24A)-H(24A)	1.002(19)
N(3A)-C(20A)	1.3587(18)	C(24A)-H(24B)	0.985(16)
N(3A)-C(10A)	1.4638(19)	C(24A)-H(24C)	1.005(18)
N(3A)-C(11A)	1.4723(19)	C(25A)-C(26A)	1.326(2)
C(1A)-C(2A)	1.398(2)	C(25A)-H(25A)	0.983(14)
C(1A)-C(6A)	1.399(2)	C(26A)-C(28A)	1.495(2)
C(2A)-C(3A)	1.382(2)	C(26A)-C(27A)	1.496(2)
C(2A)-H(2A)	0.984(14)	C(27A)-H(27A)	0.993(15)
C(3A)-C(4A)	1.378(2)	C(27A)-H(27B)	1.045(17)
C(3A)-H(3A)	0.956(14)	C(27A)-H(27C)	0.982(15)
C(4A)-C(5A)	1.385(2)	C(28A)-H(28A)	0.992(16)
C(4A)-H(4A)	0.994(14)	C(28A)-H(28B)	1.027(16)
C(5A)-C(6A)	1.387(2)	C(28A)-H(28C)	1.033(17)
C(5A)-H(5A)	0.981(13)	O(1B)-C(20B)	1.2202(18)
C(6A)-C(7A)	1.501(2)	O(2B)-C(20B)	1.3503(18)
C(7A)-C(8A)	1.543(2)	O(2B)-C(21B)	1.4804(18)
C(7A)-H(7A1)	1.071(14)	N(1B)-C(1B)	1.3853(19)
C(7A)-H(7A2)	0.966(14)	N(1B)-C(18B)	1.4360(19)
C(8A)-C(19A)	1.523(2)	N(1B)-H(1B)	0.910(15)
C(8A)-C(9A)	1.527(2)	N(2B)-C(16B)	1.3929(19)
C(8A)-C(18A)	1.542(2)	N(2B)-C(17B)	1.458(2)
C(9A)-C(10A)	1.521(2)	N(2B)-C(18B)	1.4811(19)
C(9A)-H(9A1)	1.013(14)	N(3B)-C(20B)	1.3623(19)
C(9A)-H(9A2)	1.053(14)	N(3B)-C(10B)	1.4643(19)
C(10A)-H(10A)	1.037(13)	N(3B)-C(11B)	1.4794(19)
C(10A)-H(10B)	0.983(13)	C(1B)-C(6B)	1.392(2)
C(11A)-C(25A)	1.513(2)	C(1B)-C(2B)	1.399(2)
C(11A)-C(12A)	1.522(2)	C(2B)-C(3B)	1.378(2)
C(11A)-H(11A)	0.964(13)	C(2B)-H(2B)	0.994(14)
C(12A)-C(19A)	1.384(2)	C(3B)-C(4B)	1.380(3)
C(12A)-C(13A)	1.402(2)	C(3B)-H(3B)	0.969(15)
C(13A)-C(14A)	1.380(2)	C(4B)-C(5B)	1.387(2)
C(13A)-H(13A)	0.965(14)	C(4B)-H(4B)	0.959(17)
C(14A)-C(15A)	1.384(2)	C(5B)-C(6B)	1.386(2)
C(14A)-H(14A)	0.988(14)	C(5B)-H(5B)	0.975(15)
C(15A)-C(16A)	1.380(2)	C(6B)-C(7B)	1.500(2)
C(15A)-H(15A)	0.977(13)	C(7B)-C(8B)	1.548(2)
C(16A)-C(19A)	1.4101(19)	C(7B)-H(7B1)	1.023(15)
C(17A)-H(17A)	1.000(16)	C(7B)-H(7B2)	0.973(14)
C(17A)-H(17B)	1.019(17)	C(8B)-C(19B)	1.525(2)
C(17A)-H(17C)	1.042(16)	C(8B)-C(9B)	1.528(2)
C(18A)-H(18A)	1.048(12)	C(8B)-C(18B)	1.545(2)
C(21A)-C(23A)	1.513(2)	C(9B)-C(10B)	1.518(2)

C(9B)-H(9B1)	1.017(13)	C(33)-C(34)#1	0.952(5)
C(9B)-H(9B2)	1.021(14)	C(33)-C(35)#1	1.251(6)
C(10B)-H(10C)	1.033(14)	C(33)-C(34)	1.5478(10)
C(10B)-H(10D)	1.014(14)	C(33)-C(36)#1	1.700(5)
C(11B)-C(25B)	1.514(2)	C(33)-H(33A)	0.9600
C(11B)-C(12B)	1.517(2)	C(33)-H(33B)	0.9600
C(11B)-H(11B)	1.002(13)	C(34)-C(34)#1	0.725(5)
C(12B)-C(19B)	1.385(2)	C(34)-C(33)#1	0.952(5)
C(12B)-C(13B)	1.403(2)	C(34)-C(35)	1.5479(10)
C(13B)-C(14B)	1.380(2)	C(34)-C(35)#1	1.623(5)
C(13B)-H(13B)	0.992(14)	C(34)-H(34A)	0.9597
C(14B)-C(15B)	1.385(2)	C(34)-H(34B)	0.9601
C(14B)-H(14B)	0.955(16)	C(35)-C(32)#1	0.957(5)
C(15B)-C(16B)	1.385(2)	C(35)-C(33)#1	1.251(6)
C(15B)-H(15B)	1.000(14)	C(35)-C(36)	1.5448(10)
C(16B)-C(19B)	1.407(2)	C(35)-C(34)#1	1.623(5)
C(17B)-H(17D)	1.007(16)	C(35)-H(35A)	0.9601
C(17B)-H(17E)	0.997(16)	C(35)-H(35B)	0.9598
C(17B)-H(17F)	1.022(17)	C(36)-C(32)#1	0.799(6)
C(18B)-H(18B)	1.020(13)	C(36)-C(31)#1	1.242(5)
C(21B)-C(23B)	1.508(2)	C(36)-C(37)	1.5455(10)
C(21B)-C(22B)	1.513(2)	C(36)-C(33)#1	1.700(5)
C(21B)-C(24B)	1.517(2)	C(36)-H(36A)	0.9599
C(22B)-H(22D)	0.991(19)	C(36)-H(36B)	0.9600
C(22B)-H(22E)	1.022(17)	C(37)-C(31)#1	0.707(6)
C(22B)-H(22F)	1.014(18)	C(37)-C(32)#1	1.707(6)
C(23B)-H(23D)	0.969(17)	C(37)-H(37A)	0.9600
C(23B)-H(23E)	0.998(18)	C(37)-H(37B)	0.9602
C(23B)-H(23F)	0.984(17)	C(37)-H(37C)	0.9599
C(24B)-H(24D)	1.008(16)		
C(24B)-H(24E)	0.996(17)	C(20A)-O(2A)-C(21A)	119.99(12)
C(24B)-H(24F)	1.001(18)	C(1A)-N(1A)-C(18A)	123.40(14)
C(25B)-C(26B)	1.322(2)	C(1A)-N(1A)-H(1A)	121.4(10)
C(25B)-H(25B)	1.001(14)	C(18A)-N(1A)-H(1A)	115.2(10)
C(26B)-C(27B)	1.505(2)	C(16A)-N(2A)-C(17A)	118.21(13)
C(26B)-C(28B)	1.502(2)	C(16A)-N(2A)-C(18A)	104.96(11)
C(27B)-H(27D)	0.997(19)	C(17A)-N(2A)-C(18A)	117.77(13)
C(27B)-H(27E)	0.977(18)	C(20A)-N(3A)-C(10A)	116.78(13)
C(27B)-H(27F)	1.028(18)	C(20A)-N(3A)-C(11A)	123.32(13)
C(28B)-H(28D)	0.998(18)	C(10A)-N(3A)-C(11A)	119.00(13)
C(28B)-H(28E)	0.955(17)	N(1A)-C(1A)-C(2A)	120.04(14)
C(28B)-H(28F)	1.009(16)	N(1A)-C(1A)-C(6A)	120.32(14)
C(31)-C(37)#1	0.707(6)	C(2A)-C(1A)-C(6A)	119.64(14)
C(31)-C(36)#1	1.242(5)	C(3A)-C(2A)-C(1A)	119.84(16)
C(31)-C(32)	1.5511(10)	C(3A)-C(2A)-H(2A)	122.7(8)
C(31)-H(31A)	0.9599	C(1A)-C(2A)-H(2A)	117.4(8)
C(31)-H(31B)	0.9599	C(2A)-C(3A)-C(4A)	121.00(17)
C(31)-H(31C)	0.9601	C(2A)-C(3A)-H(3A)	117.0(9)
C(32)-C(36)#1	0.799(6)	C(4A)-C(3A)-H(3A)	122.0(9)
C(32)-C(35)#1	0.957(5)	C(3A)-C(4A)-C(5A)	119.11(16)
C(32)-C(33)	1.5450(10)	C(3A)-C(4A)-H(4A)	122.9(9)
C(32)-C(37)#1	1.707(6)	C(5A)-C(4A)-H(4A)	117.9(9)
C(32)-H(32A)	0.9600	C(6A)-C(5A)-C(4A)	121.39(16)
C(32)-H(32B)	0.9600	C(6A)-C(5A)-H(5A)	117.6(8)

C(4A)-C(5A)-H(5A)	121.0(8)	H(17B)-C(17A)-H(17C)	108.2(12)
C(5A)-C(6A)-C(1A)	119.00(15)	N(1A)-C(18A)-N(2A)	114.75(12)
C(5A)-C(6A)-C(7A)	121.80(14)	N(1A)-C(18A)-C(8A)	114.09(13)
C(1A)-C(6A)-C(7A)	119.07(14)	N(2A)-C(18A)-C(8A)	102.43(12)
C(6A)-C(7A)-C(8A)	112.68(13)	N(1A)-C(18A)-H(18A)	107.0(7)
C(6A)-C(7A)-H(7A1)	111.3(7)	N(2A)-C(18A)-H(18A)	108.6(7)
C(8A)-C(7A)-H(7A1)	109.9(7)	C(8A)-C(18A)-H(18A)	109.9(7)
C(6A)-C(7A)-H(7A2)	108.2(9)	C(12A)-C(19A)-C(16A)	119.59(14)
C(8A)-C(7A)-H(7A2)	107.1(8)	C(12A)-C(19A)-C(8A)	133.34(14)
H(7A1)-C(7A)-H(7A2)	107.5(11)	C(16A)-C(19A)-C(8A)	106.97(13)
C(19A)-C(8A)-C(9A)	118.08(13)	O(1A)-C(20A)-O(2A)	124.81(15)
C(19A)-C(8A)-C(18A)	99.60(12)	O(1A)-C(20A)-N(3A)	123.53(15)
C(9A)-C(8A)-C(18A)	110.85(12)	O(2A)-C(20A)-N(3A)	111.65(14)
C(19A)-C(8A)-C(7A)	108.45(12)	O(2A)-C(21A)-C(23A)	111.21(13)
C(9A)-C(8A)-C(7A)	111.36(13)	O(2A)-C(21A)-C(24A)	108.66(13)
C(18A)-C(8A)-C(7A)	107.51(12)	C(23A)-C(21A)-C(24A)	112.64(16)
C(10A)-C(9A)-C(8A)	114.36(14)	O(2A)-C(21A)-C(22A)	101.56(13)
C(10A)-C(9A)-H(9A1)	109.6(8)	C(23A)-C(21A)-C(22A)	111.06(15)
C(8A)-C(9A)-H(9A1)	108.4(8)	C(24A)-C(21A)-C(22A)	111.17(16)
C(10A)-C(9A)-H(9A2)	108.7(7)	C(21A)-C(22A)-H(22A)	108.3(9)
C(8A)-C(9A)-H(9A2)	108.2(7)	C(21A)-C(22A)-H(22B)	108.7(8)
H(9A1)-C(9A)-H(9A2)	107.4(11)	H(22A)-C(22A)-H(22B)	109.4(12)
N(3A)-C(10A)-C(9A)	112.86(13)	C(21A)-C(22A)-H(22C)	110.4(10)
N(3A)-C(10A)-H(10A)	106.4(7)	H(22A)-C(22A)-H(22C)	112.0(13)
C(9A)-C(10A)-H(10A)	112.6(7)	H(22B)-C(22A)-H(22C)	108.0(13)
N(3A)-C(10A)-H(10B)	109.7(8)	C(21A)-C(23A)-H(23A)	112.4(9)
C(9A)-C(10A)-H(10B)	108.4(8)	C(21A)-C(23A)-H(23B)	110.2(9)
H(10A)-C(10A)-H(10B)	106.6(10)	H(23A)-C(23A)-H(23B)	107.2(12)
N(3A)-C(11A)-C(25A)	112.86(13)	C(21A)-C(23A)-H(23C)	111.1(9)
N(3A)-C(11A)-C(12A)	112.94(13)	H(23A)-C(23A)-H(23C)	110.5(13)
C(25A)-C(11A)-C(12A)	109.90(13)	H(23B)-C(23A)-H(23C)	105.1(13)
N(3A)-C(11A)-H(11A)	104.1(8)	C(21A)-C(24A)-H(24A)	108.8(10)
C(25A)-C(11A)-H(11A)	110.3(8)	C(21A)-C(24A)-H(24B)	110.4(9)
C(12A)-C(11A)-H(11A)	106.3(8)	H(24A)-C(24A)-H(24B)	106.7(13)
C(19A)-C(12A)-C(13A)	118.04(15)	C(21A)-C(24A)-H(24C)	109.8(10)
C(19A)-C(12A)-C(11A)	123.83(14)	H(24A)-C(24A)-H(24C)	113.3(14)
C(13A)-C(12A)-C(11A)	118.04(14)	H(24B)-C(24A)-H(24C)	107.9(13)
C(14A)-C(13A)-C(12A)	121.62(16)	C(26A)-C(25A)-C(11A)	126.31(16)
C(14A)-C(13A)-H(13A)	119.3(9)	C(26A)-C(25A)-H(25A)	117.6(8)
C(12A)-C(13A)-H(13A)	119.0(9)	C(11A)-C(25A)-H(25A)	115.9(8)
C(13A)-C(14A)-C(15A)	120.78(16)	C(25A)-C(26A)-C(28A)	124.28(16)
C(13A)-C(14A)-H(14A)	118.0(9)	C(25A)-C(26A)-C(27A)	121.39(16)
C(15A)-C(14A)-H(14A)	121.2(9)	C(28A)-C(26A)-C(27A)	114.33(16)
C(16A)-C(15A)-C(14A)	118.07(16)	C(26A)-C(27A)-H(27A)	113.1(9)
C(16A)-C(15A)-H(15A)	120.4(8)	C(26A)-C(27A)-H(27B)	112.7(9)
C(14A)-C(15A)-H(15A)	121.5(8)	H(27A)-C(27A)-H(27B)	106.5(12)
C(15A)-C(16A)-N(2A)	127.37(14)	C(26A)-C(27A)-H(27C)	113.0(9)
C(15A)-C(16A)-C(19A)	121.89(15)	H(27A)-C(27A)-H(27C)	106.8(12)
N(2A)-C(16A)-C(19A)	110.74(13)	H(27B)-C(27A)-H(27C)	104.0(12)
N(2A)-C(17A)-H(17A)	108.4(9)	C(26A)-C(28A)-H(28A)	114.0(9)
N(2A)-C(17A)-H(17B)	109.3(9)	C(26A)-C(28A)-H(28B)	111.1(8)
H(17A)-C(17A)-H(17B)	110.9(13)	H(28A)-C(28A)-H(28B)	106.1(12)
N(2A)-C(17A)-H(17C)	111.1(9)	C(26A)-C(28A)-H(28C)	109.9(9)
H(17A)-C(17A)-H(17C)	108.8(12)	H(28A)-C(28A)-H(28C)	110.7(13)

H(28B)-C(28A)-H(28C)	104.5(12)	N(3B)-C(11B)-C(12B)	111.86(13)
C(20B)-O(2B)-C(21B)	121.02(12)	C(25B)-C(11B)-C(12B)	112.79(14)
C(1B)-N(1B)-C(18B)	123.14(15)	N(3B)-C(11B)-H(11B)	104.8(7)
C(1B)-N(1B)-H(1B)	117.2(10)	C(25B)-C(11B)-H(11B)	107.0(7)
C(18B)-N(1B)-H(1B)	115.8(10)	C(12B)-C(11B)-H(11B)	108.7(7)
C(16B)-N(2B)-C(17B)	119.04(14)	C(19B)-C(12B)-C(13B)	118.08(15)
C(16B)-N(2B)-C(18B)	105.64(12)	C(19B)-C(12B)-C(11B)	123.60(15)
C(17B)-N(2B)-C(18B)	115.81(14)	C(13B)-C(12B)-C(11B)	118.32(15)
C(20B)-N(3B)-C(10B)	117.64(13)	C(14B)-C(13B)-C(12B)	121.00(17)
C(20B)-N(3B)-C(11B)	121.68(13)	C(14B)-C(13B)-H(13B)	117.9(8)
C(10B)-N(3B)-C(11B)	118.31(13)	C(12B)-C(13B)-H(13B)	121.1(9)
N(1B)-C(1B)-C(6B)	120.41(15)	C(15B)-C(14B)-C(13B)	121.35(17)
N(1B)-C(1B)-C(2B)	119.74(16)	C(15B)-C(14B)-H(14B)	120.9(10)
C(6B)-C(1B)-C(2B)	119.84(16)	C(13B)-C(14B)-H(14B)	117.7(10)
C(3B)-C(2B)-C(1B)	120.10(18)	C(16B)-C(15B)-C(14B)	118.08(17)
C(3B)-C(2B)-H(2B)	120.7(8)	C(16B)-C(15B)-H(15B)	119.5(8)
C(1B)-C(2B)-H(2B)	119.2(9)	C(14B)-C(15B)-H(15B)	122.3(8)
C(4B)-C(3B)-C(2B)	120.43(18)	C(15B)-C(16B)-N(2B)	127.66(16)
C(4B)-C(3B)-H(3B)	120.0(9)	C(15B)-C(16B)-C(19B)	121.21(16)
C(2B)-C(3B)-H(3B)	119.5(9)	N(2B)-C(16B)-C(19B)	111.09(14)
C(3B)-C(4B)-C(5B)	119.41(18)	N(2B)-C(17B)-H(17D)	109.4(9)
C(3B)-C(4B)-H(4B)	122.1(11)	N(2B)-C(17B)-H(17E)	109.3(9)
C(5B)-C(4B)-H(4B)	118.4(11)	H(17D)-C(17B)-H(17E)	108.2(12)
C(4B)-C(5B)-C(6B)	121.23(19)	N(2B)-C(17B)-H(17F)	111.3(10)
C(4B)-C(5B)-H(5B)	119.3(9)	H(17D)-C(17B)-H(17F)	109.1(13)
C(6B)-C(5B)-H(5B)	119.4(9)	H(17E)-C(17B)-H(17F)	109.5(13)
C(5B)-C(6B)-C(1B)	118.98(16)	N(1B)-C(18B)-N(2B)	113.79(13)
C(5B)-C(6B)-C(7B)	122.47(16)	N(1B)-C(18B)-C(8B)	114.89(13)
C(1B)-C(6B)-C(7B)	118.55(15)	N(2B)-C(18B)-C(8B)	102.95(12)
C(6B)-C(7B)-C(8B)	111.90(14)	N(1B)-C(18B)-H(18B)	108.7(8)
C(6B)-C(7B)-H(7B1)	109.7(8)	N(2B)-C(18B)-H(18B)	106.6(7)
C(8B)-C(7B)-H(7B1)	110.2(8)	C(8B)-C(18B)-H(18B)	109.5(8)
C(6B)-C(7B)-H(7B2)	110.4(8)	C(12B)-C(19B)-C(16B)	120.27(15)
C(8B)-C(7B)-H(7B2)	105.7(8)	C(12B)-C(19B)-C(8B)	132.26(15)
H(7B1)-C(7B)-H(7B2)	108.8(12)	C(16B)-C(19B)-C(8B)	107.31(14)
C(19B)-C(8B)-C(9B)	116.86(13)	O(1B)-C(20B)-O(2B)	125.13(15)
C(19B)-C(8B)-C(18B)	100.39(12)	O(1B)-C(20B)-N(3B)	123.76(15)
C(9B)-C(8B)-C(18B)	109.69(13)	O(2B)-C(20B)-N(3B)	111.07(14)
C(19B)-C(8B)-C(7B)	109.09(13)	O(2B)-C(21B)-C(23B)	108.87(14)
C(9B)-C(8B)-C(7B)	112.35(13)	O(2B)-C(21B)-C(22B)	111.66(14)
C(18B)-C(8B)-C(7B)	107.46(13)	C(23B)-C(21B)-C(22B)	112.33(17)
C(10B)-C(9B)-C(8B)	115.82(14)	O(2B)-C(21B)-C(24B)	101.44(14)
C(10B)-C(9B)-H(9B1)	108.6(8)	C(23B)-C(21B)-C(24B)	111.02(16)
C(8B)-C(9B)-H(9B1)	109.2(8)	C(22B)-C(21B)-C(24B)	111.00(17)
C(10B)-C(9B)-H(9B2)	108.6(8)	C(21B)-C(22B)-H(22D)	108.2(11)
C(8B)-C(9B)-H(9B2)	108.4(8)	C(21B)-C(22B)-H(22E)	109.3(9)
H(9B1)-C(9B)-H(9B2)	105.7(11)	H(22D)-C(22B)-H(22E)	105.9(14)
N(3B)-C(10B)-C(9B)	113.22(14)	C(21B)-C(22B)-H(22F)	112.8(10)
N(3B)-C(10B)-H(10C)	107.9(8)	H(22D)-C(22B)-H(22F)	110.7(14)
C(9B)-C(10B)-H(10C)	109.1(8)	H(22E)-C(22B)-H(22F)	109.7(14)
N(3B)-C(10B)-H(10D)	107.4(8)	C(21B)-C(23B)-H(23D)	112.2(10)
C(9B)-C(10B)-H(10D)	109.4(8)	C(21B)-C(23B)-H(23E)	108.7(10)
H(10C)-C(10B)-H(10D)	109.8(11)	H(23D)-C(23B)-H(23E)	109.0(14)
N(3B)-C(11B)-C(25B)	111.30(13)	C(21B)-C(23B)-H(23F)	109.8(10)

H(23D)-C(23B)-H(23F)	111.1(14)	C(31)-C(32)-H(32A)	110.4
H(23E)-C(23B)-H(23F)	105.8(14)	C(37)#1-C(32)-H(32A)	133.0
C(21B)-C(24B)-H(24D)	110.4(10)	C(36)#1-C(32)-H(32B)	159.6
C(21B)-C(24B)-H(24E)	110.3(10)	C(35)#1-C(32)-H(32B)	76.9
H(24D)-C(24B)-H(24E)	108.4(14)	C(33)-C(32)-H(32B)	110.8
C(21B)-C(24B)-H(24F)	109.5(10)	C(31)-C(32)-H(32B)	110.0
H(24D)-C(24B)-H(24F)	111.3(14)	C(37)#1-C(32)-H(32B)	104.2
H(24E)-C(24B)-H(24F)	107.0(14)	H(32A)-C(32)-H(32B)	108.5
C(26B)-C(25B)-C(11B)	125.60(16)	C(34)#1-C(33)-C(35)#1	88.2(3)
C(26B)-C(25B)-H(25B)	118.5(8)	C(34)#1-C(33)-C(32)	126.3(4)
C(11B)-C(25B)-H(25B)	115.9(8)	C(35)#1-C(33)-C(32)	38.2(2)
C(25B)-C(26B)-C(27B)	123.19(17)	C(34)#1-C(33)-C(34)	19.6(4)
C(25B)-C(26B)-C(28B)	120.78(17)	C(35)#1-C(33)-C(34)	70.0(2)
C(27B)-C(26B)-C(28B)	116.02(17)	C(32)-C(33)-C(34)	108.16(10)
C(26B)-C(27B)-H(27D)	111.9(11)	C(34)#1-C(33)-C(36)#1	140.0(5)
C(26B)-C(27B)-H(27E)	108.9(10)	C(35)#1-C(33)-C(36)#1	60.9(2)
H(27D)-C(27B)-H(27E)	104.6(14)	C(32)-C(33)-C(36)#1	28.0(2)
C(26B)-C(27B)-H(27F)	114.0(10)	C(34)-C(33)-C(36)#1	127.5(2)
H(27D)-C(27B)-H(27F)	107.2(14)	C(34)#1-C(33)-H(33A)	106.1
H(27E)-C(27B)-H(27F)	109.8(14)	C(35)#1-C(33)-H(33A)	125.5
C(26B)-C(28B)-H(28D)	108.6(10)	C(32)-C(33)-H(33A)	109.5
C(26B)-C(28B)-H(28E)	112.2(10)	C(34)-C(33)-H(33A)	110.4
H(28D)-C(28B)-H(28E)	105.3(14)	C(36)#1-C(33)-H(33A)	112.4
C(26B)-C(28B)-H(28F)	111.8(9)	C(34)#1-C(33)-H(33B)	94.0
H(28D)-C(28B)-H(28F)	109.1(13)	C(35)#1-C(33)-H(33B)	123.0
H(28E)-C(28B)-H(28F)	109.6(14)	C(32)-C(33)-H(33B)	110.8
C(37)#1-C(31)-C(36)#1	101.4(6)	C(34)-C(33)-H(33B)	109.6
C(37)#1-C(31)-C(32)	90.2(5)	C(36)#1-C(33)-H(33B)	84.1
C(36)#1-C(31)-C(32)	30.8(3)	H(33A)-C(33)-H(33B)	108.5
C(37)#1-C(31)-H(31A)	136.2	C(34)#1-C(34)-C(33)#1	134.3(9)
C(36)#1-C(31)-H(31A)	115.6	C(34)#1-C(34)-C(35)	82.7(5)
C(32)-C(31)-H(31A)	109.4	C(33)#1-C(34)-C(35)	53.9(3)
C(37)#1-C(31)-H(31B)	27.6	C(34)#1-C(34)-C(33)	26.1(5)
C(36)#1-C(31)-H(31B)	127.9	C(33)#1-C(34)-C(33)	160.4(4)
C(32)-C(31)-H(31B)	109.7	C(35)-C(34)-C(33)	107.63(9)
H(31A)-C(31)-H(31B)	109.5	C(34)#1-C(34)-C(35)#1	71.0(4)
C(37)#1-C(31)-H(31C)	99.4	C(33)#1-C(34)-C(35)#1	150.9(5)
C(36)#1-C(31)-H(31C)	79.2	C(35)-C(34)-C(35)#1	153.72(19)
C(32)-C(31)-H(31C)	109.3	C(33)-C(34)-C(35)#1	46.40(17)
H(31A)-C(31)-H(31C)	109.5	C(34)#1-C(34)-H(34A)	114.1
H(31B)-C(31)-H(31C)	109.5	C(33)#1-C(34)-H(34A)	75.1
C(36)#1-C(32)-C(35)#1	123.0(8)	C(35)-C(34)-H(34A)	110.8
C(36)#1-C(32)-C(33)	86.9(4)	C(33)-C(34)-H(34A)	110.4
C(35)#1-C(32)-C(33)	54.0(3)	C(35)#1-C(34)-H(34A)	81.1
C(36)#1-C(32)-C(31)	52.7(4)	C(34)#1-C(34)-H(34B)	127.3
C(35)#1-C(32)-C(31)	161.2(4)	C(33)#1-C(34)-H(34B)	85.0
C(33)-C(32)-C(31)	107.68(10)	C(35)-C(34)-H(34B)	109.8
C(36)#1-C(32)-C(37)#1	64.8(4)	C(33)-C(34)-H(34B)	109.7
C(35)#1-C(32)-C(37)#1	138.1(6)	C(35)#1-C(34)-H(34B)	87.0
C(33)-C(32)-C(37)#1	88.7(3)	H(34A)-C(34)-H(34B)	108.5
C(31)-C(32)-C(37)#1	24.5(2)	C(32)#1-C(35)-C(33)#1	87.8(4)
C(36)#1-C(32)-H(32A)	73.2	C(32)#1-C(35)-C(36)	25.7(4)
C(35)#1-C(32)-H(32A)	82.5	C(33)#1-C(35)-C(36)	74.1(2)
C(33)-C(32)-H(32A)	109.5	C(32)#1-C(35)-C(34)	125.6(3)

C(33)#1-C(35)-C(34)	37.9(2)
C(36)-C(35)-C(34)	108.19(10)
C(32)#1-C(35)-C(34)#1	151.3(5)
C(33)#1-C(35)-C(34)#1	63.6(3)
C(36)-C(35)-C(34)#1	133.7(3)
C(34)-C(35)-C(34)#1	26.28(19)
C(32)#1-C(35)-H(35A)	113.6
C(33)#1-C(35)-H(35A)	140.0
C(36)-C(35)-H(35A)	110.5
C(34)-C(35)-H(35A)	110.6
C(34)#1-C(35)-H(35A)	91.8
C(32)#1-C(35)-H(35B)	84.9
C(33)#1-C(35)-H(35B)	106.8
C(36)-C(35)-H(35B)	109.5
C(34)-C(35)-H(35B)	109.6
C(34)#1-C(35)-H(35B)	100.2
H(35A)-C(35)-H(35B)	108.4
C(32)#1-C(36)-C(31)#1	96.6(5)
C(32)#1-C(36)-C(35)	31.3(5)
C(31)#1-C(36)-C(35)	125.1(3)
C(32)#1-C(36)-C(37)	87.4(6)
C(31)#1-C(36)-C(37)	26.7(3)
C(35)-C(36)-C(37)	108.13(10)
C(32)#1-C(36)-C(33)#1	65.1(3)
C(31)#1-C(36)-C(33)#1	115.5(3)
C(35)-C(36)-C(33)#1	45.04(17)
C(37)-C(36)-C(33)#1	88.9(3)
C(32)#1-C(36)-H(36A)	139.9
C(31)#1-C(36)-H(36A)	113.4
C(35)-C(36)-H(36A)	109.6
C(37)-C(36)-H(36A)	107.3
C(33)#1-C(36)-H(36A)	77.7
C(32)#1-C(36)-H(36B)	98.8
C(31)#1-C(36)-H(36B)	87.1
C(35)-C(36)-H(36B)	110.0
C(37)-C(36)-H(36B)	113.2
C(33)#1-C(36)-H(36B)	152.7
H(36A)-C(36)-H(36B)	108.4
C(31)#1-C(37)-C(36)	52.0(4)
C(31)#1-C(37)-C(32)#1	65.3(5)
C(36)-C(37)-C(32)#1	27.9(2)
C(31)#1-C(37)-H(37A)	71.8
C(36)-C(37)-H(37A)	109.2
C(32)#1-C(37)-H(37A)	134.0
C(31)#1-C(37)-H(37B)	161.4
C(36)-C(37)-H(37B)	112.6
C(32)#1-C(37)-H(37B)	106.1
H(37A)-C(37)-H(37B)	109.5
C(31)#1-C(37)-H(37C)	86.7
C(36)-C(37)-H(37C)	106.6
C(32)#1-C(37)-H(37C)	84.3
H(37A)-C(37)-H(37C)	109.5
H(37B)-C(37)-H(37C)	109.5

_____
Symmetry transformations used to generate equivalent atoms:
#1 -x+1,-y+2,-z

Table 4.   Anisotropic displacement parameters (Å²x 10⁴) for 475 (CCDC 220259). The anisotropic displacement factor exponent takes the form: -2π² [h² a*²U ¹¹ + ... + 2 h k a* b* U¹²]

	U^{11}	U^{22}	U^{33}	U^{23}	U^{13}	U^{12}
O(1A)	277(7)	238(7)	200(6)	-11(5)	31(5)	-22(5)
O(2A)	307(7)	171(6)	219(6)	-32(5)	-5(5)	-38(5)
N(1A)	183(8)	152(8)	245(8)	0(6)	-31(7)	-4(7)
N(2A)	206(8)	216(8)	140(7)	19(6)	-17(6)	-16(6)
N(3A)	221(8)	178(8)	180(7)	-16(6)	-6(6)	-30(6)
C(1A)	234(10)	168(9)	114(8)	-24(7)	16(7)	2(8)
C(2A)	228(10)	235(10)	169(9)	-17(7)	-4(8)	-19(8)
C(3A)	308(11)	212(10)	220(10)	-10(8)	4(8)	-84(9)
C(4A)	344(11)	167(10)	210(10)	13(8)	4(8)	7(9)
C(5A)	250(11)	200(10)	161(9)	-6(7)	-10(8)	35(8)
C(6A)	218(9)	184(9)	103(8)	-28(7)	-3(7)	-6(7)
C(7A)	200(10)	185(9)	169(9)	-9(7)	-8(8)	5(8)
C(8A)	178(9)	165(9)	162(9)	-1(7)	-2(7)	1(7)
C(9A)	218(10)	152(9)	176(9)	-4(7)	-4(8)	7(8)
C(10A)	260(10)	172(9)	164(9)	16(7)	2(8)	-22(8)
C(11A)	220(10)	186(10)	202(9)	-14(7)	-21(8)	-44(8)
C(12A)	207(9)	167(9)	185(9)	-11(7)	10(7)	21(7)
C(13A)	215(10)	239(10)	252(10)	-12(8)	-15(8)	-54(8)
C(14A)	269(11)	222(10)	238(10)	24(8)	36(8)	-42(8)
C(15A)	289(11)	195(9)	163(9)	17(7)	0(8)	11(8)
C(16A)	205(9)	170(9)	161(9)	-17(7)	6(7)	13(7)
C(17A)	271(11)	301(12)	205(10)	44(9)	-58(9)	-25(9)
C(18A)	200(9)	167(9)	150(9)	-19(7)	-2(7)	-8(8)
C(19A)	197(9)	140(8)	153(8)	1(7)	29(7)	28(7)
C(20A)	266(10)	186(9)	161(9)	11(7)	-71(8)	-23(8)
C(21A)	339(11)	175(9)	212(10)	-45(7)	-38(8)	7(8)
C(22A)	360(13)	215(11)	400(13)	-59(10)	-42(10)	-39(10)
C(23A)	349(12)	249(11)	335(12)	-44(10)	-5(10)	8(9)
C(24A)	539(15)	270(12)	256(11)	-40(9)	-89(10)	-34(11)
C(25A)	260(10)	191(10)	227(10)	-3(8)	-5(8)	-2(8)
C(26A)	229(10)	255(10)	241(10)	46(8)	26(8)	-13(8)
C(27A)	257(12)	342(12)	370(13)	58(10)	-25(10)	52(10)
C(28A)	305(12)	366(12)	281(11)	16(10)	-46(9)	27(10)
O(1B)	226(7)	307(7)	254(7)	10(5)	14(5)	50(6)
O(2B)	228(7)	328(7)	246(7)	95(5)	-10(5)	14(6)
N(1B)	225(9)	271(9)	232(8)	24(6)	-26(7)	2(7)
N(2B)	273(9)	195(8)	255(8)	-19(6)	-29(7)	18(7)
N(3B)	198(8)	229(8)	199(8)	21(6)	8(6)	26(6)
C(1B)	323(11)	206(10)	164(9)	-26(7)	21(8)	54(8)
C(2B)	349(12)	286(11)	217(10)	-29(8)	-18(9)	32(9)
C(3B)	442(13)	310(11)	208(10)	9(9)	-28(9)	120(10)
C(4B)	485(14)	282(11)	251(11)	73(9)	55(10)	62(10)
C(5B)	341(12)	262(11)	270(11)	18(8)	79(9)	40(9)
C(6B)	291(11)	232(10)	164(9)	1(7)	55(8)	50(8)
C(7B)	256(11)	216(10)	225(10)	10(8)	33(8)	20(9)
C(8B)	218(10)	185(9)	186(9)	16(7)	10(7)	17(8)

C(9B)	198(10)	214(10)	212(9)	18(8)	10(8)	30(8)
C(10B)	215(10)	227(10)	201(9)	28(8)	17(8)	33(8)
C(11B)	201(10)	245(10)	243(10)	16(8)	-14(8)	28(8)
C(12B)	198(9)	226(9)	229(9)	20(7)	53(8)	-1(8)
C(13B)	228(11)	261(11)	330(11)	50(8)	-23(9)	22(9)
C(14B)	314(11)	206(10)	404(12)	53(9)	-5(9)	46(9)
C(15B)	340(11)	203(10)	308(11)	-12(8)	-5(9)	18(9)
C(16B)	227(10)	238(10)	236(10)	25(8)	26(8)	7(8)
C(17B)	375(12)	252(11)	272(11)	-35(9)	-45(10)	-15(10)
C(18B)	229(10)	224(10)	191(9)	14(8)	5(8)	15(8)
C(19B)	201(9)	192(9)	218(9)	23(7)	30(8)	10(8)
C(20B)	233(10)	212(10)	235(10)	-11(8)	-40(8)	-27(8)
C(21B)	257(10)	257(10)	284(10)	77(8)	-2(8)	-26(8)
C(22B)	397(13)	363(12)	257(11)	42(10)	9(10)	-44(11)
C(23B)	313(13)	288(12)	490(14)	-9(11)	-60(11)	-51(10)
C(24B)	322(13)	412(14)	435(14)	182(12)	-24(11)	34(11)
C(25B)	198(10)	261(10)	262(10)	3(8)	13(8)	41(8)
C(26B)	204(10)	261(10)	317(11)	23(8)	-13(8)	18(8)
C(27B)	307(13)	360(13)	371(13)	-21(10)	-58(10)	-29(11)
C(28B)	291(13)	392(14)	422(14)	-5(11)	23(10)	-89(11)
C(31)	380(30)	440(30)	440(30)	20(30)	120(30)	90(20)
C(32)	620(50)	1370(70)	840(50)	-530(50)	-570(40)	850(50)
C(33)	440(30)	590(40)	320(30)	50(20)	20(20)	120(30)
C(34)	350(30)	780(50)	480(40)	350(30)	-200(20)	180(30)
C(35)	1490(70)	500(40)	1900(80)	300(50)	-80(60)	20(50)
C(36)	390(40)	1340(60)	710(40)	-30(40)	-40(30)	0(40)
C(37)	1080(50)	1410(60)	360(40)	-140(30)	200(40)	900(50)

Table 5. **Hydrogen coordinates (x 10⁴) and isotropic displacement parameters (Å²x 10 ³) for 475 (CCDC 220259).**

	x	y	z	U$_{iso}$
H(1A)	3201(5)	2708(17)	1919(4)	31(5)
H(2A)	3426(4)	5271(15)	1859(4)	20(4)
H(3A)	3258(4)	7781(16)	1714(4)	20(4)
H(4A)	2552(4)	8472(16)	1537(4)	25(4)
H(5A)	2051(4)	6524(14)	1497(3)	9(4)
H(7A1)	1851(4)	3855(15)	1479(4)	21(4)
H(7A2)	1983(4)	3564(15)	1893(4)	24(4)
H(9A1)	2586(4)	913(16)	1171(4)	26(4)
H(9A2)	2616(4)	2789(16)	1140(3)	20(4)
H(10A)	1853(4)	2764(15)	966(3)	14(4)
H(10B)	2177(4)	1986(14)	693(4)	16(4)
H(11A)	1315(4)	-513(15)	1139(3)	14(4)
H(13A)	1156(5)	-1375(16)	1700(4)	25(4)
H(14A)	1327(5)	-1759(16)	2288(4)	26(5)
H(15A)	1941(4)	-572(15)	2533(4)	19(4)
H(17A)	2528(5)	981(17)	2685(4)	40(5)
H(17B)	2962(5)	1491(17)	2475(4)	39(5)
H(17C)	2773(5)	-260(19)	2430(4)	39(5)
H(18A)	2816(4)	777(14)	1755(3)	9(4)
H(22A)	1476(5)	-4604(17)	948(4)	39(5)
H(22B)	1371(5)	-5206(17)	540(4)	31(5)
H(22C)	1109(6)	-3751(19)	695(4)	48(6)
H(23A)	2375(5)	-3364(17)	455(4)	35(5)
H(23B)	2142(5)	-5033(19)	438(4)	44(5)
H(23C)	2234(5)	-4244(17)	820(4)	41(5)
H(24A)	1332(6)	-2180(20)	198(4)	55(6)
H(24B)	1589(5)	-3533(18)	24(4)	33(5)
H(24C)	1841(6)	-1990(20)	100(5)	52(6)
H(25A)	1229(4)	2519(15)	1378(4)	19(4)
H(27A)	655(5)	3981(16)	1210(4)	27(5)
H(27B)	259(6)	2998(17)	1062(4)	43(5)
H(27C)	559(5)	3902(17)	800(4)	30(5)
H(28A)	911(5)	-35(18)	679(4)	31(5)
H(28B)	743(5)	1389(17)	453(4)	34(5)
H(28C)	419(6)	564(18)	722(4)	44(5)
H(1B)	2901(5)	9532(17)	635(4)	34(5)
H(2B)	2763(5)	11441(16)	216(4)	24(5)
H(3B)	3009(5)	13626(16)	-76(4)	29(5)
H(4B)	3721(5)	14368(19)	-17(4)	49(6)
H(5B)	4170(5)	13019(16)	349(4)	29(5)
H(7B1)	4276(5)	11147(16)	812(4)	25(4)
H(7B2)	4135(4)	9617(16)	608(4)	21(4)
H(9B1)	3442(4)	10673(15)	1483(3)	16(4)
H(9B2)	3479(4)	11885(15)	1163(4)	18(4)
H(10C)	4208(4)	12341(15)	1329(4)	17(4)
H(10D)	3863(4)	12819(15)	1641(4)	19(4)
H(11B)	4707(4)	9690(14)	1852(3)	9(4)

H(13B)	4807(5)	7127(16)	1706(4)	25(4)
H(14B)	4567(5)	4947(18)	1450(4)	39(5)
H(15B)	4006(4)	4920(16)	1022(4)	21(4)
H(17D)	3451(5)	5375(18)	653(4)	34(5)
H(17E)	3099(5)	6633(17)	554(4)	33(5)
H(17F)	3130(5)	5997(18)	962(5)	49(6)
H(18B)	3210(4)	8764(14)	1121(4)	17(4)
H(22D)	4150(6)	10690(20)	2936(5)	61(6)
H(22E)	3853(5)	9389(19)	3091(5)	50(5)
H(22F)	3659(6)	10620(20)	2800(4)	54(6)
H(23D)	3481(5)	8584(19)	2353(4)	41(5)
H(23E)	3621(5)	7300(20)	2626(5)	50(6)
H(23F)	3827(5)	7340(19)	2247(5)	45(6)
H(24D)	4528(5)	7327(18)	2509(4)	38(5)
H(24E)	4349(5)	7387(19)	2909(5)	49(6)
H(24F)	4664(6)	8696(19)	2786(4)	49(6)
H(25B)	4866(4)	10533(15)	1151(4)	25(4)
H(27D)	4953(6)	13530(20)	1904(5)	64(7)
H(27E)	5395(6)	12796(18)	1949(4)	45(6)
H(27F)	4979(5)	11830(20)	2064(5)	53(6)
H(28D)	5687(6)	12469(18)	1324(4)	45(6)
H(28E)	5378(5)	13810(20)	1272(4)	47(6)
H(28F)	5341(5)	12401(18)	1006(5)	40(5)
H(31A)	5640	14357	-76	63
H(31B)	5536	13422	-416	63
H(31C)	5175	14209	-205	63
H(32A)	5290	12519	275	113
H(32B)	5649	11737	65	113
H(33A)	5133	11091	-382	54
H(33B)	4784	11706	-134	54
H(34A)	4986	9866	303	64
H(34B)	5308	9210	36	64
H(35A)	4696	8867	-368	156
H(35B)	4427	9039	-28	156
H(36A)	5072	6900	9	98
H(36B)	4677	6417	-205	98
H(37A)	4618	5711	405	143
H(37B)	4673	7397	524	143
H(37C)	4274	6911	309	143

6.7 Notes and References

---

(1) Numata, A.; Takahashi, C.; Ito, Y.; Takada, T.; Kawai, K.; Usami, Y.; Matsumura, E.; Imachi, M.; Tadayoshi, I.; Hasegawa, T. *Tetrahedron Lett*. **1993**, *34*, 2355.

(2) Ratnayake, A. S.; Yoshida, W. Y.; Mooberry, S. L.; Hemsheidt, T. K. *J. Org. Chem.* **2001**, *66*, 8717.

(3) See also Chapter 5 in this thesis.

(4) (a) Soloveva, T. F.; Kuvichkina, T. N.; Baskunov, B. P.; Kozlovskii, A. G. *Microbiol*. **1995**, *64*, 550. (b) Kozlovskii, A. G.; Soloveva, T. F.; Sakharovskii, V. G.; Adanin, V. M. *Dokl. Akad. Nauk. SSSR* **1981**, *260*, 230.

(5) For ^{1}H NMR data, see Refs. 1, 2, and; (a) Jackson, A. H.; Smith, A. E. *J. Chem. Soc*. **1964**, 5510. (b) Dachriyanus; Sargent, M. V.; Wahyuni, F. S. *Aust. J. Chem.* **2000**, *53*, 159. (c) Horne, S.; Taylor, N.; Collins, S.; Rodrigo, R. *J. Chem. Soc*., *Perkin Trans*. 1 **1991**, 3047. (d) Nyerges, M.; Rudas, M.; Bitter, I.; Töke, L. *Tetrahedron* **1997**, *53*, 3269. (e) Spande, T. F.; Wilchek, M.; Witkop, B. *J. Am. Chem. Soc*. **1968**, 3256. (f) Chan, T.-L.; Schellenberg, K. A. *J. Biol. Chem*. **1968**, *243*, 6284. (g) Decodts, G.; Wakselman, M.; Vilkas, M. *Tetrahedron* **1970**, 26, 3313. (h) Britten, A. Z.; Bardsley, W. G.; Hill, C. M. *Tetrahedron* **1971**, *27*, 5631. (i) Lyle, F. R. US Patent 5 973 257, 1985; *Chem. Abstr*. **1985**, *65*, 2870. (j) Lindquist, N.; Fenical, W.; Van Duyne, G. D.; Clardy, J. *J. Am. Chem. Soc*. **1991**, *113*, 2303. (k) Li, J.; Burgett, A. W. G.; Esser, L.; Amezcua, C.; Harran, P. G. *Angew. Chem*., *Int. Ed*. **2001**, *40*, 4770. (l) Li, J.; Jeong, S.; Esser, L.; Harran, P. G. *Angew. Chem*., *Int. Ed*. **2001**, *40*, 4765.

(6) For ^{13}C NMR data, see Refs. 1, 2, 5b, and 5d.

(7) Recently, the novel polycyclic alkaloid perophoramidine (**425**) was isolated.[8]   A similar tryptamine oxidative dimerization would account for its biogenesis as well.

425
Perophoramidine
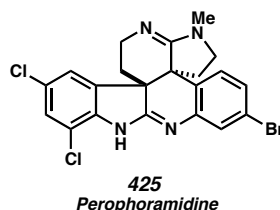
(8) Verbitski, S. M.; Mayne, C. L.; Davis, R. A.; Concepcion, G. P.; Ireland, C. M. *J. Org. Chem.* **2002**, *67*, 7124.

(9) Steinhagen, H.; Corey, E. J. *Angew. Chem.*, *Int. Ed.* **1999**, *38*, 1928.

(10) (a) Yamada, F.; Makita, Y.; Suzuki, T.; Somei, M. *Chem. Pharm. Bull.* **1985**, *33*, 2162. (b) Somei, M.; Yamada, F. Jpn. Patent JP 85-47044 19850308, 1986. (c) Iwao, M.; Motoi, O. *Tetrahedron Lett.* **1995**, *36*, 5929.

(11) The biosynthetic proposal depicted in Scheme 6.2.1 is only one of a number of potential scenarios. Another possibility might involve a combination of the clavicipitic acid/aurantioclavine and chimonanthine biosyntheses. Nonetheless, these routes would also involve two molecules of tryptamine or tryptophan undergoing an oxidative coupling, see: (a) Kirby, G. W.; Shah, S. W.; Herbert, E. J. *J. Chem. Soc. C* **1969**, 1916. (b) Robbers, J. E.; Otsuka, H.; Floss, H. G.; Arnold, E. V.; Clardy, J. *J. Org. Chem.* **1980**, 45, 1117.

APPENDIX TWO

Spectra Relevant to Chapter 6:

**Evaluating the Structure of and Proposing a Biomimetic Approach to
Communesin B (a.k.a. Nomofungin)**
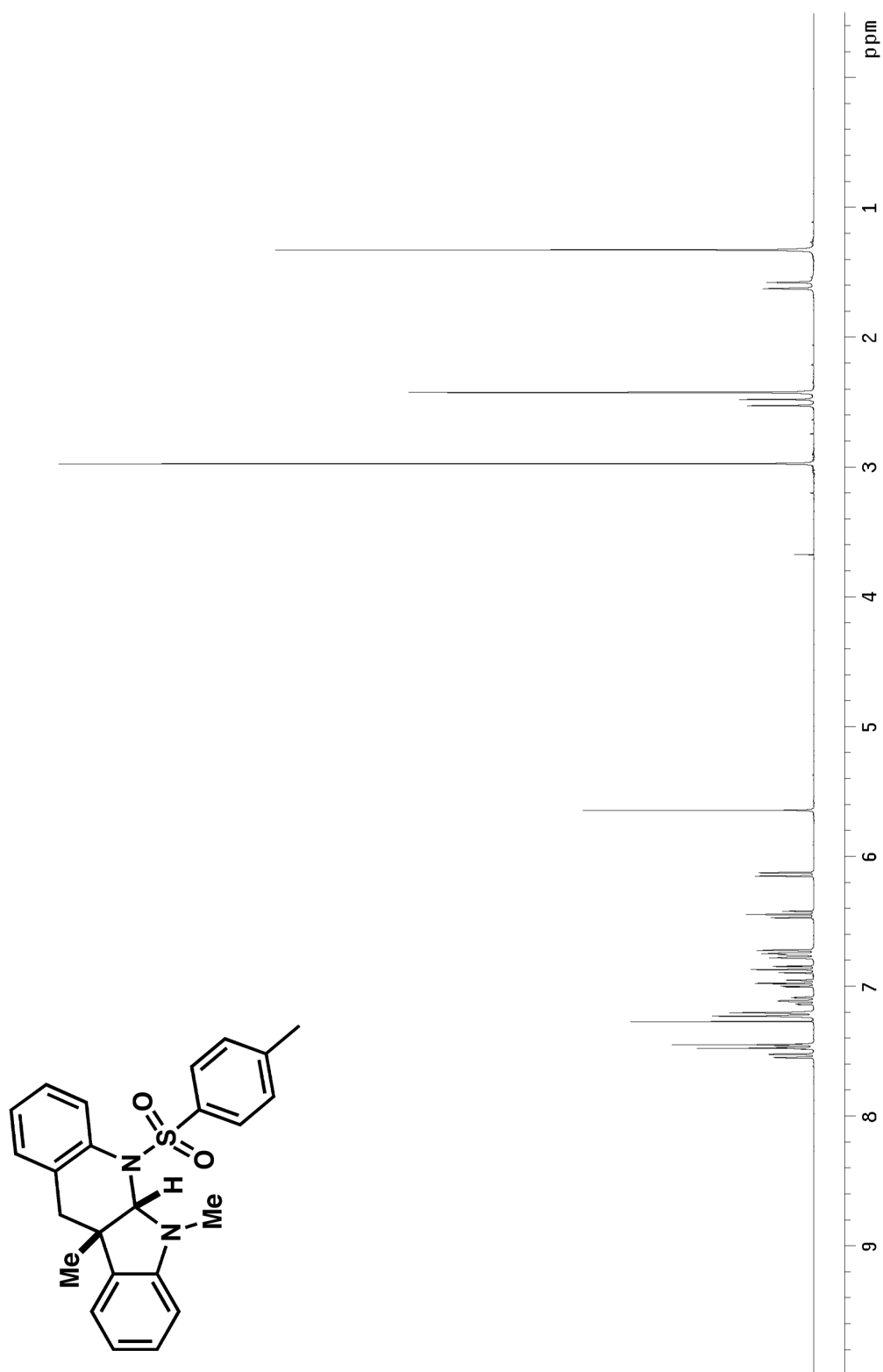
Figure A.2.1 ^{1}HNMR (300 MHz, CDCL$_3$) of compound **470**.
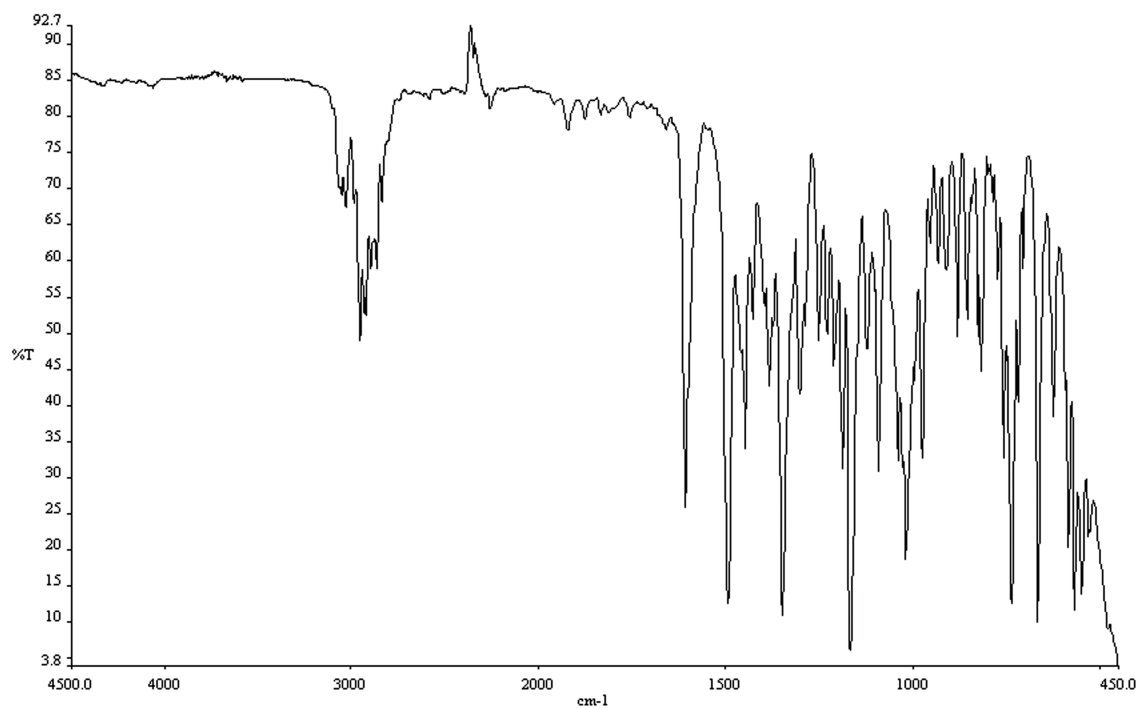
Figure A.2.2 Infrared spectrum (thin film/NaCl) of compound **470**.

Figure A.2.3 ^{13}CNMR (75 Mhz, CDCl$_3$) of compound **470**.
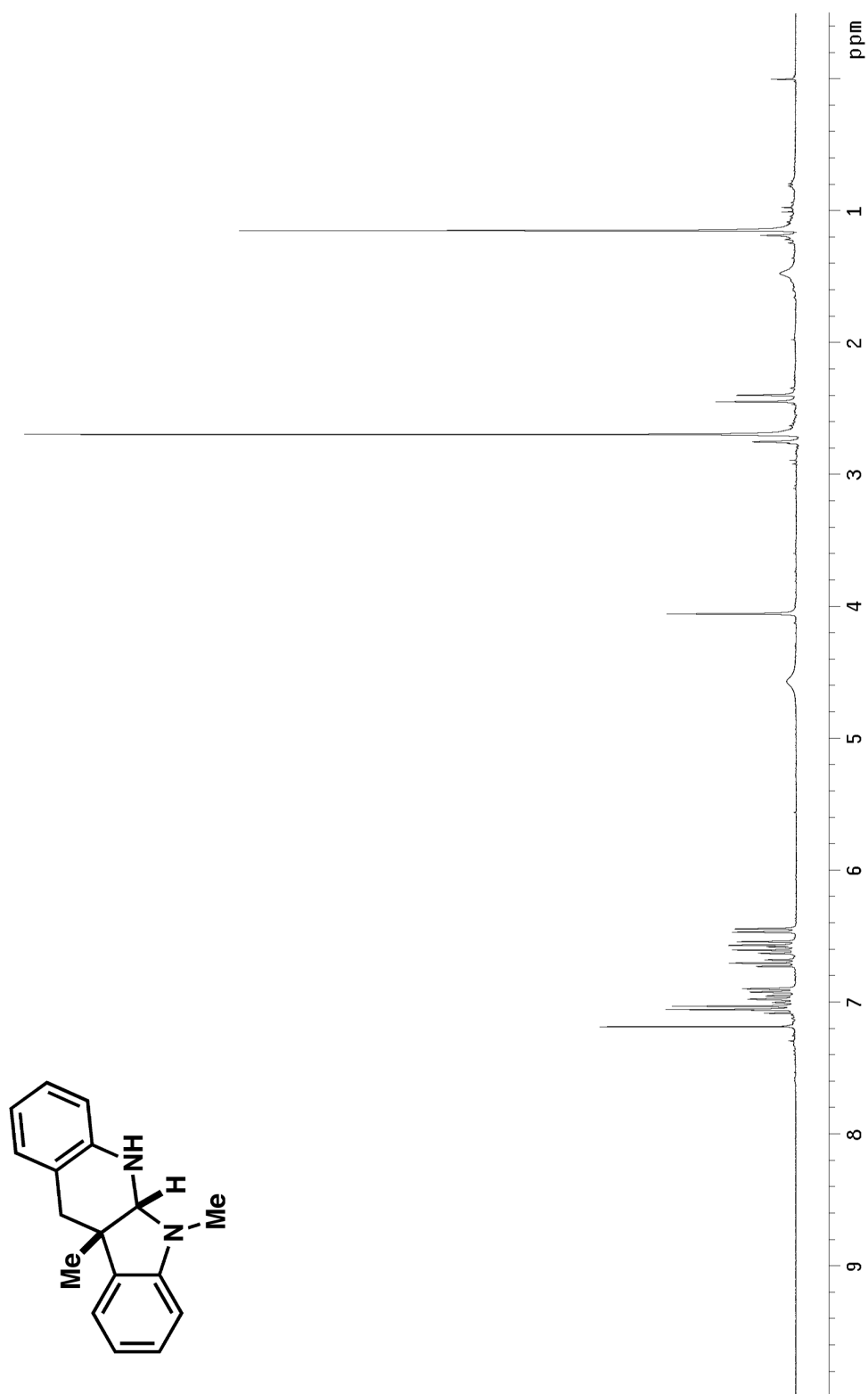
Figure A.2.4 ¹HNMR (300 MHz, CDCL₃) of compound **471**.
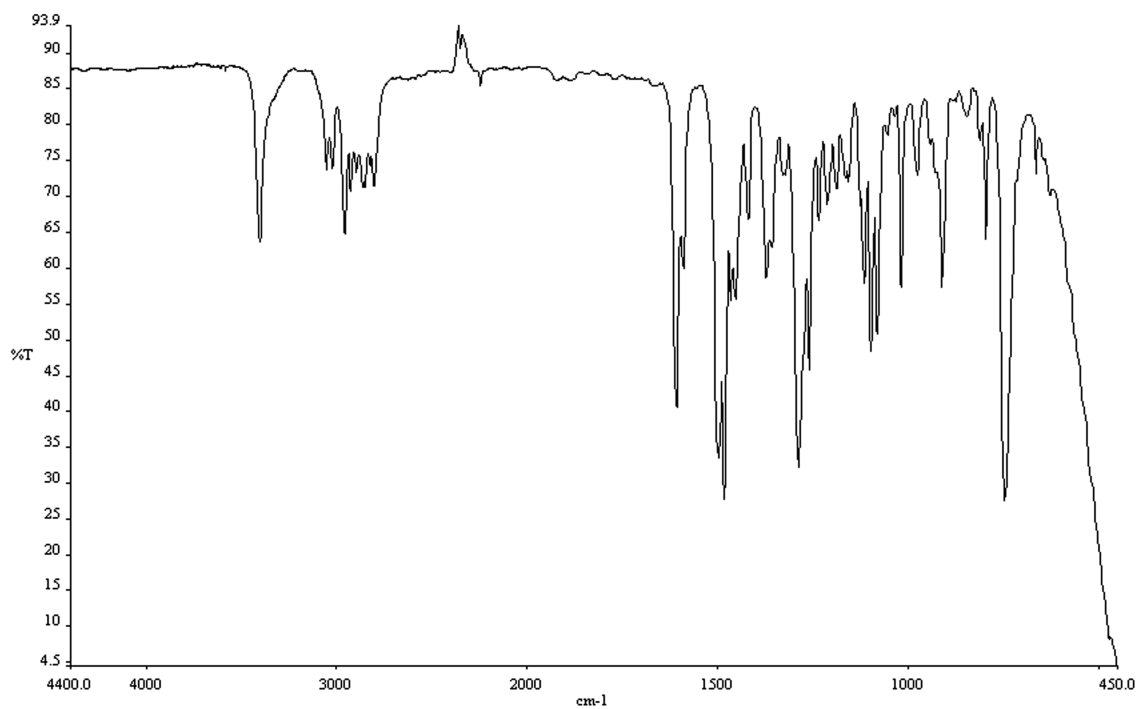
Figure A.2.5 Infrared spectrum (thin film/NaCl) of compound **471**.
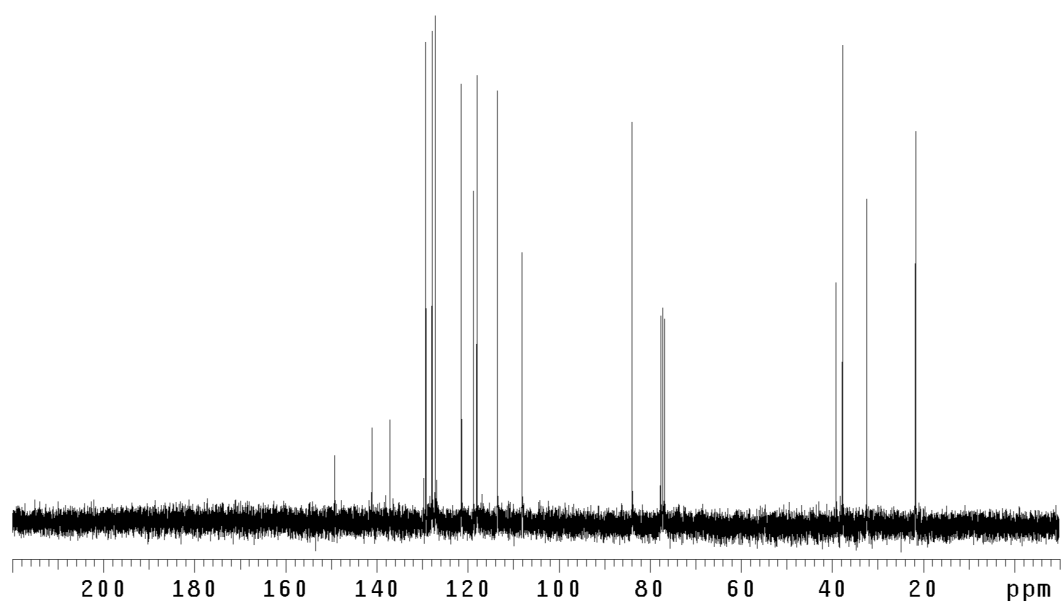
Figure A.2.6 ^{13}CNMR (75 Mhz, CDCl$_3$) of compound **471**.
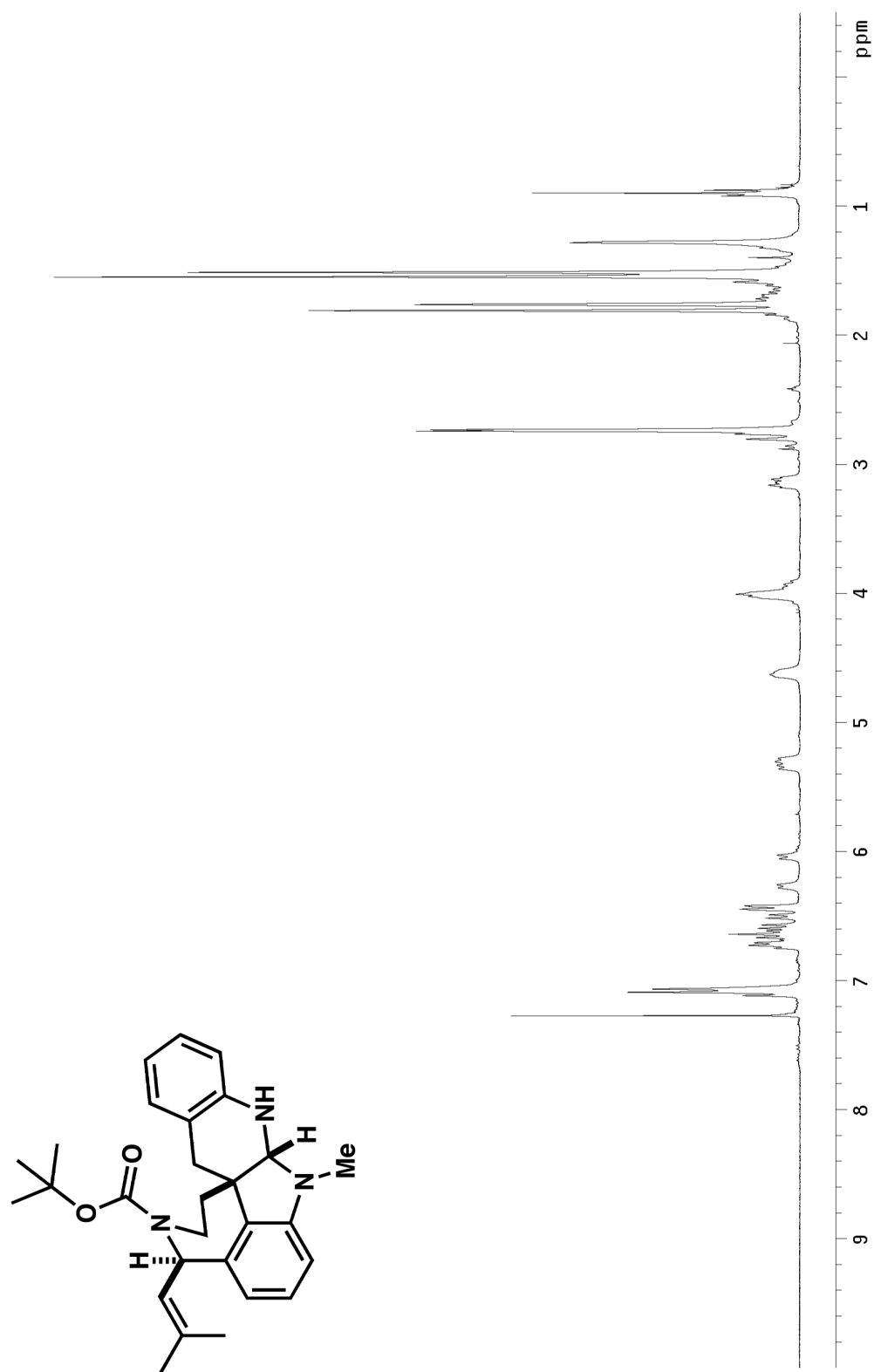
Figure A.2.7 ¹HNMR (300 MHz, CDCL₃) of compound **474**.
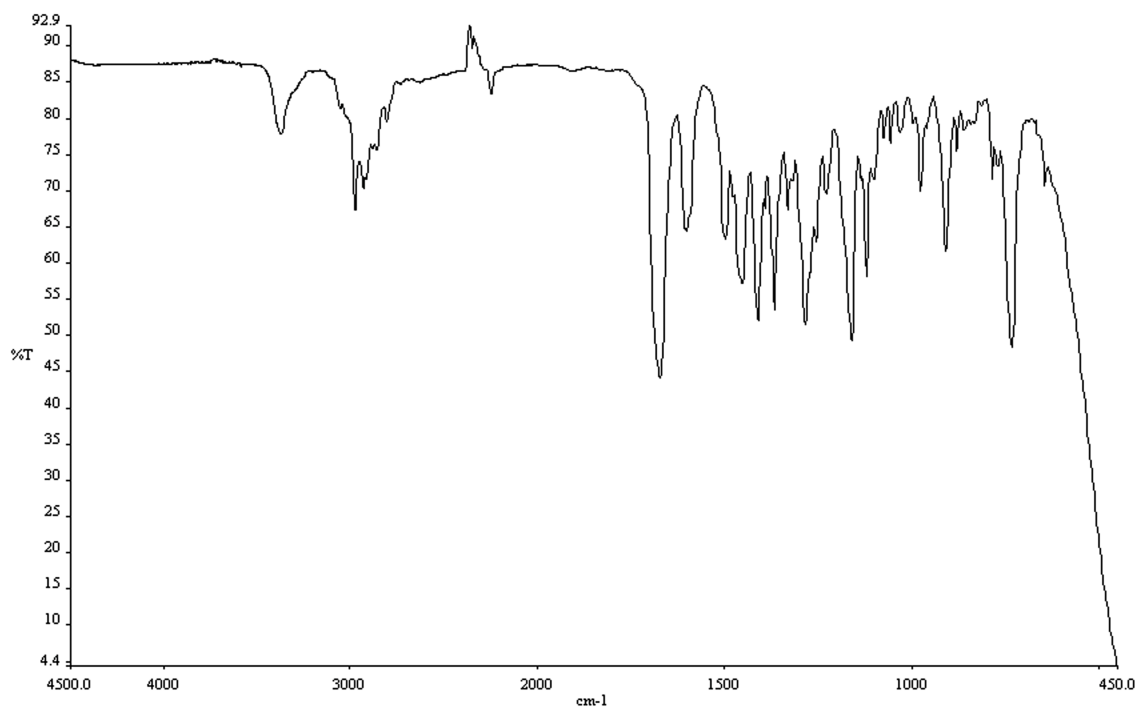
Figure A.2.8 Infrared spectrum (thin film/NaCl) of compound **474**.
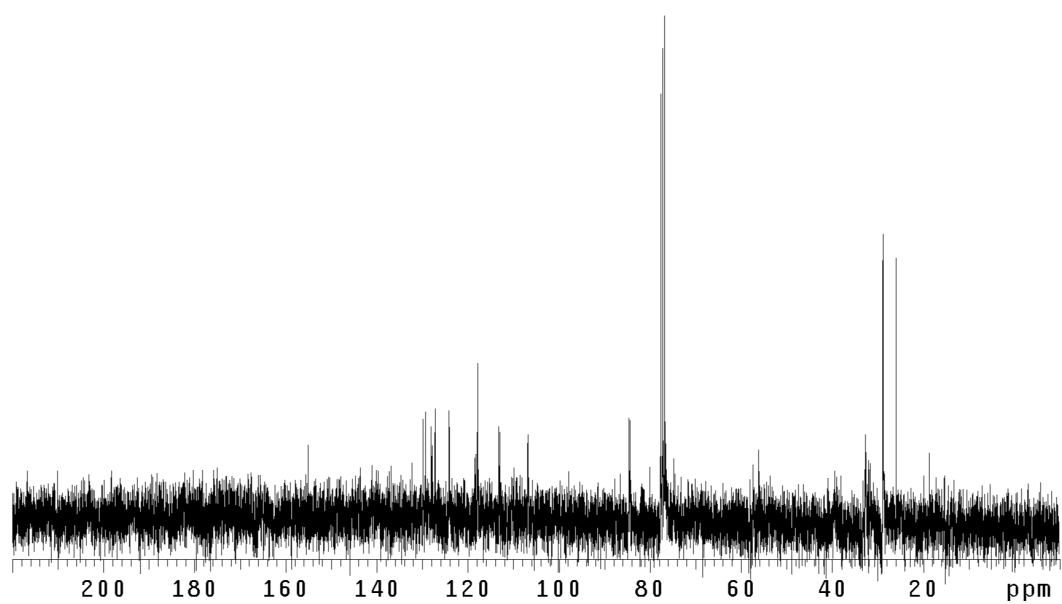
Figure A.2.9 ^{13}CNMR (75 Mhz, CDCl$_3$) of compound **474**.
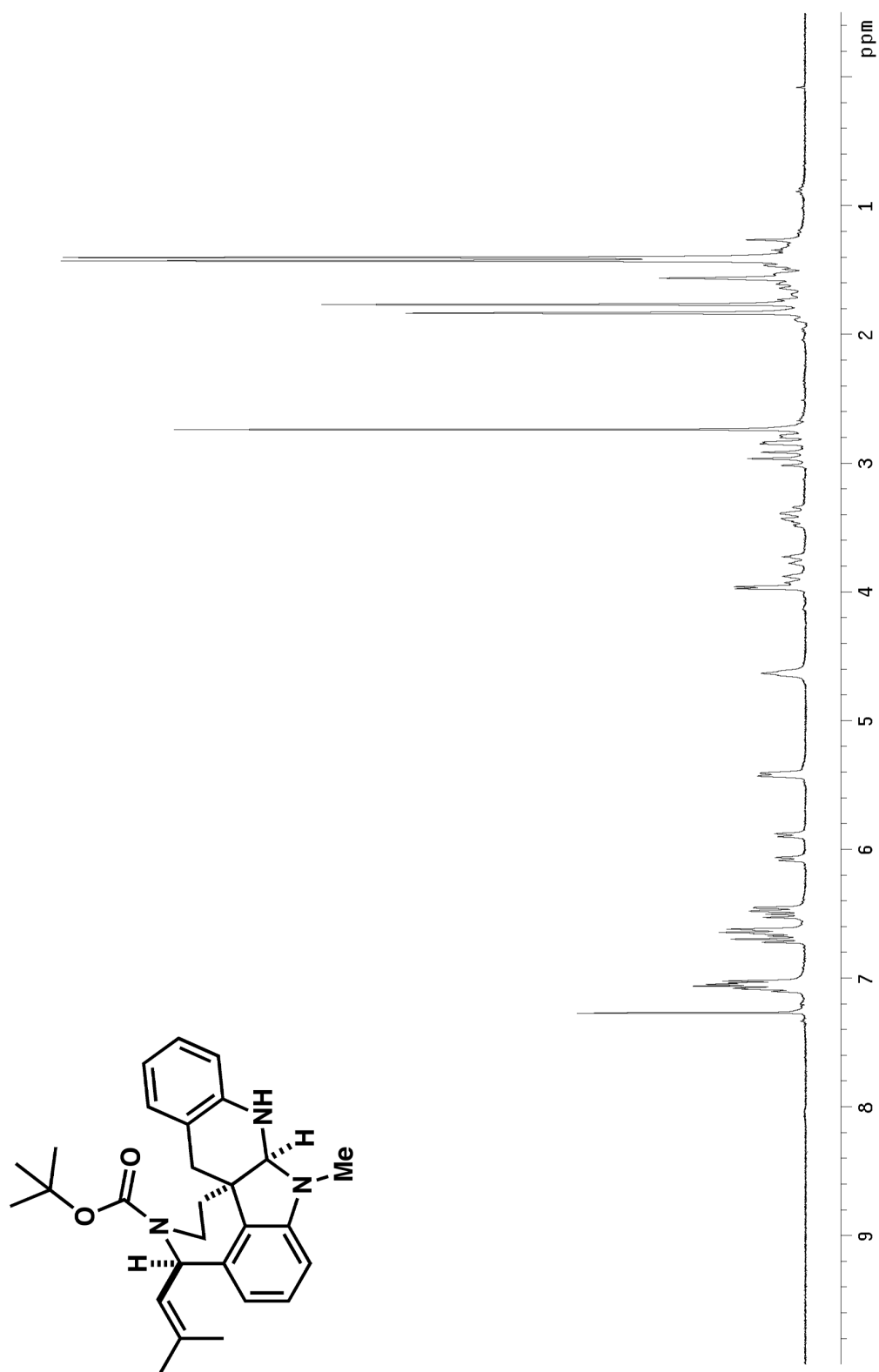
Figure A.2.10 ¹HNMR (300 MHz, CDCL₃) of compound **475**.
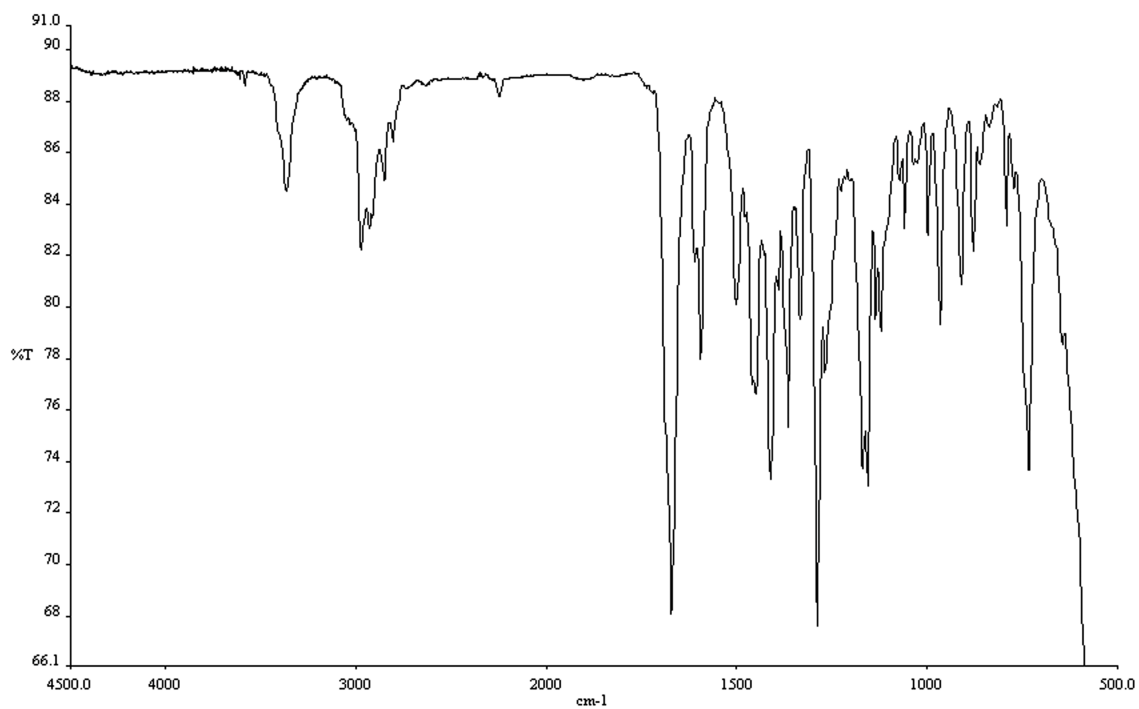
Figure A.2.11 Infrared spectrum (thin film/NaCl) of compound **475**.
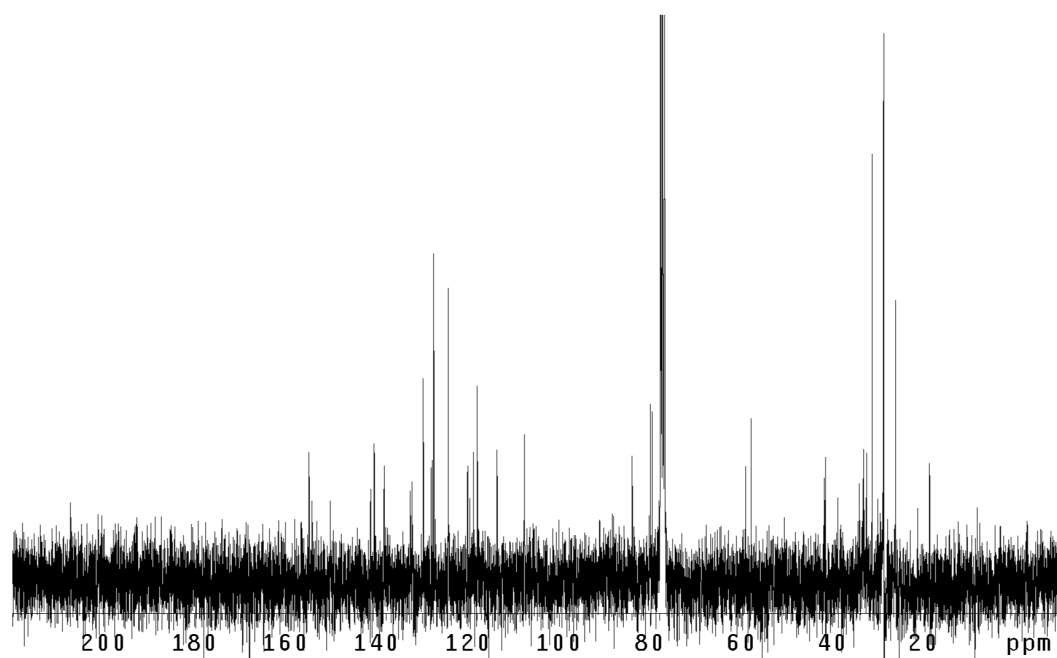
Figure A.2.12 ^{13}CNMR (75 Mhz, CDCl$_3$) of compound **475**.

Chapter 7

Recent Discoveries toward the Synthesis of the
Communesin Family of Indole Alkaloids

7.1 Background

7.1.1 Natural Product Synthesis

Natural Product Synthesis has long occupied a position of importance in the structural elucidation of compounds isolated from natural sources. In many cases, synthetic efforts have allowed correction of a flawed assignment. Despite many powerful spectroscopic techniques available for structure assignment, mistakes can still be made with the highly complex molecules found in the environment.[1] Synthetic efforts toward these natural products are thus critical to understand the chemistry and architecture of these compounds more in depth, as well as provide strategies for modifying their structures and activities as desired.

7.1.2 Nomofungin

In 2001, an intriguing natural product was isolated from a fungus (unidentified) growing on trees on the University of Hawaii campus by the research group of Dr. Thomas Hemsheidt.[2] The group cultured the fungus to be able to produce sufficient amounts of compound for analysis. Unfortunately, the culture ceased production of the novel compound, but the Hemsheidt group was still able to perform structural elucidation studies on the sample previously obtained. The chemical structure assigned to this compound, **434**, is shown in Figure 7.1.1, and the name nomofungin was given to the

isolation to reflect that the active fungal culture for the compound had been lost. Nomofungin showed interesting microfilament disrupting activity when used to treat cultured LoVo and KB cells.

7.1.3 The Communesins

The structure assigned to nomofungin closely resembles that of communesin B (**427**), one of two alkaloids isolated in 1993 from a strain of *Penicillium* sp. found on a marine algae.[3] These two structures are illustrated in Figure 7.1.1, also. Later, in 2004, communesins B (**427**), C (**428**), and D (**429**) were isolated from a strain of *Penicillium* sp. growing on a Mediterranean sponge.[4] The same year, from cultured *Penicillium expansum* Link MK-57, communesins D (**429**), E (**430**), and F (**433**) were extracted.[5] In 2005, two more communesins, G (**431**) and H (**432**), were isolated from *Penicillium rivulum* Frisvad.[6] With the exception of G and H, the communesins showed insecticidal activity and antiproliferative activity against cancerous cell lines.

Figure 7.1.1: Nomofungin and the Communesins.

Communesin		R	R'
426	A	CH₃	CH₃
427	B	CH₃	
428	C	H	
429	D	CHO	
430	E	H	CH₃
431	G	CH₃	CH₂CH₃
432	H	CH₃	CH₂CH₂CH₃
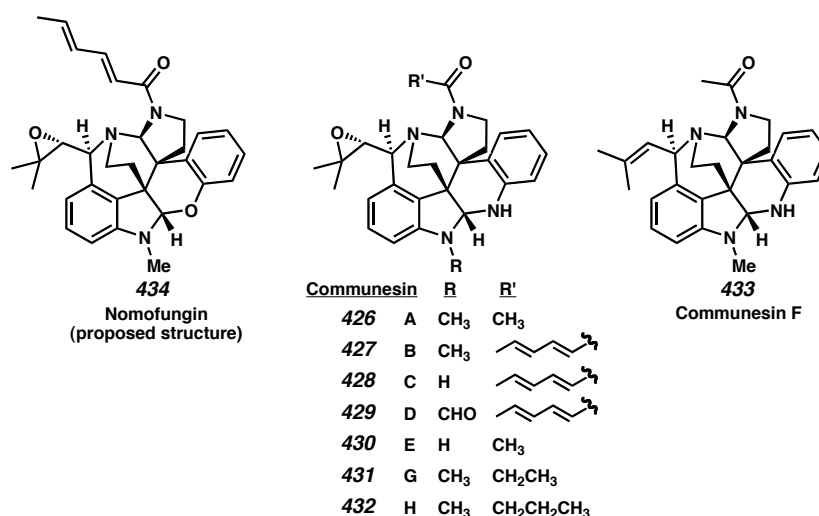
A related compound, perophoramidine (**425**, Figure 7.1.2) was isolated in 2002 from the ascidian *Perophora namei*.[7] It contains a similar core to the communesins, but in

a higher oxidation state, and it has the opposite diastereomeric relationship about the vicinal quaternary carbons and lacks the cycle formed from *N*-prenylation. Perophoramidine exhibited activity against a human colon carcinoma cell line.

Figure 7.1.2: Perophoramidine.

245
Perophoramidine
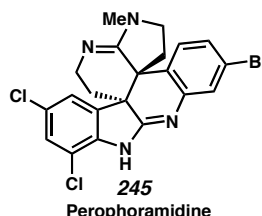
7.1.4 Comparison of Communesin B and Nomofungin

Given the similarity of the communesin B and nomofungin structures, a comparison was made of the two.[8,9] Amazingly, the reported spectroscopic data for the two compounds are practically identical (see Table 6.3.1, Chapter 6). This indicates that the two are, in fact, the same compound. Further comparison to synthetically characterized aminals and hemiaminals indicated that structure **427** was likely to represent the correct structure for both communesin B and nomofungin.[10]

When the biogenic origins of the compound are considered, the communesins can readily be derived from two tryptophan units (**439**, Figure 7.1.3). Nomofungin, however, would derive from a tryptophan and an unnatural benzofuran amino acid **476**. This consideration of the availability of biological compound precursors further supports the case for communesin B as the representative structure.

Figure 7.1.3: Biogenic Derivation of Communesin B and Nomofungin.
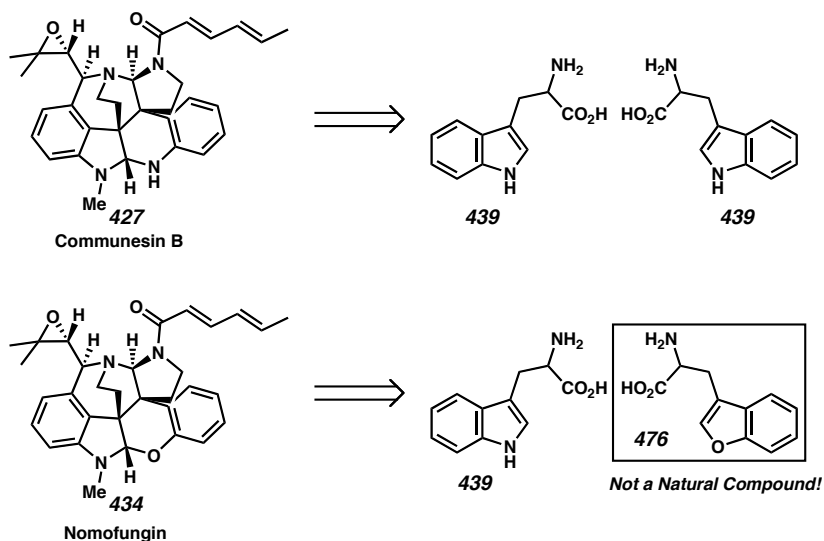
7.1.5 Biosynthesis of the Communesins

A synthetically relevant biogenetic proposal for communesin B is made in Figure 7.1.4. This hypothesis involves oxidation of tryptamine to form the oxidized oxindole **441** and a Diels-Alder reaction with the fungal natural product aurantioclavine (**435**). The newly formed bridged lactam **442** would be trans-amidated by the free primary amine to provide the spirocycle **443**. Further elaboration would provide communesin B. This inverse-demand Diels-Alder reaction proposed in the biosynthesis could also be a viable synthetic approach to the communesins.

Figure 7.1.4: Biosynthesis of Communesin B.
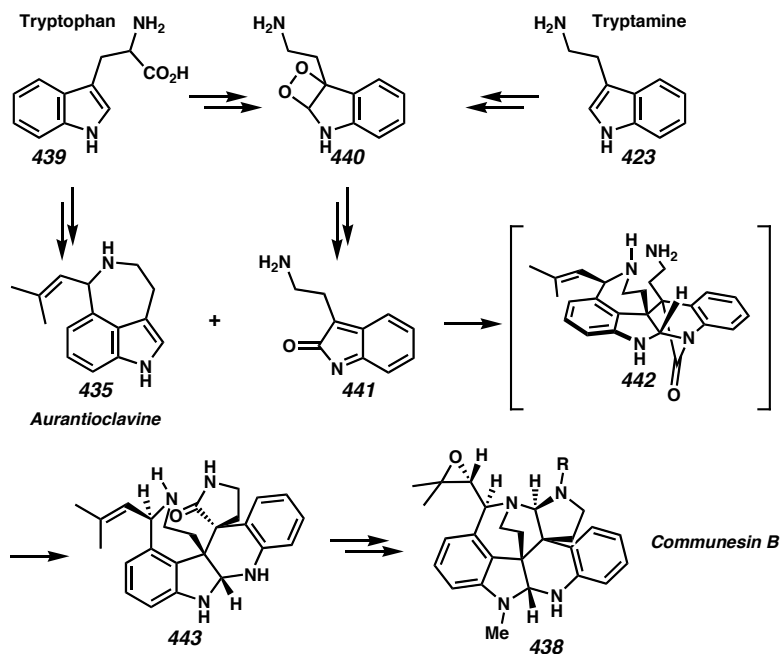
7.1.6 The Inverse-Demand Diels-Alder Reaction

7.1.6.1 General Reaction

The Diels-Alder reaction is one of the most useful and most used synthetic reactions. It has been used with complex substrates, can be used with a high degree of predictability, and is capable of constructing bonds between congested centers.

The traditional Diels-Alder reaction pairs an electron-rich diene **477** with an electron-deficient dienophile **478** (Figure 7.1.5). Thus, the HOMO of the diene reacts with the LUMO of the dienophile, and secondary orbital interactions stabilize an *endo* transition state for the reaction and thus provide selective formation of the major diastereomer **480**. Additionally, an electron-deficient diene can be paired with an electron-rich dienophile in an inverse-demand Diels-Alder reaction. The proposed reaction of an indole with an *o*-methide imine (i.e., **485** + **486** → **487**) falls into this latter category.

Figure 7.1.5: Types of Diels-Alder Reactions.
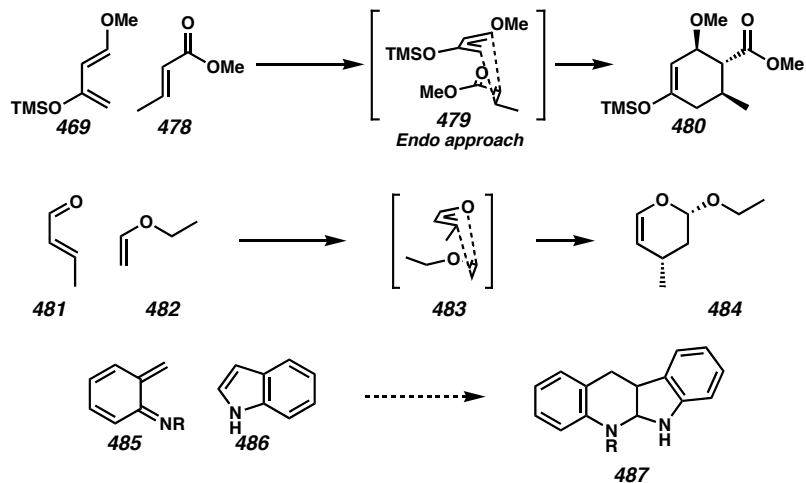
7.1.6.2 Corey's Benzylic Chloride Precursor

The Corey lab has developed a benzylic chloride precursor to an *o*-methide imine that is easy to handle and readily reacts in the presence of Cs_2CO_3 (Scheme 7.1.1).[11] A variety of electron rich dienes is tolerated in the Diels-Alder reaction to generate benzanulated piperidines. In our hands, this precursor served to generate the indoline system **470** in good yield.[8] More complex indoles also worked well in the reaction, as discussed in Chapter 6 and Section 7.2.3.

Scheme 7.1.1: The Corey Inverse-Demand Diels-Alder Reaction.
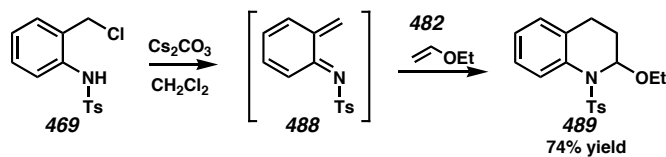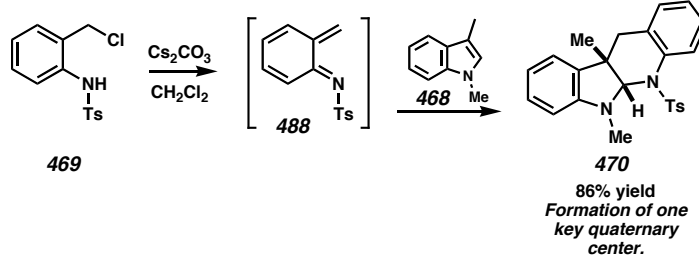
7.2 Synthetic Plan for Communesin: A Biomimetic Strategy

7.2.1 Retrosynthesis

Given our success with model systems for the Diels-Alder reaction, we anticipated that the benzopiperidine system in **438** could be dismantled via that cyclization in a biomimetic fashion (Figure 7.2.1). Such a transformation allows us to target derivative **490** of the natural product, aurantioclavine, and the *o*-methide imine **492**. The success of this cycloaddition would serve to further establish the viability of the proposed biosynthesis.

Figure 7.2.1: Biomemetic Retrosynthesis for Communesin B.
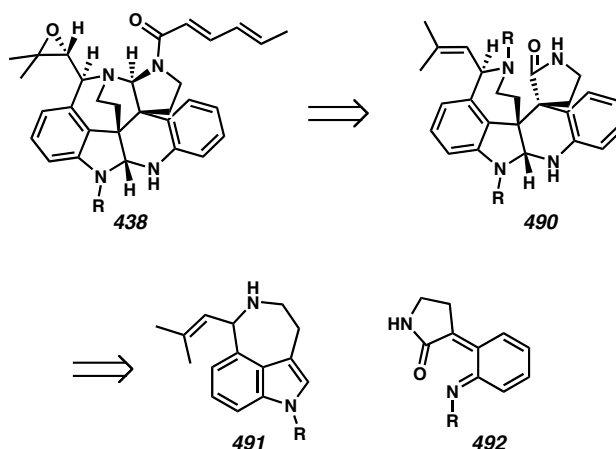
7.2.2 Synthesis of Aurantioclavine

As the retrosynthetic plan indicates, derivatives of aurantioclavine were needed. Fortunately, several approaches to this compound have been studied.[12] The sequence developed by Iwao to arrive at the nitro indole **479** was used for its ease and scaleability (Scheme 7.2.1).[13] Thus, the indole nitrogen and 2-position of gramine (**493**) were protected with a triisopropylsilyl group, so lithiation with *t*-butyllithium and reaction with the aldehyde **494** provided the benzylic alcohol **495**. This alcohol was somewhat unstable and interfered with reaction at the tertiary amine, so rearrangement to tertiary

alcohol **497** was effected with phosphoric acid. Quaternization of the amine and removal of the silyl group caused amine elimination to the α,β-unsaturated imine and allowed for conjugate nitromethane addition to generate nitro compound **497**. At this point, the heterogeneous reductive cyclization developed by Somei was used on a large scale to produce aurantioclavine (**435**) in useful amounts.[14] The secondary amine could be selectively functionalized, and then the indole nitrogen could be methylated if desired.

Scheme 7.2.1: Synthesis of Aurantioclavine.
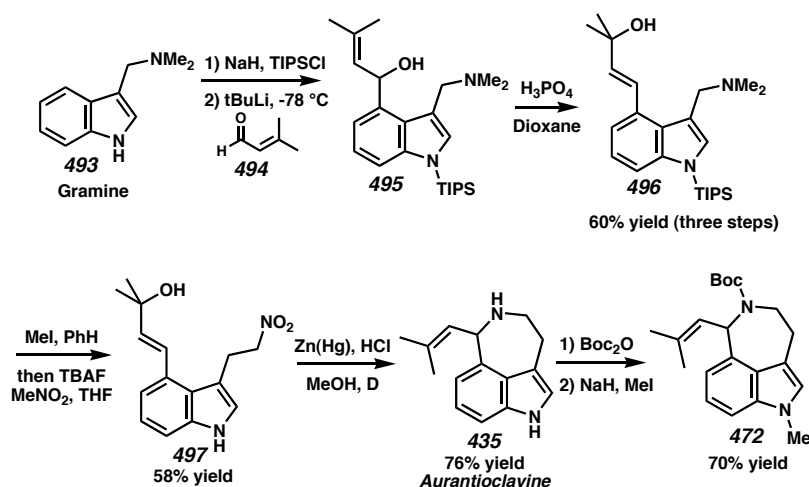
7.2.3 Reaction of Aurantioclavine with Corey's *o*-Methide Imine Precursor

Reacting aurantioclavine derivative **435** with benzyl chloride **469** provided the Diels-Alder adducts **472** and **473**. Removal of the tosyl group allowed for separation of the diastereomers and structural characterization.[8]

Scheme 7.2.2: Aurantioclavine and the Corey Benzyl Chloride.
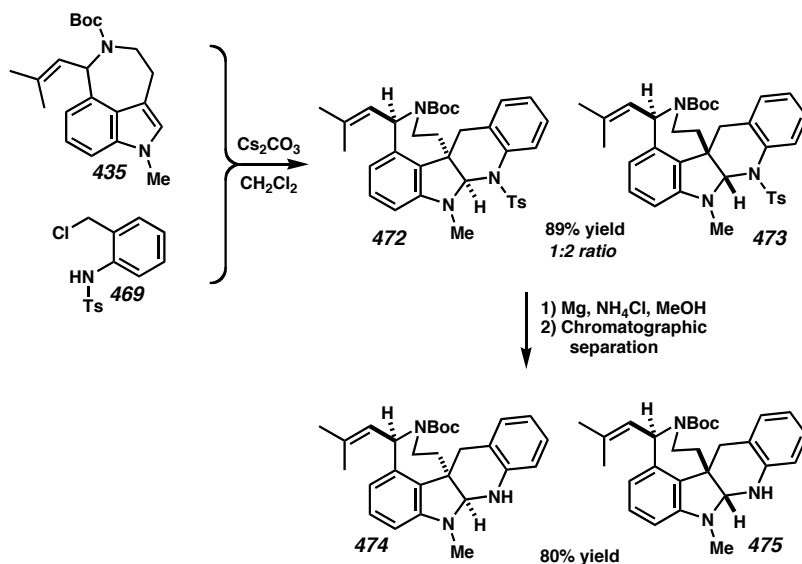
7.3 Expanded Substitution in the Diels-Alder Reaction

7.3.1 Retrosynthesis

Having successfully reacted an aurantioclavine derivative with an unsubstituted *o*-methide imine, a substituted diene was desired. Thus, reaction with aurantioclavine could provide synthetic intermediate **493**, which contains a synthetic handle to install communesin functionality (Figure 7.3.1).

Figure 7.3.1: A Retrosynthetic Study of Communesin B with a Monosubstituted Diene.
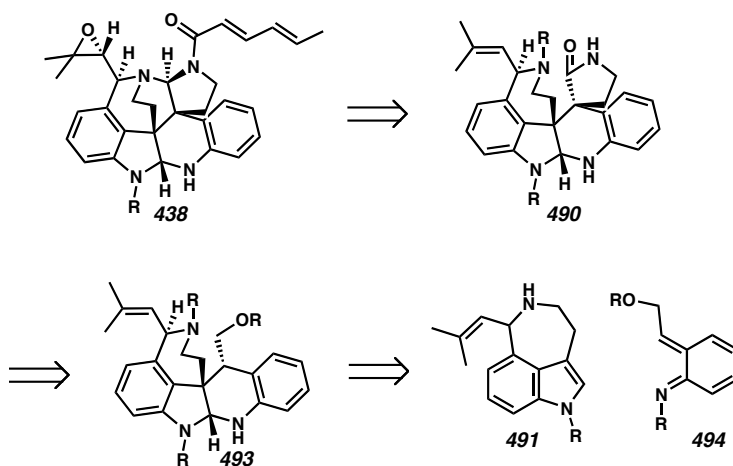
7.3.2 Diels-Alder Considerations

7.3.2.1 *Exo* versus *Endo* Reactivity

The substitution present on *o*-methide imine **494** requires consideration of Diels-Alder selectivity. In the traditional Diels-Alder reaction, *endo* selectivity is preferred as it provides secondary orbital interactions in the transition state. For these inverse-demand Diels-Alder reactions, however, these interactions are not present and do not control the transition state to the same extent. On the other hand, the aromatic reactants could gain stabilization through π-stacking interactions between the electron-rich and electron-deficient rings (Figure 7.3.2). Thus, an *endo* transition state may be favored, though steric interactions would favor the *exo* transition state. With appropriate substitution, either transition state geometry could be synthetically productive if a high level of selectivity could be obtained.

Figure 7.3.2: Transition State Geometry Considerations.
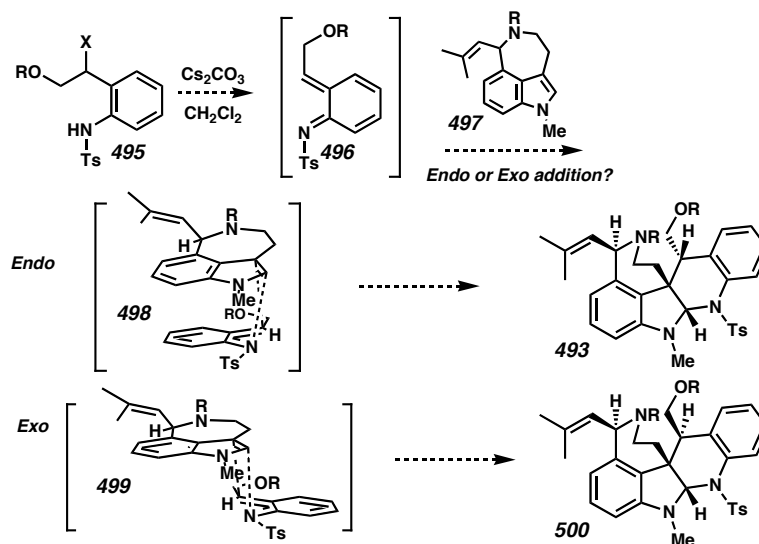
7.3.2.2 *o*-Methide Imine Geometry

The selective formation of a specific geometry is important with a substituted *o*-methide imine. For a monosubstitution, as in **496**, an *E*-olefin is favored because of steric

interactions. With disubstitution, however, selectivity could be eroded unless some sort of direction is programmed into the substrate. For the initial trials, only the monosubstitution was used for the Diels-Alder reaction.

Scheme 7.3.1: Geometry Considerations for the Diene.
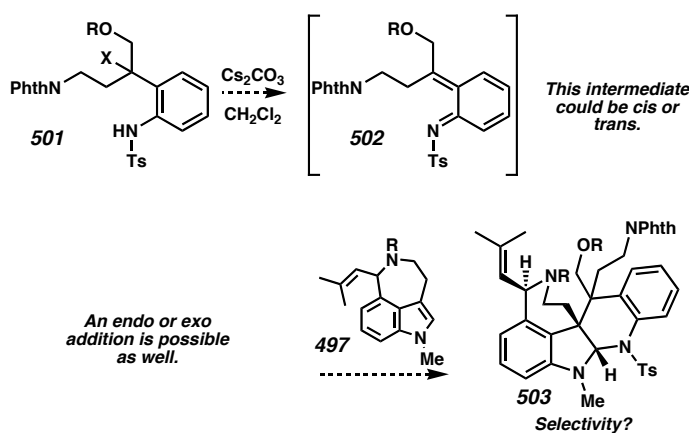
7.3.3 Monosubstituted Inverse Demand Diels-Alder Reactions

7.3.3.1 Allylic Substitution

7.3.3.1.1 Synthesis of the Diene Precursor

Initial incorporation of a benzylic substituent was approached through addition of allyl Grignard reagent to aldehyde **505** (Scheme 7.3.2). An allyl group was chosen for its lack of sensitive functionality and for the possibility of subsequent functionalization. Attempts to transform alcohol **507** to a benzylic halide were unreliable, requiring development of a novel method for *o*-methide imine formation.

Scheme 7.3.2: Synthesis of a Substituted o-Methide Imine Precursor.
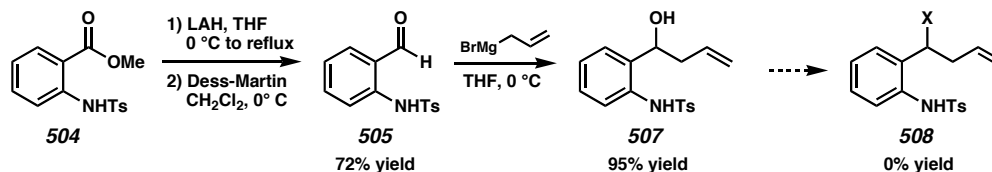
7.3.3.1.2 Reaction with 1,3-Dimethylindole

In lieu of elimination of a benzylic chloride, the secondary alcohol **507** could be converted in situ to a mesylate, and exposure to Cs_2CO_3 caused elimination of the mesylate anion to generate the *o*-methide imine **509** (Scheme 7.3.3). This diene reacted with 1,3-dimethyl indole, a useful indole dienophile for probing reactivity, to generate the annulated piperidine **510** as one diastereomer. The relative stereochemistry of the substituents was confirmed by measuring nOe interactions between the methyne and methyl protons. To achieve the relative stereochemistry shown in **510**, an *endo* transition state must be operative during the Diels-Alder reaction, as diagrammed for **509**.

Scheme 7.3.3: The Diels-Alder Reaction with a Substituted o-Methide Imine.
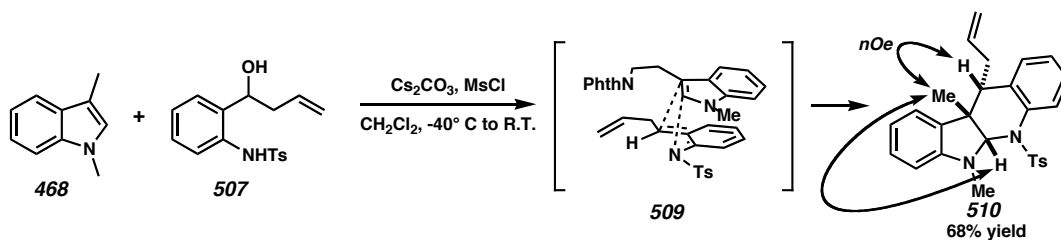
7.3.3.2 Protected Primary Alcohol Substitution

7.3.3.2.1 The *o*-Methide Imine Precursor

The success of the coupling between **468** and **567** with *endo* selectivity prompted the use of more elaborate precursors that could lead to synthesis of perophoramidine. A straightforward approach was thus taken to the silyl ether *o*-methide imine precursor **513** (Scheme 7.3.4). 2-Bromoaniline could be reacted with *p*-tolylsulfonyl chloride and then subjected to a Stille coupling in practical yield to generate styrene **512**. Dihydroxylation proceeded well, and the preferential protection of the primary alcohol was enhanced by initial formation of the tin acetal. As with the allylic substitution, a few attempts were made to convert the secondary hydroxyl group in **513** to a halide and mimic the Corey

precursor, but these attempts failed. Fortunately, the alternative approach to generate the

o-methide imine using methanesulfonyl chloride was successful and obviated the need

for an additional synthetic step to generate an alkyl halide.

Scheme 7.3.4: Generation of the o-Methide Imine Precursor.
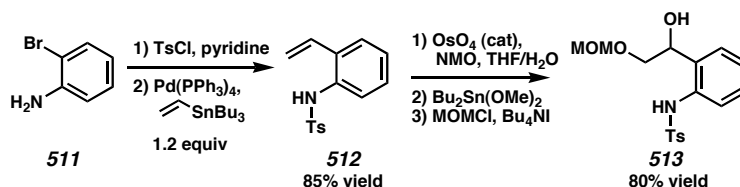
7.3.3.2.2 The Tryptamine-Derived Dienophile

As aurantioclavine could be a demanding substrate for initial trials, a less

hindered tryptamine analogue, **516** (Scheme 7.3.5), was sought. **516** would also provide

for entry into a perophoramidine-like framework. Thus, tryptamine (**423**) was protected

as the phthalimide and methylated under phase-transfer conditions.

Scheme 7.3.5: Phthalimide and Methyl Protection of Tryptamine.
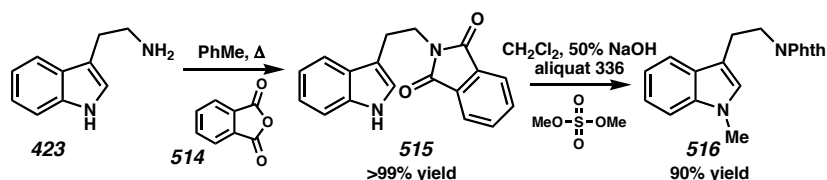
7.3.3.2.3 The Inverse Demand Diels-Alder Reaction

Secondary alcohol **513** successfully reacted under trifluoromethanesulfonic

anhydride conditions to generate the desired diene (Scheme 7.3.6) in a similar manner to

the use of methanesulfonyl chloride previously. Indole **516** then coupled to generate the

indoline annulated piperidine **518**. The relative stereochemistry obtained for both **510**

and **518** is reminiscent of the perophoramidine core, and indoline **518** could, in fact, be a

possible intermediate upon a route to perophoramidine. Further modifications to attempt such a transformation were then pursued.

*Scheme 7.3.6: Diels-Alder Reaction between Tryptamine **516** and Diene Precursor **513**.*
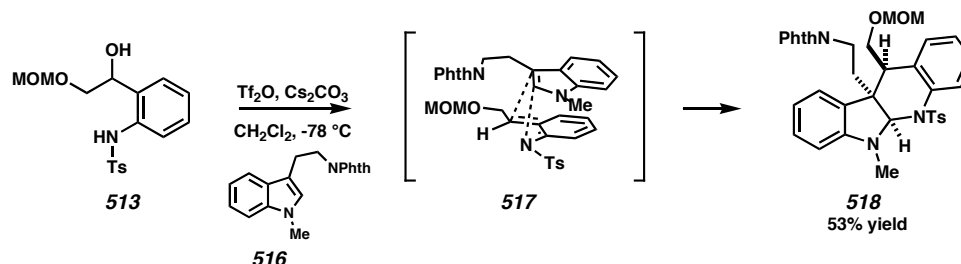
7.3.4 Elaborating the Diels-Alder Reaction Product to a Perophoramidine Core

The latent primary alcohol in **518** could be revealed with trimethylsilyl iodide, though the product had some unexpected properties (Scheme 7.3.7). The isomers **519** and **520** could be separated via flash column chromatography, but epimerized back to a 4:1 mixture of **519** to **520** within 30 min. This mixture could be oxidized with Dess-Martin periodinate (DMP) reagent to aldehyde **521**. Because only the free hydroxyl **519** was oxidized, oxidants that could not promote the equilibrium between **520** and **519** would generally cause decomposition of **520**. With oxidants other than DMP, recovery of **521** was generally less than 10% of the theoretical yield.

*Scheme 7.3.7: Manipulations of Diels-Alder Product **518***.
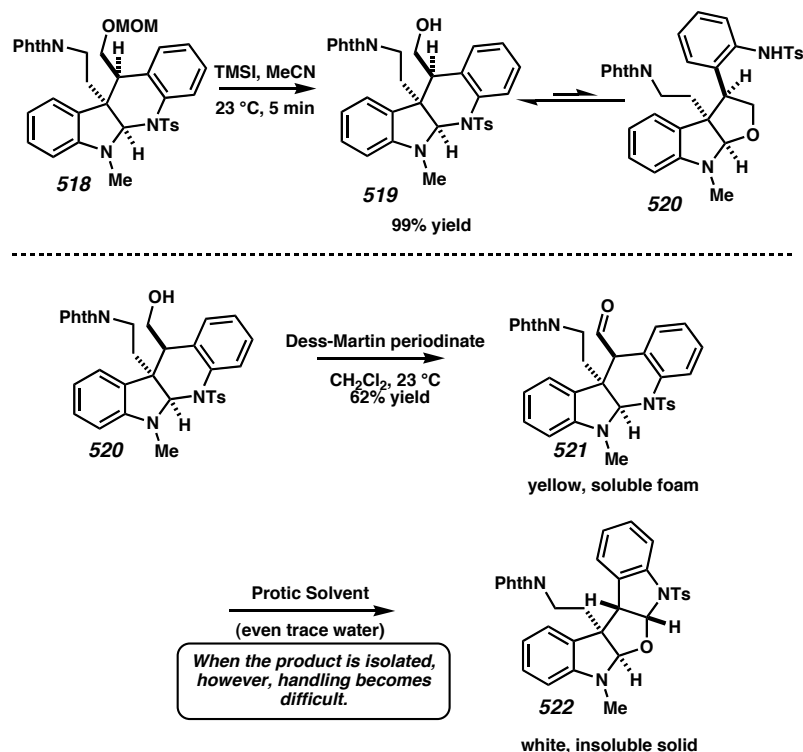
The aldehyde **521** provided its own problems. After silica-gel purification, the aldehyde was obtained as a yellow, soluble foam. When dissolved in dry deuterated chloroform, **521** could be visualized spectroscopically, but showed no evidence of an aldehydic form by ^{1}H NMR. Structure **522** was then proposed be the predominant structural form. Solubility was an issue with this compound since, over time, a white precipitant could be seen forming in the chloroform solution. Similarly, **522** could be dissolved in methanol, but after several seconds precipitated as a white solid. Generally, chloroform was the only viable solvent for handling **522**, and solubility was limited in that solvent as well. Infrared spectroscopy and ^{1}H and ^{13}C NMR further suggest that **522** is the structure of the white precipitant.

Despite the solubility problems of **522**, however, refluxing ethanol and hydrazine hydrate dissolved the tetrahydrofuran **522** and hydrazinalized the phthalimide protecting

group (Scheme 7.3.8). The ring system rearranged to form the enamine **523** in good yield. This enamine proved difficult to characterize as it readily decomposed. As with many of these indoline alkaloids, exposure to air while in solution caused the solution to turn blue-green within minutes. From the enamine, a few initial alkylations were attempted without significant results. Additionally, attempts to form the communesin framework drew our attention to a novel substrate for this reaction.

*Scheme 7.3.8 Formation of Enamine **523***.
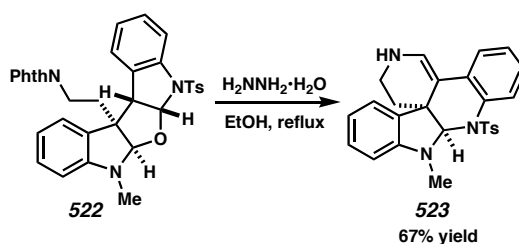
7.3.5 The Monosubstituted Diels-Alder with Aurantioclavine

The success of reacting **513** with a tryptamine derivative and of subsequent reactions prompted an attempt to react this precursor with an aurantioclavine derivative. Unfortunately, despite many trials, no adduct was detected (Scheme 7.3.9). Given that the monosubstituted *o*-methide imine wouldn't react with aurantioclavine, synthesis of a disubstituted *o*-methide imine was not attempted.

Scheme 7.3.9: Reaction of Aurantioclavine with a Monosubstituted Diene.
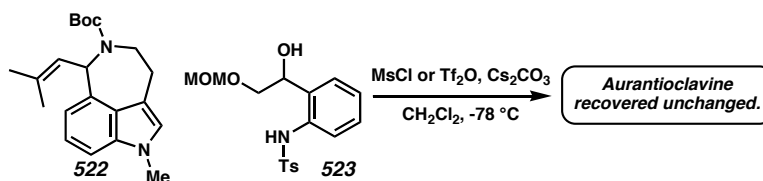
7.4 Many Diene Precursors

At this stage in the synthesis of the communesins, many potential *o*-methide imine precursors were synthesized with the goal of reacting with aurantioclavine. Most

intriguing were those that could present the possibility of undergoing an intramolecular version of the inverse-demand Diels-Alder reaction (Figure 7.4.1).[15] An intramolecular approach would allow for greater control over *o*-methide imine geometry and could react with the demanding aurantioclavine substrate by promotion through enforced proximity.

Figure 7.4.1: Retrosynthesis of Communesin B with an Intramolecular Diels-Alder.
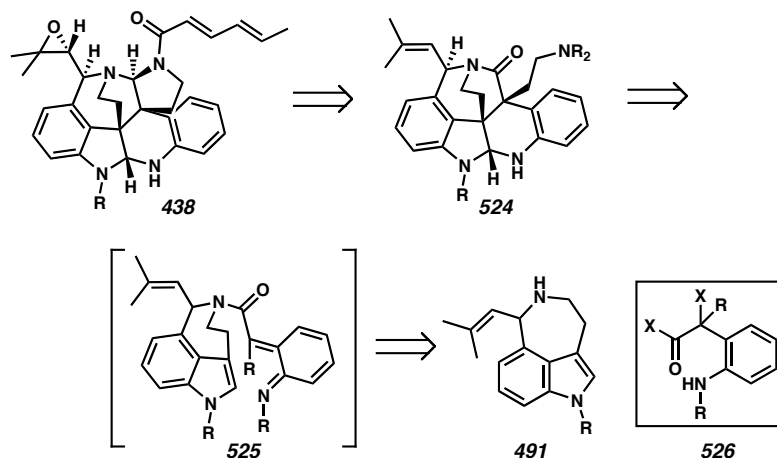
7.4.1 The First Intramolecular Diels-Alder Reaction Approach

Amide **531** is an analogue of the *o*-methide imine precursor **513** that is set up for an intramolecular Diels-Alder reaction with aurantioclavine (Scheme 7.4.1). The amide was hoped to result from opening of the imide **529** by the secondary amine of 1-methylaurantioclavine. Imide **529** was readily synthesized from isatin by addition of a vinyl or allyl Grignard reagent and subsequent protection as a carbamate. Unfortunately, acylation of aurantioclavine was unsuccessful under a variety of conditions, though control reactions with piperidine, azepane, or 2-methylpiperidine showed transamidation.

Scheme 7.4.1: Generating an Intramolecular Substrate.

527

528a n=0 84% yield
528b n=1 76% yield

529a n=0 98% yield
529b n=1 64% yield

530

531
0% yield
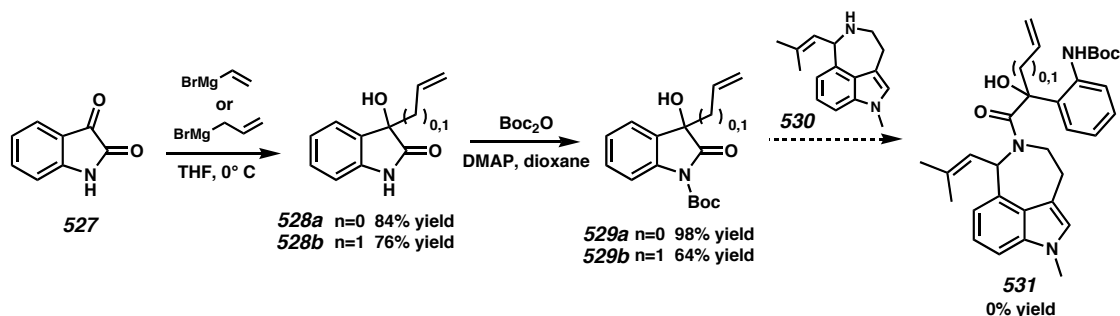
7.4.2 Another Intramolecular Diels-Alder Reaction Approach

Since opening of imide **529** by 1-methylaurantioclavine proved difficult, a more accessible route to form amide **531** was sought. A ring-opened acid or ester **535** could react with aurantioclavine, whereas imide **529** would not (Scheme 7.4.2). Thus, ketone **534** was produced from amino-ester **532** by tosylation and addition of lithiated acetonitrile. Attempts to transform **534** to **535** were largely unsuccessful because **534** was recalcitrant to reduction and the acidity of the **534** quenched nucleophiles.

Scheme 7.4.2: Formation of a Cyanoketone.

XX

XX
80% yield

XX
93% yield

XX
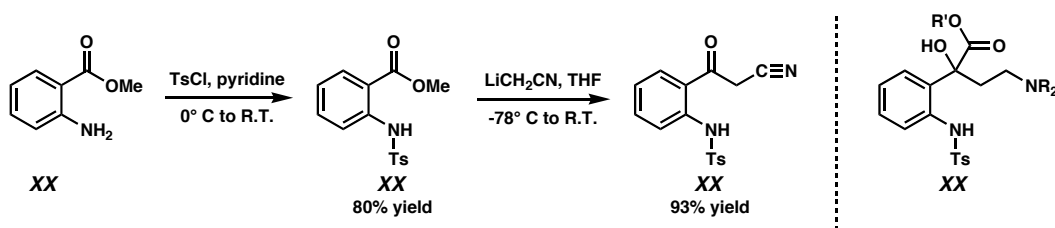
7.4.3 A Cyclopropane *o*-Methide Imine Precursor

An alternative to generating a diene from a benzylic halide or a benzylic mesylate could be the opening of a cyclopropane ester such as **538** (Scheme 7.4.3). Such an ester can be synthesized from isatin through a Horner-Wadsworth-Emmons reaction and cyclopropanation from the ylide generated from trimethyl sulfoxonium iodide.[16] Attempts to form an amide with aurantioclavine met with failure. The ability of the

cyclopropane to form the desired *o*-methide imine has not yet been tested, and reaction with a more reactive dienophile in an intermolecular sense may yet succeed.

Scheme 7.4.3: Generation of the Cyclopropyl Ester.

527

537
90% yield

538
67% yield
1.6:1 dr
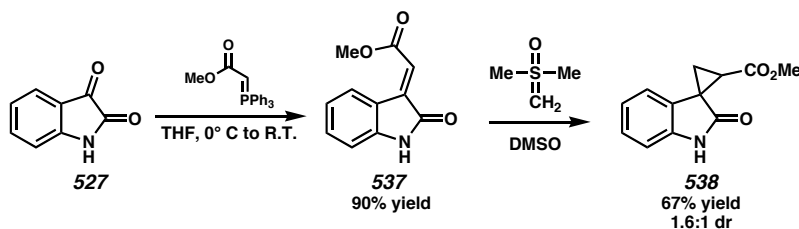
7.4.4 Epoxide Opening

One final method for *o*-methide imine generation could be opening of a benzylic epoxide such as **539**, which is formed in one step from isatin (Scheme 7.4.4).[17] Either basic or acidic conditions could potentially generate an intermittent diene. However, when the transformation was attempted in the presence of 1,3-dimethylindole, nonspecific decomposition of **539** was observed with 1,3-dimethylindole recovered unchanged.

Scheme 7.4.4: An Epoxide as an o-Methide Imine Precursor.

527

539
59% yield

540

No Reaction
Observed
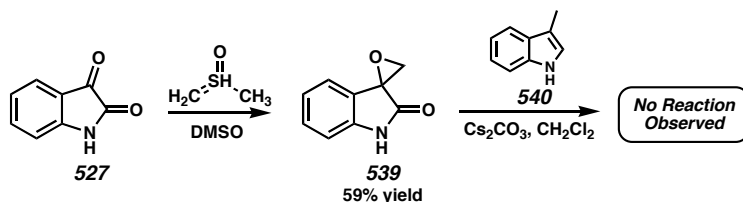
7.5 An Intramolecular Diels-Alder Reaction

7.5.1 Retrosynthesis

Given the difficulties with aurantioclavine as a dienophile, formation of the piperidine ring via an intramolecular Diels-Alder using a diene already in a reactive conformation was next considered. Such a motif is present in **542** as an appropriately substituted benzisoxazole (Figure 7.5.1). Thus, benzisoxazole **543**, when coupled to

aurantioclavine, offered a stable *o*-methide imine that could react with aurantioclavine in a controlled manner as a result of the tethered system.

Figure 7.5.1: Retrosynthesis of an Intramolecular Diels-Alder Reaction.
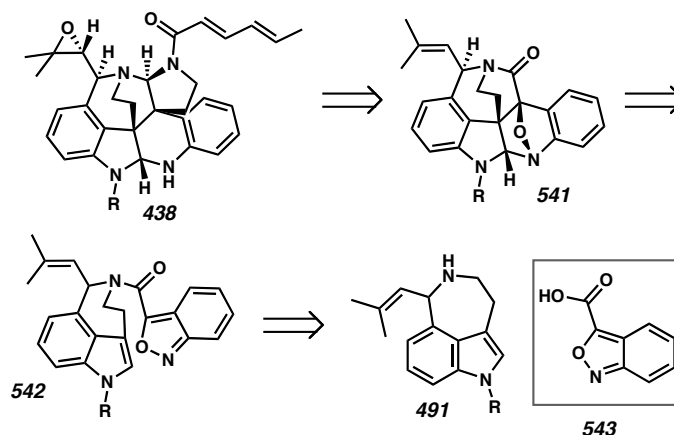
7.5.2 Benzisoxazole Synthesis

The benzisoxazole carboxylic acid **543** has been reported to be accessible through several routes (Scheme 7.5.1). The first, reported by Arndt and Eistert[18] in the 1920s, adds diazomethane to the acid chloride of 2-nitrobenzylic acid (**545**) to generate the α-diazoketone **546**. Addition of this compound to a mixture of acetic and formic acid, followed by refluxing the resulting solution for one minute, afforded a black mess, from which *N*-hydroxyisatin could be isolated in low yield. Unfortunately, half the attempts at this transformation resulted in a very rapid decomposition of the material to smoke and tar. An improvement in this reaction was obtained by adding $BF_3 \cdot OEt_2$ to a solution of **545** in dichloromethane. The resulting yield was more than double that of the previous technique, and no more reactions were lost due to an excessive exotherm. The hydroxy-isatin **546** could be rearranged to the benzisoxazole carbonate in aqueous base, and carboxylic acid **543** was recovered upon acidification. However, the multiple steps and low yield created a bottleneck for the production of **543**.

Scheme 7.5.1: Routes to Benzisoxazole Carboxylic Acid 543.
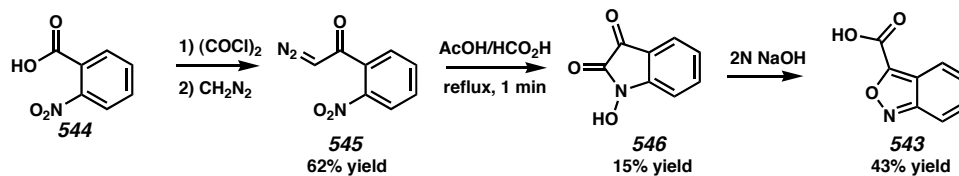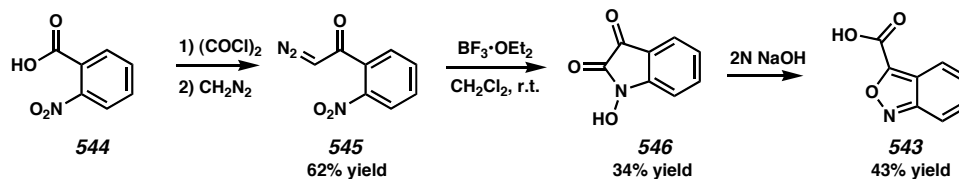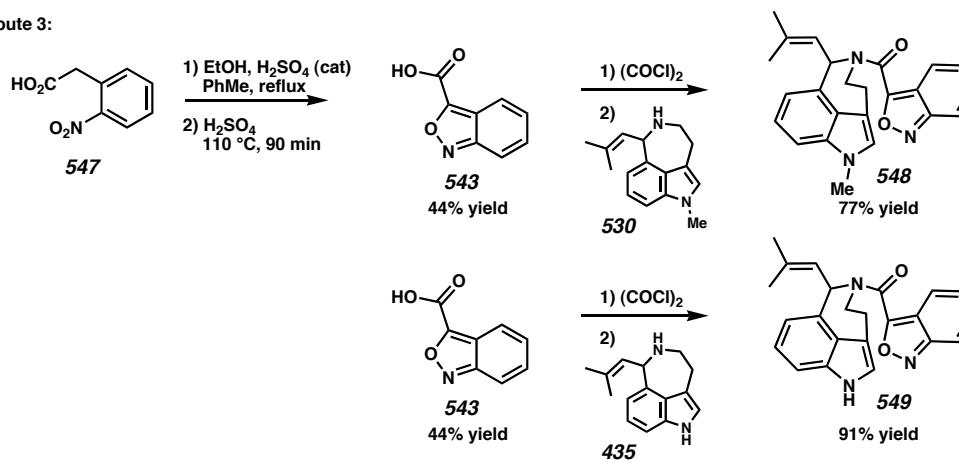
A much more practical route to **543** starts from commercially available carboxylic acid **547**.[19] Fischer esterification and then heating in neat sulfuric acid provides the benzisoxazole acid **543** in useful yield and multigram quantities. With **543** available in useful quantities, coupling to aurantioclavine could proceed through the acid chloride and generate the intramolecular Diels-Alder reaction substrate **549**. Similarly, 1-methylaurantioclavine reacted with the acid chloride to afford amide **548**.

7.5.3 Intramolecular Diels-Alder Reaction

Substrates **548** and **549** were subjected to both thermal and acidic conditions, with the acidic conditions providing for a cleaner reaction. Unfortunately, the benzisoxazole reacted completely with the butenyl side chain of the aurantioclavine to generate the bridged polycycles **550** and **551** (Scheme 7.5.2). nOe analysis demonstrated the relative stereochemistry shown for **550**, and that of **551** was assigned by analogy.

Scheme 7.5.2 Intramolecular Diels-Alder Reaction.
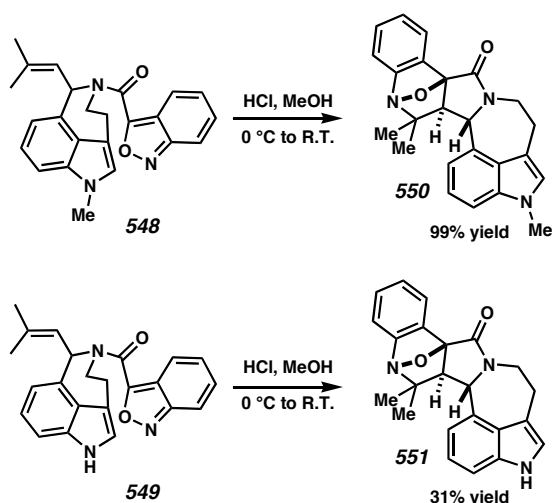
7.6 The Biomimetic Diels-Alder Reaction

7.6.1 Retrosynthesis

At this point, the original biosynthetic proposal for communesin B (Scheme 7.6.1) prompted development of oxidized oxindole **553** that would act as a precursor to an *o*-methide imine. Such a compound could allow access to a Diels-Alder product such as **442** that would allow for further functionalization.

Figure 7.6.1: Biomimetic Retrosynthesis.
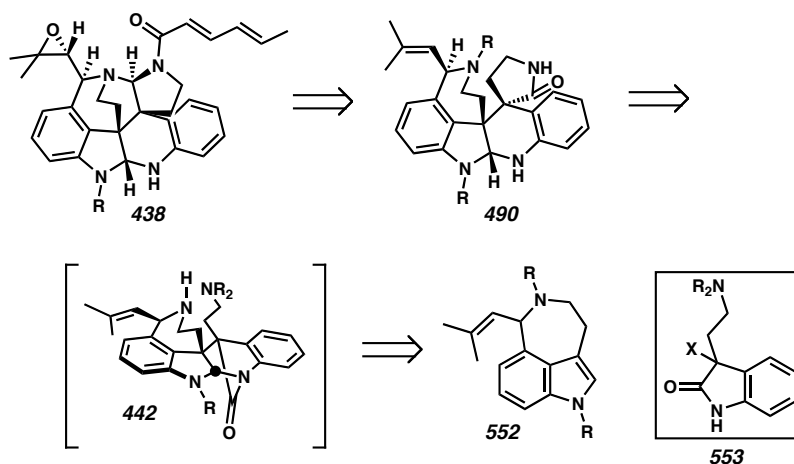
7.6.2 Initial Halooxindole Synthesis

After screening a large number of halogenating agents, suitable conditions were found to generate fluorooxindole **55** and chlorooxindole **555** from phthalimide-protected tryptamine (Scheme 7.6.1). The fluorinating agent selectfluor (Aldrich) was the only reagent to provide **554**.[20] In contrast, several reagents generated chloride **555**, but only dichlorohydantoin (**536**) allowed for a practical yield without over-oxidation to the 5-haloindole or 5-halooxindole.[21] Regrettably, no reagents could be found to generate a bromo or iodooxindole from phthalimide-protected tryptamine. Attempts to generate these compounds resulted in over-oxidation, decomposition of the substrate, or elimination of the phthalimide.

Scheme 7.6.1: Oxidation to Oxindole and Halogenation.
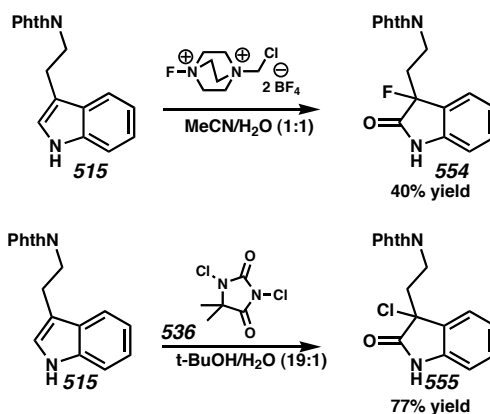
7.6.3 Attempted Diels-Alder with Halooxindoles

Unfortunately, when halooxindoles **554** and **555** were reacted with base in the presence of 1,3-dimethylindole, no generation of an *o*-methide imine was observed, and no product adduct was isolated (Scheme 7.6.2). As the oxindoles **554** and **555** were recovered unchanged from many of the attempted conditions, we hypothesized that a more reactive benzylic leaving group was needed. Thus, an attempt was made to access a bromooxindole.

Scheme 7.6.2: Fluoro and Chlorooxindoles Are Unreactive.
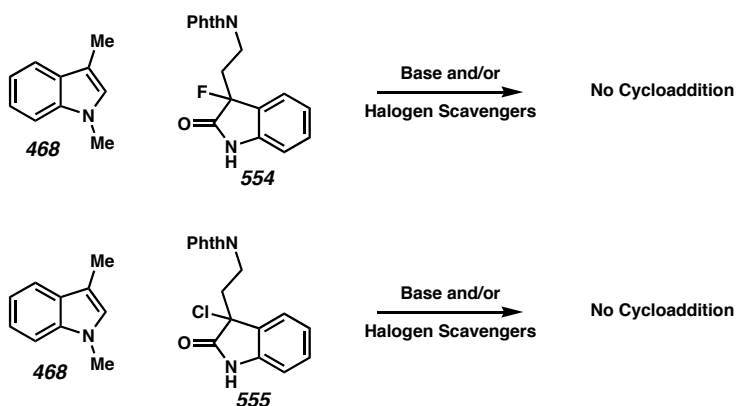
7.6.4 A More Reactive Halooxindole

As stated previously, the phthalimide protecting group interfered with the oxidation and bromination of tryptamine. To circumvent these problems, an azide was targeted as a masked nitrogen. This compound was accessed by first forming alkyliodide **557** from tryptophol (**556**), and then reacting the iodide with sodium azide (Scheme 7.6.3). Selective oxidation of indole **558** to oxindole **559** could be accomplished with one equivalent of *N*-bromosuccinimide (NBS) at low temperature, though competitive bromination at the indole 5-position was observed at temperatures above –20 °C. Avoiding formation of the 5-bromooxindole is necessary because it is inseparable from the non-brominated oxindole. The second stage of the oxidation, forming the 3-bromooxindole from the oxindole, was not as easily effected, however.

Scheme 7.6.3: Generation of a Bromooxindole.
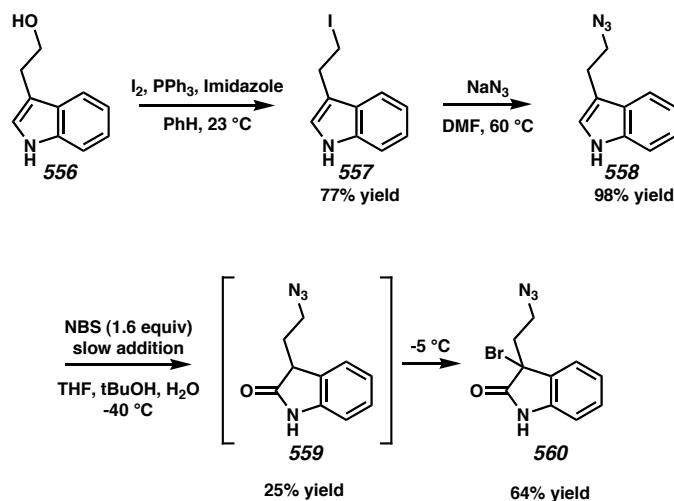
After much modification and many control experiments, several controlling factors were determined for the oxidation of oxindole **559** to 3-bromooxindole **560**. Bromination at the 3-position and bromination at the 5-position of the oxindole **559** were similar in rate; however, neither event occurred appreciably below 10 °C. Thus, the

initial oxidation to the oxindole without bromination at the 5-position could be performed at –40 °C with addition of NBS performed via cannula. The temperature is then allowed to rise to –10, –5, and 0 °C at intervals to try to maximize the 3-bromination, since, at room temperature, bromination on the aromatic ring appears favored. Additionally, because of the similarity in rates for the competing halogenations, once oxindole **559** reacts to about two-thirds completion, bromination of the aromatic ring of **560** begins to compete with bromination at the 3-position of **559** due to statistical effects. Thus, only 1.5-1.6 equiv of NBS is added to indole **558** to be certain that no 3,5-bromoindole is formed, since that product is inseparable from **560**. Under these conditions, some oxindole **559** remains, but can be easily separated from **560** via silica-gel chromatography.

Other trials demonstrated that potassium *tert*-butoxide promotes 3-bromination and accelerates the reaction rate, but it also causes *N*-bromination and complicates the workup with an aqueous extraction. Furthermore, if the reaction mixture is concentrated in the presence of *N*-bromooxindole, that compound can then brominate at the 5-position of another molecule. Therefore, the reaction was ultimately run under neutral conditions while slowly warming as described above. Once the reaction reached completion, the solvent was removed under reduced pressure, and the residue was immediately purified chromatographically. Finally, compound **560** must be chromatographed in pentane/ether, as it forms an oil with any residual higher-boiling solvent upon concentration, and then the oil decomposes within hours.

7.6.5 Reaction of Bromooxindole 560 with an Aurantioclavine Derivative

The bromooxindole **560** reacted with aurantioclavine derivative **561** to form an

adduct of the anticipated molecular weight (Scheme 7.6.4). However, differing reactivity

was observed for coordinating and noncoordinating solvents. In THF or acetonitrile, for

example, one major product was formed that demonstrated only a slightly lower R_F on

silica-gel TLC plates (2:1 hexanes/ethyl acetate eluent) than the starting compounds. On

the other hand, benzene or dichloromethane influenced the reaction so that a major and

two minor products were formed.[22] The major product from these noncoordinating

solvents had an R_F significantly lower than the starting materials and a molecular weight

corresponding to the desired adduct, and a minor product with a higher R_F was identical

to that obtained in coordinating solvent. The other minor product, having a lower R_F, had

a molecular weight corresponding to the addition of two *o*-methide imine units to

aurantioclavine derivative **561**. Initially, the two products **562** and **563** of the anticipated

formula weight were thought to be diastereomers of the desired product.

Scheme 7.6.4: Reaction of Aurantioclavine with 3-Bromooxindole.
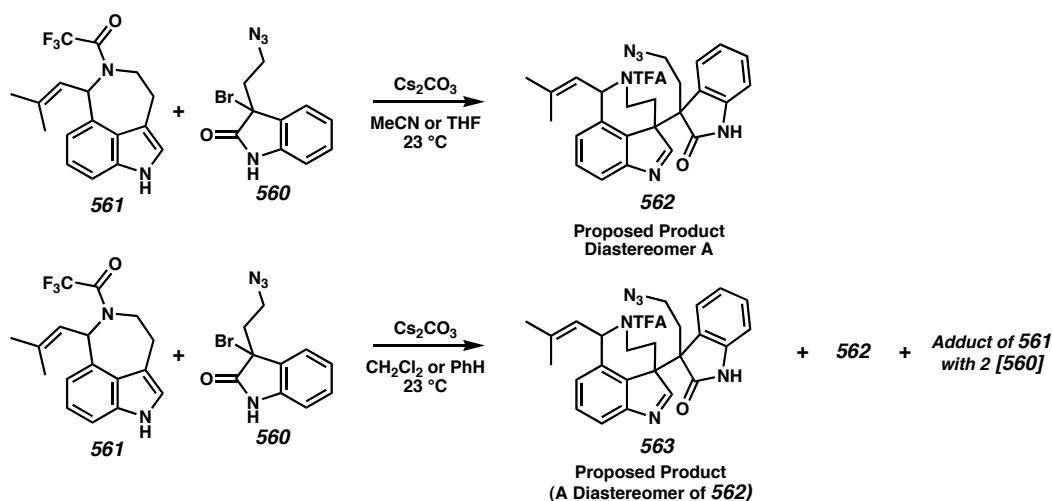
7.6.6 Stereochemical Elucidation via Spectrographic Techniques

To establish the relative stereochemistry of these compounds, they were subjected to transformations that would construct the core ring system and allow for structural characterization similar to those made for nomofungin and the communesins. Thus, the amide nitrogen of **562** would be sulfonylated to generate imide **565** (Scheme 7.6.5). Next, reduction of the azide to the amine would allow formation of the lactam and closure of the piperidine as shown in **566**. The trifluoroacetamide group could be hydrolytically cleaved, which would remove the encumbering rotamers observed in the ^{1}H and ^{13}C NMR spectra for these compounds. These transformations were pursued with both supposed diastereomers, and the postulated structures **562**, **565**, **566**, and **567** were all studied for diagnostic nOe interactions. In a maddening turn of events, however, no conclusive information was obtained from any compounds, as the key proton signals all seemed to interact with no specificity. Moreover, the signal patterns were very similar for both series of compounds, so no conclusions could be made from the studies. As a final indication that something was amiss, many reduction attempts to form the aminal **568** either failed to react or caused general decomposition, despite the use of reagents precedented for that reduction.

Scheme 7.6.5: Reaction and Manipulation of the Adducts of the Diels-Alder Reaction.
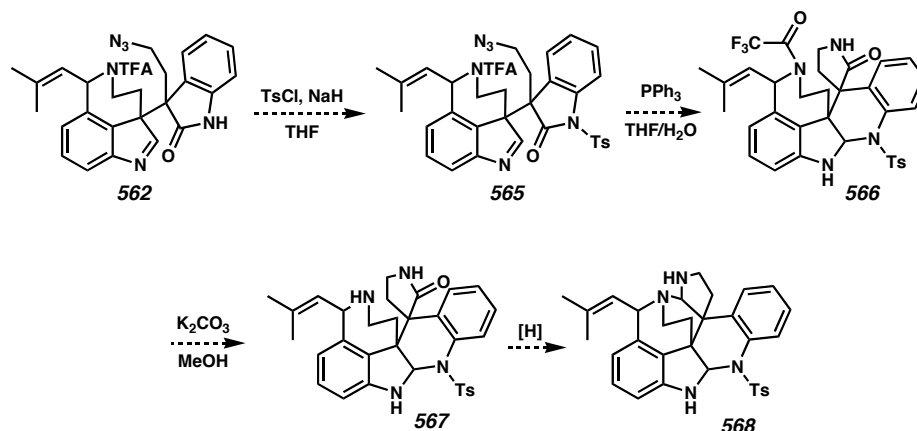
7.6.7 Functionalization to Generate a Crystalline Derivative

7.6.7.1 Modification of the Major Product in THF

Because of the failure of NMR techniques to elucidate the structure of the Diels-Alder and subsequent products, many attempts were made to elaborate the products of the *o*-methide imine addition so that single crystals could be grown that were suitable for X-ray diffraction studies. The major product from reaction in THF was first studied.

A serendipitous reaction with excess nosyl chloride in the presence of sodium hydride reacted with the amide to generate the sulfonimide and oxidized the core of the indole to a 3-chloroindolenine (Scheme 7.6.7). The observed oxidation was competitive with imide formation, as one equivalent of nosyl chloride generated both the expected imide and some oxidized indole. In the presence of hydroxide ion, hydroxyl incorporation was observed as well as chloride addition.

Scheme 7.6.7: Transformation that Lead to a Crystalline Compound.
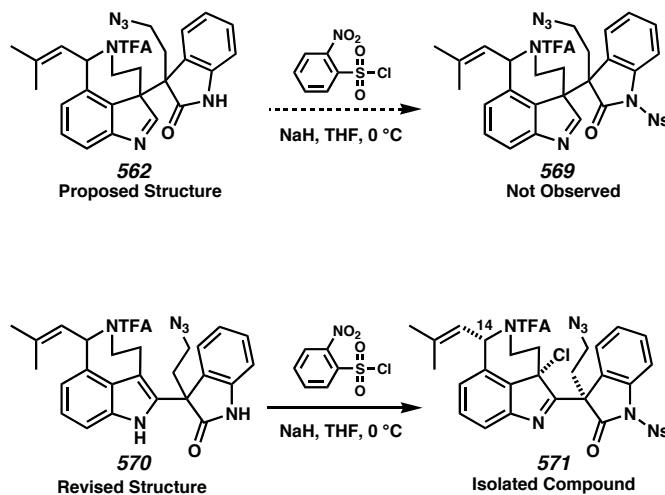
The isolate from the reaction with nosyl chloride a highly crystalline compound **571** that formed crystals suitable for X-ray diffraction in the collection tubes from chromatographic purification. To our surprise and dismay, the atomic map thus obtained clearly showed a 2-3' connection between the indolenine and oxindole rather than the desired **562** (Figure 7.6.2). Spectroscopic data of the indole addition product also favor the structure presented as **570**. Unfortunately, **570** is not a productive intermediate in the synthesis of the communesins. Furthermore, the relative stereochemistry between the quaternary carbon center and butenyl group at C(14) was that obtained from an *endo* transition state and was therefore opposite that needed for synthesis of the communesins.

*Figure 7.6.2: Crystal Structure of **571***.
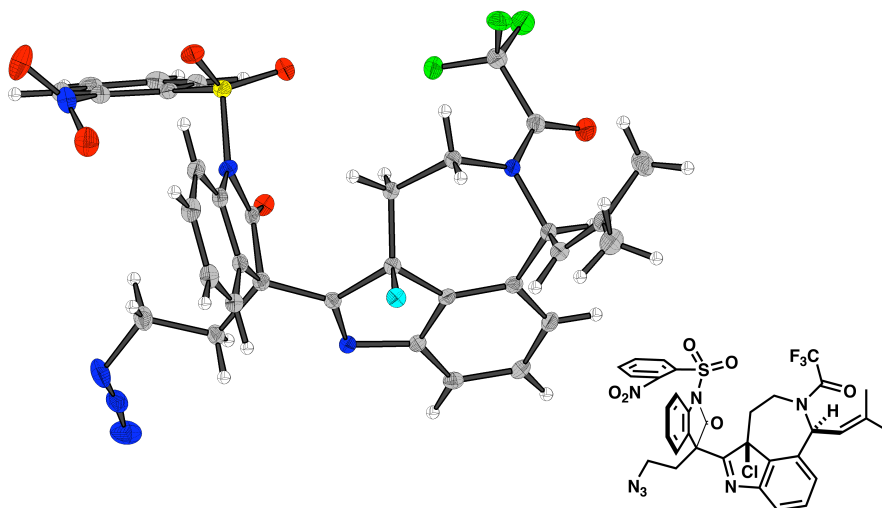
7.6.7.2 Modification of the Major Product in CH$_2$Cl$_2$

With the hope that the major product from the *o*-methide imine addition run in CH$_2$Cl$_2$ would prove to be the desired 3-3' linked compound, modifications were initiated that could provide a suitable version of that product in a crystalline form. Again, a nosyl group provided a suitable crystal. In this case, excess sodium hydride and nosyl chloride were used to functionalize both the amide and indole nitrogen (Scheme 7.6.8). Subsequent reduction of the azide allowed for cyclization to the crystalline lactam **575**. As the X-ray diffraction showed, this compound contained a 6-3' connection (Figure 7.6.3). Aurantioclavine derivatives appear reluctant to form the desired vicinal quaternary centers under electrophilic reaction conditions.

Scheme 7.6.8: Formation of a Second Crystalline Compound.
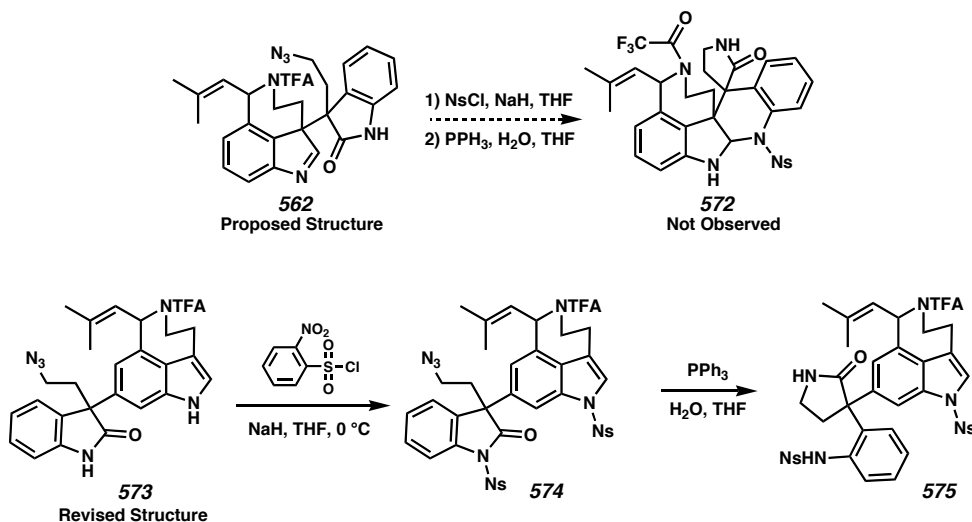
Figure 7.6.3: X-Ray Structure of the 6-3' Product.
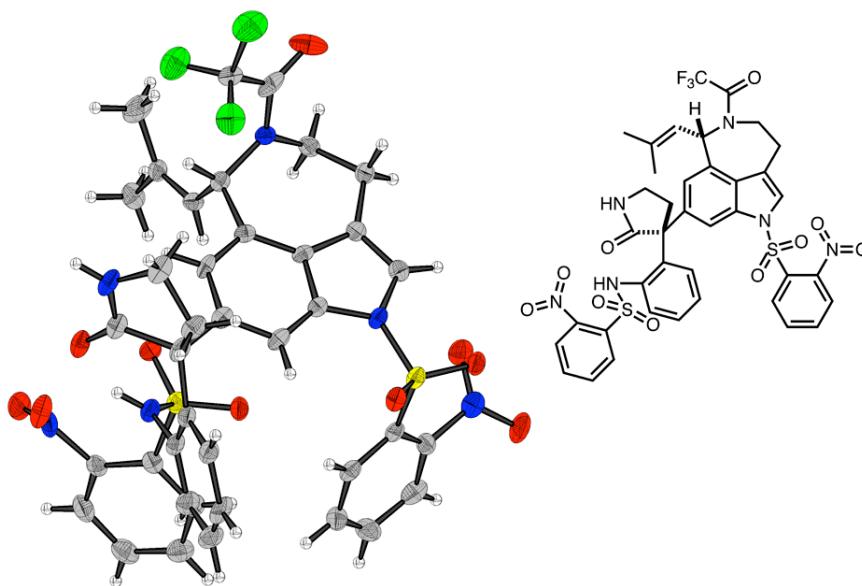
The resulting bond formations for the preceding compounds indicate that a Diels-Alder mechanism is not operative for this reaction. Instead, nucleophilic addition to the highly reactive *o*-methide imine is more likely. This conclusion is supported by work from the Funk laboratories using similar *o*-methide imines.[23]

7.6.7.3 Proposed Structures of the Minor Product in CH$_2$Cl$_2$

The third product from this addition, [**561** + 2**577**], that contains two *o*-methide imine additions could be a combination of the other two major products. In other words, it could contain both 2 and 6 additions of the electrophile (i.e., **576**, Figure 7.6.4). Alternatively, the case could be that an *o*-methide imine unit first reacts with a bromooxindole to form **578**, a product observed via mass spectrometry, which then forms a new *o*-methide imine and reacts with the aurantioclavine starting material at either the 2 or 6 position.

Figure 7.6.4: Possible Double Electrophilic Substitution Structures.
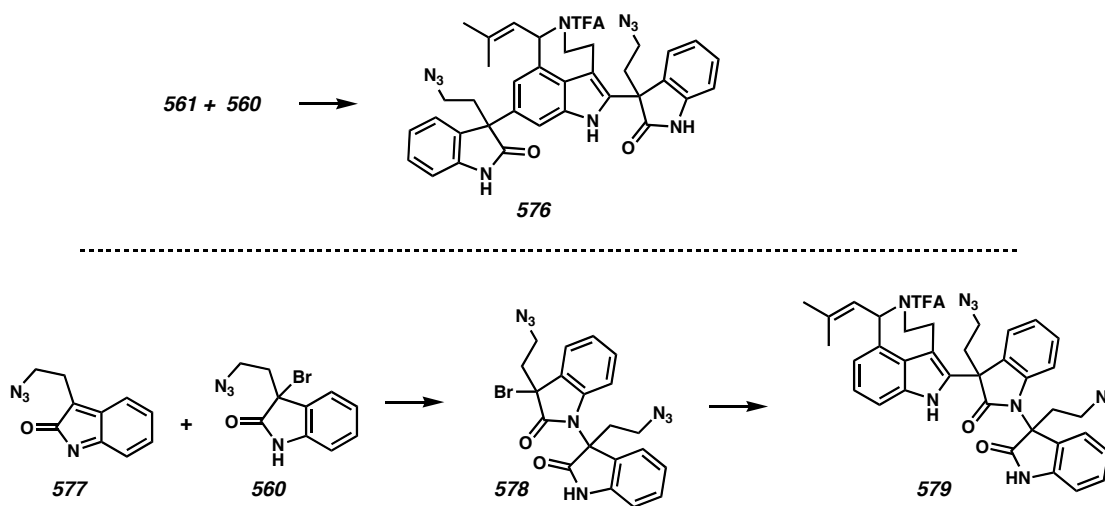
7.7 Conclusion

Several variants of electrophilic dienes have been developed to react with indoles in inverse Diels-Alder reactions. Many of these *o*-methide imine precursors have been reacted with simple indoles as dienophiles to generate new carbon-carbon bonds, including quaternary carbon center formation. Unfortunately, aurantioclavine, the desired nucleophile to pursue a synthesis of the communesins, has not displayed similar reactivity. In the presence of the potent electrophile **577** reaction is seen, but the reaction

forms a bond at the 3 or 6 position of aurantioclavine rather than form the key vicinal quaternary carbon centers. An alternate strategy must then be devised for the synthesis of the communesins.

7.8 Experimental

7.8.1 Materials and Methods

Reactions were performed in flame-dried glassware under a nitrogen atmosphere. Solvents were dried and purified using activated alumina columns. All other reagents were used as received from commercial sources. Reaction temperatures were controlled by an IKAmag temperature modulator. Thin-layer chromatography (TLC) was performed using E. Merck silica gel 60 F254 precoated plates (0.25 mm) and visualized by UV and *p*-anisaldehyde staining. ICN silica gel (particle size 0.032-0.063 mm) was used for flash chromatography. ^{1}H and ^{13}C NMR spectra were recorded on a Varian Mercury 300 spectrometer (at 300 MHz and 75 MHz, respectively) in $CDCl_3$ and are internally referenced to the residual chloroform peak (7.27 ppm and 77.23 ppm, respectively) relative to Me_4Si. Data for ^{1}H NMR spectra are reported as follows: chemical shift (δ ppm), multiplicity, coupling constant (Hz), and integration. Data for ^{13}C NMR spectra are reported in terms of chemical shift. IR spectra were recorded on a Perkin Elmer Paragon 1000 spectrometer and are reported in frequency of absorption (cm^{-1}). High resolution mass spectra were obtained from the California Institute of Technology Mass Spectrometry Facility.

7.8.2 Synthesis of Compounds

7.8.2.1 Model Studies for the Inverse Demand Diels-Alder
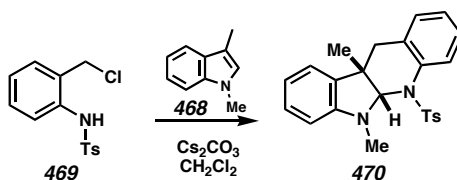
Indoline 470: The synthesis of indoline **470** is described in Section 6.6.2 of this thesis.
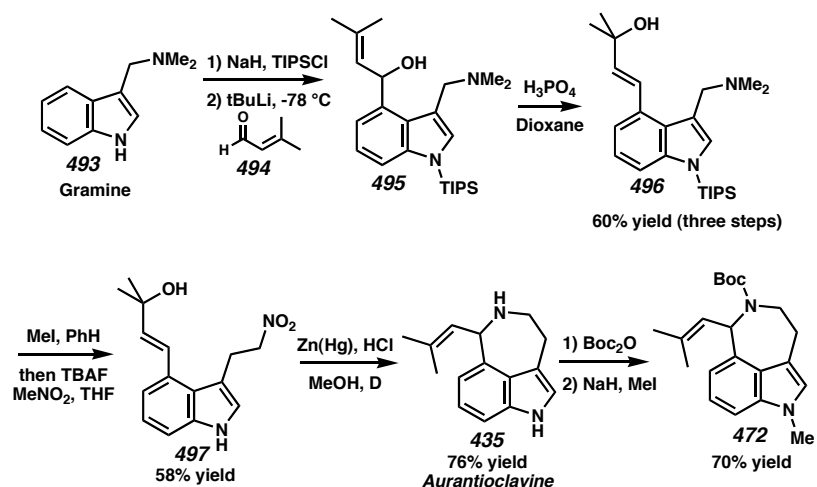
Aurantioclavine 435: A flame-dried flask (50 mL) equipped with a teflon stirbar was charged with indole **496** (20.4 g, 49.19 mmol), which was subsequently dissolved in benzene (100 mL). To the resulting solution was added methyl iodide (12.4 mL, 199 mmol) was added. The mixture was stirred for 12 hours. The reaction was then concentrated under reduced pressure. The resulting salt was redissolved in THF (100 mL) and dry nitromethane (30 mL). A solution of TBAF (1 M in THF, 74 mL, 74 mmol) was added slowly after the reaction had been cooled to 0 °C. After allowing the reaction

to come to room temperature and stir for 15 minutes, the reaction was quenched with water and extracted three times with ether. The organic layers were combined, the solution was dried over magnesium sulfate, and the solvent was then removed under reduced pressure. Purification was performed via flash column chromatography (5:1 to 0:1 gradient of hexanes/ethyl acetate) and washing the resulting solid with dichloromethane to afford nitro compound **497** (3.25 g, 11.85 mmol, 24% yield) as a yellow solid.

A flame-dried flask (250 mL) equipped with a teflon stirbar was charged with nitro compound **497** (400.1 mg, 1.458 mmol), which was subsequently dissolved in MeOH (104 mL) and 2*N* HCl (36 mL). To this solution was added amalgamated zinc, which had been formed from zinc dust (5.33 g, 62.42 mmol) and mercuric chloride (793 mg, 2.92 mmol) in 2*N* HCl (36 mL) and subsequently rinsed with MeOH. The mixture was stirred at reflux for 3 h. The reaction was then decanted from the remaining amalgam and basified to pH >10. The solid was removed by filtration, and the resulting solution was extracted 5 times with dichloromethane. The organic layers were combined, the solution was dried over magnesium sulfate, and the solvent was then removed under reduced pressure. Purification was performed via flash column chromatography (18:1 dichloromethane/methanol with 0.5% NH_4OH) to afford aurantioclavine **435** (204.7 mg, 0.904 mmol, 62% yield) as a yellow foam that had spectral characteristics identical to those previously reported.[13,14]

472 Me
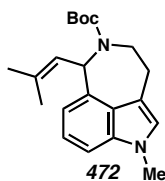
***N*-Boc-1-Methylaurantioclavine (472):** The synthesis of *N*-Boc-1-methylaurantioclavine is described in Section 6.6.2 of this thesis.

474   **Me 475**
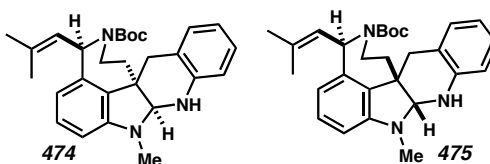
Indolines 474 and 475: The synthesis of indolines **474** and **475** is described in Section 6.6.2 of this thesis.

7.8.2.2 Strategies with Monosubstituted *o*-Methide Imines

504   **505** **507**
      72% yield **95% yield**
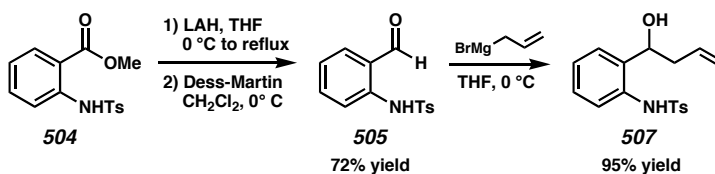
Alcohol 507: A flame-dried flask (25 mL) equipped with a teflon stirbar was charged with THF (10 mL), the solvent was cooled to 0 °C, and then lithium aluminum hydride (547 mg, 14.4 mmol) was added. To this solution was added ester **504** (2.00 g, 6.55 mmol) in small portions. After addition, reaction was fitted with a condenser and refluxed for 60 min. Sat. NH₄Cl solution was added to the mixture. The resulting solution was extracted 3 times with ethyl acetate, the organic layers were combined and dried over sodium sulfate, and the solvent was removed under reduced pressure.

Purification was performed via crystallization from dichloromethane and hexanes to afford an alcohol (1.6908 g, 6.10 mmol, 93% yield) as a white solid. R_F 0.34 (1:1 hexane/ethyl acetate eluent). A flame-dried flask (50 mL) equipped with a teflon stirbar was charged with the alcohol product of the previous reaction (432.7 mg, 1.560 mmol), which was subsequently dissolved in dichloromethane (18 mL). This solution was cooled to 0 °C, and Dess-Martin periodinate (991.6 mg, 2.34 mmol) was added to the solution. After addition, reaction was stirred for 45 min, and then sat. $NaCO_3$ and $Na_2S_2O_4$ solutions were added in a 1:1 ratio to quench excess oxidant. The resulting solution was extracted 3 times with diethyl ether, the organic layers were combined and dried over magnesium sulfate, and the solvent was removed under reduced pressure. Purification was performed via flash column chromatography (3:1 hexanes/ethyl acetate eluent) to afford aldehyde **505** (328.9 mg, 1.19 mmol, 77% yield) as a white solid. R_F 0.51 (1:1 hexane/ethyl acetate eluent);

A flame-dried vial (20 mL) equipped with a teflon stirbar was charged with aldehyde **505** (323 mg, 1.174 mmol), which was subsequently dissolved in THF (2.7 mL). This solution was cooled to 0 °C, and allylmagnesiumbromide (1.0 M in THF, 2.6 mL, 2.6 mmol) was added to the solution dropwise. After addition, reaction was complete, so sat. NH_4Cl solution added to the mixture. The resulting solution was extracted 3 times with diethyl ether, the organic layers were combined and dried over magnesium sulfate, and the solvent was removed under reduced pressure. Purification was performed via flash column chromatography (3:1 hexanes/ethyl acetate eluent) to afford **507** (352.1 mg, 1.109 mmol, 95% yield) as a white solid. R_F 0.18 (3:1 hexane/ethyl acetate eluent); ^{1}H NMR (300 MHz, CDCl$_3$) δ 8.40 (s, 1H), 7.73 (d, J = 8.5

Hz, 2H), 7.49 (d, J = 8.0 Hz, 1H), 7.28-7.19 (comp. m, 3H), 7.06-7.04 (comp. m, 1H),

5.74-5.6 (m, 1H), 5.15 (d, J = 10.5 Hz, 2H), 5.08 (d, J = 15.5 Hz, 1H), 4.66 (t, J = 7.0

Hz, 1H), 2.39 (s, 3H), 2.37-2.31 (m, 2H); ^{13}C NMR (75 MHz, CDCl$_3$) δ 151.0, 143.9,

136.9, 135.8, 134.0, 132.7, 129.8, 128.6, 128.0, 127.2, 124.7, 122.1, 118.9, 73.3, 41.4,

21.6; IR (neat) 3488, 3246, 1598, 1496, 1332, 1161 cm^{-1}.   MS m/e calc'd for

C$_{17}$H$_{19}$NO$_3$S$^+$: 317.1086, found 317.1085.
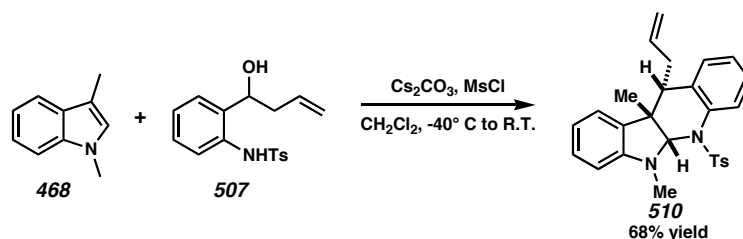
Indoline 510: A flame-dried flask (25 mL) equipped with a teflon stirbar was

charged with cesium carbonate (141.0 mg, 0.433 mmol), alcohol **507** (50 mg, 0.158

mmol), and indole **468** (19 μL, 0.131 mmol), which were subsequently dissolved in

dichloromethane (1.5 mL). This solution was cooled to -40 °C, and methanesulfonyl

chloride (51 μL, 0.659 mmol) dissolved in dichloromethane (1 mL) was added to the

solution dropwise. After addition, the reaction was stirred at –40 °C for 2.5 h and then

allowed to warm to room temperature over two h. The reaction was quenched by

addition of water, the resulting solution was extracted 3 times with ethyl acetate, the

organic layers were combined and dried over magnesium sulfate, and the solvent was

removed under reduced pressure. Purification was performed via flash column

chromatography (9:1 hexanes/ethyl acetate eluent) to afford indoline **510** (39.7 mg, 0.089

mmol, 68% yield) as a white solid. R_F 0.42 (3:1 hexane/ethyl acetate eluent); ^{1}H NMR

(300 MHz, CDCl$_3$) δ 7.57 (d, J = 8.0 Hz, 1H), 7.50 (d, J = 8.0 Hz, 2H), 7.21 (d, J = 8.0

Hz, 2H), 7.13 (t, *J* = 7.0 Hz, 1H), 7.04 (t, *J* = 7.5 Hz, 1H), 6.91-6.81 (comp. m, 3H), 6.39

(t, *J* = 7.5 Hz, 1H), 6.09 (d, *J* = 8.0 Hz, 1H), 5.66 (s, 1H), 5.49-5.35 (m, 1H), 4.90 (d, *J* =

10.5 Hz, 1H), 4.80 (d, *J* = 17.0 Hz, 1H), 2.93 (s, 3H), 2.70-2.64 (m, 2H), 2.40 (s, 3H),

1.68 (t, *J* = 6.0 Hz, 1H), 1.45 (s, 3H); ^{13}C NMR (75 MHz, CDCl$_3$) δ 150.3, 143.9, 138.0,

137.2, 137.1, 136.1, 130.9, 129.9, 128.2, 128.1, 127.1, 127.0, 126.8, 125.8, 123.4, 116.5,

115.9, 104.5, 88.4, 55.1, 44.1, 29.9, 29.1, 27.5, 21.7; IR (neat) 2924, 1607, 1494, 1351,

1167 cm^{-1}; MS *m/e* calc'd for C$_{27}$H$_{28}$N$_2$O$_2$S+H$^+$: 445.1950, found 445.1951.
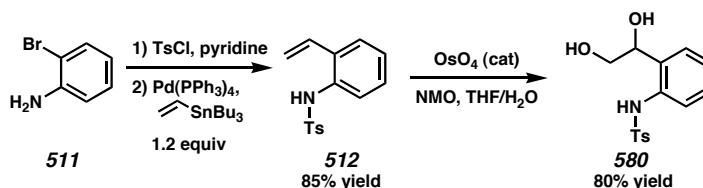
Diol 580: A flame-dried flask (25 mL) equipped with a teflon stirbar was charged

with bromide **511** (2.4370 g, 14.17 mmol), and then pyridine (3 mL). The solvent was

cooled to 0 °C, and then *p*-tolylsulfonyl chloride (3.0 g, 15.74 mmol) was added. The

reaction was complete in 30 minutes. Water was added to the mixture to precipitate

product. The resulting solution was crystallized from benzene and hexanes to afford the

tosylate (4.4044 g, 13.50 mmol, 95% yield) as a white solid. R_F 0.68 (1:1 hexane/ethyl

acetate eluent). A flame-dried flask (100 mL) equipped with a teflon stirbar was charged

with the tosylated product of the previous reaction (2.0989 g, 6.434 mmol), which was

subsequently dissolved in toluene (50 mL). This solution was cooled to -78 °C and

placed under vacuum for 15 minutes to degas the solvent. Pd(PPh$_3$)$_4$ (350 mg, 0.303

mmol) and tributylvinyl tin (4.5 ml, 15.37 mmol) were added to the reaction. After

addition, the reaction was refluxed for 120 min, and then silica gel was added to bind Pd

and gravity filtered, and solvent was removed under reduced pressure. Purification was performed via flash column chromatography (15:1 to 5:1 gradient of hexanes/ethyl acetate eluent) to afford styrene **512** (1.4411 g, 5.27 mmol, 82% yield) as a white solid. R_F 0.29 (3:1 hexane/ethyl acetate eluent). The spectral properties of **512** match those reported.[24]

A flame-dried flask (500 mL) equipped with a teflon stirbar was charged with styrene **512** (6.1093 g, 22.35 mmol), which was subsequently dissolved in THF (140 mL) and water (70 mL). To this solution was added *N*-methylmorpholine (5.9563 g, 50.84 mmol) and osmium tetroxide (11.6 mg, 0.04385 mmol). After addition, reaction was stirred for three days. The reaction was then concentrated to about 50 mL under reduced pressure, then extracted with a mixture of ether and THF three times. The organic layers were dried over sodium sulfate, and the solvent was removed under reduced pressure. Impurities were removed by washing solid with dichloromethane to afford diol **580** (5.4303 g, 17.67 mmol, 80% yield) as a white solid. R_F 0.13 (1:1 hexane/ethyl acetate eluent); ^{13}C NMR (75 MHz, CDCl$_3$) δ 144441, 137.1, 136.3, 129.9, 129.8, 129.2, 128.5, 127.4, 127.0, 122.2, 74.78, 66.0, 21.8; IR (neat) 3271, 1318, 1150 cm^{-1}. MS *m/e* calc'd for C$_{15}$H$_{18}$NO$_4$+H$^+$: 308.0957, found 308.0967.
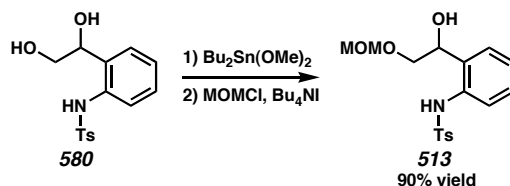
Alcohol 513: A flame-dried flask (250 mL) equipped with a teflon stirbar was charged with diol **580** (500.0 mg, 1.627 mmol), toluene (70 mL), and dibutyltin

dimethoxide (410 μL, 1.787 mmol). The flask was fit with a short path distillation apparatus, and approximately half the solvent was removed by distillation. To this solution was added MOMCl (136 μL, 1.79 mmol) and tetrabutylammonium iodide (900 mg, 2.44 mmol). After addition, the reaction was stirred for 12 h. Brine was added to this solution, the mixture was extracted 3 times with ethyl acetate, the organic layers were combined and dried over magnesium sulfate, and the solvent was removed under reduced pressure. Purification was performed via flash column chromatography (3:1 to 1:1 gradient of hexanes/ethyl acetate eluent) to afford alcohol **513** (512.6 mg, 1.46 mmol, 90% yield) as a white solid. R_F 0.27 (1:1 hexane/ethyl acetate eluent); ^{1}H NMR (300 MHz, CDCl$_3$) δ 8.76 (s, 1H), 7.72 (d, J = 8.5 Hz, 2H), 7.50 (d, J = 8.0 Hz, 1H), 7.27-7.20 (comp. m, 3H), 7.11-7.02 (comp. m, 2H), 4.83-4.78 (m, 1H), 4.64 (s, 2H), 3.60 (dd, J = 10.5, 3.5 Hz, 1H), 3.48-3.41 (m, 2H), 3.39 (s, 3H), 2.39 (s, 3H); ^{13}C NMR (75 MHz, CDCl$_3$) δ 143.9, 137.1, 136.3, 129.7, 129.5, 128.9, 128.2, 127.2, 124.7, 122.0, 97.0, 73.3, 72.4, 55.6, 21.6; IR (neat) 3233, 2932, 1598, 1497, 1335, 1161 cm^{-1}. MS m/e calc'd for C$_{17}$H$_{22}$NO$_5$S+H$^+$: 352.1219, found 352.1219.
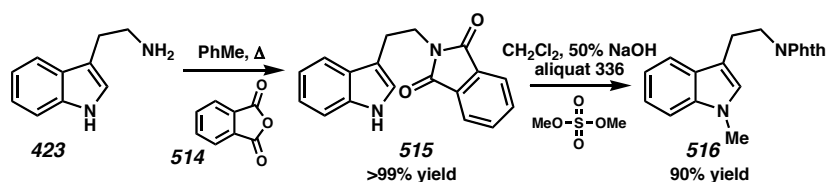
Indole 516: A flask (100 mL), equipped with a teflon stirbar and Dien-Stark apparatus, was charged with tryptamine (**423**) (1.5 g, 9.36 mmol), toluene (20 mL), and phthalic anhydride (1.4 g, 9.45 mmol). The solution was refluxed for 18 h, and the product **515** was recovered by vacuum filtration as a white solid (2.72 g, 9.36 mmol).

To a solution of tryptamine derivative **515** (1.0024 g, 3.45 mmol) in dichloromthane (8 ml) in a flask (50 ml) was added aliquat 336 (22.7 mg), a 50% solution of sodium hydroxide (3.3 mL), and dimethylsulfate (500 μL, 5.29 mmol). After 30 minutes of rapid stirring, the reaction was extracted 3 times with dichloromethane, the organic layers were combined and dried over magnesium sulfate, and the solvent was removed under reduced pressure. Purification was performed via crystallization from dichloromethane and hexanes to afford **516** (936.5 mg, 3.08 mmol, 90% yield) as a white solid. R_F 0.44 (2:1 hexane/ethyl acetate eluent); ^{1}H NMR (300 MHz, CDCl$_3$) δ 7.87-7.84 (comp. m, 2H), 7.76-7.70 (comp. m, 3H), 7.30 (d, J = 8.0 Hz, 2H), 7.23 (t, J = 7.0 Hz, 1H), 7.13 (t, J = 8.0 Hz, 1H), 6.98 (s, 1H), 4.00 (t, J = 8.0 Hz, 2H), 3.76 (s, 3H), 3.15 (t, J = 8.0 Hz, 2H); ^{13}C NMR (75 MHz, CDCl$_3$) δ 168.4, 137.1, 133.9, 132.3, 130.0, 129.8, 128.2, 127.9, 126.9, 123.2, 121.7, 119.1, 119.0, 110.9, 109.3, 38.8, 32.7, 24.5; IR (neat) 2953, 1761, 1709 cm^{-1}. MS m/e calc'd for C$_{19}$H$_{16}$N$_2$O$_2$[+]: 304.1212, found 304.1225.
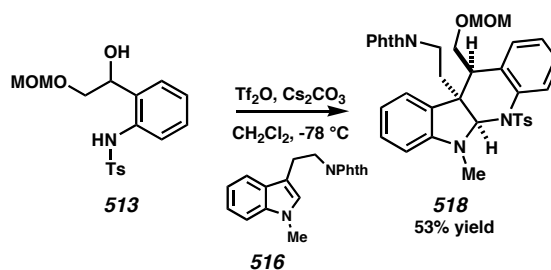
Indoline 518: A flame-dried flask (25 mL) equipped with a teflon stirbar was charged with cesium carbonate (3.951 g, 12.13 mmol), alcohol **513** (506.1 mg, 1.44 mmol), and indole **516** (295.3 mg, 0.970 mmol), which were subsequently dissolved in dichloromethane (10 mL). This solution was cooled to -78 °C and trifluoromethane sulfonic anhydride (820 μL, 4.87 mmol) was added to the solution dropwise over 4 hours.

After addition, the reaction was stirred for 4 h and then allowed to warm to –55 °C for

1.25 h. The reaction was quenched by addition of water, and the resulting solution was

extracted 3 times with dichloromethane, the organic layers were combined and dried over

magnesium sulfate, and the solvent was removed under reduced pressure. Purification

was performed via flash column chromatography (3:1 to 2:1 gradient of hexanes/ethyl

acetate eluent) to afford indoline **518** (330.2 mg, 0.518 mmol, 53% yield) as a yellow

foam. R_F 0.32 (2:1 hexane/ethyl acetate eluent); ^{1}H NMR (300 MHz, CDCl$_3$) δ 7.83-7.79

(m, 1H), 7.73-7.66 (m, 2H), 7.55 (d, J = 1.5 Hz, 1H), 7.25-7.22 (m, 2H), 7.16 (t, J = 7.5

Hz, 1H), 7.07 (t, J = 7.5 Hz, 1H), 7.00 (d, J = 8.0 Hz, 1H), 6.77 (t, J = 6.5 Hz, 2H), 6.33

(t, J = 7.5 Hz, 1H), 6.02 (d, J = 9.5 Hz, 2H), 4.53 (dd, J = 6.5, 20.5 Hz, 2H), 4.14-4.11

(m, 2H), 3.67-3.47 (m, 2H), 3.33 (s, 3H), 2.88 (s, 3H), 2.47-2.39 (m, 1H), 2.36 (s, 3H),

2.10 (t, J = 7.0 Hz, 1H), 1.93-1.83 (m, 1H); ^{13}C NMR (75 MHz, CDCl$_3$) δ 168.1, 150.6,

143.8, 138.2, 136.0, 135.5, 134.0, 132.3, 130.0, 128.5, 127.7, 127.2, 127.1, 125.7, 123.8,

123.3, 116.8, 104.7, 96.2, 84.5, 63.9, 56.9, 55.6, 43.4, 36.5, 34.0, 31.1, 29.8, 21.6; IR

(neat) 2944, 1771, 1712, 1167 cm^{-1}. MS m/e calc'd for C$_{36}$H$_{35}$N$_3$O$_6$S$^+$: 637.2247, found

637.2242.
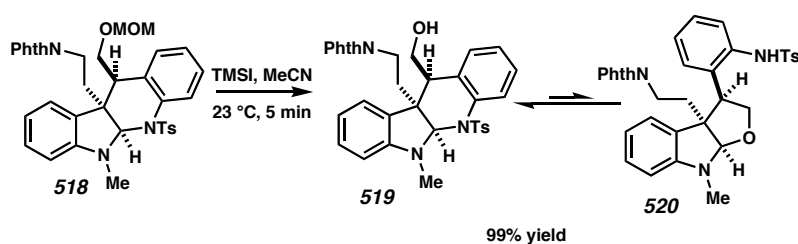
Indolines 519 and 520: A flame-dried flask (25 mL) equipped with a teflon

stirbar was charged with MOM ether **518** (330.0 mg, 0.517 mmol), which was

subsequently dissolved in acetonitrile (10 mL). This solution was cooled to 0 °C, and trimethylsilyl iodide (240 μL, 1.69 mmol) was added to the solution dropwise. After addition, the reaction was stirred for 4.5 h. The reaction was quenched by addition of a saturated solution of sodium bicarbinate, the resulting solution was extracted 3 times with dichloromethane, the organic layers were combined and dried over magnesium sulfate, and the solvent was removed under reduced pressure. Purification was performed via flash column chromatography (3:1 to 1:1 gradient of hexanes/ethyl acetate eluent) to afford indoline **519** (306.0 mg, 0.517 mmol, 99% yield) as a yellow foam or white solid. R_F 0.37 (1:1 hexane/ethyl acetate eluent); ^{1}H NMR (300 MHz, CDCl$_3$) δ 7.83-7.80 (m, 1H), 7.72-7.60 (comp. m, 5H), 7.29-7.03 (comp. m, 6H), 6.79-6.67 (m, 2H), 6.39 (d, J = 7.5 Hz, 2H), 6.32 (t, J = 7.5 Hz, 1H), 6.03-6.01 (m, 1H), 5.49 (s(br), 2H), 4.27 (d, J = 6.5 Hz, 2H), 3.89-3.86 (comp. m, 3H), 3.74-3.69 (comp. m, 2H), 3.57-3.31 (comp. m, 4H), 3.00 (s, 3H), 2.87 (s, 1H), 2.38 (s, 3H), 1.79 (s(br), 2H); ^{13}C NMR (75 MHz, CDCl$_3$) δ 168.1, 168.0, 150.7, 144.1, 143.9, 136.9, 134.1, 134.1, 133.9, 132.1, 132.0, 131.5, 130.0, 129.8, 128.9, 128.5, 127.9, 127.6, 127.3, 127.2, 127.1, 127.0, 123.7, 123.4, 123.3, 123.3, 123.1, 118.3, 116.8, 105.7, 104.7, 102.8, 84.5, 77.4, 59.7, 59.7, 59.4, 56.9, 46.2, 36.4, 35.2, 34.0, 32.0, 30.9, 29.8, 21.7; IR (neat) 3531, 3255, 2942, 2879, 2254, 1771, 1710 cm^{-1}. MS m/e calc'd for C$_{34}$H$_{31}$N$_3$O$_5$S+H$^+$: 594.2063, found 594.2074.
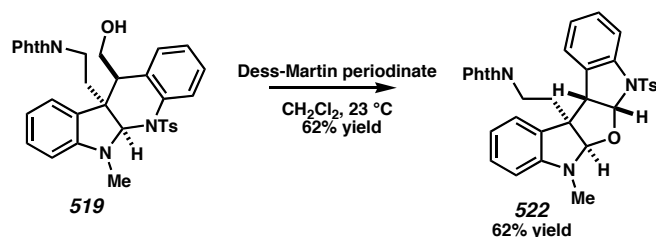
Indoline 522: A flame-dried vial (4 mL) equipped with a teflon stirbar was charged with alcohol **519** (44.7 mg, 0.0753 mmol), which was subsequently dissolved in dichloromethane (2 mL). To this solution was added Dess-Martin periodinate (65 mg, 0.153 mmol). After addition, the reaction was stirred for 15 minutes, and then sat. $NaCO_3$ and $Na_2S_2O_4$ solutions were added in a 1:1 ratio to quench excess oxidant. The resulting solution was extracted 3 times with ethyl acetate, the organic layers were combined and dried over magnesium sulfate, and the solvent was removed under reduced pressure. Purification was performed via flash column chromatography (3:1 to 2:1 gradient of hexanes/ethyl acetate eluent) to afford indoline **522** (27.3 mg, 0.0461 mmol, 62% yield) as a yellow foam or white solid. R_F 0.38 (1:1 hexane/ethyl acetate eluent); ^{1}H NMR (300 MHz, CDCl$_3$) δ 7.84 (d, 8.5, 1H), 7.77-7.66 (comp. m, 2H), 7.49 (d, J = 8.0 Hz, 1H), 7.38 (d, J = 7.5 Hz, 1H), 7.28-7.22 (comp. m, 2H), 7.17 (t, J = 7.5 Hz, 1H), 7.02 (t, J = 7.5 Hz, 1H), 6.8 (t, J = 7.5 Hz, 1H), 6.51 (d, J = 8.0 Hz, 1H), 6.04 (d, J = 6.0 Hz, 1H), 5.15 (s, 1H), 4.04 (d, J = 6.0 Hz, 1H), 3.60-3.50 (m, 1H), 3.39-3.29 (m, 1H), 2.98 (s, 3H), 2.53-2.42 (m, 1H), 2.40 (s, 3H), 1.94-1.84 (m, 1H); ^{13}C NMR (75 MHz, CDCl$_3$) δ 168.1, 149.7, 144.3, 141.4, 136.4, 134.0, 132.2, 131.7, 129.7, 129.4, 129.1, 127.9, 127.5, 123.5, 123.3, 119 (2), 114.3, 107.7, 102.7, 95.5, 57.1, 56.3, 34.5, 32.9, 31.5, 21.8, 3.7; IR (neat) 2925, 1712, 1168 cm^{-1}. MS m/e calc'd for $C_{34}H_{29}N_3O_5S+H^+$: 592.1906, found 592.1912.
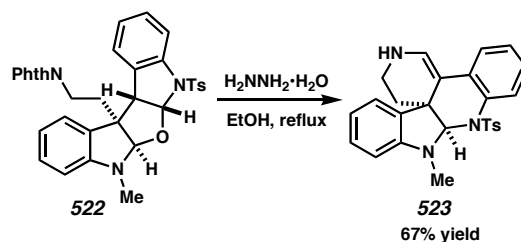
Enamine 523: A vial (20 mL) equipped with a teflon stirbar was charged with indoline **522** (160.0 mg, 0.270 mmol), which was subsequently suspended in ethanol (2.7 mL) and water (20 μL). To this solution was added hydrazine hydrate (131 μL, 2.7 mmol). After addition, the reaction was refluxed for 60 minutes, and then cooled to room temperature. The solid was removed via filtration, and the mother liquor (containing the product) was concentrated under reduced pressure. Purification was performed via flash column chromatography (5:1 to 2:1 gradient of hexanes/ethyl acetate eluent) to afford indoline **523** (80.9 mg, 0.182 mmol, 67% yield) as a white solid. R_F 0.67 (1% methanol in dichloromethane eluent); ^{1}H NMR (300 MHz, CDCl$_3$) δ 7.51-7.48 (m, 1H), 7.27 (d, J = 8.0 Hz, 2H), 7.11 (d, J = 8.0 Hz, 2H), 7.00-6.96 (m, 1H), 6.92 (d, J = 7.5 Hz, 1H), 6.82 (d, J = 7.0 Hz, 1H), 6.78-6.75 (m, 1H), 6.46 (t, J = 7.5 Hz, 1H), 6.25 (d, J = 7.5 Hz, 1H), 5.99 (s, 1H), 5.78 (s, 1H), 3.48-3.39 (comp. m, 2H), 3.14-3.05 (m, 1H), 3.06 (s, 3H), 2.37 (s, 3H), 1.91-1.83 (m, 2H); ^{13}C NMR (75 MHz, CDCl$_3$) δ 149.5, 143.3, 137.0, 136.5, 135.6, 133.3, 129.1, 128.7, 128.4, 128.0, 127.5, 127.3, 125.1, 124.5, 124.0, 116.7, 104.6, 103.9, 88.1, 49.0, 37.3, 35.6, 30.0, 21.6; IR (neat) 3430, 2945, 1645, 1604, 1493, 1347, 1164 cm^{-1}. MS m/e calc'd for C$_{26}$H$_{25}$N$_3$O$_2$S$^+$: 443.1667, found 443.1663.

7.8.2.3 Alternative Electrophile Precursors
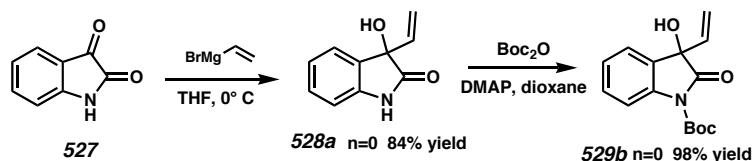
Imide 529b: A flame-dried flask (500 mL) equipped with a teflon stirbar was charged with isatin (**527**) (5.0 mg, 33.98 mmol), which was subsequently dissolved in THF (150 mL). This solution was cooled to –40 °C, and then vinylmagnesiumbromide (1.0 M in THF, 75 mL, 75 mmol) was added dropwise. After addition, the reaction was stirred for 30 minutes, and then the reaction was quenched by addition of a saturated ammonium chloride solution. The mixture was extracted three times with ethyl acetate, the organic layers were dried over magnesium sulfate, and the solvent was removed under reduced pressure. Impurities were removed by washing with dichloromethane to afford oxindole **528a** (4.9747 g, 28.4 mmol, 84% yield) as a light yellow solid that matched the reported data.[25] R_F 0.24 (1:1 hexanes/ethyl acetate eluent).

A flame-dried vial (20 mL) equipped with a teflon stirbar was charged with oxindole **528a** (500.0 mg, 2.85 mmol), which was subsequently dissolved in dioxane (5 mL). To this solution was added di-t-butyldicarbonate (930 mg, 4.04 mmol). After addition, the reaction was stirred for 30 h, and then the reaction was quenched by addition of brine. The mixture was extracted three times with ethyl acetate, the organic layers were dried over magnesium sulfate, and the solvent was removed under reduced pressure. Purification was performed via flash column chromatography (9:1 to 5:1 gradient of hexanes/ethyl acetate eluent) to afford imide **529b** (809.4 mg, 2.797 mmol, 98% yield). R_F 0.66 (1:1 hexanes/ethyl acetate eluent).
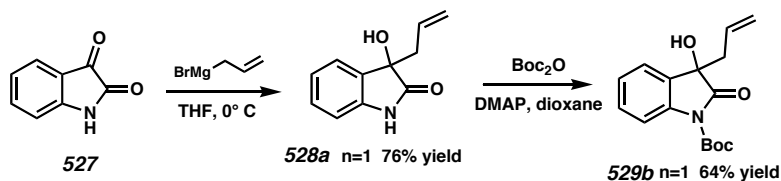
Imide 529b: A flame-dried flask (250 mL) equipped with a teflon stirbar was charged with isatin (**527**) (7.00 g, 47.58 mmol), which was subsequently dissolved in THF (100 mL). This solution was cooled to –40 °C, and then allylmagnesiumbromide (1.0 M in THF, 115 mL, 115 mmol) was added dropwise. After addition, the reaction was stirred for 30 minutes, and then the reaction was quenched by addition of a saturated ammonium chloride solution. The mixture was extracted three times with ethyl acetate, the organic layers were dried over magnesium sulfate, and the solvent was removed under reduced pressure. Impurities were removed by washing with dichloromethane to afford oxindole **528b** (6.80 g, 35.94 mmol, 76% yield) as a light yellow solid that matched the reported data.[26] R_F 0.35 (1:1 hexanes/ethyl acetate eluent).

A flame-dried flask (50 mL) equipped with a teflon stirbar was charged with oxindole **528b** (1.00 g, 5.485 mmol), which was subsequently dissolved in THF (25 mL). To this solution was added di-*t*-butyldicarbonate (1.8 g, 8.24 mmol). After addition, the reaction was stirred for 20 h, and then the reaction was quenched by addition of brine. The mixture was extracted three times with ethyl acetate, the organic layers were dried over magnesium sulfate, and the solvent was removed under reduced pressure. Purification was performed via flash column chromatography (15:1 to 5:1 gradient of hexanes/ethyl acetate eluent) to afford imide **529b** (969.8 mg, 3.35 mmol, 64% yield). R_F 0.61 (1:1 hexanes/ethyl acetate eluent).
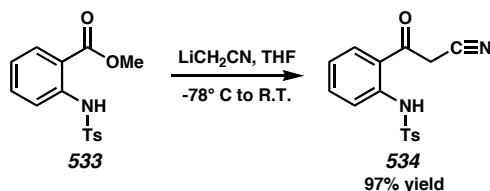
Ketone 534: A flame-dried flask (250 mL) equipped with a teflon stirbar was charged with THF (80 mL). The solvent was cooled to –78 °C, and then *n*-butyllithium (2.45 M in hexanes, 10 mL, 24.5 mmol) was added, followed by the addition of acetonitrile (1.3 mL, 24.89 mmol). To this solution was added ester **533** (2.5014 g, 8.19 mmol) in a solution of THF (80 mL) over 15 minutes. After addition, the reaction was stirred for 5 minutes, and then brought to room temperature for 40 minutes. 2 N HCl was added to quench the reaction, and then brine was added. The resulting solution was extracted 3 times with ethyl acetate, the organic layers were combined and dried over magnesium sulfate, and the solvent was removed under reduced pressure. Purification was performed via crystallization from ethyl acetate and hexanes to afford ketone **534** (2.4942 g, 7.93 mmol, 97% yield) as a white solid. R_F 0.43 (1:1 hexane/ethyl acetate eluent); ^{1}H NMR (300 MHz, CDCl$_3$) δ 10.78 (s(br), 1H), 7.79-7.74 (comp. m, 3H), 7.62 (d, J = 8.0 Hz, 1H), 7.56 (t, J = 7.0 Hz, 1H), 7.27 (d, J = 8.0 Hz, 2H), 7.13 (t, J = 7.5 Hz, 1H), 4.04 (s, 2H), 2.39 (s, 3H); ^{13}C NMR (75 MHz, CDCl$_3$) δ 190.9, 144.6, 141.0, 136.7, 136.3, 131.0, 130.0, 127.5, 123.2, 120.1, 119.8, 113.3, 30.8, 21.7; IR (neat) 3175, 1664, 1570, 1161 cm^{-1}. MS *m/e* calc'd for C$_{16}$H$_{15}$N$_2$O$_3$S+H$^+$: 315.0803, found 315.0811.

527 → **537** 90% yield → **538** 67% yield 1.6:1 dr
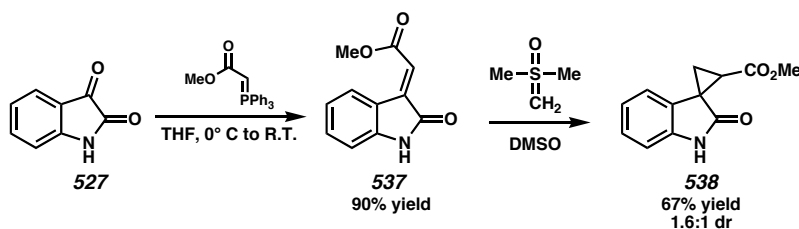
Cyclopropane 538: A flame-dried flask (250 mL) equipped with a teflon stirbar was charged with methyl(triphenylphosphoranylidene)acetate (5.00 g, 14.95 mmol), which was subsequently dissolved in THF (15.5 mL). This solution was cooled to 0 °C, and then isatin (2.00 g, 13.59 mmol) was added in a solution of THF (26 mL). After addition, the reaction was warmed to room temperature and stirred for 2.5 h, and then the reaction was quenched by addition of actone (20 mL). The solvent was removed under reduced pressure in the presence of silica gel, and the resulting solid was loaded onto a flash chromatography column. Purification was performed via flash column chromatography (9:1 to 1:1 gradient of hexanes/ethyl acetate eluent) to afford oxindole **537**, which was further purified by recrystalization from ethanol (2.4929 g, 12.27 mmol, 90% yield) as a bright orange solid that matched the reported data.[27] R_F 0.52 (1:1 hexanes/ethyl acetate eluent).

A flame-dried flask (25 mL) equipped with a teflon stirbar was charged with sodium hydride (60% dispersion in mineral oil, 22 mg, 0.55 mmol), which was washed 3 times with dry hexanes. Then DMSO (5.5 mL) and trimethyl sulfoxonium iodide (119 mg, 5.485 mmol) were added. To this solution was added oxindole **537** (100.0 mg, 0.492 mmol) in a solution of DMSO (2.5 mL). After addition, the reaction was stirred for 2 h, and then the temperature was raised to 50 °C. The reaction was complete after another hour. Brine was added, the mixture was extracted three times with ethyl acetate, the organic layers were dried over magnesium sulfate, and the solvent was removed under

reduced pressure. Purification was performed via flash column chromatography (3:1 to 1:1 gradient of hexanes/ethyl acetate eluent) to afford oxindole **538** as two diastereomers. Diastereomer 1: (44.7 mg, 0.206 mmol, 42% yield). R_F 0.52 (1:1 hexanes/ethyl acetate eluent). ^{1}H NMR (300 MHz, CDCl$_3$) δ 9.40 (s, 1H), 7.34 (d, J = 7.5 Hz, 1H), 7.23 (t, J = 7.5 Hz, 1H), 7.04-6.97 (comp. m, 2H), 3.70 (s, 3H), 2.74 (t, J = 8.0 Hz, 1H), 2.18 (dd, J = 4.5, 7.5 Hz, 1H), 2.05 (dd, J = 4.5, 8.5 Hz, 1H); ^{13}C NMR (75 MHz, CDCl$_3$) δ 177.5, 169.3, 141.8, 127.9, 126.4, 123.0, 122.4, 110.3, 52.4, 34.3, 32.9, 21.1; IR (neat) 3214, 1712, 1622, 1470, 1209 cm^{-1}. MS m/e calc'd for C$_{12}$H$_{12}$NO$_3$+H$^+$: 218.0817, found 218.0825. Diastereomer 2: (28.6 mg, 0.132 mmol, 27% yield). R_F 0.45 (1:1 hexanes/ethyl acetate eluent). ^{1}H NMR (300 MHz, CDCl$_3$) δ 9.06 (s, 1H), 7.27-7.20 (m, 1H), 7.04-6.97 (comp. m, 2H), 6.83 (d, J = 7.5 Hz, 1H), 3.75 (s, 3H), 2.68 (t, J = 8.0 Hz, 1H), 2.40 (dd, J = 5.0, 8.0 Hz, 1H), 1.84 (dd, J = 5.0, 8.5 Hz, 1H); ^{13}C NMR (75 MHz, CDCl$_3$) δ 176.0, 167.7, 141.1, 129.5, 188.0, 122.4, 118.9, 110.3, 52.6, 33.5, 32.9, 21.3; IR (neat) 3256, 1739, 1710 cm^{-1}. MS m/e calc'd for C$_{12}$H$_{12}$NO$_3$+H$^+$: 218.0817, found 218.0828.
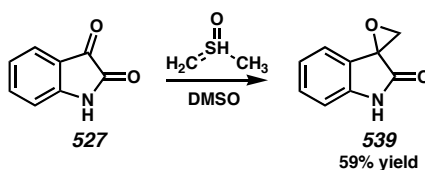
Epoxide 539: A flame-dried flask (50 mL) equipped with a teflon stirbar was charged with sodium hydride (60% dispersion in mineral oil, 1.36 g, 34.0 mmol), which was washed 3 times with dry hexanes. Then DMSO (17 mL) and trimethyl sulfonium iodide (6.95 g, 34.06 mmol) were added. To this solution was added isatin **527** (500.0

mg, 3.40 mmol) in a solution of DMSO (8 mL). After addition, the reaction was stirred

for 30 min. The reaction was quenched with saturated ammonium chloride solution.

Brine was added, the mixture was extracted three times with ethyl acetate, the organic

layers were dried over magnesium sulfate, and the solvent was removed under reduced

pressure. Impurities were removed by washing with dichloromethane to afford oxindole

539 that matched the reported data.[28].

7.8.2.4 Intramolecular Diels-Alder Reaction with Benzisoxazole

Acid 543: A flame-dried flask (500 mL) equipped with a teflon stirbar was

charged with acid **547** (10.00 g, 55.20 mmol), ethanol (60 mL), sulfuric acid (200 μL),

and toluene (280 mL). The flask was fit with a condenser, and the solution was refluxed

for 14 h. The solvent was removed under reduced pressure, and sulfuric acid (280 mL)

was added. After addition, the reaction was heated to 110 °C and stirred for 90 min. The

solution was then poured onto ice (600 g), the mixture was extracted 3 times with ether,

the organic layers were combined and dried over magnesium sulfate, and the solvent was

removed under reduced pressure. Purification was performed via crystallization from

water to afford acid **543** (3.9431 g, 24.17 mmol, 44% yield) as an off-white solid that

matched the reported data.[29] ^{1}H NMR (300 MHz, acetone-d$_6$) δ 10.82 (s(br), 1H), 7.94 (d,

J = 9.0 Hz, 1H), 7.75 (d, J = 10.0 Hz, 1H), 7.50 (dd, J = 6.5, 9.5 Hz, 1H), 7.34 (dd, J =

7.0, 8.5 Hz, 1H); ^{13}C NMR (75 MHz, acetone-d$_6$) δ 158.5, 158.1, 155.3, 132.4, 128.8,

121.4, 121.0, 116.7; IR (neat) 2360, 1731, 1301, 1231, 1189, 753 cm^{-1}. MS m/e calc'd

for C$_8$H$_6$NO$_3$+H$^+$: 164.0348, found 164.0341.
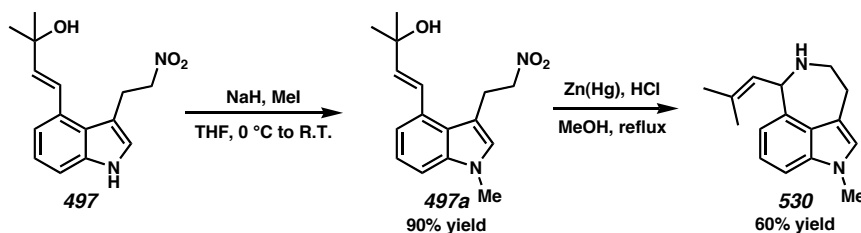
1-methylaurantioclavine 530: A flame-dried flask (50 mL) equipped with a

teflon stirbar was charged with indole **497** (385.5 mg, 1.405 mmol), which was

subsequently dissolved in THF (14 mL). The resulting solution was cooled to 0 °C, and

methyl iodide (875 μL, 14.06 mmol) was added. Sodium hydride (60% dispersion in

mineral oil, 562 mg, 14.5 mmol) was then added to the solution, and the mixture was

stirred for 25 minutes. The reaction was quenched with saturated ammonium hydride

solution and extracted three times with ethyl acetate. The organic layers were combined,

the solution was dried over magnesium sulfate, and the solvent was then removed under

reduced pressure. Purification was performed via flash column chromatography (3:1 to

2:1 gradient of hexanes/ethyl acetate) to afford nitro compound **497a** (363.5 mg, 1.26

mmol, 90% yield) as a yellow solid.

A flame-dried flask (50 mL) equipped with a teflon stirbar was charged with nitro

compound **497a** (511.7 mg, 1.775 mmol), which was subsequently dissolved in MeOH

(125 mL) and 2N HCl (40 mL). To this solution was added amalgamated zinc, which had

been formed from zinc dust (6.5 g, 98.34 mmol) and mercuric chloride (1.10 g, 3.55

mmol) in 2N HCl and subsequently rinsed with MeOH. The mixture was stirred at reflux

for 3 h. The reaction was then decanted from the remaining amalgam and then basified

to pH >10. The solid was removed by filtration, and the resulting solution was extracted 5 times with dichloromethane. The organic layers were combined, the solution was dried over magnesium sulfate, and the solvent was then removed under reduced pressure. Purification was performed via flash column chromatography (18:1 dichloromethane/methanol) to afford 1-methylaurantioclavine **530** (257.6 mg, 1.07 mmol, 60% yield) as a yellow oil. ^{1}H NMR (300 MHz, CDCl$_3$) δ 7.19-7.12 (comp. m, 2H), 6.89-6.83 (comp. m, 2H), 5.48 (d, J = 9.0 Hz, 1H), 4.92 (d, J = 9.0 Hz, 1H), 3.76 (s, 3H), 3.62-3.54 (m, 1H), 3.13-3.02 (comp. m, 3H), 2.26 (s(br), 1H), 1.86 (s, 6H); ^{13}C NMR (75 MHz, CDCl$_3$) δ 138.5, 137.8, 133.3, 127.7, 125.9, 121.1, 117.4, 114.2, 107.3, 62.6, 48.9, 32.7 (30.8), 25.9, 18.4; IR (neat) 3332, 2910, 1554, 1455 cm^{-1}. MS m/e calc'd for C$_{16}$H$_{21}$N$_2$+H$^+$: 241.1705, found 241.1712.

to pH >10. The solid was removed by filtration, and the resulting solution was extracted
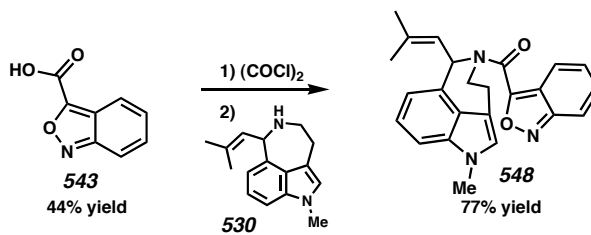
Amide 548: A flame-dried vial (20 mL) equipped with a teflon stirbar was charged with acid **543** (37.5 mg, 0.229 mmol), which was subsequently dissolved in dichloromethane (500 μL). Oxalyl chloride (59 μL, 0.676 mmol) was added and then a small amount of DMF (~1 μL). After 1 h the reaction was complete, so the solvent was removed under reduced pressure, and the residue was evaporated from benzene (1 mL) to remove excess reagent. Dichloromethane (1.1 mL) and triethylamine (30 μL, 0.215 mmol) were added, and to this solution was added 1-methylaurantioclavine **530** (50.0 mg, 0.208 mmol). After addition, the reaction was stirred for 60 minutes, and then brine was

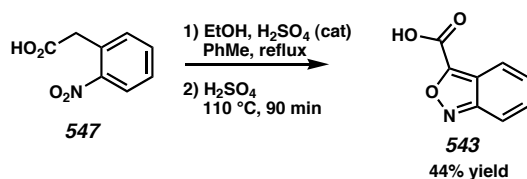added. The resulting solution was extracted 3 times with ethyl acetate, the organic layers were combined and dried over magnesium sulfate, and the solvent was removed under reduced pressure. Purification was performed via flash column chromatography (3:1 to 2:1 gradient of hexanes/ethyl acetate eluent) to afford amide **548** (61.6 mg, 0.160 mmol, 77% yield) as a white solid. R_F 0.79 (1:2 hexane/ethyl acetate eluent); ^{1}H NMR (300 MHz, CDCl$_3$) δ 7.99 (d, J = 9.0 Hz, 1H), 7.68 (d, J = 9.0 Hz, 1H), 7.62 (t, J = 10.0 Hz, 1H), 7.37-7.30 (comp. m, 1.5H), 7.22-7.18 (comp. m, 2H), 7.13-7.08 (comp. m, 2H), 7.04-6.99 (comp. m, 1H), 6.95 (s, 1H), 6.86-6.84 (m, 2H), 6.67 (d, J = 7.5 Hz, 1H), 5.46 (d, J = 7.5 Hz, 1H), 4.69 (dd, J = 15.0, 38.0 Hz, 1H), 4.04 (dt, J = 4.5, 15.5 Hz, 1H), 3.77 (s, 3H), 3.74 (s, 3H), 3.48 (t, J = 18.0 Hz, 1H), 3.25 (3.11, J = comp. m Hz, 2H), 1.92 (s, 3H), 1.78 (s, 3H), 1.72 (s, 3H), 1.60 (s, 3H); ^{13}C NMR (75 MHz, CDCl$_3$) δ 158.5, 158.5, 157.7, 157.6, 156.9, 156.8, 137.8, 137.7, 137.6, 136.8, 135.7, 135.6, 131.3, 131.2, 126.5, 126.3, 125.9, 124.8, 124.4, 124.3, 124.2, 122.1, 121.6, 121.5, 121.2, 121.1, 120.0, 118.1, 117.3, 115.0, 114.9, 112.3, 111.7, 107.9, 107.7, 60.9, 57.3, 44.5, 43.1, 32.6, 29.0, 25.9, 25.7, 18.9, 18.2; IR (neat) 2913, 2245, 1615, 1455, 1410 cm^{-1}. MS *m/e* calc'd for C$_{24}$H$_{23}$N$_3$O$_2$S$^+$: 385.1790, found 385.1775.
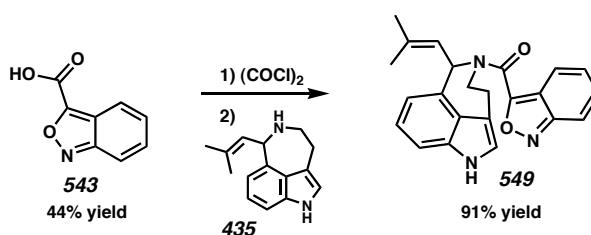
Amide 549: A flame-dried vial (20 mL) equipped with a teflon stirbar was charged with acid **543** (262 mg, 1.604 mmol), which was subsequently dissolved in dichloromethane (5 mL). Oxalyl chloride (420 μL, 4.81 mmol) was added and then a

small amount of DMF (~20 μL). After 1 h the reaction was complete, so the solvent was removed under reduced pressure, and the residue was evaporated from benzene (2 mL) to remove excess reagent. Dichloromethane (10 mL) and triethylamine (537 μL, 3.85 mmol) were added, and to this solution was added aurantioclavine **435** (290.4 mg, 1.283 mmol). After addition, the reaction was stirred for 60 minutes, and then brine was added. The resulting solution was extracted 3 times with ethyl acetate, the organic layers were combined and dried over magnesium sulfate, and the solvent was removed under reduced pressure. Purification was performed via flash column chromatography (3:1 to 1:1 gradient of hexanes/ethyl acetate eluent) to afford amide **549** (434.6 mg, 1.17 mmol, 91% yield) as a white solid. R_F 0.72 (1:2 hexane/ethyl acetate eluent); ^{1}H NMR (300 MHz, CDCl$_3$) δ 8.93 (d, J = 18.0 Hz, 1H), 8.99 (d, J = 9.0 Hz, 1H), 7.70-7.60 (comp. m, 2H), 7.35-6.96 (comp. m, 12H), 6.90-6.85 (comp. m, 2H), 6.72 (d, J = 7.5 Hz, 1H), 5.49 (d, J = 7.5 Hz, 1H), 4.74 (t, J = 15.5 Hz, 1H), 4.13-4.03 (m, 1H), 3.83 (t, J = 13.0 Hz, 1H), 3.54 (t, J = 14.5 Hz, 1H), 3.23-3.15 (comp. m, 2H), 1.98 (s, 1.5H), 1.80 (s, 1.5H), 1.74 (s, 1.5H), 1.65 (s, 1.5H); ^{13}C NMR (75 MHz, CDCl$_3$) δ 158.5, 158.4, 157.9, 157.8, 156.9, 156.8, 137.7, 137.4, 137.2, 136.9, 135.2, 135.1, 131.5, 131.4, 126.4, 126.1, 124.7, 124.3, 123.9, 123.8, 122.1, 121.9, 121.8, 121.7, 121.1, 121.0, 119.9, 118.3, 117.5, 114.9, 113.3, 112.6, 110.1, 109.9, 61.0, 57.5, 44.5, 43.1, 29.1, 25.9, 25.8, 25.7, 18.9, 18.2; IR (neat) 3325, 2914, 2246, 1730, 1616, 1447 cm^{-1}.
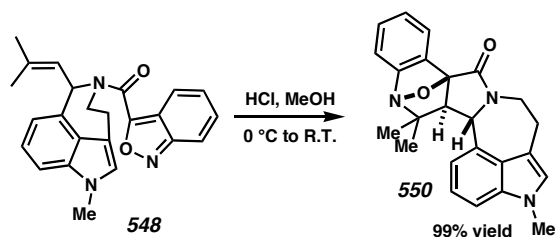
Lactam 550: A flame-dried vial (20 mL) equipped with a teflon stirbar was charged with amide **548** (100 mg, 0.259 mmol) and cooled to 0°C. A 0.5 M solution of HCl in MeOH (2.6 mL, generated from addition of acetyl chloride to methanol at 0 °C) cooled to 0 °C was then added, and the mixture was stirred for 1 hour and then warmed to room temperature for 30 min. The solvent was then removed under reduced pressure. Purification was performed via flash column chromatography (3:1 to 1:1 gradient of hexanes/ethyl acetate eluent) to afford lactam **550** (101.0 mg, 0.259 mmol, 99% yield) as a white solid. R_F 0.29 (1:1 hexane/ethyl acetate eluent); ^{1}H NMR (300 MHz, CDCl$_3$) δ 7.37-7.17 (comp. m, 6H), 7.00 (s, 1H), 6.76-6.73 (m, 1H), 5.51 (d, J = 6.5 Hz, 1H), 4.57-4.50 (m, 1H), 3.80 (s, 3H), 3.50-3.15 (comp. m, 3H), 2.57 (d, J = 6.5 Hz, 1H), 1.95 (s, 3H), 1.18 (s, 3H); ^{13}C NMR (75 MHz, CDCl$_3$) δ 165.4, 153.5, 139.8, 137.9, 135.6, 127.5, 127.0, 126.9, 124.6, 121.9, 119.1, 118.4, 115.9, 113.4, 108.4, 97.2, 70.9, 64.1, 61.9, 45.2, 33.0, 27.5, 27.2, 26.6; IR (neat) 3315, 2932, 1699, 1456, 1317, 754 cm^{-1}. MS *m/e* calc'd for C$_{24}$H$_{22}$N$_3$O$_2$+H$^+$: 385.1790, found 385.1809.
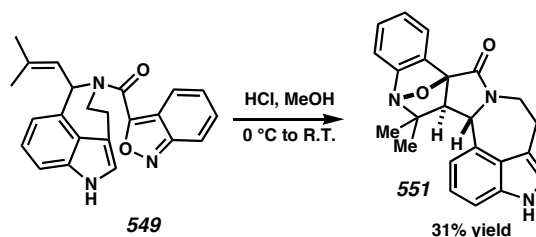
Lactam 551: A flame-dried vial (20 mL) equipped with a teflon stirbar was charged with amide **549** (100 mg, 0.269 mmol) and cooled to 0°C. A 0.5 M solution of HCl in MeOH (2.7 mL, generated from addition of acetyl chloride to methanol at 0 °C) cooled to 0 °C was then added, and the mixture was stirred for 1 hour and then warmed to room temperature for 30 min. The solvent was then removed under reduced pressure. Purification was performed by washing the solid with dichloromethane to afford lactam **551** (31.1 mg, 0.084 mmol, 31% yield) as a white solid. R_F 0.22 (1:1 hexane/ethyl acetate eluent); ^{1}H NMR (300 MHz, acetone-d_6) δ 7.34-7.17 (comp. m, 6H), 7.09 (t, J = 7.5 Hz, 1H), 6.61 (d, J = 7.5 Hz, 1H), 5.47 (d, J = 6.5 Hz, 1H), 4.21 (d, J = 13.0 Hz, 1H), 3.44 (t, J = 11.0 Hz, 1H), 3.18-2.98 (comp. m, 2H), 2.37 (d, J = 6.5 Hz, 1H), 1.77 (s, J = 3, 1.04, s Hz, 3H); ^{13}C NMR (75 MHz, acetone-d_6) δ 164.3, 153.0, 139.6, 137.0, 134.6, 127.3, 126.6, 123.7, 122.6, 121.4, 118.6, 118.0, 115.2, 112.7, 110.2, 96.4, 70.1, 63.1, 61.2, 44.4, 30.7, 26.9, 26.5, 26.0; IR (neat) 3314, 1681, 753 cm^{-1}. MS m/e calc'd for C$_{23}$H$_{22}$N$_3$O$_2$+H$^+$: 372.1712, found 372.1710.

7.8.2.5 Halo Oxindoles as Precursors
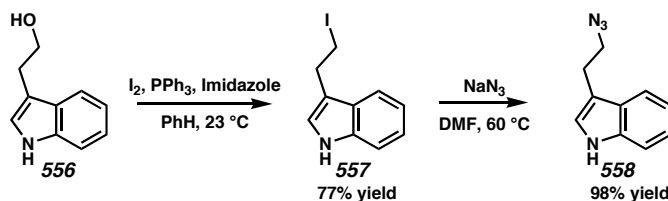
Azide 558: A flame-dried flask (2000 mL) equipped with a teflon stirbar was charged with tryptophol **556** (10.20 g, 63.275 mmol), imidazole (5.08 g, 74.62 mmol), and triphenylphosphine (17.88 g, 68.17 mmol), which were subsequently dissolved in benzene (600 mL). Iodine (17.20 g, 67.77 mmol) was dissolved in benzene (600 mL) and then added dropwise to the tryptophol solution. At 1 h intervals imidazole, triphenylphosphine, and iodine were added until the reaction was complete. Saturated $NaCO_3$ and $Na_2S_2O_4$ solutions were added in a 1:1 ratio to quench excess oxidant, and then the organic layer was washed with brine. The organic layer was dried over magnesium sulfate, and the solvent was removed under reduced pressure. The residue was purified via flash column chromatography (15:1 to 2:1 gradient of hexanes/ethyl acetate eluent) to afford iodide **557** (13.45 g, 48.72 mmol, 77% yield) as a white solid. R_F 0.54 (2:1 hexane/ethyl acetate eluent).

A flame-dried flask (100 mL) equipped with a teflon stirbar was charged with iodide **557** (4.3728 g, 15.84 mmol), which was subsequently dissolved in DMF (32 mL). Sodium azide (2.06 g, 31.69 mmol) was then added. After addition, the reaction was stirred at 50 °C for 120 minutes, and then water was added. The resulting solution was extracted 3 times with ether, the organic layers were combined and dried over magnesium sulfate, and the solvent was removed under reduced pressure. Purification was performed via flash column chromatography (9:1 to 5:1 gradient of hexanes/ethyl acetate eluent) to

afford azide **558** (2.5832 g, 15.54 mmol, 98% yield) as a yellow oil. R_F 0.48 (2:1

hexane/ethyl acetate eluent); the characteristics of **558** were identical to those previously

reported.
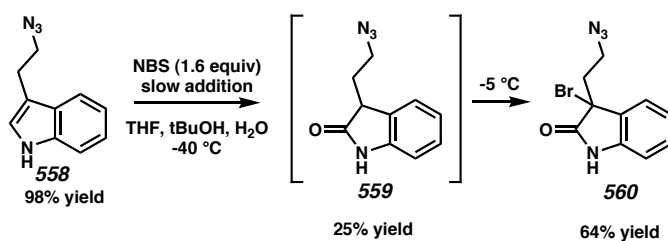
Bromooxindole 560: A flame-dried flask (1000 mL) equipped with a teflon

stirbar was charged with azide **558** (5.03 g, 30.26 mmol), to which was subsequently

added THF (150 mL), *t*-BuOH (150 mL), and water (3.75 mL) and cooled to -40°C. A 0

°C solution of NBS (8.03 g, 45.11 mmol) in THF (450 mL) was then added via cannula

over 30 minutes, and the resulting solution was allowed to warm to –10 °C over 2 h.

Warming continued slowly over 30 min to 0 °C. After 20 min at 0 °C, the solvent was

removed under reduced pressure. Purification was performed via flash column

chromatography (9:1 to 1:2 gradient of pentane/ether eluent) to afford bromooxindole

559 (5.4577 g, 19.41 mmol, 64% yield) as a yellow solid: R_F 0.46 (2:1 hexane/ethyl

acetate eluent); ^{1}H NMR (300 MHz, CDCl$_3$) δ 8.12 (s(br), 1H), 7.28-7.23 (comp. m, 2H),

7.06 (t, J = 7.5 Hz, 1H), 6.91 (d, J = 7.5 Hz, 1H), 3.61-3.44 (comp. m, 3H), 2.32-2.17

(m, 2H); ^{13}C NMR (75 MHz, CDCl$_3$) δ 180.5, 141.7, 128.4, 128.1, 123.8, 123.8, 122.3,

110.2, 48.0, 43.3, 29.5; IR (neat) 3228, 2100, 1693, 1620, 1470 cm^{-1}. MS *m/e* calc'd for

C$_{10}$H$_{10}$N$_4$OBr$^+$: 281.0038, found 281.0040. Oxindole **560** (1.4965 g, 7.40 mmol, 25%

yield) was also isolated as a light yellow solid: R_F 0.37 (2:1 hexane/ethyl acetate eluent);

^{1}H NMR (300 MHz, CDCl$_3$) δ 8.21 (s(br), 1H), 7.40 (d, *J* = 7.5 Hz, 1H), 7.32 (t, *J* = 8.0

Hz, 1H), 7.13 (t, *J* = 7.5 Hz, 1H), 6.95 (d, *J* = 8.0 Hz, 1H), 3.41-3.20 (m, 2H), 2.84-2.57

(m, 2H); ^{13}C NMR (75 MHz, CDCl$_3$) δ 176.6, 139.8, 130.6, 129.1, 124.6, 123.5, 111.4,

54.5, 47.6, 38.0; IR (neat) 3252, 2102, 1732, 1619, 1471 cm^{-1}. MS *m/e* calc'd for

C$_{10}$H$_{11}$N$_4$O+H$^+$: 203.0933, found 203.0933.
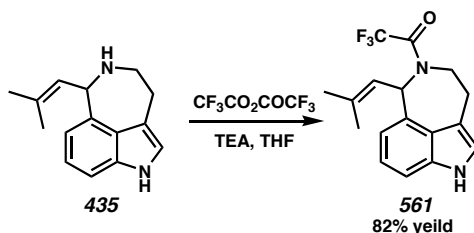
N-trifluoroacetate-aurantioclavine 561: A flame-dried flask (50 mL) equipped

with a teflon stirbar was charged with indole **435** (882.3 mg, 3.898 mmol), which was

subsequently dissolved in THF (14 mL). The resulting solution was cooled to 0 °C and

to it was added triethylamine (820 μL, 5.88 mmol) and then trifluoroacetic anhydride

(606 μL, 4.288 mmol). The reaction was complete immediately, so it was quenched with

methanol. The solvent was then removed under reduced pressure. Purification was

performed via flash column chromatography (9:1 to 3:1 gradient of hexanes/ethyl

acetate) to afford the aurantioclavine **561** (1.034 g, 3.204 mmol, 82% yield) as a yellow

foam; ^{1}H NMR (300 MHz, CDCl$_3$) δ 8.51 (s(br), 1H), 7.29-7.26 (m, 1H), 7.02-6.97

(comp. m, 2H), 6.90 (t, *J* = 7.0 Hz, 1H), 6.23 (d, *J* = 8.0 Hz, 1H), 5.40 (dd, *J* = 7.5, 19.5

Hz, 1H), 4.40 (d, *J* = 13.0 Hz, 1H), 4.16-4.10 (m, 1H), 4.04-3.94 (comp. m, 2H), 3.83 (t,

J = 13.0 Hz, 1H), 3.43 (t, *J* = 16.5 Hz, 1H), 3.27-3.23 (m, 1H), 3.09 (d, *J* = 16.5 Hz, 1H),

1.91 (s, 3H), 1.86 (s, 3H), 1.78 (s, 6H); ^{13}C NMR (75 MHz, CDCl$_3$) δ 157.5, 157.0,

156.8, 156.3, 138.5, 137.4, 137.2, 137.2, 135.1, 134.4, 124.3, 123.9, 123.5, 123.3, 122.1, 121.9, 121.8, 119.0, 118.8, 118.5, 117.1, 115.2, 115.0, 113.1, 112.6, 110.3, 110.1, 60.7, 60.6, 58.6, 43.7, 43.7, 28.4, 26.2, 25.7, 25.0, 18.9, 18.2; IR (neat) 3361, 2917, 1667, 1441, 1205 cm^{-1}; MS m/e calc'd for $C_{17}H_{17}N_2OF_3^+$: 322.1293, found 322.1308.
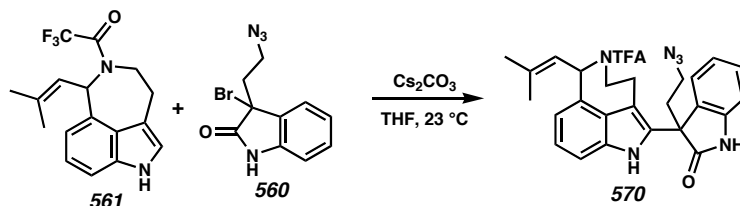
Adduct 570: A flame-dried vial (20 mL) equipped with a teflon stirbar was charged with indole **561** (120.0 mg, 0.372 mmol) and bromooxindole **560** (157.0 mg, 0.559 mmol), which were subsequently dissolved in THF (4 mL). Cesium carbonate (243 mg, 0.746 mmol) was then added. After addition, the reaction was stirred for 12 h, and then water was added. The resulting solution was extracted 3 times with ethyl acetate, the organic layers were combined and dried over magnesium sulfate, and the solvent was removed under reduced pressure. Purification was performed via flash column chromatography (9:1 to 2:1 gradient of hexanes/ethyl acetate eluent) to afford adduct **570** (134.3 mg, 0.257 mmol, 69% yield) as a yellow foam. R_F 0.34 (2:1 hexane/ethyl acetate eluent run twice); ^{1}H NMR (300 MHz, CDCl$_3$) δ 8.74 (s(br), 2H), 8.59 (s(br), 1H), 8.97 (s(br), 1H), 7.34-6.86 (comp. m, 12H), 6.78 (t, J = 7.0 Hz, 1H), 6.11 (d, J = 8.0 Hz, 1H), 5.33 (dd, J = 7.5, 20.5 Hz, 2H), 4.16 (d, J = 13.5 Hz, 1H), 3.96-3.90 (m, 1H), 3.80 (t, J = 16.0 Hz, 1H), 3.63 (t, J = 13.5 Hz, 1H), 3.25-3.12 (comp. m, 5H), 3.09-2.86 (comp. m, 3H), 2.65-2.53 (comp. 3), 1.84 (s, 3H), 1.80 (s, 3H), 1.71 (s, 6H); ^{13}C NMR (75 MHz, CDCl$_3$) δ 178.8, 178.7, 157.1, 156.7, 156.5, 156.0, 141.4,

141.3, 138.4, 137.0, 136.0, 135.6, 135.1, 134.4, 130.1, 129.9, 129.8, 129.5, 129.5, 125.5,

125.0, 124.9, 124.8, 124.4, 123.7, 123.3, 122.4, 122.2, 119.5, 119.0, 118.7, 118.1, 114.9,

111.8, 111.5, 111.2, 111.2, 110.1, 109.8, 60.5, 58.3, 52.7, 52.6, 47.3, 47.3, 43.5, 43.4,

35.0, 34.8, 28.1, 26.3, 25.8, 24.5, 19.0, 18.3; IR (neat) 3335, 2102, 1713, 1674 cm^{-1}; MS

m/e calc'd for $C_{27}H_{25}N_6O_2F_3^+$: 522.1991, found 522.1982.
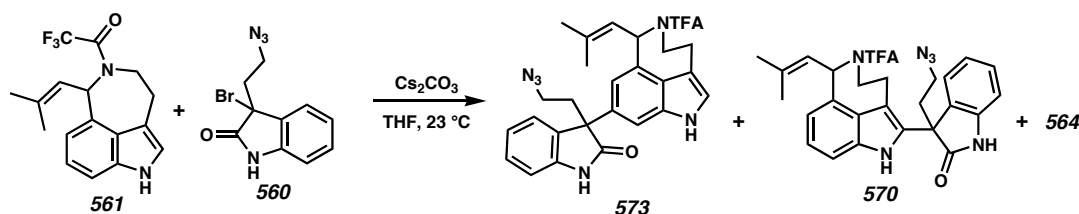
Adducts 570, 573, and 564: A flame-dried flask (100 mL) equipped with a

teflon stirbar was charged with indole **561** (1.0337 g, 3.207 mmol) and bromooxindole

560 (2.254 mg, 8.02 mmol), which were subsequently dissolved in dichloromethane (32

mL). Cesium carbonate (3.135 g, 9.62 mmol) was then added. After addition, the

reaction was stirred for 3 h, and then water was added. The resulting solution was

extracted 3 times with ethyl acetate, the organic layers were combined and dried over

magnesium sulfate, and the solvent was removed under reduced pressure. Purification

was performed via flash column chromatography (18:1 to 1:2 gradient of hexanes/ethyl

acetate eluent) to afford adduct **570** (404.1 mg, 0.773 mmol, 24% yield) as a yellow

foam: R_F 0.34 (2:1 hexane/ethyl acetate eluent run twice). Adduct **573** (538.0 mg, 1.03

mmol, 32% yield) as a yellow foam: R_F 0.18 (2:1 hexane/ethyl acetate eluent run twice);

^{1}H NMR (300 MHz, CDCl$_3$) δ 8.91 (d, J = 13.0 Hz, 2H), 8.33 (d, J = 6.0 Hz, 2H), 7.28-

6.86 (comp.m, 9H), 6.75 (d, J = 7.5 Hz, 1H), 6.11 (d, J = 7.5 Hz, 1H), 5.31 (dd, J = 7.5,

29.5 Hz, 2H), 4.30 (d, J = 13.5 Hz, 1H), 4.06-4.01 (m, 1H), 3.94-3.84 (m, 1H), 3.71 (t, J

= 13.0 Hz, 1H), 3.29 (t, J = 13.0 Hz, 1H), 3.17-3.13 (comp. m, 4H), 2.98 (d, J = 16.5 Hz,

1H), 2.89-2.75 (comp. m, 2H), 2.53-2.44 (comp. m, 2H), 1.76 (s, 3H), 1.72 (s, 9H); ^{13}C

NMR (75 MHz, CDCl$_3$) δ 181.1, 180.9, 157.4, 157.0, 156.7, 156.2, 141.1, 138.5, 137.5,

137.3, 137.1, 135.5, 134.8, 133.4, 133.2, 132.2, 132.1, 128.8, 128.7, 125.1, 124.0, 123.6,

123.2, 123.1, 122.8, 122.5, 119.0, 118.7, 117.0, 115.7, 115.1, 114.9, 113.3, 112.6, 110.7,

108.6, 108.5, 60.6, 58.6, 55.5, 55.4, 47.9, 43.8, 43.7, 36.6, 36.3, 28.4, 26.3, 25.8, 25.0,

18.9, 18.3; IR (neat) 3328, 2100, 1712, 1682 cm^{-1}; MS m/e calc'd for C$_{27}$H$_{25}$N$_6$O$_2$F$_3$$^+$:

522.1991, found 522.2002. Adduct **564** (548.2 mg, 0.759 mmol, 24% yield) as a yellow

foam: R_F 0.09 (2:1 hexane/ethyl acetate eluent run twice); ^{1}H NMR (300 MHz, acetone-

d$_6$) δ 10.43 (d, J = 11.5 Hz, 1H), 9.80 (d, J = 8.0 Hz, 1H), 9.59 (s, 1H), 7.36-7.23 (comp.

m, 7H), 7.19-6.97 (comp. m, 8H), 5.36 (dd, J = 7.0, 40.0 Hz, 2H), 4.02-3.50 (comp. m,

6H), 3.25-3.10 (comp. m, 8H), 3.04 (s, 2H), 3.01-2.44 (comp. m, 8H), 1.76 (s, 3H), 1.73

(s, 3H), 1.68 (s, 6H); ^{13}C NMR (75 MHz, acetone-d$_6$) δ 180.2, 180.1, 177.9, 177.8,

143.1, 143.0, 142.9, 138.3, 137.4, 137.2, 136.8, 135.3, 134.8, 134.6, 134.4, 133.6, 133.3,

133.2, 133.0, 131.3, 129.9, 129.3, 129.2, 126.1, 125.3, 125.2, 125.0, 124.8, 123.9, 123.6,

122.9, 118.0, 147.1, 111.0, 110.9, 110.3, 109.9, 109.4, 109.2, 61.2, 59.2, 55.8, 55.7, 52.7,

52.7, 48.6, 47.6, 44.0, 37.0, 36.9, 35.4, 28.2, 26.1, 25.7, 24.8, 18.8, 18.3; IR (neat) 3305,

2101, 1713, 1472 cm^{-1}; MS m/e calc'd for C$_{37}$H$_{33}$N$_{10}$F$_3$O$_3$$^+$: 722.2689, found 722.2689.
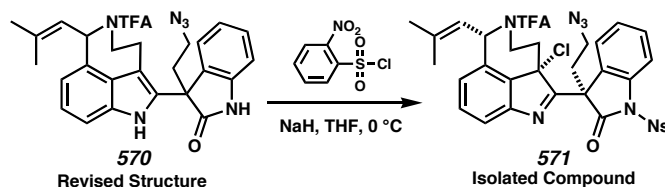
Chloride 571: A flame-dried vial (20 mL) equipped with a teflon stirbar was charged with adduct **570** (183.0 mg, 0.350 mmol), which was subsequently dissolved in THF (4 mL). The solution was cooled to 0 °C, and then sodium hydride (60% dispersion in mineral oil, 42 mg, 1.05 mmol) was added. 5 min after the sodium hydride addition, *o*-nitrobenzylsulfonyl chloride (116 mg, 0.523 mmol) was added. The reaction was stirred for 10 min, and then a saturated solution of ammonium chloride was added. The resulting solution was extracted 3 times with ethyl acetate, the organic layers were combined and dried over magnesium sulfate, and the solvent was removed under reduced pressure. Purification was performed via flash column chromatography (15:1 to 2:1 gradient of hexanes/ethyl acetate eluent) to afford alkyl chloride **571** (142.1 mg, 0.256 mmol, 73% yield) as a white crystalline solid. R_F 0.26 (2:1 hexane/ethyl acetate eluent); ^{1}H NMR (300 MHz, CDCl$_3$) δ 8.64-8.59 (m, 2H), 7.95-7.84 (comp. m, 8H), 7.55-7.47 (comp. m, 6H), 7.37-7.26 (comp. m, 5H), 7.15 (d, J = 7.0 Hz, 2H), 6.95 (d, J = 8.0 Hz, 1H), 6.31 (d, J = 7.5 Hz, 2H), 5.76-5.72 (m, 2H), 5.61 (d, J = 7.5 Hz, 1H), 4.20-4.08 (comp. m, 2H), 3.94-3.67 (comp. m, 3H), 3.31-3.19 (comp. m, 2H), 2.99-2.74 (comp. m, 6H), 2.29 (dd, J = 3.0, 10.5 Hz, 1H), 1.75 (s, 6H), 1.65 (s, 3H); ^{13}C NMR (75 MHz, CDCl$_3$) δ 175.9, 175.8, 173.8, 173.6, 156.3, 155.9, 151.7, 151.6, 148.2, 147.9, 141.6, 140.7, 139.9, 139.7, 139.2, 138.2, 137.4, 136.9, 136.4, 136.0, 135.3, 135.2, 132.6, 130.9, 130.8, 130.4, 130.4, 128.3, 126.8, 126.6, 126.4, 126.3, 125.8, 125.4, 125.3, 125.2, 124.9, 121.7, 121.6, 120.6, 119.8, 118.6, 115.4, 115.3, 114.8, 77.7, 77.4, 77.2, 76.8, 75.7, 75.5,

60.1, 57.6, 55.7, 55.6, 46.5, 46.4, 40.0, 39.1, 37.8, 37.6, 36.1, 32.6, 26.5, 26.0, 18.6, 18.1; IR (neat) 2102, 1755, 1686, 1544, 1146 cm^{-1}; MS m/e calc'd for C$_{33}$H$_{27}$O$_6$N$_7$F$_3$SCl+H$^+$: 742.1462, found 742.1442. MS m/e calc'd for C$_{33}$H$_{28}$N$_7$O$_6$F$_3$ClS+H$^+$: 445.1950, found 445.1951.

573
Revised Structure

574
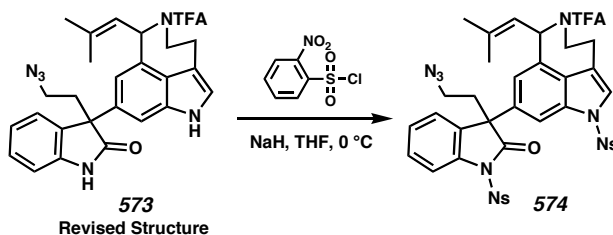
Nosylate 574: A flame-dried vial (4 mL) equipped with a teflon stirbar was charged with adduct **573** (43.7 mg, 0.0836 mmol), which was subsequently dissolved in THF (800 μL). The solution was cooled to 0 °C, and then sodium hydride (60% dispersion in mineral oil, 17 mg, 0.425 mmol) was added. 5 min after the sodium hydride addition, o-nitrobenzylsulfonyl chloride (93 mg, 0.420 mmol) was added. The reaction was stirred for 10 min, and then a saturated solution of ammonium chloride was added. The resulting solution was extracted 3 times with ether, the organic layers were combined and dried over magnesium sulfate, and the solvent was removed under reduced pressure. Purification was performed via flash column chromatography (9:1 to 1:1 gradient of hexanes/ethyl acetate eluent) to afford the bisnosylate **594** (49.0 mg, 0.0549 mmol, 66% yield) as a yellow solid. R_F 0.42 (1:1 hexane/ethyl acetate eluent); ^{1}H NMR (300 MHz, CDCl$_3$) δ 8.54-8.51 (m, 2H), 8.03-8.00 (m, 2H), 7.88-7.56 (comp. m, 10H), 7.50 (s, 1H), 7.42-7.35 (comp. m, 5H), 7.18-7.12 (comp. m, 3H), 6.95 (s, 1H), 6.61 (d, J = 7.5 Hz, 1H), 5.97 (d, J = 7.5 Hz, 1H), 5.23-5.16 (m, 2H), 4.27 (d, J = 13.5 Hz, 1H), 4.02 (d, J = 15.0 Hz, 1H), 3.89-3.79 (m, 1H), 3.64 (t, J = 11.0 Hz, 1H), 3.32-2.80 (comp. m, 10H),

2.48-2.33 (m, 2H), 1.73 (s, 12H); ^{13}C NMR (75 MHz, CDCl$_3$) δ 176.2, 176.0, 157.3, 156.9, 156.5, 148.0, 148.0, 140.2, 140.1, 140.0, 138.6, 137.2, 136.6, 136.2, 136.0, 135.7, 135.5, 134.8, 134.7, 132.8, 132.8, 132.4, 131.2, 131.2, 131.1, 130.9, 130.6, 129.9, 129.8, 129.5, 129.2, 127.4, 127.0, 125.7, 125.7, 125.4, 125.4, 125.2, 125.1, 124.9, 122.8, 121.9, 121.1, 120.0, 118.8, 118.5, 117.9, 115.5, 114.9, 110.6, 60.2, 58.1, 55.0, 55.0, 47.5, 42.8, 42.7, 36.6, 36.6, 39.9, 28.0, 26.3, 25.8, 25.0, 18.9, 18.3; IR (neat) 2930, 2101, 1754, 1684, 1544 cm^{-1}; MS m/e calc'd for C$_{39}$H$_{31}$N$_8$O$_{10}$F$_3$S$_2$+H$^+$: 893.1635, found 893.1613.
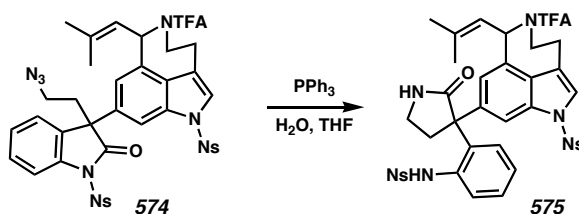
Lactam 575: A vial (4 mL) equipped with a teflon stirbar was charged with nosylate **574** (43.1 mg, 0.0483 mmol), which was subsequently dissolved in THF (1 mL) and water (250 μL). To this solution, triphenylphosphine (25 mg, 0.0953 mmol) was added. The reaction was stirred for 3 h at 50 °C, and then the solvent was removed under reduced pressure. Purification was performed via flash column chromatography (3:1 to 1:1 gradient of hexanes/ethyl acetate eluent) to afford the lactam **575** (49.0 mg, 0.0549 mmol, 66% yield) as a yellow crystalline solid. R_F 0.14 (1:1 hexane/ethyl acetate eluent); ^{1}H NMR (300 MHz, CDCl$_3$) δ 7.75-7.50 (comp. m, 6H), 7.43 (t, J = 7.5 Hz, 1H), 7.34-7.22 (comp. m, 4H), 7.14 (d, J = 7.5 Hz, 1H), 6.81 (d, J = 7.5 Hz, 2H), 6.55 (d, J = 6.5 Hz, 2H), 6.01 (d, J = 7.5 Hz, 1H), 5.32 (d, J = 8.0 Hz, 1H), 5.20 (d, J = 8.0 Hz, 1H), 4.26 (d, J = 13.5 Hz, 1H), 4.02 (d, J = 15.5 Hz, 1H), 3.81 (t, J = 11.5 Hz, 1H), 3.30-3.00 (comp. m, 3H), 2.35-2.28 (m, 2H), 1.67 (s, 3H), 1.62 (s, 3H); ^{13}C NMR (75 MHz,

CDCl$_3$) δ 180.0, 180.0, 157.3, 156.8, 156.7, 156.2, 147.9, 147.8, 147.7, 147.7, 139.5, 139.4, 137.8, 137.5, 137.4, 136.9, 136.5, 136.4, 136.2, 136.1, 135.6, 135.3, 135.1, 133.6, 132.9, 132.5, 132.5, 132.2, 132.2, 132.0, 131.0, 130.9, 130.5, 129.0, 129.0, 127.9, 127.8, 126.3, 126.2, 125.2, 125.1, 125.0, 124.9, 124.8, 124.5, 124.4, 124.3, 123.3, 122.4, 121.4, 120.5, 119.2, 118.9, 118.5, 118.4, 115.1, 110.2, 109.7, 77.7, 77.4, 77.2, 76.8, 60.1, 58.2, 57.7, 43.0, 42.8, 39.8, 38.8, 38.8, 28.5, 26.1, 25.7, 25.3, 18.9, 18.3; IR (neat) 3098, 2916, 1682, 1545, 1368, 1170, 732 cm^{-1}; MS m/e calc'd for C$_{39}$H$_{33}$N$_6$O$_{10}$F$_3$S$_2$+H$^+$: 867.1730, found 867.1731.

7.8.3 Crystallographic Data

CALIFORNIA INSTITUTE OF TECHNOLOGY
BECKMAN INSTITUTE
X-RAY CRYSTALLOGRAPHY LABORATORY

Date 25 July 2005

Crystal Structure Analysis of:

571

Note: The crystallographic data have been deposited in the Cambridge Database (CCDC) and has been placed on hold pending further instructions from me. The deposition number is 266777. Ideally the CCDC would like the publication to contain a footnote of the type: "Crystallographic data have been deposited at the CCDC, 12 Union Road, Cambridge CB2 1EZ, UK and copies can be obtained on request, free of charge, by quoting the publication citation and the deposition number 266777."

Table 1. Crystal data and structure refinement for 571 (CCDC 266777).

Empirical formula	$C_{33}H_{27}ClF_3N_7O_6S$
Formula weight	742.13
Crystal Habit	Fragment
Crystal size	0.39 x 0.37 x 0.13 mm^3
Crystal color	Colorless

Data Collection

Type of diffractometer	Bruker SMART 1000	
Wavelength	0.71073 Å MoKα	
Data Collection Temperature	100(2) K	
θ range for 16089 reflections used in lattice determination	2.20 to 31.97°	
Unit cell dimensions	a = 10.9264(5) Å	α= 73.0330(10)°
	b = 12.1779(6) Å	β= 67.6620(10)°
	c = 14.2739(7) Å	γ = 67.3760(10)°
Volume	1597.82(13) Å^3	
Z	2	
Crystal system	Triclinic	
Space group	P-1	
Density (calculated)	1.543 Mg/m^3	
F(000)	764	
Data collection program	Bruker SMART v5.630	
θ range for data collection	1.57 to 32.63°	
Completeness to θ = 32.63°	88.9 %	
Index ranges	-16 ≤ h ≤ 16, -18 ≤ k ≤ 16, -20 ≤ l ≤ 21	
Data collection scan type	ω scans at 8 φ settings	
Data reduction program	Bruker SAINT v6.45A	
Reflections collected	37699	
Independent reflections	10400 [R$_{int}$= 0.0577]	
Absorption coefficient	0.262 mm^{-1}	
Absorption correction	None	
Max. and min. transmission	0.9667 and 0.9047	

Table 1 (cont.)

Structure Solution and Refinement

Structure solution program	Bruker XS v6.12
Primary solution method	Direct methods
Secondary solution method	Difference Fourier map
Hydrogen placement	Geometric positions
Structure refinement program	Bruker XL v6.12
Refinement method	Full matrix least-squares on F^2
Data / restraints / parameters	10400 / 0 / 462
Treatment of hydrogen atoms	Riding
Goodness-of-fit on F^2	1.637
Final R indices [I>2σ(I), 7425 reflections]	R1 = 0.0454, wR2 = 0.0773
R indices (all data)	R1 = 0.0690, wR2 = 0.0795
Type of weighting scheme used	Sigma
Weighting scheme used	$w=1/\sigma^2(Fo^2)$
Max shift/error	0.001
Average shift/error	0.000
Largest diff. peak and hole	0.887 and -0.658 e.Å^{-3}

Special Refinement Details

Refinement of F^2 against ALL reflections. The weighted R-factor (wR) and goodness of fit (S) are based on F^2, conventional R-factors (R) are based on F, with F set to zero for negative F^2. The threshold expression of $F^2 > 2\sigma(F^2)$ is used only for calculating R-factors(gt) etc. and is not relevant to the choice of reflections for refinement. R-factors based on F^2 are statistically about twice as large as those based on F, and R-factors based on ALL data will be even larger.

All esds (except the esd in the dihedral angle between two l.s. planes) are estimated using the full covariance matrix. The cell esds are taken into account individually in the estimation of esds in distances, angles and torsion angles; correlations between esds in cell parameters are only used when they are defined by crystal symmetry. An approximate (isotropic) treatment of cell esds is used for estimating esds involving l.s. planes.

Table 2. Atomic coordinates (x 10⁴) and equivalent isotropic displacement parameters (Å²x 10³) for 571 (CCDC 266777). U(eq) is defined as the trace of the orthogonalized U^{ij} tensor.

	x	y	z	U_{eq}
S(1)	6743(1)	-231(1)	818(1)	16(1)
Cl(1)	942(1)	-99(1)	3598(1)	16(1)
O(1)	5897(1)	29(1)	3010(1)	18(1)
O(2)	6074(1)	1034(1)	786(1)	21(1)
O(3)	6993(1)	-772(1)	-26(1)	20(1)
O(4)	10273(1)	-3117(1)	-29(1)	39(1)
O(5)	8240(1)	-2949(1)	1113(1)	31(1)
O(6)	766(1)	5270(1)	2429(1)	24(1)
F(1)	3742(1)	3405(1)	1166(1)	24(1)
F(2)	2938(1)	5340(1)	877(1)	28(1)
F(3)	2323(1)	4289(1)	261(1)	26(1)
N(1)	6917(2)	-3499(1)	6299(1)	34(1)
N(2)	6864(1)	-3701(1)	5590(1)	25(1)
N(3)	6851(1)	-4089(1)	4877(1)	29(1)
N(4)	2959(1)	-97(1)	5003(1)	15(1)
N(5)	952(1)	3332(1)	2438(1)	14(1)
N(6)	5780(1)	-933(1)	1872(1)	15(1)
N(7)	9295(1)	-2649(1)	665(1)	24(1)
C(1)	6355(2)	-3160(1)	4053(1)	22(1)
C(2)	5039(2)	-2165(1)	4468(1)	18(1)
C(3)	4394(1)	-1276(1)	3627(1)	15(1)
C(4)	3142(1)	-274(1)	4110(1)	13(1)
C(5)	2097(1)	683(1)	3569(1)	13(1)
C(6)	2706(1)	1248(1)	2461(1)	14(1)
C(7)	1630(2)	2230(1)	1980(1)	15(1)
C(8)	1334(2)	4342(1)	2069(1)	16(1)
C(9)	2600(2)	4332(1)	1084(1)	20(1)
C(10)	-240(1)	3325(1)	3415(1)	15(1)
C(11)	-1289(1)	2842(1)	3354(1)	17(1)
C(12)	-2160(2)	3444(1)	2791(1)	19(1)
C(13)	-2171(2)	4663(1)	2142(1)	27(1)
C(14)	-3179(2)	2931(2)	2746(1)	26(1)
C(15)	325(1)	2665(1)	4319(1)	14(1)
C(16)	-136(1)	3229(1)	5172(1)	16(1)
C(17)	377(2)	2688(1)	6007(1)	17(1)
C(18)	1390(1)	1566(1)	6014(1)	16(1)
C(19)	1857(1)	1010(1)	5169(1)	14(1)
C(20)	1319(1)	1536(1)	4339(1)	13(1)
C(21)	5442(1)	-625(1)	2843(1)	14(1)
C(22)	4210(1)	-1931(1)	2959(1)	15(1)
C(23)	3446(2)	-2719(1)	3237(1)	18(1)
C(24)	3511(2)	-3284(1)	2497(1)	20(1)
C(25)	4330(2)	-3049(1)	1481(1)	20(1)
C(26)	5110(2)	-2267(1)	1189(1)	17(1)
C(27)	5052(1)	-1732(1)	1943(1)	14(1)
C(28)	8318(1)	-577(1)	1094(1)	15(1)
C(29)	8505(2)	345(1)	1360(1)	18(1)

C(30)	9730(2)	168(1)	1547(1)	21(1)
C(31)	10784(2)	-923(1)	1459(1)	21(1)
C(32)	10633(2)	-1835(1)	1162(1)	20(1)
C(33)	9405(2)	-1658(1)	986(1)	17(1)

Table 3. Bond lengths [Å] and angles [°] for 571 (CCDC 266777).

Bond	Length	Bond	Length
S(1)-O(2)	1.4240(10)	C(28)-C(33)	1.3936(19)
S(1)-O(3)	1.4262(10)	C(29)-C(30)	1.388(2)
S(1)-N(6)	1.6843(11)	C(30)-C(31)	1.385(2)
S(1)-C(28)	1.7770(15)	C(31)-C(32)	1.382(2)
Cl(1)-C(5)	1.8334(14)	C(32)-C(33)	1.383(2)
O(1)-C(21)	1.2015(16)		

Bond/Angle	Value
O(4)-N(7) 1.2260(16) — O(2)-S(1)-O(3)	120.01(6)
O(5)-N(7) 1.2240(16) — O(2)-S(1)-N(6)	107.28(6)
O(6)-C(8) 1.2187(16) — O(3)-S(1)-N(6)	107.23(6)
F(1)-C(9) 1.3400(16) — O(2)-S(1)-C(28)	107.05(6)
F(2)-C(9) 1.3369(16) — O(3)-S(1)-C(28)	110.36(6)
F(3)-C(9) 1.3384(16) — N(6)-S(1)-C(28)	103.69(6)
N(1)-N(2) 1.1362(18) — N(1)-N(2)-N(3)	171.19(15)
N(2)-N(3) 1.2467(18) — N(2)-N(3)-C(1)	115.84(13)
N(3)-C(1) 1.4808(18) — C(4)-N(4)-C(19)	107.30(11)
N(4)-C(4) 1.2826(16) — C(8)-N(5)-C(7)	125.26(11)
N(4)-C(19) 1.4307(17) — C(8)-N(5)-C(10)	117.08(11)
N(5)-C(8) 1.3475(18) — C(7)-N(5)-C(10)	117.64(11)
N(5)-C(7) 1.4683(17) — C(21)-N(6)-C(27)	110.75(11)
N(5)-C(10) 1.5039(16) — C(21)-N(6)-S(1)	119.57(9)
N(6)-C(21) 1.4160(16) — C(27)-N(6)-S(1)	129.14(9)
N(6)-C(27) 1.4384(18) — O(5)-N(7)-O(4)	125.07(14)
N(7)-C(33) 1.4689(19) — O(5)-N(7)-C(33)	117.60(12)
C(1)-C(2) 1.5229(19) — O(4)-N(7)-C(33)	117.33(13)
C(2)-C(3) 1.5518(18) — N(3)-C(1)-C(2)	112.83(12)
C(3)-C(22) 1.5151(19) — C(1)-C(2)-C(3)	113.61(11)
C(3)-C(4) 1.5250(19) — C(22)-C(3)-C(4)	118.06(12)
C(3)-C(21) 1.5487(19) — C(22)-C(3)-C(21)	102.26(10)
C(4)-C(5) 1.5429(19) — C(4)-C(3)-C(21)	104.90(11)
C(5)-C(20) 1.5120(18) — C(22)-C(3)-C(2)	111.98(11)
C(5)-C(6) 1.5279(17) — C(4)-C(3)-C(2)	109.39(11)
C(6)-C(7) 1.5276(18) — C(21)-C(3)-C(2)	109.53(11)
C(8)-C(9) 1.5519(19) — N(4)-C(4)-C(3)	120.43(12)
C(10)-C(11) 1.514(2) — N(4)-C(4)-C(5)	113.83(12)
C(10)-C(15) 1.5196(18) — C(3)-C(4)-C(5)	125.42(11)
C(11)-C(12) 1.3378(19) — C(20)-C(5)-C(6)	116.08(11)
C(12)-C(14) 1.498(2) — C(20)-C(5)-C(4)	100.03(10)
C(12)-C(13) 1.502(2) — C(6)-C(5)-C(4)	116.65(11)
C(15)-C(20) 1.3869(18) — C(20)-C(5)-Cl(1)	108.91(9)
C(15)-C(16) 1.4014(18) — C(6)-C(5)-Cl(1)	109.25(9)
C(16)-C(17) 1.3904(19) — C(4)-C(5)-Cl(1)	105.03(9)
C(17)-C(18) 1.3888(19) — C(7)-C(6)-C(5)	114.39(11)
C(18)-C(19) 1.3837(18) — N(5)-C(7)-C(6)	114.75(11)
C(19)-C(20) 1.3991(18) — O(6)-C(8)-N(5)	125.99(12)
C(22)-C(23) 1.384(2) — O(6)-C(8)-C(9)	116.88(12)
C(22)-C(27) 1.4007(18) — N(5)-C(8)-C(9)	117.12(12)
C(23)-C(24) 1.388(2) — F(2)-C(9)-F(3)	107.14(11)
C(24)-C(25) 1.3977(19) — F(2)-C(9)-F(1)	106.70(12)
C(25)-C(26) 1.389(2) — F(3)-C(9)-F(1)	107.39(11)
C(26)-C(27) 1.3833(19) — F(2)-C(9)-C(8)	109.93(12)
C(28)-C(29) 1.390(2) — F(3)-C(9)-C(8)	111.99(12)

F(1)-C(9)-C(8)	113.36(11)
N(5)-C(10)-C(11)	112.45(11)
N(5)-C(10)-C(15)	109.42(11)
C(11)-C(10)-C(15)	113.48(11)
C(12)-C(11)-C(10)	123.71(13)
C(11)-C(12)-C(14)	122.06(14)
C(11)-C(12)-C(13)	122.82(14)
C(14)-C(12)-C(13)	115.11(13)
C(20)-C(15)-C(16)	117.22(12)
C(20)-C(15)-C(10)	123.57(12)
C(16)-C(15)-C(10)	119.18(12)
C(17)-C(16)-C(15)	121.85(13)
C(18)-C(17)-C(16)	120.64(13)
C(19)-C(18)-C(17)	117.71(12)
C(18)-C(19)-C(20)	121.94(13)
C(18)-C(19)-N(4)	125.82(12)
C(20)-C(19)-N(4)	112.16(11)
C(15)-C(20)-C(19)	120.61(12)
C(15)-C(20)-C(5)	132.79(12)
C(19)-C(20)-C(5)	106.49(11)
O(1)-C(21)-N(6)	125.18(12)
O(1)-C(21)-C(3)	127.13(12)
N(6)-C(21)-C(3)	107.69(12)
C(23)-C(22)-C(27)	119.66(13)
C(23)-C(22)-C(3)	129.41(12)
C(27)-C(22)-C(3)	110.73(12)
C(22)-C(23)-C(24)	119.25(13)
C(23)-C(24)-C(25)	120.17(14)
C(26)-C(25)-C(24)	121.41(14)
C(27)-C(26)-C(25)	117.48(13)
C(26)-C(27)-C(22)	121.99(13)
C(26)-C(27)-N(6)	129.48(12)
C(22)-C(27)-N(6)	108.53(12)
C(29)-C(28)-C(33)	118.43(14)
C(29)-C(28)-S(1)	116.44(11)
C(33)-C(28)-S(1)	124.93(11)
C(28)-C(29)-C(30)	120.25(14)
C(31)-C(30)-C(29)	120.37(14)
C(32)-C(31)-C(30)	120.09(14)
C(31)-C(32)-C(33)	119.26(14)
C(32)-C(33)-C(28)	121.55(14)
C(32)-C(33)-N(7)	117.33(13)
C(28)-C(33)-N(7)	121.11(13)

Table 4. Anisotropic displacement parameters ($\mathring{A}^2$x 10^4) for 571 (CCDC 266777). The anisotropic displacement factor exponent takes the form: $-2\pi^2$ [h^2 $a^{*2}U^{11}$ + ... + 2 h k a* b* U^{12}]

	U^{11}	U^{22}	U^{33}	U^{23}	U^{13}	U^{12}
S(1)	154(2)	167(2)	139(2)	-20(1)	-47(1)	-45(2)
Cl(1)	157(2)	164(2)	173(2)	-25(1)	-62(1)	-59(1)
O(1)	168(5)	204(6)	195(5)	-65(4)	-52(4)	-62(5)
O(2)	209(6)	166(5)	231(5)	-16(4)	-92(4)	-27(5)
O(3)	217(6)	249(6)	137(5)	-50(4)	-39(4)	-90(5)
O(4)	295(7)	393(7)	454(7)	-285(6)	-37(6)	-7(6)
O(5)	266(7)	224(6)	451(7)	-63(5)	-91(5)	-105(5)
O(6)	272(6)	160(5)	247(5)	-75(4)	-28(5)	-58(5)
F(1)	175(5)	206(5)	271(4)	-33(4)	-26(4)	-27(4)
F(2)	280(5)	193(5)	329(5)	-46(4)	2(4)	-123(4)
F(3)	344(5)	256(5)	147(4)	-10(4)	-66(4)	-85(4)
N(1)	325(9)	461(10)	254(7)	36(7)	-141(6)	-174(7)
N(2)	176(7)	239(7)	282(7)	41(6)	-99(6)	-55(6)
N(3)	322(8)	195(7)	330(7)	-45(6)	-198(6)	30(6)
N(4)	134(6)	149(6)	137(5)	-21(5)	-36(5)	-34(5)
N(5)	135(6)	137(6)	120(5)	-28(5)	-38(4)	-14(5)
N(6)	145(6)	174(6)	118(5)	-38(5)	-29(5)	-50(5)
N(7)	223(7)	183(7)	293(7)	-54(6)	-111(6)	-12(6)
C(1)	213(8)	209(8)	228(7)	-49(6)	-111(6)	6(7)
C(2)	178(8)	164(7)	154(7)	-22(6)	-72(6)	-5(6)
C(3)	137(7)	151(7)	142(6)	-28(5)	-49(5)	-25(6)
C(4)	121(7)	130(7)	138(6)	-6(5)	-43(5)	-48(6)
C(5)	125(7)	137(7)	138(6)	-28(5)	-40(5)	-43(6)
C(6)	133(7)	132(7)	131(6)	-31(5)	-31(5)	-23(6)
C(7)	170(7)	130(7)	136(6)	-34(5)	-45(5)	-33(6)
C(8)	167(8)	166(7)	149(6)	-24(6)	-70(6)	-34(6)
C(9)	223(8)	160(8)	199(7)	-21(6)	-52(6)	-53(7)
C(10)	135(7)	153(7)	130(6)	-28(5)	-31(5)	-13(6)
C(11)	166(8)	164(7)	155(7)	-31(6)	-28(6)	-39(6)
C(12)	156(8)	214(8)	163(7)	-69(6)	-40(6)	-5(6)
C(13)	304(10)	250(9)	243(8)	-32(7)	-156(7)	-13(7)
C(14)	209(9)	344(9)	242(8)	-88(7)	-93(6)	-49(7)
C(15)	111(7)	165(7)	140(6)	-17(5)	-24(5)	-55(6)
C(16)	124(7)	162(7)	176(7)	-49(6)	-16(5)	-33(6)
C(17)	164(8)	203(8)	136(6)	-72(6)	-10(6)	-51(6)
C(18)	167(8)	194(8)	121(6)	-16(6)	-44(5)	-69(6)
C(19)	116(7)	144(7)	138(6)	-18(5)	-24(5)	-46(6)
C(20)	121(7)	147(7)	117(6)	-25(5)	-15(5)	-48(6)
C(21)	121(7)	142(7)	144(6)	-28(6)	-62(5)	10(6)
C(22)	145(7)	139(7)	140(6)	-34(5)	-59(5)	-1(6)
C(23)	163(8)	157(7)	177(7)	-21(6)	-37(6)	-33(6)
C(24)	160(8)	158(7)	286(8)	-43(6)	-77(6)	-49(6)
C(25)	184(8)	203(8)	233(7)	-85(6)	-83(6)	-32(7)
C(26)	142(7)	192(8)	157(7)	-54(6)	-50(6)	-18(6)
C(27)	118(7)	126(7)	182(7)	-30(6)	-52(5)	-22(6)
C(28)	134(7)	181(7)	116(6)	-8(5)	-28(5)	-50(6)

C(29)	205(8)	163(7)	155(7)	-3(6)	-44(6)	-57(6)
C(30)	257(9)	233(8)	176(7)	2(6)	-80(6)	-131(7)
C(31)	175(8)	282(9)	179(7)	23(6)	-66(6)	-105(7)
C(32)	162(8)	207(8)	179(7)	-2(6)	-43(6)	-30(6)
C(33)	186(8)	172(8)	143(6)	-13(6)	-33(6)	-61(6)

_____

CALIFORNIA INSTITUTE OF TECHNOLOGY
BECKMAN INSTITUTE
X-RAY CRYSTALLOGRAPHY LABORATORY

Date 22 July 2005

Crystal Structure Analysis of:

575

(shown below)

For   Investigator: Jeremy May   ext. 6131

Advisor: B. M. Stoltz   ext. 6064

Account Number: BMS.JandJ-2.21-GRANT.000010

By   Michael W. Day   116 Beckman   ext. 2734
e-mail: mikeday@caltech.edu

Contents

575

Note: The crystallographic data have been deposited in the Cambridge Database (CCDC) and has been placed on hold pending further instructions from me. The deposition number is 279131. Ideally the CCDC would like the publication to contain a footnote of the type: "Crystallographic data have been deposited at the CCDC, 12 Union Road, Cambridge CB2 1EZ, UK and copies can be obtained on request, free of charge, by quoting the publication citation and the deposition number 279131."

Table 1. Crystal data and structure refinement for 575 (CCDC 279131).

Empirical formula	$C_{39}H_{33}F_3N_6O_{10}S_2 \cdot C_3H_6O$
Formula weight	924.91
Crystallization Solvent	Acetone/H_2O
Crystal Habit	Needle
Crystal size	0.44 x 0.07 x 0.04 mm^3
Crystal color	Yellow

Data Collection

Type of diffractometer	Bruker SMART 1000
Wavelength	0.71073 Å MoKα
Data Collection Temperature	100(2) K
θ range for 5619 reflections used in lattice determination	2.18 to 22.18°
Unit cell dimensions	a = 17.6754(7) Å
	b = 11.5184(5) Å β= 110.488(2)°
	c = 22.3282(9) Å
Volume	4258.3(3) Å^3
Z	4
Crystal system	Monoclinic
Space group	P2$_1$/n
Density (calculated)	1.443 Mg/m^3
F(000)	1920
Data collection program	Bruker SMART v5.630
θ range for data collection	1.27 to 22.54°
Completeness to θ = 22.54°	99.2 %
Index ranges	-19 ≤ h ≤ 17, -12 ≤ k ≤ 12, -24 ≤ l ≤ 23
Data collection scan type	ω scans at 3 ϕ settings
Data reduction program	Bruker SAINT v6.45A
Reflections collected	22570
Independent reflections	5566 [R$_{int}$= 0.1110]
Absorption coefficient	0.207 mm^{-1}
Absorption correction	None
Max. and min. transmission	0.9918 and 0.9145

Table 1 (cont.)

Structure Solution and Refinement

Structure solution program	Bruker XS v6.12
Primary solution method	Direct methods
Secondary solution method	Difference Fourier map
Hydrogen placement	Geometric positions
Structure refinement program	Bruker XL v6.12
Refinement method	Full matrix least-squares on F^2
Data / restraints / parameters	5566 / 0 / 581
Treatment of hydrogen atoms	Riding
Goodness-of-fit on F^2	1.647
Final R indices [I>2σ(I), 3657 reflections]	R1 = 0.0610, wR2 = 0.1142
R indices (all data)	R1 = 0.0994, wR2 = 0.1220
Type of weighting scheme used	Sigma
Weighting scheme used	$w=1/\sigma^2(Fo^2)$
Max shift/error	0.000
Average shift/error	0.000
Largest diff. peak and hole	1.089 and -0.740 e.Å^{-3}

Special Refinement Details

Refinement of F^2 against ALL reflections. The weighted R-factor (wR) and goodness of fit (S) are based on F^2, conventional R-factors (R) are based on F, with F set to zero for negative F^2. The threshold expression of $F^2 > 2\sigma(F^2)$ is used only for calculating R-factors(gt) etc. and is not relevant to the choice of reflections for refinement. R-factors based on F^2 are statistically about twice as large as those based on F, and R-factors based on ALL data will be even larger.

All esds (except the esd in the dihedral angle between two l.s. planes) are estimated using the full covariance matrix. The cell esds are taken into account individually in the estimation of esds in distances, angles and torsion angles; correlations between esds in cell parameters are only used when they are defined by crystal symmetry. An approximate (isotropic) treatment of cell esds is used for estimating esds involving l.s. planes.

Table 2. Atomic coordinates (x 10⁴) and equivalent isotropic displacement parameters (Å²x 10³) for 575 (CCDC 279131). U(eq) is defined as the trace of the orthogonalized U^{ij} tensor.

	x	y	z	U_{eq}
S(1)	796(1)	1154(1)	2298(1)	23(1)
S(2)	1837(1)	2436(1)	5010(1)	25(1)
F(1)	-2426(2)	3645(3)	3244(1)	46(1)
F(2)	-2916(2)	3349(3)	3989(2)	51(1)
F(3)	-3670(2)	3148(3)	3000(2)	56(1)
O(1)	-3290(2)	1016(3)	3111(2)	47(1)
O(2)	971(2)	2303(3)	2148(1)	25(1)
O(3)	515(2)	295(3)	1811(1)	27(1)
O(4)	726(2)	-1502(3)	2714(2)	33(1)
O(5)	1637(2)	-2205(3)	2359(2)	43(1)
O(6)	893(2)	5526(3)	4940(2)	30(1)
O(7)	1790(2)	1760(3)	4461(1)	27(1)
O(8)	1256(2)	2273(3)	5321(1)	25(1)
O(9)	2232(2)	3906(3)	6240(2)	41(1)
O(10)	2447(2)	2664(3)	7011(2)	39(1)
N(1)	110(2)	1260(3)	2637(2)	23(1)
N(2)	-1954(2)	1372(3)	3723(2)	23(1)
N(3)	1385(3)	-1474(4)	2645(2)	30(1)
N(4)	-182(3)	6301(4)	4131(2)	31(1)
N(5)	1821(2)	3784(3)	4840(2)	26(1)
N(6)	2525(3)	3010(4)	6515(2)	30(1)
C(1)	-471(3)	406(4)	2606(2)	23(1)
C(2)	-889(3)	679(4)	2987(2)	22(1)
C(3)	-1587(3)	-31(4)	3036(2)	26(1)
C(4)	-1767(3)	156(4)	3647(2)	25(1)
C(5)	-1282(3)	2126(4)	4115(2)	21(1)
C(6)	-728(3)	2468(4)	3754(2)	20(1)
C(7)	-305(3)	3503(4)	3923(2)	23(1)
C(8)	262(3)	3874(4)	3661(2)	22(1)
C(9)	459(3)	3170(4)	3233(2)	24(1)
C(10)	46(3)	2125(4)	3071(2)	20(1)
C(11)	-556(3)	1763(4)	3307(2)	20(1)
C(12)	-2718(4)	1699(5)	3416(2)	34(1)
C(13)	-2897(3)	2987(5)	3422(2)	28(1)
C(14)	-807(3)	1539(4)	4743(2)	21(1)
C(15)	-1064(3)	1359(4)	5226(2)	23(1)
C(16)	-1879(3)	1699(5)	5233(3)	48(2)
C(17)	-527(3)	795(4)	5829(2)	31(1)
C(18)	1699(3)	641(4)	2892(2)	22(1)
C(19)	2257(3)	1460(4)	3232(2)	26(1)
C(20)	3012(3)	1131(5)	3636(2)	31(1)
C(21)	3239(3)	-13(5)	3702(2)	36(1)
C(22)	2691(3)	-866(5)	3354(2)	34(1)
C(23)	1936(3)	-528(4)	2969(2)	24(1)
C(24)	662(3)	5096(4)	3802(2)	26(1)
C(25)	168(3)	5916(4)	3246(2)	30(1)
C(26)	-551(3)	6277(5)	3434(2)	32(1)

C(27)	487(3)	5657(4)	4365(3)	28(1)
C(28)	1556(3)	5005(4)	3882(2)	23(1)
C(29)	1867(3)	5513(4)	3458(2)	27(1)
C(30)	2645(3)	5333(5)	3485(3)	35(2)
C(31)	3166(3)	4630(5)	3957(3)	35(2)
C(32)	2877(3)	4122(4)	4394(2)	31(1)
C(33)	2094(3)	4307(4)	4368(2)	27(1)
C(34)	2805(3)	2082(4)	5594(2)	23(1)
C(35)	3027(3)	2303(4)	6255(2)	25(1)
C(36)	3726(3)	1881(5)	6679(3)	36(1)
C(37)	4252(3)	1260(5)	6463(3)	38(2)
C(38)	4066(3)	1045(5)	5820(3)	35(1)
C(39)	3332(3)	1441(4)	5390(2)	29(1)
O(11)	4894(3)	1449(7)	4720(2)	135(3)
C(41)	5216(4)	2230(7)	3884(4)	93(3)
C(42)	5270(4)	2185(8)	4564(4)	77(2)
C(43)	5851(6)	2895(10)	5031(5)	161(5)

Table 3. **Bond lengths [Å] and angles [°] for 575 (CCDC 279131).**

_____

S(1)-O(2)	1.426(3)	C(24)-C(27)	1.538(7)
S(1)-O(3)	1.425(3)	C(24)-C(25)	1.561(7)
S(1)-N(1)	1.644(4)	C(25)-C(26)	1.528(6)
S(1)-C(18)	1.781(5)	C(28)-C(29)	1.379(6)
S(2)-O(7)	1.429(3)	C(28)-C(33)	1.416(7)
S(2)-O(8)	1.438(3)	C(29)-C(30)	1.372(6)
S(2)-N(5)	1.597(4)	C(30)-C(31)	1.392(7)
S(2)-C(34)	1.798(5)	C(31)-C(32)	1.380(6)
F(1)-C(13)	1.287(5)	C(32)-C(33)	1.381(6)
F(2)-C(13)	1.344(5)	C(34)-C(39)	1.386(6)
F(3)-C(13)	1.375(5)	C(34)-C(35)	1.412(6)
O(1)-C(12)	1.272(6)	C(35)-C(36)	1.356(7)
O(4)-N(3)	1.227(5)	C(36)-C(37)	1.387(7)
O(5)-N(3)	1.231(5)	C(37)-C(38)	1.379(7)
O(6)-C(27)	1.241(6)	C(38)-C(39)	1.393(7)
O(9)-N(6)	1.220(5)	O(11)-C(42)	1.201(8)
O(10)-N(6)	1.230(5)	C(41)-C(42)	1.487(10)
N(1)-C(1)	1.406(5)	C(42)-C(43)	1.436(10)
N(1)-C(10)	1.422(6)		
N(2)-C(12)	1.338(6)	O(2)-S(1)-O(3)	120.74(19)
N(2)-C(4)	1.462(6)	O(2)-S(1)-N(1)	107.17(19)
N(2)-C(5)	1.484(6)	O(3)-S(1)-N(1)	106.7(2)
N(3)-C(23)	1.472(6)	O(2)-S(1)-C(18)	105.8(2)
N(4)-C(27)	1.337(6)	O(3)-S(1)-C(18)	108.6(2)
N(4)-C(26)	1.462(6)	N(1)-S(1)-C(18)	107.2(2)
N(5)-C(33)	1.437(6)	O(7)-S(2)-O(8)	120.4(2)
N(6)-C(35)	1.465(6)	O(7)-S(2)-N(5)	109.6(2)
C(1)-C(2)	1.344(6)	O(8)-S(2)-N(5)	106.59(19)
C(2)-C(11)	1.457(6)	O(7)-S(2)-C(34)	104.6(2)
C(2)-C(3)	1.517(6)	O(8)-S(2)-C(34)	106.2(2)
C(3)-C(4)	1.520(6)	N(5)-S(2)-C(34)	109.0(2)
C(5)-C(14)	1.518(6)	C(1)-N(1)-C(10)	107.0(3)
C(5)-C(6)	1.522(6)	C(1)-N(1)-S(1)	124.7(3)
C(6)-C(7)	1.388(6)	C(10)-N(1)-S(1)	127.9(3)
C(6)-C(11)	1.401(6)	C(12)-N(2)-C(4)	116.0(4)
C(7)-C(8)	1.393(6)	C(12)-N(2)-C(5)	126.4(4)
C(8)-C(9)	1.388(6)	C(4)-N(2)-C(5)	117.5(4)
C(8)-C(24)	1.557(6)	O(4)-N(3)-O(5)	125.4(4)
C(9)-C(10)	1.389(6)	O(4)-N(3)-C(23)	116.9(4)
C(10)-C(11)	1.404(6)	O(5)-N(3)-C(23)	117.6(4)
C(12)-C(13)	1.519(7)	C(27)-N(4)-C(26)	114.2(4)
C(14)-C(15)	1.326(6)	C(33)-N(5)-S(2)	126.8(3)
C(15)-C(17)	1.496(6)	O(9)-N(6)-O(10)	124.5(4)
C(15)-C(16)	1.498(6)	O(9)-N(6)-C(35)	118.8(4)
C(18)-C(19)	1.385(6)	O(10)-N(6)-C(35)	116.7(4)
C(18)-C(23)	1.403(6)	C(2)-C(1)-N(1)	111.0(4)
C(19)-C(20)	1.377(7)	C(1)-C(2)-C(11)	107.1(4)
C(20)-C(21)	1.370(7)	C(1)-C(2)-C(3)	124.1(4)
C(21)-C(22)	1.406(7)	C(11)-C(2)-C(3)	128.8(4)
C(22)-C(23)	1.367(6)	C(4)-C(3)-C(2)	114.8(4)
C(24)-C(28)	1.531(6)	N(2)-C(4)-C(3)	111.5(4)

N(2)-C(5)-C(14)	110.7(4)	C(30)-C(29)-C(28)	122.7(5)
N(2)-C(5)-C(6)	111.7(4)	C(29)-C(30)-C(31)	120.6(5)
C(14)-C(5)-C(6)	110.7(4)	C(32)-C(31)-C(30)	118.1(5)
C(7)-C(6)-C(11)	117.4(4)	C(31)-C(32)-C(33)	121.2(5)
C(7)-C(6)-C(5)	117.6(4)	C(32)-C(33)-C(28)	121.0(4)
C(11)-C(6)-C(5)	124.7(4)	C(32)-C(33)-N(5)	119.6(5)
C(6)-C(7)-C(8)	123.2(4)	C(28)-C(33)-N(5)	119.5(4)
C(9)-C(8)-C(7)	120.1(5)	C(39)-C(34)-C(35)	117.9(5)
C(9)-C(8)-C(24)	117.5(4)	C(39)-C(34)-S(2)	117.5(4)
C(7)-C(8)-C(24)	122.3(4)	C(35)-C(34)-S(2)	124.3(4)
C(8)-C(9)-C(10)	116.7(4)	C(36)-C(35)-C(34)	121.2(5)
C(9)-C(10)-C(11)	124.0(4)	C(36)-C(35)-N(6)	116.9(5)
C(9)-C(10)-N(1)	128.6(4)	C(34)-C(35)-N(6)	121.9(5)
C(11)-C(10)-N(1)	107.4(4)	C(35)-C(36)-C(37)	119.9(5)
C(6)-C(11)-C(10)	118.5(4)	C(38)-C(37)-C(36)	120.8(5)
C(6)-C(11)-C(2)	134.0(4)	C(37)-C(38)-C(39)	118.9(5)
C(10)-C(11)-C(2)	107.4(4)	C(34)-C(39)-C(38)	121.3(5)
O(1)-C(12)-N(2)	124.8(5)	O(11)-C(42)-C(43)	121.3(8)
O(1)-C(12)-C(13)	118.7(5)	O(11)-C(42)-C(41)	118.4(7)
N(2)-C(12)-C(13)	116.5(5)	C(43)-C(42)-C(41)	119.7(7)
F(1)-C(13)-F(2)	109.9(4)		
F(1)-C(13)-F(3)	107.7(4)		
F(2)-C(13)-F(3)	105.0(4)		
F(1)-C(13)-C(12)	114.4(4)		
F(2)-C(13)-C(12)	112.7(4)		
F(3)-C(13)-C(12)	106.6(4)		
C(15)-C(14)-C(5)	125.8(4)		
C(14)-C(15)-C(17)	120.6(4)		
C(14)-C(15)-C(16)	124.9(4)		
C(17)-C(15)-C(16)	114.5(4)		
C(19)-C(18)-C(23)	117.5(4)		
C(19)-C(18)-S(1)	117.6(4)		
C(23)-C(18)-S(1)	124.1(4)		
C(20)-C(19)-C(18)	120.9(5)		
C(21)-C(20)-C(19)	121.0(5)		
C(20)-C(21)-C(22)	119.6(5)		
C(23)-C(22)-C(21)	118.7(5)		
C(22)-C(23)-C(18)	122.3(5)		
C(22)-C(23)-N(3)	115.6(5)		
C(18)-C(23)-N(3)	122.1(4)		
C(28)-C(24)-C(27)	115.3(4)		
C(28)-C(24)-C(8)	109.8(4)		
C(27)-C(24)-C(8)	109.7(4)		
C(28)-C(24)-C(25)	113.7(4)		
C(27)-C(24)-C(25)	100.3(4)		
C(8)-C(24)-C(25)	107.4(4)		
C(26)-C(25)-C(24)	103.5(4)		
N(4)-C(26)-C(25)	101.1(4)		
O(6)-C(27)-N(4)	125.7(5)		
O(6)-C(27)-C(24)	125.9(5)		
N(4)-C(27)-C(24)	108.4(5)		
C(29)-C(28)-C(33)	116.4(4)		
C(29)-C(28)-C(24)	122.2(4)		
C(33)-C(28)-C(24)	121.1(4)		

Table 4.   Anisotropic displacement parameters (Å²x 10⁴) for 575 (CCDC 279131). The anisotropic displacement factor exponent takes the form: $-2\pi^2$ [h^2 $a^{*2}U^{11}$ + ... + 2 h k a* b* U^{12}]

	U^{11}	U^{22}	U^{33}	U^{23}	U^{13}	U^{12}
S(1)	281(8)	239(8)	214(8)	-7(6)	131(6)	2(6)
S(2)	272(8)	267(8)	216(8)	-7(6)	105(6)	-21(6)
F(1)	540(20)	420(20)	410(20)	58(16)	130(17)	42(17)
F(2)	590(20)	540(20)	430(20)	68(17)	198(17)	180(18)
F(3)	460(20)	690(30)	480(20)	152(18)	106(18)	235(18)
O(1)	250(20)	520(30)	610(30)	210(20)	100(20)	-70(20)
O(2)	360(20)	170(20)	250(20)	16(15)	167(16)	-23(16)
O(3)	330(20)	290(20)	210(20)	-57(16)	131(16)	-22(17)
O(4)	410(20)	330(20)	310(20)	18(17)	193(19)	-44(18)
O(5)	510(30)	380(30)	450(30)	-150(20)	220(20)	100(20)
O(6)	450(20)	280(20)	240(20)	-25(18)	196(19)	-10(18)
O(7)	320(20)	300(20)	210(20)	-61(16)	106(16)	-17(17)
O(8)	264(19)	260(20)	250(20)	20(16)	116(16)	-3(16)
O(9)	690(30)	280(20)	370(20)	-40(20)	330(20)	-10(20)
O(10)	490(20)	500(30)	230(20)	-41(19)	182(18)	-100(20)
N(1)	270(20)	230(30)	230(20)	-10(20)	148(19)	10(20)
N(2)	190(20)	300(30)	180(20)	20(20)	63(19)	20(20)
N(3)	390(30)	270(30)	270(30)	50(20)	160(20)	30(20)
N(4)	430(30)	220(30)	380(30)	-10(20)	260(20)	70(20)
N(5)	330(30)	270(30)	210(20)	-30(20)	140(20)	-10(20)
N(6)	420(30)	260(30)	240(30)	-100(20)	150(20)	-110(20)
C(1)	260(30)	190(30)	230(30)	0(20)	90(20)	-20(20)
C(2)	230(30)	240(30)	180(30)	20(20)	70(20)	-30(20)
C(3)	250(30)	340(30)	190(30)	-30(20)	90(20)	-40(20)
C(4)	240(30)	300(30)	220(30)	20(20)	90(20)	-40(20)
C(5)	230(30)	190(30)	200(30)	0(20)	80(20)	20(20)
C(6)	200(30)	250(30)	160(30)	70(20)	80(20)	30(20)
C(7)	330(30)	240(30)	160(30)	40(20)	140(20)	80(30)
C(8)	230(30)	230(30)	200(30)	50(20)	70(20)	70(30)
C(9)	270(30)	260(30)	240(30)	60(20)	140(20)	70(30)
C(10)	210(30)	210(30)	180(30)	40(20)	80(20)	50(20)
C(11)	180(30)	260(30)	160(30)	70(20)	60(20)	70(20)
C(12)	410(40)	500(40)	210(30)	120(30)	230(30)	150(30)
C(13)	210(30)	540(40)	80(30)	110(30)	50(20)	40(30)
C(14)	170(30)	260(30)	210(30)	20(20)	60(20)	-10(20)
C(15)	250(30)	250(30)	200(30)	-20(20)	90(20)	-20(20)
C(16)	470(40)	750(50)	290(40)	80(30)	240(30)	60(30)
C(17)	360(30)	360(40)	190(30)	20(30)	70(30)	-40(30)
C(18)	250(30)	300(30)	150(30)	0(20)	120(20)	-10(30)
C(19)	300(30)	260(30)	280(30)	0(30)	190(30)	20(30)
C(20)	340(30)	340(40)	270(30)	-60(30)	140(30)	-60(30)
C(21)	270(30)	490(40)	280(30)	-10(30)	40(30)	-20(30)
C(22)	360(40)	370(40)	330(40)	80(30)	180(30)	120(30)
C(23)	270(30)	290(30)	170(30)	-20(20)	90(20)	-40(30)
C(24)	360(30)	220(30)	260(30)	20(20)	200(30)	10(30)

C(25)	390(30)	230(30)	350(30)	60(30)	240(30)	20(30)
C(26)	450(40)	250(30)	310(40)	60(30)	190(30)	60(30)
C(27)	430(40)	170(30)	330(40)	-20(30)	260(30)	-80(30)
C(28)	300(30)	200(30)	240(30)	-40(20)	150(30)	-40(30)
C(29)	360(30)	240(30)	260(30)	-70(20)	160(30)	-60(30)
C(30)	520(40)	340(40)	360(40)	-20(30)	370(30)	-110(30)
C(31)	360(40)	340(40)	440(40)	-50(30)	260(30)	-70(30)
C(32)	340(30)	310(40)	320(30)	0(30)	190(30)	-40(30)
C(33)	350(30)	220(30)	320(30)	-80(30)	230(30)	-120(30)
C(34)	270(30)	230(30)	180(30)	20(20)	70(20)	-60(20)
C(35)	290(30)	240(30)	230(30)	-40(30)	110(30)	-110(30)
C(36)	380(40)	410(40)	230(30)	-70(30)	60(30)	-170(30)
C(37)	300(30)	450(40)	320(40)	20(30)	20(30)	-30(30)
C(38)	310(30)	400(40)	340(40)	40(30)	110(30)	50(30)
C(39)	310(30)	380(40)	230(30)	-20(30)	140(30)	-60(30)
O(11)	1080(50)	2530(80)	470(40)	-270(40)	320(30)	-990(50)
C(41)	650(50)	1260(80)	930(70)	470(50)	340(50)	150(50)
C(42)	370(40)	1260(80)	680(60)	100(50)	170(40)	-210(50)
C(43)	1220(90)	1720(120)	1550(110)	-740(80)	80(80)	-580(80)

Table 5. Hydrogen bonds for 575 (CCDC 279131) [Å and °].

D-H...A	d(D-H)	d(H...A)	d(D...A)	<(DHA)
N(4)-H(4)...O(8)#1	0.88	2.23	3.072(5)	160.1
N(5)-H(5)...O(6)	0.88	1.91	2.651(5)	141.0
N(5)-H(5)...O(9)	0.88	2.51	2.955(5)	112.1

Symmetry transformations used to generate equivalent atoms:
#1 -x,-y+1,-z+1

7.9 References and Notes

(1) Nicolaou, K. C.; Snyder, S. A. *Angew. Chem. Int. Ed.* **2005**, *44*, 1012-1044.

(2) Ratnayake, A. S.; Yoshida, W. Y.; Mooberry, S. L.; Hemsheidt, T. K. *J. Org. Chem.* **2001**, *66*, 8717.

(3) Numata, A.; Takahashi, C.; Ito, Y.; Takada, T.; Kawai, K.; Usami, Y.; Matsumura, E.; Imachi, M.; Tadayoshi, I.; Hasegawa, T. *Tetrahedron Lett.* **1993**, 34, 2355.

(4) Jadulco, R.; Edrada, R. A.; Ebel, R.; Berg, A.; Schaumann, K.; Wray, V.; Steube, K; Proksch, P. *J. Nat. Prod.* 2004, *67*, 78-81.

(5) Hayashi, H.; Matsumoto, H.; Akiyama, K. *Biosci. Biotechnol. Biochem.* **2004**, *68*(3), 753-756.

(6) Dalsgaard, P. W.; Blunt, J. W.; Munro, M. H. G.; Frisvad, J. C.; Christophersen, C. *J. Nat. Prod.* **2005**, *68*, 258-261.

(7) Verbitski, S. M.; Mayne, C. L.; Davis, R. A.; Concepcion, G. P.; Ireland, C. M. *J. Org. Chem.* **2002**, *67*, 7124.

(8) May, J. A.; Zeidan, R. K.; Stoltz, B. M. *Tetrahedron Lett.* **2003**, *44*, 1203. This work is also presented in Chapter 6 of this thesis.

(9) See also Chapter 5 of this thesis for comparison to the calycanthaceous alkaloids.

(10) (a) Jackson, A. H.; Smith, A. E. *J. Chem. Soc.* **1964**, 5510. (b) Dachriyanus; Sargent, M. V.; Wahyuni, F. S. *Aust. J. Chem.* **2000**, *53*, 159. (c) Horne, S.; Taylor, N.; Collins, S.; Rodrigo, R. *J. Chem. Soc., Perkin Trans.* 1 **1991**, 3047. (d) Nyerges, M.; Rudas, M.; Bitter, I.; Töke, L. *Tetrahedron* **1997**, *53*, 3269. (e) Spande, T. F.; Wilchek, M.; Witkop, B. *J. Am. Chem. Soc.* **1968**, 3256. (f) Chan, T.-L.; Schellenberg, K. A. *J. Biol. Chem.* **1968**, *243*, 6284. (g) Decodts, G.; Wakselman, M.; Vilkas, M. *Tetrahedron*

1970, *26*, 3313. (h) Britten, A. Z.; Bardsley, W. G.; Hill, C. M. *Tetrahedron* **1971**, *27*, 5631. (i) Lyle, F. R. US Patent 5 973 257, 1985; *Chem. Abstr.* **1985**, *65*, 2870. (j) Lindquist, N.; Fenical, W.; Van Duyne, G. D.; Clardy, J. *J. Am. Chem. Soc.* **1991**, *113*, 2303. (k) Li, J.; Burgett, A. W. G.; Esser, L.; Amezcua, C.; Harran, P. G. *Angew. Chem., Int. Ed.* **2001**, *40*, 4770. (l) Li, J.; Jeong, S.; Esser, L.; Harran, P. G. *Angew. Chem., Int. Ed.* **2001**, *40*, 4765.

(11) Corey, E. J. *Angew. Chem., Int. Ed.* **1999**, *38*, 1928.

(12) (a) Soloveva, T. F.; Kuvichkina, T. N.; Baskunov, B. P.; Kozlovskii, A. G. *Microbiol.* **1995**, 64, 550. (b) Kozlovskii, A. G.; Soloveva, T. F.; Sakharovskii, V. G.; Adanin, V. M. *Dokl. Akad. Nauk. SSSR* **1981**, *260*, 230.

(13) Somei, M. *Chem. Pharm. Bull.* **1985**, *33*, 2162.

(14) Iwao, M. *Tetrehedron Lett.* **1995**, *36*, 5929.

(15) The lab of Raymond Funk used a similar approach in a model system for nomofungin.

(16)

(17)

(18) Arndt, ; Eistert, *Chem. Ber.* **1927**, *60*, 1269.

(19) *J. Med Chem.* **1994**, *37*(15), 2308.

(20) Takeuchi, Y.; Tarui, T; Shibata, N. *Org. Lett.* **2000**, *2*(5), 639-642.

(21) Weert, M.; Lagerwerf, F. M. *J. Mass Spectrom.* **1998**, *33*(9), 884-891.

(22) Studies by the Moore lab at the University of Illinois have shown that acetonitrile is a superb solvent to promote π-stacking interactions between aromatic rings. THF is similar to acetonitrile, but CH_2Cl_2 and other chlorinated solvents disrupt π-stacking. This

phenomenon may explain the selectivity for one product observed in THF and a different, non-selective product distribution as seen in CH_2Cl_2. See: Hill, D. J.; Mio, M. J.; Prince, R. B.; Hughes, T. S.; Moore, J. S. *Chem. Rev*. **2001**, *101*, 3893-4012.

(23) Fuchs, J. R.; Funk, R. L *Org*. *Lett*. **2004**, *7*(4), 677-680.

(24) Krolski, M. E.; Renaldo, A. F.; Rudisill, D. E.; Stille; J. K. *J*. *Org*. *Chem*. **1988**; *53*(6); 1170-1176.

(25) Sharma, V. M.; Prasanna, P.; Adi Seshu, K. V.; Renuka, B.; Rao, L.; Kumar, G. S.; Narasimhulu, C. P.; Babu, P. A.; Puranik, R. C.; Subramanyam, D. *Biorg*. *Med*. *Chem*. *Lett*. **2002**, *12*(17), 2303-2308.

(26) Kawasaki; Nagaoka; Satoh; Okamoto *Tetrahedron* **2004**, *60*(15), 3493-3504.

(27) Gabriela; Salermo; Veltri; Costa *Eur*. *J*. *Org*. *Chem*. **2001**, *24*, 4607-4614.

(28) Kennewell; Miller; Scrowston; Westwood *J*. *Chem*. *Res*. *Miniprint* **1995**, *10*, 2380-2388.

(29) (a) Spence, T. *J*. *Chem*. *Soc*. *C* **1971**, 3712-3718. (b) Eckroth, C. *J*. *Chem*. *Soc*. *C* **1970**, 2660. (c) *J*. *Med Chem*. **1994**, *37*(15), 2308.

APPENDIX THREE

Spectra Relevant to Chapter 7:

**Recent Discoveries toward the Synthesis of the
Communesin Family of Indole Alkaloids**

450
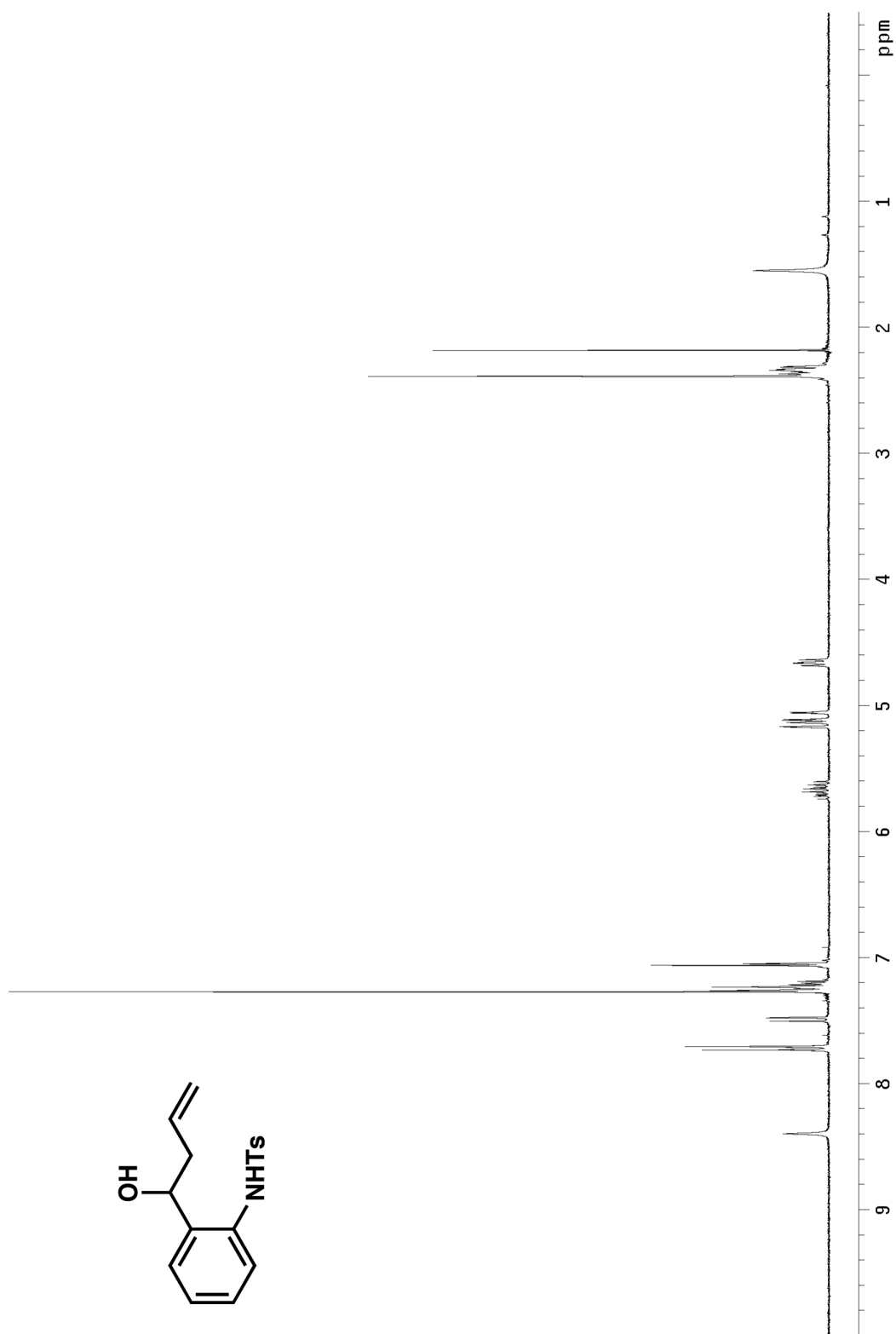
Figure A.3.1 ¹HNMR (300 MHz, CDCL₃) of compound **507**.
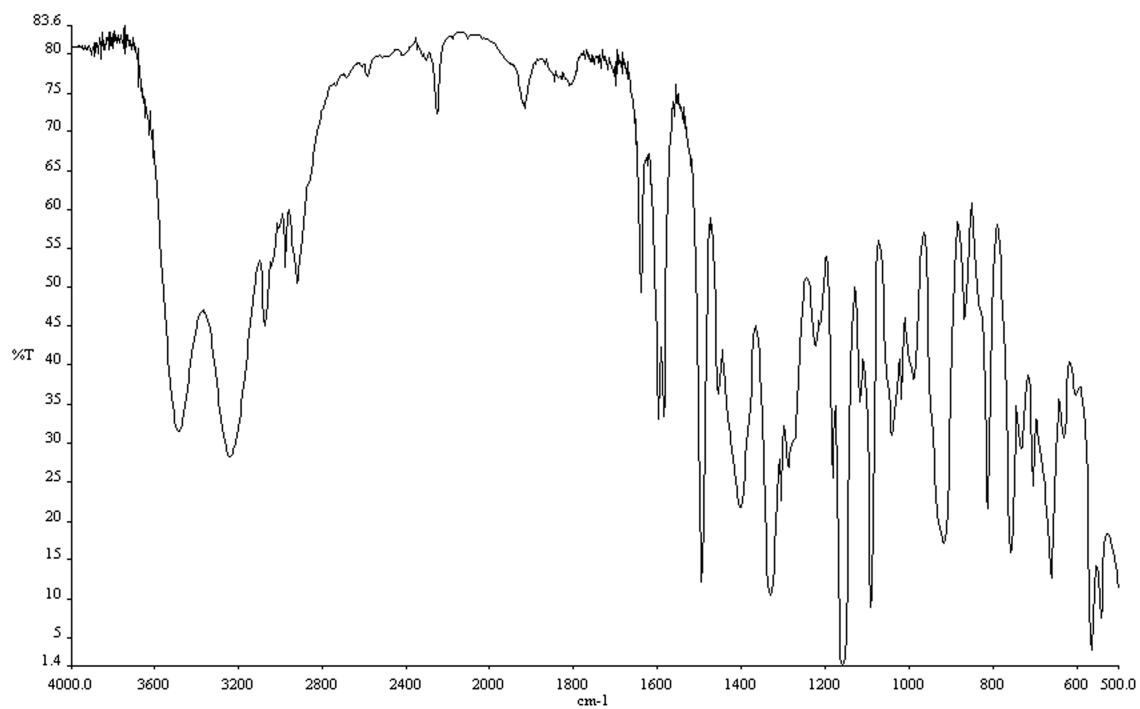
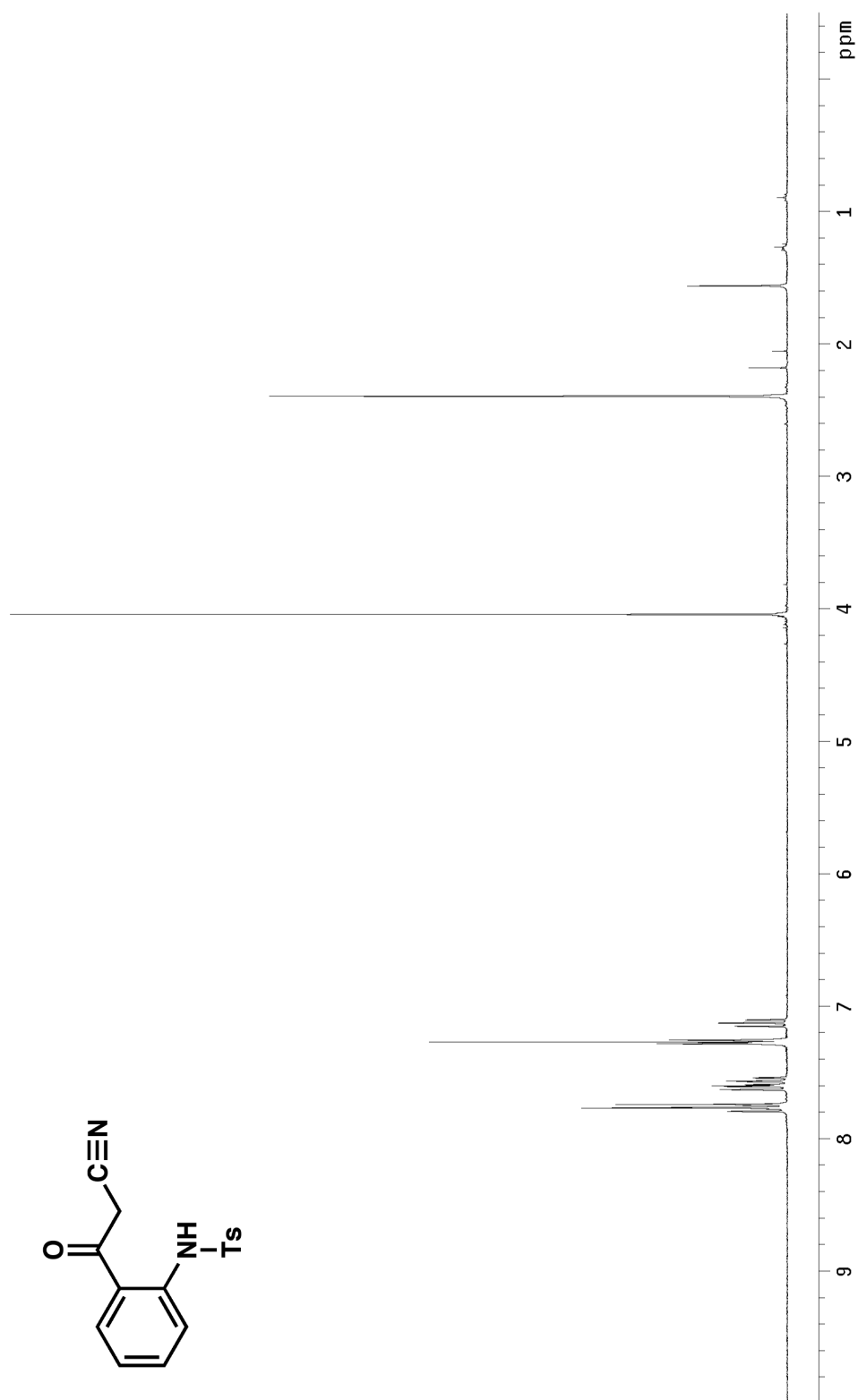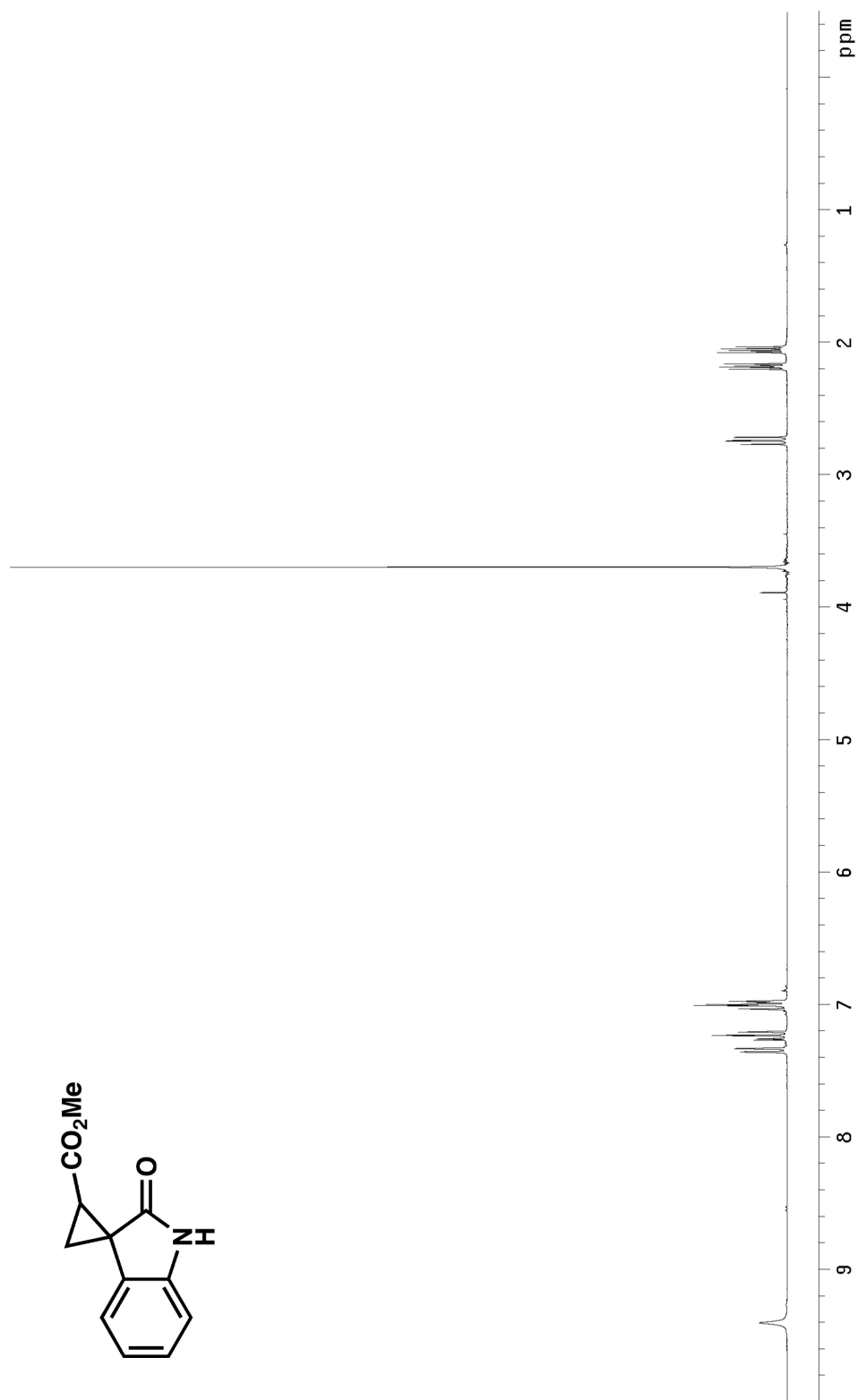*Figure A.3.2* Infrared spectrum (thin film/NaCl) of compound **507**.
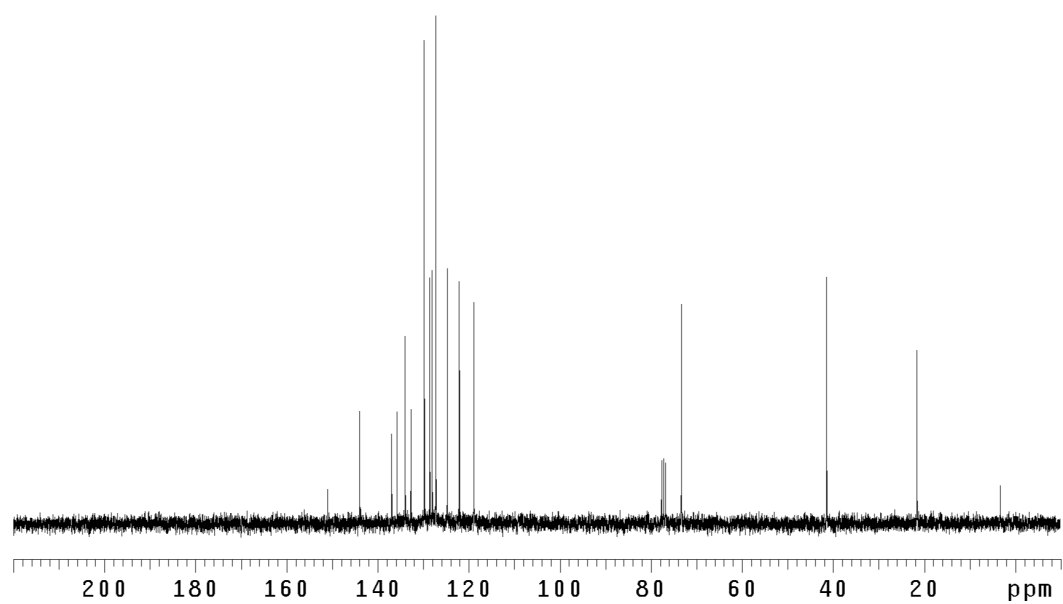
Figure A.3.3 ^{13}CNMR (75 Mhz, CDCl$_3$) of compound **507**.

452
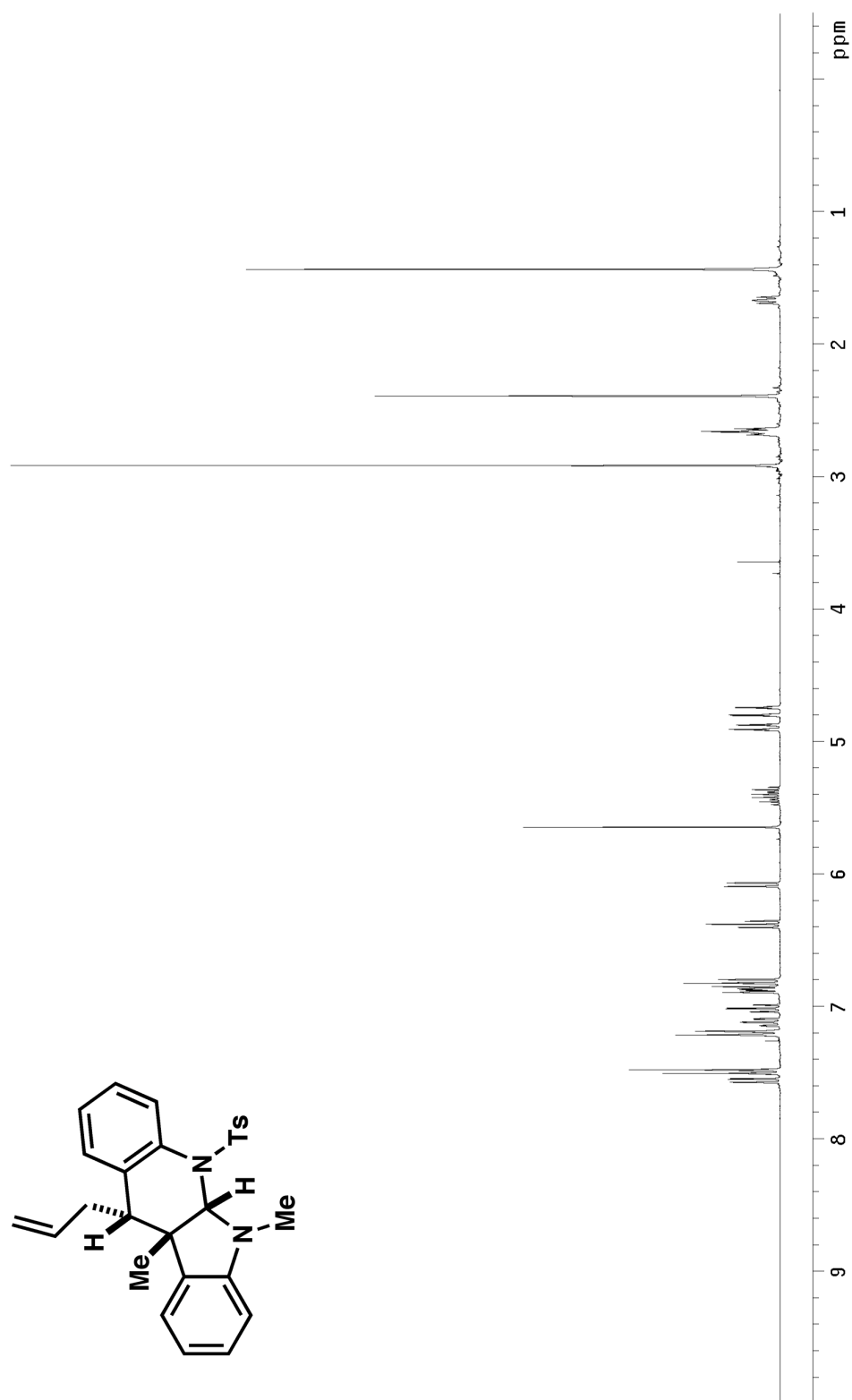
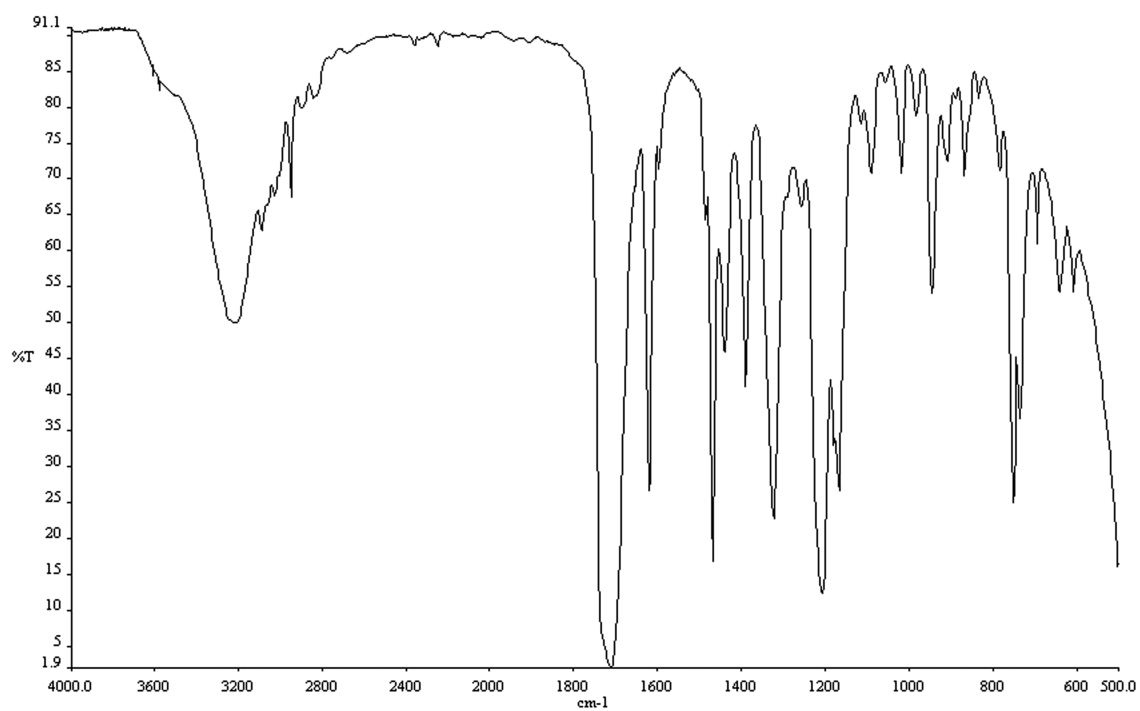*Figure A.3.4* ^{1}HNMR (300 MHz, CDCL$_3$) of compound **510**.
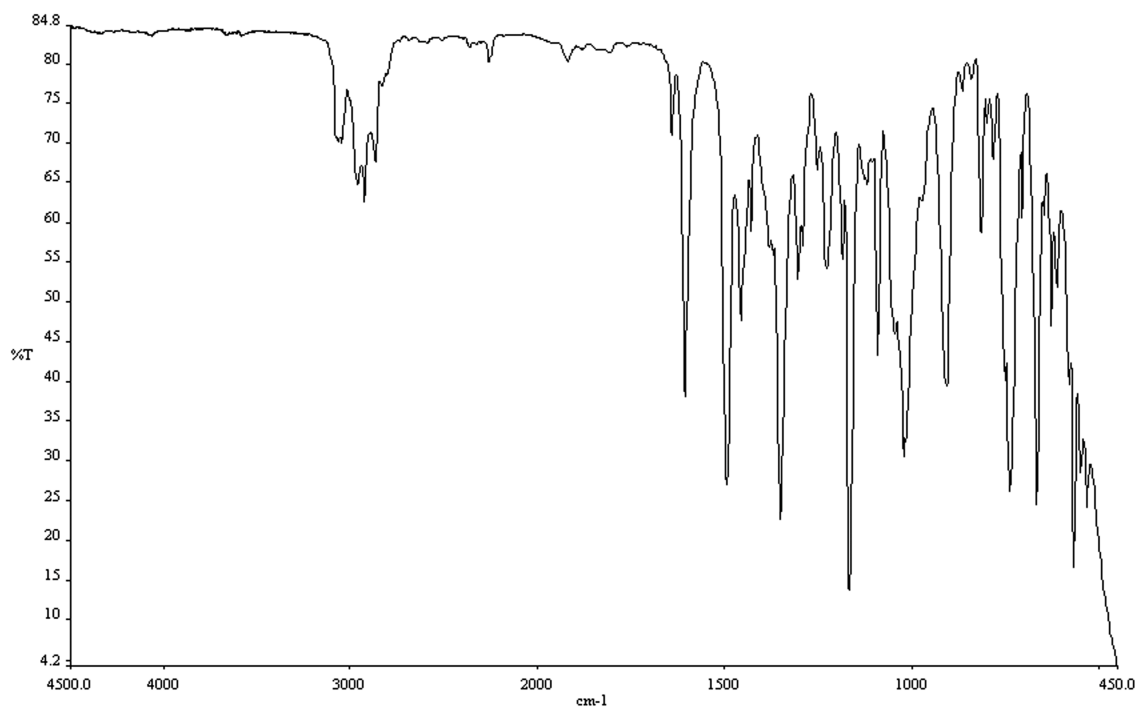
Figure A.3.5 Infrared spectrum (thin film/NaCl) of compound **510**.
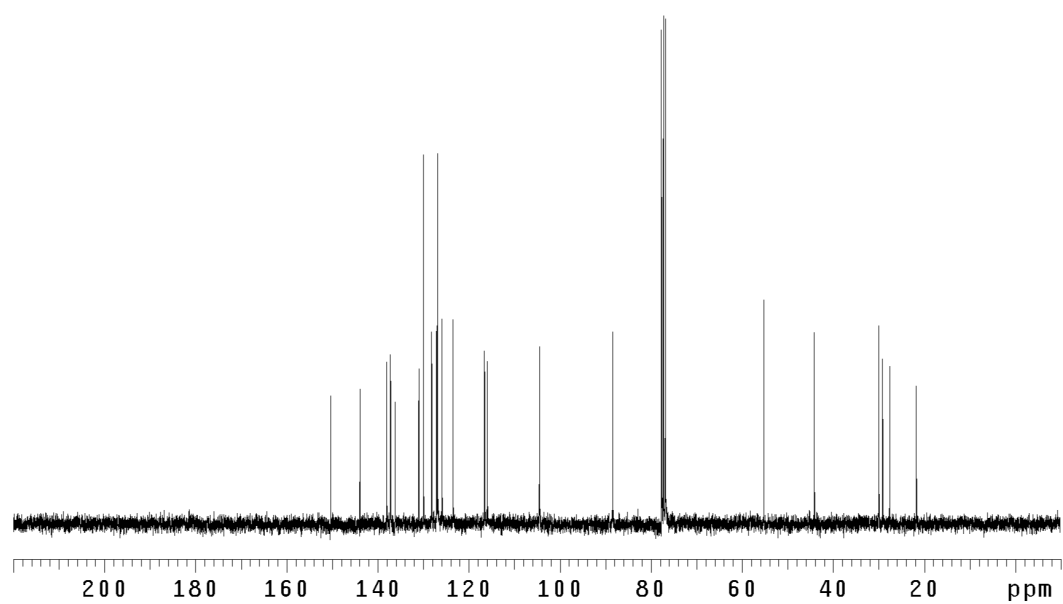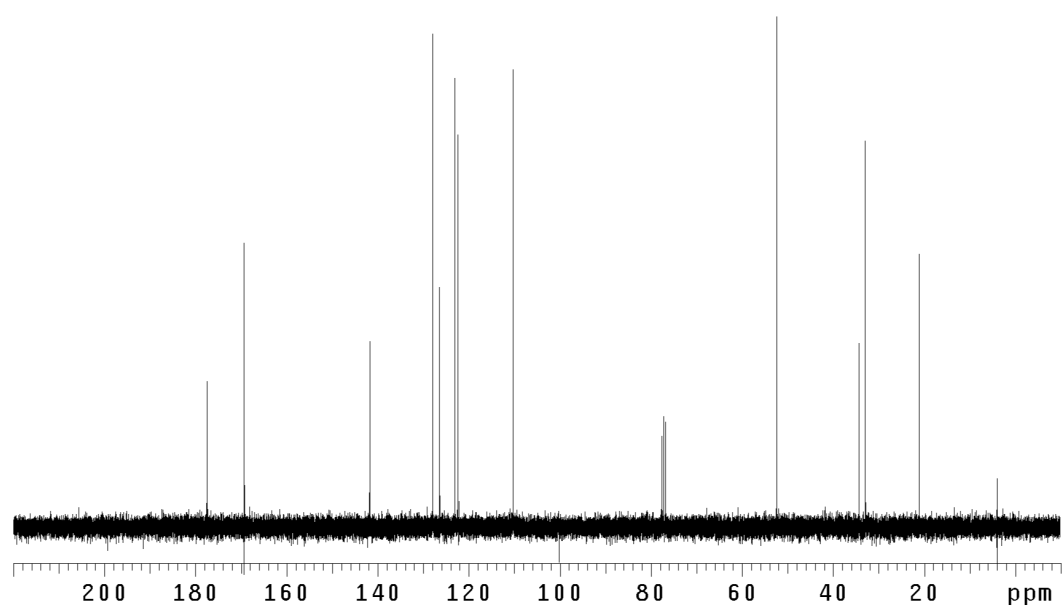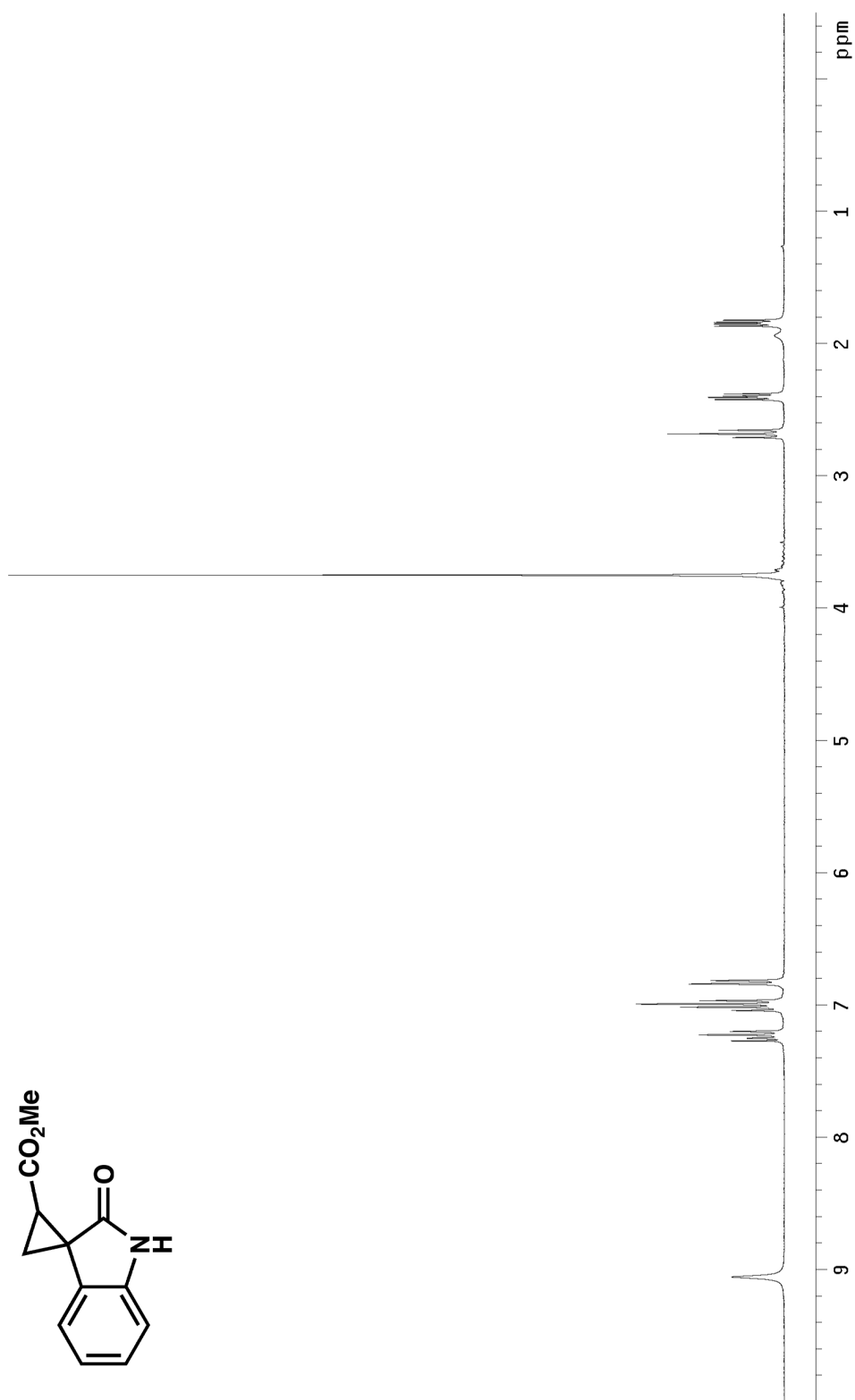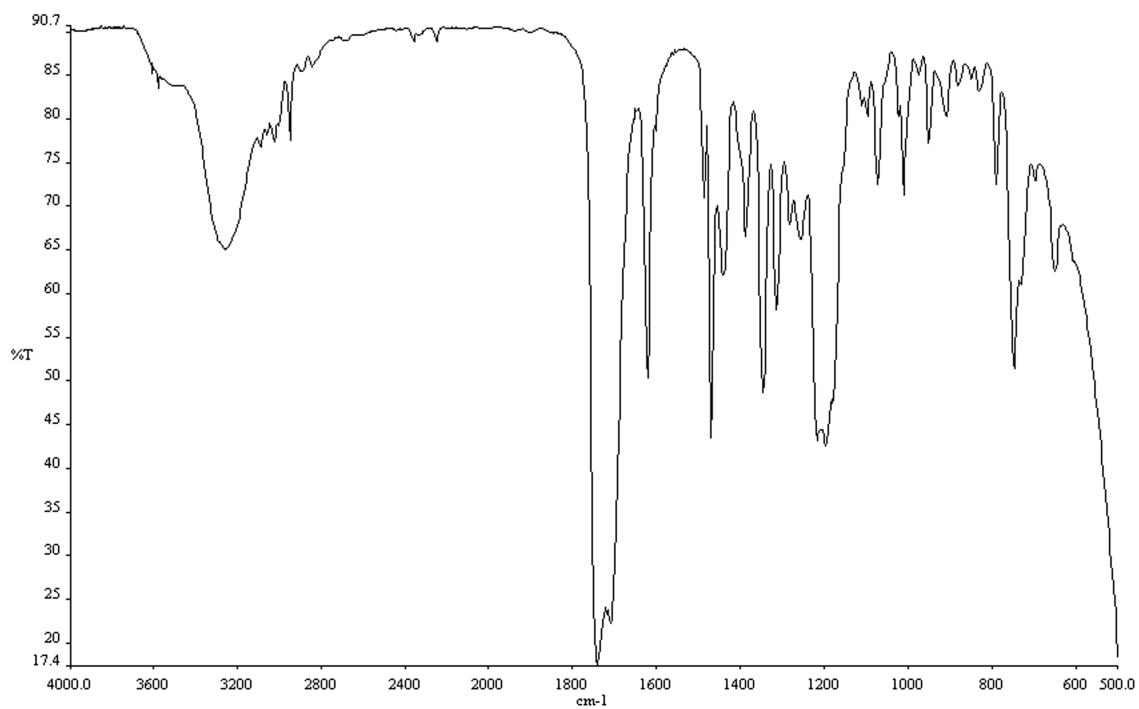

Figure A.3.6 ¹³CNMR (75 Mhz, CDCl₃) of compound **510**.
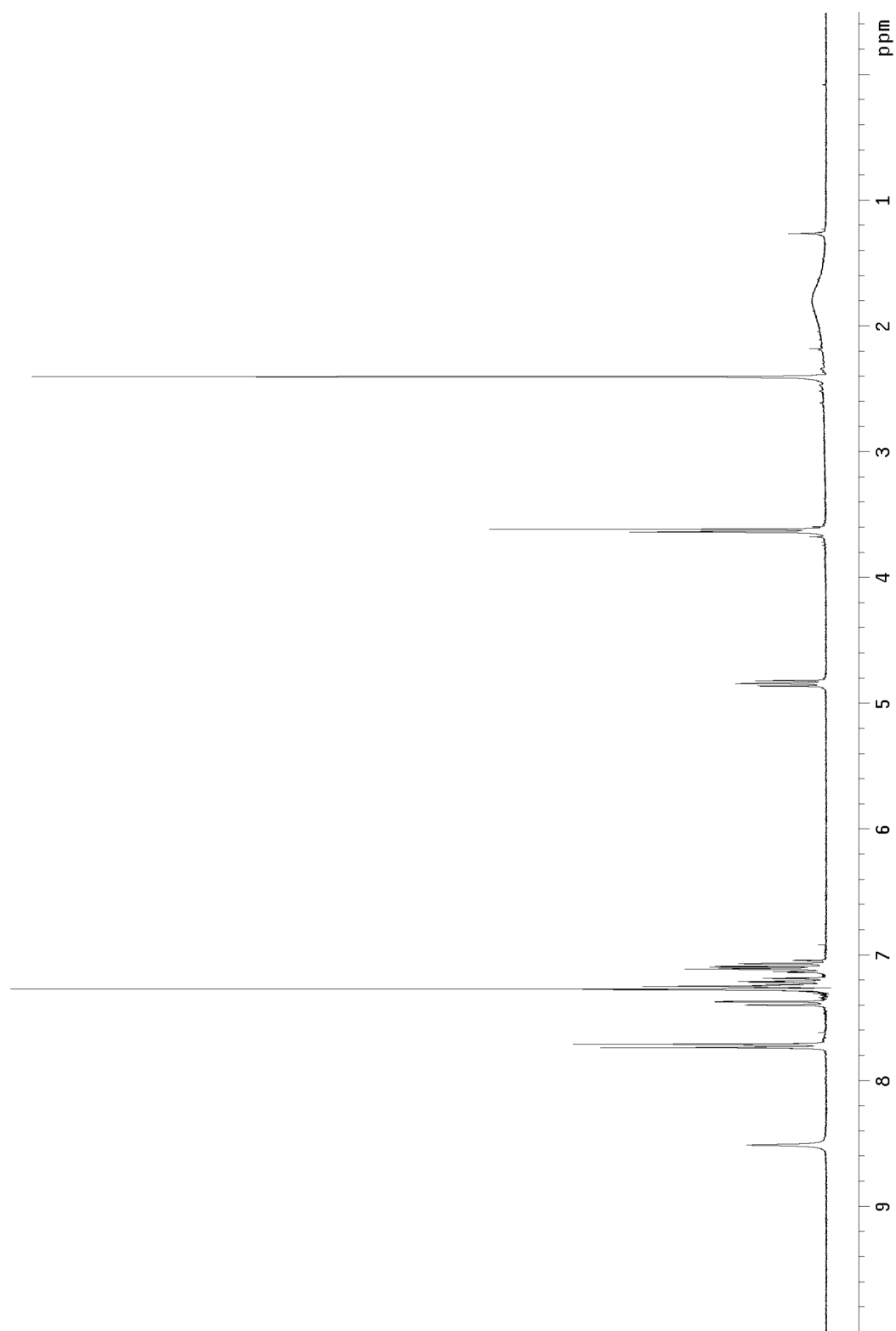
Figure A.3.7 ^{1}HNMR (300 MHz, CDCL$_3$) of compound **580**.

Figure A.3.8 Infrared spectrum (thin film/NaCl) of compound **580**.
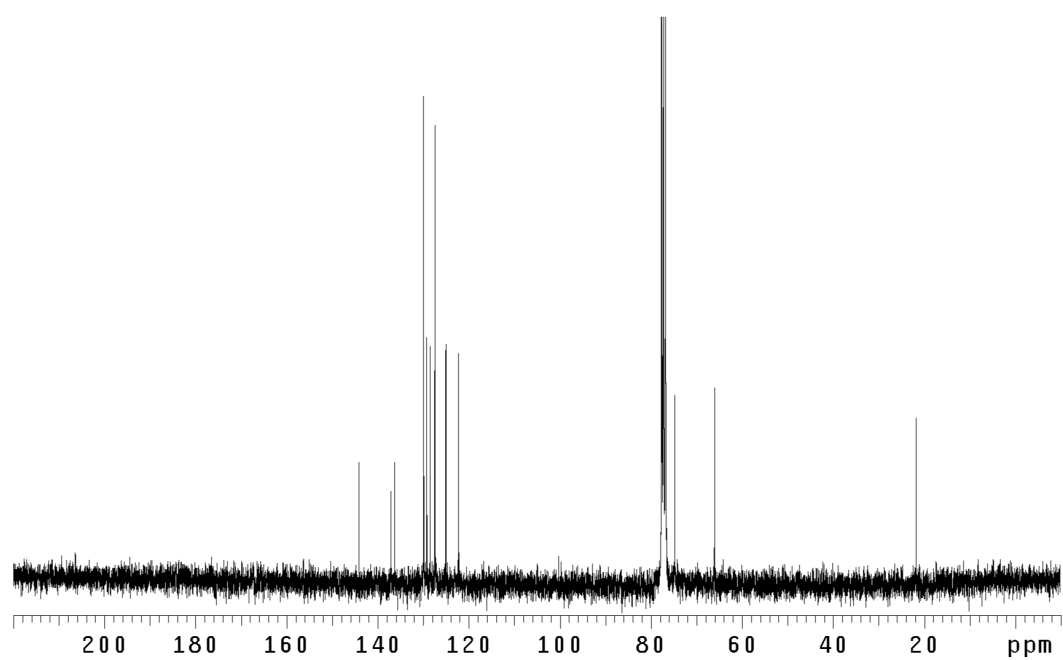
Figure A.3.9 ^{13}CNMR (75 Mhz, CDCl$_3$) of compound **580**.
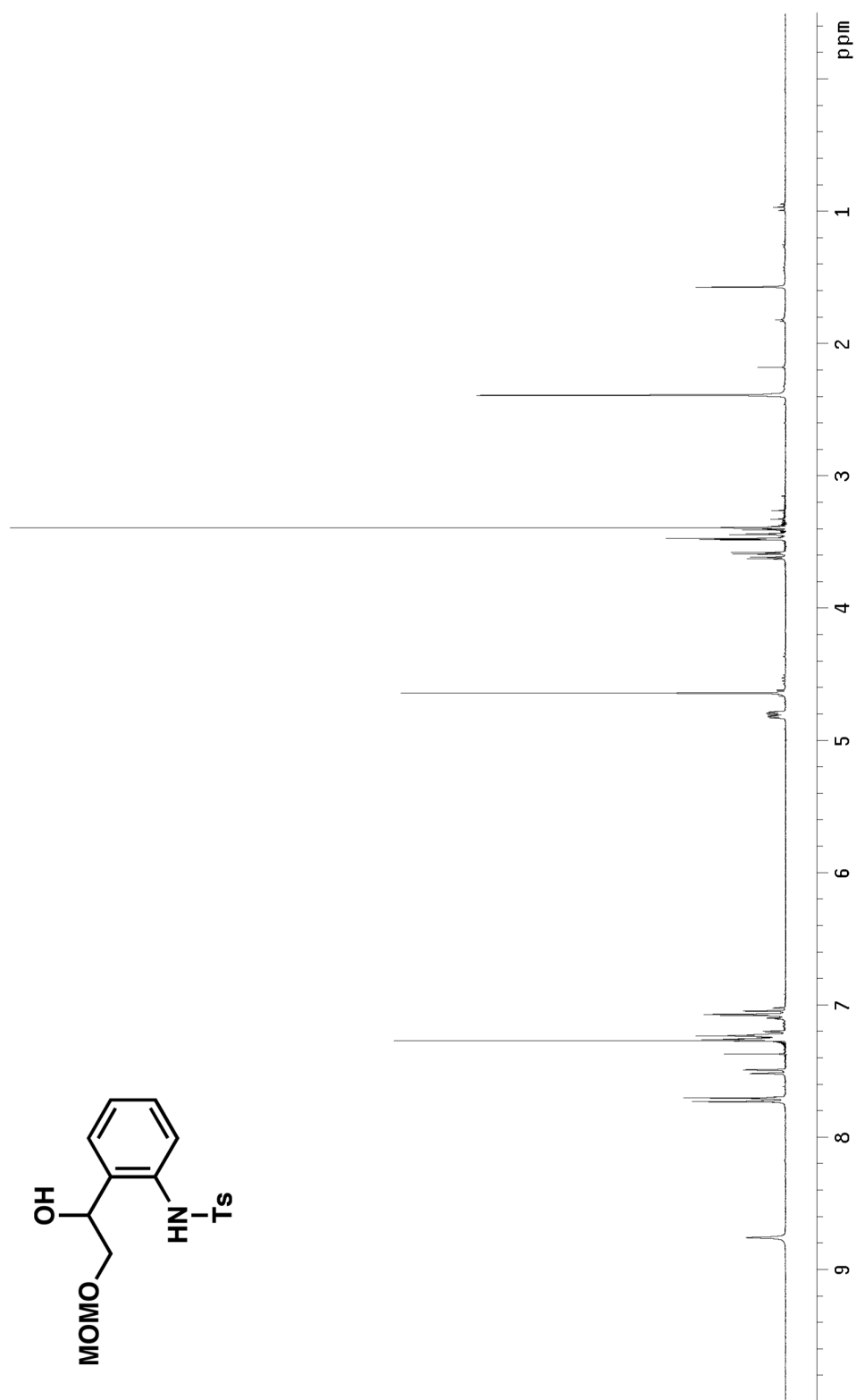
Figure A.3.10 ^{1}HNMR (300 MHz, CDCL$_3$) of compound **513**.
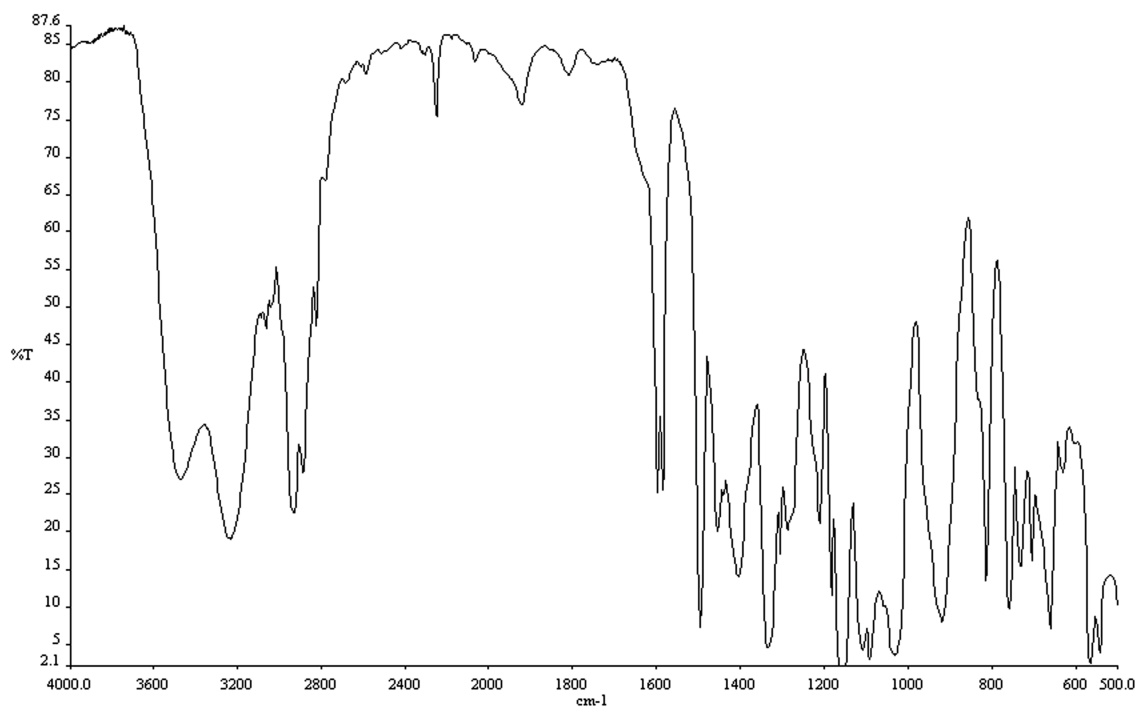
Figure A.3.11 Infrared spectrum (thin film/NaCl) of compound **513**.
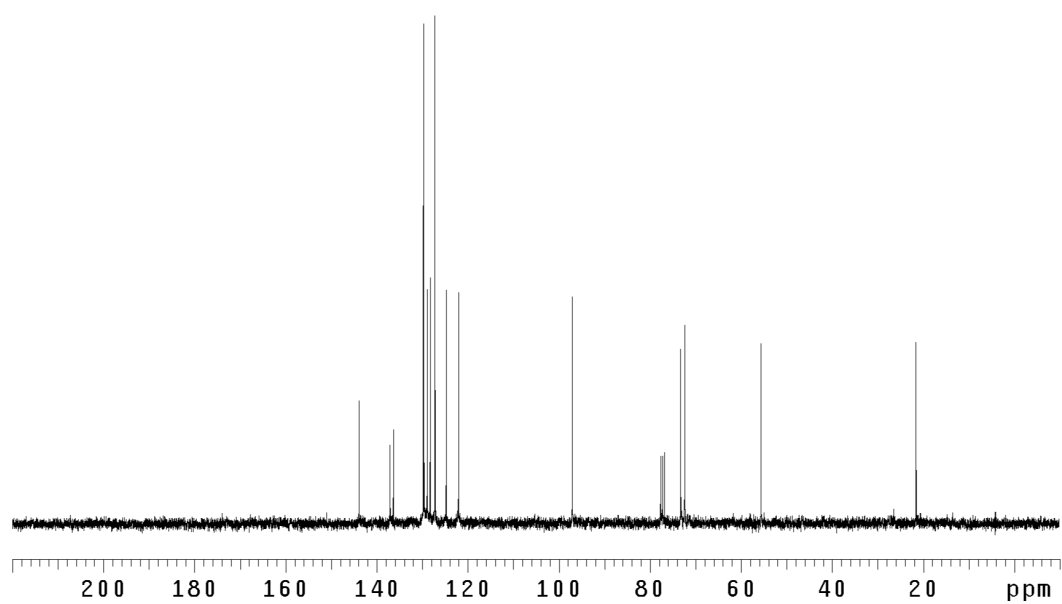
Figure A.3.12 ^{13}CNMR (75 Mhz, CDCl$_3$) of compound **513**.
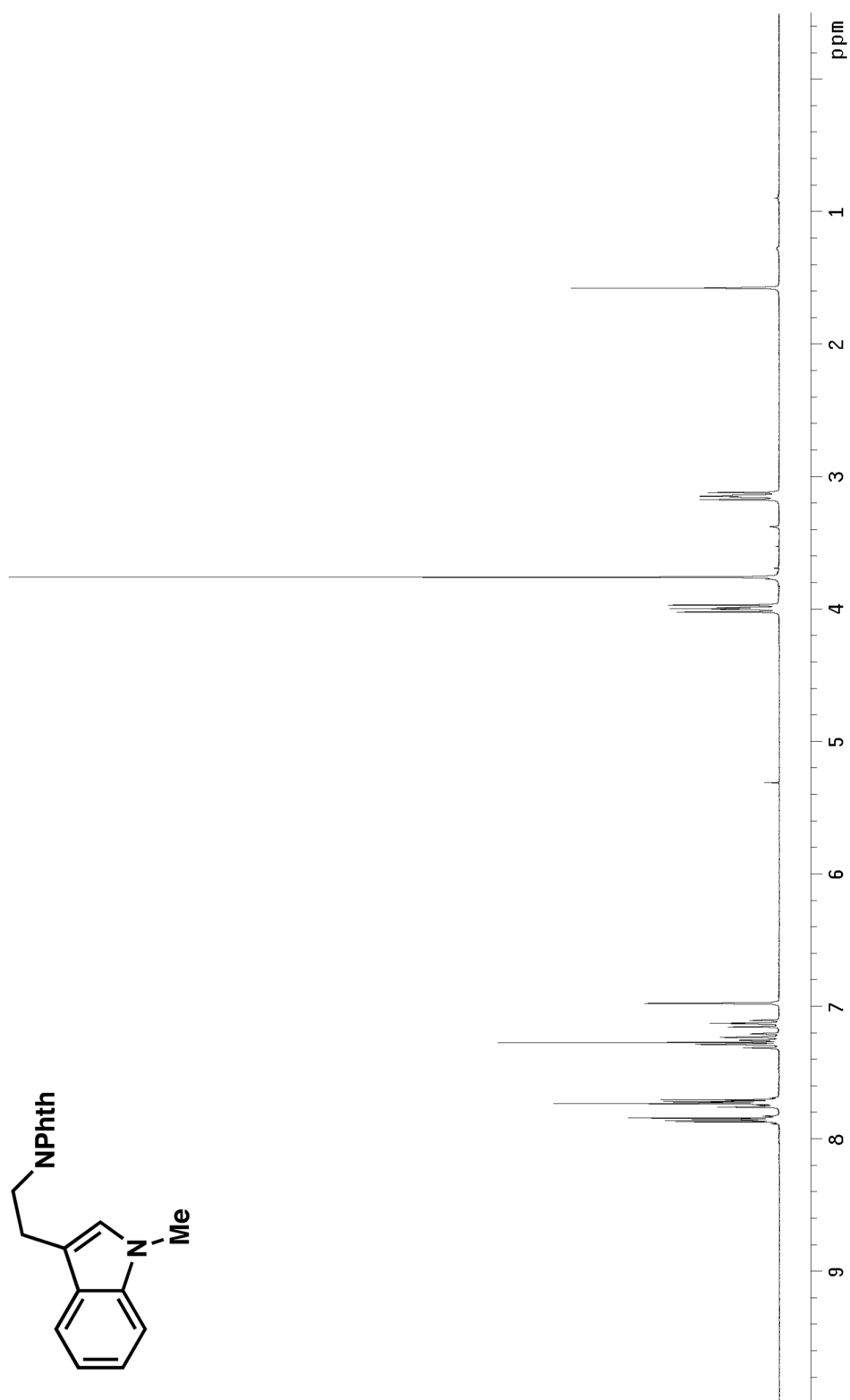
Figure A.3.13 ¹HNMR (300 MHz, CDCL₃) of compound **516**.
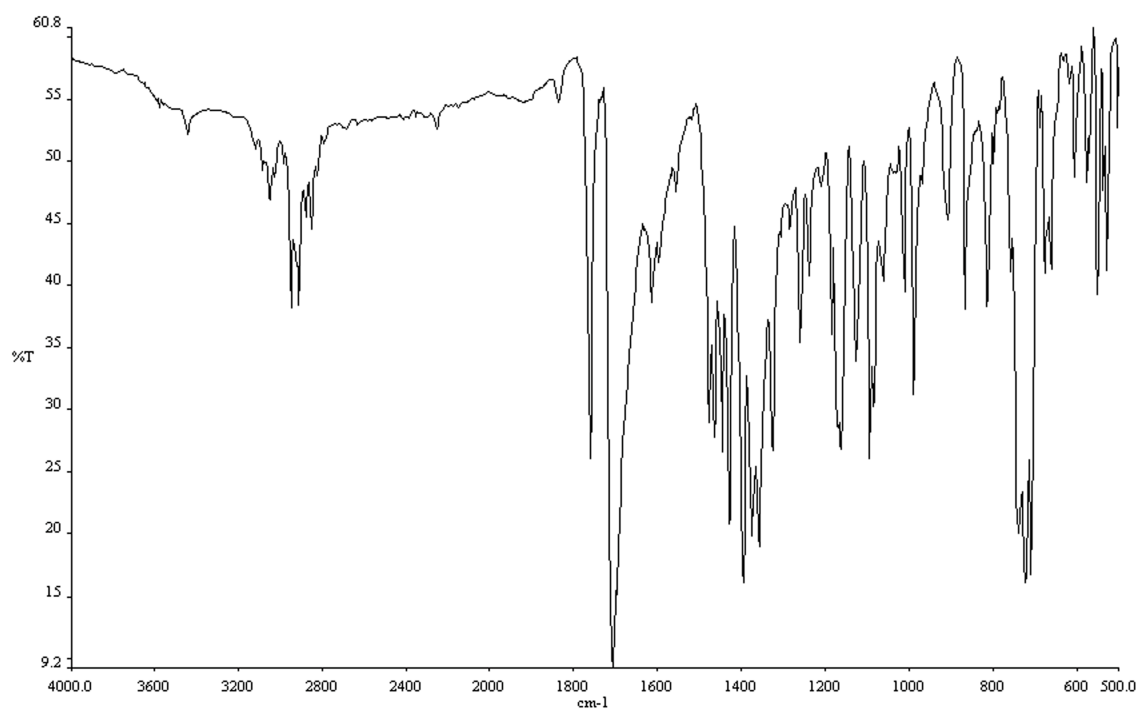
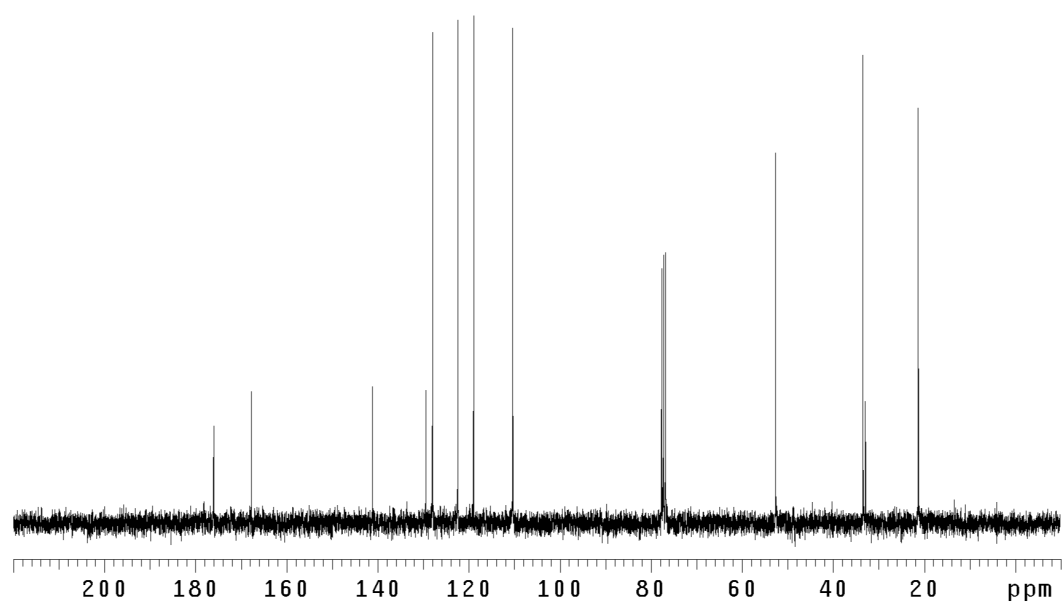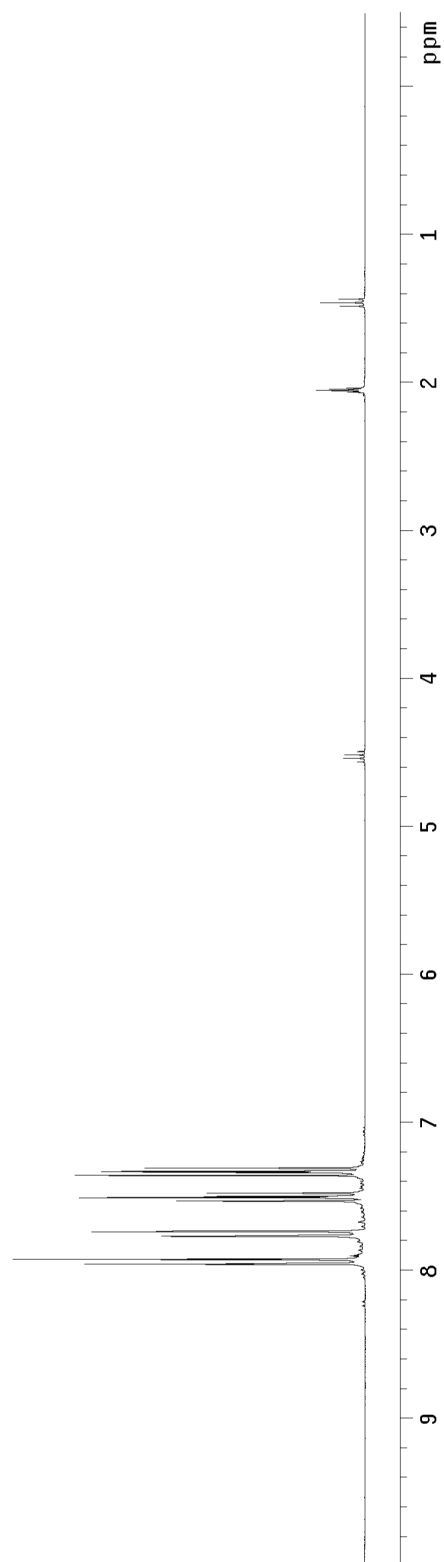*Figure A.3.14* Infrared spectrum (thin film/NaCl) of compound **516**.
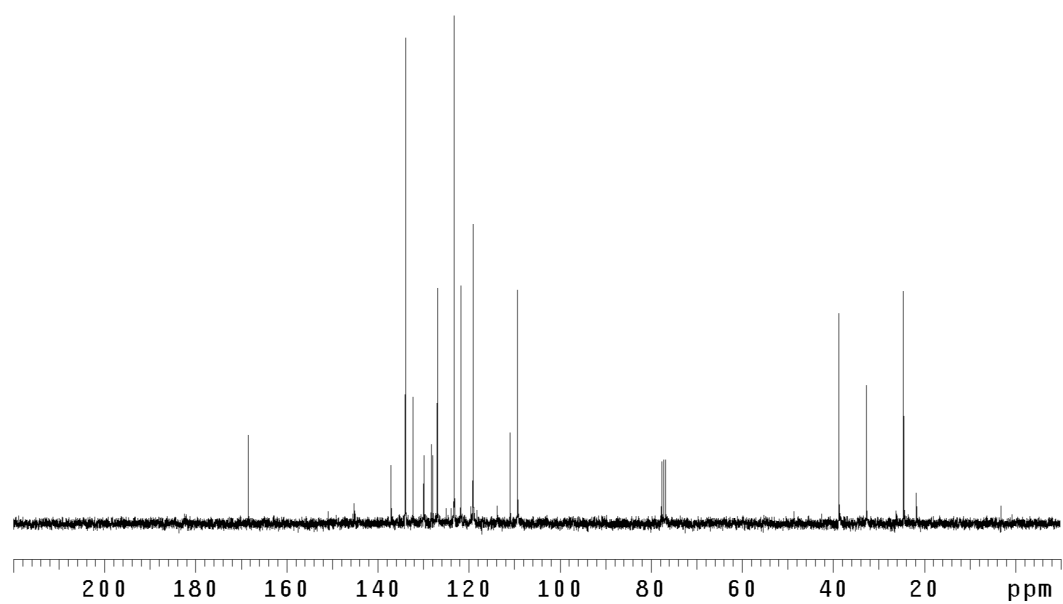
Figure A.3.15 ^{13}CNMR (75 Mhz, CDCl$_3$) of compound **516**.
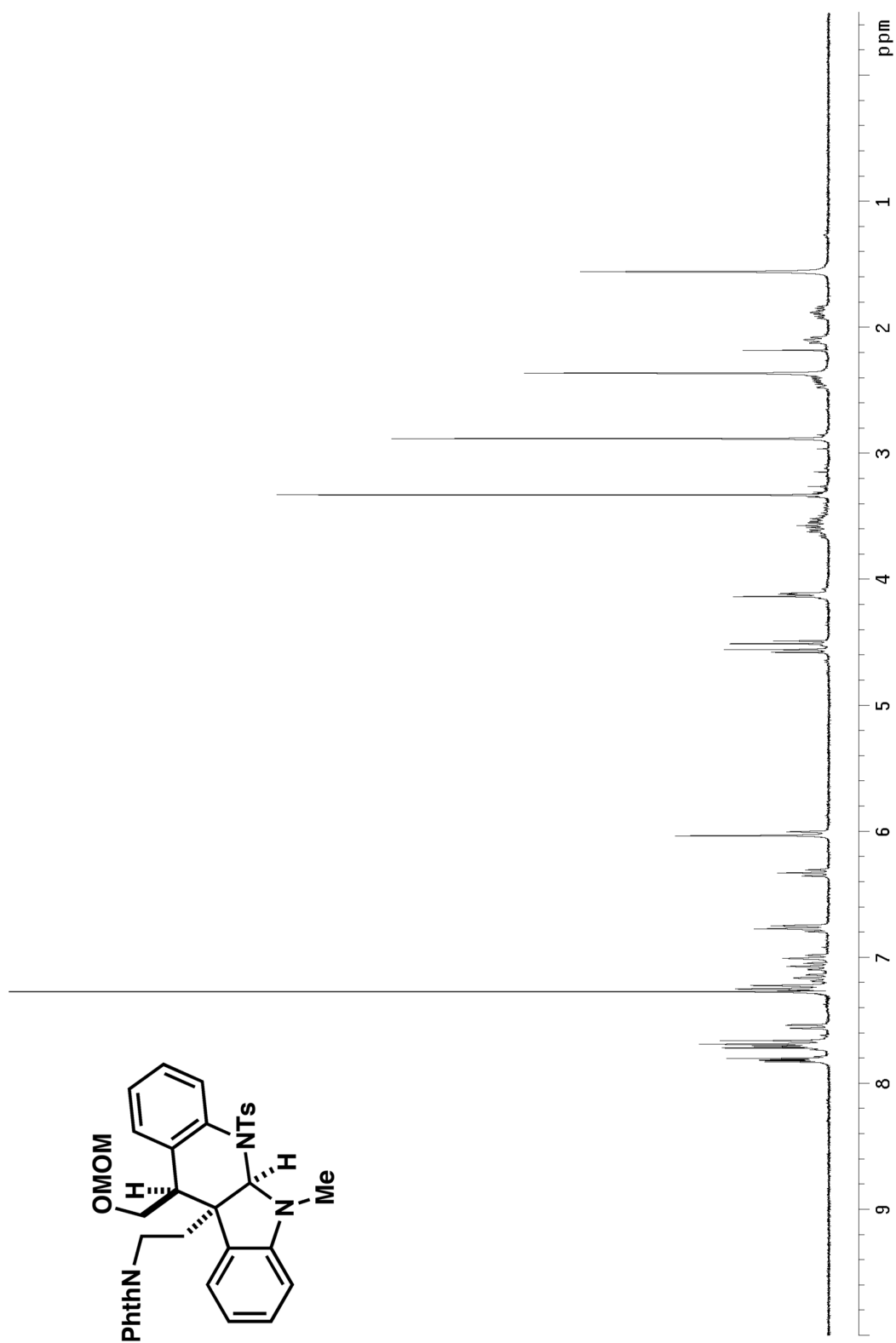
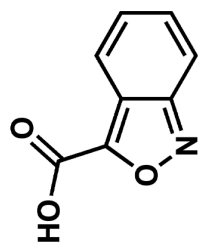*Figure A.3.16* ¹HNMR (300 MHz, CDCL₃) of compound **518**.
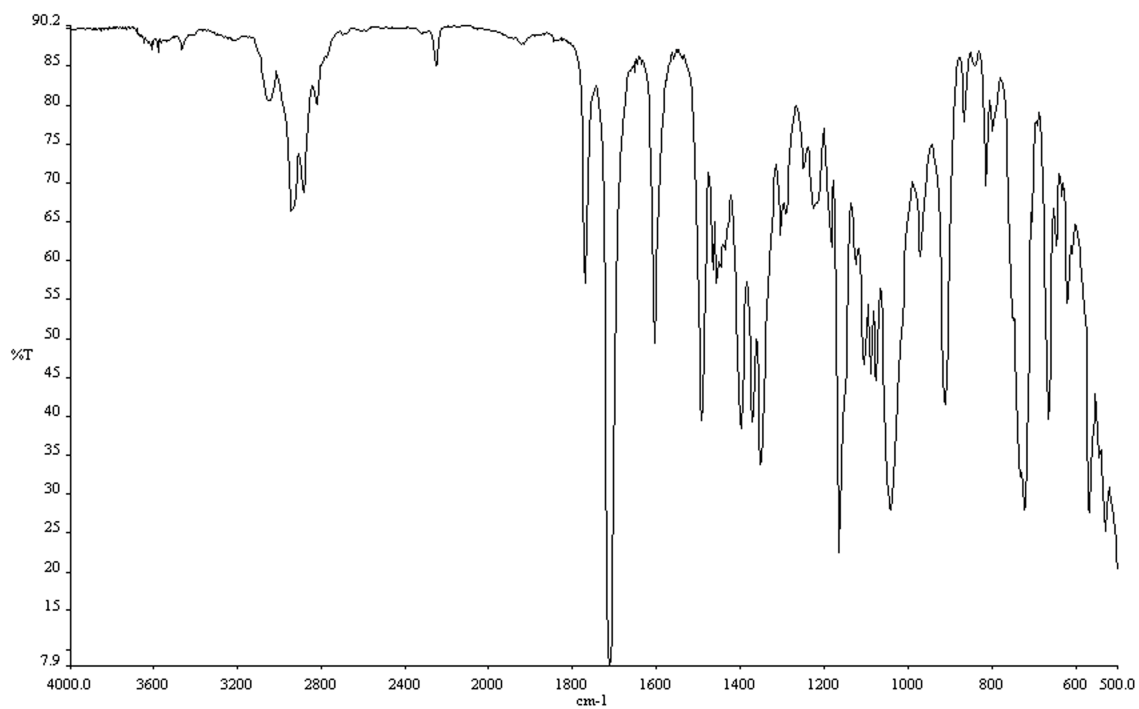
Figure A.3.17 Infrared spectrum (thin film/NaCl) of compound **518**.
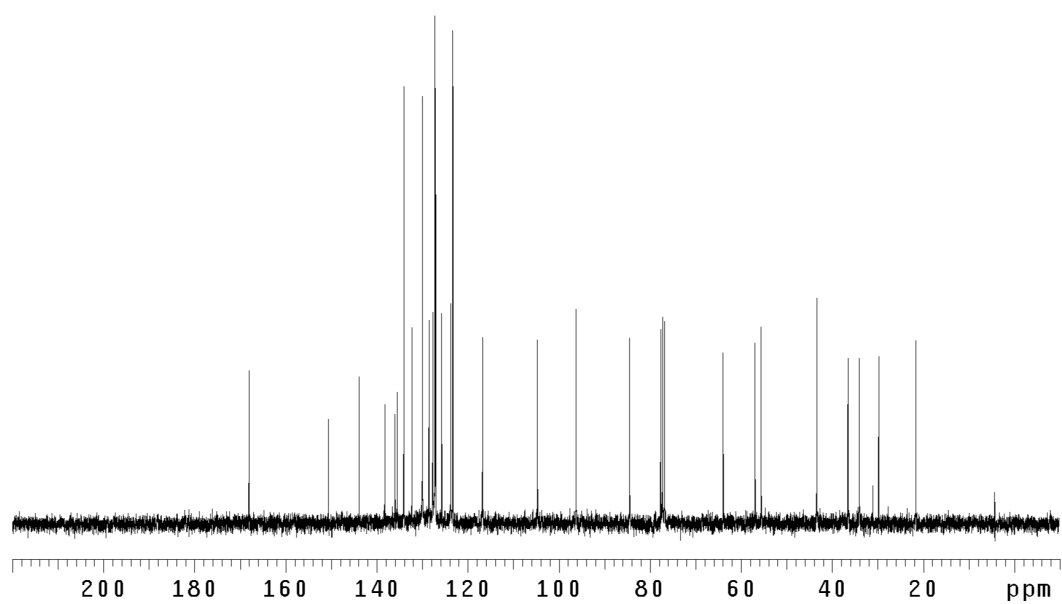
Figure A.3.18 ^{13}CNMR (75 Mhz, CDCl$_3$) of compound **518**.
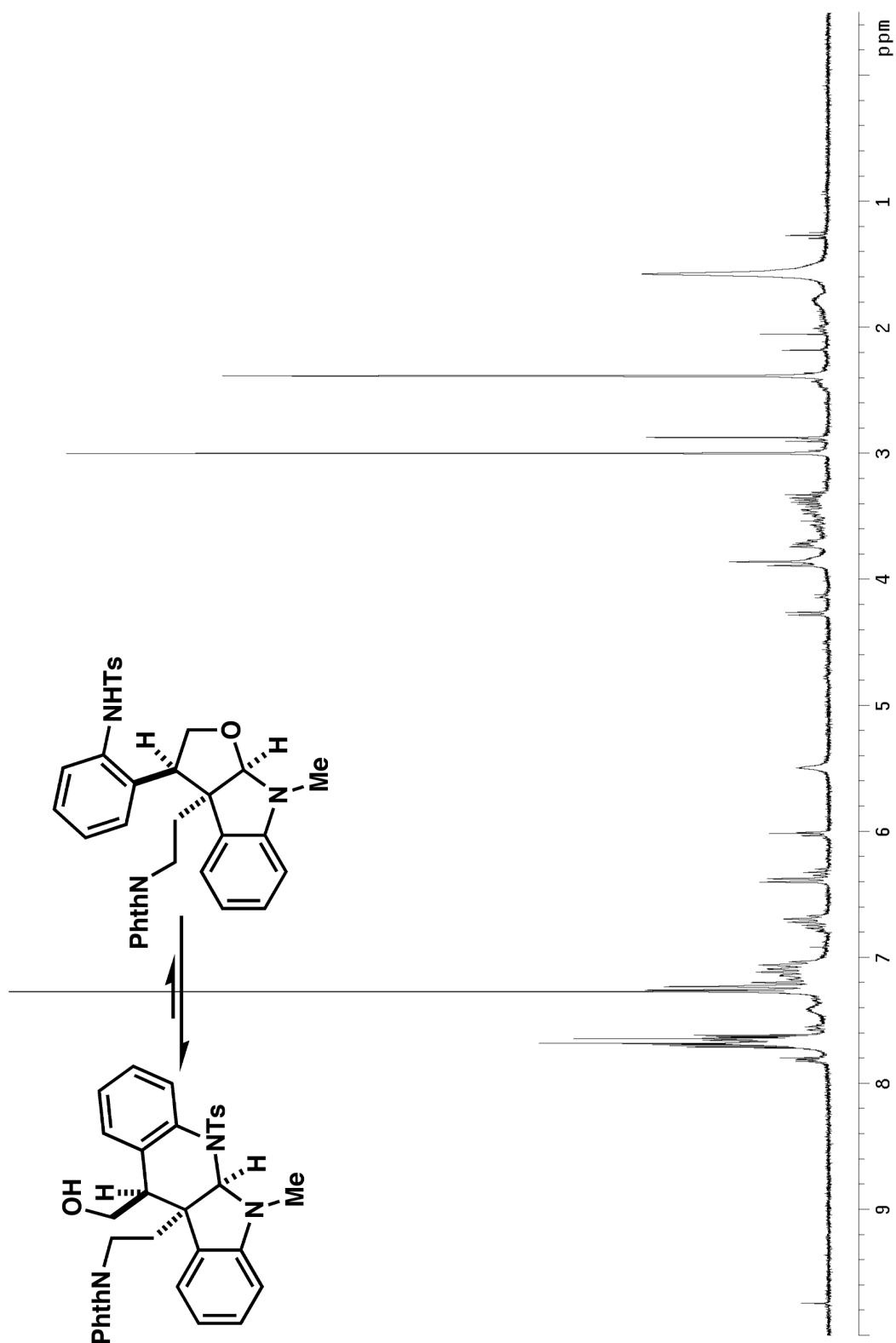
Figure A.3.19 ¹HNMR (300 MHz, CDCL₃) of compounds **519** and **520**.
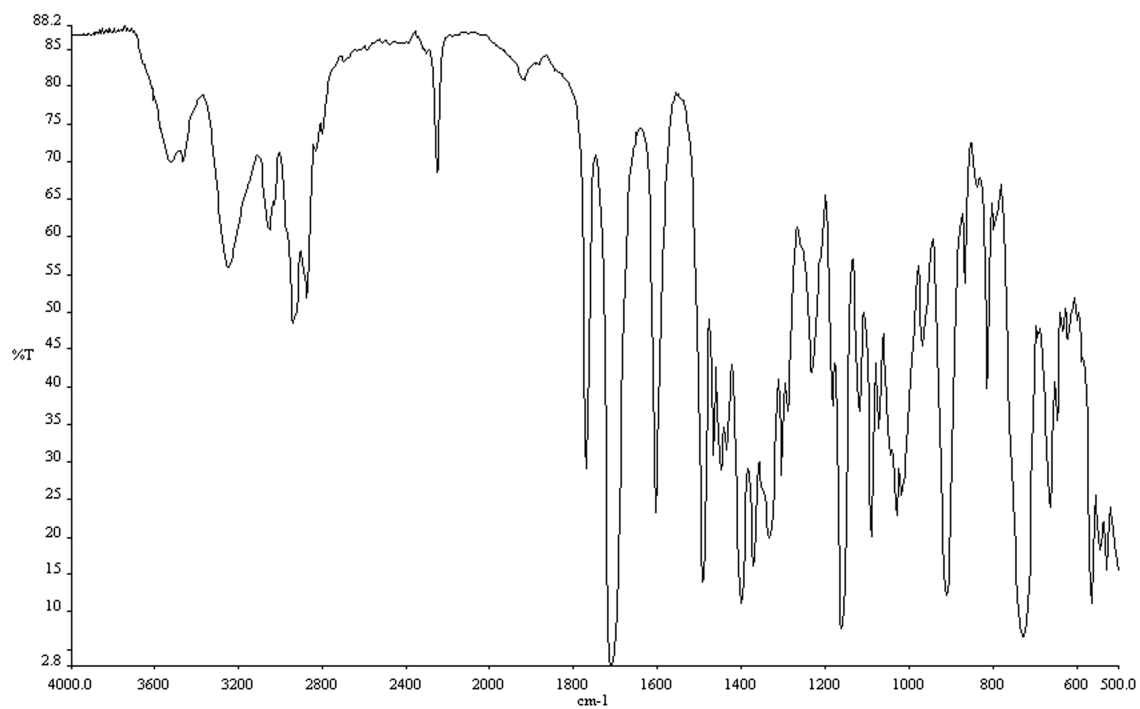
Figure A.3.20 Infrared spectrum (thin film/NaCl) of compounds **519** and **520**.
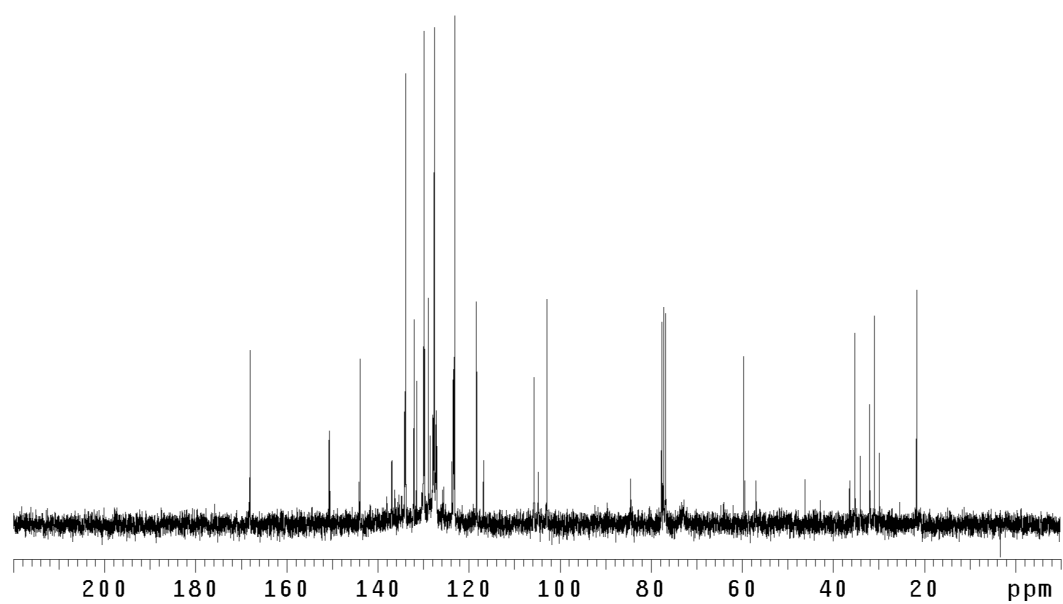
Figure A.3.21 ^{13}CNMR (75 Mhz, CDCl$_3$) of compounds **519** and **520**.
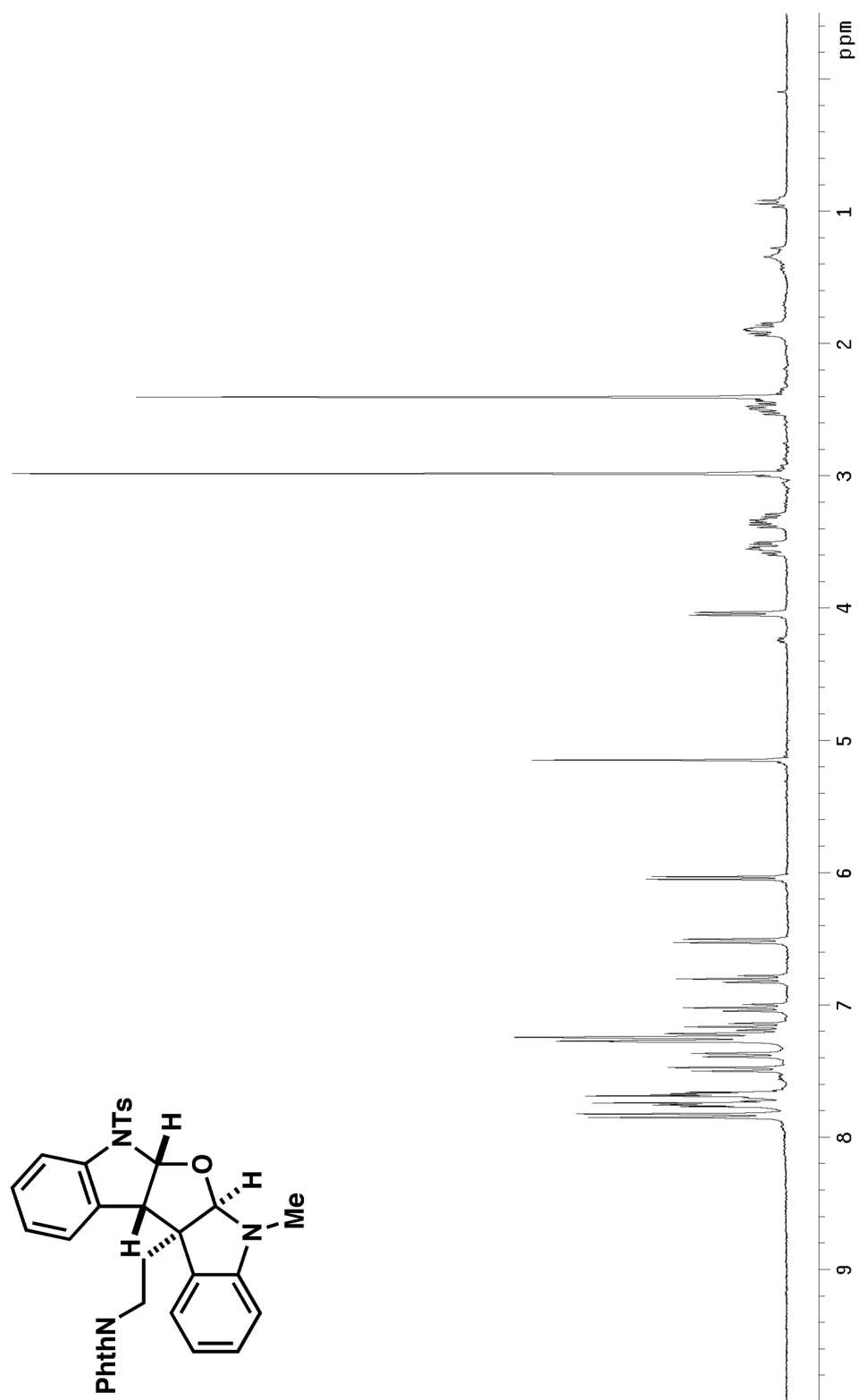
Figure A.3.22 ¹HNMR (300 MHz, CDCL₃) of compound **522**.

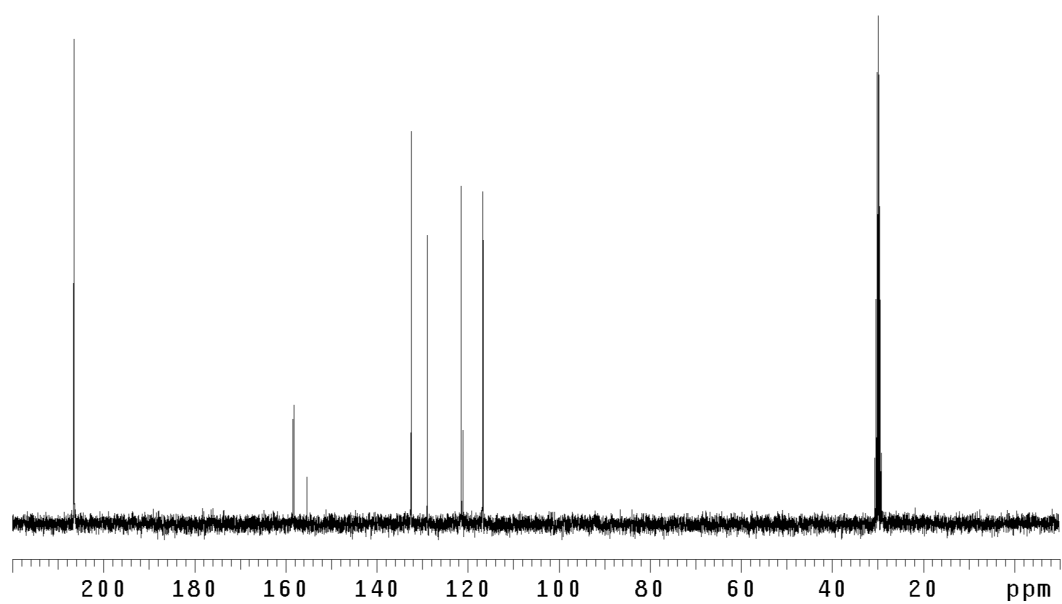*Figure A.3.23* Infrared spectrum (thin film/NaCl) of compound **522**.
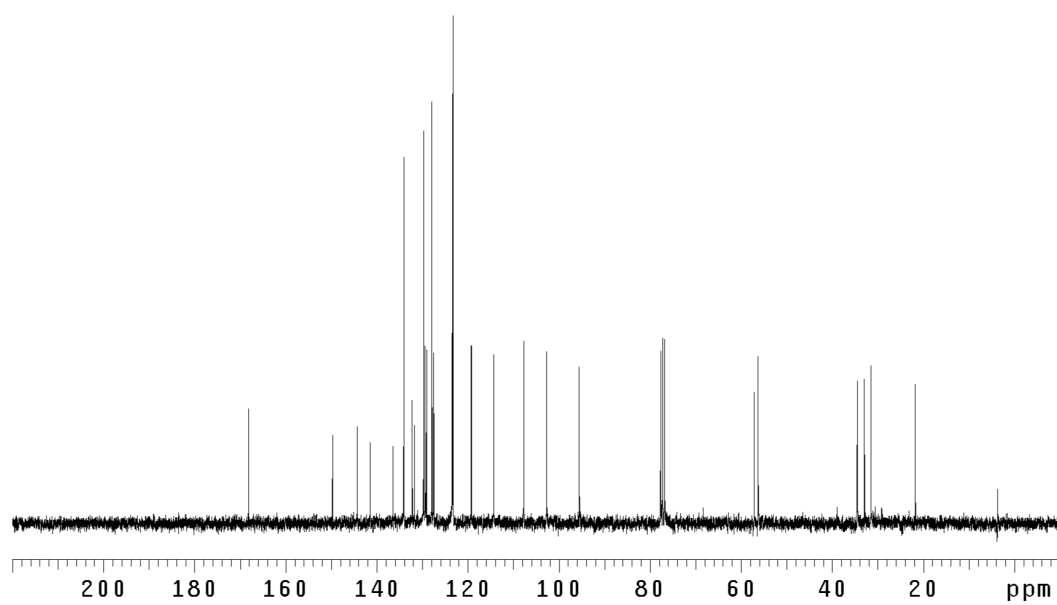
Figure A.3.24 ¹³CNMR (75 Mhz, CDCl₃) of compound **522**.
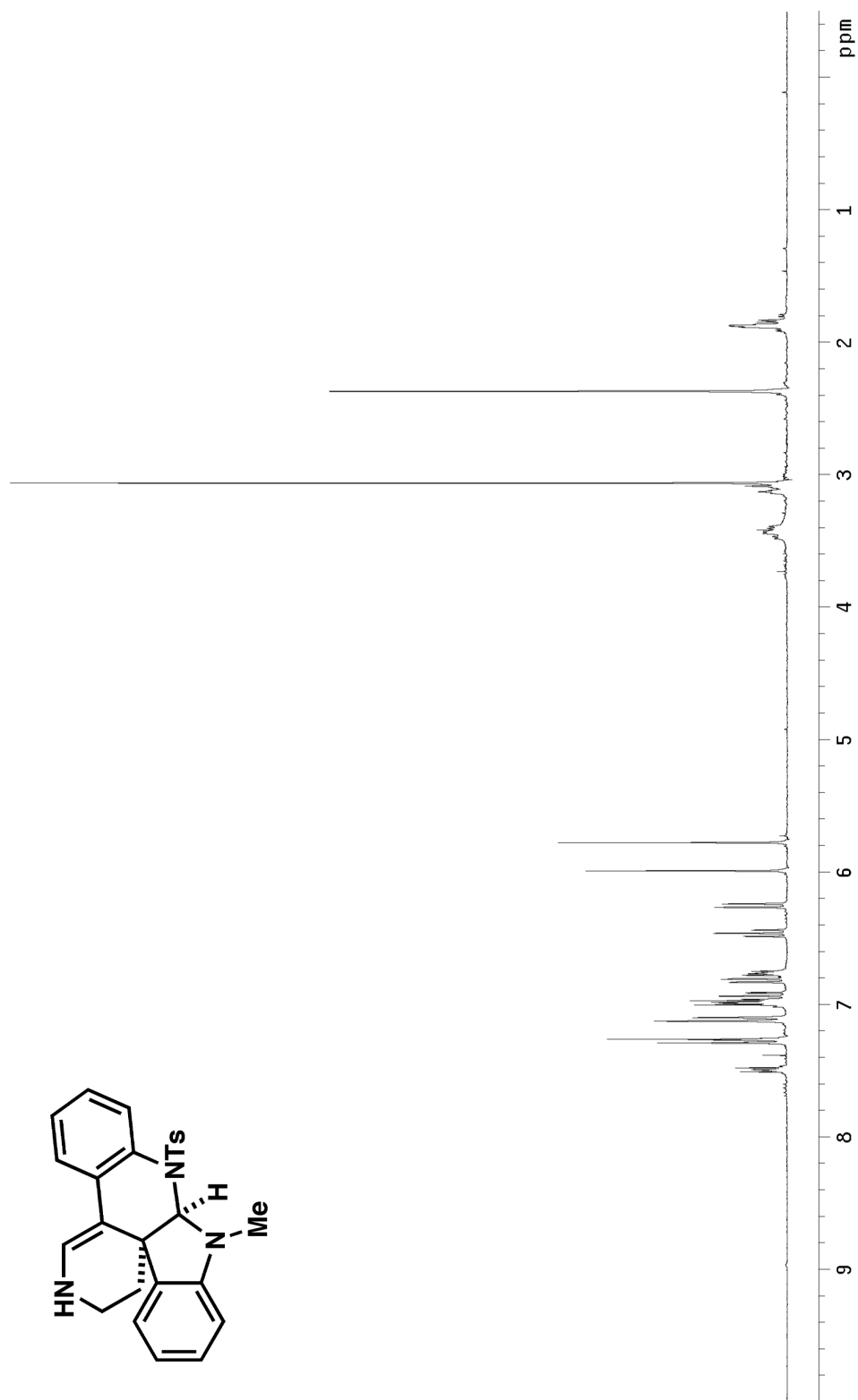
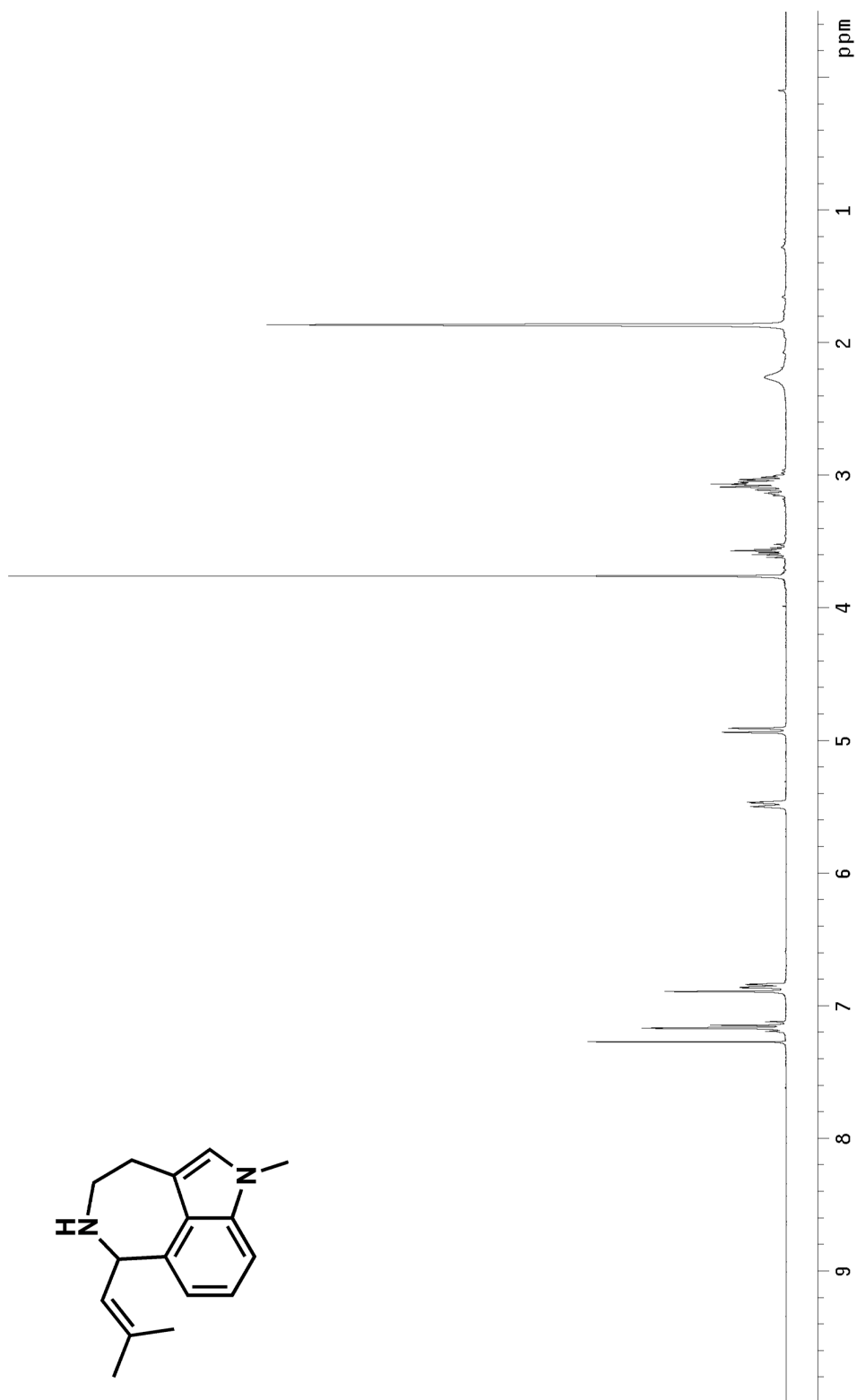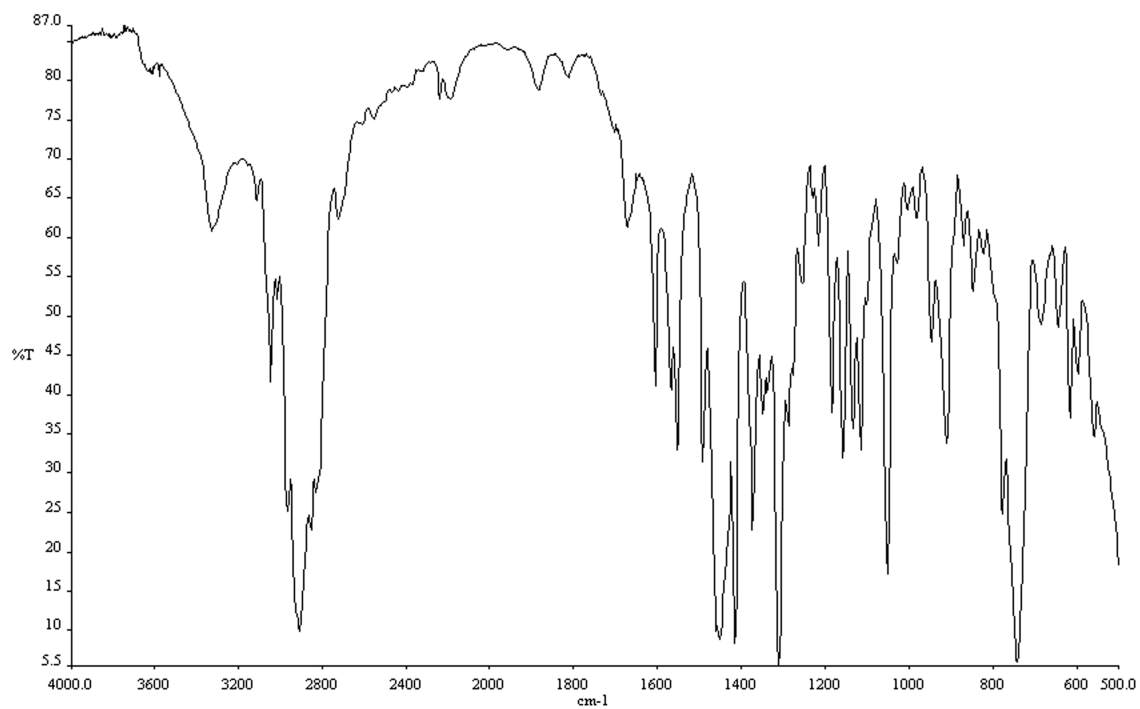*Figure A.3.25* ¹HNMR (300 MHz, CDCL₃) of compound **523**.
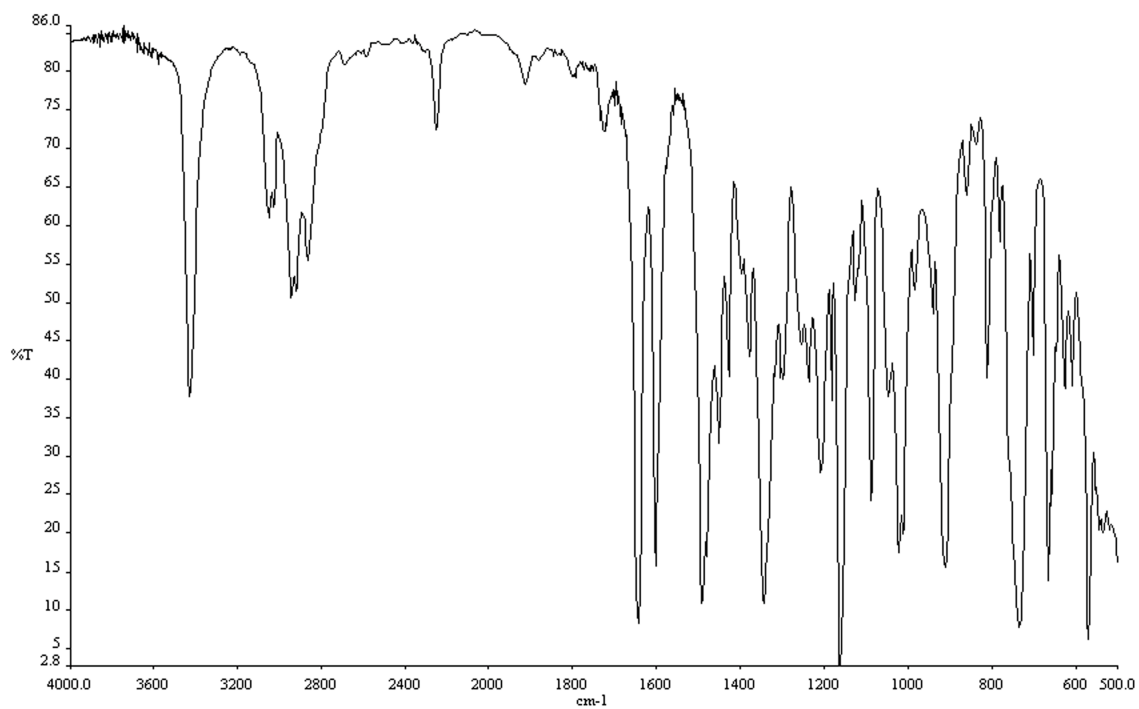
Figure A.3.26 Infrared spectrum (thin film/NaCl) of compound **523**.
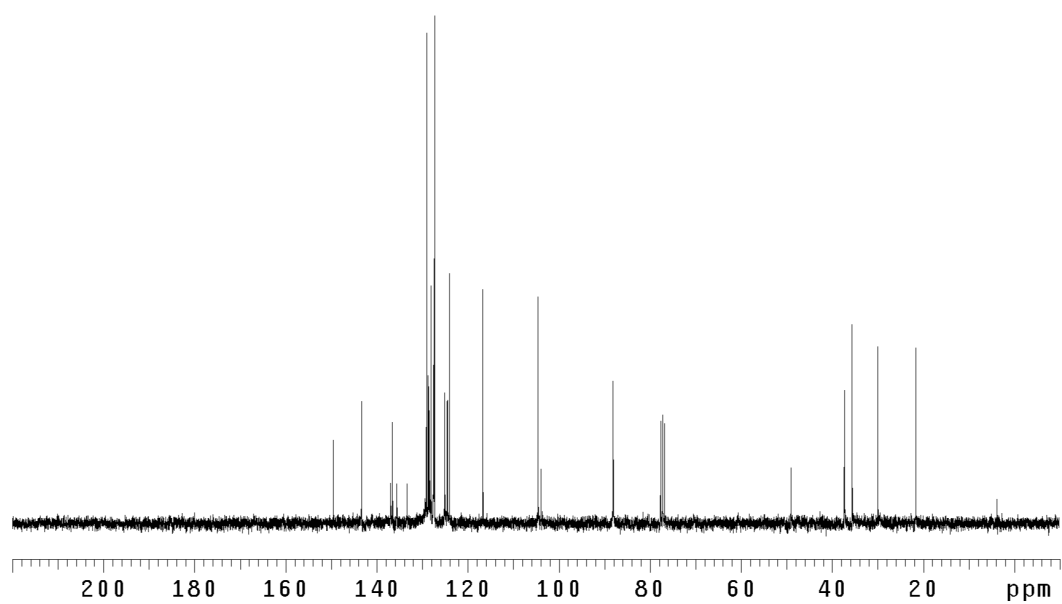
Figure A.3.27 ^{13}CNMR (75 Mhz, CDCl$_3$) of compound **523**.

Figure A.3.28 ¹HNMR (300 MHz, CDCL₃) of compound **534.**
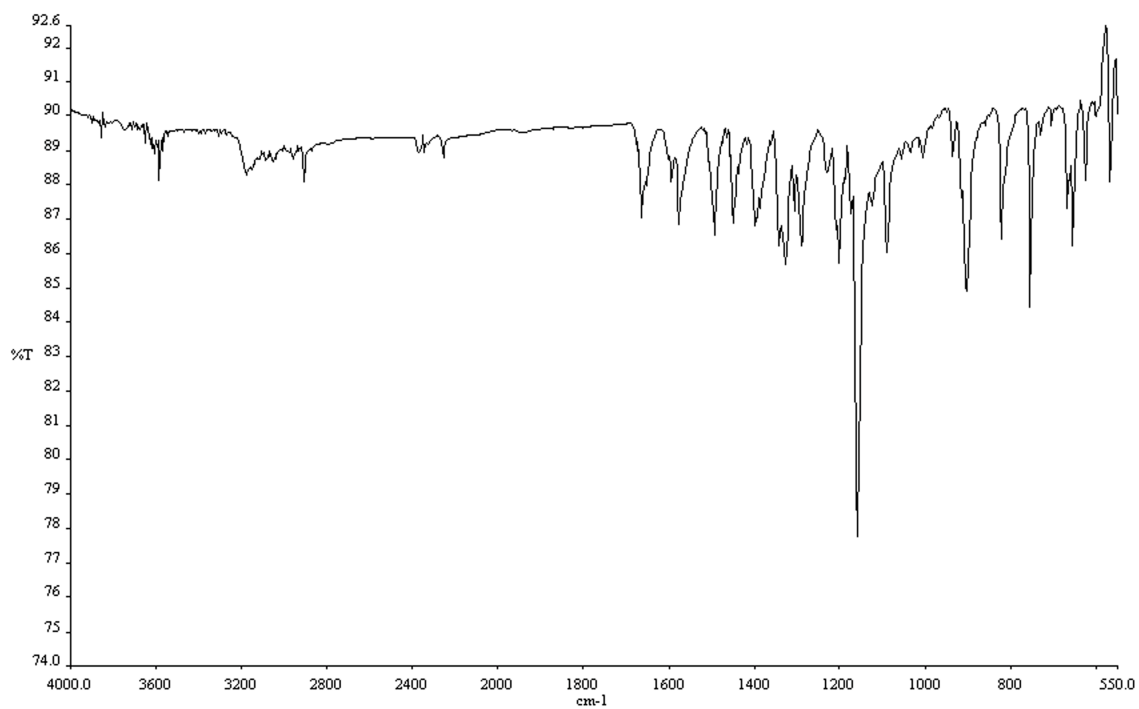
Figure A.3.29 Infrared spectrum (thin film/NaCl) of compound **534**.
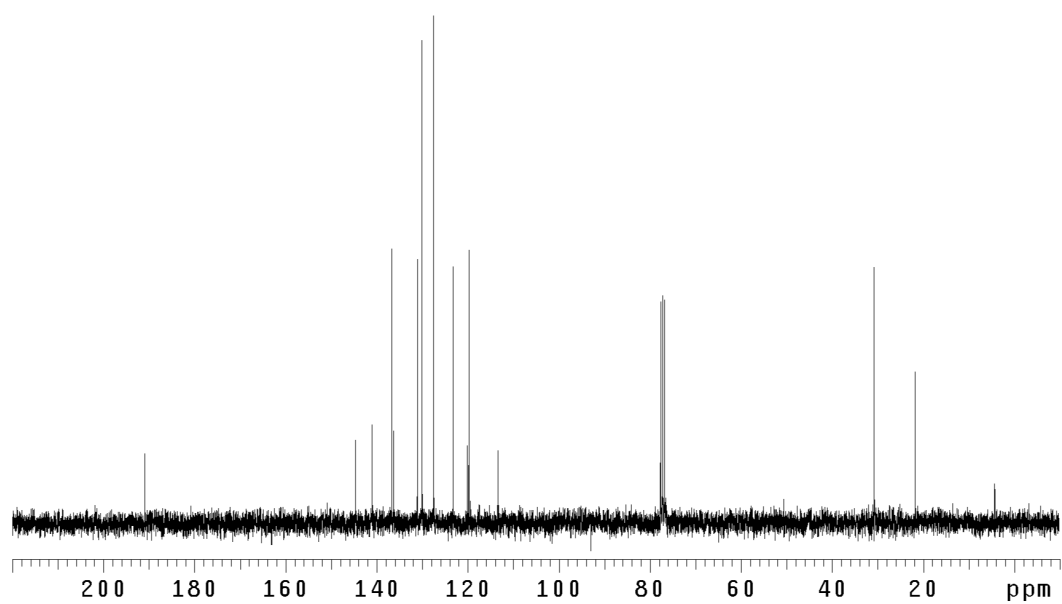
Figure A.3.30 ^{13}CNMR (75 Mhz, CDCl$_3$) of compound **534**.

Figure A.3.31 ¹HNMR (300 MHz, CDCL₃) of compound **538a**.

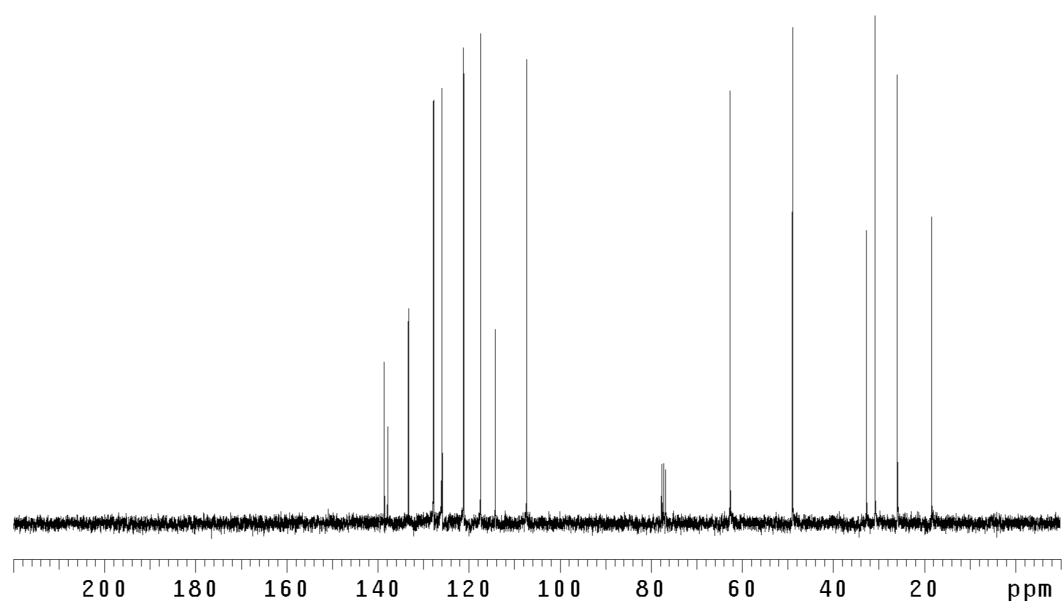*Figure A.3.32* Infrared spectrum (thin film/NaCl) of compound **538a**.

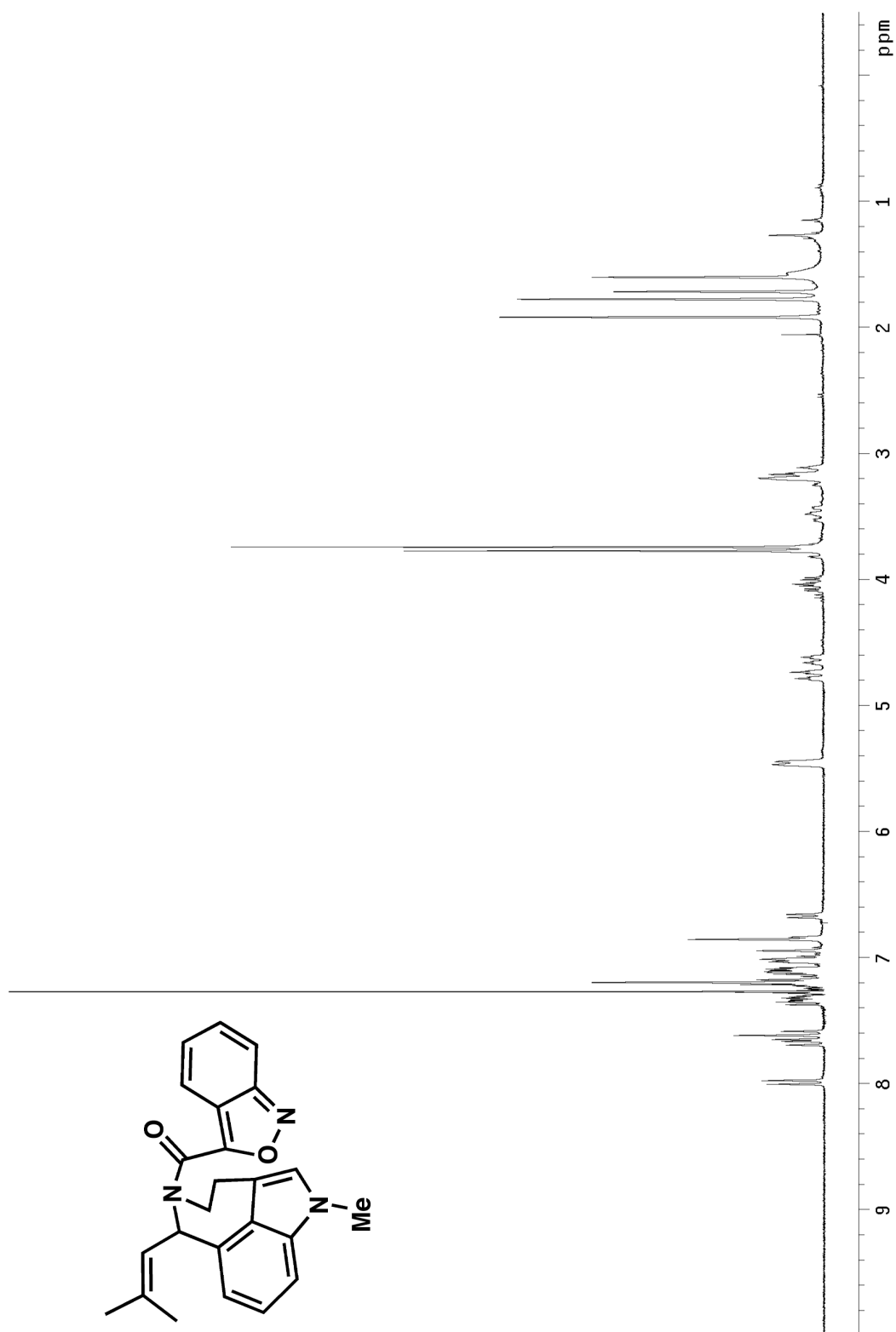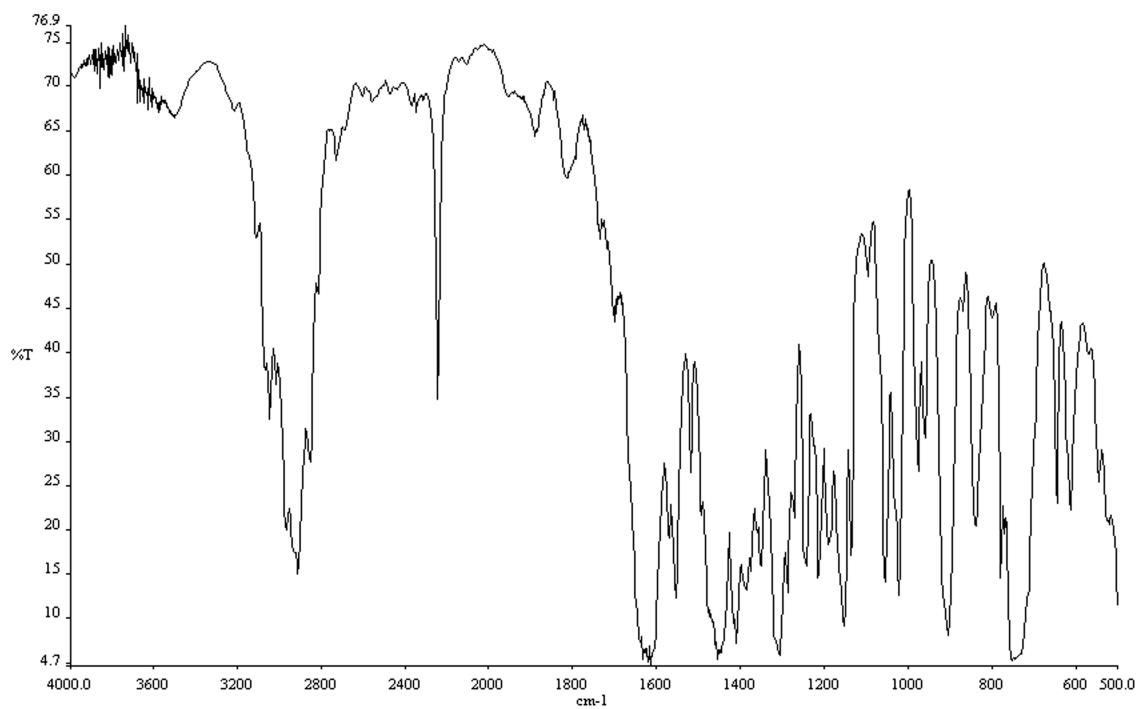*Figure A.3.33* ¹³CNMR (75 Mhz, CDCl₃) of compound **538a**.

Figure A.3.34 ^{1}HNMR (300 MHz, CDCL$_3$) of compound **538b**.

Figure A.3.35 Infrared spectrum (thin film/NaCl) of compound **538b**.

Figure A.3.36 ^{13}CNMR (75 Mhz, CDCl$_3$) of compound **538b**.

Figure A.3.37 ^{1}HNMR (300 MHz, acetone-d$_6$) of compound **543**.
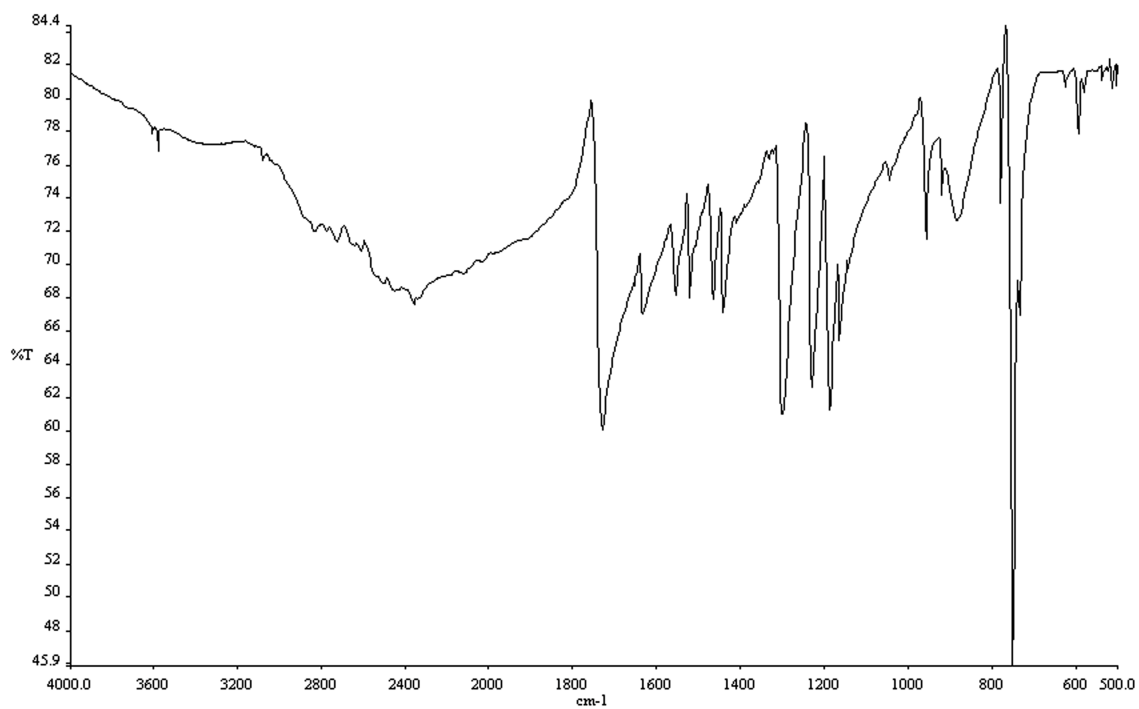
Figure A.3.38 Infrared spectrum (thin film/NaCl) of compound **543**.

Figure A.3.39 ^{13}CNMR (75 Mhz, acetone-d$_6$) of compound **543**.

Figure A.3.40 ^{1}HNMR (300 MHz, CDCL$_3$) of compound **530**.

Figure A.3.41 Infrared spectrum (thin film/NaCl) of compound **530**.

Figure A.3.42 ^{13}CNMR (75 Mhz, CDCl$_3$) of compound **530**.

Figure A.3.43 ¹HNMR (300 MHz, CDCL₃) of compound **548**.

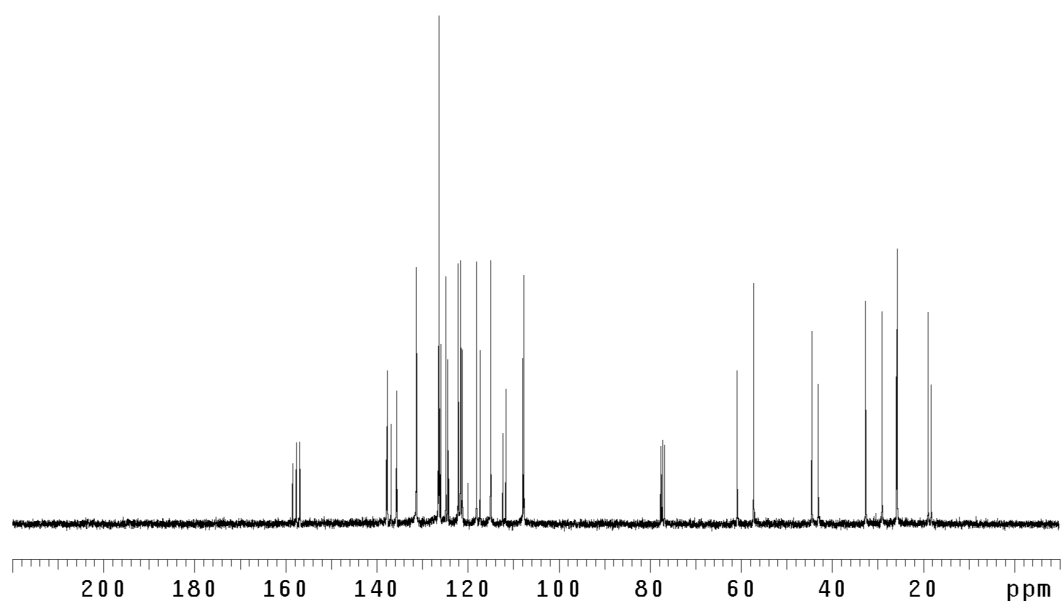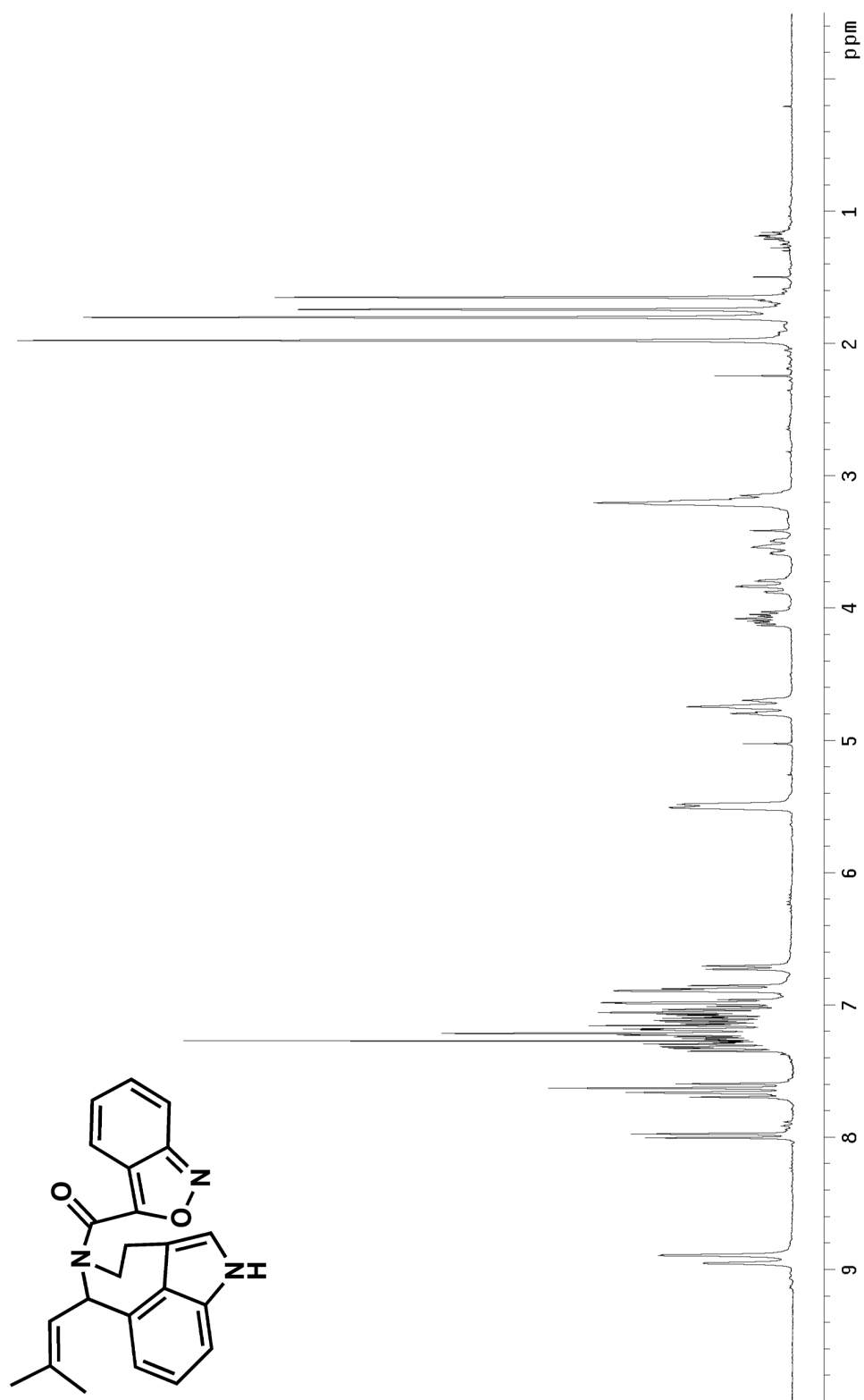*Figure A.3.44* Infrared spectrum (thin film/NaCl) of compound **548**.

Figure A.3.45 ^{13}CNMR (75 Mhz, CDCl$_3$) of compound **548**.

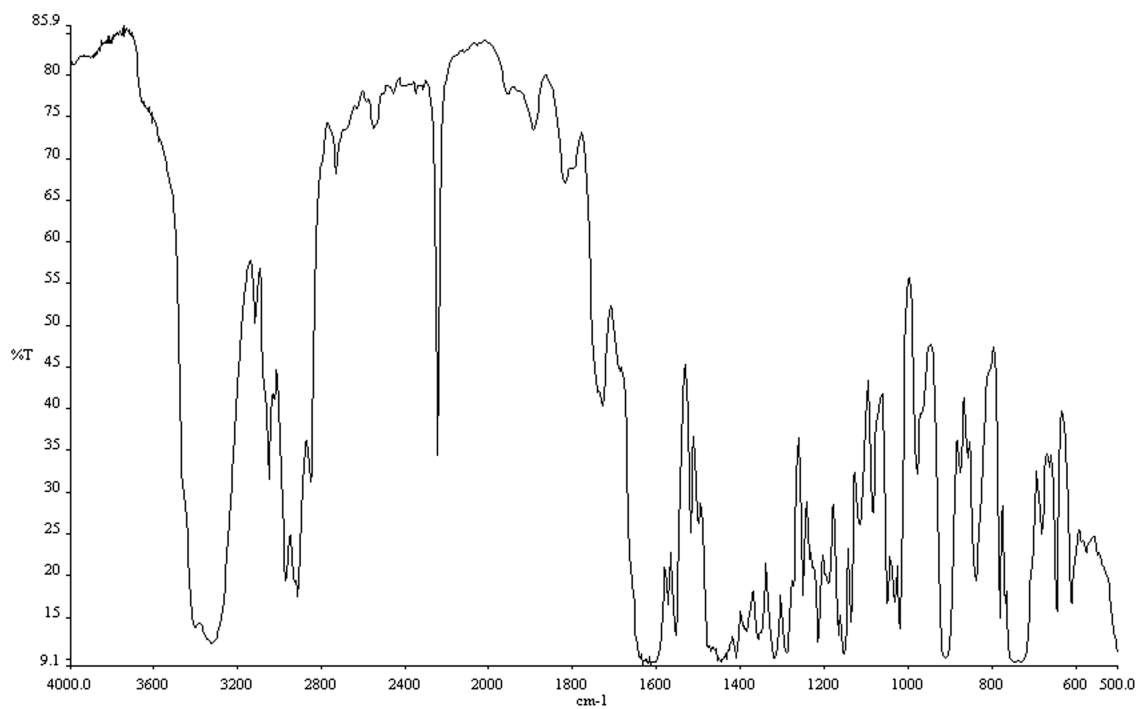*Figure A.3.46* ¹HNMR (300 MHz, CDCL₃) of compound **549**.

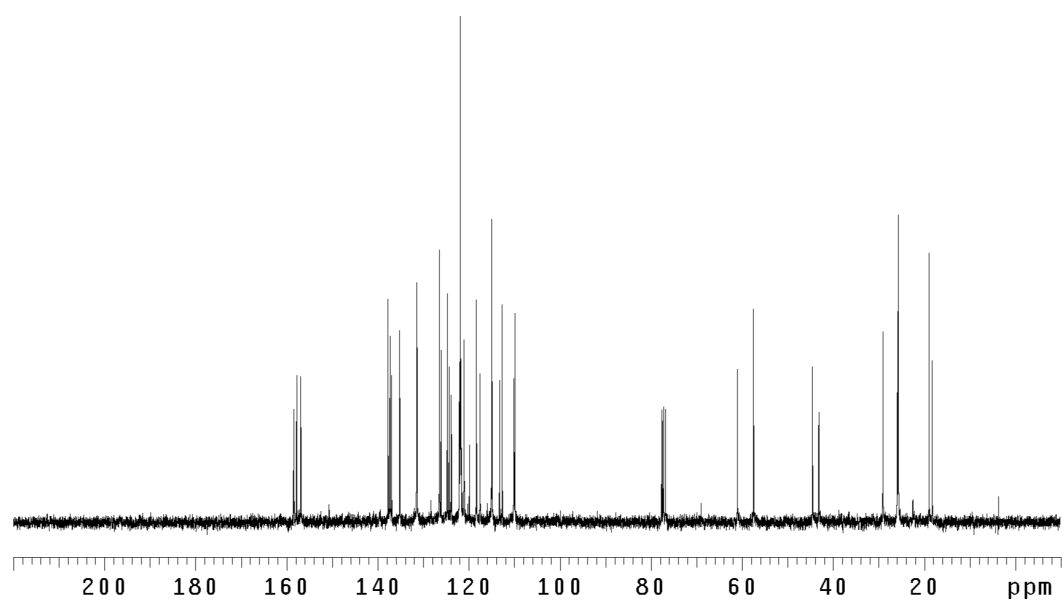*Figure A.3.47* Infrared spectrum (thin film/NaCl) of compound **549**.

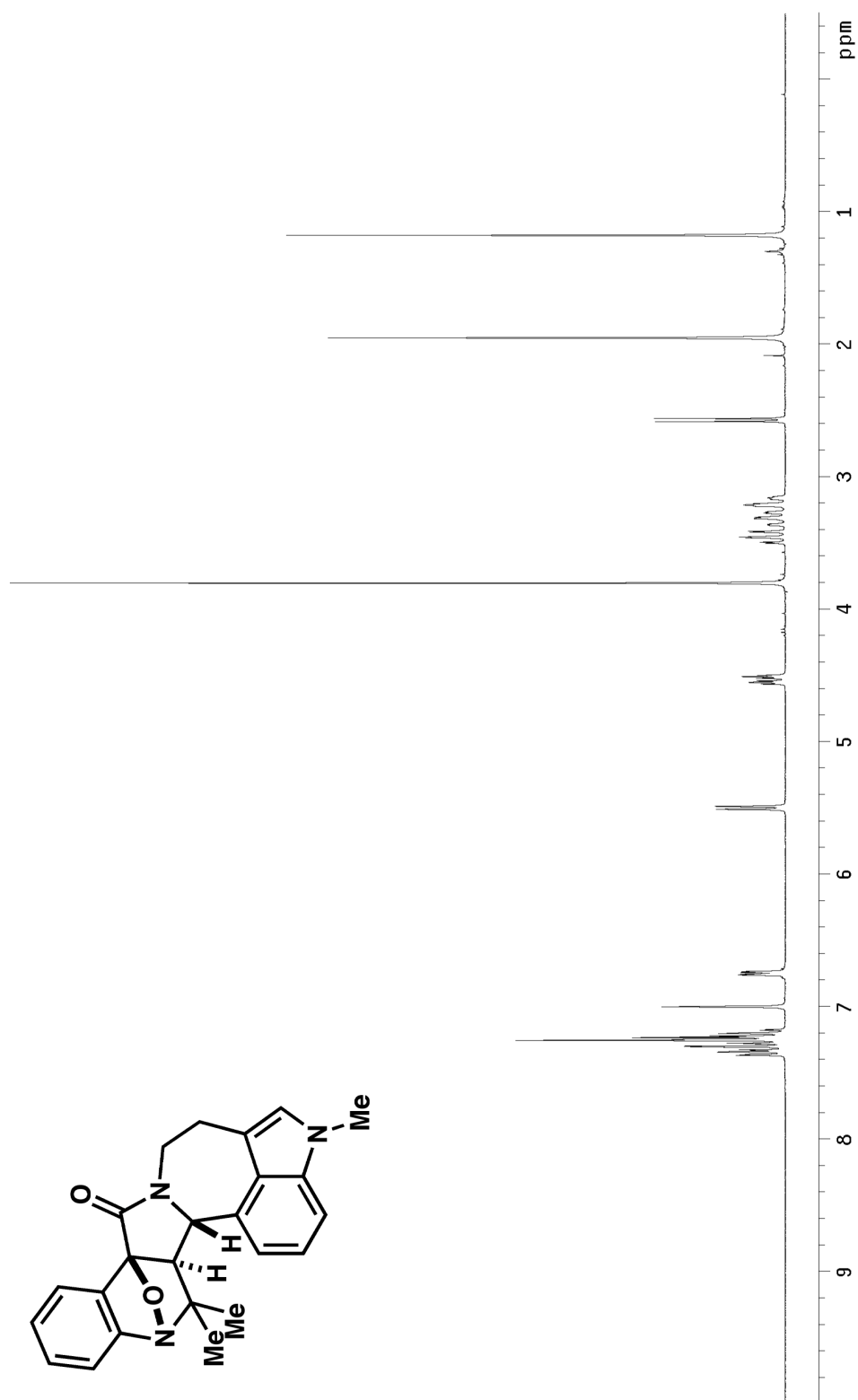*Figure A.3.48* ^{13}CNMR (75 Mhz, CDCl$_3$) of compound **549**.

Figure A.3.49 ¹HNMR (300 MHz, CDCL₃) of compound **550**.

Figure A.3.50 Infrared spectrum (thin film/NaCl) of compound **550**.

Figure A.3.51 ^{13}CNMR (75 Mhz, CDCl$_3$) of compound **550**.

Figure A.3.52 ^{1}HNMR (300 MHz, acetone-d$_6$) of compound **551**.

Figure A.3.53 Infrared spectrum (KBr) of compound **551**.
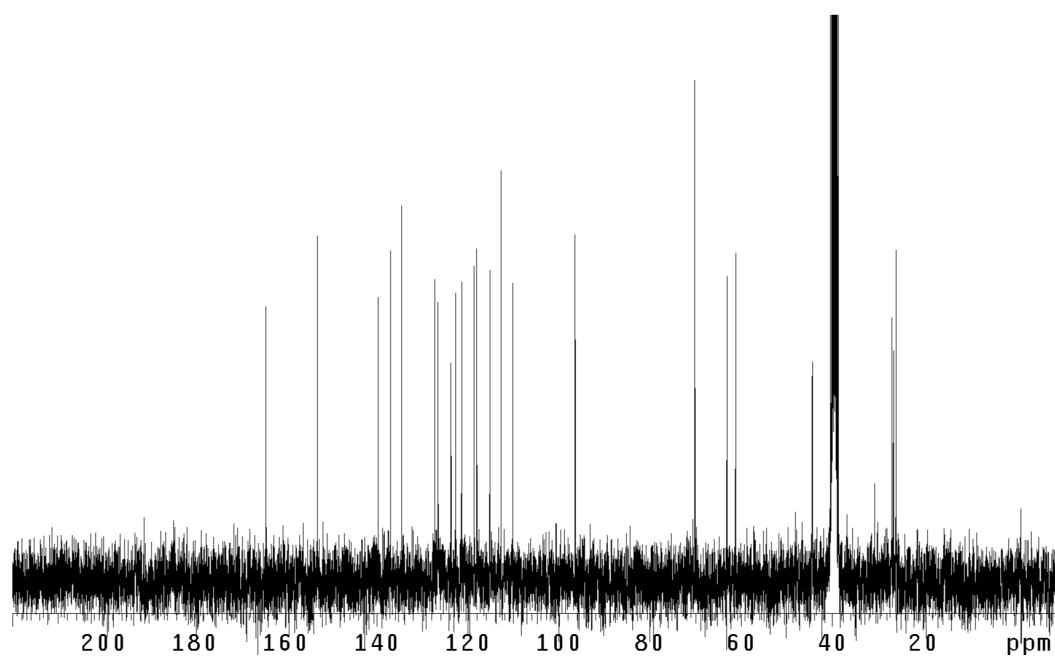
Figure A.3.54 ^{13}CNMR (75 Mhz, acetone-d$_6$) of compound **551**.

Figure A.3.55 ¹HNMR (300 MHz, CDCL₃) of compound **559**.

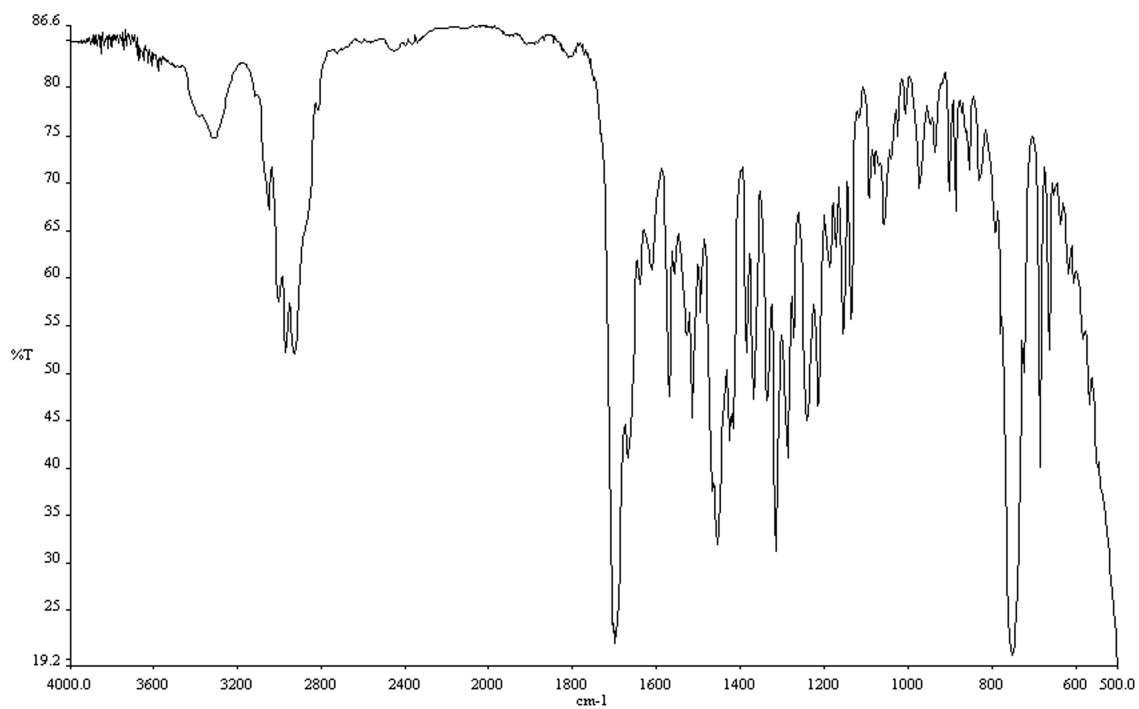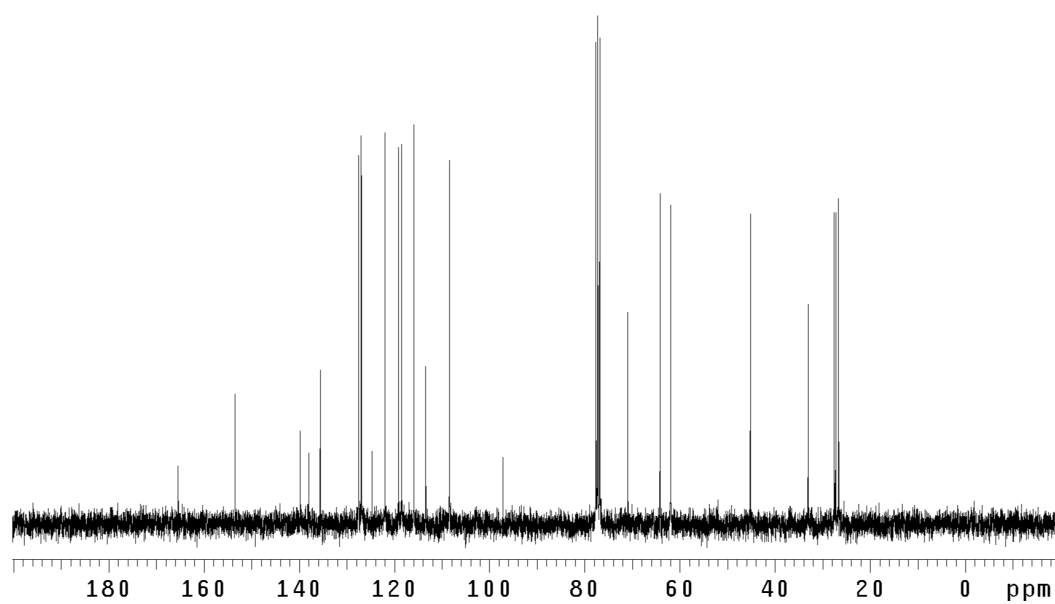*Figure A.3.56* Infrared spectrum (thin film/NaCl) of compound **559**.

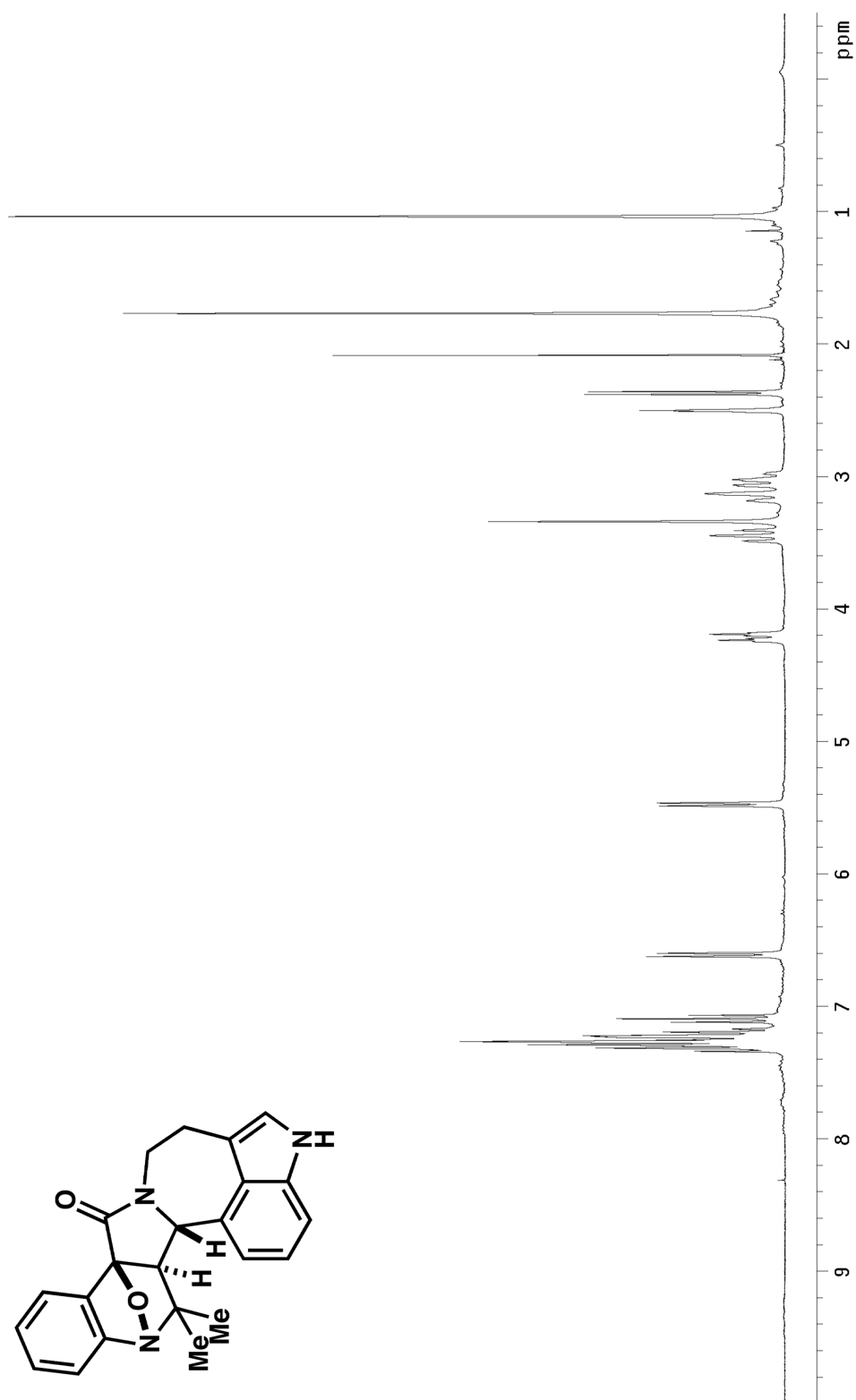
Figure A.3.57 ¹³CNMR (75 Mhz, CDCl₃) of compound **559**.

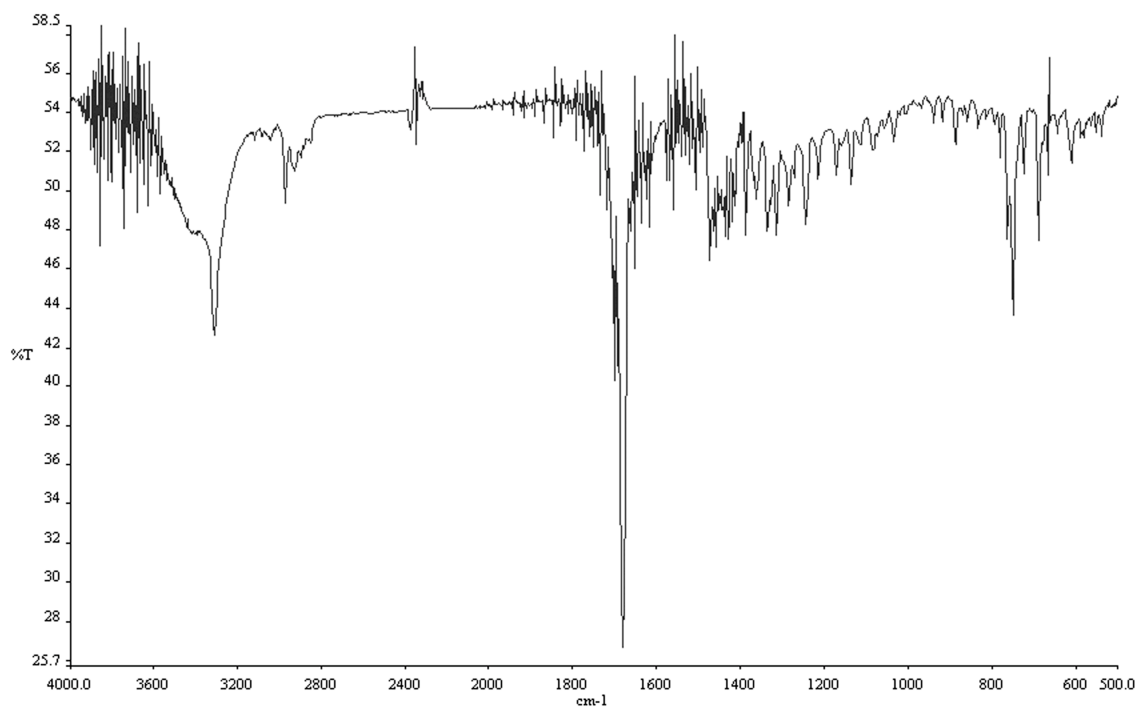*Figure A.3.58* ^{1}HNMR (300 MHz, CDCL$_3$) of compound **560**.

Figure A.3.59 Infrared spectrum (thin film/NaCl) of compound **560**.

Figure A.3.60 ^{13}CNMR (75 Mhz, CDCl$_3$) of compound **560**.

Figure A.3.61 ¹HNMR (300 MHz, CDCL₃) of compound **561**.

Figure A.3.62 Infrared spectrum (thin film/NaCl) of compound **561**.

Figure A.3.63 ^{13}CNMR (75 Mhz, CDCl$_3$) of compound **561**.

Figure A.3.64 ¹HNMR (300 MHz, CDCL₃) of compound **570**.

Figure A.3.65 Infrared spectrum (thin film/NaCl) of compound **570**.

Figure A.3.66 ^{13}CNMR (75 Mhz, CDCl$_3$) of compound **570**.
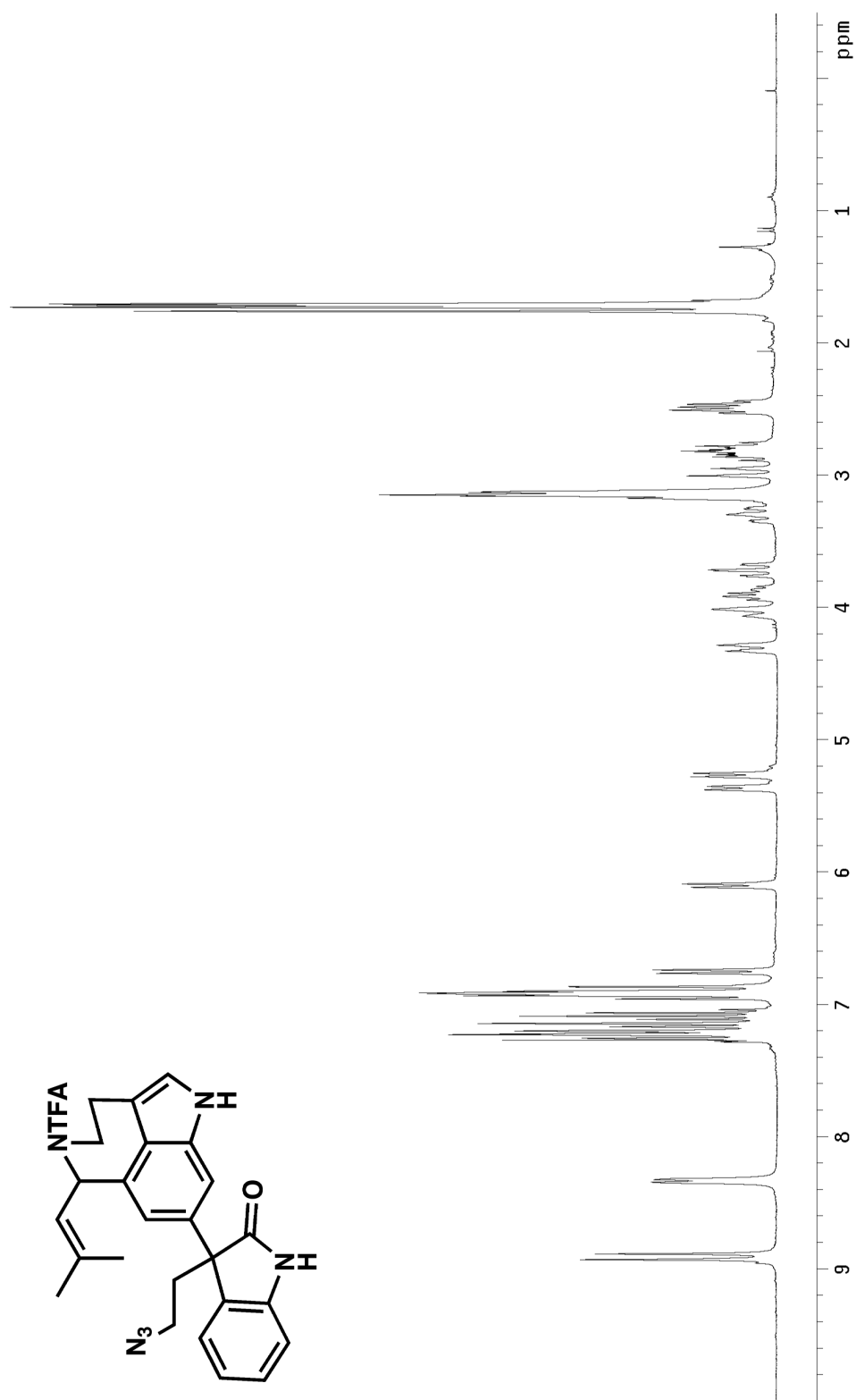
Figure A.3.67 ¹HNMR (300 MHz, CDCL₃) of compound **573**.
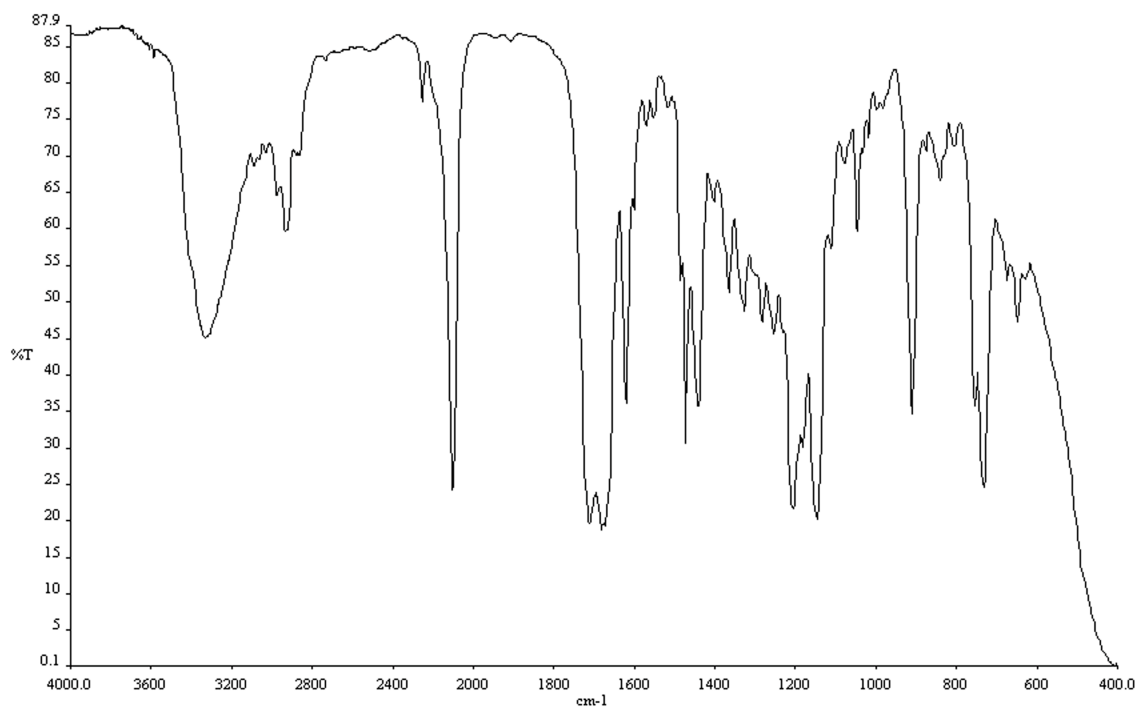
Figure A.3.68 Infrared spectrum (thin film/NaCl) of compound **573**.
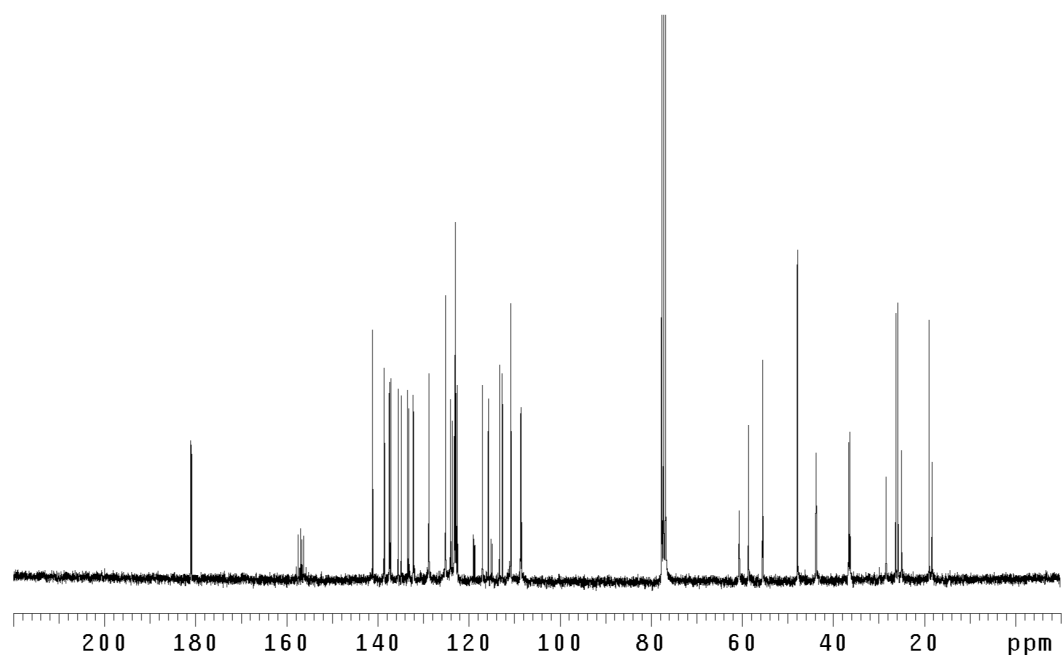
Figure A.3.69 ^{13}CNMR (75 Mhz, CDCl$_3$) of compound **573**.
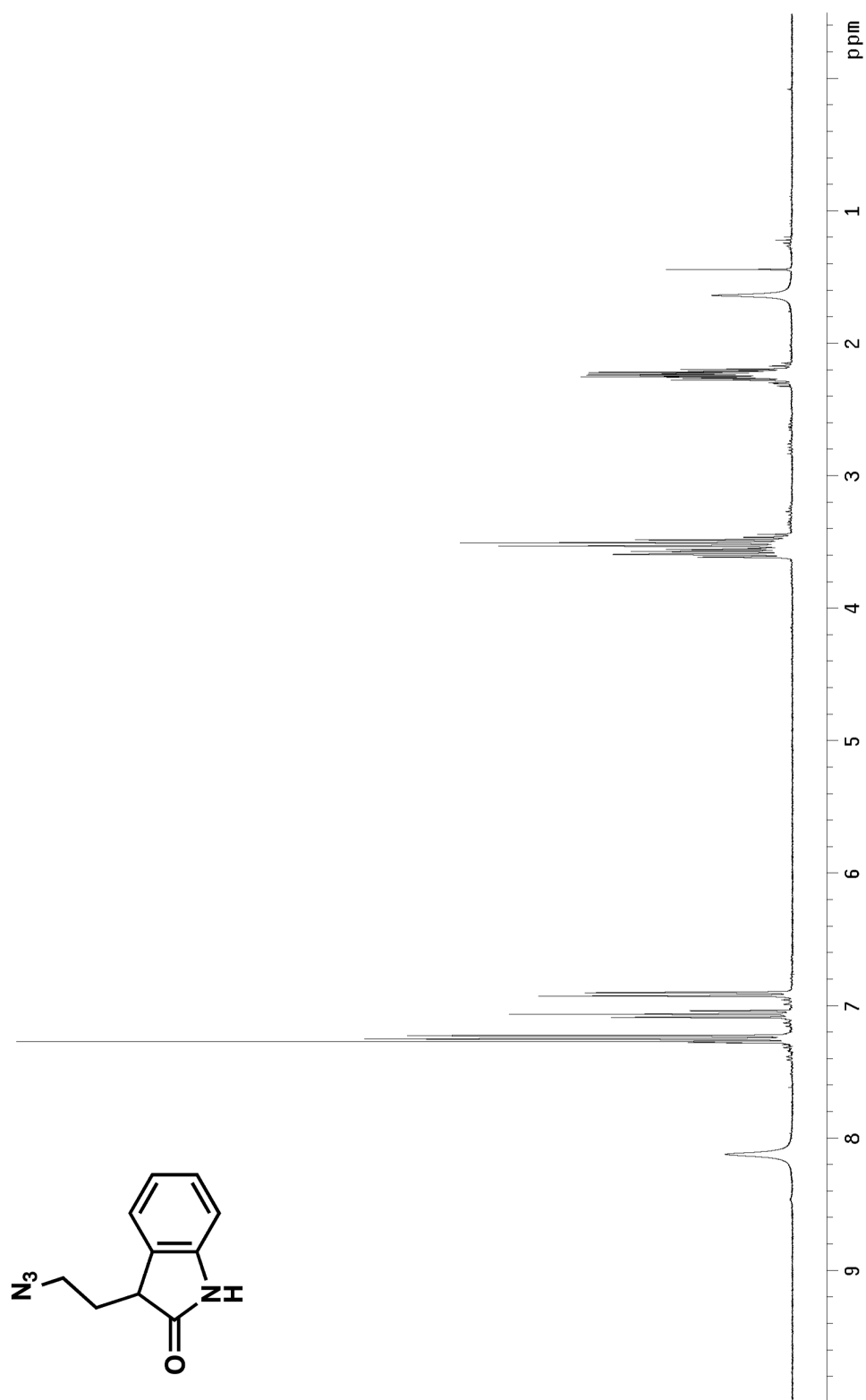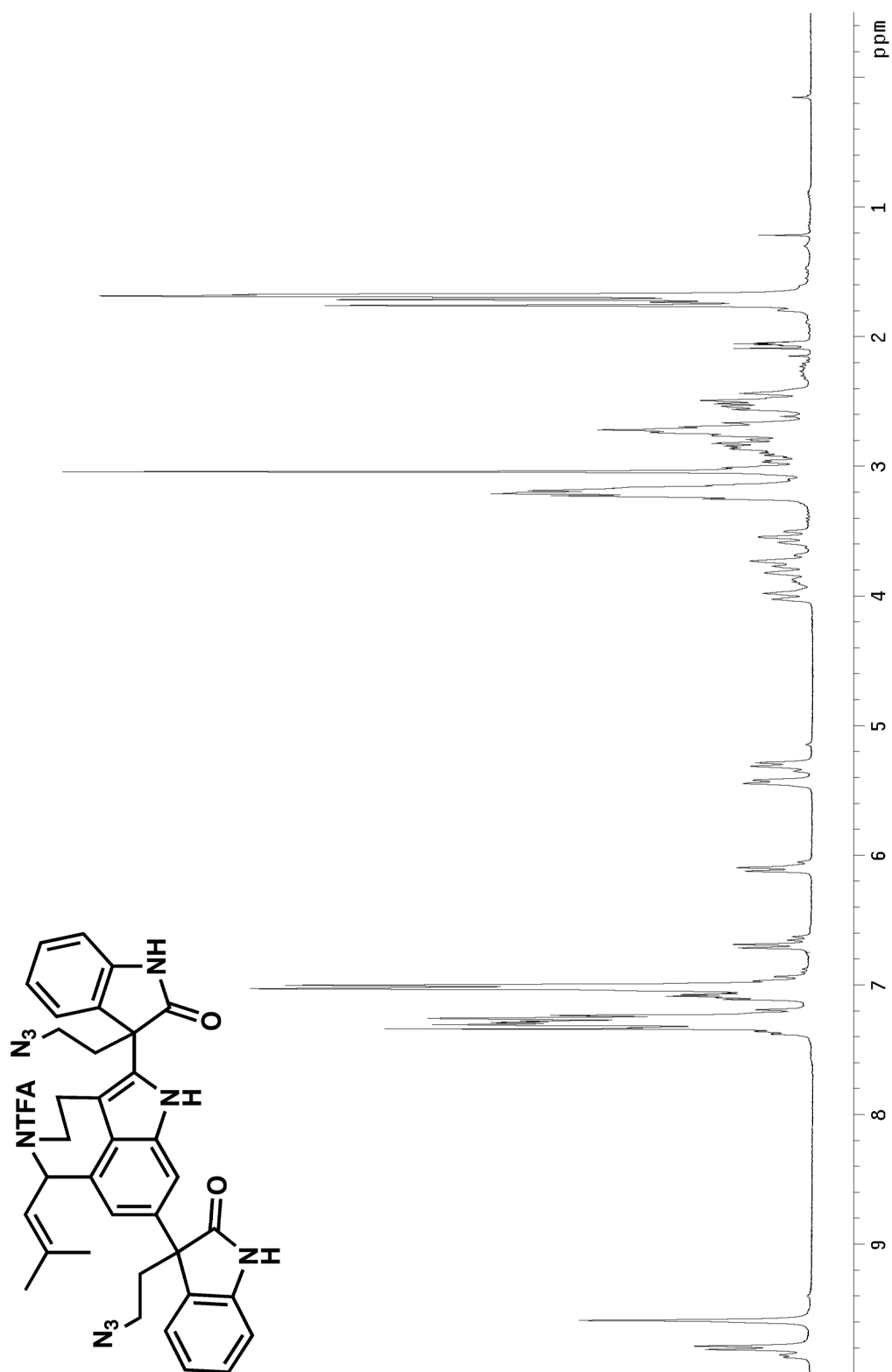
Figure A.3.70 ^{1}HNMR (300 MHz, CDCL$_3$) of compound **564**.
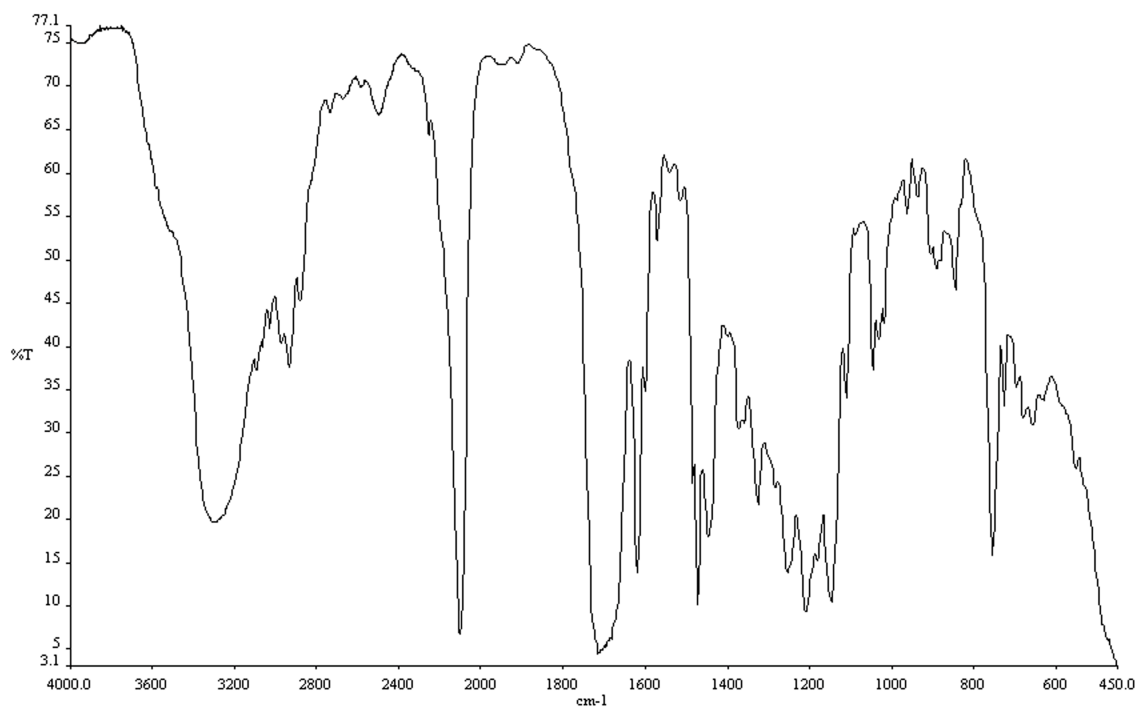
Figure A.3.71 Infrared spectrum (thin film/NaCl) of compound **564**.
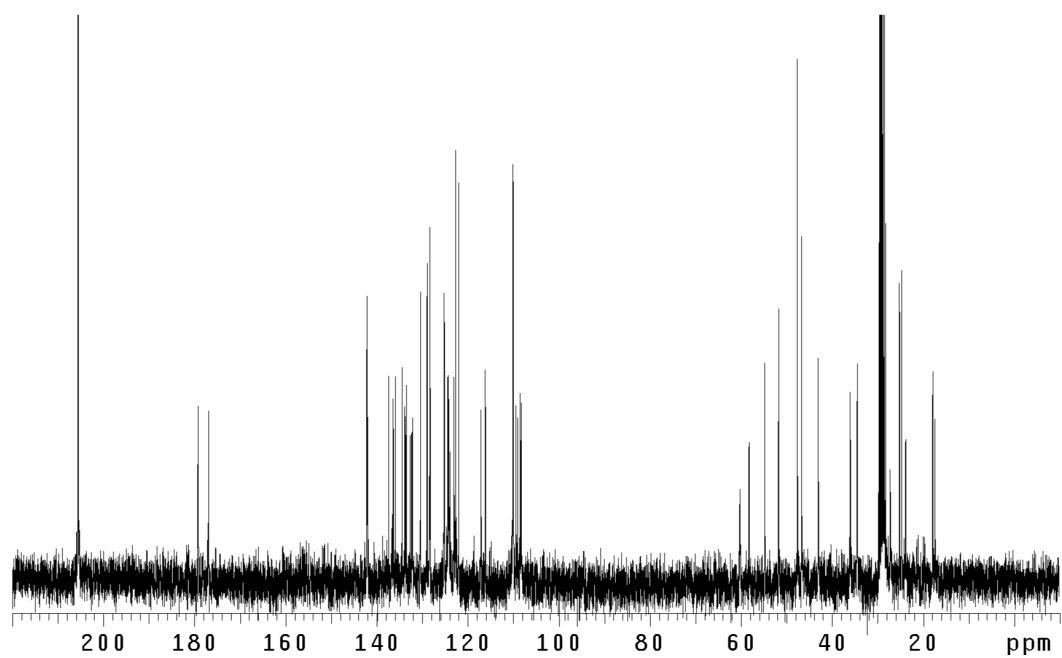
Figure A.3.72 ^{13}CNMR (75 Mhz, CDCl$_3$) of compound **564**.
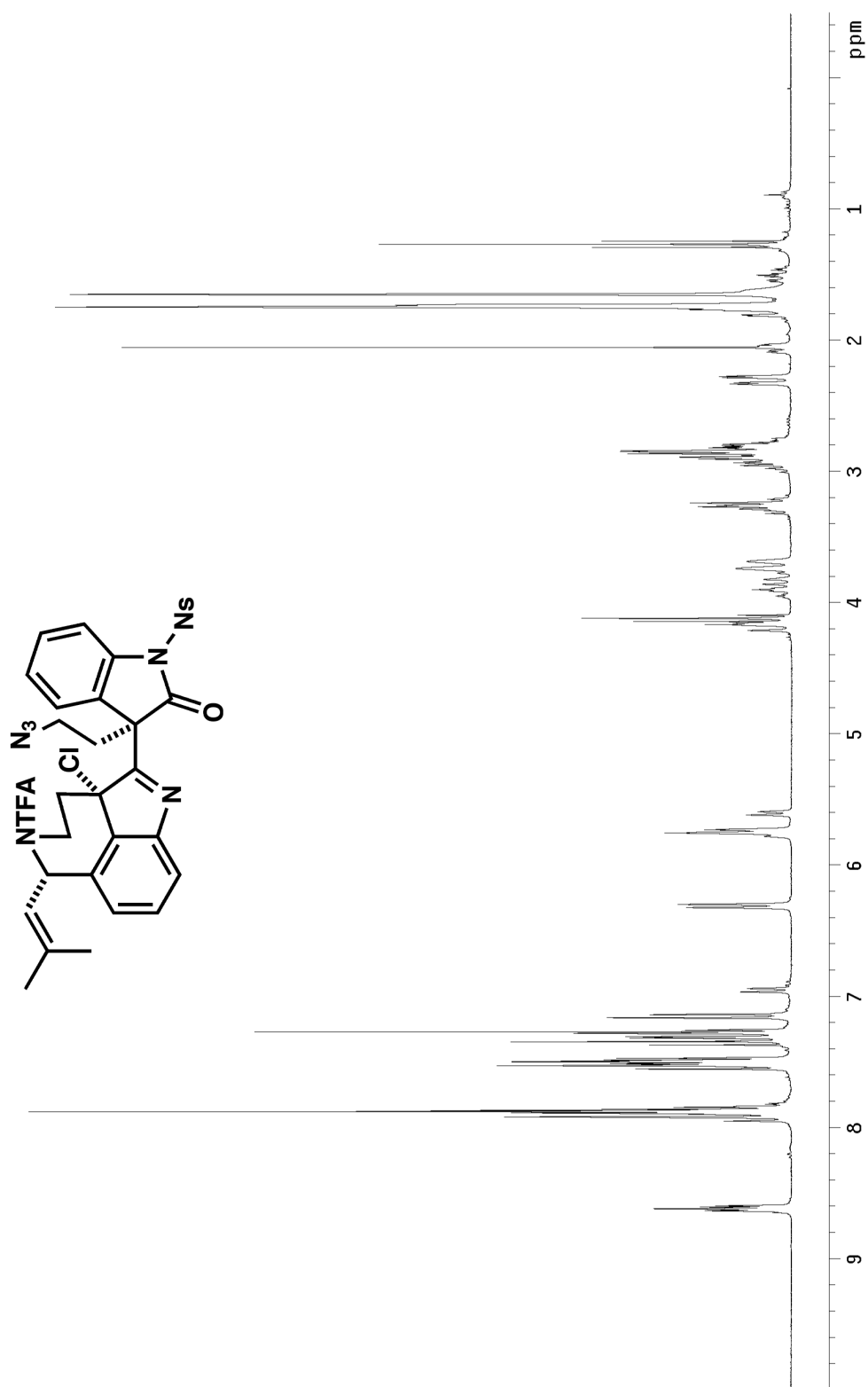
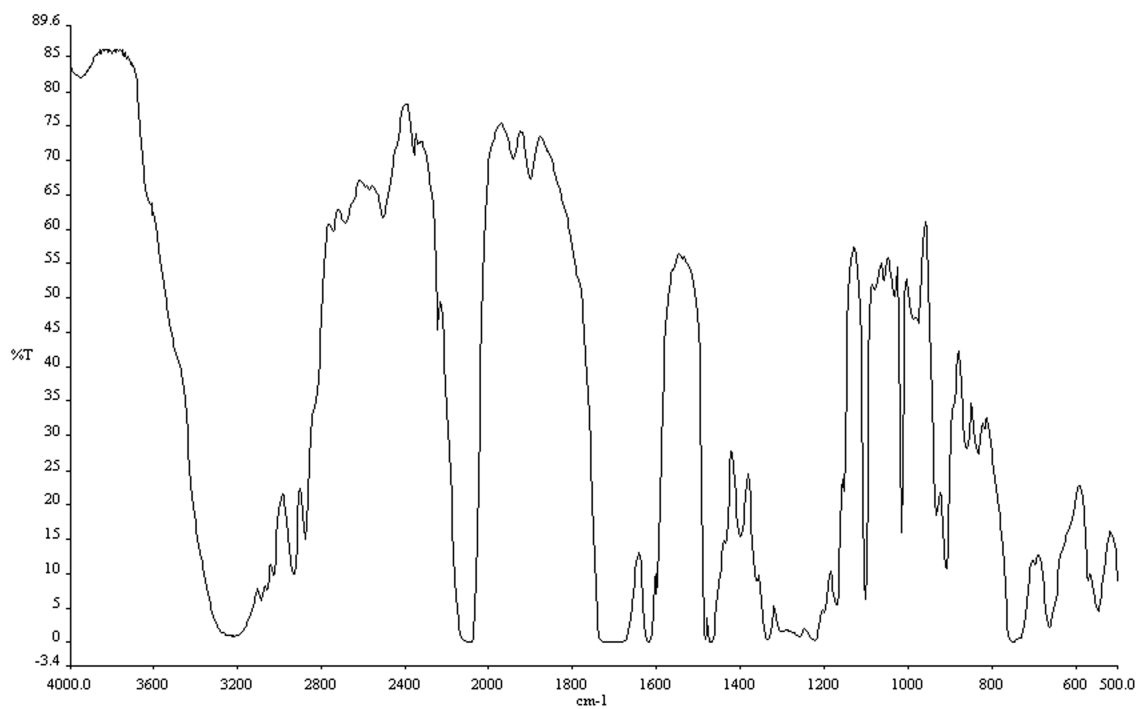*Figure A.3.73* ¹HNMR (300 MHz, CDCL₃) of compound **571**.
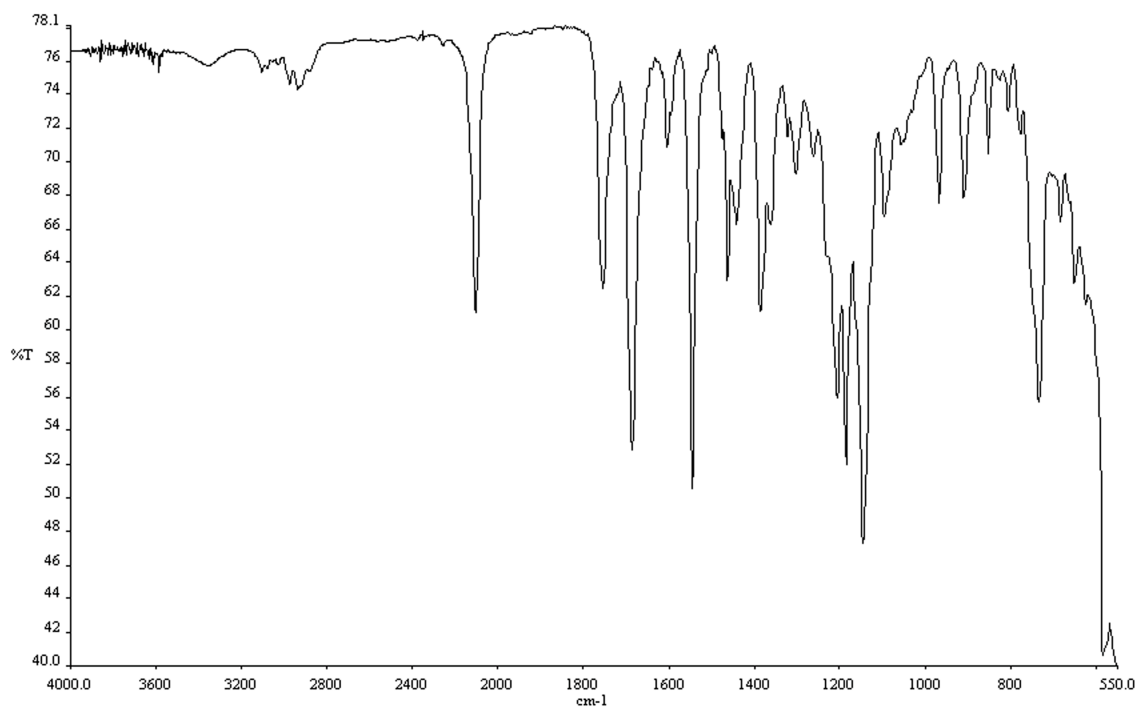
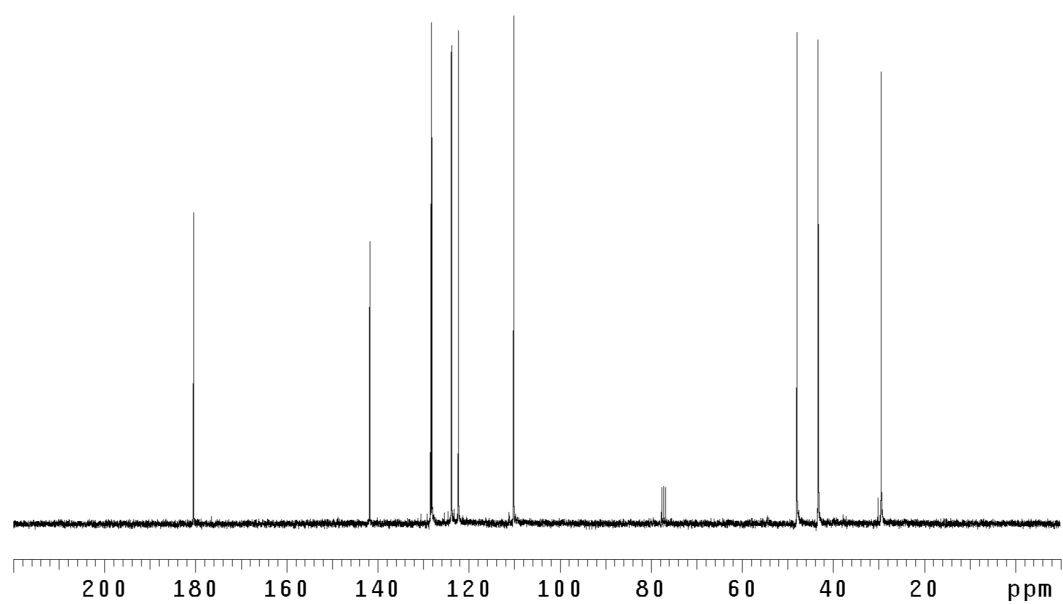*Figure A.3.74* Infrared spectrum (thin film/NaCl) of compound **571**.
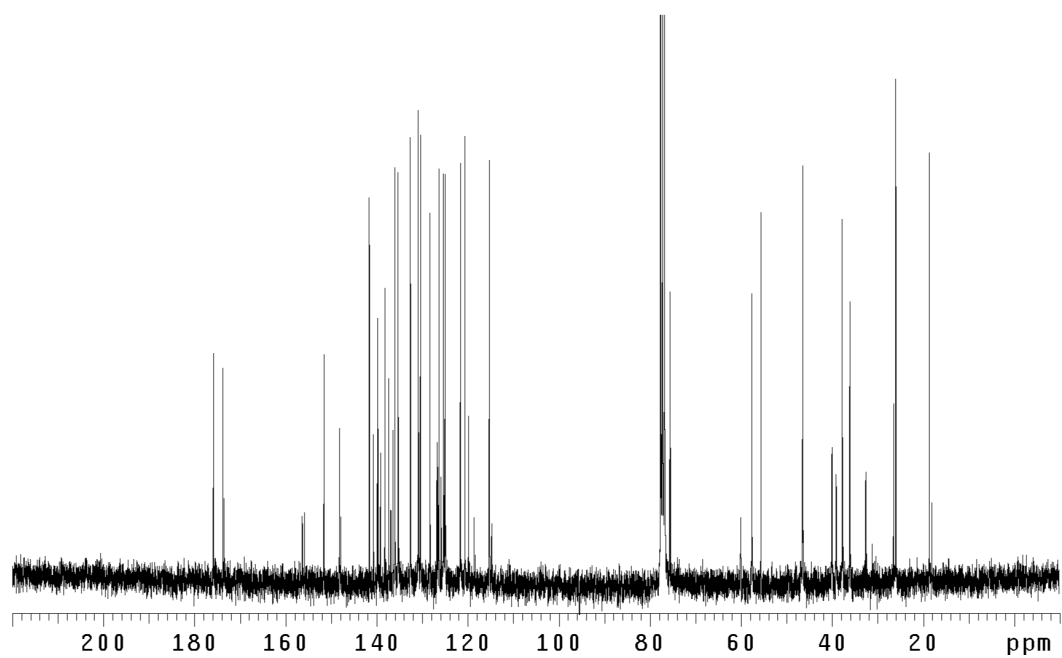
Figure A.3.75 ¹³CNMR (75 Mhz, CDCl₃) of compound **571**.
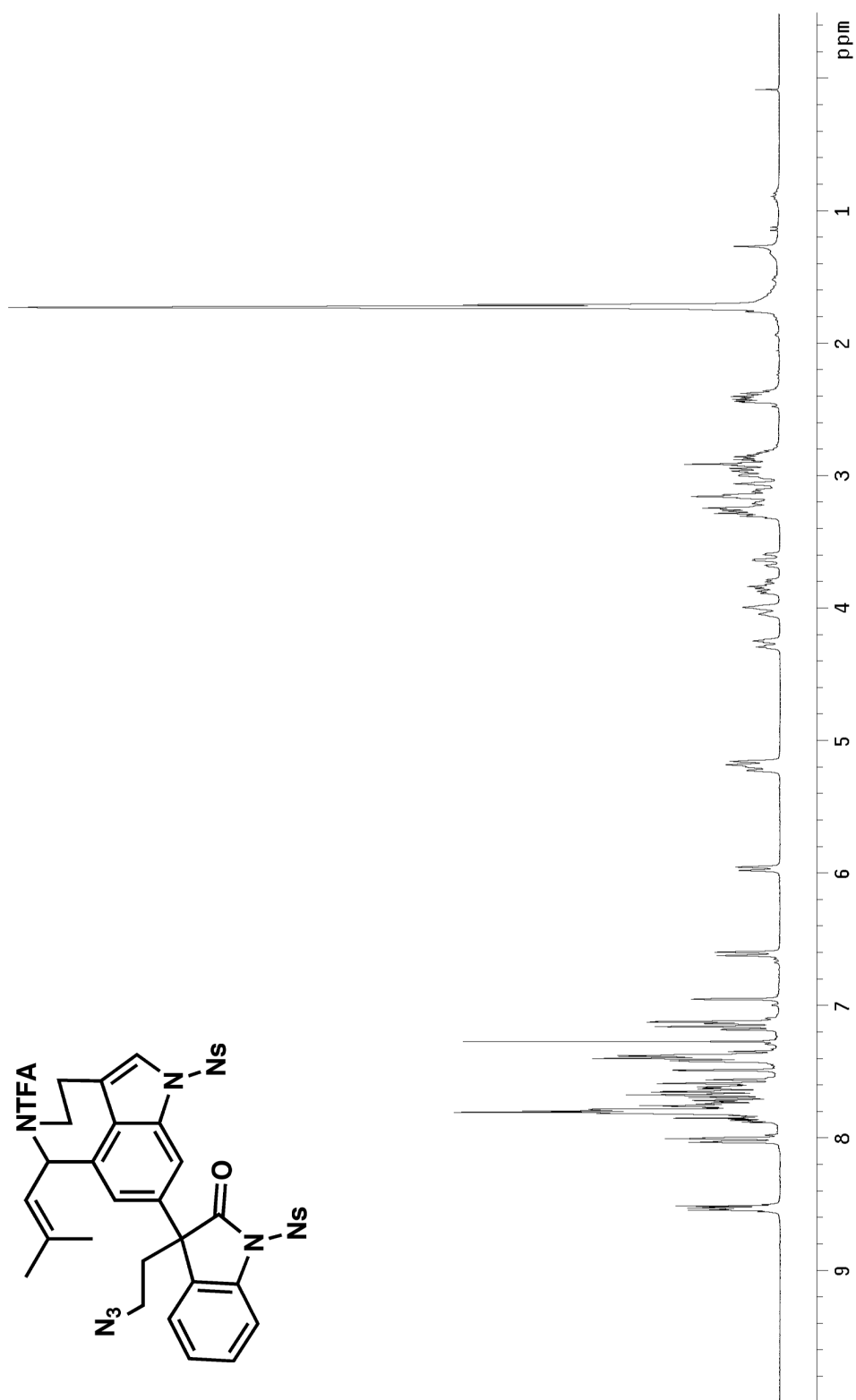
Figure A.3.76 ^{1}HNMR (300 MHz, CDCL$_3$) of compound **574**.
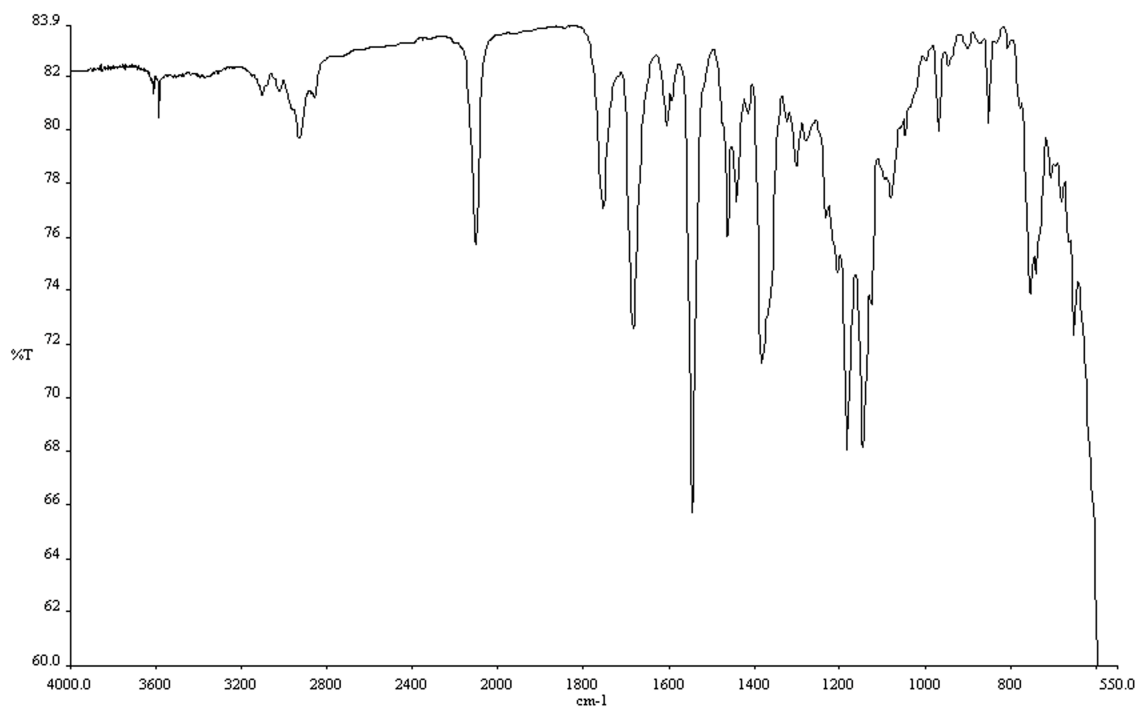
Figure A.3.77 Infrared spectrum (thin film/NaCl) of compound **574**.
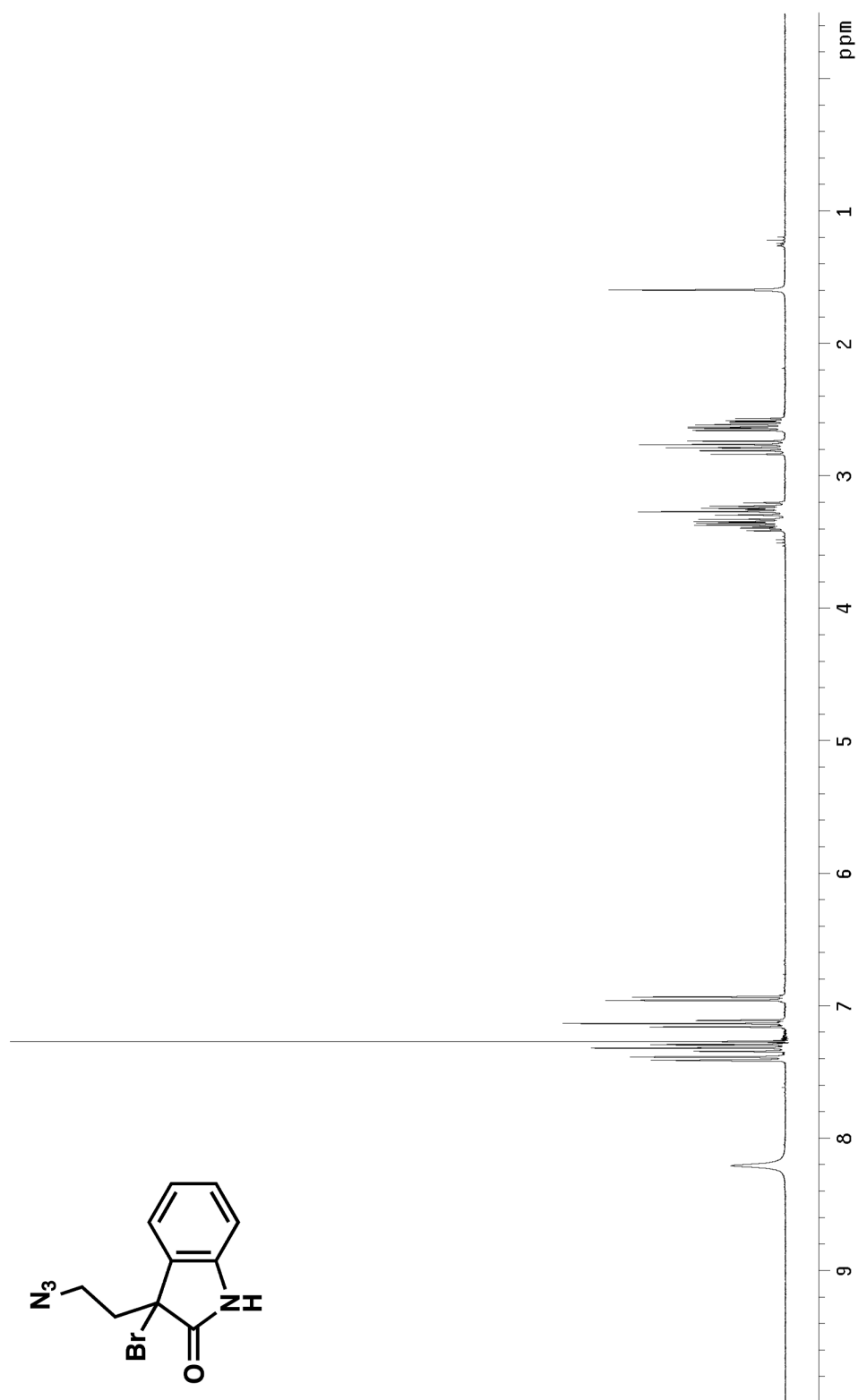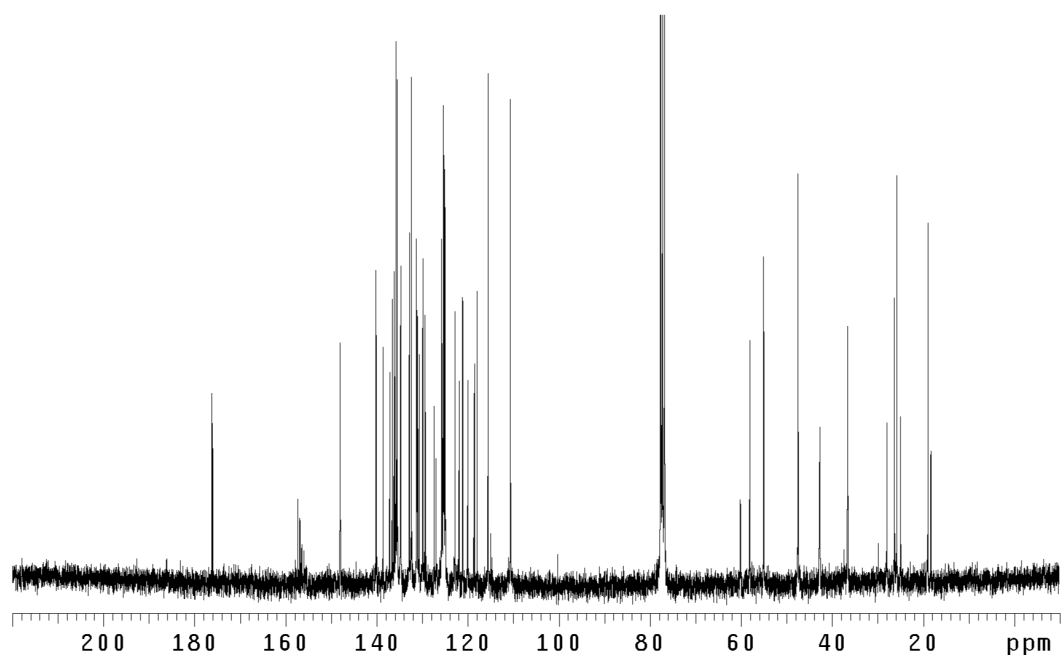

Figure A.3.78 ¹³CNMR (75 Mhz, CDCl₃) of compound **574**.
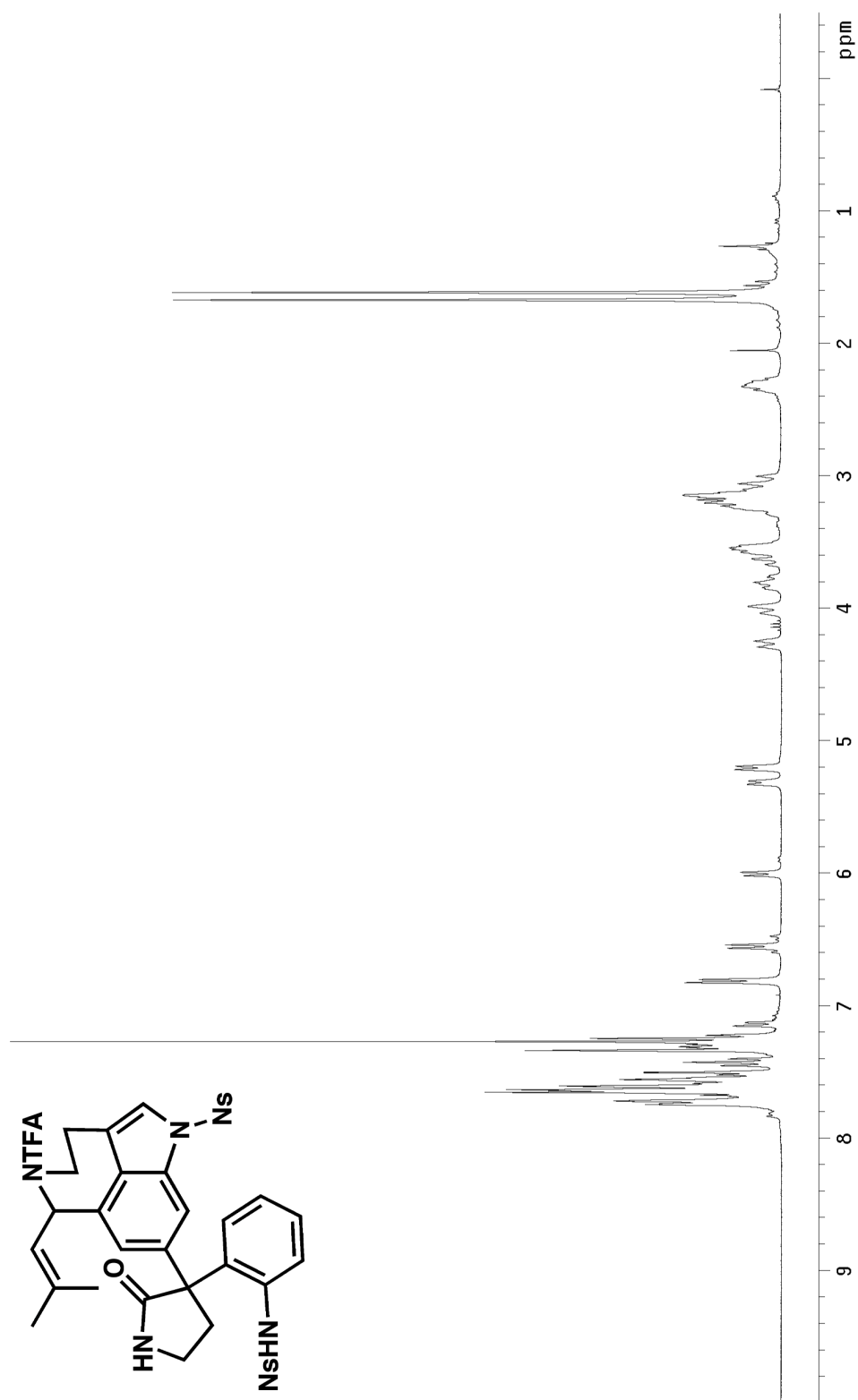
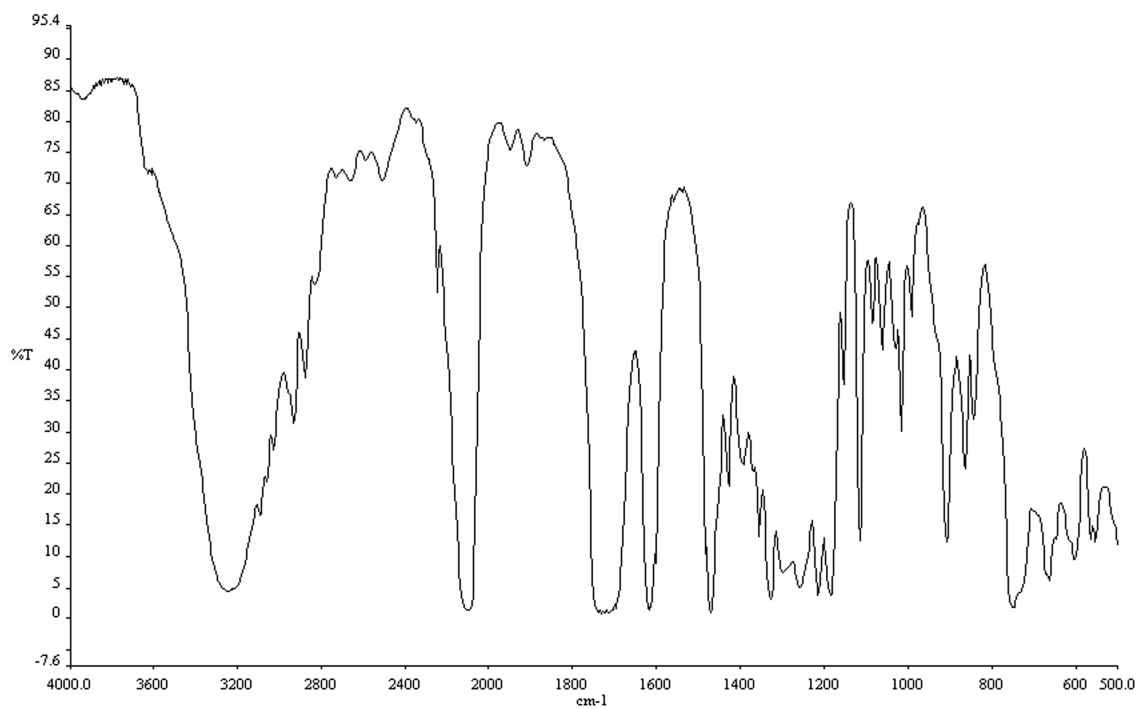*Figure A.3.79* ¹HNMR (300 MHz, CDCL₃) of compound **575**.

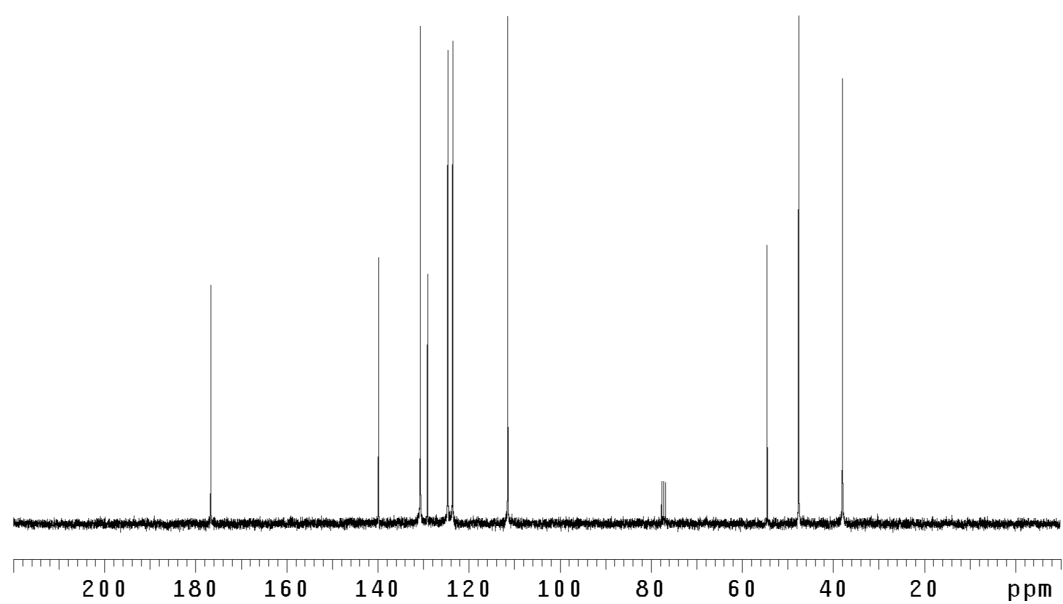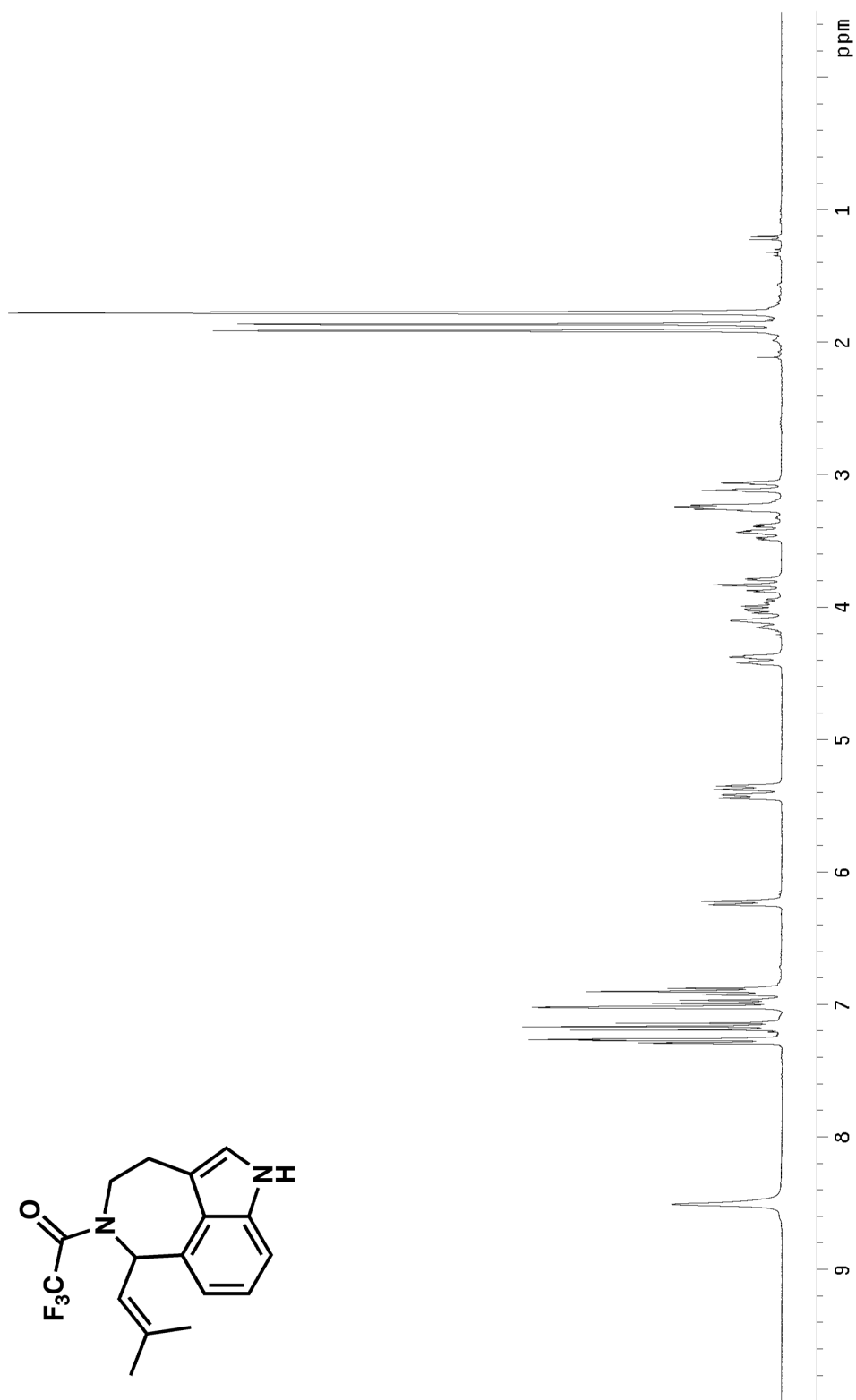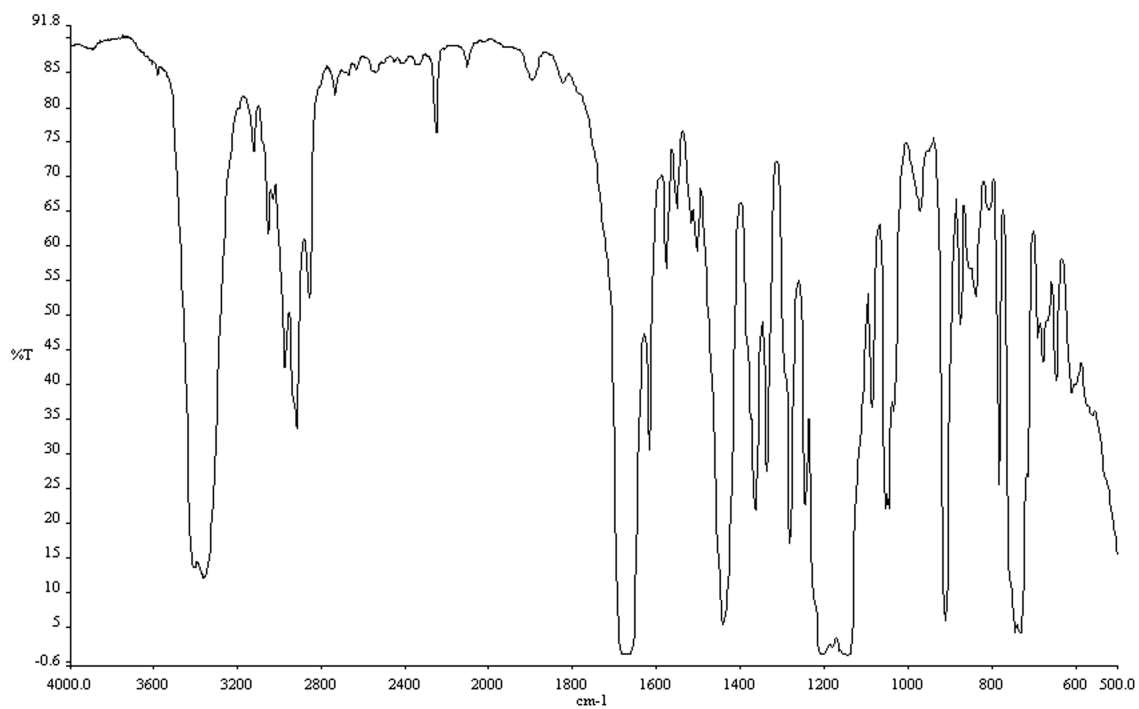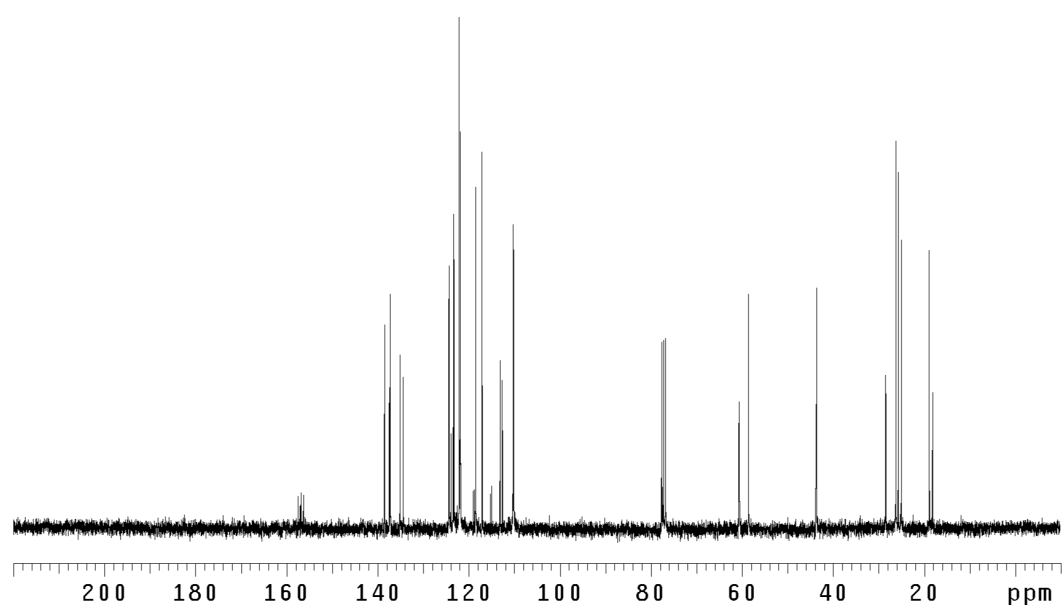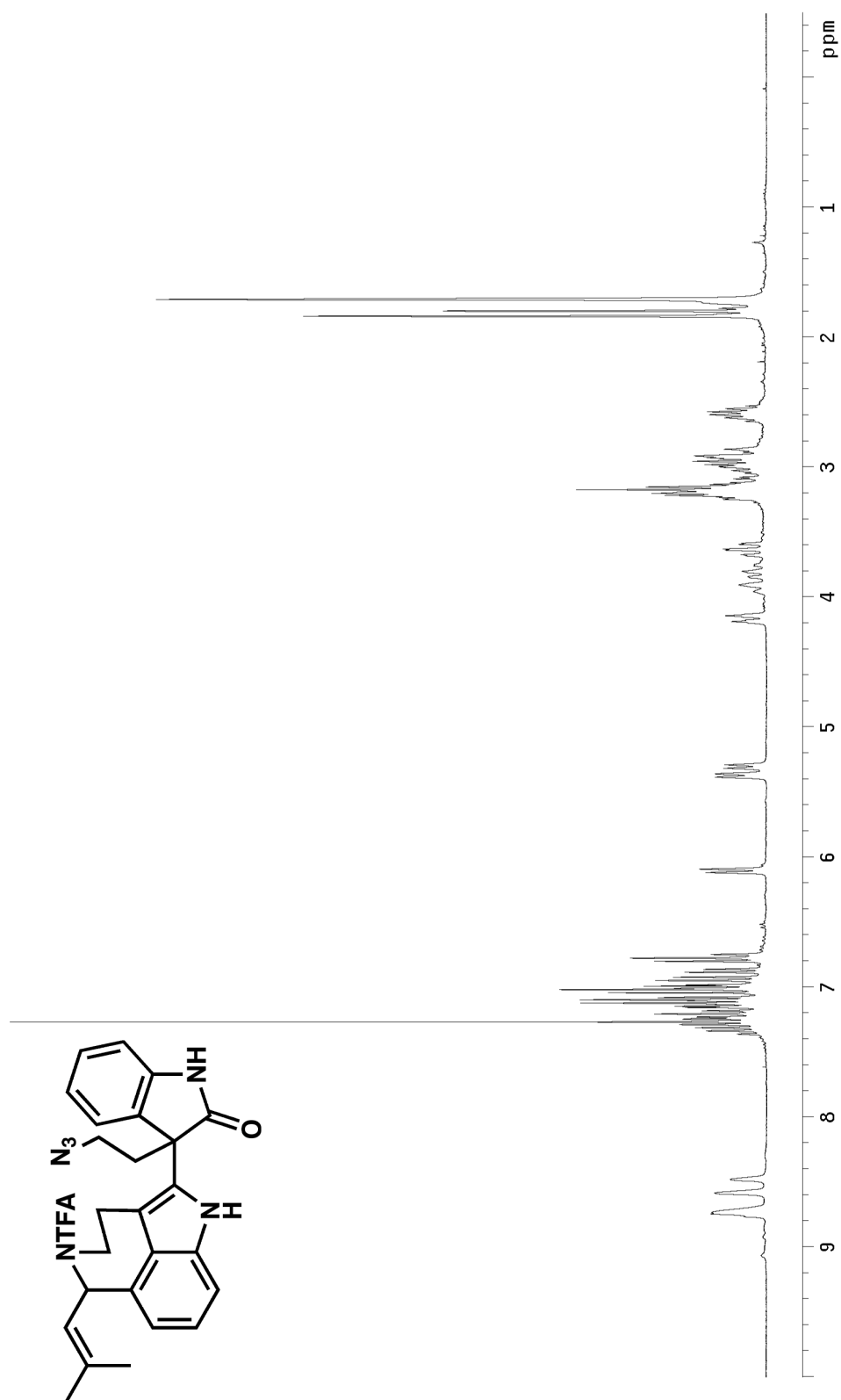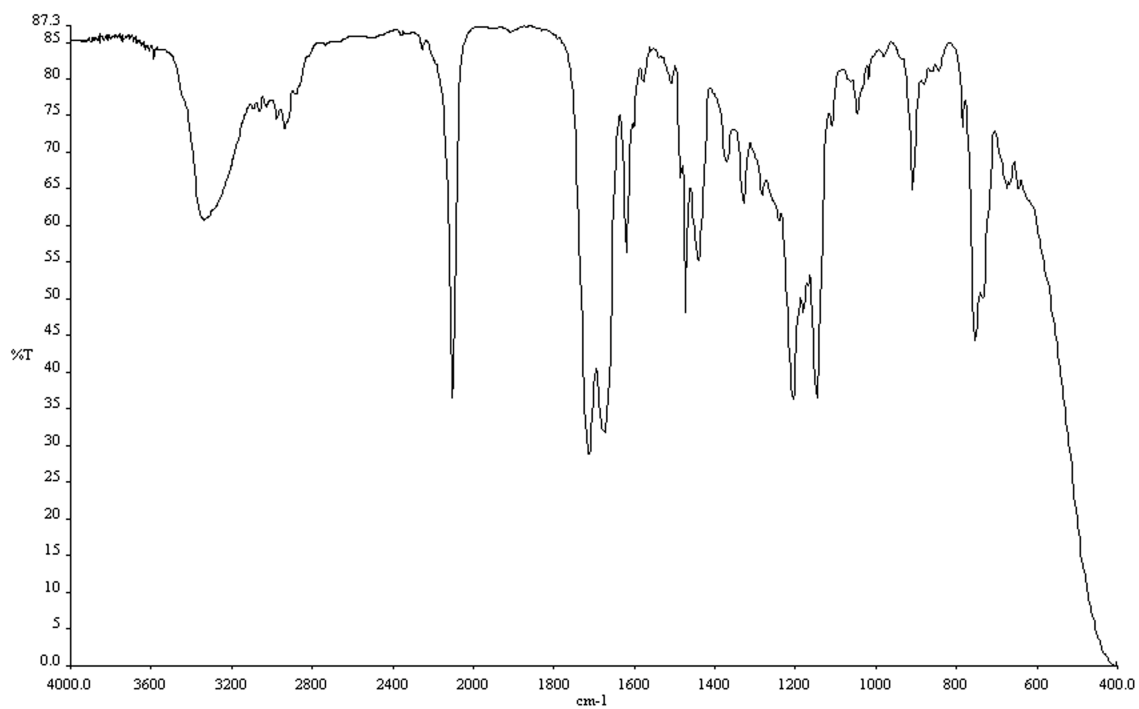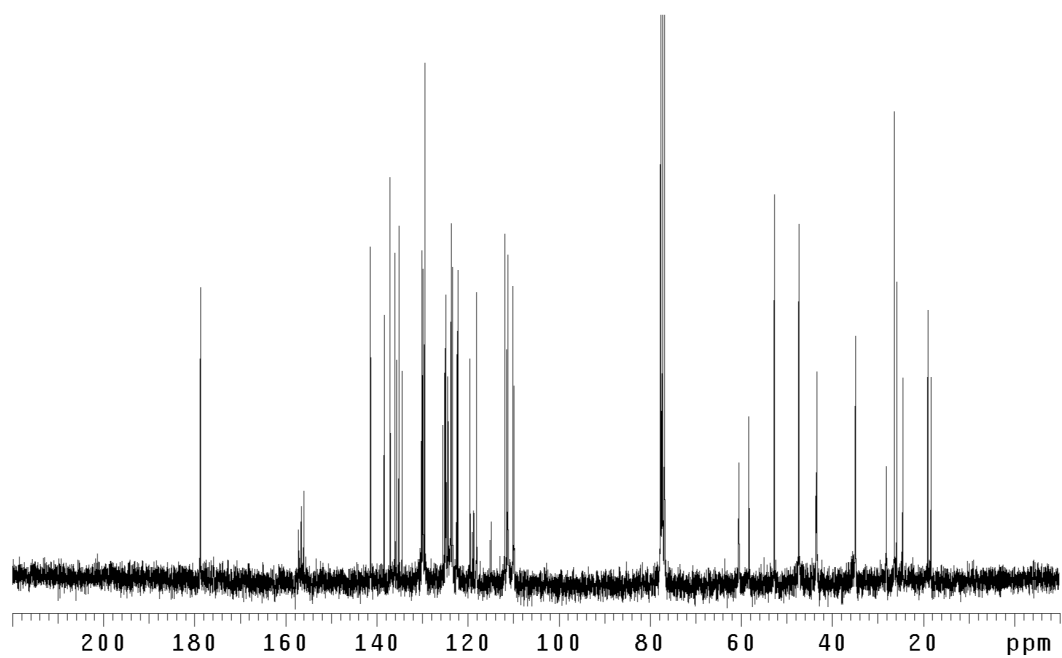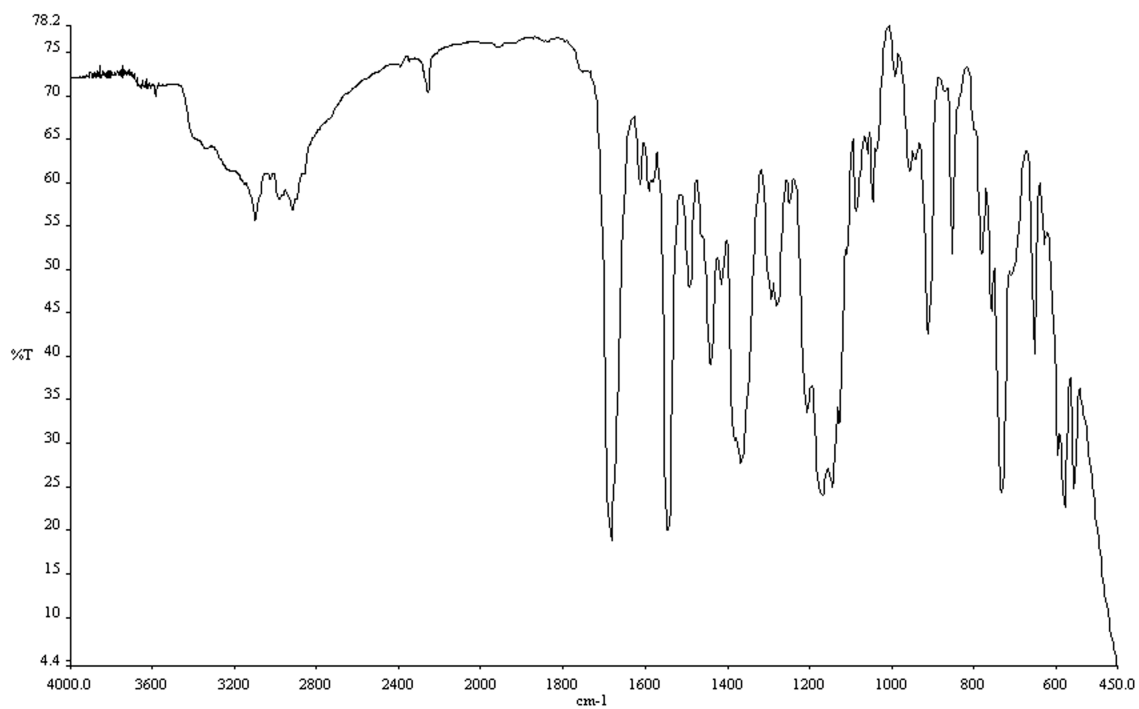*Figure A.3.80* Infrared spectrum (thin film/NaCl) of compound **575**.
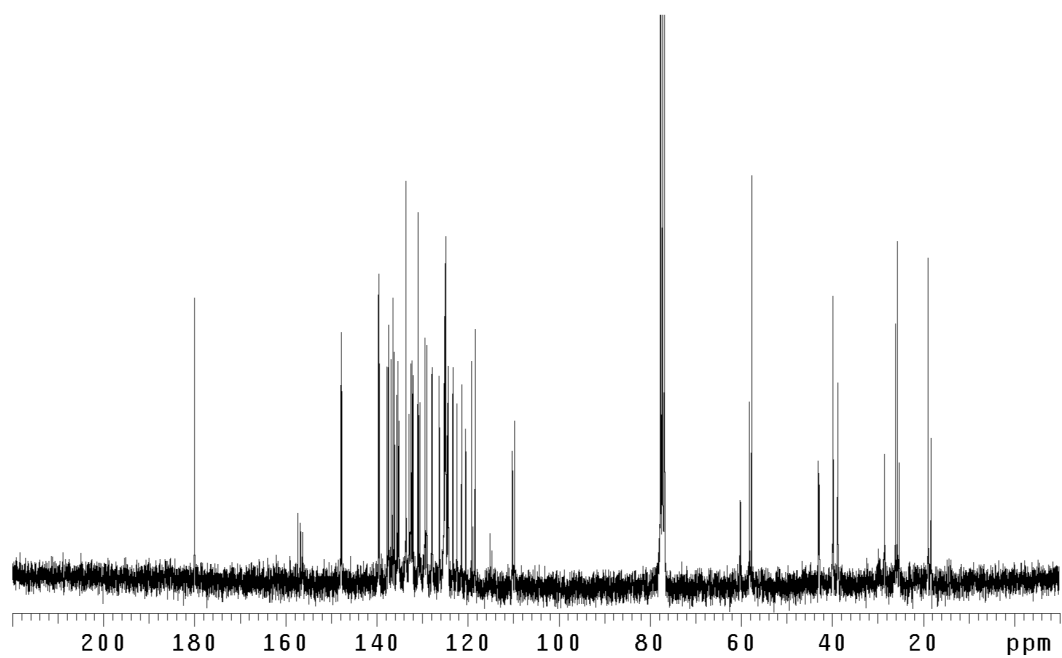
Figure A.3.81 ^{13}CNMR (75 Mhz, CDCl$_3$) of compound **575**.

APPENDIX FOUR

Notebook Cross-Reference

The following notebook cross-reference has been included to facilitate access to the original spectroscopic data obtained for the compounds presented in this thesis. For each compound, both hardcopy and electronic characterization folders have been created that contain copies of the original ^{1}H NMR, ^{13}C NMR, and IR spectra. All notebooks and spectral data are stored in the Stoltz archives.

Table A.4.1 Compounds Appearing in Chapter 1:
Non-Carbonyl Stabilized Diazo Compounds in the Tandem Bamford-Stevens/Claisen Reaction

Compound	^{1}H NMR	^{13}C NMR	IR
261	JAMIV-185i	JAMIV-185i	JAMIV-185i
263	JAMV-301	JAMV-301	JAMV-301
264	JAMIII-199	JAMIII-199	JAMIII-199
265	JAMVI-297i	JAMVI-297i	JAMVI-297i
267	JAMIV-115	JAMIV-115	JAMIV-115
268	JAMIII-285	JAMIII-285	JAMIII-285
269	JAMIII-221	JAMIII-221	JAMIII-221
270	JAMIV-167	JAMIV-167	JAMIV-167
271	JAMIV-165	JAMIV-165	JAMIV-165
272	JAMV-51	JAMV-51	JAMV-51
273	JAMVII-101	JAMVII-101	JAMVII-101
163	JAMIII-147	JAMIII-147	JAMIII-147
104	JAMIV-111i	JAMIV-111i	JAMIV-111i
106	JAMVI-227i	JAMVI-227i	JAMVI-227i

Compound	¹H NMR	¹³C NMR	IR
95	JAMI-206ii	JAMI-206ii	
165	JAMVII-151ii	JAMVII-151ii	JAMVII-151ii
167	JAMIV-95i	JAMIV-95i	JAMIV-95i
169	JAMVI-227i	JAMVI-227i	JAMVI-227i
171	JAMIII-201	JAMIII-201	JAMIII-201
173	JAMVII-41i	JAMVII-41i	JAMVII-41i
179	JAMIII-279	JAMIII-279	JAMIII-279
181	JAMIV-117i	JAMIV-117i	JAMIV-117i
183	JAMIII-287	JAMIII-287	JAMIII-287
185	JAMVI-143i	JAMVI-143i	JAMVI-143i
189	JAMIV-173i	JAMIV-173i	JAMIV-173i
192	JAMIV-171i	JAMIV-171i	JAMIV-171i
199	JAMV-53ii	JAMV-53ii	JAMV-53ii
202	JAMVII-103iib	JAMVII-103iib	JAMVII-103iib
105	JAMIV-139	JAMIV-139	JAMIV-139
107	JAMVI-259ii	JAMVI-259ii	JAMVI-259ii
98	JAMI-211iv	JAMI-211iv	
164	JAMIII-205	JAMIII-205	JAMIII-205
166	JAMVII-153a	JAMVII-153a	JAMVII-153a
168	JAMIV-127ii	JAMIV-127ii	JAMIV-127ii
170	JAMVII-177	JAMVII-177	JAMVII-177
172	JAMIII-269	JAMIII-269	JAMIII-269
180	JAMIII-295i	JAMIII-295i	JAMIII-295i
182	JAMIV-141i	JAMIV-141i	JAMIV-141i
174	JAMVII-183	JAMVII-183	JAMVII-183
213	JAMIV-59i	JAMIV-59i	JAMIV-59i
186	JAMVII-281	JAMVII-281	JAMVII-281
184	JAMVII-215	JAMVII-215	JAMVII-215
191	JAMIV-197iii	JAMIV-197iii	JAMIV-197iii
188	JAMVII-215	JAMVII-215	JAMVII-215
194	JAMIV-189ii	JAMIV-189ii	JAMIV-189ii
197	JAMVI-287i	JAMVI-287i	JAMVI-287i
198	JAMVII-133iii	JAMVII-67	JAMVII-133ii

Compound	^{1}H NMR	^{13}C NMR	IR
203	JAMVII-109	JAMVII-109	JAMVII-109
201	JAMVII-117ii	JAMVII-117ii	JAMVII-117ii
205	JAMVII-209a	JAMVII-209a	JAMVII-209a
208	JAMVI-283ii	JAMVI-283ii	JAMVI-283ii

Table A.4.2 Compounds Appearing in Chapter 6:
Evaluating the Structure of and Proposing a Biomimetic Approach to Communesin
B (a.k.a Nomofungin)

Compound	^{1}H NMR	^{13}C NMR	IR
470	JAMIX-43	JAMIX-43	JAMIX-43
471	JAMIX-73	JAMIX-73	JAMIX-73
474	JAMIX-125i	JAMIX-125i	JAMIX-125i
475	JAMIX-125ii	JAMIX-125ii	JAMIX-125ii

Table A.4.3 Compounds Appearing in Chapter 7:
Recent Discomeries toward the Synthesis of the Communesin Family of Indole
Alkaloids

Compound	^{1}H NMR	^{13}C NMR	IR
507	JAMVIII-293	JAMVIII-293	JAMVIII-293
510	JAMIX-49ii	JAMIX-49ii	JAMIX-49ii
580	JAMX-95	JAMX-95	JAMX-95
513	JAMX-75ii	JAMX-75ii	JAMX-75ii
516	JAMX-249ii	JAMX-249ii	JAMX-249ii
518	JAMXI-83ii	JAMXI-83ii	JAMXI-83ii
519 and 520	JAMX-213	JAMX-213	JAMX-213
522	JAMXVI-169i	JAMXVI-169i	JAMX-205
523	JAMXVI-171	JAMXVI-171	JAMXVI-171
534	JAMXII-179	JAMXII-179	JAMXII-179
538a	JAMXII-75ii	JAMXII-75ii	JAMXII-75ii

Compound	^{1}H NMR	^{13}C NMR	IR
538b	JAMXII-75iii	JAMXII-75iii	JAMXII-75iii
543	JAMXVI-201	JAMXVI-201	JAMXVI-201
530	JAMXIII-45i	JAMXIII-45i	JAMXIII-45i
548	JAMXVI-155	JAMXVI-155	JAMXVI-155
549	JAMXVI-157	JAMXVI-157	JAMXVI-157
550	JAMXVI-159	JAMXVI-159	JAMXVI-159
551	JAMXVI-161	JAMXVI-161	JAMXVI-161
559	JAMXV-243iii	JAMXV-243iii	JAMXV-243iii
560	JAMXV-243i	JAMXV-243i	JAMXV-243i
561	JAMXVI-41i	JAMXVI-41i	JAMXVI-41i
570	JAMXVI-85iib	JAMXVI-35iib	JAMXVI-35iib
573	JAMXVI-47iiib	JAMXVI-47iiib	JAMXVI-47iiib
564	JAMXVI-85iv	JAMXVI-85iv	JAMXVI-85iv
571	JAMXV-233	JAMXV-233	JAMXV-233
574	JAMXVI-75	JAMXVI-75	JAMXVI-75
575	JAMXVI-93	JAMXVI-93	JAMXVI-93

COMPREHENSIVE BIBLIOGRAPHY

Adlhart, C.; Hinderling, C.; Baumann, H.; Chen, P. *J. Am. Chem. Soc*. **2000**, *122*, 8204-8214.

Aggarwal, V. K.; Vicente, J.; Bonnert, R. V. *Org*. *Lett*. **2001**, *3*, 2785.

Aitken, R. A.; Thomas, A. W. *Synlett* **1998**, *1,* 102.

Arduengo, A. J.; Dias, H. V. R.; Calabrese, J. C.; Davidson, F. *Organometallics* **1993**, *12*, 3405.

Armentrout, P. B.; Sunderlin, L. S.; Fisher, E. R. *Inorg*. *Chem.* **1989**, *28*, 4436-4437.

Arndt, ; Eistert, *Chem. Ber*. **1927**, *60*, 1269.

Artman III, G. D.; Weinreb, S. M. *Org*. *Lett*. **2003**, *5*(9), 1523-1526.

Ashimori, A.; Bachand, B.; Calter, M. A.; Govek, S. P.; Overman, L. E.; Poon, D. J. *J. Am. Chem. Soc*. **1998**, *120*, 6488.

Ashimori, A.; Bachand, B.; Overman, L. E.; Poon, D. J. *J. Am. Chem. Soc*. **1998**, *120*, 6477.

Ashimori, A.; Bachand, B.; Overman, L. E.; Poon, D. J. *J. Am. Chem. Soc*. **2000**, *122*, 192.

Ashimori, A.; Overman, L. E. *J. Synth. Org. Chem. Jpn*. **2000**, *58*, 718

Austin, J. F.; Kim, S.-G.; Sinz, C. J.; Xiao, W.-J.; MacMillan, D. W. C. *Proc. Nat. Acad. Sci,* **2004**, *101*, 5482-5487.

Ban, E. M.; Gil, S.; Mestres, R.; Parra, M. *Tetrahedron* **1998**, *54*, 15305.

Barluenga, J.; Lopez, L. A.; Lober, O.; Tomas, M.; Garcia-Granda, S.; Alvarez-Rua, C.; Borge, *J. Angew. Chem., Int. Ed*. **2001**, *40*, 3392-3394.

Beer, P.D.; Gale, P.A.; Smith, D.K. *Supramolecular Chemistry*, Oxford University Press, New York, 1999.

Bell, T.W.; Khasanov, A.B.; Drew, M.G.B.; Filikov, A.; James, T.L. *Angew. Chem. Int. Ed*. **1999**, *38*, 2543;

Bertani, R.; Michelin, R. A.; Mozzon, M.; Traldi, P.; Seraglia, R.; Busetto, L.; Cassani, M. C.; Tagliatesta, P.; D'Arcangelo, G. *Organometallics* **1997**, *16*, 3229-3233.

de Boer, T. J.; Backer, H. *J. Org. Synth. Coll. Vol. 4*, Rabjohn, N., Ed.; John Wiley & Sons: New York, 1963, 250-53.

Bradshaw, J. S.; Izatt, R. M.; Bordunov, A. V.; Zhu, C. Y.; Hathaway, J. K. *Comprehensive Supramolecular Chemistry*; Gokel, G. W., Ed., Pergamon/Elsevier: Oxford, U.K., 1996; Vol. 1, pp 35-95.

Britten, A. Z.; Bardsley, W. G.; Hill, C. M. *Tetrahedron* **1971**, *27*, 5631.

Brodbelt, J.S. *Int. J. Mass Spectrom.* **2000**, *200*, 57.

Burgstahler and Nordin *J. Am. Chem. Soc.* **1961**, *83*, 198

Byhlmann; Mannhardt *Prog. Chem. Org. Nat. Prod.* **1957**, *14*, 1.

Carbenes, Vols. 1 and 2 (Eds.: R. A. Moss, M. Jones, Jr.), Wiley, New York, 1973, 1975;

Chan, T.-L.; Schellenberg, K. A. *J. Biol. Chem.* **1968**, *243*, 6284.

Chandler, C.J.; Deady, L.W.; Reiss, J.A. *J. Heterocycl. Chem.* **1981**, *18*, 599.

Chang, S.-C.; Kafafi, Z. H.; Hauge, R. H.; Billups, W. E.; Margrave, J. L. *J. Am. Chem. Soc.* **1987**, *109*, 4508-4513.

Chu, Y.; Yang, Z.; Rodgers, M. T. *J. Am. Mass Spectrom.* **2002**, *13*, 453-468.

Corey, E. J. *Angew. Chem., Int. Ed.* **1999**, *38*, 1928.

Corey, E. J.; Lee, D.-H. *J. Am. Chem. Soc.* **1991**, *113*, 4026.

Corey, E. J.; Roberts, B. E.; Dixon, B. R. *J. Am. Chem. Soc.* **1995**, *117*, 193.

Crawley, S. L.; Funk, R. L. *Org. Lett.* **2003**, *5*(18), 3169-3171.

Dachriyanus; Sargent, M. V.; Wahyuni, F. S. *Aust. J. Chem.* **2000**, *53*, 159.

Dalsgaard, P. W.; Blunt, J. W.; Munro, M. H. G.; Frisvad, J. C.; Christophersen, C. *J. Nat. Prod.* **2005**, *68*, 258-261.

Dattelbaum, A. M.; Martin, J. D. *Inorg. Chem.* **1999**, *38*, 6200-6205.

Daub, G. W.; Sanchez, M. G.; Cromer, R. A.; Gibson, L. L. *J. Org. Chem.* **1982**, *47*, 745.

Davies, J. M. L.; McAfee, M. J.; Oldenburg, C. E. M. *J. Org. Chem.* **1989**, *54*, 930-936.

Dearden, C.; Dejsupa, Y.; Liang, J. S.; Bradshaw, R. M.; Izatt, *J. Am. Chem. Soc*. **1997**, *119*, 353–359.

Decodts, G.; Wakselman, M.; Vilkas, M. *Tetrahedron* **1970**, *26*, 3313.

Denmark, S. E.; Thorarensen, A. *Chem. Rev*. **1996**, *96*, 137-165.

Dias, H. V. R.; Polach, S. A. *Inorg. Chem.* **2000**, *39*, 4676-4677.

Doyle, M. P.; High, K. G.; Su-Min, O.; Osborn, A. K. *Tetrahedron Lett*. **1989**, *30*, 3049.

Doyle, M. P.; McKervey, M. A.; Ye, T. *Modern Catalytic Methods for Organic Synthesis with Diazo Compounds: From Cyclopropanes to Ylides*; Wiley & Sons: New York, 1998.

Eckart, K.; Spiess, J. *J. Am. Soc. Mass Spectrom.* **1995**, *6*, 912.

Eckroth, C. *J. Chem. Soc. C* **1970**, 2660.

Eiter, K.; Svierak, O. *Monatsh. Chem.* **1951**, *82*, 186.

Eschenmoser, A. *Helv. Chim. Acta,* **1970**, *53*, 1479.

Falorni, M.; Dettori, G.; Giacomelli, G. *Tetrahedron: Asymmetry* **1998**, *9*, 1419.

Fang, C-L; Horne, S.; Taylor, N.; Rodrigo, R. *J. Am. Chem. Soc.* **1994**, *116*, 9480.

Fang, F. G.; Maier, M. E.; Danishefsky, S. J.; Schulte, G. *J. Org. Chem.* **1990**, *55*, 831.

Felix, D.; Müller, R. K.; Horn, U.; Joos, R.; Schreiber, J.; Eschenmoser, A. *Helv. Chim. Acta* **1972**, *55*, 1276.

Fenwick, J.; Frater, G.; Ogi, K.; Strausz, O. P. *J. Am. Chem. Soc.* **1973**, *95*, 124-132.

Flammang, R.; Nguyen, M. T.; Bouschoux, G.; Gerbaux, P. *Int. J. Mass Spectrom.* **2002**, *202*, A8–A25.

Friess, S.D.; Zenobi, R. *J. Am. Soc. Mass Spectrom.* **2001**, *12*(7), 810.

Fuchs, J. R.; Funk, R. L. *J. Am. Chem. Soc.* **2004**, *126*, 5068.

Fuchs, J. R.; Funk, R. L *Org. Lett.* **2004**, *7*(4), 677-680.

Gabriela; Salermo; Veltri; Costa *Eur. J. Org. Chem.* **2001**, *24*, 4607-4614.

Galan, A.; Andreu, D.; Echavarren, A.M.; Prados, P.; de Mendoza, J. *J. Am. Chem. Soc.* **1992**, *114*, 1511.

Grant, I. J.; Hamor, T. A.; Robertson, J. M.; Sim, G. A. *J. Chem. Soc.* **1965**, 5678.

Grant, I. J.; Hamor, T. A.; Robertson, J. M.; Sim, G. A. *Proc. Chem. Soc.* **1962**, 148.

Halle, L. F.; Armentrout, P. B.; Beauchamp, J. L. *J. Am. Chem. Soc.* **1981**, *103*, 962-963.

Hamor, T. A.; Robertson, J. M. *J. Chem. Soc.* **1962**, 194.

Hauser, S.L.; Johanson, E.W.; Green, H.P.; Smith, P.J. *Org. Lett.* **2000**, *2*(23), 3575.

Hayashi, H.; Matsumoto, H.; Akiyama, K. *Biosci. Biotechnol. Biochem.* **2004**, *68*(3), 753-756.

Hayes, R. N.; Gross, M. L. *Methods Enzymol.* **1990**, *193*, 237-263.

Hendrickson, J. B.; Rees, R.; Goschke *Proc. Chem. Soc.* **1962**, 383.

Herzberg, G. *Proc. R. Soc. London Ser. A* **1961**, *262*, 291 – 317;

Hill, D. J.; Mio, M. J.; Prince, R. B.; Hughes, T. S.; Moore, J. S. *Chem. Rev.* **2001**, *101*,

3893-4012.

Horne, S.; Taylor, N.; Collins, S.; Rodrigo, R. *J. Chem. Soc., Perkin Trans. 1* **1991**, 3047.

Hu, P.; Loo, J.A. *J. Am. Chem. Soc.* **1995**, *117*, 11314.

Ilikhotvorik, Z.; Zhendong, E. L.; Tae, E.; Tippmann, B. T.; Hill, M. S.; Platz, *J. Am. Chem. Soc.* **2001**, *123*, 6061–6068.

Iwao, M.; Motoi, O. *Tetrahedron Lett.* **1995**, *36*, 5929.

J. Med Chem. **1994**, *37*(15), 2308.

Jackson, A. H.; Smith, A. E. *J. Chem. Soc.* **1964**, 5510.

Jadulco, R.; Edrada, R. A.; Ebel, R.; Berg, A.; Schaumann, K.; Wray, V.; Steube, K; Proksch, P. *J. Nat. Prod.* **2004**, *67*, 78-81.

Julian, R. R.; Akin, M.; May, J. A.; Stoltz, B. M.; Beauchamp, J. L. *Int. J. Mass Spectrom.* **2002**, *220*, 87-96.

Julian, R. R.; Beauchamp, J. L. *Int. J. Mass. Spectrom.* **2001**, *210*, 613-623.

Julian, R.R.; Beauchamp, J.L. *J. Am. Soc. Mass Spectrom.* **2002**, *13*, 493.

Julian, R. R.; May, J. A.; Stoltz, B. M.; Beauchamp, J. L. *Angew. Chem., Int. Ed.* **2003**, *42*(9), 1012-1015.

Julian, R. R.; May, J. A.; Stoltz, B. M.; Beauchamp. J. L. *Int. J. Mass Spectrom.* **2003**, *228*(2-3), 851-864.

Julian, R. R.; May, J. A.; Stoltz, B. M.; Beauchamp. J. L. *J. Am. Chem. Soc.* **2003**, *125*, 4478.

Kachinski, J. L. C.; Salomon, R. G. *J. Org. Chem.* **1986**, *51*, 1393.

Kametani, T.; Yukawa, H.; Honda, T. *J. Chem Soc., Perkin Trans. 1* **1990**, *3*, 571-577.

Katritzky, A. R.; Watson, C. H.; Dega-Szafran, Z.; Eyler, J. R. *J. Am. Chem. Soc.* **1990**, *112*, 2471-2478.

Kawasaki; Nagaoka; Satoh; Okamoto *Tetrahedron* **2004**, *60*(15), 3493-3504.

Kennewell; Miller; Scrowston; Westwood *J. Chem. Res. Miniprint* **1995**, *10*, 2380-2388.

Kirby, G. W.; Shah, S. W.; Herbert, E. J. *J. Chem. Soc. C* **1969**, 1916.

Kirmse, W. *Eur. J. Org. Chem.* **1998**, *2*, 201.

Kozlovskii, A. G.; Soloveva, T. F.; Sakharovskii, V. G.; Adanin, V. M. *Dokl. Akad. Nauk. SSSR* **1981**, *260*, 230.

Krishna, P.; Prabhakar, S.; Manoharan, M.; Jemmis, E.D.; Vairamani, M. *Chem. Commun.* **1999**, 1215.

Krolski, M. E.; Renaldo, A. F.; Rudisill, D. E.; Stille, J. K. *J. Org. Chem.* **1988**; *53*(6); 1170-1176.

Lamb, J. D.; Izatt, R. M.; Swain, C. S.; Bradshaw, J. S.; Christensen, J. J. *J. Am. Chem. Soc.* **1980**, *102*, 479-482.

Lebedev, A. T. *Rev. Mass Spectrom.* **1991**, *10*, 91-132.

Lebedev, A. T.; Bakulev, V. A.; Hayes, R. N.; Bowie, J. H. *Rapid Commun. Mass. Spectrom.* **1991**, *5*, 234-237.

Lee, H.-N.; Lee, H. S.; Kim, J. L.; Beauchamp, *J. Am. Chem. Soc.* **1998**, *120*, 5800 – 5805.

Lee, S.-W.; Kim, S.K.; Beauchamp, J.L. *J. Am. Chem. Soc*. **1998**, *120*, 3188.

Leopold, K. K.; Murray, A. E. S.; Miller, W. C.; Lineberger, *J. Chem. Phys*. **1985**, *83*, 4849–4865.

Li, J.; Burgett, A. W. G.; Esser, L.; Amezcua, C.; Harran, P. G. *Angew. Chem., Int. Ed.* **2001**, *40*, 4770.

Li, J.; Jeong, S.; Esser, L.; Harran, P. G. *Angew. Chem., Int. Ed.* **2001**, *40*, 4765.

Likhotvorik, I.; Zhu, Z.; Tae, E. L.; Tippmann, E.; Hill, B. T.; Platz, M. S. *J. Am. Chem. Soc*. **2001**, *123*, 6061-6068.

Lin, T.; Glish, G.L. *Anal. Chem.* **1998**, *70*, 5162.

Lindquist, N.; Fenical, W.; Van Duyne, G. D.; Clardy, J. *J. Am. Chem. Soc*. **1991**, *113*, 2303.

Link, J. T.; Overman, L. E. *CHEMTECH* **1998**, *28*, 19.

Loo, J. A. *Int. J. Mass Spectrom*. **2000**, *200*, 175–186.

Ludwig, R.; Fresen, *J. Anal. Chem*. **2000**, *367*, 103.

Lyle, F. R. US Patent 5 973 257, 1985; *Chem. Abstr.* **1985**, *65*, 2870.

Maleknia, J.; Brodbelt, *J. Am. Chem. Soc.* **1993**, *115*, 2837–2843;

Marfisi, C.; Verlaque, P.; Davidovics, G.; Pourcin, J.; Pizzala, L.; Aycard, J.-P.; Bodot, H. *J. Org Chem.* **1983**, *48*, 533-537.

Marzluff, E. M.; Beauchamp, J. L. In *Large Ions: Their Vaporization, Detection, and Structural Analysis*; Baer, T., Ng, C. Y., Powis, I.; Eds.; John Wiley & Sons Ltd.: New York, 1996; pp 115-143.

Mason, S. F. *Proc. Chem. Soc.* **1962**, 362.

May, J. A.; Stoltz, B. M. *J. Am. Chem. Soc.* **2002**, *124*, 12426.

May, J. A.; Zeidan, R. K.; Stoltz, B. M. *Tetrahedron Lett.* **2003**, *44*,1203.

McLuckey, S. A. *J. Am. Soc. Mass Spectrom.* **1992**, *3*, 599-614.

McMahon, R. J.; Chapman, O. L.; Hayes, R. A.; Hess, T. C.; Krimmer, H. P. *J. Am. Chem. Soc.* **1985**, *107*, 7597-7606.

Moody, C. J.; Whitham, G. H. *Reactive Intermediates*; Oxford University Press: New York, 1992; pp 26-50.

Moss, R.A.; Jones Jr., M. (Eds.), *Carbenes*, vols. 1 and 2, Wiley, New York, 1973, 1975.

Namamura, Chi, Yan, Nakasugi, Yoshizawa, Irino, Hashimoto, Kinjo, Nohara, and Sakurada *J. Nat. Prod.* **1999**, *62*, 1293.

Nemirovskiy, O.V.; Gross, M.L. *J. Am. Soc. Mass Spectrom.* **1998**, *9*, 1285.

Nemirovskiy, O.V.; Ramanathan, R.; Gross, M.L. *J. Am. Soc. Mass Spectrom.* **1997**, *8*, 809.

Ngola, S.M.; Kearney, P.C.; Mecozzi, S.; Russell, K.; Dougherty, D.A. *J. Am. Chem. Soc.* **1999**, *121*, 1192.

Nicolaou, K. C.; Snyder, S. A. *Angew. Chem. Int. Ed.* **2005**, *44*, 1012-1044.

Numata, A.; Takahashi, C.; Ito, Y.; Takada, T.; Kawai, K.; Usami, Y.; Matsumura, E.; Imachi, M.; Tadayoshi, I.; Hasegawa, T. *Tetrahedron Lett.* **1993**, *34*, 2355.

Nyerges, M.; Rudas, M.; Bitter, I.; Töke, L. *Tetrahedron* **1997**, *53*, 3269.

Odson, H. F.; Robinson, B.; Smith, G. F. *Proc. Chem. Soc*. **1961**, 465.

Oestrich, M.; Dennison, P. R.; Kodanko, J. J.; Overman, L. E. *Angew. Chem., Int. Ed.* **2001**, *48*, 1439.

Oh, T.; Wrobel, Z.; Rubenstein, S. M. *Tetrahedron Lett*. **1991**, *32*, 4647.

Overman, L. E. *Pure Appl. Chem.* **1994**, *66*, 1423.

Overmann, L. E.; Larrow, J. F.; Stearns, B. A.; Vance, J. M. *Angew. Chem. Int. Ed*. **2000**, *39*(1) 213.

Overmann, L. E.; Paone, D. V.; Stearns, B. A *J. Am. Chem. Soc*. **1999**, *121*, 7702-7703.

Padwa, A.; Straub, C. S. *J. Org. Chem*. **2003**, *68*(2), 227-239.

Paulino, R. R.; Squires, *J. Am. Chem. Soc*. **1991**, *113*, 5573–5580;

Pliego J. R.; De Almeida, W. B. *J. Chem. Soc., Faraday Trans*. **1997**, *93*, 1881-1883.

Pliego J. R.; De Almeida, W. B. *J. Phys. Chem. A* **1999**, *103*, 3904–3909.

Pomerantz, M.; Levanon, M. *Tetrahedron Lett*. **1991**, *32*, 995-998.

Poutsma, J. J. Nash, J. A. Paulino, R. R. Squires, *J. Am. Chem. Soc.* **1997**, *119*, 4686–4697;

Ramirez, J.; He, F.; Lebrilla, C.B. *J. Am. Chem. Soc.* **1998**, *120*, 7387.

Ratnayake, A. S.; Yoshida, W. Y.; Mooberry, S. L.; Hemscheidt, T. K. *J. Org. Chem.* **2001**, *66*, 8717. Note that this publication has since been withdrawn.

Regitz, M.; Hocker, J.; Liedhegener, A. *Org. Synth. Coll. Vol. 5*, Baumgarten, J. E., Ed.; John Wiley & Sons: New York, 1973, 179-83.

Rensing, S.; Arendt, A.; Springer, A.; Grawe, T.; Schrader, T. *J. Org. Chem.* **2001**, *66*, 5814.

Rice, F. O.; Glasebrook, A. L. *J. Am. Chem. Soc.* **1934**, *56*, 2381–2383.

Richardson, D. C.; Hendrick, M. E.; Jones, M. *J. Am. Chem. Soc.* **1971**, *93*, 3790-3791.

Robbers, J. E.; Otsuka, H.; Floss, H. G.; Arnold, E. V.; Clardy, J. *J. Org. Chem.* **1980**, *45*, 1117.

Robinson, R.; Teuber, H. *J. Chem. Ind.* **1954**, 783.

Rynbrandt, J. D.; Rabinovitch, B. S. *J. Phys. Chem.* **1970**, *74*, 4175–4176.

Sakharovskii, V. G.; Aripovskii, A. V.; Baru, M. B.; Kozlovskii, A. G. *Khim. Prir. Soedin.* **1983**, 656.

Salih, B.; Zenobi, R. *Anal. Chem.* **1998**, *70*, 1536.

Santelli, M.; Pons, J.-M. *Lewis Acids and Selectivity in Organic Synthesis*; CRC Press: New York, 1996.

Sarko, C. R.; Guch, I. C.; Dimare, M. *J. Org. Chem.* **1994**, *59*, 705.

Sarpong, R.; Su, J. T.; Stoltz, B. M. *J. Am. Chem. Soc.* **2003**, *125*, 13624.

Sawada, M.; Shizuma, M.; Takai, Y.; Adachi, H.; Takeda, T.; Uchiyama, T. *Chem. Commun.* **1998**, 1453.

Saxton, J. E.; Bardsley, W. G.; Smith, G. F. *Proc. Chem. Soc.* **1962**, 148.

Schalley, C.A. *Int. J. Mass Spectrom.* **2000**, *194*, 11.

Schalley, C.A. *Mass Spectrom. Rev.* **2001**, *20*, 253-309.

Schrader, T.H. *Tetrahedron Lett*. **1998**, *39*, 517.

Schwartz, B.L.; Light-Wahl, K.J.; Smith, R.D. *J. Am. Soc. Mass Spectrom*. **1994**, *5*, 201;

Scott, A. I.; McCapra, F.; Hall, E. S. *J. Am. Chem. Soc*. **1964**, *86*, 302.

Scott, A. P.; Platz, M. S.; Radom, L. *J. Am. Chem. Soc*. **2001**, *123*, 6069-6076.

Sharma, V. M.; Prasanna, P.; Adi Seshu, K. V.; Renuka, B.; Rao, L.; Kumar, G. S.; Narasimhulu, C. P.; Babu, P. A.; Puranik, R. C.; Subramanyam, D. *Biorg*. *Med*. *Chem*. *Lett*. **2002**, *12*(17), 2303-2308.

Shoeib, T.; Aribi, H. E.; Siu, K. W. M.; Hopkinson, A. C. *J. Phys*. *Chem. A* **2001**, *105*, 710-719.

Sibi, M. P.; Stessman, C. C.; Schultz, J. A.; Christensen, J. W.; Lu, J; Marvin, M. *Synth*. *Comm*. **1995**, *25*, 1255.

Sigmund, U. *Monatsh*. *Chem*. **1929**, *51*, 245.

Smith, R.D.; Bruce, J.E.; Wu, Q.Y.; Lei, Q.P. *Chem*. *Soc*. *Rev*. **1997**, *26*, 191.

Soloveva, T. F.; Kuvichkina, T. N.; Baskunov, B. P.; Kozlovskii, A. G. *Microbiol*. **1995**, *64*, 550.

Somei, M.; *Chem. Pharm. Bull*. **1985**, *33*, 2162.

Somei, M.; Yamada, F. Jpn. Patent JP 85-47044 19850308, 1986.

Spande, T. F.; Wilchek, M.; Witkop, B. *J. Am. Chem. Soc*. **1968**, 3256.

Spence, T. *J. Chem. Soc. C* **1971**, 3712-3718.

Steen, H.; Jensen, O.N. *Mass Spectrom. Rev*. **2002**, *21*, 163.

Steinhagen, H.; Corey, E. J. *Angew. Chem., Int. Ed*. **1999**, *38*, 1928.

Stevens, A. E.; Beauchamp, J. L. *J. Am. Chem. Soc*. **1979**, *101*, 6449-6450.

Straub, B. F.; Hofmann, P. *Angew. Chem., Int. Ed*. **2001**, *40*, 1288-1290.

Sudrik, S. G.; Chavan, S. P.; Chandrakumar, K. R. S.; Pal, S.; Date, S. K.; Chavan, S. P.; Sonawane, H. R. *J. Org. Chem*. **2002**, *67*, 1574-1579.

Takai, Mori, Oshima, and Nozaki *Bull. Chem. Soc. Jpn*. **1984**, *57*, 446.

Takeuchi, Y.; Tarui, T; Shibata, N. *Org. Lett.* **2000**, *2*(5), 639-642.

Tokuyama, T.; Daly, J. W. *Tetrahedron* **1983**, *39*, 41.

Toscano, J.P.; Platz, M.S.; Nikolaev, V.; Popic, V. *J. Am. Chem. Soc.* **1994**, *116*, 8146.

Tsaprailis, G.; Arpad, S.; Nikolaev, E.N.; Wysocki, V.H. *Int. J. Mass Spectrom.* **2000**, *195/196*, 467.

Tsaprailis, G.; Nair, H.; Somogyi, A.; Wysocki, V.H.; Zhong, W.; Futrell, J.H.; Summerfield, S.G.; Gaskell, S.J. *J. Am. Chem. Soc.* **1999**, *121*, 5142.

Tulloch, A. A. D.; Danopoulos, A. A.; Kleinhenz, S.; Light, M. E.; Hursthouse, M. B.; Eastham, G. *Organometallics* **2001**, *20*, 2027-2031.

Veenstra, T.D. *Biophys. Chem.* **1999**, *79*, 63.

Verbitski, S. M.; Mayne, C. L.; Davis, R. A.; Concepcion, G. P.; Ireland, C. M. *J. Org. Chem.* **2002**, *67*, 7124.

Vihinen, M. *Biomol. Eng.* **2001**, *18*, 241.

Vitale, G.; Valina, A. B.; Huang, H.; Amunugama, R.; Rodgers, M. T. *J. Phys. Chem. A* **2001**, *105*, 11351-11364.

Vogt, J.; Beauchamp, J. L. *J. Am. Chem. Soc*. **1975**, *97*, 6682-6685.

Weert, M.; Lagerwerf, F. M. *J. Mass Spectrom.* **1998**, *33*(9), 884-891.

Weijnen, J.G.J.; Koudijs, A.; Schellekens, G.A.; Engbersen, J.F.J. *J. Chem. Soc. Perkin Trans*. **1992**, *2*, 830.

Wen, M.; Munakata, M.; Suenaga, Y.; Kuroda-Sowa, T.; Maekawa, M. *Inorg. Chim. Acta* **2002**, *332*, 18-24.

Wentrup, C. *Reactive Molecules: The Neutral Reactive Intermediates in Organic Chemistry*; John Wiley & Sons: New York, 1984; pp 177-264.

Wipf, P. In *Comprehensive Organic Synthesis*; Trost, B. M., Fleming, I., Eds.; Pergamon Press: Oxford, 1991; Vol. 5, Chapter 7.2; p 827.

Wolff, L. *Justus Liebigs Ann. Chem*. **1902**, *325*, 129.

Wood, J. L.; Moniz, G. A.; Pflum, D. A.; Stoltz, B. M.; Holubec, A. A.; Dietrich, H.-J. *J. Am. Chem. Soc*. **1999**, *121*, 1748.

Woodward, R. B.; Yand, N.; Katz, T. *J. Proc. Chem. Soc*. **1960**, 76.

Yamada, F.; Makita, Y.; Suzuki, T.; Somei, M. *Chem. Pharm. Bull*. **1985**, *33*, 2162.

Ziegler, F. E. *Chem. Rev*. **1988**, *88*, 1423.

Ziegler, F. E.; Piwinski, J. J. *J. Am. Chem. Soc*. **1982**, *104*, 7181.

ABOUT THE AUTHOR

Jeremy A. May was born October 26, 1975 in Bozeman, Montana to David and Roselyn May. He was followed by a sister, Kristen, and two brothers, Benjamin and Aaron. At three years of age, he and his family moved to Great Falls, Montana, where he lived until he started high school. At that time, the family moved to Tallahassee, Florida, and then two years later to Midvale, Utah. When Jeremy graduated from high school in 1994, he served an LDS mission in Campinas, Brasil and in Marilia, Brazil for two years.

Upon returning home, Jeremy attended the University of Utah and obtained a Bachelor of Science degree in chemistry with an emphasis in biochemistry. The time at "the U" was well spent, as he actively participated in mountain biking, rock climbing, ultimate frisbee, basketball, skiing (downhill and cross-country), snowboarding, backpacking, kayaking, and squash. There was even time to study while working as a computer lab manager for the biology department.

In 2000, Jeremy moved to Pasadena, CA to pursue a Ph. D. in chemistry at the California Institute of Technology. There, he joined the lab of Brian Stoltz and researched a thesis on the synthesis and application of diazocompounds in solution and in the gas phase, as well as the synthesis of the communesin indole alkaloids. This thesis was completed in 2005.

While in Pasadena, Jeremy met Sarah Monahan and then married her in the spring of 2004. They will move to New York City in the summer of 2005 and Jeremy will work as a post-doctoral fellow in the labs of Samuel Danishefsky and Sarah will pursue a career in photography.